PRACA DOKTORSKA

Institute of Organic Chemistry
Polish Academy of Sciences

Chiral Cyclotriveratrylene-Based Molecular Cages with Sucrose Unit – Synthesis and Molecular Recognition Properties

mgr inż. Łukasz Szyszka

Ph.D. Thesis in the form of monothematic collection of research articles with a commentary, presented to the Scientific Council of the Institute of Organic Chemistry of the Polish Academy of Sciences for the degree of Doctor of Philosophy in Chemistry

Supervisor: Professor Sławomir Jarosz
Co-supervisor: Dr. Mykhaylo A. Potopnyk

Warsaw 2021

This doctoral research was a part of the OPUS 11 project funded by the National Science Centre (UMO-2016/21/B/ST5/03382).

NATIONAL SCIENCE CENTRE
POLAND

I would like to thank:

Prof. Sławomir Jarosz *for kind supervision, comprehensive support, extensive guidance during my work, and independence in my experimmmental work;*

Dr. Mykhaylo Potopnyk *for valuable advice and knowledge, inspirations, fruitful discussions, and significant contribution to realization of this project;*

Dr. Marcin Górecki *and* ***Dr. Piotr Cmoch*** *for their collaboration, great help in determining the structures of molecular cages and priceless knowledge of ECD and NMR spectroscopies;*

All my colleagues from ***Team IV***:
Patrycja, ***Karolina***, ***Ania***, ***Kinga***, ***Ola***, ***Kasia***, *and* ***Bartek*** *for the friendly atmosphere and exchanging their experience;*

All my colleagues from ***IOC PAS*** *for all discussions and sharing their knowledge;*

My closest ***friends*** *and* ***family*** *for huge support, patience, and believing in me.*

Table of Contents

1. List of publications

Publications included in the doctoral thesis:

1. Łukasz Szyszka, Piotr Cmoch, Aleksandra Butkiewicz, Mykhaylo A. Potopnyk,* and Sławomir Jarosz* "Synthesis of Cyclotriveratrylene-Sucrose-Based Capsules" *Org. Lett.* **2019**, *21*, 6523–6528.
2. Łukasz Szyszka,* Piotr Cmoch, Marcin Górecki, Magdalena Ceborska, Mykhaylo A. Potopnyk, and Sławomir Jarosz* "Chiral Molecular Cages Based on Cyclotriveratrylene and Sucrose Units Connected with *p*-Phenylene Linkers" *Eur. J. Org. Chem.* **2021**, 897–906. (**Front Cover**)
3. Łukasz Szyszka,* Marcin Górecki, Piotr Cmoch, and Sławomir Jarosz* "Fluorescent Molecular Cages with Sucrose and Cyclotriveratrylene Units for the Selective Recognition of Choline and Acetylcholine" *J. Org. Chem.* **2021**, *86*, 5129–5141.
4. Sławomir Jarosz, Patrycja Sokołowska, and Łukasz Szyszka "Synthesis of fine chemicals with high added value from sucrose: Towards sucrose-based macrocycles" *Tetrahedron Lett.* **2020**, *61*, 151888. (Digest paper)

Other publications:

5. Grzegorz Witkowski, Michał Kowalski, Łukasz Szyszka, Mykhaylo A. Potopnyk, and Sławomir Jarosz "Synthesis of 5-*epi*-deoxynojirimycin from methyl α-D-glucoside" *Tetrahedron: Asymmetry* **2016**, *27*, 747–752.
6. Łukasz Szyszka, Anna Osuch-Kwiatkowska, Mykhaylo A. Potopnyk, and Sławomir Jarosz "An efficient synthesis of a C_{12}-higher sugar aminoalditol" *Beilstein J. Org. Chem.* **2017**, *13*, 2146–2152.

2. Participation in conferences

1. 19th European Carbohydrate Symposium (EUROCARB 2017), Barcelona, Spain, 2–6.07.2017, poster presentation
2. 60. Zjazd Naukowy Polskiego Towarzystwa Chemicznego, Wrocław, Poland, 17–21.09.2017, poster presentation
3. XI Ogólnopolskie Sympozjum Chemii Organicznej, Warszawa, Poland, 8–11.04.2018, oral communication
4. German-Polish-Baltic Conference on Organic Chemistry, Hamburg, Germany, 15–19.05.2018, oral communication
5. 29th International Carbohydrate Symposium, Lisbon, Portugal, 15–19.07.2018, poster presentation
6. 61. Zjazd Naukowy Polskiego Towarzystwa Chemicznego, Kraków, Poland, 17–21.09.2018, oral communication
7. 14th International Symposium on Macrocyclic and Supramolecular Chemistry, Lecce, Italy, 2–6.06.2019, poster presentation

3. Abstract

Molecular recognition involves non-covalent specific interactions usually between two molecules (host-guest) and it is responsible for almost all biological processes occurring in Nature. In addition, molecular recognition is crucial for understanding molecular biology systems as well as enzymatic catalysis or drug design. The selective recognition of neutral or charged guests by synthetic receptors is one of the biggest challenge in supramolecular chemistry nowadays.

Among numerous artificial receptors, hemicryptophanes seem to be particularly interesting. These ditopic host molecules are capable of the selective recognition of various guest (*e.g.* carbohydrates, ammonium salts, zwitterions, anions, or ion-pairs) mainly due to their inherently chiral rigid cyclotriveratrylene (CTV) scaffold. Nowadays, we can observe the continuous search for novel hemicryptophanes being able to selective recognition of guest molecules.

The aim of this doctoral research was the synthesis of novel chiral sucrose-based hemicryptophanes and to explore their molecular recognition ability. The first part of my work concerned the synthesis of four unique enantiopure molecular cages (two of them are water-soluble) consisting of the CTV and sucrose units linked by short ethylene linkers and their structural characterization. These compounds are the first reported water-soluble hemicryptophanes with the C_1-symmetry so far. Their absolute configuration was determined by both NMR and ECD spectroscopies supported by DFT calculations. The second part of my work involved the facile synthesis of four CTV-sucrose-based diastereoisomeric cages (two pairs of regioisomers) containing *p*-phenylene linkers. For one of the diatereoisomers I obtained the X-Ray crystal structure. Moreover, such hemicryptophanes exhibit moderate binding ability towards 1-methylpyridinium and 1,3-dimethylimidazolium cations. The last part is focused on four fluorescent diastereoisomeric sucrose-based hemicryptophanes with naphthyl linkers. These molecular cages were found to be efficient and selective receptors for choline and acetylcholine. The highest selectivity was observed for one of the *M*-stereoisomers towards acetylcholine (K_{ACh}/K_{Ch} = 3.1). Additional ^{1}H NMR studies and DFT calculations allowed for investigation of its recognition properties and selectivity towards acetylcholine over choline.

4. Streszczenie

Rozpoznanie molekularne polega na specyficznych oddziaływaniach niekowalencyjnych zazwyczaj między dwiema cząsteczkami (gospodarz-gość) i jest ono odpowiedzialne za prawie wszystkie procesy biologiczne zachodzące w przyrodzie. Ponadto, rozpoznanie molekularne jest kluczowe dla zrozumienia mechanizmów działania w biologii molekularnej, jak również katalizy enzymatycznej czy projektowania leków. Selektywne rozpoznanie neutralnych lub naładowanych cząsteczek gościa przez syntetyczne receptory jest obecnie jednym z największych wyzwań w chemii supramolekularnej.

Spośród wielu sztucznych receptorów, hemikryptofany wydają się szczególnie interesujące. Te ditopowe cząsteczki gospodarza są zdolne do selektywnego rozpoznania różnych gości (*np*. węglowodanów, soli amoniowych, zwitterjonów, anionów lub par jonowych), głównie ze względu na ich inherentnie chiralne, sztywne rusztowanie cyklotriweratrylenu (CTV). Obecnie obserwuje się ciągłe poszukiwania nowych hemikryptofanów zdolnych do selektywnego rozpoznawania cząsteczek gości.

Celem mojej pracy doktorskiej była synteza nowych chiralnych hemikryptofanów na bazie sacharozy oraz zbadanie ich zdolności kompleksujących. Pierwsza część pracy dotyczyła syntezy czterech unikalnych enancjomerycznie czystych klatek molekularnych (dwie z nich są rozpuszczalne w wodzie) składających się z jednostek CTV i sacharozy połączonych krótkimi łącznikami etylenowymi oraz ich charakterystyki strukturalnej. Związki te są pierwszymi jak dotąd opisanymi rozpuszczalnymi w wodzie hemikryptofanami o symetrii C_1. Ich konfiguracja absolutna została określona zarówno za pomocą spektroskopii NMR, jak i ECD wspomaganej obliczeniami DFT. Druga część mojej pracy polegała na prostej, efektywnej syntezie czterech diastereoizomerycznych klatek (dwie pary regioizomerów) opartych na CTV i sacharozie zawierających łączniki *p*-fenylenowe. Za pomocą analizy X-Ray dla jednego z diastereoizomerów uzyskałem strukturę krystaliczną. Ponadto, te hemikryptofany wykazują umiarkowaną zdolność wiązania kationów 1-metylopirydyniowego i 1,3-dimetyloimidazoliowego. Ostatnia część pracy dotyczy czterech fluorescencyjnych diastereoizomerycznych hemikryptofanów na bazie sacharozy zawierających łączniki naftalenowe. Te klatki molekularne okazały się być efektywnymi i selektywnymi receptorami dla choliny i acetylocholiny. Największą selektywność obserwowano dla jednego z *M*-stereoizomerów w stosunku do acetylocholiny (K_{ACh}/K_{Ch} = 3.1). Dodatkowe badania ^{1}H NMR i obliczenia DFT pozwoliły na zbadanie jego właściwości wiążących i selektywności wobec acetylocholiny względem choliny.

5. Abbreviations

$\Delta G^{\neq}$	activation Gibbs free energy
ACh	acetylcholine
Aliquat 336	trioctylmethylammonium chloride
ATP	adenosine-5'-triphosphate
BINOL	1,1'-bi-2-naphthol
Boc	*tert*-butyloxycarbonyl group
Cbz	carboxybenzyl group
Ch	choline
COSY	correlation spectroscopy
CTC	cyclotricatechylene
CTG	cyclotriguaiacylene
aCTG	cyclotriaminoguaiacylene
tCTG	cyclotrithioguaiacylene
CTP	cyclotriphenolene
CTV	cyclotriveratrylene
CuAAC	copper(I)-catalyzed alkyne-azide cycloaddition
DCE	1,2-dichloroethane
DCM	dichloromethane
DFT	density functional theory
DHP	3,4-dihydro-2*H*-pyran
DIPEA	*N*,*N*-diisopropylethylamine
DOSY	diffusion-ordered spectroscopy
ECD	electronic circular dichroism
FG	functional group
G	guest
Gal	galactose
Glc	glucose
H	host
HBTU	*O*-(benzotriazol-1-yl)-*N,N,N',N'*-tetramethyluronium hexafluorophosphate
HMBC	heteronuclear multiple bond coherence
HMPA	hexamethylphosphoramide

HRMS	high-resolution mass spectrometry
HSQC	heteronuclear single quantum coherence
ITC	isothermal titration calorimetry
K_a	association constant
Man	mannose
MRI	magnetic resonance imaging
Ms	methanesulfonyl group
NaAsc	(+)-sodium L-ascorbate
NBS	*N*-bromosuccinimide
NIS	*N*-iodosuccinimide
NOESY	nuclear Overhauser effect spectroscopy
PPTS	pyridinium *p*-toluenesulfonate
PTC	phase-transfer catalysis
Py	pyridine
PyBOP	(benzotriazol-1-yloxy)tripyrrolidinophosphonium hexafluorophosphonate
R	alkyl group
ROESY	rotating-frame nuclear Overhauser effect correlation spectroscopy
S_NAr	nucleophilic aromatic substitution
TBDMS	*tert*-butyldimethylsilyl group
TBTA	tris[(1-benzyl-1*H*-1,2,3-triazol-4-yl)methyl]amine
TFAA	trifluoroacetic anhydride
THP	tetrahydropyranyl group
TMS	trimethylsilyl group
TOCSY	total correlation spectroscopy
TPA	tris(2-pyridylmethyl)amine
TREN	tris(2-aminoethyl)amine
Ts	*p*-toluenesulfonyl group
VT	variable temperature
XPhos	2-dicyclohexylphosphino-2',4',6'-triisopropylbiphenyl
XRD	X-ray diffraction

6. Hypothesis and aim of the research

Supramolecular chemistry is the discipline that deals with the creating and studying the properties of chemical systems obtained by a combining of at least two molecular components with reversible non-covalent „host-guest" interactions (*e.g.* hydrogen bonds, metal-ligand coordination or van der Waals forces). These weak forces are crucial for better understanding of biological processes, self-assembling systems, creating molecular machinery and complex materials.[1,2] The importance of supramolecular chemistry is reflected in the awards of the Nobel Prize in 1987 (Pedersen, Cram, Lehn – for pioneering works on crown-ethers and cryptands) and in 2016 (Feringa, Stoddart, Sauvage – for molecular machines).

Supramolecular chemistry, since its beginning, is interdisciplinary research area across chemistry, biology, physics, nanotechnology, and material science. In medicine, almost all interactions between drug and receptor are supramolecular in nature. Two enantiomers of chiral compound often show significant differences in toxicity, biochemical activity, transport, mechanism, and pathways of metabolism. Therefore, they will react differently with the complementary receptor or enzyme. While one enantiomer of a drug has the desired effect, the other may be inactive or cause adverse side effects.[3] Thus, development of the effective receptors with high stereoselective discrimination properties is of great significance.

Due to the interdisciplinary nature of supramolecular chemistry, for several decades, we observe constant development of functional supramolecular architectures of impressive size and properties. Supramolecular species such as cavitands,[4] cages,[5] capsules,[6] carcerands,[7] catenanes,[8] or rotaxanes[9] are some of them. These compounds can find various applications as sensors,[10] catalysts,[11] transporters,[12] separators,[13] nanoreactors,[14] polymers,[15] or porous materials.[16] Although the examples show that it is possible to prepare extremely sophisticated and functional systems in supramolecular chemistry so far, it is still a long way to completely understand the process of a controlled synthesis of supramolecular architectures with the precise physicochemical parameters (*e.g.* size, shape, function).[17,18,19] Furthermore, the synthesis of compounds able to selective binding cations, anions or neutral compounds is an important challenge in supramolecular chemistry.[20,21,22]

One of the interesting building blocks for creating molecular cages is cyclotriveratrylene (CTV) and its derivatives – the C_3-symmetrical macrocyclic compounds capable of binding small guests. An important aspect is that most of the CTV derivatives are inherently chiral (if

each aromatic ring contains at least two different substituents) and thus exist as the *M* and *P* enantiomers (Fig. 6.1).[23]

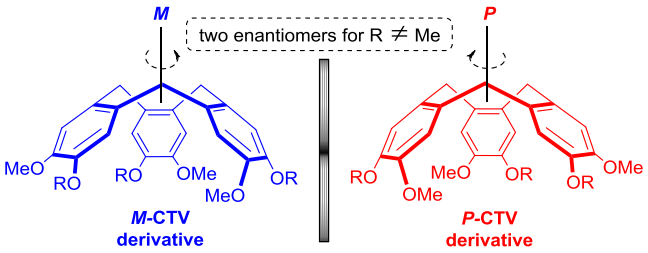

Figure 6.1. Structures of two enantiomers (*M* and *P*) of CTV-derivatives separated by mirror.

This C_3 symmetrical unit is effectively used for the synthesis of various host molecules, named cryptophanes – in which two CTV molecules are connected together[24] – and hemicryptophanes – where the CTV unit is connected with other C_3-symmetrical moiety.[25] Most of the molecular cages containing the CTV unit are synthesized as racemic mixtures with the *M* and *P* configurations. Therefore, in order to obtain enantiomerically pure cages, expensive chiral HPLC resolution is necessary, which usually provides small amount of target compounds. Another approach requires using optically pure *M* and *P* stereoisomers of CTV substrate. However, in this case, racemization is possible during further synthetic steps.[26] The alternative method, leading to enantiopure cages, requires an introduction of a chiral platform to form diastereoisomers. Nevertheless, there are only few reports, in which the CTV scaffold is triply connected with a chiral molecule creating diastereoisomers, which are possible to separate.[26] In general, difficult resolution and low yield are major limitations in the synthesis of enantiopure CTV-based molecular cages.

For many years Prof. Jarosz's group is involved in the synthesis of chiral macrocyclic receptors with sucrose scaffold, able to recognize different guests. In our group, several macrocyclic compounds containing sucrose scaffold, in which two terminal positions (C-6 and C-6') are connected together *via* different linkers were prepared (Figure 6.2., *e.g.* **1**). Some of the synthesized receptors consisted of two carbohydrate units linked together (Figure 6.2., **2**).[27] Recently, our group also obtained the first sucrose-based cryptands (Figure 6.2., **3**)[28] as well as visible-light responsive sucrose-based receptors (Figure 6.2. *cis/trans*-**4**).[29]

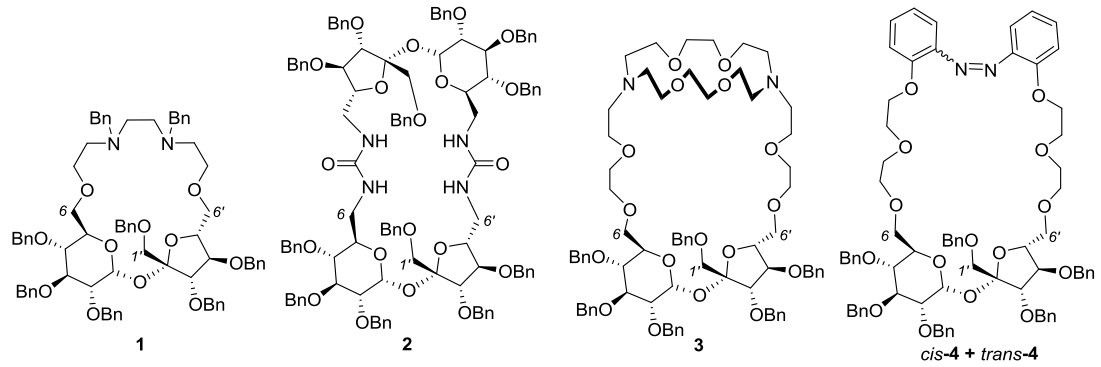

Figure 6.2. Examples of macrocyclic sucrose-based compounds prepared in our laboratory.

In view of the above, **the aim of this doctoral research was the synthesis of new chiral molecular cages with cyclotriveratrylene and sucrose units and to investigate their molecular recognition properties**. I planned to connect all three terminal positions of sucrose triol **5** with a cyclotriveratrylene unit **(±)-6** to create unprecedented C_1-symmetrical hemicryptophanes. I assumed that the triple connection of the terminal positions of both species with different linkers, should lead to the pair of at least two diastereoisomers with a different shape and size of the cavity (Scheme 6.1).

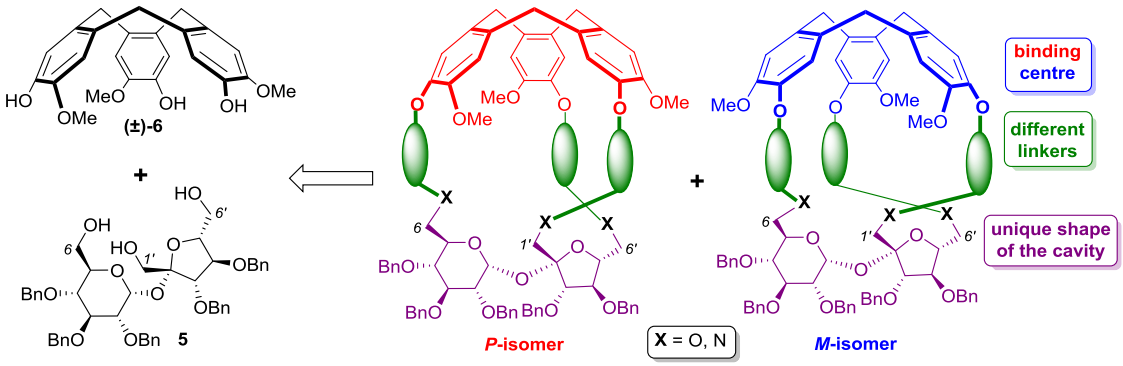

Scheme 6.1. The aim of the research: synthesis of chiral CTV-sucrose-based molecular cages connected *via* different linkers.

The chemistry of the C_1-symmetrical hemicryptophanes is unexplored to this day. For the best of my knowledge, only one example of the C_1-symmetrical hemicryptophanes is described in the literature. Namely, in 1989, the mixture of four CTV-based stereoisomers was obtained by Nolte *et al.* (see Chapter 7.4.2.7).[30] However, these molecular cages were impossible to separate, and thus they were not studied in the host-guest chemistry. The vast majority of the CTV-based cages are C_3-symmetrical and exist as racemic mixture of – difficult to separate – *P* and *M* enantiomers. Therefore, the synthesis of chiral enantiopure C_1-symmetrical receptors that I have proposed, seemed to be very interesting, particularly in

view of potential molecular recognition. Moreover, molecular cages, in which the CTV unit is triply connected to a disaccharide, are not known in the literature.

I assumed that the main advantages of the combination of chiral sucrose fragment with the CTV unit leading to molecular cages will be:

- access to the unprecedented C_1-symmetrical hemicryptophanes,
- formation of diastereoisomers, which could be separated by a classical chromatography or preparative HPLC (due to their different polarities) without using expensive chiral columns,
- ensure a unique shape of the cavity, which should allow for a better selectivity in the recognition studies,
- sucrose platform (after deprotection) will provide water-soluble receptors, which is very important because most of the recognition phenomena in Nature takes place in water.

Additionally, in further studies I planned to enlarge the cavity of these cages applying *e.g.* aromatic-type linkers, which should provide the additional π-type host-guest interactions and thus would result in an increased discrimination of guest molecules.

The greatest challenge of my research plan seemed to be the [1+1] coupling reactions as most of these type of synthetic pathways towards molecular cages generally proceed with low yield due to steric and entropic reasons. Moreover, the resulting products might be difficult to separate as more than two diastereoisomers could be formed due to the possibility of different connections between sucrose and CTV units. However, I believed that preparation of such novel, chiral, water-soluble and unprecedented C_1-symmetrical hemicryptophanes with original shape of the cavity is of great significance.

7. Literature background

7.1. Introduction

The first part of this chapter provides a short overview of basic information on the synthesis of cyclotriveratrylene (CTV) and its key derivatives. Next, the examples of the carbohydrate-based CTV derivatives are described. In the second part of this section I describe the basic information about hemicryptophanes and historical background of these molecular cages. Then, I present different approaches for the syntheses of hemicryptophanes based on the type of scaffold, linked to the CTV unit. I believe that sorting their syntheses by the nature of moieties seems to be more adequate than division by their synthetic pathways. In the last part of this chapter I describe the application of hemicryptophanes in supramolecular chemistry as artificial receptors for the complexation of various guest molecules.

I focused on this topic because CTV is the main unit – beside sucrose – in the structure of molecular cages that I have synthesized during my doctoral studies. In addition, these molecular cages are part of the C_1-symmetrical hemicryptophane group.

Cryptophanes and CTV-based metallocages, even if they are related to the CTV chemistry, will be not discussed here, as they are not connected with my doctoral research. Several reviews concerning them can be found in the literature.[24,31,32,33] Basic information and functionalization of sucrose as well as macrocyclic receptors with sucrose scaffold will be also not discussed here as they are described in the review, which I am co-author.[27] A commentary on this review is included in the next chapter.

7.2. Cyclotriveratrylene and its derivatives

7.2.1. Basic information

Cyclotriveratrylene (**7**, CTV) is a rigid bowl-shaped macrocyclic compound consisting of three veratrole units. This comparatively shape-persistent C_{3v}-symmetrical compound with tribenzo[*a*,*d*,*g*]cyclononatriene core has two conformations: crown and saddle (Scheme 7.1). The predominant crown conformation is more thermodynamically stable and adopts a pyramidal shape.[32] Its saddle conformation is thermodynamically unstable because of steric crowding of the methylene proton (H_{in}) with the aromatic ring. This disfavoured conformation is very rare and its macroscopic quantities were obtained only from quenching of melt or hot solutions of CTV.[34] Nevertheless, the crown-to-crown interconversion of CTV

is possible through a pseudorotating saddle form.[35] The rate for inversion varies with lower-rim substitution and the solvent effects, with the half-life evaluated to be approximately one month at 20°C, based on the racemization of chiral deuterated CTV derivatives.[32,36] However, the huge barrier for the crown-to-crown inversion ($\Delta G^{\neq}$ 26-27 kcal/mol) makes this process slow enough at room temperature.[35]

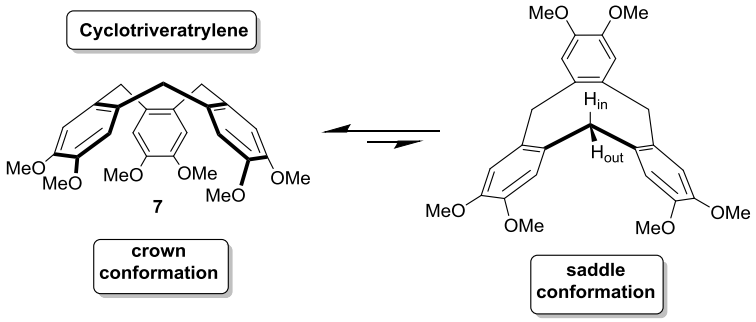

Scheme 7.1. Crown and saddle conformations of CTV.

As mentioned before, the vast majority of the CTV derivatives are inherently chiral and thus they exist as the *M* and *P* enantiomers (see Figure 6.1).[37] While both enantiomers could be separated by chiral HPLC, interconversion between the crown conformations may cause racemization in solution. Thus, a racemic mixture of the CTV analogues is usually used as a substrate in further transformations.[32]

Most of the CTV-based supramolecular architectures were obtained from the functionalized CTV analogues such as achiral hexameric cyclotricatechylene (**8**, CTC), or chiral C_3-symmetrical cyclotriguaiacylene [**(±)-6**, CTG], and cyclotriphenolene [**(±)-9**, CTP]. Other important building blocks are: tris-amino [**(±)-10**, aCTG] and tris-thiol [**(±)-11**, tCTG] derivatives (Figure 7.1).[32] These structures could be further transformed through a functionalization of the lower-rim to various CTV-based compounds.

Cyclotriveratrylene has small, hydrophobic, and electron-rich cavity, which could bound guest molecules non-covalently.[23,32] Indeed, the CTV core is efficiently used for the preparation of numerous host molecules due to its stable conformation and easy functionalization.[23] Therefore, much of the CTV chemistry is focused on molecular recognition. The CTV unit is very attractive for the formation of cages due to its crown conformation, which naturally forms capsule or container architectures with internal well-defined cavity, capable of binding guest molecules.[33] The lower rim substituents allow for further modifications of CTV moiety towards molecular receptors. Thus, it is not surprising that the vast majority of CTV functionalization takes place at the lower rim.

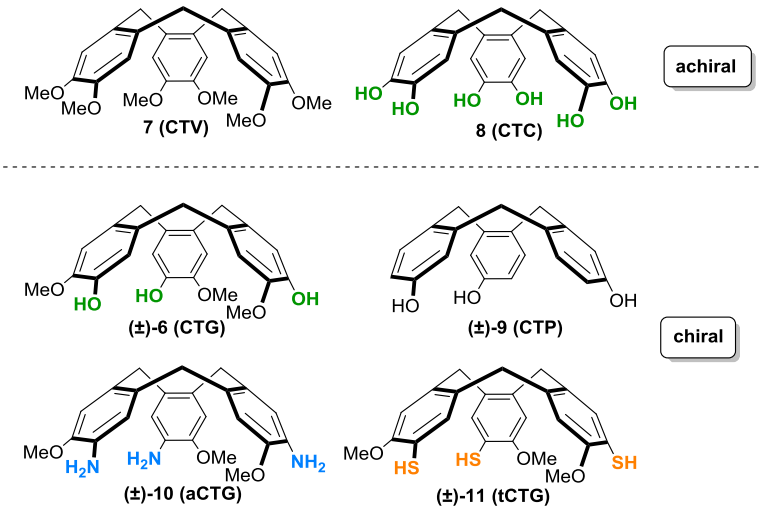

Figure 7.1. Molecular structures of the CTV analogues.

The rigid crown structure of the CTV derivatives, consisting of three benzene chromophores, makes them interesting to study chiroptical properties by electronic circular dichroism (ECD). In a pioneered work, Collet and Gottarelli discovered that the absolute configuration of various chiral CTV derivatives could be determined using the ECD spectroscopy regarding to excitonic coupling between transition moments of the CTV aromatic rings.[38] Namely, the *M* or *P* configuration of the CTV derivative could be assigned by the ^1L_a transition pattern, which gives two characteristic opposite bands with a negative to positive sequence from low to high energy in case of *M* stereoisomer, or positive to negative sequence from low to high energy for *P* stereoisomer.

7.2.2. Synthesis of CTV and its analogues

Cyclotriveratrylene was synthesized for the first time approximately one century ago by Ewins[39] and Robinson,[40] but its structure was incorrectly assigned as a dimer. The proper trimeric macrocyclic structure was proposed in the 1960s by Erdtman,[41] Lindsey,[42] and Goldup.[43] There are two main synthetic pathways towards CTV and its derivatives: 1) acid-catalyzed condensation of formaldehyde with 1,2-disubstituted benzenes, or more common 2) acid-catalyzed condensation of 3,4-disubstituted benzylic alcohols (Scheme 7.2).

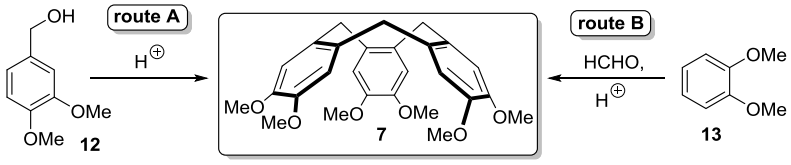

Scheme 7.2. Two possible routes towards CTV.

The condensation of veratryl alcohol (**12**) towards cyclotriveratrylene generally requires strong dehydrating acids as $HClO_4$ in MeOH,[44] H_3PO_4,[45] H_2SO_4 in glacial AcOH,[42] TFA in $CHCl_3$,[46] or concentrated HCl[42] (Table 7.1, route A). However, milder reaction conditions with a catalytic amount of $Sc(OTf)_3$ as a Lewis acid,[47] or including *green* syntheses[48] have also been reported. Similar reagents are also used for the trimerization of veratrole (**13**).[42] Interestingly, replacement of the aqueous solution of formaldehyde with solid paraformaldehyde as well as changing the mineral acid to Lewis or organic acid provided much better yields of final CTV product (Table 7.1, route B).[49,50]

Table 7.1. Reaction conditions of the synthesis of cyclotriveratrylene.

Entry	Route A		Entry	Route B	
	Conditions	**Yield [%]**		**Conditions**	**Yield [%]**
1.	H_2SO_4, AcOH, 90°C	87[42]	**1.**	conc. HCl, rt	21[42]
2.	60% $HClO_4$, MeOH	35[44]	**2.**	70% H_2SO_4, rt	21[42]
3.	conc. HCl, 0°C→rt	21[42]	**3.**	paraformaldehyde,	55[49]
4.	H_3PO_4, 80°C	31[45]		$BF_3{\cdot}OEt_2$, DCE, rt	
5.	TFA, $CHCl_3$, 0°C→rt	19[46]	**4.**	paraformaldehyde,	85[50]
6.	cat. $Sc(OTf)_3$, MeCN, 60°C	44[47]		MsOH, DCM, rt	

CTV derivatives are mostly prepared by the aromatic electrophilic substitution of 3,4-disubstituted benzyl alcohols. While this trimerization of benzyl alcohol containing the electron donating groups in the *para* and *meta* positions is mostly efficient (Table 7.2, Entries 1-5, 10, and 11), the same strategy for the corresponding benzyl alcohols with the electron withdrawing groups in the *para* and *meta* positions is usually ineffective. The importance of the electron donating group in the *meta* position is demonstrated by comparing the 4-bromo-3-methoxybenzyl alcohol (**20**) with its regioisomer 3-bromo-4-methoxybenzyl alcohol (**21**), where only the first one can be successfully transformed into cyclic compound **(±)-31** (Table 7.2, Entries 7 and 8).[31,51] The substituent at the *para* position of hydroxymethyl function probably prevents side reaction at this position.[31] It was noticed that 3-methoxybenzyl alcohol (**19**) gives trimeric product **(±)-30** in poor yield; polymeric compounds are the main products (Table 7.2, Entry 6).[31,52] However, in some cases, weak deactivating groups (*e.g.* Br, I)

directly attached to the aromatic ring at the *para* position in respect to hydroxymethyl function, could be used in the trimerization reaction providing trihalogenated CTV analogues in moderate yields (Table 7.2. Entries 7 and 9).[51,53,54] These trihalogenated compounds are very attractive intermediates towards the extended-cavity CTV derivatives particularly for the synthesis of the CTV analogues containing electron withdrawing groups, which cannot be obtained *via* a typical trimerization.[55,56]

Table 7.2. Reaction conditions of the synthesis of CTV derivatives.

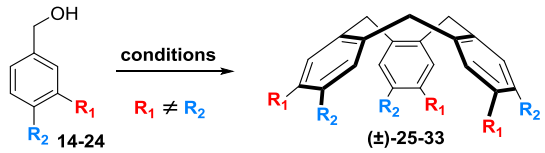

Entry	Substrate	R_1	R_2	Conditions	Product	Yield [%]
1.	**14**	OMe	*O*-allyl	$Sc(OTf)_3$, DCM, 60°C	**(±)-25**	55[47]
2.	**15**	OEt	*O*-allyl	$Sc(OTf)_3$, DCM, 60°C	**(±)-26**	47[47]
3.	**16**	OMe	OEt	H_3PO_4, 80-90°C	**(±)-27**	59[57]
4.	**17**	OMe	OCH_2CO_2H	65% $HClO_4$, 0°C→rt	**(±)-28**	45[58]
5.	**18**	OMe	OCH_2CH_2Br	$Sc(OTf)_3$, DCM, 35°C	**(±)-29**	67[59]
6.	**19**	OMe	H	P_2O_5, Et_2O, reflux	**(±)-30**	9[52]
7.	**20**	OMe	Br	P_2O_5, Et_2O	**(±)-31**	40[51]
8.	**21**	Br	OMe	65% $HClO_4$, 0°C→rt	**(±)-31**	0[31]
9.	**22**	OMe	I	P_2O_5, Et_2O, reflux	**(±)-32**	50[53]
10.	**23**	SMe	OMe	HCOOH, 70°C	**(±)-33**	70[60]
11.	**24**	OMe	SMe	HCOOH, 70°C	**(±)-33**	60[64]

The most important approach towards CTV analogues with the extended cavity, is the functionalization of the hydroxyl groups of cyclotriguaiacylene [(±)-CTG] or cyclotricatechylene (CTC). The CTC is synthesized *via* a demethylation of CTV induced by BBr_3[61] (Scheme 7.3 a), while removal of the allyl protections from **(±)-25** affords (±)-CTG up to 92% yield (Scheme 7.3 b).[62,63,64,65]

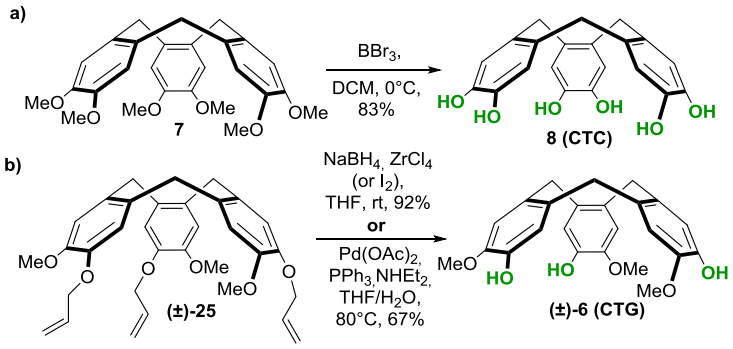

Scheme 7.3. Convienient synthesis of a) CTC and b) (±)-CTG.

It is noteworthy that both compounds [(±)-CTG and CTC], cannot be prepared *via* a direct cyclization of the corresponding benzylic alcohols (4-hydroxy-3-methoxybenzyl and 3,4-dihydroxybenzyl alcohol, respectively).

The CTV derivatives with the amino [(±)-aCTG] or thio [(±)-tCTG] functional groups represent another important macrocyclic compounds, particularly useful for the synthesis of nitrogen or sulfur containing supramolecular hosts. Cyclotriaminoguaiacylene [**(±)-10**] can be prepared in a multi-step procedure from the commercially available compound **34** as shown in Scheme 7.4. This synthetic pathway was reported for the first time in 1993 by Collet and there is still no alternative method for the preparation of (±)-aCTG.[66]

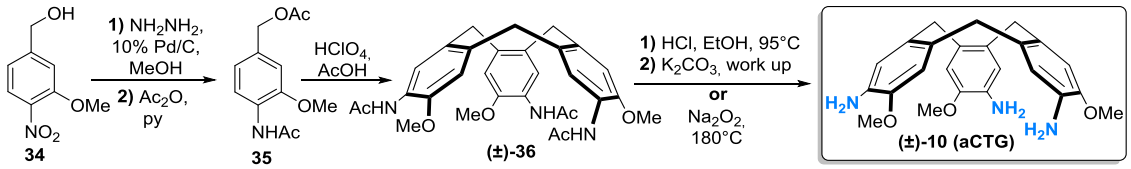

Scheme 7.4. Synthesis of (±)-aCTG.

The thio-derivative – cyclotrithioguaiacylene [(±)-tCTG] – might be successfully synthesized on two different pathways: the Pummerer or Newman-Kwart rearrangements as shown in Scheme 7.5.[67]

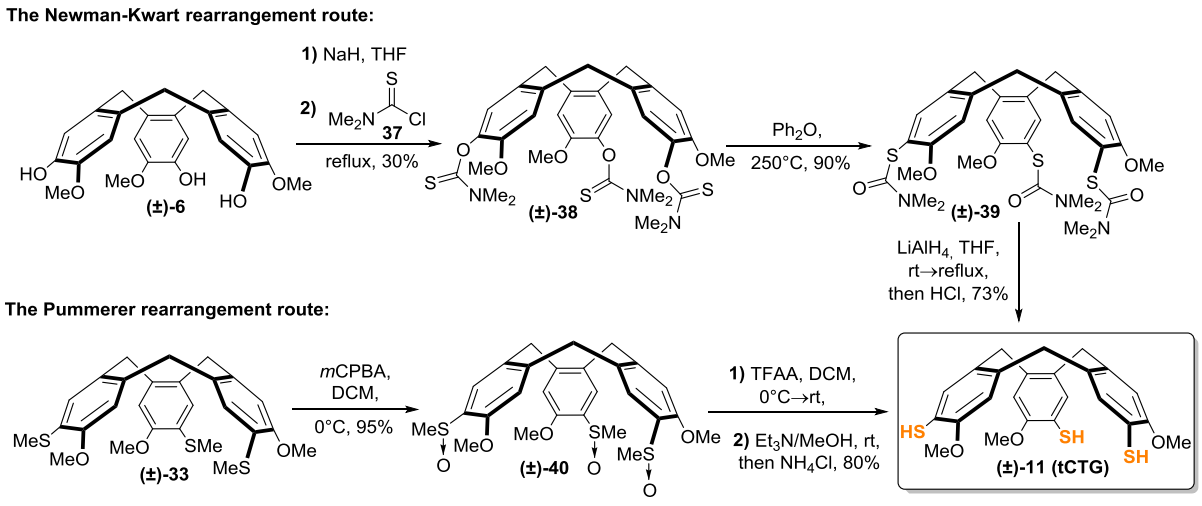

Scheme 7.5. Two possible synthetic routes towards (±)-tCTG.

While most of the CTV derivatives are trifunctionalized and thus they are C_3-symmetrical, the C_1-symmetrical mono- or difunctionalized species are relatively rare and only several of them were reported in the literature so far.[68, 69] For example,

monohalogenation of cyclotriphenolene [(±)-CTP] using *N*-iodo- or *N*-bromosuccinimide afforded C_1-symmetrical (±)-CTP derivatives **(±)-42** and **(±)-43** in very good yield (Scheme 7.6).[69] These monohalogenated CTV analogues could be a suitable platform for further transformations leading to novel C_1-symmetrical hosts.

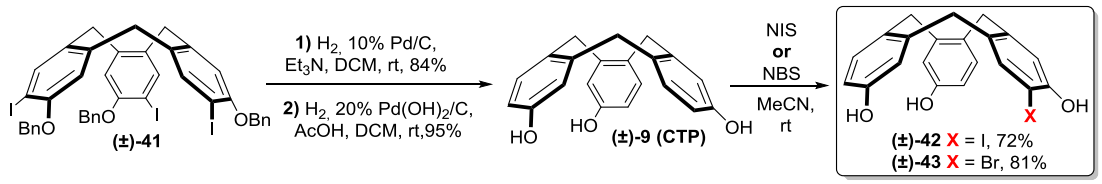

Scheme 7.6. Synthesis of monohalogenated CTV analogues.

Recently, Martinez *et al.* reported the straightforward convenient synthesis of the enantiopure C_1-symmetrical (±)-CTG.[70] Reaction of a 1:1 mixture of regioisomers **14** and **44** catalyzed with $Sc(OTf)_3$ afforded the C_1- and C_3-symmetrical CTV derivatives in 46% yield and 4:1 ratio, respectively. Subsequent removal of the allyl groups from the main C_1-symmetrical product **45** provided the C_1-symmetrical (±)-CTGs ***M*-46** and ***P*-46** in 90% yield (Scheme 7.7). These compounds can be easily prepared in a gram scale and separated by chiral HPLC. This synthetic approach might open new routes to the C_1-symmetrical CTV-based hosts with original shape of the cavity.

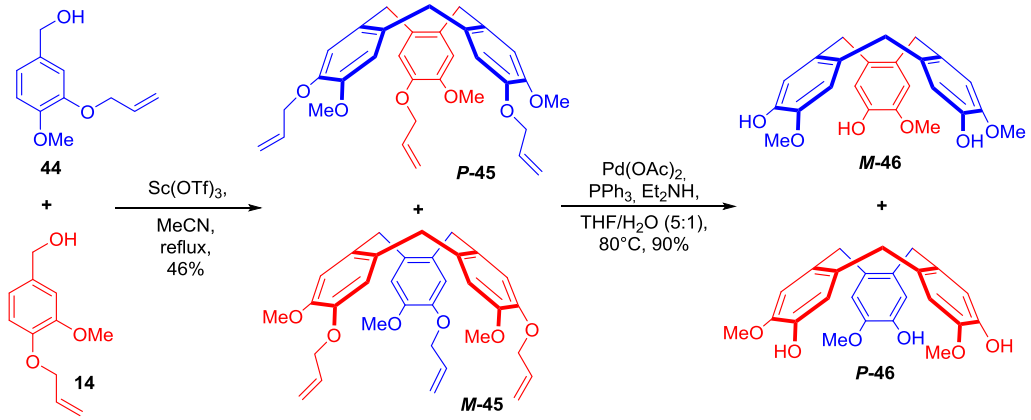

Scheme 7.7. Synthesis of C_1-symmetrical (±)-CTGs.

Cyclotriveratrylene derivatives are widely used in supramolecular chemistry due to their electron-rich cavity capable of binding guest molecules non-covalently. Indeed, these bowl-shaped macrocycles have found an application as the efficient and selective receptors towards various anions,[71,72,73] cations,[74,75] fullerenes,[76,77] carboranes,[78,79] carbohydrates,[80] and other organic compounds.[81,82,83] In addition, they are able to form coordination polymers and

networks,[84,85,86] self-assembled dendritic columns and spheres,[87,88] organo- and hydrogels,[89,90] porous materials,[91,92] and liquid crystals,[93,94] thus finding an application as soft materials. The CTV derivatives, in particular the metal complexes, were also successfully used as catalysts in the Knoevenagel condensation,[95] Michael addition,[96] or Suzuki-Miyaura coupling.[97]

7.3. Carbohydrate-based cyclotriveratrylene derivatives

There are only few reports in the literature about the CTV unit combined with carbohydrates so far. The first example concerning the connection of a simple sugar to the CTV platform was described in 1999 by Iyengar and Thomas.[98] In this paper, the authors presented the facile synthesis of the water-soluble diastereoisomeric mixture of the CTV derivative with peripheral glycosyl units. Treatment of racemic **(±)-47** with bromide **48** in the presence of NaH followed by removal of the acetyl groups afforded a mixture of two diastereoisomers ***M*-49** and ***P*-49** in 93% (Scheme 7.8). However, attempts to separate both diastereoisomers as well as studies on their complexing capacity using 1-anilinonaphthalene-8-sulfonate (ANS) as a guest were unsuccessful.

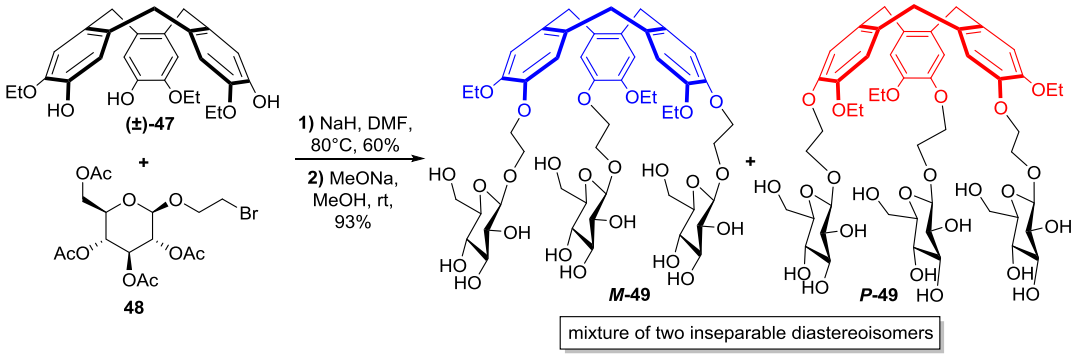

Scheme 7.8. Synthesis of water-soluble CTV derivative with peripheral glycosyl residues.

The small library of trivalent CTV-based amino acid glycoconjugates was synthesized by Liskamp and Ameijde.[99] These glycoconjugates varied in the length of the linkers (different polyethylene glycols) as well as the type of amino acid (alanine, lysine, or glutamic acid), and carbohydrate (galactose, glucose, or lactose) units. The general synthetic pathway is shown in Scheme 7.9. Alkylation of (±)-CTG with tosylate **50** under basic conditions gave triol **(±)-51**, which was further activated by transforming into the *p*-nitrophenyl carbonate derivative **(±)-53**. Subsequent coupling reaction between **(±)-53** and corresponding glyco-amino acid monomers **54** in the presence of $NaHCO_3$ in THF led to the CTV-based glycoconjugates in moderate yields (15-48%). Finally, removal of protecting

groups from the carbohydrate units provided target products **55** as diastereoisomeric mixtures with 1:3 up to 1:7 ratio. The authors suggested that this class of molecules could find an application as antibiotics due to their potential ability to block the trimeric general bacterial porins. However, the biological activity of such prepared glycoconjugates has not been investigated.

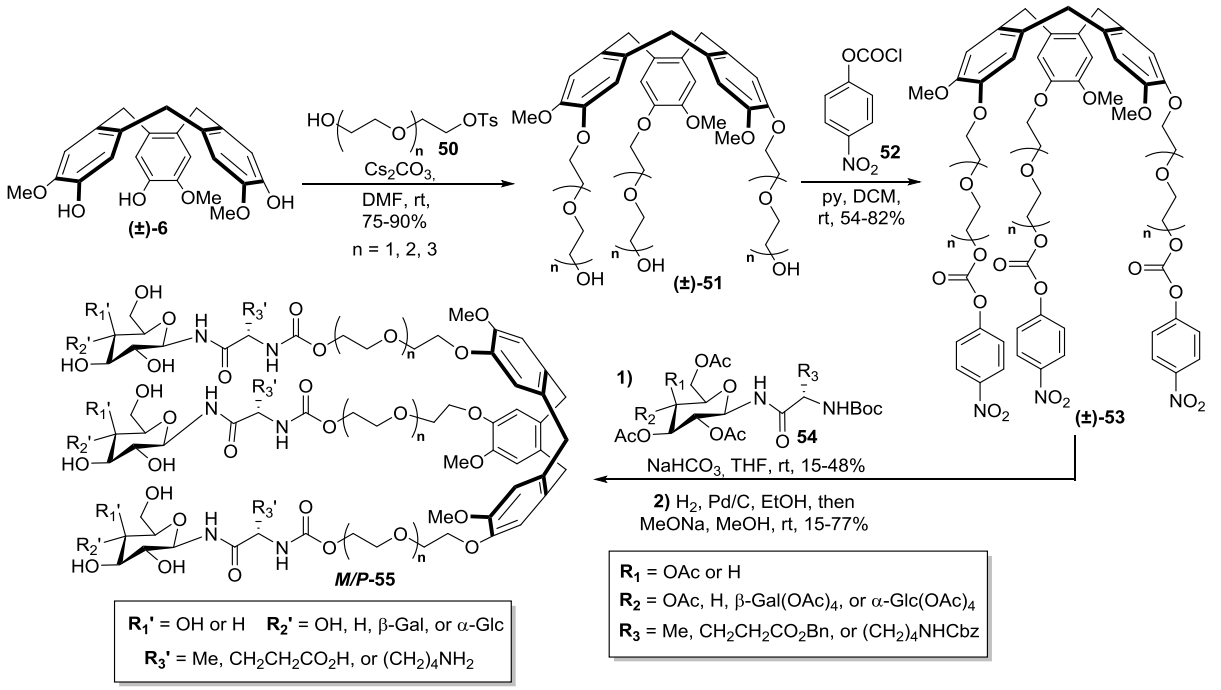

Scheme 7.9. General synthesis pathway towards CTV-based amino acid glycoconjugates.

In 2012 and 2013, Han and co-workers described the syntheses of four water-soluble CTV-based glycoconjugates containing peripheral glucose, glucosamine hydrochloride, or lactose units, and studied their binding properties with C_{60} in both organic and aqueous media.[100,101] The trivalent sugar-containing compounds ***M/P*-59** and ***M/P*-60** were obtained *via* a Huisgen 1,3-dipolar cycloaddition reaction between propargylated CTV derivative **(±)-56** and corresponding azido-functionalized carbohydrates (**57** or **58**) using $CuSO_4$ and (+)-sodium L-ascorbate in excellent yields (Scheme 7.10a). The final one-pot cleavage of all acetyl and Boc protecting groups afforded the desired, water-soluble compounds ***M/P*-61** and ***M/P*-62**. Similar strategy was employed for the preparation of hexavelent CTV-based glycoconjugates **65** and **66** (Scheme 7.10b); all four compounds have fluorescence properties. The authors explained that the enhanced planar conformation of the CTV ring originating from the spatial effect of large-volume sugar scaffolds could be responsible for the fluorescence properties of these carbohydrate-extended CTV derivatives.

The binding properties of all four CTV-based glycoconjugates towards C_{60} were performed by the fluorescence spectroscopy titrations in the mixture of toluene/DMSO (1:1).

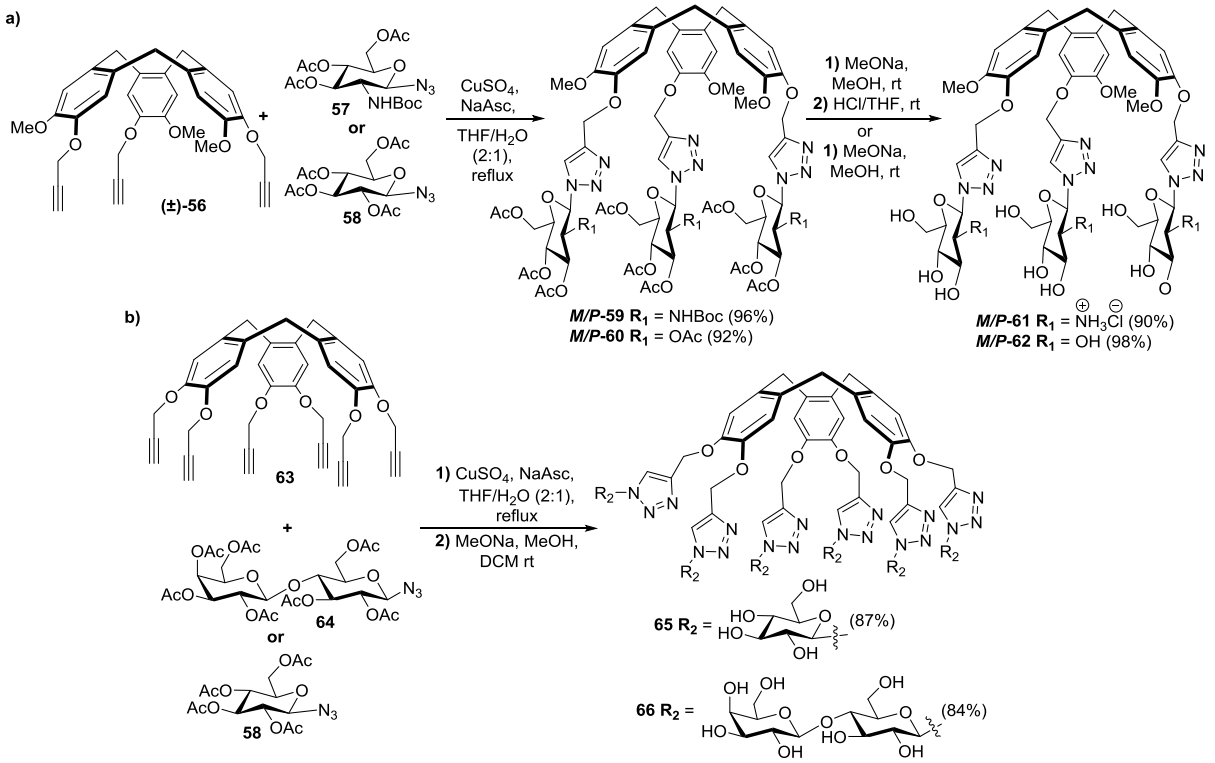

Scheme 7.10. Synthesis of a) trivalent and b) hexavalent CTV-based glycoconjugates.

All hosts demonstrated very good binding abilities towards C_{60} with particular emphasis on the cationic receptor ***M/P*-61,** which displayed the best complexing properties (K_a = 4.36 × 10^5 M^{-1} for ***M/P*-61**, 1.38 × 10^5 M^{-1} for ***M/P*-62**, and 5.09 × 10^4 M^{-1} for **66**). Moreover, additional experiments showed that these sugar-bearing compounds are able to transfer fullerene into the aqueous solution through non-covalent interactions leading to water-soluble supramolecular complexes. While multiple hydroxyl functions from carbohydrates provided water-soluble complexes, both 1,2,3-triazole rings and sugar scaffolds could increase the hydrophobic interactions as well as van der Waals forces between the host and guest molecules.

Similar synthetic pathway involving azide-alkyne cycloaddition towards trivalent and hexavalent CTV-based glucoconjugates were reported by Vidal *et al.*[102] Nevertheless, these compounds differed from the previous ones by an additional triethylene glycol chain and carbohydrate edges (galactose and fucose). Moreover, they interact non-covalently with bacterial lectins, which point them as possible adhesion-blocking agents that could prevent bacterial infections.

Combinations of the CTV scaffold with α-cyclodextrin are also known in the literature. They are described in details in Chapter 7.4.2.6.

7.4. Hemicryptophanes

7.4.1. Basic information and historical background

Hemicryptophanes are inherently chiral, covalently bound cage-type molecular receptors with ditopic cavity, consisting of the C_3-symmetrical cyclotriveratrylene scaffold triply connected to another different C_3-symmetrical unit.[25] Their inherent chirality results from the C_3-symmetrical CTV unit and thus these compounds exist in the *P* and *M* configurations. Basically, hemicryptophanes differ from each other by the type and length of the linkers as well as the nature of the lower C_3-symmetrical moiety. Their most important advantage is, undoubtedly, the ability to recognize various neutral or charged guests molecules.

First synthesis of hemicryptophane was published in 1982 by Collet, Lehn *et al.*[103] The authors described two molecular cages constructed from the CTV unit and aza-crown ether [**(±)-67** and **(±)-68**], which were named *speleands* (Figure 7.2). However, there was almost no interest in studying this class of molecular hosts during next two decades. Only few articles, focused on hemicryptophane chemistry, were published before 2005.

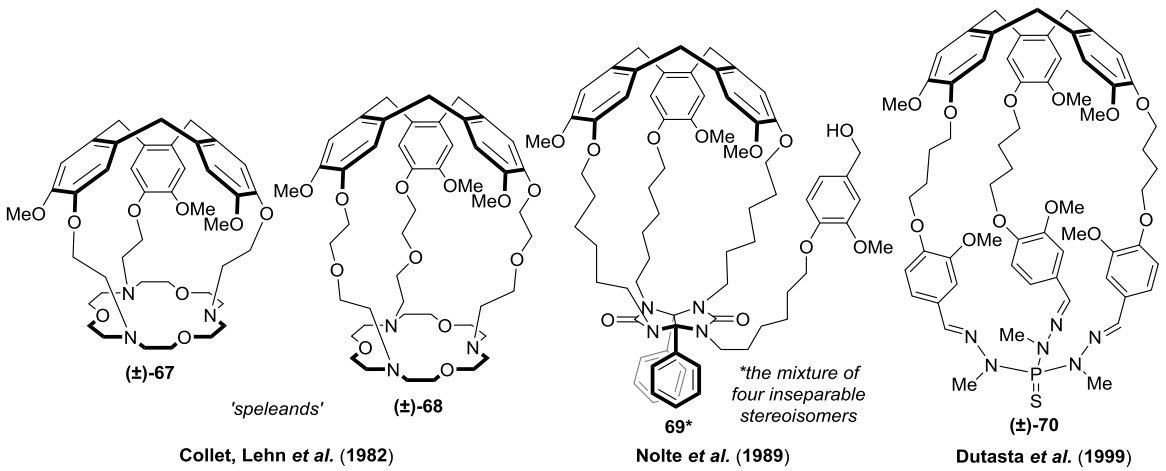

Figure 7.2. Structures of first hemicryptophanes synthesized from 1982 to 2005.

In 1989 Nolte's group reported the first synthesis of four inseparable stereoisomers of the C_1-symmetrical hemicryptophanes containing diphenylglycoluril moiety and additional pendant arm designed for potential catalytic functions (**69**, Figure 7.2).[30] Ten years later,

Dutasta *et al.* presented the synthetic pathway leading to thiophosphorylated hemicryptophane **(±)-70** (Figure 7.2) and reported its crystal structure with encapsulated toluene molecule.[104] In the same paper, the authors proposed – for the first time – the name *hemicryptophane* for the structurally related cage compounds, which is widely used since then. Hemicryptophanes have attracted growing attention in the last 16 years, which is manifested by constant increasing of a number of publications describing these molecular cages. A number of various hemicryptophanes were synthesized and successfully applied in the selective recognition of different guest molecules, supramolecular catalysis, or molecular motions, so far.[25]

The greatest contribution to the design and development of hemicryptophanes was made by Dutasta and Martinez group.[25] There are only several examples of hemicryptophanes reported by other groups. This research area seems to be interesting particularly in the case of chirality and selective recognition properties of these host cages.

7.4.2. Synthesis of hemicryptophanes

While the connection of the inherently chiral CTV unit with an achiral C_3-symmetrical scaffold leads to a racemic mixture of the *P* and *M* enantiomers of hemicryptophane, the combination of the CTV unit with a chiral molecule provides appropriate *P* and *M* diastereoisomers. In the literature, most of hemicryptophanes are synthesized as racemic mixtures without its further separation.[25] The fast and easy preparation of enantiopure cages is very challenging due to their high complexity and thus limits its application in chiral recognition studies. In general, the enantiopure cages could be prepared by three different methods:

1) chiral resolution of a racemic mixture by HPLC,
2) synthesis of diastereoisomers by an introduction of additional stereogenic center(s),
3) employing optically pure *M* and *P* stereoisomers of the CTV substrate.

The first method is expensive and usually provides as little as few milligrams of optically pure cages. The second one could afford enantiopure products, but their separation might be unsuccessful, or difficult and tedious in most cases. In the last method, very mild reaction conditions (*e.g.* avoiding heating) are required, since racemization of the product on each synthetic step can occur. Moreover, the synthesis is time consuming due to additional reactions with each *P* and *M* enantiomer.[26]

From a synthetic point of view, three different strategies could be used to obtain hemicryptophanes (Scheme 7.11):

1) the cage-closing reaction to construct the CTV scaffold from veratryl precursors,

2) the cage-closing reaction at the lower part of appropriate CTV-based precursor,

3) the [1+1] coupling between the CTV unit and other C_3-symmetrical moiety.

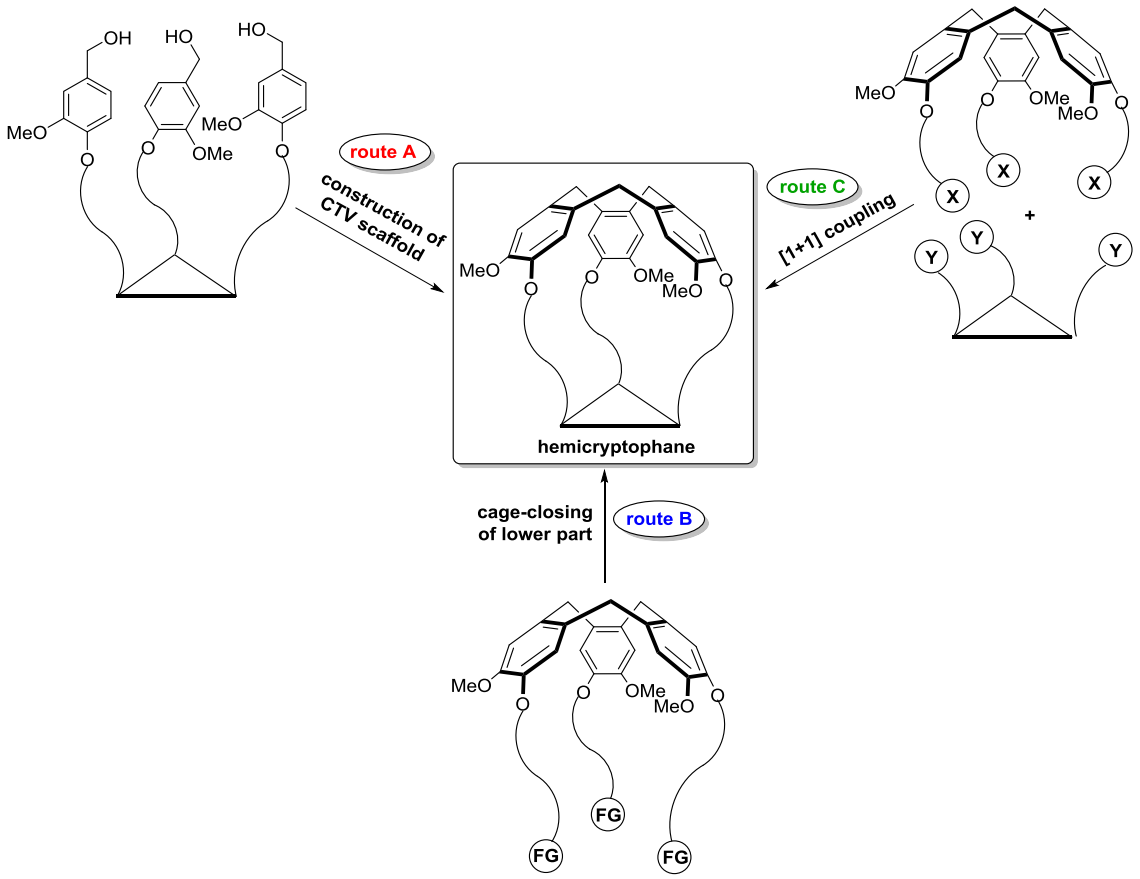

Scheme 7.11. Three different synthetic routes for the synthesis of hemicryptophane.

The first pathway – the *template method* – involves the acid-catalyzed cyclization of the veratryl precursors, which will form the CTV moiety in the last step of hemicryptophane synthesis (Scheme 7.11, route A). This reaction is commonly applied for the construction of numerous CTV derivatives. Nevertheless, the use of this cyclodehydration reaction depends on the structure and character of the cage precursors (acid-sensitive compounds cannot be employed in this synthetic method).

In the second pathway, the CTV unit contains three linkers with the appropriate functional groups for intramolecular reaction forming hemicryptophanes (Scheme 7.11, route B); this method is rarely used in practice.

The last approach, which is the most widely used pathway leading to hemicryptophanes, deals with the [1+1] coupling between the CTV derivative and other C_3-symmetrical unit (Scheme 7.11, route C). This strategy is very effective for the preparation of many CTV-based molecular cages due to the vast array of different C_3-symmetrical molecules, which could be employed. An important advantage of this synthetic route results from various types of reactions that could be used for a triple connection of both units (*e.g.* alkylation, amidation, imination, esterification, *etc.*) as well as introducing other host molecules, such as crown ethers, cyclodextrins, or calixarenes.

It is noteworthy that all three synthetic strategies require high-dilution conditions to prevent the formation of polymeric by-products. In some cases, addition of template (*e.g.* cation with suitable size) might improve the efficiency of the macrocyclization reaction.[25,26]

In the next sections, I describe different approaches leading to hemicryptophanes based on the type of scaffolds, which are linked to the CTV unit, such as triethanolamine, nitrilotriacetamide, tris(2-aminoethyl)amine (TREN), tris(2-pyridylmethyl)amine (TPA), 1,3,5-tripodal benzene, and various macrocycle units. Other examples of hemicryptophanes with diphenylglycoluril, phosphotrihydrazone, tribenzylamine, and tris(benzyltriazolylmethyl)amine (TBTA) moieties, which do not fit to any of above categories, will be presented in the last part of this chapter.

7.4.2.1. Hemicryptophanes containing triethanolamine scaffold

In 2005, after a long break in hemicryptophane chemistry, Dutasta and co-workers reported the synthesis of four chiral, enantiopure CTV-based molecular cages containing triethanolamine moiety.[105] The synthesis of the first diastereoisomeric pair was initiated from vanillyl alcohol (**71**), which was transformed in a few steps into veratryl precursor **72**. Regioselective nucleophilic substitution of compound **72** with (*R*)-(–)-glycidyl nosylate, provided the enantiopure epoxide (*R*)-**73** (Scheme 7.12). Reaction of compound (*R*)-**73** with an excess of ammonia caused the opening of the epoxide ring giving aminoalcohol (*R*)-**74**. Next, reaction of aminoalcohol (*R*)-**74** with epoxide (*R*)-**73** afforded C_3-symmetrical veratryl precursor (*R*,*R*,*R*)-**75**, which was further acetylated. The target diastereoisomeric hemicryptophanes ***M***-(*R*,*R*,*R*)-**77** and ***P***-(*R*,*R*,*R*)-**77** were prepared by a Lewis acid-catalyzed intramolecular cage-closing reaction of veratryl precursor (*R*,*R*,*R*)-**76** in 22% and 17% yields, respectively. Finally, removal of the acetyl functions in methanolic NaOH afforded hemicryptophanes ***M***-(*R*,*R*,*R*)-**78** and ***P***-(*R*,*R*,*R*)-**78** in quantitative yield.

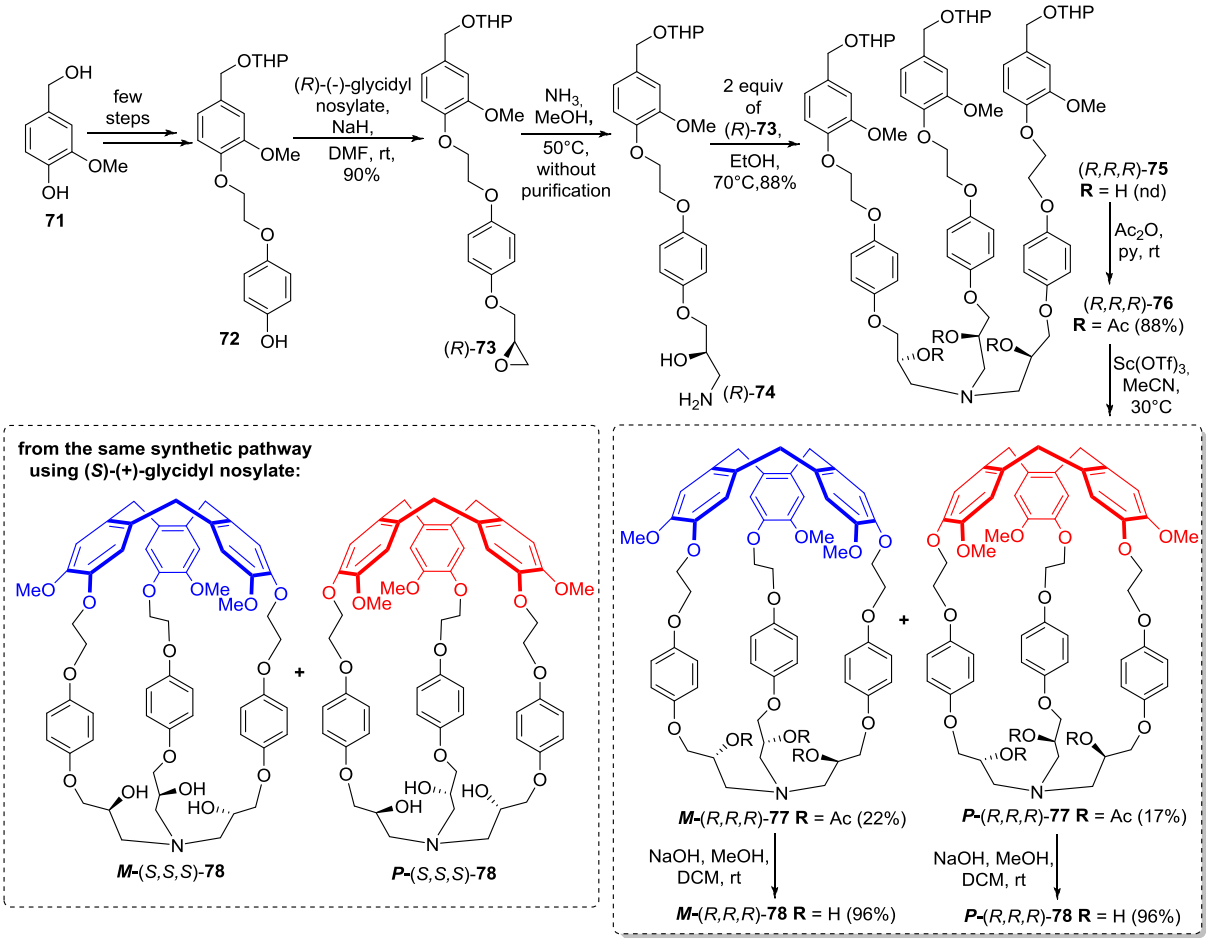

Scheme 7.12. Synthetic pathway towards four chiral diastereoisomeric hemicryptophanes.

The other pair of diastereoisomeric hemicryptophanes [***M***-(*S*,*S*,*S*)-**78** and ***P***-(*S*,*S*,*S*)-**78**] were similarly obtained using (*S*)-(+)-glycidyl nosylate. It should be pointed out that both optically pure hemicryprophanes ***M***-(*R*,*R*,*R*)-**77** and ***P***-(*R*,*R*,*R*)-**77** as well as their enantiomers ***M***-(*S*,*S*,*S*)-**77** and ***P***-(*S*,*S*,*S*)-**77**, were separated by a classical silica gel chromatography.

In another study, Guy, Gao and Martinez described the synthesis of eight enantiopure hemicryptophanes containing three different types of stereogenic elements: 1) helically chiral CTV unit, 2) axially chiral 1,1'-bi-2-naphthol linkers, and 3) central chirality of the stereogenic centers located on carbon atoms on the triethanolamine moiety.[106] Four diastereoisomeric pairs of enantiomers [***M***-(*S*,*S*,*S*)-(*S*,*S*,*S*)-**84** and ***P***-(*S*,*S*,*S*)-(*S*,*S*,*S*)-**84**; ***M***-(*R*,*R*,*R*)-(*R*,*R*,*R*)-**84** and ***P***-(*R*,*R*,*R*)-(*R*,*R*,*R*)-**84**; ***M***-(*S*,*S*,*S*)-(*R*,*R*,*R*)-**84** and ***P***-(*S*,*S*,*S*)-(*R*,*R*,*R*)-**84**; ***M***-(*R*,*R*,*R*)-(*S*,*S*,*S*)-**84** and ***P***-(*R*,*R*,*R*)-(*S*,*S*,*S*)-**84**] were obtained on the similar route by changing the stereochemistry of either 1,1'-bi-2-naphthol or glycidyl nosylate as shown in Scheme 7.13a.

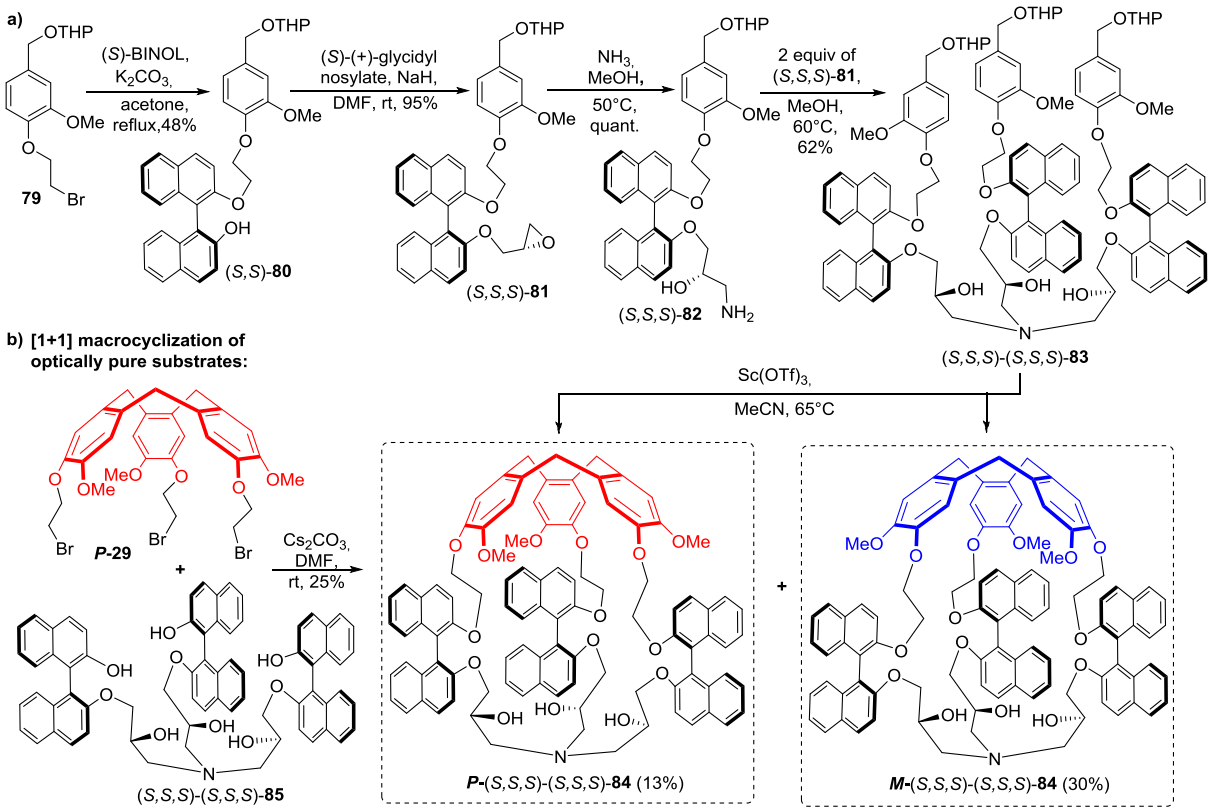

Scheme 7.13. Synthetic pathway to hemicryptophanes with triethanolamine scaffold bearing multiple stereogenic elements.

In all cases, the final intramolecular cyclization reaction induced by $Sc(OTf)_3$ afforded the *M*- and *P*-isomers with *ca.* 2:1 diastereoselectivity, respectively. All four diastereoisomeric pairs were separated by classical column chromatography followed by preparative TLC. In addition, the authors also prepared enantiopure hemicryptophane ***P*-(*S*,*S*,*S*)-(*S*,*S*,*S*)-84** by a [1+1] coupling reaction of optically pure substrates ***P*-29** and (*S*,*S*,*S*)-(*S*,*S*,*S*)-**85** under mild conditions in order to avoids racemization of product (Scheme 7.13b).

7.4.2.2. Hemicryptophanes containing nitrilotriacetamide scaffold

The first hemicryptophanes containing nitrilotriacetamide moiety were synthesized by Martinez, Dutasta *et al.*[107,108,109] In all cases, the synthesis was initiated from vanillyl alcohol (**71**), which was converted into bromide **79** in a two-step procedure involving nucleophilic substitution with 1,2-dibromoethane followed by a protection of the primary hydroxyl group in compound **18** as tetrahydropyranyl ether. At the same time, nitrilotriacetic acid (**86**) was condensed with *p*-methoxy benzylamine (**87a**) [using $P(OPh)_3$ in pyridine] and subsequently demethylated with BBr_3, which afforded triphenol derivative **88**. This intermediate was further reacted with bromide **79** under the basic conditions (Cs_2CO_3) giving

hemicryptophane precursor **89** in 58% yield. The final intramolecular macrocyclization of tripodal precursor **89** induced by HCOOH provided the racemic mixture of hemicryptophane **(±)-90** in 30% yield.[107]

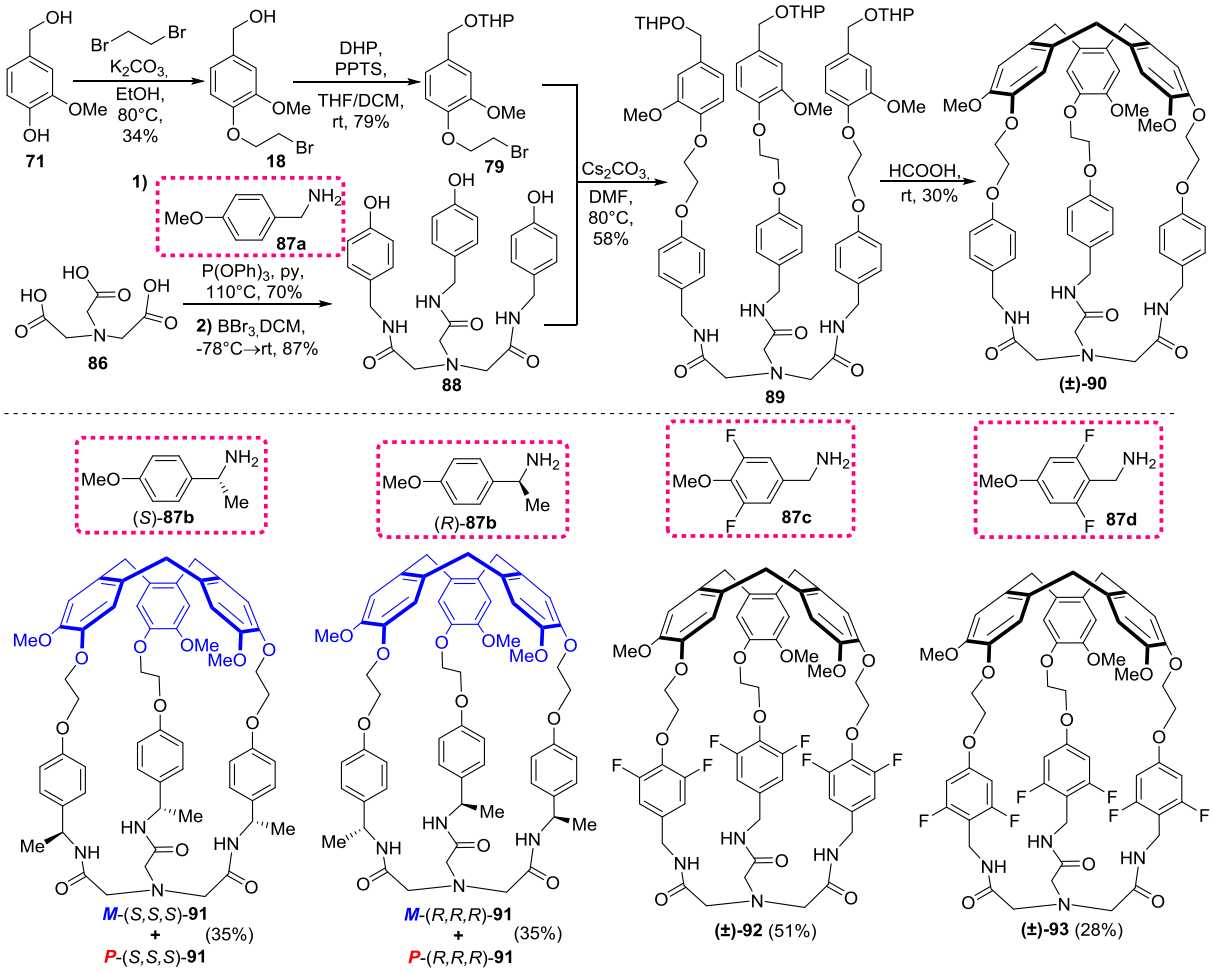

Scheme 7.14. Synthesis pathway towards hemicryptophanes bearing nitrilotriacetamide moiety.

The formation of the CTV moiety in the presence of $Sc(OTf)_3$ as a Lewis acid in MeCN or DCM was unsuccessfull. The authors suggested that triamide functions in compound **89** are capable of complexing proton from formic acid, and thus the template effect might be responsible for the formation of the CTV unit.[107]

Four years later, the same authors proposed an analogous pathway to four enantio- and diastereomerically pure hemicryptophanes ***M***-(*S*,*S*,*S*)-**91**, ***P***-(*S*,*S*,*S*)-**91**, ***M***-(*R*,*R*,*R*)-**91**, and ***P***-(*R*,*R*,*R*)-**91**.[108] In contrast to the previously prepared racemic cages, they introduced additional stereogenic centers to the hemicryptophane structure employing (*S*)- or (*R*)-4-methoxy-α-methylbenzylamine (**87b**) as a substrate (Scheme 7.14). In both cases, the cage-

closing reaction led to the mixture of diastereoisomeric pairs, which were purified by silica gel column chromatography (35% yield) and then successfully separated on alumina preparative TLC thus avoiding chiral HPLC.

Similar strategy was used for the synthesis of two racemic cages containing differently positioned fluorine atoms in the phenyl linkers.[109] While cage **(±)-92** with fluorine atoms located closer to the CTV unit was obtained in 51% yield, cage **(±)-93** with fluorine atoms located closer to the triamide moiety was synthesized only in 28% yield; the authors, however, did not comment this difference.

Different approach to hemicryptophane containing triamide moiety was presented by Makita and co-workers.[110] The authors applied the [1+1] coupling reaction between the CTV and nitrilotriacetic acid derivative, instead of the acid catalyzed CTV cage-closing reaction. Thus, the racemic cyclotriguaiacylene was reacted with tosylate **94** in DMF providing hemicryptophane precursor **(±)-95** in very good yield (84%). Removal of the Boc protecting groups from **(±)-95** with trifluoroacetic acid followed by [1+1] cyclization with nitrilotriacetic acid tris(*p*-nitrophenyl ester) (‘*active ester*’, **96**) under the basic conditions gave racemic hemicryptophane **(±)-97** in 31% after two steps (Scheme 7.15).

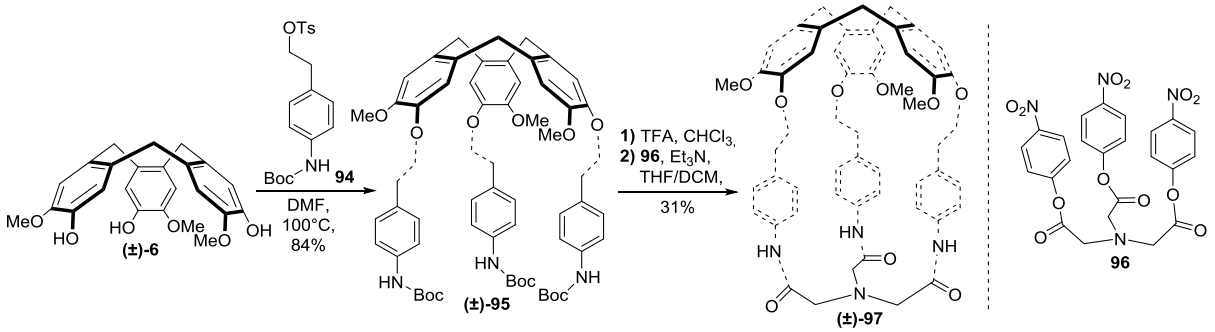

Scheme 7.15. Synthesis of hemicryptophane **(±)-97** containing nitrilotriacetamide scaffold.

7.4.2.3. Hemicryptophanes containing tris(2-aminoethyl)amine scaffold

The vast majority of hemicryptophanes, described in the literature so far, contain tris(2-aminoethyl)amine (TREN) moiety. In 2011, Martinez and Dutasta developed short, convenient, gram-scale synthesis of this kind of hemicryptophanes.[111] The four-step sequence initiated from cheap, commercially available vanillyl alcohol allowed to prepare a library of hemicryptophanes with different linkers, which results in various shapes, sizes, and functionalities of the cages. An important advantage of this synthetic strategy is undoubtedly its modular character that could open the access to molecular cages with various functional

groups attached to the linkers. The model synthesis of hemicryptophanes was based on the [1+1] coupling approach and was initiated from CTV-based tribromide **(±)-29**, which reacted with 4-hydroxybenzaldehyde (**98a**) under the basic conditions providing hemicryptophane precursor **(±)-99** in excellent yield (92%; Scheme 7.16). Condensation of trialdehyde **(±)-99** with tris(2-aminoethyl)amine (TREN, **100**) followed by reduction of an *in-situ* generated intermediate imine with $NaBH_4$ afforded target hemicryptophane **(±)-101** in 77% yield.

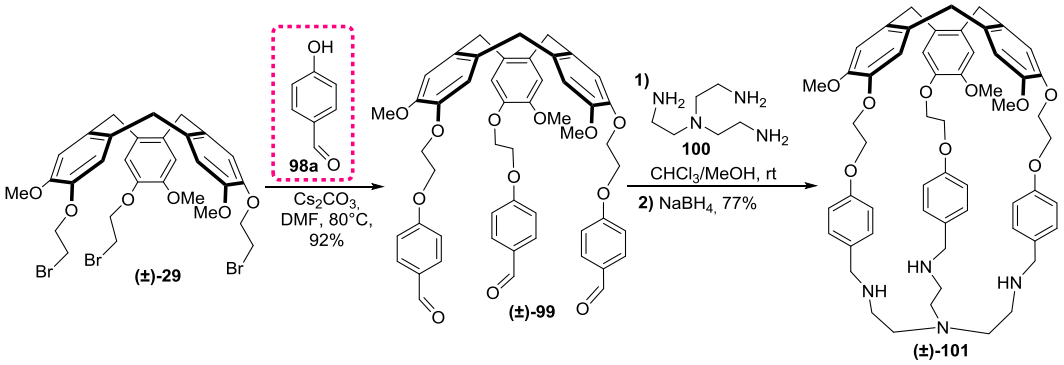

Scheme 7.16. Synthesis of hemicryptophane containing TREN moiety.

Based on this synthetic strategy, the authors prepared additional eight analogues of hemicryptophane **(±)-101**.[111,112] The structures of these hemicryptophanes are presented in Table 7.3. They modified the shape and size of the cavity by varying the position of the hydroxy and aldehyde functions located on the phenyl linkers [**(±)-102, (±)-103**]. Hemicryptophanes with different nature of the linkers *e.g.* with electron donating [**(±)-104** and **(±)-105**] or electron withdrawing [**(±)-106**] groups in the aromatic ring as well as with large naphthyl moieties [**(±)-107**, **(±)-108**, and **(±)-109**)], were successfully synthesized by changing hydroxyaldehyde substrates. The macrocyclization reactions of hemicryptophane precursors containing strong electron withdrawing groups, such as nitro or fluorine functions, in the aromatic linkers were unsuccessfull. Additionally, in another paper, the same group obtained enantiopure hemicryptophanes **101**, **104, 106,** and **109** from optically pure bromide ***M*-29** or ***P*-29** (previously separated on chiral HPLC) following synthetic strategy described in Scheme 7.16, but avoided heating in order to prevent racemization of the products.[113]

Table 7.3. Different hydroxyaldehyde substrates used in reaction from Scheme 7.16 and corresponding hemicryptophane products.

Aldehyde	Hemicryptophane	Aldehyde	Hemicryptophane
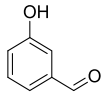 **98b**	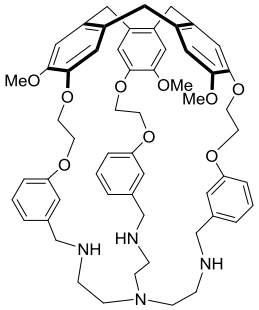 **(±)-102** (58%)	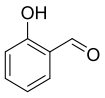 **98c**	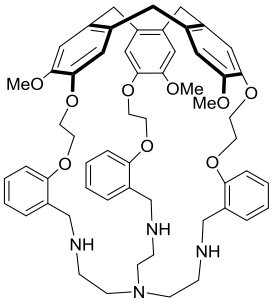 **(±)-103** (54%)
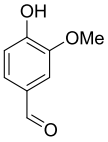 **98d**	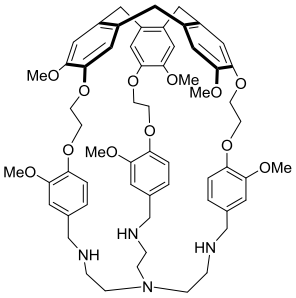 **(±)-104** (25%)	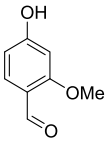 **98e**	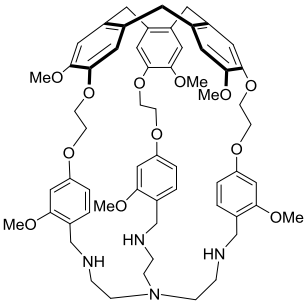 **(±)-105** (55%)
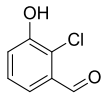 **98f**	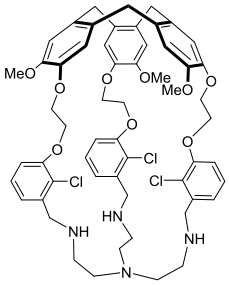 **(±)-106** (33%)	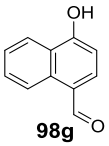 **98g**	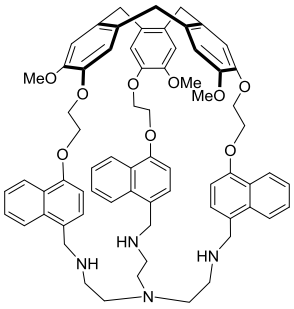 **(±)-107** (30%)
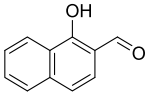 **98h**	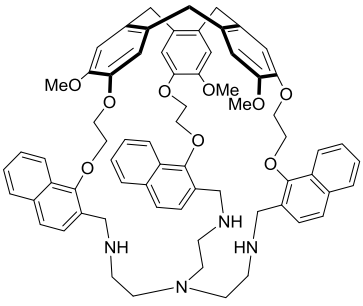 **(±)-108** (50%)	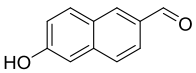 **98i**	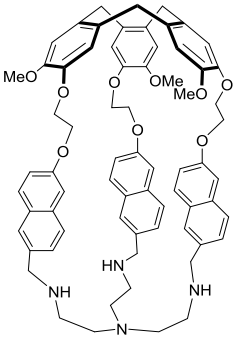 **(±)-109** (42%)

In 2015 Martinez *et al.* described a facile synthesis of enantiomerically pure cages with TREN moiety obtained *via* thermodynamic resolution of racemic CTV-based substrate.[114] The authors observed that the reductive amination of racemic CTV trialdehyde **(±)-99** with enantiopure derivative of TREN: (*S,S,S*)-**110a** afforded only one diastereoisomer ***M***-(*S,S,S*)-**111a** in 15% yield (Scheme 7.17). They discovered that substituents attached to TREN skeleton are able to transfer their stereochemical information providing single enantiopure diastereoisomer. Additionally, the authors confirmed that this thermodynamic resolution is more likely independent on the nature of the substituents located on the tris(2-aminoethyl)amine's stereogenic centers, as both methyl and benzyl groups gave similar results and only one diastereoisomer (*M*) was obtained exclusively. This remote control of the helical chirality of the CTV-based unit *via* stereogenic centers of TREN moiety is meaningful since it could provide exclusively one enantiopure diastereoisomer.

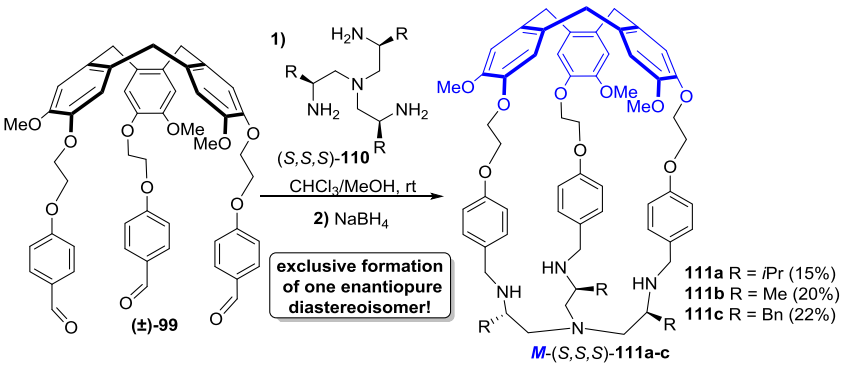

Scheme 7.17. Synthesis of one diastereoisomer ***M***-(*S,S,S*)-**111** *via* thermodynamic resolution.

Another hemicryptophane containing TREN moiety with a smaller cavity was reported by Makita *et al.*[115] Proposed synthetic pathway was similar to the previous ones and included only two steps starting from (±)-CTG: 1) nucleophilic aromatic substitution, and 2) reductive amination (Scheme 7.18). Importantly, the final cyclization reaction proceeded in excellent, almost quantitative yield.

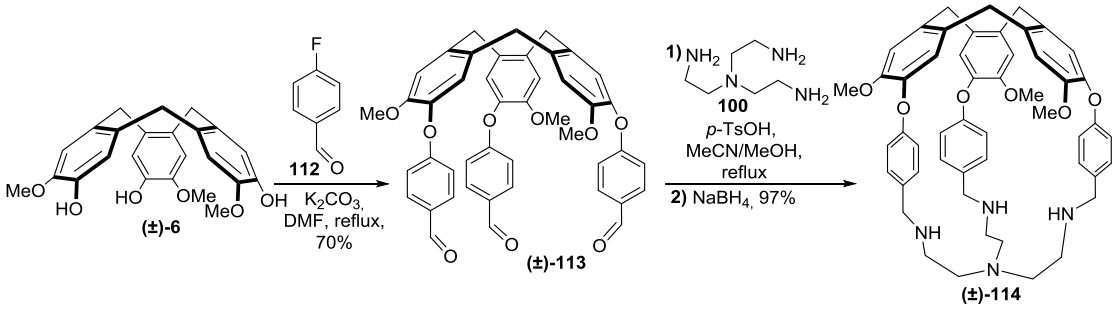

Scheme 7.18. Synthesis of racemic hemicryptophane **(±)-114**.

In the next study, Makita and co-workers decided to enlarge the host's cavity and introduced biphenyl linkers to the hemicryptophane structure.[116] For this purpose, (±)-CTG was firstly reacted with 4-bromobenzyl bromide (**115**) under the basic conditions giving CTV tribromide **(±)-116**, which was further transformed into cage precursor **(±)-118** by a Suzuki-Miyaura coupling reaction (Scheme 7.19). Next, biphenyl-extended trialdehyde **(±)-118** was reacted with TREN under the reductive amination conditions providing hemicryptophane **(±)-119** in 60% yield. It is worth mentioning that this molecular cage is able to form endohedral complex with Co (II) ion.

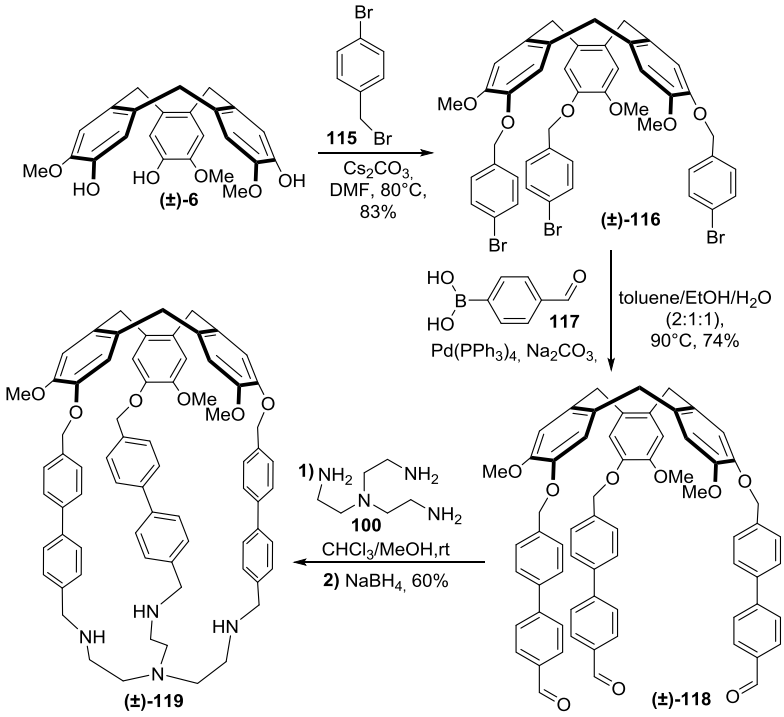

Scheme 7.19. Synthesis of biphenyl-linked hemicryptophane **(±)-119**.

Another methodology for the synthesis of hemicryptophane that contains TREN moiety was developed by Rivera and Wessjohann.[117] They used a one-pot multicomponent Ugi reaction to form molecular cage with peptoid linkers [**(±)-123**] as shown in Scheme 7.20. This Ugi reaction represents a completely different approach to hemicryptophanes and allows to incorporate the peptoid chains into their structure. Additionally, the simplicity of this method makes it an interesting procedure for the combinatorial generation of host macrocycles.

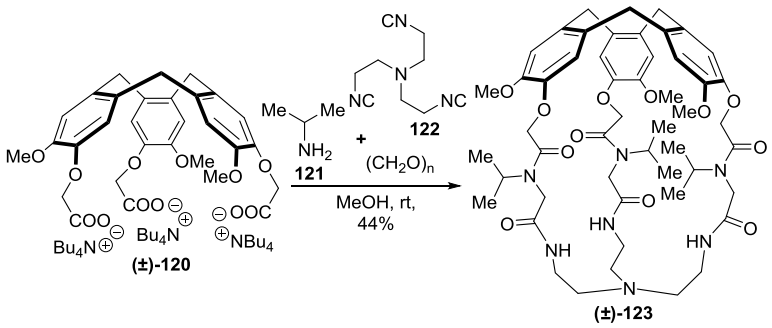

Scheme 7.20. Synthesis of TREN-hemicryptophane with peptoid backbones *via* multicomponent Ugi reaction.

In 2019, Martinez group reported the synthesis of a water-soluble polytopic hemicryptophane consisting of the CTV unit triple connected to TREN moiety *via* 2-hydroxyisophthalamide linkers.[118] This highly functionalized molecular cage [**(±)-133**] was prepared using cage-closing strategy to construct the CTV scaffold from veratryl precursors as shown in Scheme 7.21.

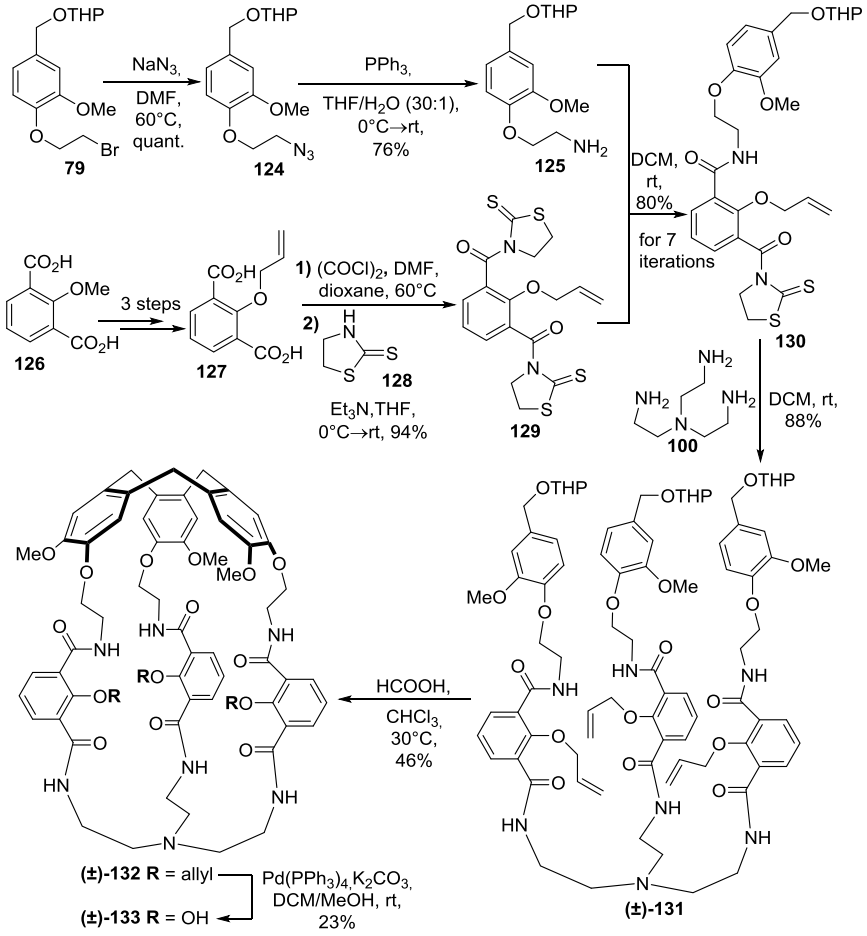

Scheme 7.21. Synthesis of polytopic hemicryptophane with 2-hydroxyisophthalamide linkers.

While the majority of the synthetic steps designed by the authors proceeded in good yields, some difficulties were noted during the preparation of compound **130** and a palladium-catalyzed cleavage of the allyl protections from hemicryptophane **(±)-132**. In the first case, reaction between amine **125** and compound **129** was time-consuming and was repeated several times in order to obtain sufficient amount of intermediate **130**. In the second case, the steric hindrance around the allyl groups and difficult purification of hemicryptophane **(±)-133** were responsible for the relative low yield (23%) of the final deprotection step. Moreover, the main disadvantage of this synthetic route is the number of steps (13 steps from comercially available vanillyl alcohol and 2-methoxyisophthalic acid). Nonetheless, this water-soluble cage is able to form complex with Gd (III) ions that exhibits a high relaxivity properties in comparison with gadoteric acid – commercial MRI agent.

Recently, the same group developed the synthesis of two hemicryptophanes, which contain three urea functions.[119,120] The authors introduced additional urea groups to the cage structure because of their well-known remarkable affinity for anions. Moreover, combining the CTV unit, capable of binding cationic species, with the urea functions provided heteroditopic ion-pair receptors that could simultaneously recognize both anions and cations. The synthetic routes leading to the CTV-based molecular cages **(±)-136** and **(±)-138** with urea motifs are shown in Scheme 7.22.

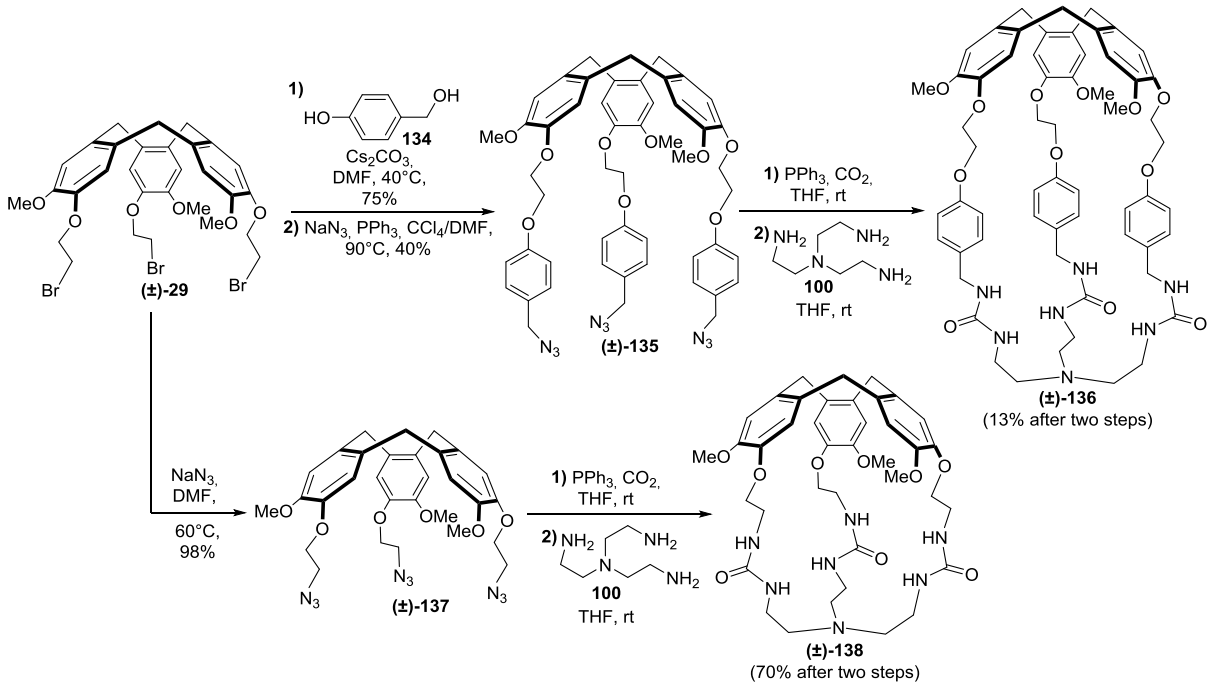

Scheme 7.22. Synthetic pathways to hemicryptophanes with TREN units and three urea functions.

Hemicryptophane **(±)-136** was obtained in four steps from tribromide **(±)-29**. Reaction of **(±)-29** with *p*-hydroxybenzyl alcohol (**134**) under the basic conditions followed by a one-pot reaction of the resulting triol with CCl_4 and NaN_3 in the presence of PPh_3 gave intermediate **(±)-135** in moderate yield (40%). Transformation of all three azide functions of **(±)-135** into isocyanate groups (with CO_2/PPh_3) followed by the [1+1] cyclization with TREN afforded target cage **(±)-136**. The smaller cage **(±)-138** was prepared in a similar manner, except the initial alkylation step. While cage **(±)-138** with shorter ethylene linkers was obtained in 70% yield, its larger analogue **(±)-136** was synthesized in only 13% yield.

In 2020, a different approach to hemicryptophanes with TREN motif was proposed by Pinet and Gosse.[121] They developed fluorescent hemicryptophane **(±)-145,** in which the methoxy groups of the CTV scaffold were replaced by phenylacetylene units. This molecular cage, due to the introduced π-conjugated moieties, shows fluorescence properties with red-shifted excitation and emission wavelengths. In contrast to the synthesis of a majority of hemicryptophanes initiated from vanillyl alcohol, this pathway started from 3-hydroxy-4-iodobenzoic acid as shown in Scheme 7.23.

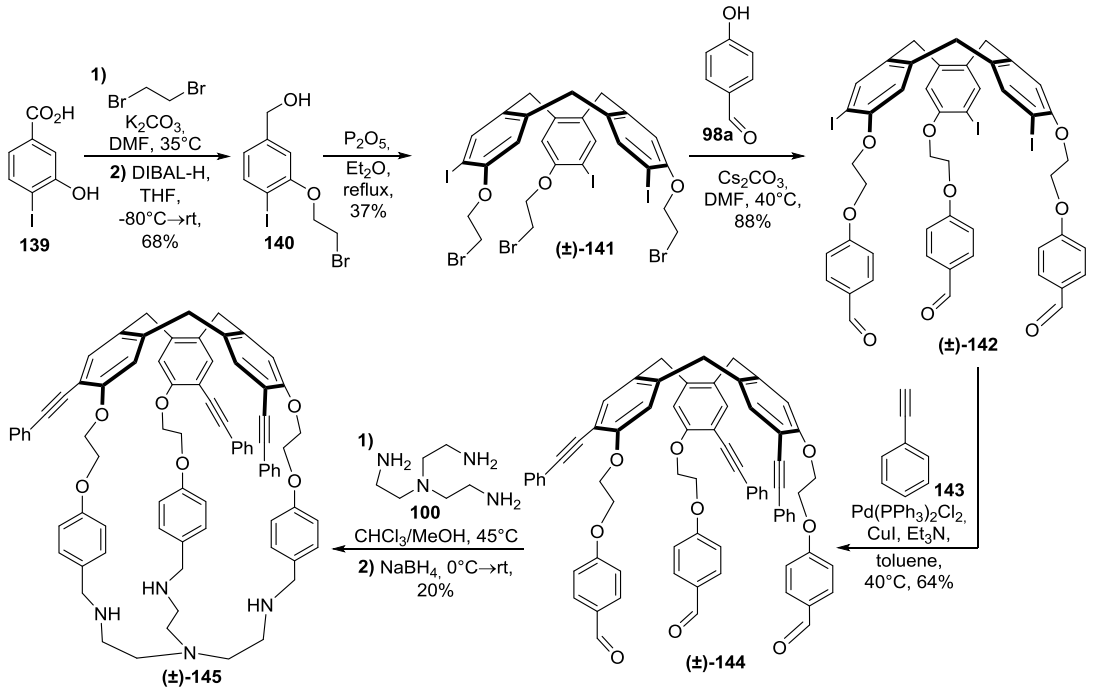

Scheme 7.23. Synthesis of hemicryptophane with phenylacetylene fluorophores.

Alkylation of **139** with 1,2-dibromoethane followed by reduction with diisobutylaluminium hydride afforded compound **140** in 68% yield after two steps. Cyclization reaction of **140** induced by P_2O_5 in refluxing diethyl ether gave CTV derivative **(±)-141** in 37% yield, which reacted with 4-hydroxybenzaldehyde affording intermediate **(±)-142.** This derivative was

treated with phenylacetylene under the classical Sonogashira cross-coupling conditions giving hemicryptophane precursor **(±)-144** in 64% yield. The last step, involving [1+1] conjugation of **(±)-144** with TREN under reductive amination conditions, afforded the desired fluorescent hemicryptophane **(±)-145** in 20% yield. This synthetic method has two main advantages: 1) the possibility of introducing various fluorophores (or other functional groups), instead of the methoxy groups attached to the CTV unit, by using cross-coupling reaction; 2) the possibility of modifying the size of the host's cavity without considering the incorporated to the structure fluorophore.

It should be pointed out that TREN function could be also easily obtained by a reduction of amide moieties in the previously described hemicryptophanes **(±)-90** and **91,** which will change the character of the cavity (Scheme 7.24).[107,122]

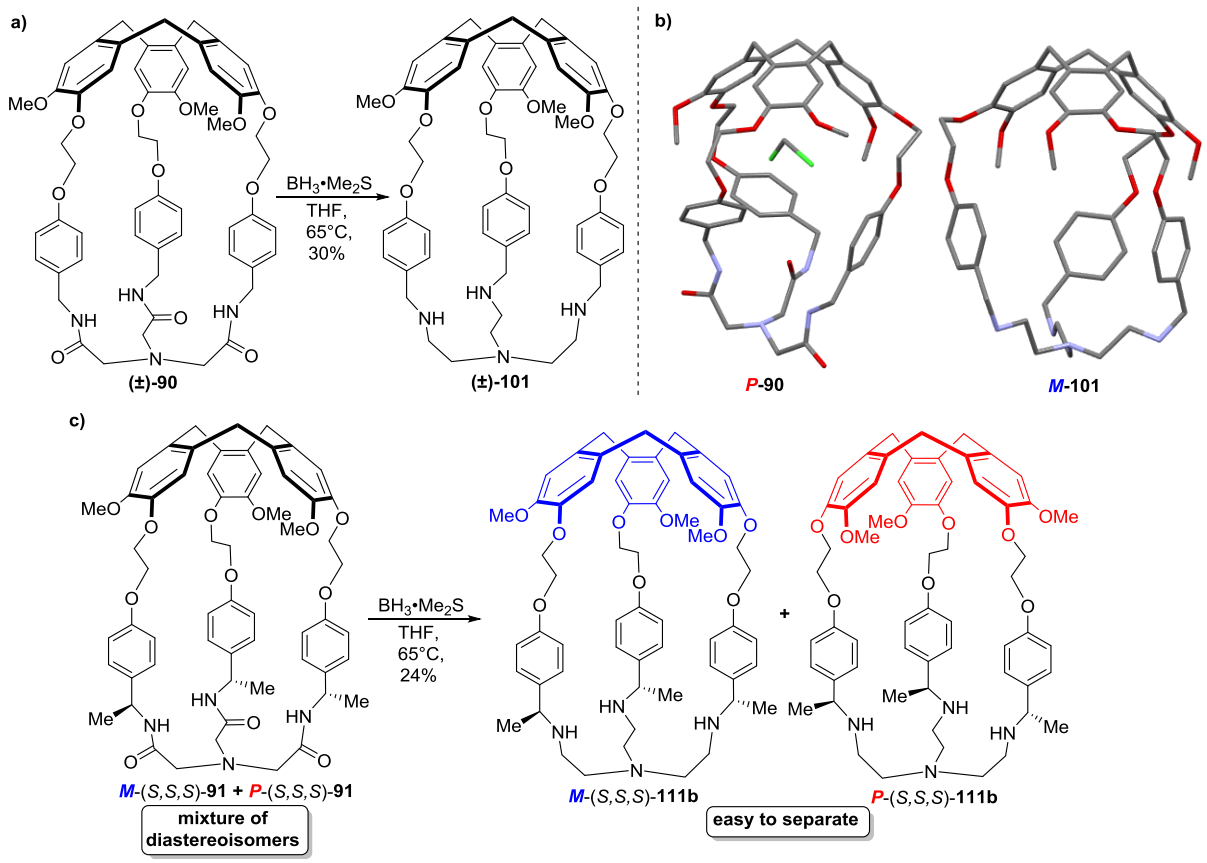

Scheme 7.24. a) and c) Preparation of TREN-hemicryptophanes *via* reduction of amide functions. b) X-ray crystal structures of ***P*-90** and ***M*-101** (hydrogen atoms are omitted for clarity) Ref. 107.

Indeed, this reduction was successfully carried out using borane dimethylsulfide ($BH_3 \cdot Me_2S$) and afforded cages **(±)-101** and **111b** in 30% and 24% yield, respectively. Moreover, the purification of hemicryptophanes ***P*-(*S*,*S*,*S*)-111b** and ***M*-(*S*,*S*,*S*)-111b** as well as its

enantiomers ***P***-(*R*,*R*,*R*)-**111b** and ***M***-(*R*,*R*,*R*)-**111b**, was much easier when comparing to the purification of the crude mixture of its triamide analogues.[122] However, this reduction is very time-consuming and required more than one week to be completed. Unfortunately, reduction with $LiAlH_4$ instead of $BH_3 \cdot Me_2S$ provided the mixture of inseparable products consisted of both reduced and demethylated compounds.

7.4.2.4. Hemicryptophanes containing tris(2-pyridylmethyl)amine scaffold

In 2017, Martinez group described the straightforward synthesis of two hemicryptophanes consisting of tris(2-pyridylmethyl)amine (TPA) and naphthyl or phenyl linkers.[123] The authors decided to introduce the TPA unit into the hemicryptophane structure due to its well-known complexing abilities towards various metals. The initial steps of the synthesis included two separated pathways: 1) reaction between bromide **79** and naphthalene derivative **146** in the presence of Cs_2CO_3 followed by a palladium-catalyzed deprotection of the allyl group (→ 147; Scheme 7.25a), and 2) conversion of pyridine derivative **148** into trimeric triester **149** (NH_3/K_2CO_3), followed by reduction of ester groups with $NaBH_4$ and subsequent triple chlorination with $SOCl_2$ (Scheme 7.25b). Hemicryptophane precursor **(±)-151** was obtained by reaction of **147** with TPA trichloride **150** under the basic conditions (98% yield; Scheme 7.25c). Finally, the intramolecular cyclization of **(±)-151** using stoichiometric amount of $Sc(OTf)_3$ as a Lewis acid in MeCN afforded TPA-based hemicryptophane **(±)-152** in 49% yield. In this case, the cyclization was also performed in HCOOH, nevertheless several by-products were formed, which caused difficulties in the purification process and lowered the yield of the desired cage. However, employing formic acid for the synthesis of its phenyl analogue **(±)-155** proved to be a good choice because cyclization of precursor **(±)-154** under these conditions afforded target product in 90% yield (Scheme 7.26). Additionally, this molecular cage was isolated without column chromatography by a precipitation from the mixture DCM/Et_2O. It is noteworthy that both molecular cages **(±)-152** and **(±)-155** could be easily obtained in a gram scale. It was also possible to separate these racemic products into pure enantiomers by HPLC resolution on chiral columns.

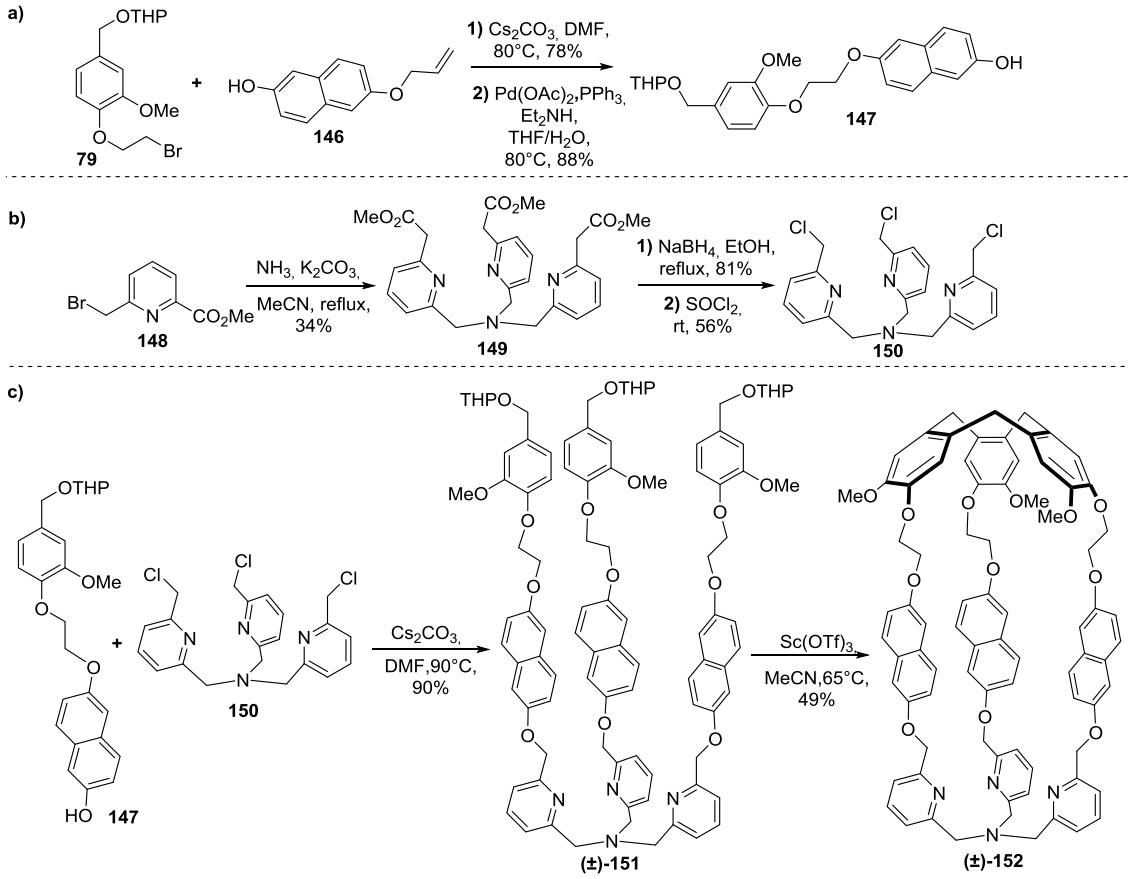

Scheme 7.25. Synthesis of a) intermediate **147**; b) TPA derivative **150**; c) TPA-based hemicryptophane with naphthyl linkers.

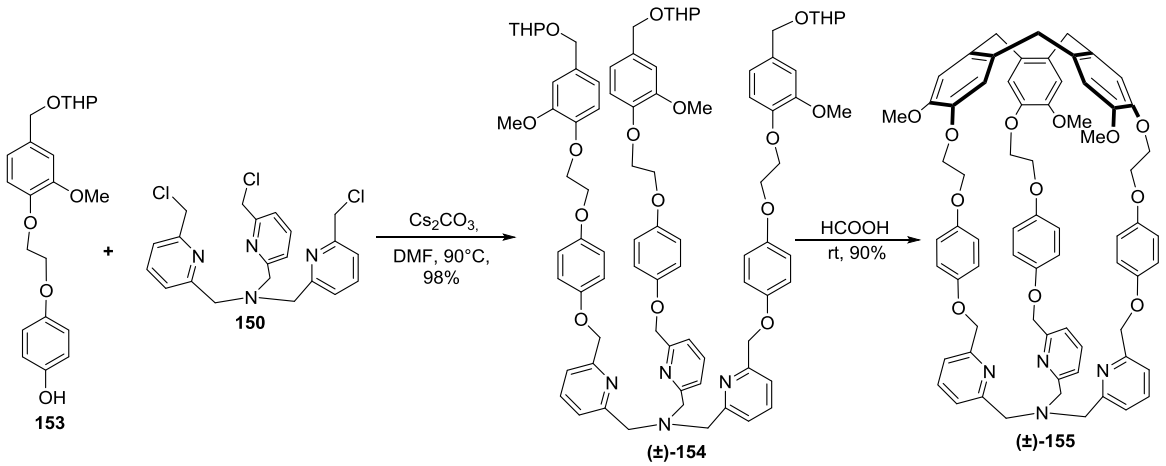

Scheme 7.26. Synthesis of TPA-based hemicryptophane with phenyl linkers.

Two years later, the same group developed the synthesis of the smallest TPA-based hemicryptophane.[124] The [1+1] coupling of (±)-CTG with TPA-based trichloride **150** in the presence of Cs_2CO_3 afforded hemicryptophane **(±)-156** in 66% yield (Scheme 7.27). This molecular cage was then separated into individual enantiomers: *P* and *M* hemicryptophanes by HPLC on chiral column.

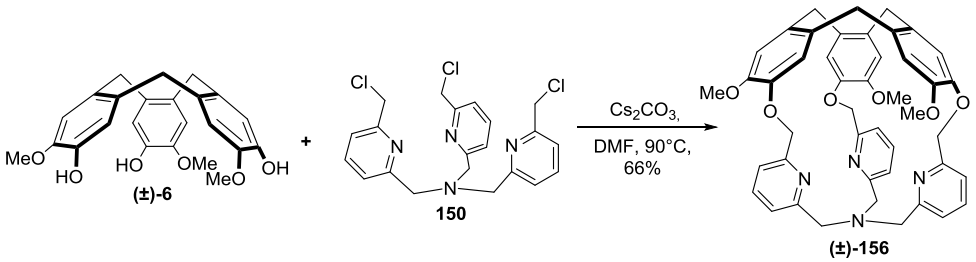

Scheme 7.27. Synthesis of the smallest TPA-based hemicryptophane.

7.4.2.5. Hemicryptophanes containing 1,3,5-tripodal benzene scaffold

The second very commonly used moiety linked to cyclotriveratrylene unit besides tris(2-aminoethyl)amine is 1,3,5-tripodal benzene scaffold. This platform is an attractive cage closing unit, in particular due to the wide range of possibilities of its functionalization. Furthermore, the benzene ring itself can interact with neutral or charged guests by CH-π, π-π, cation-π, or anion-π interactions. Additionally, the introduction of different type of substituents to the benzene ring (*e.g.* electron donating or withdrawing groups) could also improve its host-guest properties.

The first hemicryptophane containing 1,3,5-tripodal benzene moiety was prepared in 2006 by Rivera and Wessjohann.[117] These authors successfully applied the multicomponent Ugi-type macrocyclization reaction for the synthesis of hemicryptophane with a tripodal benzene unit and peptoid backbones. They combined four components [CTV-based carboxylate salt **(±)-120**, tripodal isocyanide **157**, primary amine **121**, and paraformaldehyde] in a one-pot approach and obtained hemicryptophane **(±)-158** in 32% yield (Scheme 7.28).

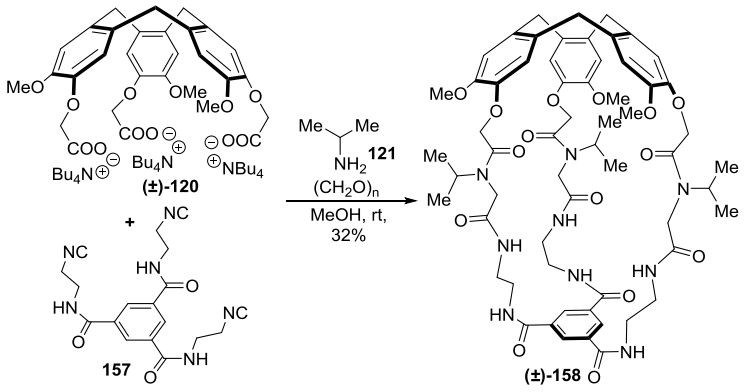

Scheme 7.28. Synthesis of hemicryptophane with tripodal benzene moiety and peptoid linkers *via* multicomponent Ugi reaction.

Few years later, Dutasta and Martinez reported the four-step synthesis of hemicryptophane **(±)-165,** in which the CTV unit was triply connected with C_3-symmetrical aromatic ring *via* electron deficient linkers.[125] In contrast to the previously described nitrilotriacetamide-based hemicryptophanes, this molecular cage contained three additional amide functions in its structure, which increased the number of hydrogen bonds that could be formed between host and guest. Treatment of vanillyl alcohol with chloroacetic acid in the presence of NaOH and NaI in refluxing ethanol afforded carboxylate salt **160** in 73% yield (Scheme 7.29), which was engaged in a subsequent one-pot cyclization (followed by esterification) to afford triester **(±)-161** in 42% yield after two steps. The condensation reaction of this triester with ethylenediamine afforded hemicryptophane precursor **(±)-163**. The final [1+1] coupling between triamine **(±)-163** and 1,3,5-benzenetricarbonyl trichloride (**164**) under the basic conditions provided hemicryptophane **(±)-165** in 22% yield. It should be mentioned that all intermediates as well as the target product were isolated by crystallization.

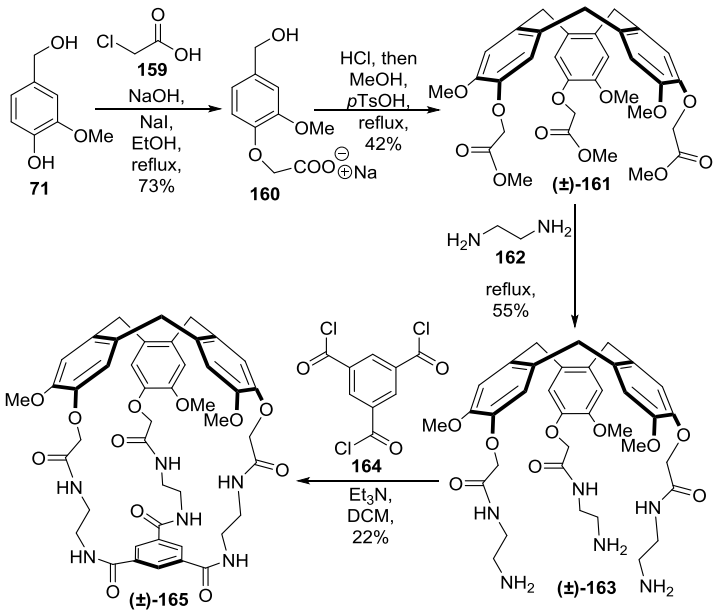

Scheme 7.29. Synthesis of hemicryptophane containing six amide functions and 1,3,5-tripodal benzene scaffold.

The 1,3,5-trisubstituted benzene ring was also employed for the synthesis of four diastereoisomerically and enantiomerically pure hemicryptophanes with three axially chiral binaphthol linkers.[126] First, bromide **79** was reacted with (*S*)-BINOL derivative **166** in the presence of K_2CO_3 to give compound (*S*)-**167** in 77% yield (Scheme 7.30). Subsequent cleavage of the allyl protections from (*S*)-**167** using palladium catalyst, provided binaphthol (*S*)-**168**, which was alkylated with 1,3,5-tris(bromomethyl)benzene under the basic

conditions, which afforded hemicryptophane precursor (*S*,*S*,*S*)-**170** in 79% yield. The intramolecular cage-closing reaction of this tripodal precursor induced by $Sc(OTf)_3$ afforded the first diastereoisomeric pair of hemicryptophanes: ***M***-(*S*,*S*,*S*)-**171** and ***P***-(*S*,*S*,*S*)-**171** in *ca.* 1:1 ratio in excellent 80% yield.

The second pair of stereoisomers ***M***-(*R*,*R*,*R*)-**171** and ***P***-(*R*,*R*,*R*)-**171** were similarly prepared from (*R*)-binaphthol derivative of **166**. All four diastereoisomers were successfully separated by silica gel column chromatography.

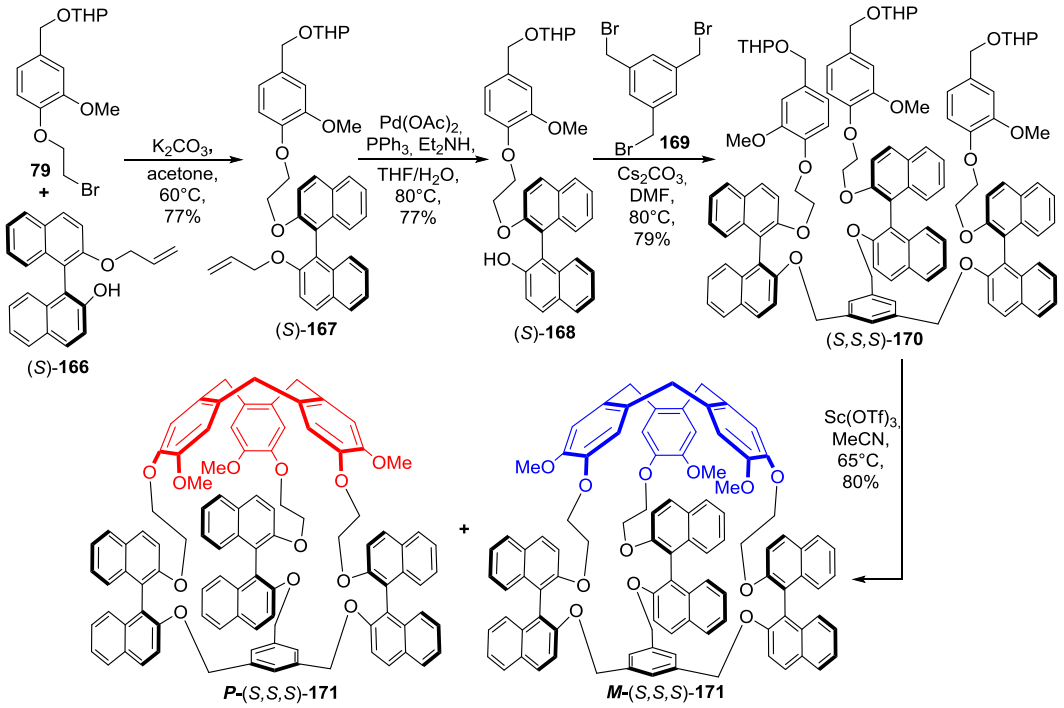

Scheme 7.30. Synthetic pathway towards two diastereoisomers of BINOL-based hemicryptophanes with tripodal benzene moiety.

In 2018, the Martinez group described another synthesis of enantiopure hemicryptophanes bearing tripodal benzene moiety using the [1+1] macrocyclization strategy.[127] Reaction of CTV tribromide **(±)-29** with sodium azide, followed by a Staudinger reduction of the azido groups, afforded CTV triamine **(±)-172** in 91% yield (Scheme 7.31). Meanwhile, they transformed 1,3,5-tris(bromomethyl)benzene into tripodal trialdehyde **173** by reaction with 2-hydroxybenzaldehyde under the basic conditions. Both C_3-symmertical intermediates were then reacted under reductive amination conditions providing the racemic mixture of hemicryptophane **(±)-174** in 42% yield. Such prepared racemic product was resolved by chiral HPLC to optically pure cages ***M***-**174** and ***P***-**174**.

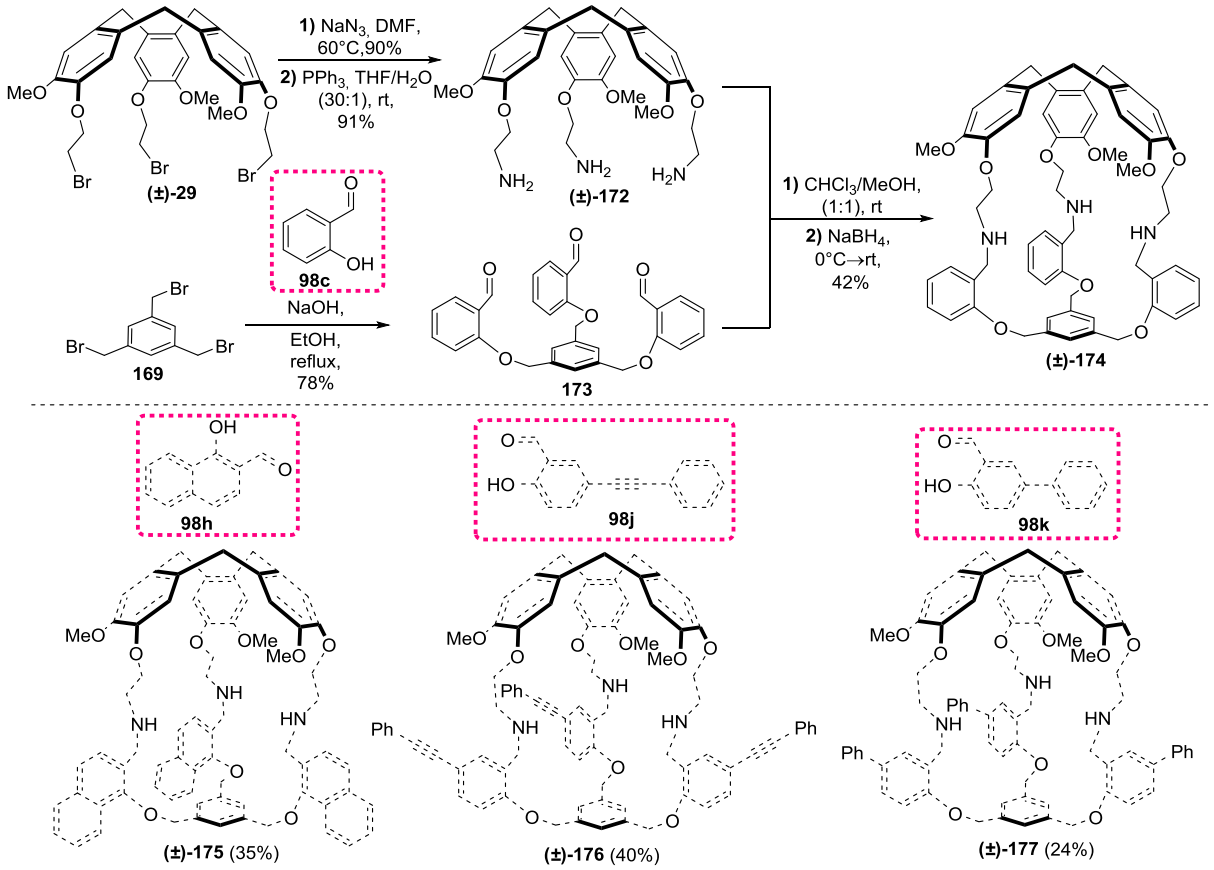

Scheme 7.31. Synthesis pathway towards hemicryptophanes bearing tripodal benzene moiety.

Recently, the same strategy was used for the synthesis of three fluorescent hemicryptophanes containing naphthalene, diphenylacetylene, and biphenyl groups in the linkers.[128, 129] In this case, the replacement of 2-hydroxybenzaldehyde with 1-hydroxy-2-naphthaldehyde, 2-hydroxy-5-(phenylethynyl)benzaldehyde or 2-hydroxy-5-phenylbenzaldehyde in the nucleophilic substitution reaction step, resulted in molecular cages **(±)-175, (±)-176,** and **(±)-177** in 35%, 40%, and 24% yield (Scheme 7.31). It should be pointed out that both hemicryptophanes with diphenylacetylene and biphenyl groups [**(±)-176,** and **(±)-177**] exhibited improved fluorescent properties in the mixture of 2% H_2O in DMSO, when compared to its naphthalene analogue **(±)-175**. Indeed, not only their quantum yields (Φ) are higher [from 1.8% for host **(±)-175** to 5.4% and 7.5% for cages **(±)-176,** and **(±)-177**), but also their maximum emission wavelengths are in both cases red-shifted [from 326 nm for cage **(±)-175** to 352 nm and 334 nm for cages **(±)-176,** and **(±)-177**].

Hemicryptophane consisting of tripodal benzene platform and both amine and amide functions in the linkers was also synthesized *via* a reductive amination reaction.[130] In this case, the authors combined already prepared precursors **(±)-163** and **173** and obtained hemicryptophane **(±)-178** in excellent yield (92%; Scheme 7.32). The authors suggested that

such high yield was achieved by possible hydrogen bonds between the imine and amide functions present in the linkers, which led to a highly stable intermediate resulting in an efficient macrocyclization reaction.

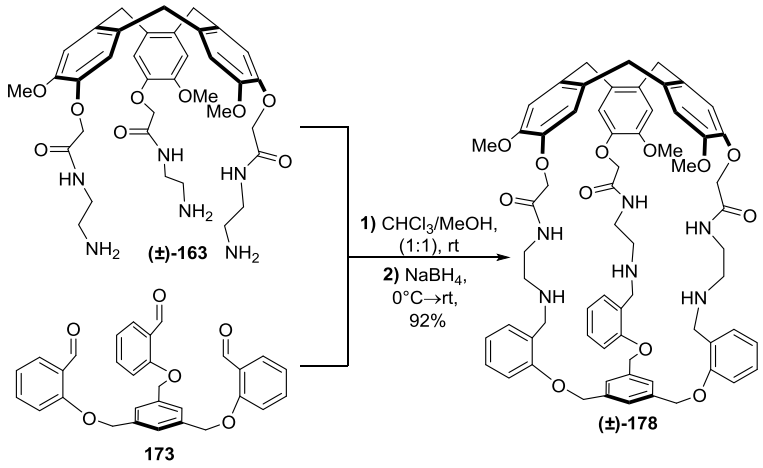

Scheme 7.32. Synthesis of hemicryptophane with C_3-symmetrical benzene unit and both amine and amide functions in the linkers.

7.4.2.6. Hemicryptophanes containing macrocyclic scaffold

Macrocyclic compounds are other units, which could be efficiently introduced to the hemicryptophanes structure. They undoubtedly have one key advantage, being an additional independent host for binding different guest molecules. In other words, macrocyclic unit linked to the CTV platform, depending on its nature, might lead to heteroditopic receptor with two binding sites capable of complexing ion-pairs or two different molecules at the same time. Several molecular cages with various macrocyclic units, *e.g.* aza-crown ethers, calix[6]arenes, α-cyclodextrins, cyclic peptides *etc.*, connected with the CTV moiety in close proximity were reported so far.

The first hemicryptophanes containing macrocyclic units were developed in 1982 by Collet and Lehn.[103] The authors combined CTV derivatives **(±)-179** and **(±)-182** with aza-crown ether **180** in a [1+1] coupling reaction and obtained two molecular cages **(±)-181** and **(±)-183** in 35% and 40% yield (Scheme 7.33). The reduction of the amide functions in **(±)-181** and **(±)-183** afforded target hemicryptophanes **(±)-67** and **(±)-68**, named by the authors as *speleands*.

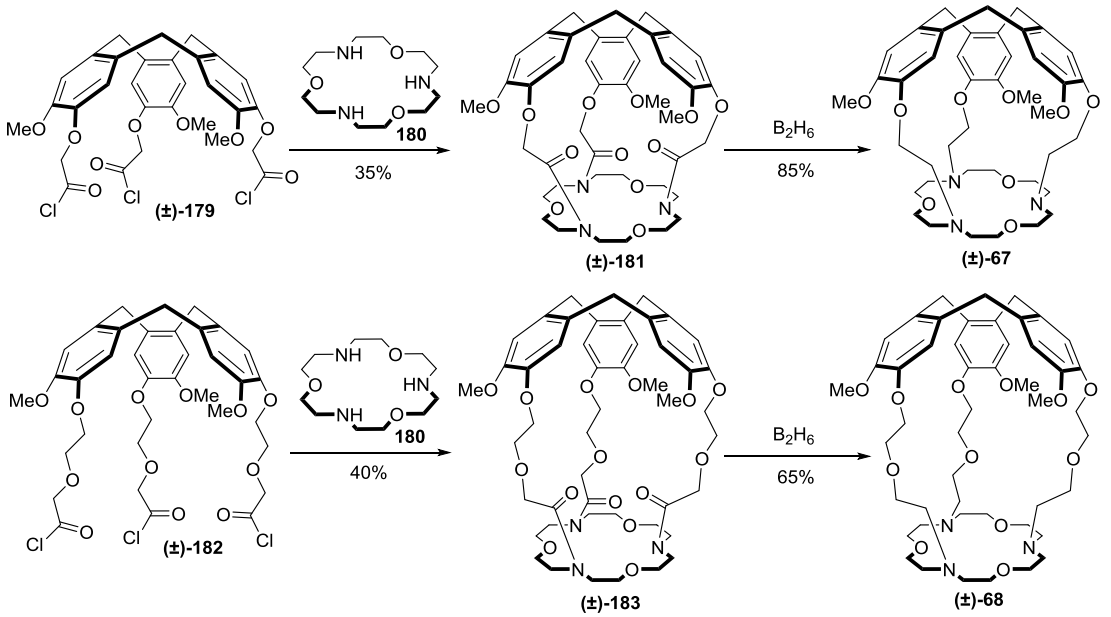

Scheme 7.33. Synthesis of aza-crown-based hemicryptophanes.

Another hemicryptophanes bearing macrocyclic scaffold were not described until 2008, when Le Gac and Jabin presented the synthesis of bifunctional cages (called calix[6]cryptamides), composed of the CTV unit triply connected with calix[6]arene derivative (Scheme 7.34).[131] In both cases, the key [1+1] macrocyclization step was realized by a peptide coupling reaction between calix[6]trisamine **184** and CTV-based triscarboxylic acids **(±)-28** or **(±)-186** in the presence of Et_3N and peptide coupling reagents (PyBOP or HBTU). This reaction, carried out under high-dilution conditions, provided receptors **(±)-185** and **(±)-187** in 46% and 33% yield, respectively (Scheme 7.34). Similarly, employing CTV-based tris-acyl chloride **(±)-179** (obtained quantitatively *via* a chlorination of **(±)-28** using oxalyl chloride) as a substrate in the [1+1] coupling reaction with calix[6]trisamine **184** also provided the corresponding multitopic receptor **(±)-185**, however with lower efficiency (15% yield). It should be pointed out that these molecular cages have two binding sites for the cooperative complexation of ion-pairs: tripodal calix[6]arene and cryptamide platforms.

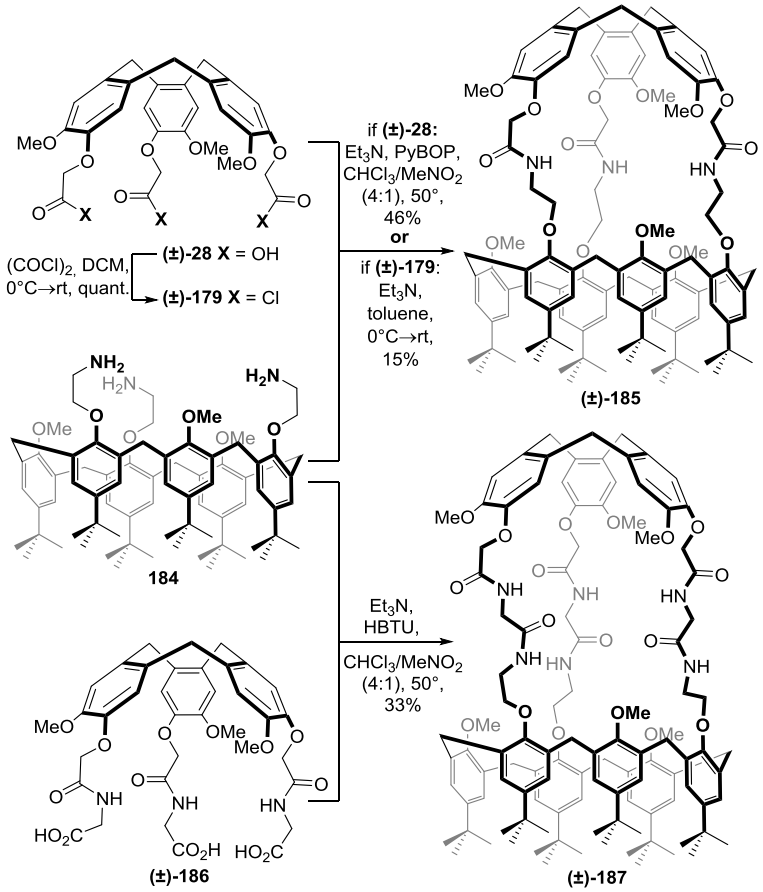

Scheme 7.34. Synthesis pathways towards calix[6]cryptamides.

Different approach to the synthesis of macrocycle-based hemicryptophanes was presented by Zhao and Li.[132] In this case, the authors used seldom used synthetic strategy consisting of the intramolecular cage-closing reaction at the lower part of the appropriate CTV-based precursor. The 1,3-dipolar cycloaddition between triazides **(±)-137** or **(±)-194** with alkyne **193** (obtained independently in a four-step sequence from **188** as shown in Scheme 7.35), in the presence of CuI and DIPEA, gave arylamide-derived precursors **(±)-195a** or **(±)-195b**, in very good yields. Treatment of precursors **(±)-195a** or **(±)-195b** with trifluoroacetic acid, allowed for the formation of preorganized, imine-bonded macrocyclic arylamide framework leading to hemicryptophanes **(±)-196a** or **(±)-196b**. Interestingly, this rare cage-closing strategy resulted in a quantitative formation of both target receptors. Moreover, although four possible isomers of each cage may be obtained during the final cyclization step (depending on the orientation of the triimine macrocyclic platform and the CTV unit), only one of them (or a pair of enantiomers) was formed.

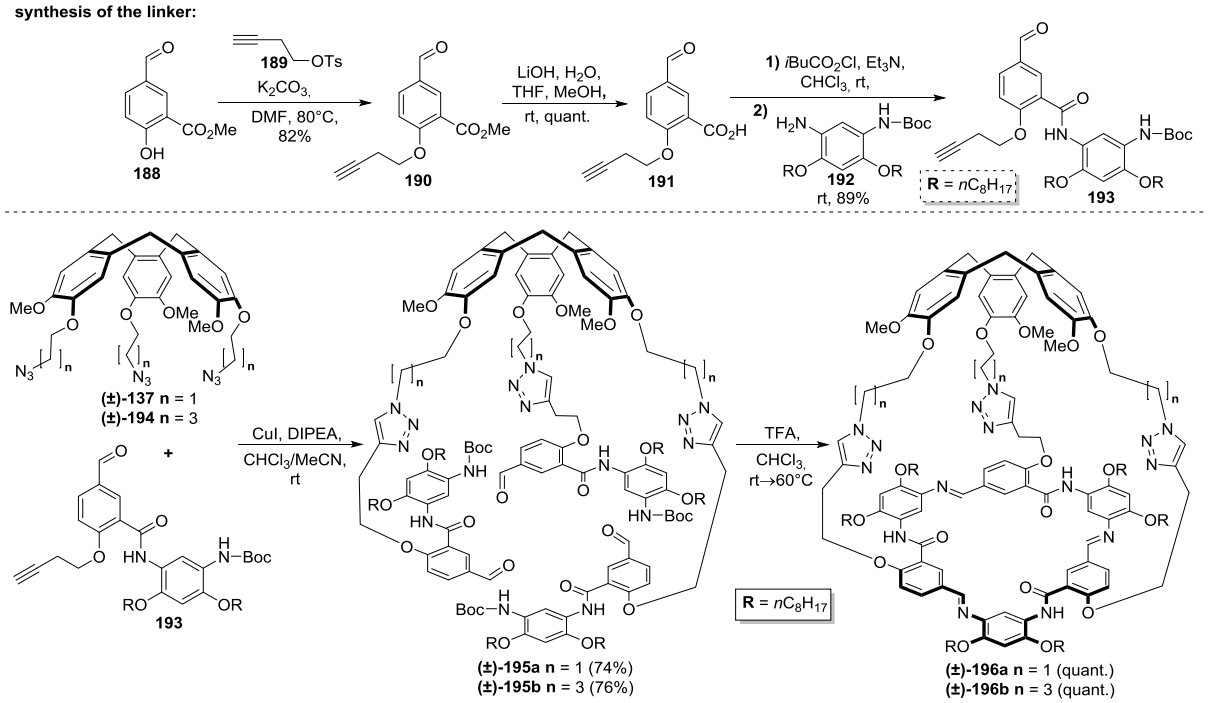

Scheme 7.35. Synthesis of hemicryptophanes with macrocyclic arylamide scaffold.

Two C_3-symmetrical diastereoisomeric hemicryptophanes containing macrocyclic peptide moiety were prepared by Hutton *et al.*[133] The authors designed such macrocyclic hexapeptide scaffold with a three-fold symmetry to match the CTV unit. This hexapeptide was composed of three L-tyrosine and glycine amino acids (Scheme 7.36). While L-tyrosine units served mainly as hydrophobic linkers between macrocyclic peptide and CTV platform, three glycine residues were chosen to simplify the macrocyclic peptide synthesis and to prevent the steric hindrance inside the cavity. Macrocyclization of **197**, obtained by a standard synthesis on solid support, afforded cyclic peptide **198**, which was further reacted with bromide **79** under the basic conditions giving hemicryptophane precursor **199** in 55% yield (Scheme 7.36). The final cage-formation step, realized by an intramolecular cyclodehydration induced by formic acid, provided two diastereoisomeric hemicryptophanes ***P*-200** and ***M*-200** in 43% and 21% yield, respectively, after classical chromatography. The 2:1 ratio suggests that inherent chirality of the macrocyclic hexapeptide had a moderate influence on the selectivity of the generation of the *P* isomer.

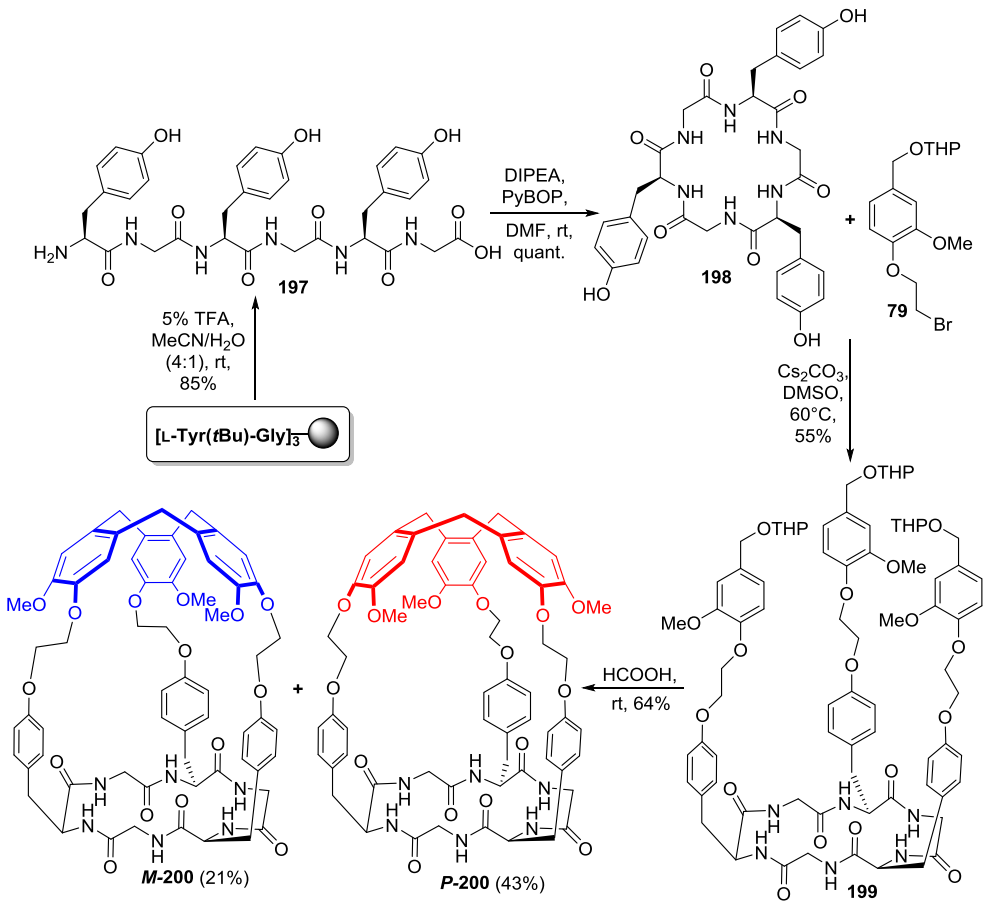

Scheme 7.36. Synthesis of macrocyclic peptide-based hemicryptophanes.

Chambron *et al*. described the synthesis of two C_3-symmetrical diastereoisomeric hemicryptophanes, in which the CTV unit was triple connected to permethylated α-cyclodextrin *via* ethylene bridges.[134] The synthetic procedure involved the triple alkylation of α-cyclodextrin **201** by iodide **202**, followed by an acid-catalyzed intramolecular cage-closing of hemicryptophane precursor **203** (Scheme 7.37). The cyclization step was performed under two different reaction conditions using formic acid or scandium triflate as promoters. In both cases, authors obtained the 6:1 mixture of two expected diastereoisomers: ***P*-204** and ***M*-204**, however in poor yields [8% for HCOOH and 5% for $Sc(OTf)_3$]. Moreover, the purification of the crude diastereoisomeric mixture allowed to isolate only one major isomer ***P*-204** in pure form. The authors tested also the [1+1] coupling reaction between the properly functionalized substrates (trimesylate derivative of permethylated α-cyclodextrin **201** and racemic cyclotriphenolene [**(±)-9**]), however they did not observe the formation of the desired products.

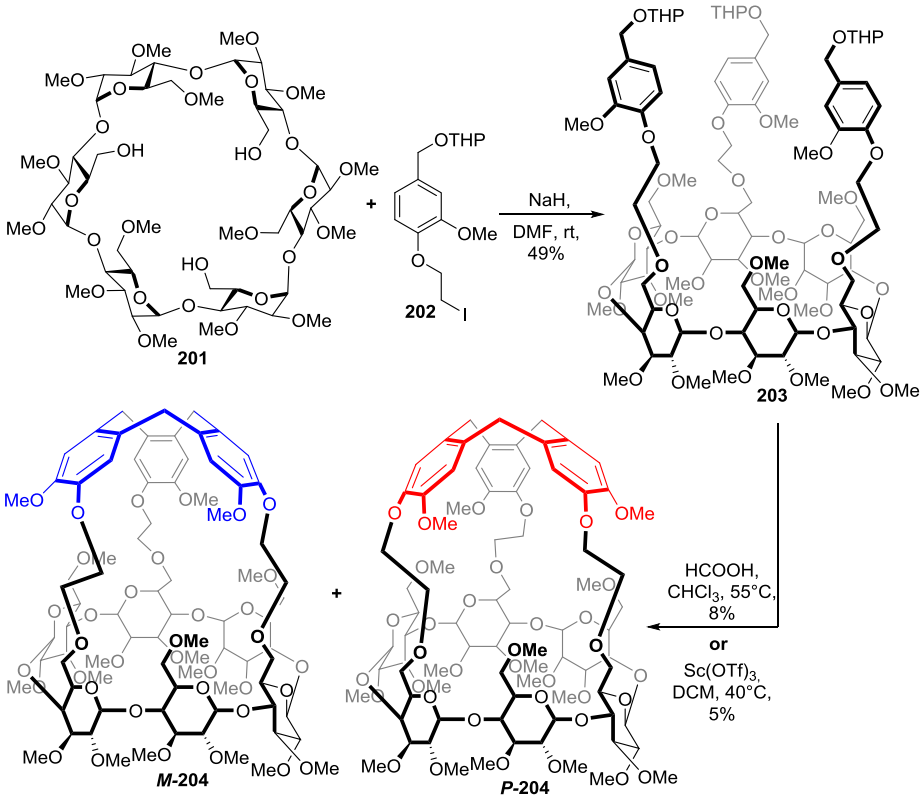

Scheme 7.37. Synthesis of α-cyclodextrin-based molecular cages with ethylene bridges.

Permethylated α-cyclodextrin platform was also used for the preparation of macrocycle-based hemicryptophanes with disulfide bonds.[135] The [1+1] coupling reaction between racemic cyclotrithiophenolene [**(±)-205**] and trithiol-α-cyclodextrin derivative **206** in the presence of iodine, potassium iodide, and triethylamine provided an inseparable mixture of two diastereoisomers ***M*-207** and ***P*-207** in 11% yield in a 5:3 ratio (Scheme 7.38). Moreover, the assignment of the *M*/*P* configuration of each cage could not be done by authors at this stage.

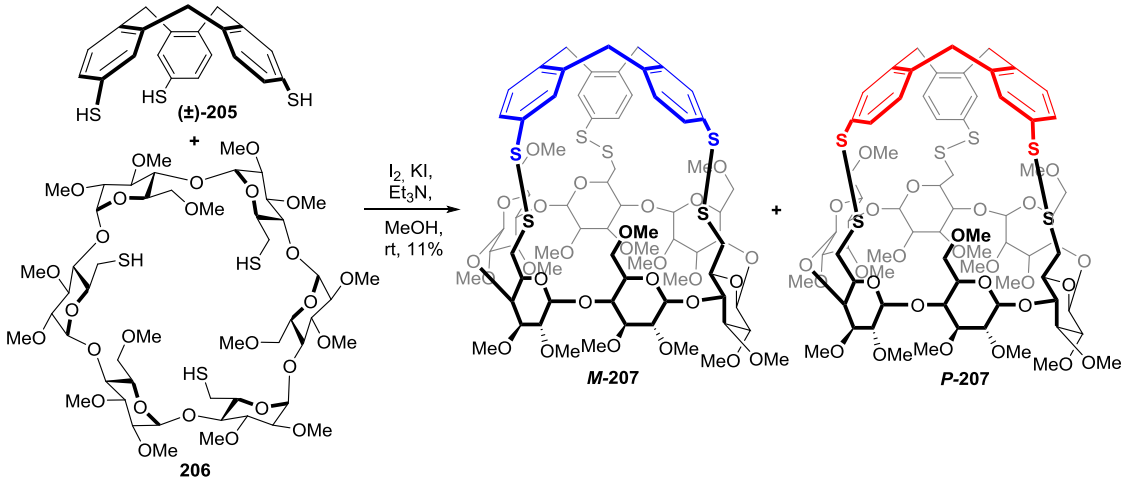

Scheme 7.38. Synthesis of α-cyclodextrin-based molecular cages with disulfide linkers.

7.4.2.7. Hemicryptophanes containing other scaffolds

The first synthesis of the mixture of four inseparable C_1-symmetrical hemicryptophanes containing diphenylglycoluril moiety and an additional pendant arm was described in 1989 by Nolte group.[30] The authors designed such unusual molecular cages due to their further possible application as metal-based catalysts. The synthesis was initiated from vanillin (**208**), which was reacted with 1,6-dibromohexane under the PTC (phase-transfer catalysis) conditions giving bromide **209** in very good yield (81%; Scheme 7.39). Subsequent reaction of **209** with diphenylglycoluril (**210**) in the presence of NaH, provided intermediate **211** with four vanillin-based extended arms in 50% yield. Then, the quantitative reduction of the aldehyde functions of **211** with $NaBH_4$ gave the corresponding tetraol **212**. The final cage-closing reaction of **212** induced by formic acid afforded the mixture of four inseparable stereoisomers of hemicryptophane **69**. It is worth to note that the possible cyclic tetramer (cyclotetraveratrylene unit) was not detected.

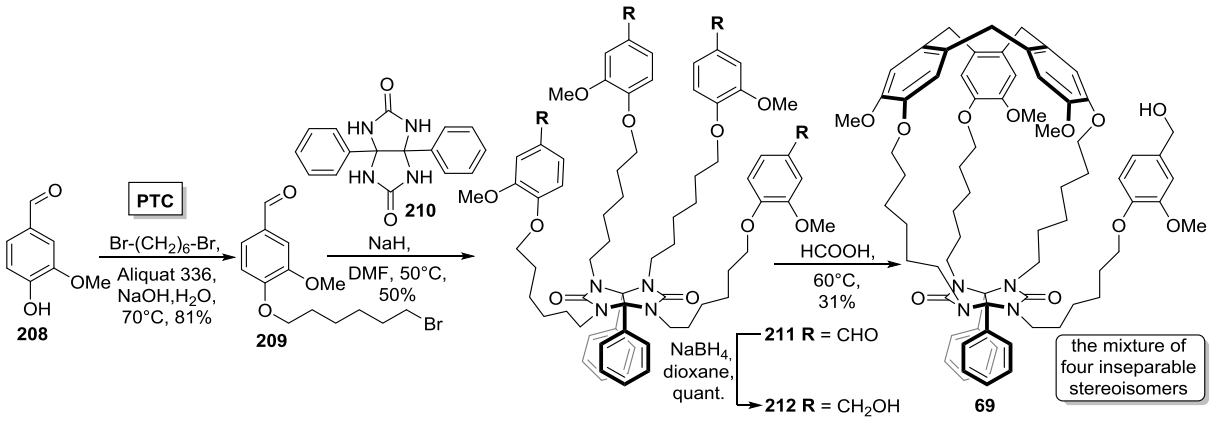

Scheme 7.39. Synthesis of the mixture of C_1-symmetrical hemicryptophanes with phenylglycouril moiety and additional pendant arm.

Different approach to the synthesis of hemicryptophanes was presented by Dutasta and co-workers.[104] The authors developed the straightforward pathway to thiophosphorylated molecular cages as shown in Scheme 7.40. The initial alkylation of (±)-CTG with bromide **213** under the basic conditions provided the corresponding cage precursor **(±)-214** in 63% yield. The [1+1] coupling between trialdehyde **(±)-214** and thiophosphotrihydrazide (**215**) afforded the expected hemicryptophane **(±)-216** in 23% yield. The authors suggested that such macrocyclization was successful probably due to the rigid conformation of the thiophospho-trihydrazide subunit. Similar strategy was employed for the synthesis of its analogue **(±)-220**, which contains three phenol functions (Scheme 7.40).[136]

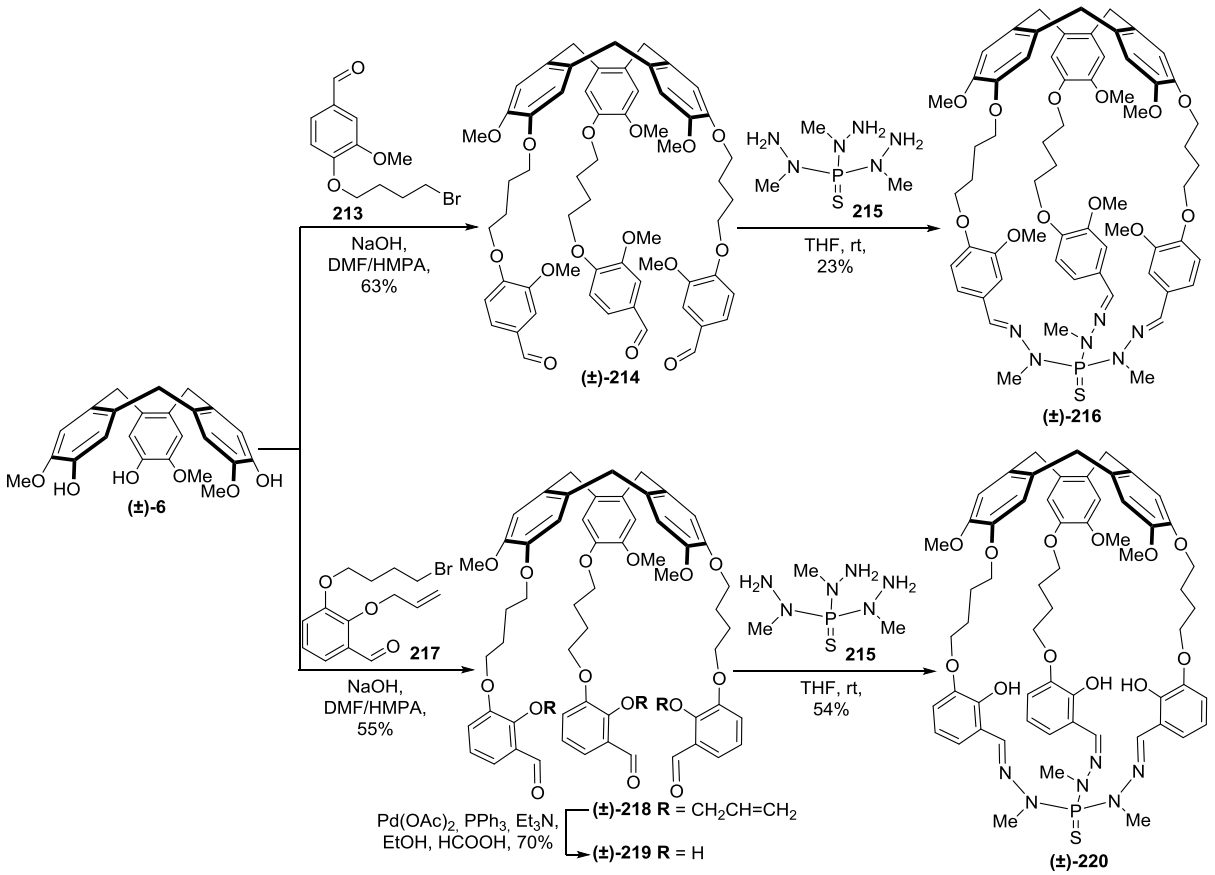

Scheme 7.40. Synthesis of hemicryptophanes containing thiophosphotrihydrazide unit.

A facile three steps synthesis towards tribenzylamine hemicryptophane **(±)-224** was proposed by Dmochowski *et al.*[137] The authors decided to cyclize the appropriate linkers to form the rigid CTV platform and then close the hemicryptophane precursor with amine constructing thus the cage-like structure. Indeed, the reaction of vanillyl alcohol (**71**) with 1,4-bis(bromomethyl)benzene (**221**) in the presence of K_2CO_3 led to compound **222**, which was cyclized to tribromide CTV derivative **(±)-223** in 29% yield using catalytic amount of $Sc(OTf)_3$ (Scheme 7.41). Treatment of tribromide **(±)-223** with 7N ammonia solution in MeOH afforded hemicryptophane **(±)-224** in 67% yield. It is noteworthy that the overall yield for all these three steps was 13%.

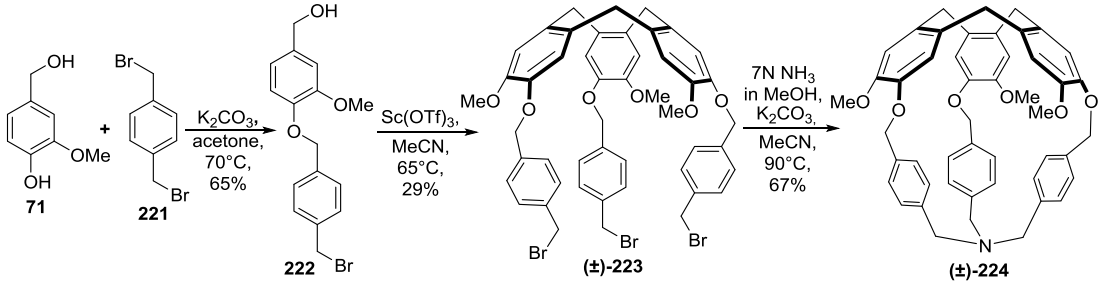

Scheme 7.41. Synthesis of tribenzylamine hemicryptophane **(±)-224**.

Recently, an efficient synthesis of hemicryptophane containing three 1,2,3-triazole rings was developed by Colomban *et al.*[138] Alkylation of (±)-CTG with 1-(azidomethyl)-4-(bromomethyl)benzene (**225**) in the presence of Cs_2CO_3 provided triazido CTV derivative **(±)-226** in very good yield (79%; Scheme 7.42). The final [1+1] macrocyclization step was performed *via* an azide-alkyne Huisgen cycloaddition between triazide **(±)-226** and tripropargylamine (**227**) giving hemicryptophane **(±)-228** in 22% yield.

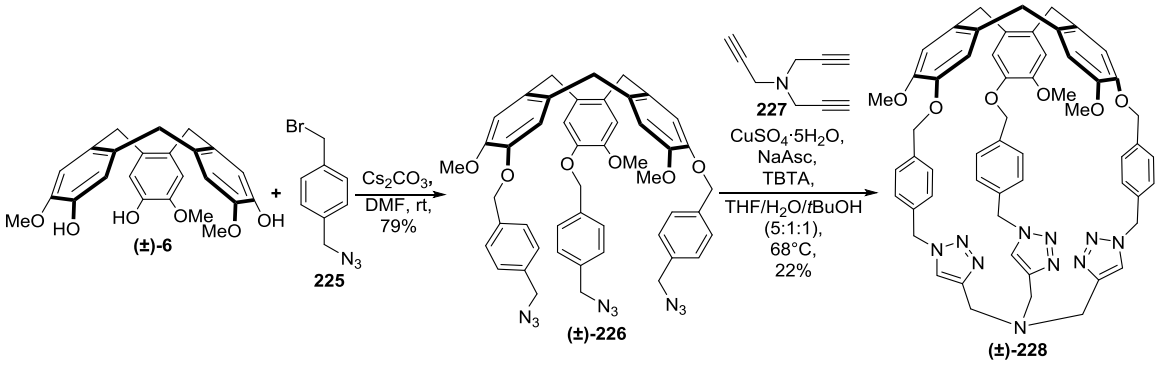

Scheme 7.42. Synthesis of hemicryptophane containing three 1,2,3-triazole rings.

7.4.3. Application of hemicryptophanes in the host-guest chemistry

The interesting host-guest properties of hemicryptophanes are mostly related to the inherently chiral, rigid CTV scaffold, which could be easily functionalized creating chiral molecular hosts with the original shape of the cavity. Introducing various lower subunits with additional binding sites (which could individually match to the guest molecule) to the hemicryptophane structure leads to heteroditopic receptors capable of complexing ion-pairs. Therefore, hemicryptophanes are effectively used as receptors for binding a vast array of charged or neutral, as well as chiral or achiral guests including carbohydrates, ammonium salts, zwitterions, ion-pairs, or fullerenes. The examples of their application are described in the following sections. To make the text below easier to follow, the structures of the described receptors are attached at the end of this Chapter (see Chapter 7.4.3.7).

7.4.3.1. Recognition of carbohydrates

Carbohydrates are essential biological molecules widely distributed in Nature. They are the most information-rich biomolecules due to their numerous steregenic centers. Apart from their primary role of providing energy to living organisms, these chiral compounds, like proteins or nucleic acids, are able to store information (glycocode) and thus they are used as

labels by living systems. The selective recognition of carbohydrates by natural receptors through non-covalent interactions plays a crucial role in various processes, such as infection by pathogens, cancer metastases, cellular recognition, or protein folding.[139] Nevertheless, selective recognition of these biomolecules by synthetic receptors is very demanding and difficult to achieve due to their sophisticated structures (often demonstrated by subtle configuration changes at just one stereogenic center). Structures of carbohydrate guest involved in the recognition studies of hemicryptophanes are shown in Figure 7.3.

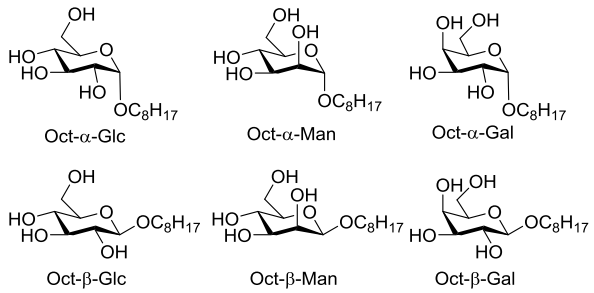

Figure 7.3. Structures of carbohydrate guests.

The first enantioselective recognition of carbohydrates by hemicryptophane receptors was reported in 2011 by Dutasta *et al.*[140] The authors investigated the complexing ability of two optically pure hemicryptophanes ***M*-90** and ***P*-90** towards carbohydrate guests [*n*-octyl-α- and *n*-octyl-β-D-glucopyranosides (Oct-α-Glc and Oct-β-Glc) shown in Figure 7.3] by the ^{1}H NMR spectroscopy in $CDCl_3$ (Table 7.4; Entries 1 and 2). Two important information could be noticed by comparison of their binding constants: 1) while host ***M*-90** showed almost three times higher selectivity for the Oct-α-Glc in relation to Oct-β-Glc, host ***P*-90** was able to bind exclusively the α-anomer of the glucoside; and 2) while the Oct-α-Glc was recognized by both hosts with 7:1 enantioselectivity, the Oct-β-Glc was complexed only by ***M*-90** enantiomer. These results suggest that both the inherent chirality of the CTV unit and the hydrogen bonds between the host and the guest, play an important role in recognition of carbohydrate derivatives. To further explore the influence of chirality of the CTV platform on the selective recognition of carbohydrates, the authors studied the binding properties of enantiopure cages ***M*-(*S*,*S*,*S*)-78**, ***P*-(*S*,*S*,*S*)-78**, ***M*-(*R*,*R*,*R*)-78**, and ***P*-(*R*,*R*,*R*)-78** with the same guests (Table 7.4; Entries 3–6). In this case, the results showed that the Oct-β-Glc is preferably recognized over its α-anomer by these cages, except cage ***P*-(*R*,*R*,*R*)-78**, which did not demonstrate any binding properties. However, its stereoisomer ***P*-(*S*,*S*,*S*)-78** exhibited exclusively complexation of the β-glucoside. In general, hemicryptophanes with the

M-configuration showed higher association constants towards octylglucosides than those with the *P* stereodescriptor, which confirms the important role of the CTV's inherent chirality in recognition of carbohydrate derivatives.

In the next paper, the same authors investigated the recognition properties of other four enantiopure cages of type **91,** bearing three additional stereogenic groups towards glucopyranosides. This would allow getting more information about the role of the CTV's inherent chirality on the stereoselectivity.[108] These additional stereogenic centers modified the shape of the host's cavity and hence improved the recognition properties comparing to the related receptors ***M*-90** and ***P*-90** (Table 7.4, Entries 1–2 *vs* 7–10).

Table 7.4. Binding constants of selected hemicryptophanes with carbohydrates.

Entry	Host	K_a (M^{-1})[a]			
		Oct-α-Glc	Oct-β-Glc	Oct-α-Man	Oct-β-Man
1.	***M*-90**	216	64	n.d.	n.d.
2.	***P*-90**	31	–	n.d.	n.d.
3.	***M*-(*S*,*S*,*S*)-78**	155	184	–	–
4.	***P*-(*S*,*S*,*S*)-78**	–	115	–	–
5.	***M*-(*R*,*R*,*R*)-78**	123	226	–	–
6.	***P*-(*R*,*R*,*R*)-78**	–	–	–	–
7.	***M*-(*S*,*S*,*S*)-91**	595	1660	n.d.	n.d.
8.	***P*-(*S*,*S*,*S*)-91**	–	183	n.d.	n.d.
9.	***M*-(*R*,*R*,*R*)-91**	56	192	n.d.	n.d.
10.	***P*-(*R*,*R*,*R*)-91**	34	384	n.d.	n.d.
11.	***M*-(*S*,*S*,*S*)-(*R*,*R*,*R*)-84**	105	83	58	–
12.	***P*-(*S*,*S*,*S*)-(*R*,*R*,*R*)-84**	–	–	100	–
13.	***M*-(*R*,*R*,*R*)-(*S*,*S*,*S*)-84**	–	–	50	–
14.	***P*-(*R*,*R*,*R*)-(*S*,*S*,*S*)-84**	89	537	135	48
15.	***M*-(*S*,*S*,*S*)-171**	41	–	–	61
16.	***P*-(*S*,*S*,*S*)-171**	174	–	–	118
17.	***M*-(*R*,*R*,*R*)-171**	223	287	55	40
18.	***P*-(*R*,*R*,*R*)-171**	29	72	182	458

[a] The K_a values were determined by the ^{1}H NMR titration experiments in $CDCl_3$ assuming the 1:1 (H:G) stoichiometry; estimated error 10%; „–" - no complexation was detected; n.d. (no data) - complexation was not measured.

Moreover, the change in the selectivity of the recognition of carbohydrate guests was observed. In all cases, the Oct-β-Glc guest was more effectively recognized than its α-anomer, which suggested that the additional stereogenic centers bearing the methyl groups were responsible for this selectivity. It could be also noticed that host ***M*-(*S*,*S*,*S*)-91** bound both carbohydrates more strongly than its stereoisomers. In addition, ***M*-(*S*,*S*,*S*)-91** can successfully recognize the Oct-α-Glc guest comparing to ***P*-(*S*,*S*,*S*)-91**, which did not exhibit any binding properties towards this carbohydrate anomer. All these results clearly showed that both the

CTV platform and the stereogenic centers were involved in the control of the selectivity of carbohydrate recognition.

The binding properties of structurally related hemicryptophanes of types **78** and **84** towards carbohydrate derivatives were compared with each other.[106] In this case, besides the Oct-α-Glc and Oct-β-Glc, two additional carbohydrate guests, *n*-octyl-α- and *n*-octyl-β-D-mannopyranoside (Oct-α-Man and Oct-β-Man), were employed for the recognition experiments (Table 7.4; Entries 3–6 *vs* 11–14). The authors noticed few correlations during host-guest interactions studies: 1) ***M***-(*S,S,S*)-(*R,R,R*)-**84** and ***P***-(*R,R,R*)-(*S,S,S*)-**84** were the only receptors able to bind glucopyranosides comparing to their stereoisomers, 2) ***P***-(*R,R,R*)-(*S,S,S*)-**84** exhibited very good selectivity towards Oct-β-Glc much better than for its enantiomer, 3) in contrast to receptors **78**, hosts **84** were capable of binding the α-anomers of mannose, 4) while ***P***-(*R,R,R*)-(*S,S,S*)-**84** isomer was able to exclusively bind the Oct-β-Man guest, the other three stereoisomers could selectively recognize Oct-α-Man, 5) hemicryptophanes of type **84** could differentiate glucopyranosides from mannopyranosides and demonstrated improved binding properties when compared to receptors **78**.

Four enantiopure hemicryptophanes containing 1,3,5-tripodal benzene scaffold and 1,1'-bi-2-naphthol linkers (**171**) were also investigated towards the selective discrimination of glucose and mannose derivatives.[126] The binding experiments showed that the K_a values of the complexation of all four sugars by these cages depended on the *M* and *P* configuration of their structures (Table 7.4; Entries 15–18). Indeed, receptors ***M***-(*R,R,R*)-**171** and ***P***-(*R,R,R*)-**171** showed higher binding constants than their stereoisomers towards both glucose and mannose derivatives. While ***M***-(*R,R,R*)-**171** and ***P***-(*R,R,R*)-**171** cages were able to bind Oct-β-Glc (K_a = 287 M^{-1}) and Oct-α-Man (K_a = 182 M^{-1}), their counterparts exhibited no complexing properties towards these guests. The authors observed the following selectivity of the recognition trend: Oct-α-Man > Oct-β-Glc > Oct-β-Man ≈ Oct-α-Glc.

An interesting conclusion was drawn from the binding experiments of hemicryptophane hosts ***M*-174** and ***P*-174** with six carbohydrate guests (α- and β- anomers of glucose, mannose, and galactose).[127] The change in the helical chirality of cyclotriveratrylene moiety led to a switch of the substrate-selectivity. Namely, receptor ***M*-174** exhibited significant selectivity for the β-glucose guest, whereas host ***P*-174** displayed better binding abilities towards the β-mannose derivative (Table 7.5; Entries 1 and 2). The high enantioselectivity between ***M*-174** and ***P*-174** (controlled only by the inherent chirality of the CTV scaffold) was observed in case of the Oct-β-Glc and the Oct-β-Man guests. Furthermore, the authors observed an exclusive discrimination of both galactose anomers by cage ***M*-174**.

In contrast with other CTV-based cages, these two receptors presented significant selectivities in the complexation of carbohydrate guests as well as good binding constants in particular for Oct-β-Glc and Oct-β-Man.

Table 7.5. Binding constants of hemicryptophanes **174** and **111b** with carbohydrates.

Entry	Host	K_a (M^{-1})[a]					
		Oct-α-Glc	Oct-β-Glc	Oct-α-Man	Oct-β-Man	Oct-α-Gal	Oct-β-Gal
1.	***M*-174**	100	993	218	7	245	274
2.	***P*-174**	30	45	508	856	–	–
3.	***M*-(*S*,*S*,*S*)-111b**	213	378	1410	804	29	13
4.	***P*-(*S*,*S*,*S*)-111b**	141	400	1648	387	112	68
5.	***M*-(*R*,*R*,*R*)-111b**	83	270	2511	641	22	–
6.	***P*-(*R*,*R*,*R*)-111b**	95	722	1544	967	142	59

[a] The K_a values were determined by the ^{1}H NMR titration experiments in $CDCl_3$ assuming the 1:1 (H:G) stoichiometry; estimated error 10%; „–“ - no complexation was detected

Similar binding experiments, including six carbohydrate guests were performed with four enantiopure hemicryptophanes **111b**.[122] In this case, all hosts displayed high association constants towards α-mannose derivative (Table 7.5; Entries 3–6). Moreover, the selectivity between these structurally related guests varied, depending on the hemicryptophane host. The authors suggested that the chirality of the receptors had a strong impact on the binding selectivity between these guests. For example, ***M*-(*R*,*R*,*R*)-111b** was more suitable for the recognition of Oct-α-Man from Oct-α-Gal or Oct-β-Gal than ***P*-(*R*,*R*,*R*)-111b**. On the other hand, ***M*-(*S*,*S*,*S*)-111b** was a better host than ***M*-(*R*,*R*,*R*)-111b** for the selective complexation of Oct-α-Glc in the presence of Oct-α-Gal or Oct-β-Gal.

To summarize the molecular recognition of carbohydrates by hemicryptophanes two main conclusions could be drawn: 1) the hydrogen bonds between hemicryptophane host and carbohydrate guest are crucial for the molecular recognition; 2) the inherent chirality of the CTV platform as well as additional stereogenic centers plays important role for the selective discrimination of carbohydrates.

7.4.3.2. Recognition of alkylammonium cations

The selective recognition of biologically relevant compounds by synthetic receptors is significant for understanding this phenomenon occurring in living organisms. Many neurotransmitters involved in key biological processes have the amino functions and exist in an ionic form (ammonium cations) at the physiological pH. One of the neurotransmitters of

broad interest is acetylcholine (ACh). This compound plays a significant role in peripheral and central nervous systems.[141] Another biologically essential compound is structurally similar choline and its derivatives (choline phosphate, betaine aldehyde, and glycine betaine; see Figure 7.4). The selective recognition of all these guests are challenging due to its similar trimethylammonium head and only slightly different tail. Therefore, the effective and selective recognition of these alkylammonium species is of great importance. Structures of alkylammonium cationic guest involved in the recognition studies of hemicryptophanes are shown in Figure 7.4.

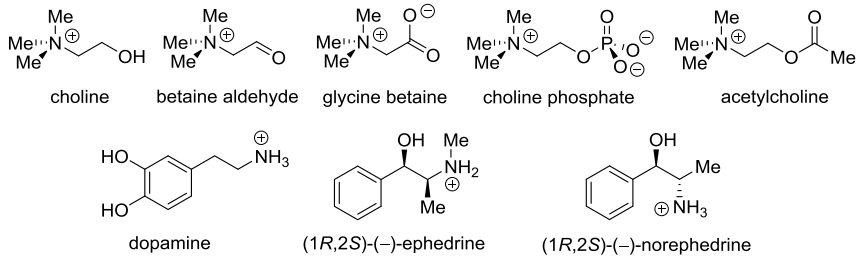

Figure 7.4. Structures of alkylammonium cationic guests.

The binding properties of hemicryptophane **(±)-97**, containing triamide moiety, towards various tetraalkylammonium salts were investigated by Makita *et al.*[110] The complexation experiments of the racemic host **(±)-97** with four tetraalkylammonium cationic guests (Me_4N^+, $Et_2Me_2N^+$, Et_3MeN^+, and acetylcholine) were studied in the mixture of $CDCl_3/CD_3OD$ (20:1) by the ^1H NMR titration method. Although the cavity of the Makita's host was smaller than most hemicryptophanes prepared by Martinez group,[25] this receptor was able to bind tetraalkylammonium salts, including acetylcholine, with very good association constants (K_a) ranging from 10^3–10^4 (Table 7.6).

Table 7.6. Association constants between hemicryptophane **(±)-97** and alkylammonium cations.

Entry	Guest	K_a (M^{-1})[a]
1.	Me_4N^+	$6.5 \pm 1.2 \times 10^4$
2.	$Et_2Me_2N^+$	$7.9 \pm 1.3 \times 10^3$
3.	Et_3MeN^+	$4.7 \pm 1.4 \times 10^3$
4.	ACh	$1.4 \pm 0.8 \times 10^4$

[a]The K_a values were determined by the ^1H NMR titration experiments in $CDCl_3/CD_3OD$ (20:1) assuming the 1:1 (H:G) stoichiometry; counterion: Cl^-.

Comparing the K_a values of all tested guests, we can observe that the highest binding constant was noted for Me_4N^+ and then by ACh (Table 7.6). These results clearly demonstrated that the

host's cavity was more suitable for tetramethylammonium unit than for its more branched ethyl analogues ($Et_2Me_2N^+$ and Et_3MeN^+). Moreover, the analysis of the X-Ray structure of **(±)-97⊂ACh** complex showed that the ammonium part of the guest is encapsulated inside the cavity, whereas the acetyl group is located outside the binding center.

Several primary alkylammonium cations of different size ($MeNH_3^+$, *n*$PrNH_3^+$, *t*$BuNH_3^+$, $BnNH_3^+$, and dopamine) were effectively encapsulated by hemicryptophane **(±)-101** bearing tris(2-aminoethyl)amine unit.[142] In this case, the complexation experiments of the ammonium picrate guests by racemic receptor **(±)-101** were studied by the ^{1}H NMR titrations in the mixture of $CDCl_3$/MeOD (95:5). The affinity of the ammonium guests to host **(±)-101** decreased in the following sequence: $BnNH_3^+$ > dopamine > $MeNH_3^+$ > *t*$BuNH_3^+$ > *n*$PrNH_3^+$ (Table 7.7).

Table 7.7. Association constants between hemicryptophane **(±)-101** and alkylammonium cations.

Entry	Guest	K_a (M^{-1})[a]
1.	$MeNH_3^+$	6.3×10^4
2.	*n*$PrNH_3^+$	1.0×10^4
3.	*t*$BuNH_3^+$	1.6×10^4
4.	$BnNH_3^+$	2.5×10^5
5.	dopamine	2.5×10^4

[a] The K_a values were determined by the ^{1}H NMR titration experiments in $CDCl_3$/MeOD (95:5) assuming the 1:1 (H:G) stoichiometry; estimated error 10%; counterion: picrate anion.

The authors explained that the highest association constant was observed for benzylammonium cation, probably because of both CH-π and π-π interactions between the host and guest molecules. In contrast to $BnNH_3^+$, tetramethylammonium cation was bound weaker by host **(±)-101,** most likely due to the lack of the π-stacking interactions. The weakest host-guest interactions were found for the sterically crowded ammonium cation *t*$BuNH_3^+$ and *n*$PrNH_3^+$. Interestingly, the binding affinity between receptor **(±)-101** and dopamine (which should ensure good matching for the host cavity due to the possible hydrogen bonds between polar functions as well as additional CH-π and π-π interactions) was one order of magnitude weaker as compared with benzylammonium ion. The DFT-optimized structures of these two host-guest complexes showed that in both cases the ammonium part is bound to TREN moiety, whereas the aromatic ring is located at the upper part of the cage. Furthermore, based on the results of the DFT calculations, the authors suggest that such selectivity between $BnNH_3^+$ and dopamine might be possible due to: 1) the additional ArH-π interactions between host's aromatic linkers and benzylammonium's phenyl ring, which did not occurr in case of

(±)-101⊂dopamine complex, and 2) the steric hindrance, which was more visible between dopamine and **(±)-101**.

Two years later, the same authors investigated the recognition properties of the water-soluble variant of **(±)-101** towards structurally similar ammonium guest (choline, glycine betaine, and betaine aldehyde) in aqueous media.[143] The synthesis of the water-soluble receptor **(±)-230** is shown in Scheme 7.43 and relies on the cleavage of the methoxy groups of the CTV scaffold with lithium diphenylphosphide.

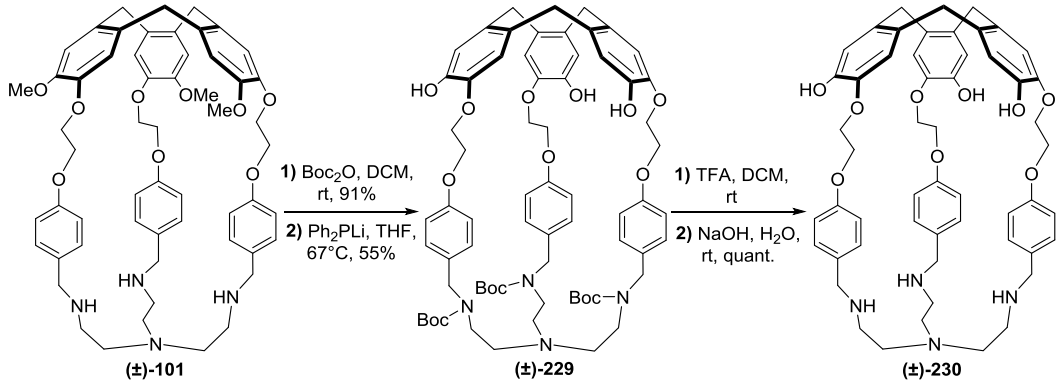

Scheme 7.43. Preparation of water-soluble hemicryptophane **(±)-230**.

The binding studies of choline, betaine aldehyde, and glycine betaine chlorides by receptor **(±)-230** were examined in the mixture of D_2O/NaOD at pD = 12 by the ^{1}H NMR titration method supported with the isothermal titration calorimetry (ITC) experiments. The results indicated that only choline was effectively recognized by this receptor (K_a = 2300 M^{-1}). The authors linked such selectivity to the zwitterionic character of both choline metabolites at pH = 12 (betaine aldehyde exist as a geminal diol in basic aqueous solution). Additional DFT studies of **(±)-230⊂Ch** complex demonstrated that choline is encapsulated within host's cavity in such a manner that the ammonium part of the guest interacts with the CTV platform, whereas its hydroxyl function interacts with the nitrogen atoms from TREN platform.

Enantiomerically pure variants of hemicryptophane **(±)-101** were used in the recognition studies towards chiral ammonium guest.[113] The complexing properties of cages ***M*-101** and ***P*-101** with (1*R*,2*S*)-(–)-norephedrine picrate salt were investigated by the ^{1}H NMR spectroscopy in the mixture of $CDCl_3$/MeOD (95:5). The results showed that such chiral guest was effectively encapsulated by both enantiopure receptors (Table 7.8; Entries 1 and 2). While host ***M*-101** could bind (1*R*,2*S*)-(–)-norephedrine with $K_a = 4.9 \times 10^7$ M^{-2}, its enantiomer ***P*-101** was able to recognize this ammonium guest with $K_a = 5.1 \times 10^6$ M^{-2},

assuming the 1:2 (H:G) stoichiometry. Moreover, the enantioselectivity for the recognition of (1*R*,2*S*)-(–)-norephedrine by these two optically pure cages was excellent (K_{a}***M*-101**/ K_{a}***P*-101** = 9.6) and resulted from the inherent chirality of the CTV scaffold.

Table 7.8. Binding constants of enantiopure cages **101** and **111b** with neurotransmitters.

Entry	Host	K_a (M^{-2})[a]	
		(1*R*,2*S*)-(–)-norephedrine	(1*R*,2*S*)-(–)-ephedrine
1.	***M*-101**	4.9×10^7	n.d.
2.	***P*-101**	5.1×10^6	n.d.
3.	***M*-(*S*,*S*,*S*)-111b**	2.6×10^9	2.2×10^8
4.	***P*-(*S*,*S*,*S*)-111b**	2.2×10^7	2.5×10^7
5.	***M*-(*R*,*R*,*R*)-111b**	1.4×10^7	4.6×10^6
6.	***P*-(*R*,*R*,*R*)-111b**	2.0×10^9	7.9×10^7

[a] The K_a values were determined by the ^{1}H NMR titration experiments in $CDCl_3$/MeOD (95:5) assuming the 1:2 (H:G) stoichiometry; estimated error 10%; n.d. (no data) - complexation was not measured; counterion: picrate anion.

Four enantiopure hemicryptophanes ***M*-(*S*,*S*,*S*)-111b**, ***P*-(*S*,*S*,*S*)-111b**, ***M*-(*R*,*R*,*R*)-111b**, and ***P*-(*R*,*R*,*R*)-111b** were succesfully employed in the recognition of (1*R*,2*S*)-(–)-ephedrine and (1*R*,2*S*)-(–)-norephedrine picrates.[144] The binding experiments were performed under the same conditions analogously as described above. The association constants of each receptor with the ammonium guest are presented in Table 7.8 (Entries 3–6). It could be noticed that all four diastereoisomers proved to be efficient hosts in chiral recognition of both bioactive compounds. The higher binding constants were observed for (1*R*,2*S*)-(–)-norephedrine than (1*R*,2*S*)-(–)-ephedrine, which could be related to their different ammonium functions (primary *vs* secondary). Whilst primary ammonium group of (1*R*,2*S*)-(–)-norephedrine might be involved in creating three hydrogen bonds with host structure, the secondary ammonium fragment of (1*R*,2*S*)-(–)-ephedrine can ensure only two hydrogen bonds. Additionally, good diastereoselectivities were observed for the recognition of both guests with the higher values for (1*R*,2*S*)-(–)-norephedrine. These results clearly showed that both CTV's inherent chirality and additional stereogenic centers have the significant impact on the diastereoselectivity in the chiral recognition.

Recently, three different fluorescent hemicryptophanes were used for the selective recognition of acetylcholine over choline.[128,129] The recognition studies of ACh and Ch by receptors **(±)-175**, **(±)-176**, and **(±)-177** were performed by fluorescence specroscopy in the mixture of 2% H_2O in DMSO. While hemicryptophanes **(±)-175** and **(±)-177** displayed a remarkable increase of the fluorescence intensity ("turn on" signal), molecular cage **(±)-176** exhibited decrease of the fluorescence intensity ("turn off" signal) after each addition of the

guest solutions. The authors suggested that this opposite behaviour might occur due to the higer rigidity of hemicryptophane **(±)-176**. The association constants of all three receptors with neurotransmitter are listed in Table 7.9. It could be noticed that acetylcholine was selectively differentiated over choline by cages **(±)-175** and **(±)-176**, and additionally in case of host **(±)-175** even over choline phosphate. The authors explained that this selectivity most likely results from the fact that ACh, as compared to Ch, has an ester function, which provides additional interactions with the host molecule. Further ^{1}H NMR titration experiments as well as DFT calculations of the host-guest complexes showed that all three receptors partially encapsulated the guest molecules within their cavities in such a way that the ammonium part of the guests is located in the center of the cavity interacting with the CTV unit, whereas "tail" of the guest molecule is positioned outside the cavity.

Table 7.9. Association constants of the fluorescent cages with neurotransmitters.

Entry	Host	K_a (M^{-1})[a]		
		acetylcholine (ACh)	choline (Ch)	choline phosphate
1.	**(±)-175**	2.4×10^4	5.9×10^3	4.2×10^3
2.	**(±)-176**	1.2×10^4	4.3×10^3	n.d.
3.	**(±)-177**	4.4×10^4	1.0×10^4	n.d.

[a] The K_a values were determined by fluorescence spectroscopy titration experiments in 2% H_2O in DMSO excited at 290 nm assuming the 1:1 (H:G) stoichiometry; estimated error 10%; n.d. (no data) - complexation was not measured; counterion: Cl^- and in addition for choline phosphate: Ca^{2+}.

7.4.3.3. Recognition of zwitterions

In most cases, hemicryptophanes are heteroditopic, which means that they have two different binding sites in their structure capable of simultaneous binding of ion-pairs or zwitterions. In comparison to ammonium neurotransmitters, the selective recognition of biologically important zwitterionic guests by artificial receptors is much less explored. This is due to the fact that recognition of zwitterionic guests is often energetically unfavorable because these strongly solvated bifunctional molecules have to be removed from water to the solution of much lower dielectric constant, which is a huge barrier to cross. Thus, strong coordination bonds along with ionic interactions are usually involved to bind zwitterionic species. Moreover, the distance between cationic and anionic binding sites in the receptor should be coordinated with the shape and size of bifunctional guest molecule.[145]

A numerous zwitterionic species (Figure 7.5) play an important role in human body. For example, taurine participates in various physiological processes including neurotransmission, modulation of calcium movements, or osmoregulation. In addition, taurine, glycine, and GABA are inhibitory neurotransmitters in the spinal cord, brain, and retina.[146] Choline phosphate is an important intermediate in the biosynthesis of phosphatidylcholine, main component of the eukaryotic cell membrane.[147] Another zwitterionic compound, L-carnitine, plays the crucial role in the metabolism and participates in the transport of long chain fatty acids.[148] Considering all these significant roles of the zwitterionic species, their selective recognition by molecular cages is of great importance.

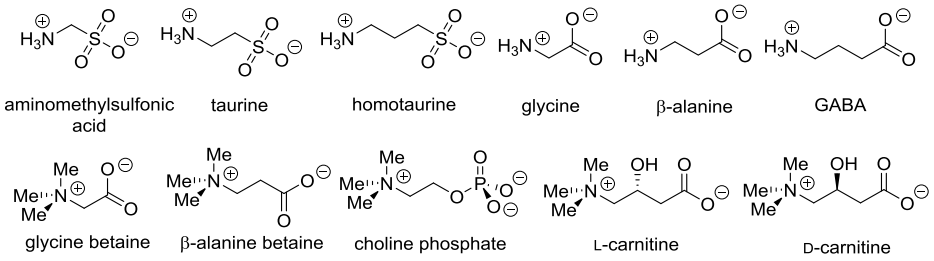

Figure 7.5. Structures of zwitterionic guests.

Heteroditopic hemicryptophane **(±)-90** with nitrilotriacetamide moiety was successfully used as a selective receptor for the encapsulation of taurine over other related zwitterionic compounds in competitive polar environment.[145] The complexation ability of host **(±)-90** towards several structurally related zwitterionic guest such as taurine, homotaurine, glycine, glycine betaine, β-alanine, β-alanine betaine, choline phosphate, aminomethylsulfonic acid, and γ-aminobutyric acid (GABA) was investigated by the ^{1}H NMR titration studies in the mixture of CD_3CN/D_2O (90:10). The results demonstrated that such receptor was able to selectively complex taurine inside its cavity. The association constants of hemicryptophane **(±)-90** with all tested zwitterions are listed in Table 7.10. In most cases, the guest molecules were too bulky or too small to fit properly to the host's cavity. For example, aminomethylsulfonic acid is too small for dual interaction with heteroditopic host, whereas GABA is too big for encapsulation. The DFT calculations of the complex of host **(±)-90** with taurine displayed full encapsulation of the guest molecule within host's cavity in such a way that the ammonium part of neurotransimitter is located in the center of the gap and interacts with the CTV scaffold through the cation-π interactions, while the negatively charged SO_3^- group is stabilized by three amide functions *via* hydrogen bonds.

Table 7.10. Binding constants of hemicryptohanes **(±)-90** and **(±)-165** with zwitterions.

Entry	Guest	K_a (M^{-1})[a]	
		(±)-90	**(±)-165**[b]
1.	aminomethylsulfonic acid	–	n.d.
2.	taurine	1.4×10^4	5.0×10^5
3.	homotaurine	5.3×10^2	1.1×10^5
4.	glycine	–	n.d.
5.	β-alanine	8.5×10^3	1.5×10^4
6.	GABA	5.1×10^2	2.3×10^5
7.	glycine betaine	0.8×10^2	n.d.
8.	β-alanine betaine	–	n.d.
9.	choline phosphate	–	n.d.

[a] The K_a values were determined by the ^{1}H NMR titration experiments in CD_3CN/D_2O (90:10) assuming the 1:1 (H:G) stoichiometry; estimated error 10%; n.d. (no data) - complexation was not measured; „–" - no complexation was detected. [b] the ^{1}H NMR titration experiments were performed in CD_3CN/D_2O (80:20).

One year later, the same authors designed heteroditopic hemicryptophane **(±)-165** with a modified cavity, which could simultaneously bind both negatively and positively charged parts of the zwitterionic guests by the anion-π and cation-π interactions.[149] The recognition studies were performed by the ^{1}H NMR titrations of host **(±)-165** with four zwitterionic neurotransmitters (taurine, homotaurine, β-alanine, and GABA) in a competitive aqueous medium (CD_3CN/D_2O = 80:20). Compared to the previously described receptor **(±)-90**, the complexation abilities of **(±)-165** were considerably improved, nevertheless still with affinity to taurine (Table 7.10). These high binding constants in such polar solvent might result from three additional hydrogen-bond donor amide functions in the linkers as well as from the π-acidic aromatic ring, which stabilize the anionic part of zwitterion. The DFT calculation of **(±)-165⊂taurine** complex showed that the positively charged ammonium part occupies the center of the CTV scaffold, whereas the negatively charged sulfonate function is located at the lower part of the host's cavity.

The recognition properties of diastereoisomerically pure hemicryptophanes ***M*-200** and ***P*-200** containing cyclic peptide moiety were investigated using L- and D-carnitine as guests.[133] The ^{1}H NMR titration experiments of diastereoisomers ***M*-200** and ***P*-200** with both enantiomers of carnitine in CD_3CN (assumed 1:1 binding model) showed that both hosts were selective towards L-carnitine ($K_a = 4.1 \times 10^3$ M^{-1} and 9.1×10^2 M^{-1}); the association constant of ***M*-200** and ***P*-200** for L-carnitine is 1.5 and 1.3 times greater than for its D-enantiomer ($K_a = 2.7 \times 10^3$ $M^{-1}$and 6.9×10^2 M^{-1}, respectively). The additional DFT calculations of ***P*-200⊂L-carnitine** complex demonstrated that guest molecule is fully encapsulated within host's cavity in ditopic fashion. While the ammonium part of the guest interacts with the CTV

unit *via* cation-π and CH-π interactions, the carboxylate function forms hydrogen bonds with cyclic peptide scaffold.

In another study, the Zn(II)-based fluorescent racemic hemicryptophane **(±)-231** was used as a selective receptor for choline phosphate in polar media.[150] The authors prepared such metal-based heteroditopic host by a coordination of Zn^{2+} cation with TREN moiety of ligand **(±)-109** using $Zn(ClO_4)_2$ (Scheme 7.44).

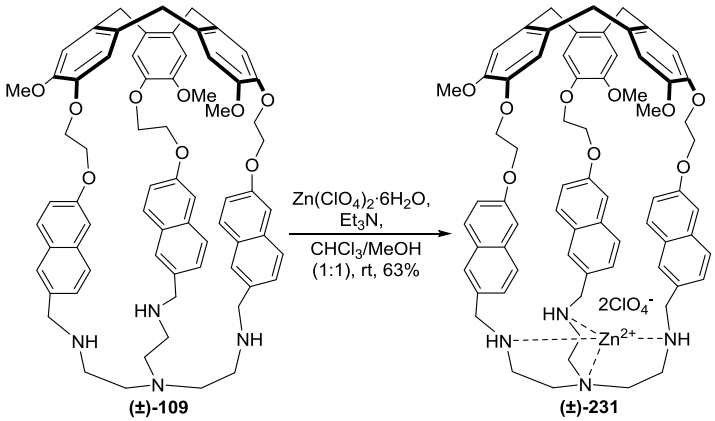

Scheme 7.44. Synthesis of Zn(II)-based fluorescent hemicryptophane **(±)-231**.

Then, they carried out the binding experiments of the complex of **(±)-231** with choline and choline phosphate by fluorescence spectroscopy (excited at 300 nm) in the mixture of DMSO/H_2O (80:20). Upon successive addition of the guest solution to the host solution, the authors observed a remarkable fluorescence quenching. The results showed that choline ($K_a = 1.2 \times 10^2$ M^{-1}) was much less recognized than its phosphorylated anologue ($K_a = 4.1 \times 10^3$ M^{-1}). The authors explained that such selectivity towards choline phosphate may results from the high complexing affinity of the Zn(II) platform for the phosphorylated species. Indeed, the Zn(II) platform plays a crucial role in this recognition because similar experiments with cage **(±)-109** show only negligible changes in the fluorescence emission spectra. In addition, the heteroditopic character of receptor **(±)-231** had also influence on this recognition, since the fluorescence quenching as well as binding constant for zwitterionic choline phosphate was larger than for choline.

7.4.3.4. Recognition of anions

Anion sensing by artificial receptors is one of the main goals of supramolecular chemistry. Transport of anions across cell membranes, extraction of anions from complex

mixtures, or their use in supramolecular catalysis are only a few examples, which demonstrate the great importance of such phenomenon.[151] However, among non-covalent interactions, the anion-π interactions, involved in the complexation of anionic guests through interactions with the electron-deficient aromatic rings, are much less studied. Anion-π interactions are very useful in designing artificial receptors capable of binding anionic species, in particular those, which play an important role in agriculture (nitrate, phosphate), medicine (fluoride, chloride), environment (sulfate, pertechnetate), or security (perchlorate, cyanide). Despite the large progress in this field, the selective recognition of anions is still challenging, particularly in water, due to the fact that they are strongly solvated by polar solvents, and they have: 1) more diffuse charge, when compared to the corresponding isoelectronic cations, 2) greater pH dependence, and 3) a wide variety of geometries.[151,152]

The selective recognition studies of various anionic species by hemicryptophane **(±)-90**, which contains a tripodal amide moiety, were carried out by Martinez and Dutasta.[153] For this purpose, the authors tested several anions with different geometries such as spherical halide anions, V-shaped (AcO^-), and tetrahedral ($H_2PO_4^-$ and HSO_4^-), by the ^1H NMR titrations in $CDCl_3$. The results clearly showed the hydrogen-bonding interactions between the amide functions in host **(±)-90** and tested anions, which was manifested by the significant downfield chemical shift of the amide group protons (NH). The binding constants of the 1:1 host-guest complexes of **(±)-90** with anions are listed in Table 7.11 (Entry 1). In-depth analysis of these results allowed to point out few general trends. First, the affinity of the receptor **(±)-90** for the spherical halide anions increased as follows: $F^- > Cl^- > Br^- > I^-$, and was compatibile with its hydrogen-bond accepting capability. Second, the more basic $H_2PO_4^-$ anion was better recognized than HSO_4^-. Finally, the most basic AcO^- anion displayed weaker affinity for host **(±)-90** in relation to $H_2PO_4^-$. This lower binding constant might be associated with the geometry of the guests. Indeed, in comparison with the V-shaped AcO^- anion, the $H_2PO_4^-$ anion with tetrahedral geometry can bind to the three amide groups at the same time. In general, the binding affinity depends on the basicity as well as the geometry of the anionic guest.

Two hemicryptophanes **(±)-92** and **(±)-93**, which contain differently fluorinated aromatic rings in the linkers, were also studied towards anionic guests.[154] The authors assumed that the introduction of fluorinated phenyl linkers close to the anionic binding site should contribute to increase of the anion-π interactions. The complexing abilities were measured in a similar way as for previously described host **(±)-90**, have proved to be highly dependent on the position of the fluorine atoms. Namely, the K_a value was remarkably

increased in case of host **(±)-92**, whereas decreased in case of **(±)-93** (Table 7.11, Entries 2 and 3). Moreover, the analysis of the chemical shift changes during the ^{1}H NMR experiments demonstrated that the encapsulated anions are bound both to the amide groups (*via* hydrogen bonds) and to the phenyl rings of the linkers (through the anion-π interactions). When comparing the binding abilities of these two hosts towards anions, the same trend as for receptor **(±)-90** could be observed. The most significant feature was the huge change in the association constants caused by the introduction of two differently situated fluorine atoms in the phenyl rings. Indeed, the binding constants of host **(±)-92**, in which the fluorine atoms are located closer to the CTV moiety, are much higher when compared to host **(±)-90** without fluorine atoms. Similarly, the complexing abilities of host **(±)-93** towards anions are remarkably lower in relation to receptor **(±)-90**. All these results clearly indicates that the location of these two fluorine atoms has a strong impact on the recognition properties of the receptor.

Table 7.11. Binding constants of various hemicryptophanes with anions.

Entry	Host	K_a (M^{-1})[a]						
		F^-	Cl^-	Br^-	I^-	AcO^-	HSO_4^-	$H_2PO_4^-$
1.	**(±)-90**	120	100	65	20	60	45	230
2.	**(±)-92**	2330	1440	620	270	1140	400	830
3.	**(±)-93**	61	27	12	13	11	18	21
4.	**(±)-136**	3900	4100	1050	80	1400	24800	184200
5.	**(±)-138**	1200	<1	<1	<1	<1	n.d.	216

[a] The K_a values were determined by the ^{1}H NMR titration experiments in $CDCl_3$ assuming the 1:1 (H:G) stoichiometry; estimated error 10%; n.d. (no data) - complexation was not measured; couterion: nBu$_4$N$^+$

In 2019, the selective recognition of the same anions with hemicryptophane **(±)-136** bearing three urea fuctions was investigated by the ^{1}H NMR titrations in $CDCl_3$.[119] Upon gradual addition of the anionic guest solution to the host solution, a significant downfield chemical shifts of the urea protons were observed. These results demonstrated that anions were efficiently encapsulated within the host cavity by hydrogen-bonding interactions with the urea functions. The calculated association constants are shown in Table 7.11 (Entry 4). Several conclusions could be drawn from these data. First, almost all association constants for receptor **(±)-136** are remarkably higher than for other hemicryptophanes. Second, the recognition ability for spherical halide anions increases in the following order: $Cl^- \approx F^- > Br^- > I^-$, which is in agreement with their hydrogen bond accepting capacity. Third, a significant increase in selectivity is noticed when compared to host **(±)-90**, particularly in the case of discrimination $H_2PO_4^-$ from AcO^- or Cl^- from I^-. Finally, host **(±)-136** showed very high

association constant towards tetrahedral $H_2PO_4^-$ guest, probably due to the simultaneous binding of this anion with the six hydrogens of the urea groups.

Recently, a small urea-based hemicryptophane **(±)-138** was studied towards selective recognition of anions, in particular halides.[120] Compared to its previously described analogue **(±)-136** with much larger cavity, receptor **(±)-138** displayed the exclusive recognition of the fluoride anion over other competing halides (Table 7.11, Entry 5). Indeed, a number of experiments on molecular recognition, including ^1H and ^{19}F NMR titrations, ESI-HRMS measurements, and XRD analysis, clearly showed that fluoride anion was efficiently encapsulated within host **(±)-136** cavity through the hydrogen-bonding interactions (NH–F^-) with six hydrogen atoms from the urea groups. Whilst the measured binding constant of host **(±)-136** with F^- anion was 1200 M^{-1}, the K_a values for other halide anions were below 1 M^{-1}, which means that this small and rigid hemicryptophane is highly selective for fluoride guest. Moreover, this remarkable selectivity towards F^- was also observed over other anions such as V-shaped AcO^- and tetrahedral $H_2PO_4^-$. In general, the three urea functions together with the well-designed size of the host's cavity ensured the exclusive selectivity for the F^- anion over other halide anions.

7.4.3.5. Recognition of ion-pairs

Heteroditopic receptors capable of simultaneously binding both cationic and anionic guests have an important advantage, namely they could prevent the competitive pairing of the guest ions in the solution. Most of the ion-pair receptors exhibit improved selectivity and binding affinity when compared to the analogous single ion hosts. In case of ion-pairs, the binding sites of the receptors, responsible for the complexation, should be located close to each other to increase the electrostatic interactions; otherwise ion-pairs could associate outside the cage. Well designed receptors allow for a positive cooperative effect, manifested in additional or more intensified long-range electrostatic interactions, which improve affinity to ion-pairs.[22]

In 2008, Le Gac and Jabin investigated the binding ability of calix[6]cryptamide **(±)-187** towards two ion-pairs: $EtNH_3^+Cl^-$ and $PrNH_3^+Cl^-$.[131] The ^1H NMR titration experiments in $CDCl_3$ demonstrated that hemicryptophane **(±)-187** acts as heteroditopic receptor, in which the alkylammonium chain of the guest molecule occupies the calixarene cavity, whereas the chloride counterion is simultaneously bound by the three amide functions of the hosts's linkers through the strong hydrogen-bonding interactions. In addition, the

authors proved that the binding of the Cl^- anion can take place only in the presence of ammonium part and vice versa – without chloride anion the alkylammonium cation was not encapsulated. This observations indicated the significant positive cooperativity, which is probably due to the electronic and structural variations.

Martinez and Dutasta also proposed hemicryptophane **(±)-90** containing two properly located binding sites (1. the CTV scaffold, which is suitable for the complexation of ammonium cations, and 2. three amide groups able to coordinate anions *via* hydrogen-bonding interactions) capable of simultaneously recognizing ion pairs.[153] Indeed, the ^{1}H NMR recognition studies of host **(±)-90** towards various ion-pairs of type $Me_4N^+X^-$ (X = F, Cl, Br, AcO) showed that tetramethylammonium guest was effectively bound by the CTV unit, while the anionic species interact with triamide moiety. Therefore, this bifunctional receptor exhibited strong positive cooperativity effect for all studied ion-pairs, which was manifested in increased association constant values (Table 7.12, Entry 1), when compared to the K_a values for individual ions. The best cooperativity effect was observed for the $Me_4N^+Cl^-$ ion-pair (K_a = 1500 M^{-1} for ion-pair *vs* K_a = 380M^{-1} for Me_4N^+ *vs* K_a = 100 M^{-1} for Cl^-). The authors explained that this ion-pair fitted to the cavity better with its size, thus leading to the efficient hydrogen-bonding as well as CH-π and cation-π interactions.

Table 7.12. Association constants of hemicryptophanes **(±)-90** and **(±)-138** with ion-pairs.

Entry	Host	K_a (M^{-1})[a]			
		$Me_4N^+F^-$	$Me_4N^+Cl^-$	$Me_4N^+Br^-$	$Me_4N^+AcO^-$
1.	**(±)-90**	1040	1500	190	310
2.	**(±)-138**	10700	29000	13500	n.d.

[a] The K_a values were determined by the ^{1}H NMR titration experiments in $CDCl_3$ assuming the 1:1 (H:G) stoichiometry; estimated error 10%; n.d. (no data) - complexation was not measured; couterions: nBu$_4$N$^+$ for anions and picrate for cations

The cooperativity effect decreased for $Me_4N^+F^-$ ion-pair probably due to the unbalanced status of both contact- and separated-ion-pair forms inside the host's cavity. In the case of $Me_4N^+Br^-$ and $Me_4N^+AcO^-$ ion-pairs, the weaker cooperativity effect could be attributed to their volume, which results in worst matching to the cavity. The authors concluded that the close proximity of two different binding sites in such heteroditopic receptor leads to the favourable electro-static interactions between cation and anion inside the cavity, and therefore a strong positive cooperativity for the recognition of ion-pairs is observed.

Recently, the same authors studied the simultaneous complexation of ion-pairs employing hemicryptophane **(±)-138** containing three urea groups.[119] The ^{1}H NMR titrations

of cage **(±)-138** with three different ion-pairs ($Me_4N^+F^-$, $Me_4N^+Cl^-$, and $Me_4N^+Br^-$) showed that this receptor was able to bind both cations and anions at the same time with much higher association constants (Table 7.12, Entry 2), when compared to its complexation of individual ions. Similarly to host **(±)-90**, Me_4N^+ ion was effectively bound in the upper part of the electron rich CTV cavity of receptor **(±)-138** through the CH-π and cation-π interactions, whereas the anionic guests were complexed in the lower part of this receptor *via* urea hydrogen bonds. It could be noticed that this strong positive cooperativity effect might result from the additional electrostatic interactions between both ions and depends on the nature of the ion-pair. In comparison to host **(±)-90**, this urea-based receptor displayed considerably higher association constants towards ion-pairs.

7.4.3.6. Recognition of other guests

Nowadays, the selective recognition of various neutral molecules by artifical receptors through non-covalent interactions is also of great importance. For example, the selective recognition of fullerenes from its crude fullerite mixture by synthetic receptors might be crucial in their isolation process, which usually is difficult and tedious, especially due to their poor solubility in most solvents. This separtation process is of particular importance, as most of spherical nanocarbons can find an application in multiple areas including catalysis, photovoltaics, or medicinal chemistry. This results from their interesting physical and chemical properties such as electron-acceptor, electrical transport, and photosensitizing features.[155] On the other hand, recognition of the persistent organic pollutants (*e.g.* chlordecone and its analogues) is equally important, as in most cases they are extremely hard to remove from environment. Chlordecone is an organic polychlorinated pesticide that is highly toxic to humans and remains in the rivers, crops and soils.[156] Therefore, the use of host-guest approach should allow for its easier detection and removal from water. The selective recognition of different structural motifs of bioactive compounds (*e.g.* imidazol-2-one, pyrrolidin-2-one) is also noteworthy. In this case, the host-guest interactions could be involved in a drug delivery system. Structures of neutral guests involved in the recognition studies of hemicryptophanes are shown in Figure 7.6.

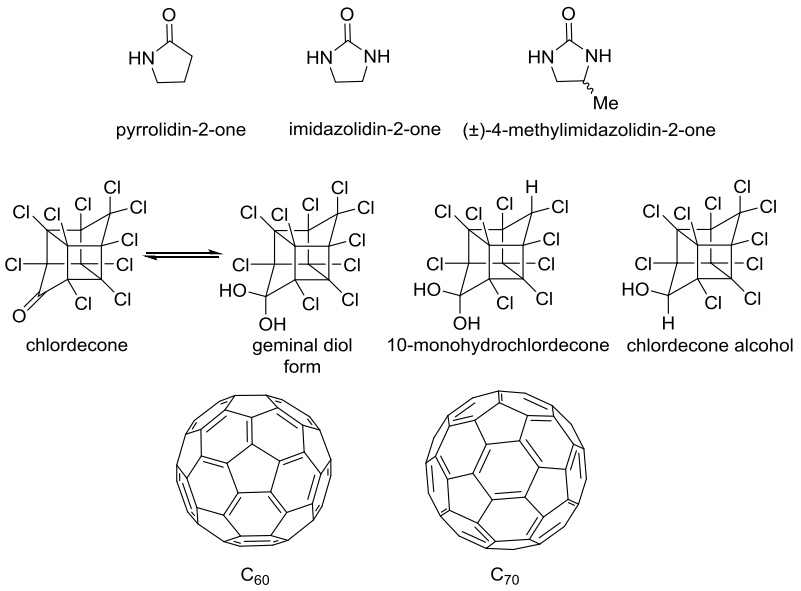

Figure 7.6. Examples of neutral guests.

The recognition properties of calix[6]cryptamide **(±)-187** towards neutral molecules such as achiral pyrrolidin-2-one and imidazolidin-2-one as well as chiral (±)-4-methyl-imidazolidin-2-one were studied by the ^{1}H NMR spectroscopy.[131] The results showed that all three guests were fully encapsulated in the calixarene cavity instead of the CTV unit. During the recognition experiments, the authors observed a remarkable downfield chemical shift of the protons from the amide functions positioned closer to the calixarene unit of host molecule. Moreover, the guest molecules are additionally stabilized by strong hydrogen bonds with the calixarene oxygen atoms of the host. These results demonstrated the specific complexation of neutral amide and urea type guests by hemicryptophane **(±)-187** involving both hydrogen bond acceptor and donor groups of the guests in the recognition process. When comparing the binding constants of calix[6]cryptamide **(±)-187** with both achiral guests, a strong preference for imidazolidin-2-one (K_a = 12800 M^{-1}) than for pyrrolidin-2-one (K_a = 250 M^{-1}) can be noticed. The authors explained that this is due to the complementary match between the calixarene unit and imidazolidin-2-one in terms of shape, size, and electronic structure. In my opinion, the additional NH group of imidazolidin-2-one could be also responsible for the higher binding constant as it can participate in the hydrogen-bonding interactions with the host molecule. It is noteworthy that in the case of chiral recognition of (±)-4-methyl-imidazolidin-2-one guest, the formation of two diastereoisomeric host-guest complexes was observed (44% *de*), however the association constant was not determined.

The encapsulation abilities of two racemic macrocycle-based hemicryptophanes **(±)-196a** and **(±)-196b** with two fullerenes (C_{60} and C_{70}) were investigated by Zhao and Li.[132]

The binding properties of hosts **(±)-196a** and **(±)-196b** were studied by the ^{1}H NMR and UV-Vis titration methodologies supported by NOESY and DOSY experiments as well as vapor pressure osmometry measurements. All these experiments confirmed the encapsulation of C_{60} and C_{70} inside the cavities of hosts **(±)-196a** and **(±)-196b**. The binding constants of both receptors towards C_{60} and C_{70} are listed in Table 7.13. It could be noted that receptor **(±)-196b** showed better recognition properties than host **(±)-196a** towards both fullerenes, which is related to its larger cavity. In addition, although these two hosts have different sized cavities, they both display better affinity for C_{60} than for C_{70}.

Table 7.13. Binding constants of the macrocycle-based hemicryptophanes **(±)-196a** and **(±)-196b** with C_{60} and C_{70} in two different solvents.

Entry	Host	K_a (M^{-1})[a]			
		chloroform		chlorobenzene	
		C_{60}	C_{70}	C_{60}	C_{70}
1.	**(±)-196a**	7.7×10^4	6.4×10^3	1.1×10^4	1.2×10^3
2.	**(±)-196b**	1.9×10^5	2.4×10^4	1.5×10^5	1.2×10^5

[a] The K_a values were determined by UV-Vis titration experiments assuming the 1:1 (H:G) stoichiometry; estimated error 10%;

Recently, two racemic hemicryptophanes: **(±)-90** and **(±)-101** were studied as receptors for chlordecone (which mainly exist as geminal diol in organic solution; Figure 7.6).[157] In both cases, the association constants were determined by the ^{1}H NMR titrations in $CDCl_3$ assuming the 1:1 binding mode. The calculated K_a value for host **(±)-101** was much higher than for **(±)-90** (2.1×10^4 M^{-1} *vs* 126 M^{-1}). The authors suggested that both the small size and high rigidity of the cavity of host **(±)-90** could have an impact on this modest binding constant. The DFT calculations of **(±)-101⊂chlordecone** complex demonstrated that this polychlorinated compound was fully encapsulated in the host cavity. Several non-covalent interactions including the hydrogen bonds between TREN unit and geminal diol functions as well as halogen-π interactions between host and guest molecules were noticed. In the next step of the studies, the authors tested the ability of hemicryptophane **(±)-101** to recognize two analogues of chlordecone, namely chlordecone alcohol and 10-monohydrochlordecone. While 10-monohydrochlordecone was recognized as good as chlordecone ($K_a = 2.6 \times 10^4$ M^{-1}), chlordecone alcohol displayed much lower affinity ($K_a = 136$ M^{-1}) than its geminal diol analogue. The authors explained that these additional recognition experiments highlights the key role of hydrogen bonds between the nitrogen atoms of TREN unit and gem diol functions of chlordecone guest.

7.4.3.7. Annex – structures of hemicryptophanes

This section contains the structures of all hemicryptophanes described in Chapter 7.4.3.

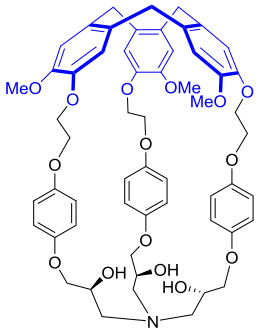

***M*-(*S*,*S*,*S*)-78**
+
***P*-(*S*,*S*,*S*)-78**

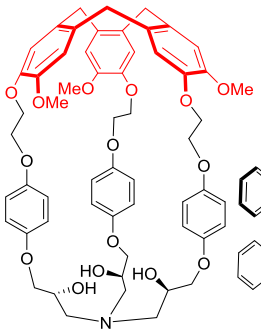

***P*-(*R*,*R*,*R*)-78**
+
***M*-(*R*,*R*,*R*)-78**

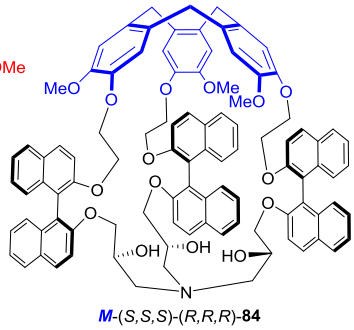

***M*-(*S*,*S*,*S*)-(*R*,*R*,*R*)-84**
+
***P*-(*S*,*S*,*S*)-(*R*,*R*,*R*)-84**

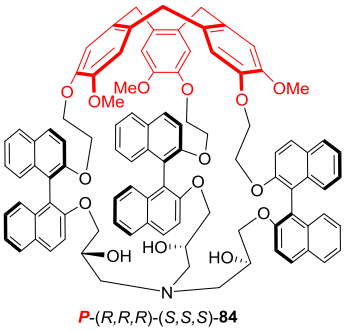

***P*-(*R*,*R*,*R*)-(*S*,*S*,*S*)-84**
+
***M*-(*R*,*R*,*R*)-(*S*,*S*,*S*)-84**

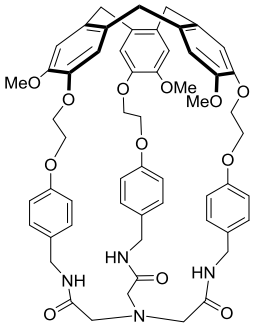

(±)-90

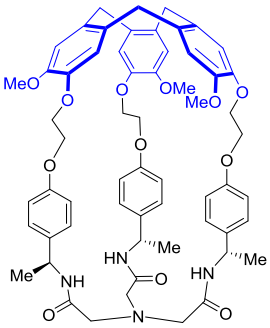

***M*-(*S*,*S*,*S*)-91**
+
***P*-(*S*,*S*,*S*)-91**

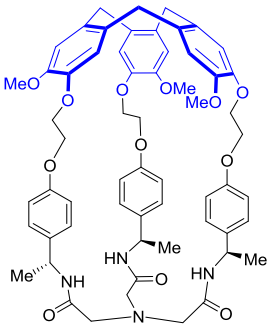

***M*-(*R*,*R*,*R*)-91**
+
***P*-(*R*,*R*,*R*)-91**

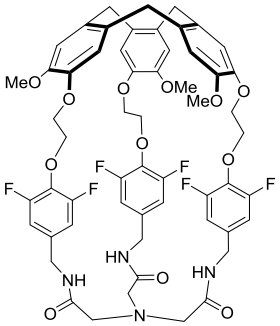

(±)-92

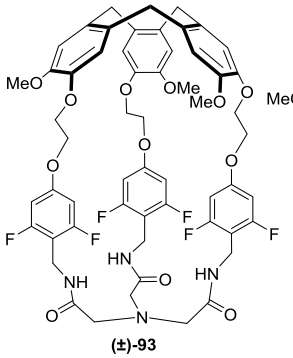

(±)-93

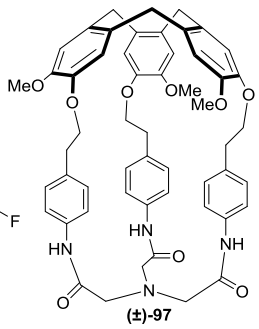

(±)-97

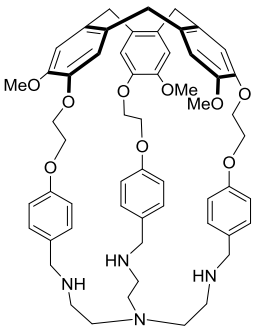

(±)-101

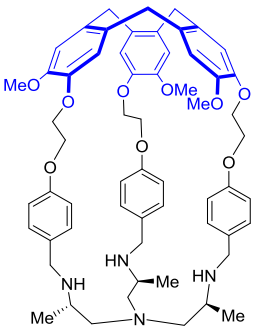

***M*-(*S*,*S*,*S*)-111b**
+
***P*-(*S*,*S*,*S*)-111b**

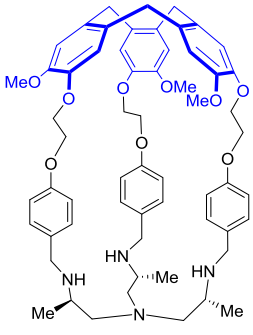

M-(*R*,*R*,*R*)-**111b**
+
P-(*R*,*R*,*R*)-**111b**

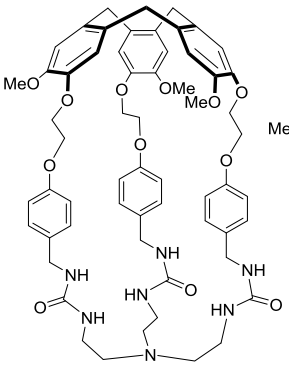

(±)-**136**

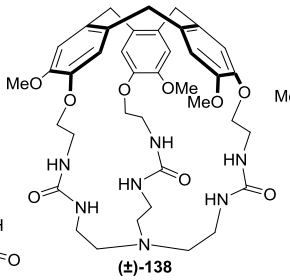

(±)-**138**

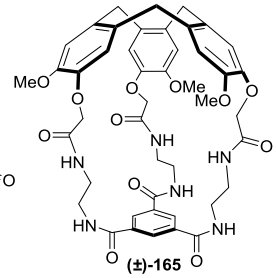

(±)-**165**

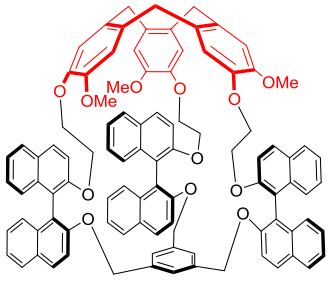

P-(*S*,*S*,*S*)-**171**
+
M-(*S*,*S*,*S*)-**171**

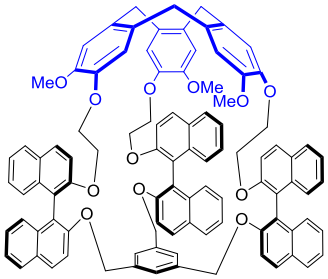

M-(*R*,*R*,*R*)-**171**
+
P-(*R*,*R*,*R*)-**171**

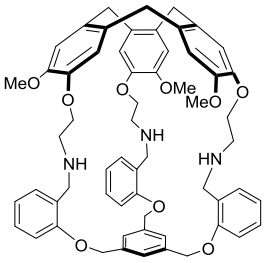

(±)-**174**

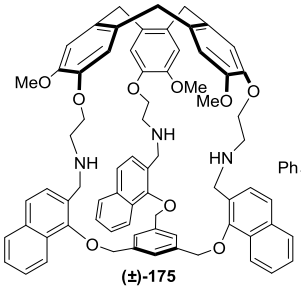

(±)-**175**

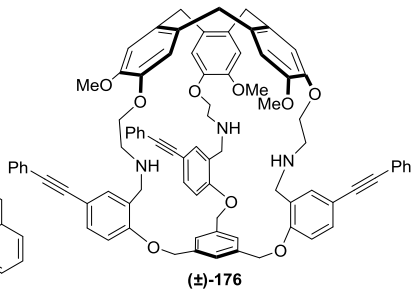

(±)-**176**

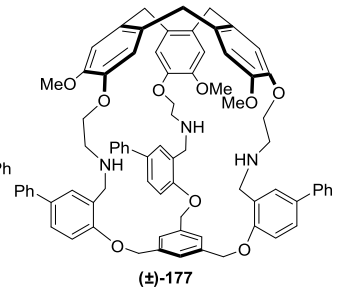

(±)-**177**

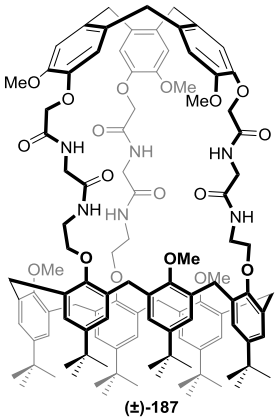

(±)-**187**

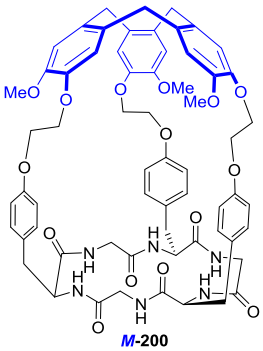

M-**200**
+
P-**200**

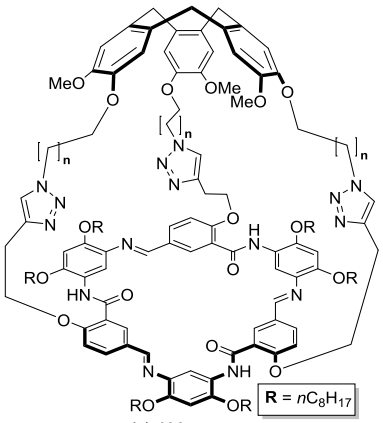

(±)-**196a** **n** = 1
(±)-**196b** **n** = 3

7.5. Summary

Cyclotriveratrylene (CTV) scaffold, a bowl-shaped macrocyclic trimer of a veratrole subunit, is widely used in supramolecular chemistry. The CTV moiety is efficiently used for the formation of numerous host molecules due to its stable crown conformation and easy functionalization at the lower rim. An important feature is its inherent chirality, which leads to the chiral receptors with *M* or *P* configuration. An interesting group of receptors based on the CTV moiety is represented by inherently chiral hemicryptophanes. These molecular cages consist of the CTV unit triply connected with another C_3-symmetrical scaffold and differ from each other by the type and the length of the linkers as well as by the nature of lower moiety. Three different synthetic strategies could be used to prepare hemicryptophanes:

1) the cage-closing reaction to construct the CTV scaffold from veratryl precursors,
2) the cage-closing reaction at the lower part of the appropriate CTV-based precursor,
3) the [1+1] coupling between the CTV unit and other C_3-symmetrical moiety.

A number of different platforms such as triethanolamine, nitrilotriacetamide, tris(2-amino-ethyl)amine, tris(2-pyridylmethyl)amine, 1,3,5-tripodal benzene, and various macrocyclic compounds were successfully attached to the CTV unit to form hemicryptophanes.
Nevertheless, the fast and easy preparation of such molecular cages in enantiopure form is very challenging due to their high complexity. Therefore, most of them are synthesized as racemic mixtures. Difficult resolution and low yield are the major limitations in the synthesis of enantiopure hemicryptophanes.

A number of various hemicryptophanes were successfully applied so far, mostly in the selective recognition of various guest molecules. These hosts are capable of binding carbohydrates, alkylammonium cations, anions, zwitterions, ion-pairs, and other organic molecules.

There are only few reports, in which the CTV scaffold is triply connected with chiral molecule obtaining possible to separate diastereoisomeric cages. Moreover, the C_1-symmetrical hemicryptophanes are unexplored to this day. These molecular cages may contribute to the more selective recognition of the guest molecules, in particular chiral ones. Therefore, more research needs to be conducted in this area.

Similarly, the combination of the CTV unit with carbohydrates is rare. These papers include the synthesis of trivalent or hexavalent glycoconjugates with peripheral carbohydrate units. The connection of the CTV scaffold with sucrose is not described in the literarure yet. I believe that introducing sugar subunits, which have many stereogenic centers, into the cage

structure would result in the receptors with more complex and specific cavity and thus would improve selectivity in the recognition process.

On the basis of the literature studies and in order to fill out the deficiencies in the C_1-symmetrical hemicryptophanes, I decided to synthesize novel chiral CTV-sucrose-based molecular cages and to investigate their binding properties. The results of my studies are presented in the next chapter.

8. Results and discussion

This chapter includes the commentary on three monothematic collections of research articles of my autorship concerning the CTV-based molecular cages with sucrose scaffold. The first section involves the initial studies towards the sucrose-based hemicryptophanes including the synthesis of two novel, water-soluble molecular cages. In the next part, the synthesis of four diastereoisomeric C_1-symmetrical hemicryptophanes containing *p*-phenylene linkers and their complexing properties towards 1-methylpyridinium and 1,3-dimethyl-imidazolium cations are described. Finally, another four fluorescent diastereoisomeric sucrose-based hemicryptophanes and their selective recognition of acetylcholine and choline are presented. Other attempts to obtain such cages with different linkers, even if unsuccessfull, are also described in this chapter.

8.1. Towards water-soluble chiral molecular cages with cyclotriveratrylene and sucrose units

The main goal of my studies was the synthesis of novel C_1-symmetrical hemicryptophanes *via* a triple connection of cyclotriveratrylene (CTV) and sucrose units. According to the previously described literature review, there are two possible pathways for the synthesis of such molecular cages (Scheme 8.1).

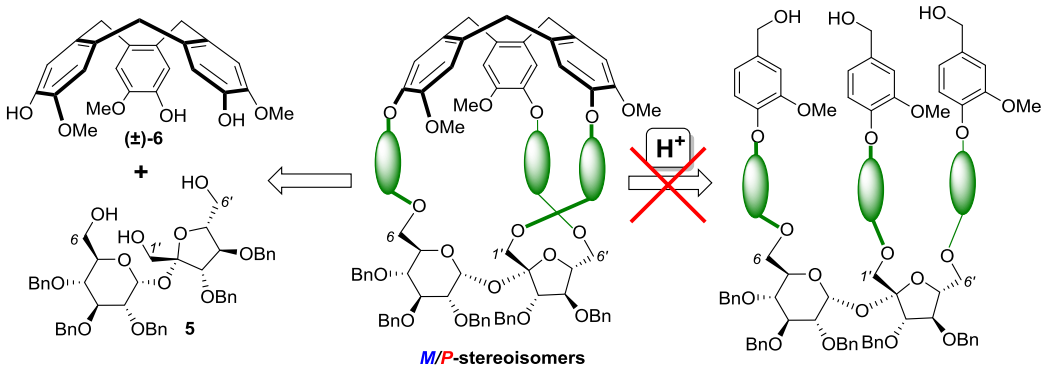

Scheme 8.1. Two synthetic routes towards sucrose-based hemicryptophanes.

The first route involves the [1+1] coupling between the appropriately functionalized CTV and sucrose derivatives. The second one consists of the condensation of the corresponding hemicryptophane precursors to form the CTV moiety in the last step of the synthetic pathway. This reaction is catalyzed by strong acids such as $HClO_4$, HCOOH,

H_3PO_4, *etc*. Sucrose and its derivatives have the α-1,2-glycosidic linkage, which is extremely sensitive to acidic conditions. Even small amounts of acid can lead to the cleavage of this bond; therefore the acidic conditions should be avoided when handling this carbohydrate. In the view of these assumptions, the second strategy cannot be employed for the preparation of sucrose-based cages. Thus, the only way to obtain the molecular cages that I propose, is the [1+1] coupling strategy.

For this purpose, I firstly synthesized two key starting materials: CTV-based tribromide **(±)-29** and 2,3,3',4,4'-penta-*O*-benzylsucrose (**5**). Both synthetic pathways are known in the literature.[64,158] I prepared tribromide **(±)-29** from the commercially available vanillyl alcohol according to Scheme 8.2. Although the yields of the alkylation and cyclization steps are moderate, the purification of the products is easy and both compounds **18** and **(±)-29** could be obtained in a gram-scale.

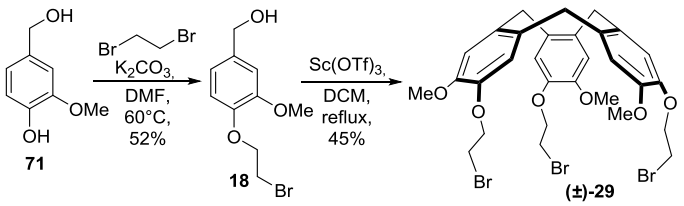

Scheme 8.2. Synthesis of CTV-based tribromide **(±)-29**.

The synthesis of 2,3,3',4,4'-penta-*O*-benzylsucrose is presented on Scheme 8.3. It is noteworthy that this compound was prepared for the first time in Prof. Jarosz group.[158] This three-steps synthesis includes the selective protection-deprotection sequence of the hydroxyl groups from sucrose unit. It is also possible to prepare triol **5** using bulky trityl protective groups instead of silyl ethers, however their cleavage requires the acidic media, which causes also the cleavage of the glycosidic bond, thus lowering the yield and making further purification of the desired triol **5** very difficult.

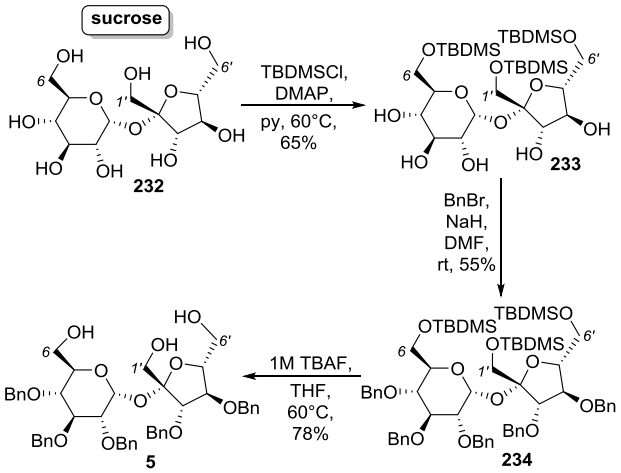

Scheme 8.3. Synthesis of 2,3,3',4,4'-penta-*O*-benzylsucrose.

In the next step, I decided to react CTV-based tribromide **(±)-29** with 2,3,3',4,4'-penta-*O*-benzylsucrose under the basic conditions (Scheme 8.4). I have chosen this synthetic strategy because the preparation and functionalization of the CTV derivatives are in most cases easier comparing to triol **5**. Indeed, the functionalization of the hydroxyl group (*e.g.* nucleophilic substitution) at the C-1' position of sucrose is usually challenging and in some cases even impossible due to its similarity to a neopentyl system structure. Therefore, the triple functionalization of triol **5** together with its further purification by column chromatography often provided low to moderate yield of the target product. Although the cyclization reactions of the appropriate 3,4-disubstituted benzyl alcohols into the CTV derivatives are also not very efficient, the purification of the main product, which can be isolated by crystallization or precipitation, is much easier.

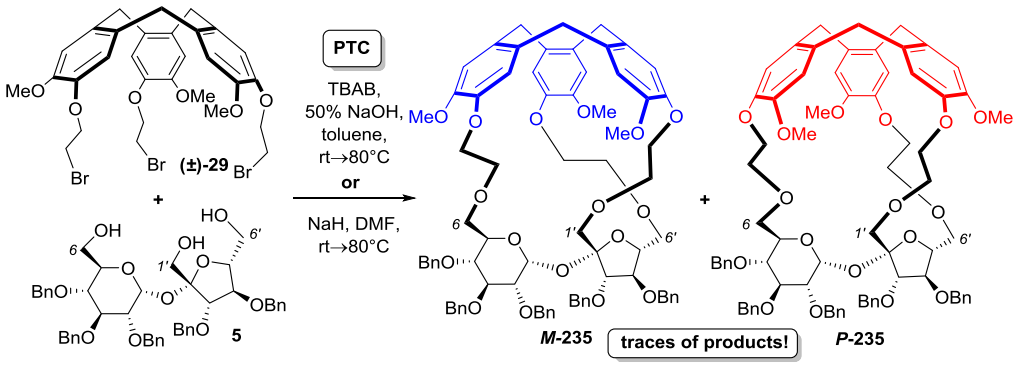

Scheme 8.4. First attempt towards sucrose-based hemicryptophanes.

This triple alkylation reaction between tribromide **(±)-29** and triol **5** under the PTC conditions or in the presence of NaH in DMF afforded only traces of target hemicryptophanes ***M*-235**

and ***P*-235** detected only by ESI-MS, which were impossible to isolate. Nevertheless, encouraged by these results, I decided to change slightly the synthetic strategy by switching the functional groups of both substrates. Namely, I prepared cyclotriguaiacylene **[(±)-6]** that has more acidic phenolic hydroxyl groups, and sucrose triiodide derivative **239**. The synthetic route towards (±)-CTG is similar to already described literature procedure[64] (Scheme 8.5). This three steps method involves the protection of the phenolic hydroxyl function by the allyl groups, followed by an acid-catalyzed trimerization of the corresponding benzylic alcohol, and finally the palladium-mediated cleavage of the allyl protections.

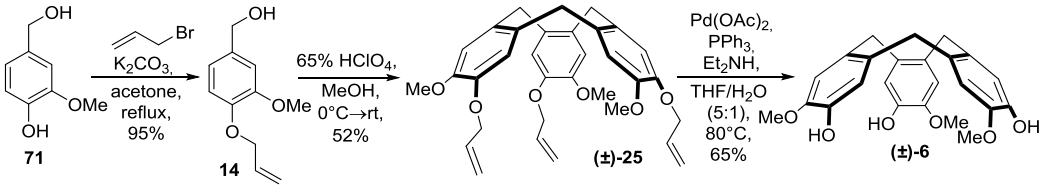

Scheme 8.5. Synthesis of cyclotriguaiacylene.

I prepared triiodosucrose derivative **239**, in a three steps sequence starting from triol **5** (Scheme 8.6). The alkylation of three primary hydroxyl groups (at the C1', C6, and C6' positions) of triol **5** with *tert*-butyl bromoacetate under the PTC conditions, afforded triester sucrose derivative **237** in 56% yield. Subsequent reduction of the ester functions in compound **237** with $LiAlH_4$ gave triol **238** in very good yield (90%). Next, the Garegg-Samuelsson iodination reaction of **238** led to target triiodide sucrose derivative **239** in 85%.

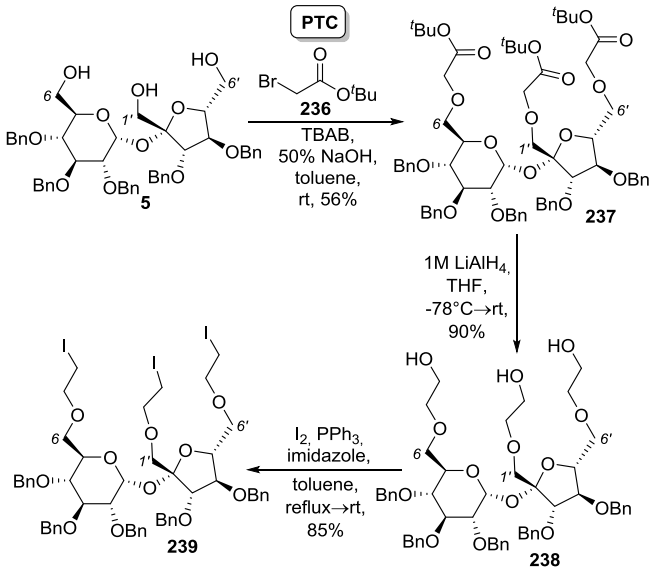

Scheme 8.6. Synthesis of triiodide sucrose derivative **239**.

In order to obtain the desired molecular cages: ***M*-235** and ***P*-235**, I conducted the reaction of intermediates **(±)-6** and **239** (1:1 ratio) in DMF under high-dilution conditions (*c* = 0.002 M) at room temperature in the presence of Cs_2CO_3 as a base. This initial [1+1] coupling reaction provided two diastereoisomeric hemicryptophanes: ***M*-235** and ***P*-235** in a 1:1 ratio in 21% total yield. Fortunately, both cages have different polarities, thus they were easily separated by a classical silica gel column chromatography.

The next goal of my work was optimization of the conditions of coupling reaction; the results are listed in Table 8.1. While the cyclization reaction carried out in DMF at room temperature afforded the desired cages in 21% yield, the increase of the temperature to 80°C resulted in lowering the efficiency of the cyclization process (Table 8.1, Entries 1 and 2). After changing the solvent to acetone, I noticed that this reaction did not proceed at room temperature (Table 8.1, Entry 3), but at reflux gave similar yield to that in DMF at rt (23%; Table 8.1, Entry 4).

Table 8.1. Optimization conditions of [1+1] coupling reaction of cages ***M*-235** and ***P*-235**.

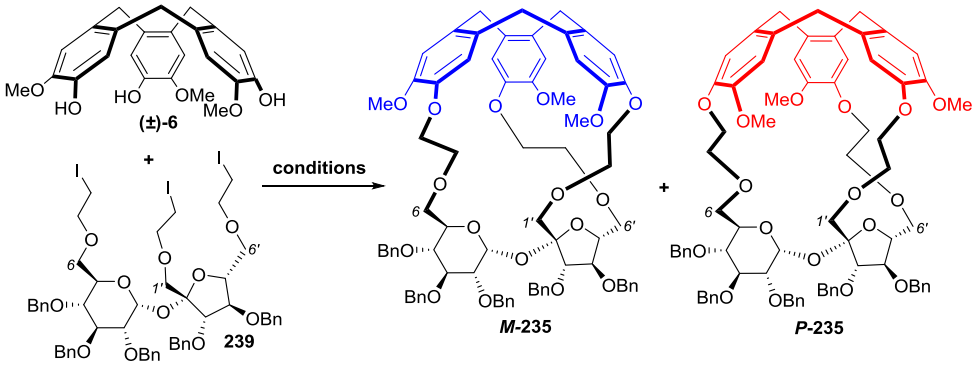

Entry	Base	Solvent	Temp. [°C]	Time [h]	Yield[c] [%]
1.	Cs_2CO_3	DMF[a]	rt	72	21
2.	Cs_2CO_3	DMF[a]	80	48	14
3.	Cs_2CO_3	acetone[a]	rt	72	–
4.	Cs_2CO_3	acetone[a]	reflux	72	23
5.	Cs_2CO_3	MeCN[a]	rt	72	–
6.	Cs_2CO_3	MeCN[a]	reflux	72	27
7.	Cs_2CO_3	EtCN[a]	reflux	96	–
8.	K_2CO_3	MeCN[a]	reflux	72	22
9.	Cs_2CO_3	MeCN[b]	reflux	72	33

[a]*c* = 0.002 M; [b]*c* = 0.001M; [c]Total yield for two diastereoisomers *M* and *P* after column chromatography (ratio 1:1); "–" - no reaction.

Next, I decided to change the solvent to MeCN. While coupling reaction in MeCN at room temperature did not work, increasing the temperature to reflux resulted in the formation of both *M*- and *P*-stereoisomers in 27% yield (Table 8.1, Entries 5 and 6). The reaction did not proceed when MeCN was changed to higher boiling EtCN (Table 8.1, Entry 7). Replacing the

base from Cs_2CO_3 to K_2CO_3 resulted in reduced total yield (Table 8.1, Entry 8). The best yield of the target products was obtained under more diluted conditions (c = 0.001 M; 33%; Table 8.1, Entry 9).

I have also tried to add the Me_4N^+ cation (as iodide salt) to the reaction mixture as a template to improve the yield of both cages; however it did not affect the final yield of products.

In order to obtain the water-soluble molecular cages, I decided to remove the benzyl protective groups from the secondary hydroxyl functions of both isolated ***M*-235** and ***P*-235**. The palladium-catalyzed hydrogenation of each diastereoisomer in THF afforded the corresponding water-soluble hemicryptophanes ***M*-240** and ***P*-240** in quantitative yield (Scheme 8.7). Next, I measured the solubility of both unprotected cages in water, which was assigned as *ca.* 6mg / 1 mL at room temperature.

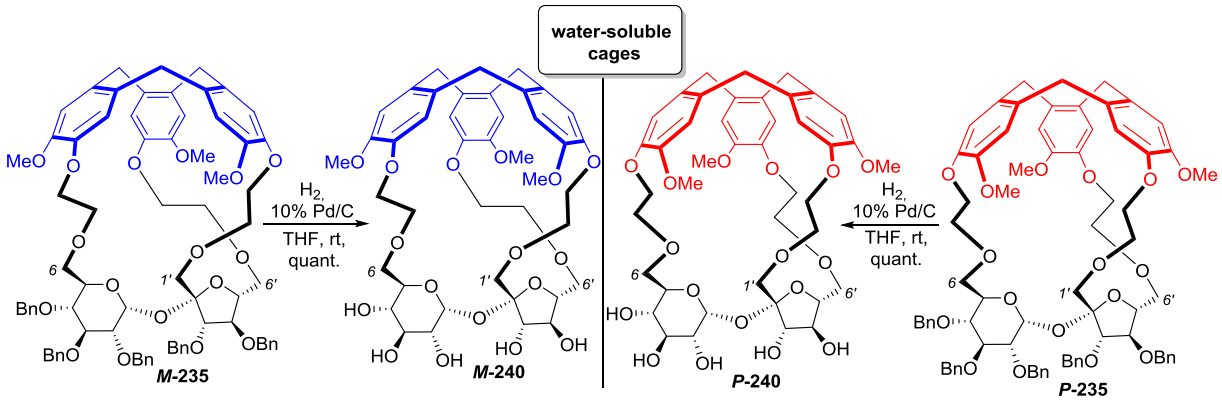

Scheme 8.7. Cleavage of the benzyl protections towards water-soluble cages ***M*-240** and ***P*-240**.

The structures of both cages ***M*-235** and ***P*-235**, as well as their water-soluble counterparts ***M*-240** and ***P*-240**, were successfully determined by the set of the NMR spectra (^{1}H, ^{13}C, COSY, TOCSY, ROESY, HSQC, HSQC-TOCSY, and HMBC) and ESI-HRMS measurements. All these NMR experiments allowed for the precise assignment of the protons of the CTV and sucrose units and their exact spatial arrangement. The most important observation, visible in the ROESY spectra, was the strong interaction of each anomeric proton (H-1) of sucrose unit from ***M*-235** or ***P*-235** with the protons of different methoxy group attached to the CTV moiety (Figure 8.1).

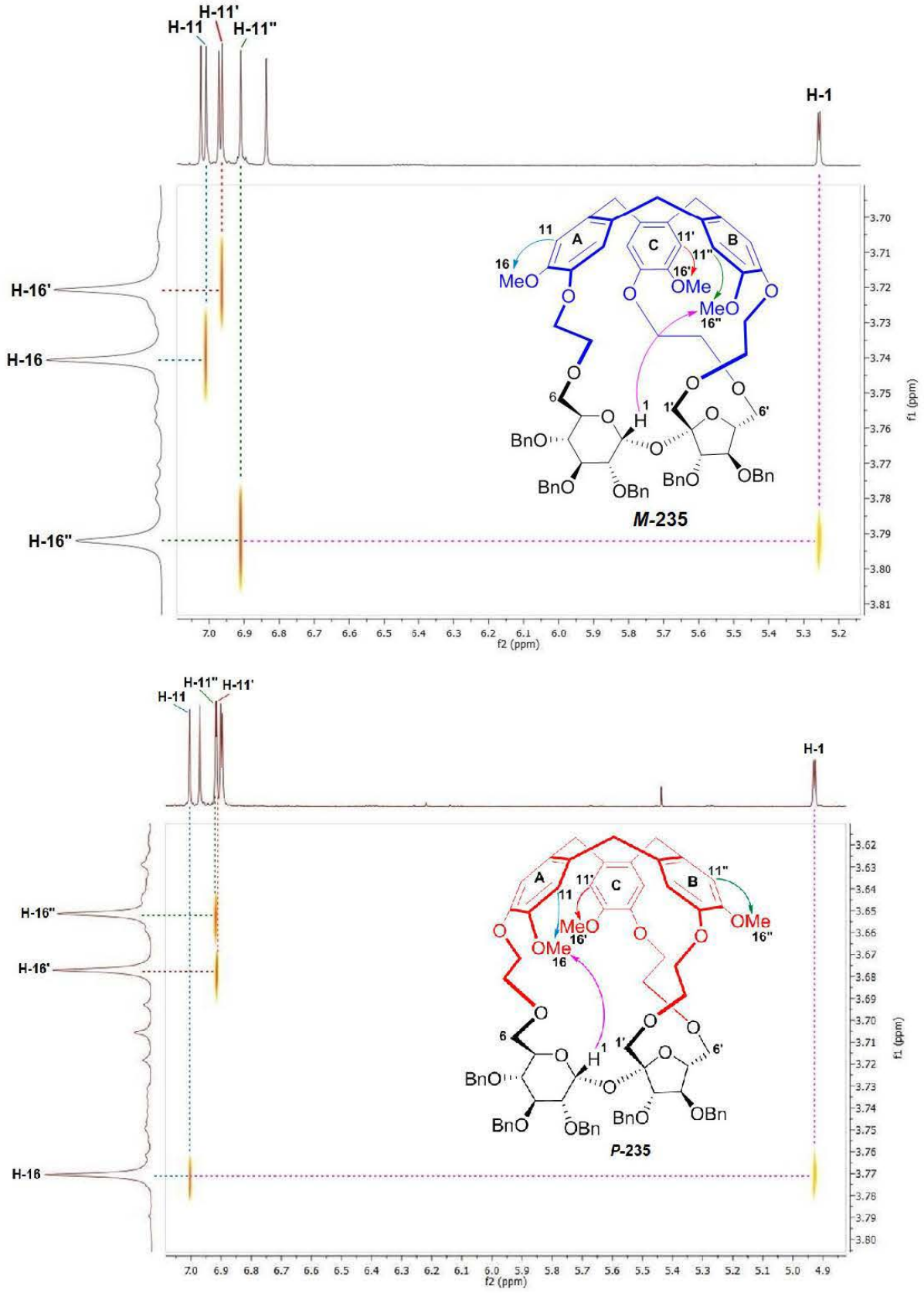

Figure 8.1. ROESY spectra of cages ***M*-235** (top) and ***P*-235** (bottom) illustrated steric interactions between anomeric proton (H-1) and protons from methoxy groups.

In order to study the *M* and *P* configuration of both compounds, the ECD spectroscopy supported by DFT calculations were performed. The ECD spectra of both cages ***M*-235** and ***P*-235** showed the symmetric bisignate pattern bands with the sequence analogous for *M* and *P* descriptors. The *M*/*P* assignment of both diastereoisomers by ECD spectroscopy was compatible with the NMR findings. The DFT-optimized structures of these two molecular cages showed different position of glucose platform most probably caused by the intermolecular interactions with the CTV scaffold. While the anomeric hydrogen atom of ***M*-235** is located outside the cavity, the same hydrogen atom of ***P*-235** is situated inside the cavity (Figure 8.2).

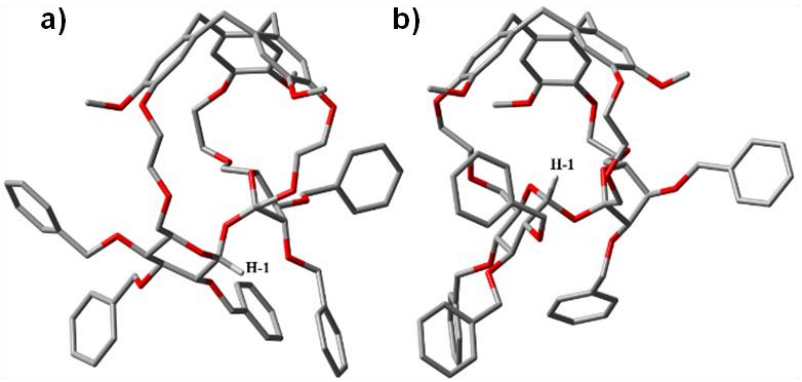

Figure 8.2. DFT-optimized structures of a) ***M*-235** and b) ***P*-235**. Hydrogen atoms, except the anomeric one, are omitted for clarity.

In the next step of the study, I decided to investigate the binding properties of cages ***M*-235** and ***P*-235** towards various small organic cations. The ^{1}H NMR titration experiments of each host: ***M*-235** or ***P*-235** with (*R*)-(+)- and (*S*)-(–)-1-phenylethylamine hydrochloride (in $CDCl_3$), L- and D-(phenylalanine, alanine, and serine) methyl ester hydrochlorides, as well as tetramethylammonium iodide and neutral guests such as methylamine and ethanolamine (in $CDCl_3/CD_3OD$ = 90:10) did not show any changes in the spectra. These results demonstrated that both cages ***M*-235** and ***P*-235** are not able to complex previously mentined guest molecules, probably due to their too small cavity. This would also explain the failed attempts to improve the yield of the cages, when I added the Me_4N^+ cation as a template to the reaction mixture. Therefore, in the next stage of my doctoral research, I decided to design the sucrose-based hemicryptophanes with larger cavity, which would allow binding small organic guests non-covalently.

The synthesis and characterization of these novel water-soluble CTV-sucrose-based molecular cages have been described in the paper: "Synthesis of Cyclotriveratrylene-Sucrose-Based Capsules" Ł. Szyszka, P. Cmoch, A. Butkiewicz, M. A. Potopnyk, S. Jarosz, *Org. Lett.* **2019**, *21*, 6523–6528.

8.2. Four chiral molecular cages containing *p*-phenylene linkers

My first idea towards the C_1-symmetrical sucrose-based hemicryptophanes with larger cavity was to introduce an aromatic linkers to their structure. I assumed that the phenyl linkers should ensure not only larger and more rigid cavity but also additional π-type interactions with guests molecules. Accordingly, there are at least two possible synthetic pathways to obtain phenyl-linked sucrose-based hemicryptophanes involving functionalization of the CTV or sucrose unit (Scheme 8.8).

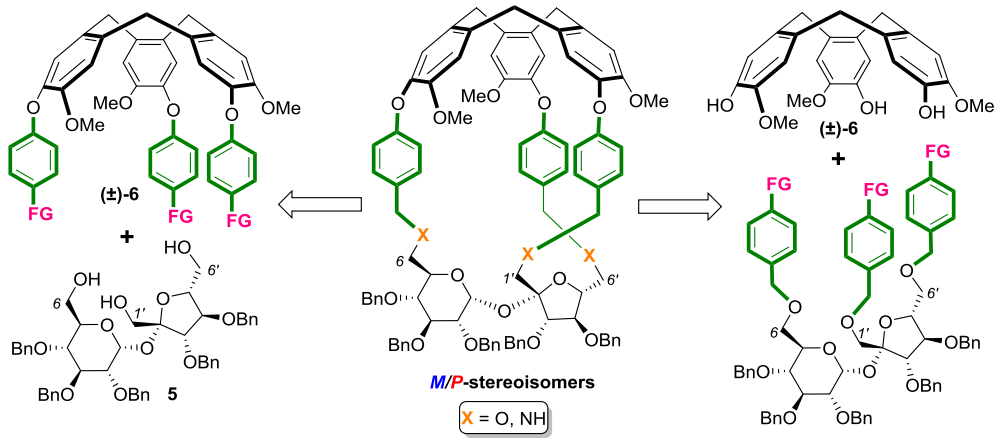

Scheme 8.8. Two possible synthetic pathways towards phenyl-linked molecular cages.

I decided to prepare the CTV derivatives due to their easier functionalization and the possibility to isolate them by precipitation or crystallization when compared to sucrose derivatives. Previous experiments showed that triol **5** is not very active in the triple alkylation cage-closing step. Thus, I decided to employ different type of reaction for [1+1] coupling of both CTV and sucrose intermediates. Reductive amination reaction seemed to be appropriate to obtain the target molecular cages, since many C_3-symmetrical hemicryptophanes were prepared by this method (see Chapter 7.4.2.3). However, it requires the additional transformation of triol into trialdehyde.

Firstly, I synthesized two different CTV derivatives with the primary [**(±)-243**] and aromatic [**(±)-246**] amino functions according to modified literature procedures.[159] The modifications consisted in carrying out both nucleophilic aromatic substitution under reduced pressure conditions and changing reducing agents (Scheme 8.9). In the case of the reduction of nitrile **(±)-242**, I obtained the target amine **(±)-243** in better yield than described in the literature[159] (85% vs 50%) by using $LiAlH_4$ instead of B_2H_6. In comparison to reduction of nitro compound **(±)-245**, replacing the palladium and hydrazine monohydride system[159] with $SnCl_2 \cdot 2H_2O$ reducing agent avoided the use of this expensive noble metal.

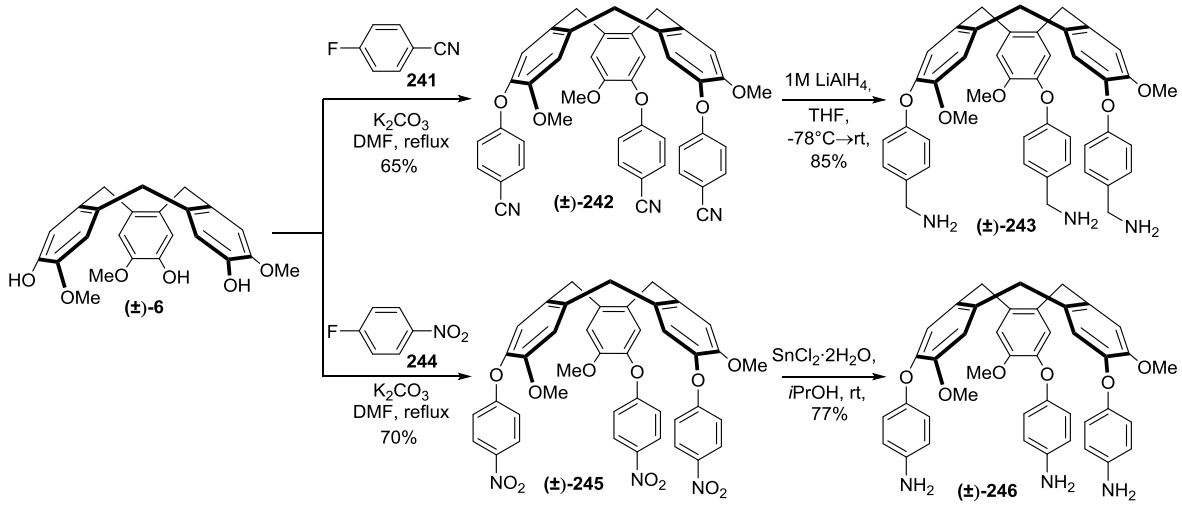

Scheme 8.9. Synthetic pathways towards primary and aromatic amino CTV derivatives **(±)-243** and **(±)-246**.

Meanwhile, I prepared trialdehyde **247** from triol **5** by the Swern oxidation method (Scheme 8.10), which was further immediately used without purification in a reductive amination reaction.

Scheme 8.10. Synthesis of trialdehyde **247**.

Two steps reaction of primary [**(±)-243**] or aromatic [**(±)-246**] CTV-based amine with crude trialdehyde **247** catalyzed with acetic acid, followed by reduction with $NaBH_4$ did not, however, afford the target compounds **(±)-248** or **(±)-249** (Scheme 8.11). Even the use of molecular sieves in order to shift the reaction equilibrium towards formation of the products has not improved the results. Each time I obtained a mixture of many differently combined

CTV- and sucrose-based compounds impossible to separate. Interestingly, the MS analysis of the crude reaction mixture did not show any *m/z* value, which corresponded to the expected main products **(±)-248** or **(±)-249**.

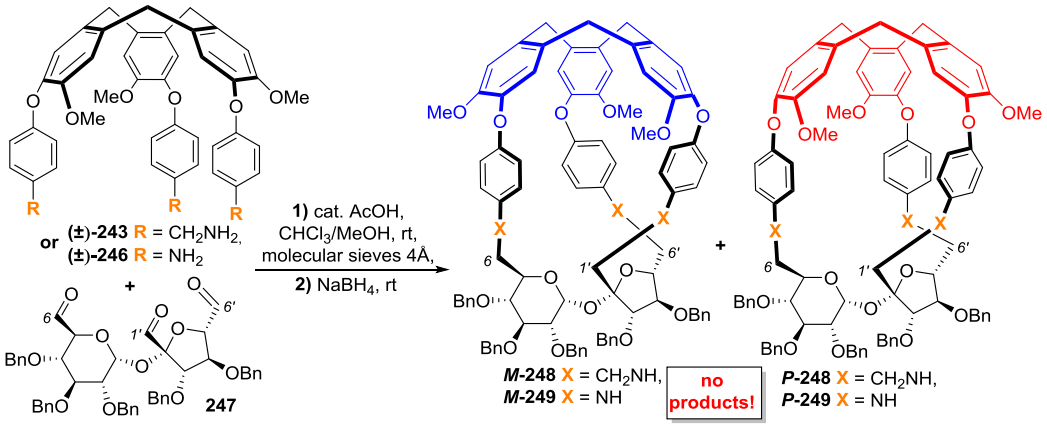

Scheme 8.11. Synthesis of sucrose-based hemicryptophanes **(±)-248** and **(±)-249** *via* a reductive amination reaction.

In view of the above, I decided to return to the triple alkylation cyclization strategy, which proved to be effective in the synthesis of sucrose-based hemicryptophanes containing ethylene linkers (***M*-235** and ***P*-235**). In order to reduce the number of the reaction steps leading to trihalogeno sucrose derivatives, I carried out a one step reaction between triol **5** and 1,4-bis(bromomethyl)benzene under the basic conditions. I used a considerable excess of such brominating reagent (9 equiv.) to prevent the formation of various polymeric by-products. The optimal reaction conditions were sodium hydride as a base in refluxing THF, which gave tribromide **250** in 45% yield (Scheme 8.12). When this reaction was carried out in DMF or under PTC conditions, lower yields of desired product were obtained (21% and 12%, respectively).

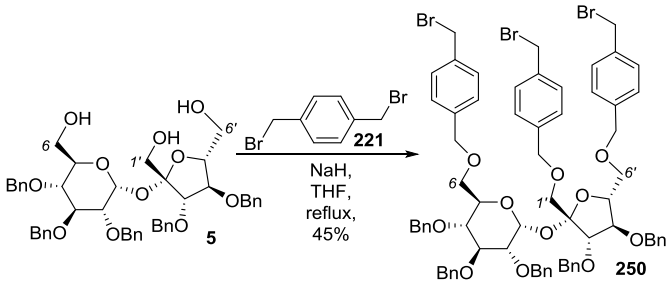

Scheme 8.12. Synthesis of tribromide sucrose derivative **250**.

The key [1+1] coupling reaction between (±)-CTG and tribromide **250** was performed in the presence of Cs_2CO_3 in refluxing MeCN under high-dilution conditions (*c* = 0.001M). Surprisingly, four diastereoisomeric hemicryptophanes containing *p*-phenylene linkers were

formed: ***P*-251a**, ***M*-251a**, ***P*-251b**, and ***M*-251b** in 18%, 17%, 9%, and 8%, respectively (52% total yield, 2:2:1:1 ratio; Scheme 8.13). I successfully isolated all these four diastereoisomers by the preparative HPLC using the hexanes/EtOAc mixture (70:30 *v/v*).

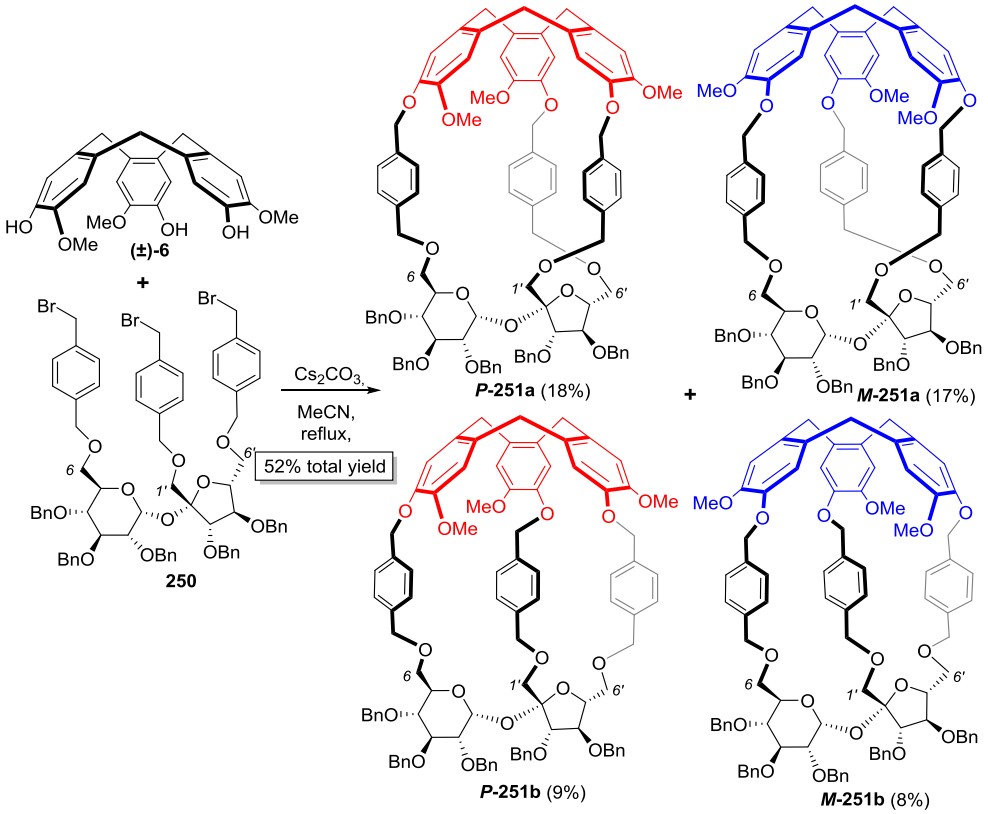

Scheme 8.13. Synthesis of four diastereoisomeric sucrose-based hemicryptophanes.

I also carried out this cyclization reaction under different conditions; however lower total yields of the desired hemicryptophanes was noted (Table 8.2). For instance, reaction performed in MeCN at room temperature gave cages **251** in 22% yield, whereas that in DMF provided these hemicryptophanes in 24% yield at room temperature, or 34% yield at 80°C. Significantly, the ratio of all four diastereoisomers was approximately the same as mentioned above.

Table 8.2. Optimization conditions of the [1+1] coupling reaction leading to cages ***P*-251a**, ***M*-251a**, ***P*-251b**, and ***M*-251b**.

Entry	Solvent[a]	Temp. [°C]	Time [h]	Yield[b] [%]
1.	DMF	rt	48	24
2.	DMF	80	48	34
3.	MeCN	rt	48	22
4.	MeCN	reflux	48	52

[a]*c* = 0.001M; [b]Total yield of four diastereoisomers after column chromatography (ratio 2:2:1:1)

The formation of four stereoisomers (instead of the expected two) results most likely from longer *p*-phenylene linkers, which are more able to generate various connections between both CTV and sucrose scaffolds, when compared to short ethylene linkers from the previously described cages ***M*-235** and ***P*-235**.

The structures of all four diastereoisomeric cages: ***P*-251a**, ***M*-251a**, ***P*-251b**, and ***M*-251b** were characterized by the set of the NMR spectra (^{1}H, ^{13}C, COSY, TOCSY, ROESY, HSQC, HSQC-TOCSY, and HMBC), ECD spectroscopy as well as the ESI-HRMS measurements. Each of these hemicryptophanes had the specific set of the ^{1}H/^{13}C chemical shifts, which allowed for the assignment of all NMR signals. Their *M/P* configurations were additionally confirmed by the ECD spectroscopy supported by TDDFT calculations, which demonstrated the typical bisignate bands, originating from the *M* or *P* CTV unit. In addition, the twisted structure of cage ***P*-251b** was confirmed by the X-ray crystallography (Figure 8.3).

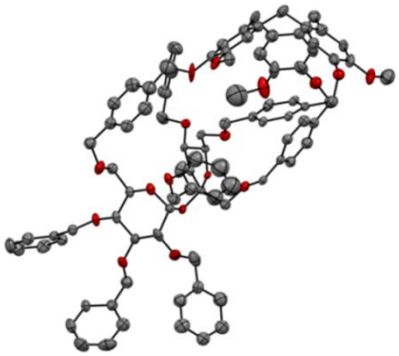

Figure 8.3. X-ray single crystal structure of ***P*-251b**. Hydrogen atoms are omitted for clarity. CCDC: 2017787.

Moreover, the VT-ECD measurements of such molecular cages were performed in the mixture of Et_2O/iC_5H_{12}/EtOH (5:5:2 v/v) in the range from +25°C to -180°C (Figure 8.4).

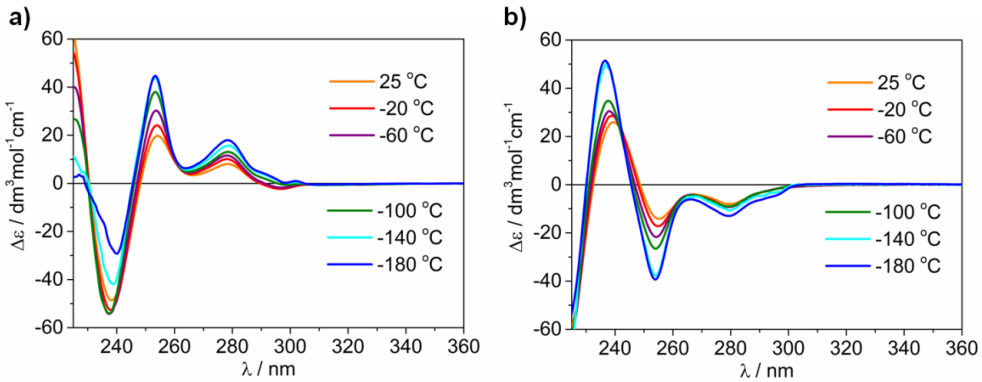

Figure 8.4. VT-ECD spectra of a) ***P*-251a** and b) ***M*-251a**.

These experiments showed the significant increase of the ECD band intensities of cages ***P*-251a** and ***M*-251a** with decreasing temperature, which is caused by the thermodynamic stabilization of the position of rotating *p*-phenylene linkers. In contrast, these ECD bands changes were less significant for both hemicryptophanes ***P*-251b** and ***M*-251b**, probably due to their twisted structure.

In the next part of my research, I investigated the binding ability of cages ***P*-251a** and ***M*-251a** towards various ammonium cations. Unfortunately, the ^{1}H NMR titration experiments of each host: ***P*-251a** or ***M*-251a** with chiral (*R*)-(+)- and (*S*)-(–)-1-phenylethylammonium chloride, (*R*)-(+)- and (*S*)-(–)-1-methylbenzyltrimethylammonium iodide (in $CDCl_3$), L- and D-alanine methyl ester hydrochlorides (in $CDCl_3/CD_3OD$ = 90:10) as well as achiral choline and acetylcholine iodides (in CD_3CN) did not show any changes in the spectra, thus suggesting that these diastereoisomers did not form the host-guest complexes with such ammonium cations. However, the recognition study of each cage ***P*-251a** or ***M*-251a** with 1,3-dimethylimidazolium (**G1**) and 1-methylpyridinium (**G2**) hexafluorophosphates in the mixture of $CD_3CN/CDCl_3$ (2:1) displayed the significant shifts of the proton signals, in particular those from the CTV unit, indicating a non-covalent interactions with both guests (Figure 8.5).

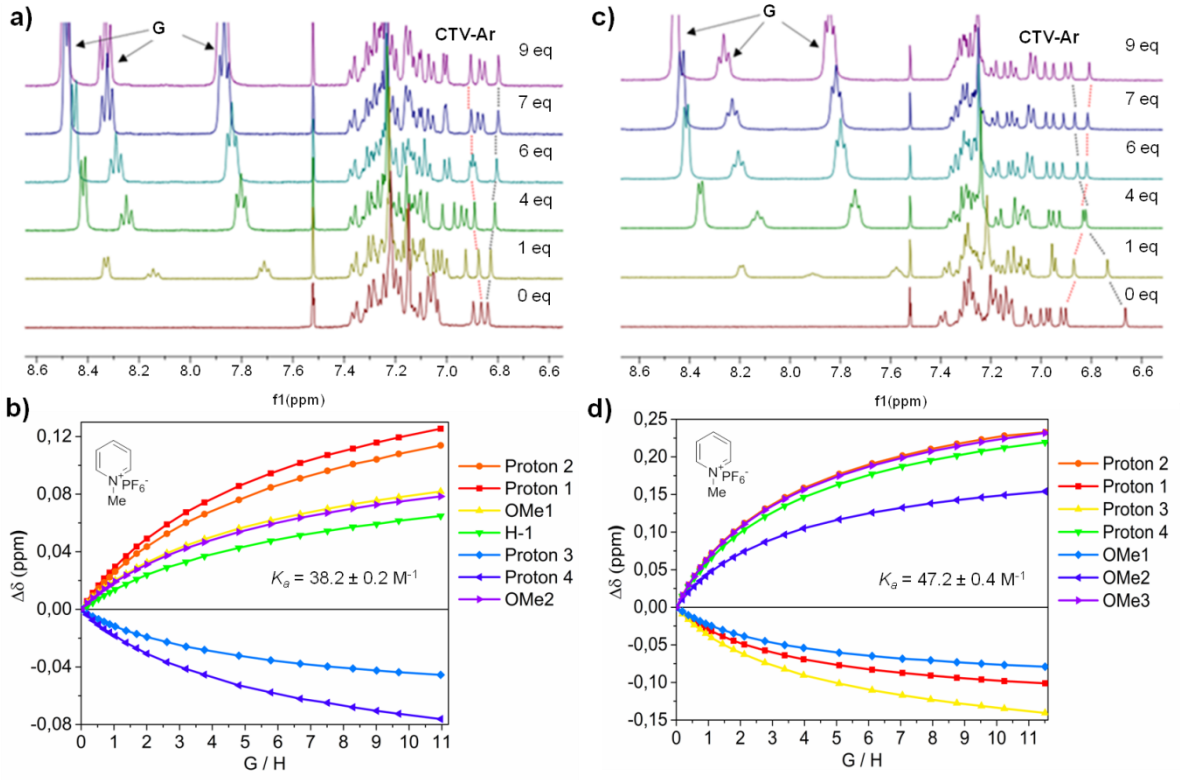

Figure 8.5. Partial ^{1}H NMR spectra of titration experiments of host a) ***M*-251a**, and b) ***P*-251a** with progressively added guest **G2**. (top) ^{1}H NMR shifts Δδ of host a) ***M*-251a**, and b) ***P*-251a** with increasing equiv. of guest **G2**. (bottom).

Additionally, the ESI-MS measurements proved the formation of the 1:1 host-guest complex of each host: ***P*-251a** and ***M*-251a** with 1-methylpyridinium salt in MeCN (*m/z* = 1601.72; for $[H+G]^+$).

The measured association constants of the complexes of receptors ***P*-251a** and ***M*-251a** with both guests are listed in Table 8.3. These values clearly showed that 1-methylpyridinium cation is more suitable for both hosts cavities than 1,3-dimethylimidazolium cation. This might be explained by their different structure. Imidazolium salt has an additional methyl group, which might provide the steric hindrance, and thus prevent the effective encapsulation. The selectivity of both hosts ***P*-251a** and ***M*-251a** towards imidazolium and pyridinium guests was, however, almost negligible.

Table 8.3. Comparison of association constants of ***P*-251a**, ***M*-251a**, ***P*-251b**, and ***M*-251b** with imidazolium and pyridinium guests.

Guest	Host	K_a (M^{-1})[a]	$K_a(P)$/ $K_a(M)$
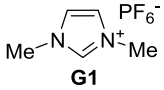 **G1**	***P*-251a**	13.9 ± 0.1	0.9:1
	***M*-251a**	14.6 ± 0.1	
 **G2**	***P*-251a**	47.2 ± 0.4	1.2:1
	***M*-251a**	38.2 ± 0.2	
	***P*-251b**	7.1 ± 0.1	1.4:1
	***M*-251b**	9.8 ± 0.6	

[a]The *K*a values were determined by fitting ^{1}H NMR titration curves using the Bindfit program.

In order to compare the binding capacity of all four cages, I performed also the recognition studies of hosts ***P*-251b** and ***M*-251b** with 1-methylpyridinium hexafluorophosphate, as this guest demonstrated the best results in the previous experiments. In both cases, the associate constants were almost 4 times lower than for their regioisomers (Table 8.3). These results might be explained by the unique structures of the hosts's cavities arising from the different connections between the CTV and sucrose moieties. Thus, hemicryptophanes ***P*-251a** and ***M*-251a** seem to have better defined cavities compared to cages ***P*-251b** and ***M*-251b**.

The synthesis and recognition properties of four diastereoisomeric sucrose-based hemicryptophanes containing *p*-phenylene linkers have been described in the paper: "Chiral Molecular Cages Based on Cyclotriveratrylene and Sucrose Units Connected with *p*-Phenylene Linkers" Ł. Szyszka, P. Cmoch, M. Górecki, M. Ceborska, M. A. Potopnyk, S. Jarosz, *Eur. J. Org. Chem.* **2021**, 897–906. These results were rated as "Very Important" by Editorial Office and the paper was highlighted with a front cover.

8.3. Fluorescent chiral molecular cages containing naphthalene linkers

In the next step of my doctoral research, I decided to further enlarge the cavity of hemicryptophanes by following previous successful triple alkylation synthetic pathway. For this purpose, I have chosen the naphthalene units as linkers due to their rigidity, possible π-type non-covalent interactions with guest molecules, and fluorescence properties. Firstly, I prepared 2,6-bis(bromomethyl)naphtahlene from the commercially available diester **252** according to the literature procedure (Scheme 8.14).[160]

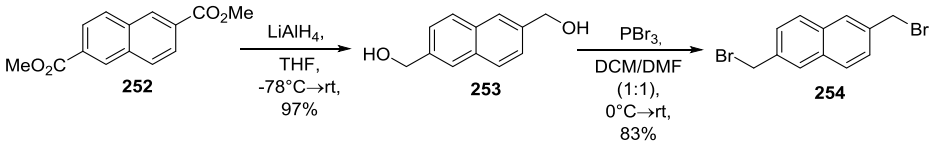

Scheme 8.14. Synthesis of 2,6-bis(bromomethyl)naphtahlene.

Then, such obtained dibromide **254** was reacted with triol **5** under the basic conditions (Scheme 8.15). Similarly to the previous alkylation reaction, I used an excess of brominating reagent **254** (6 equiv.) to prevent the formation of various polymeric by-products. The reaction was carried out at room temperature using sodium hydride as a base and THF as a solvent, afforded tribromide **255** in 24% yield. However, conducting this reaction at reflux caused the decomposition of the desired product **255**.

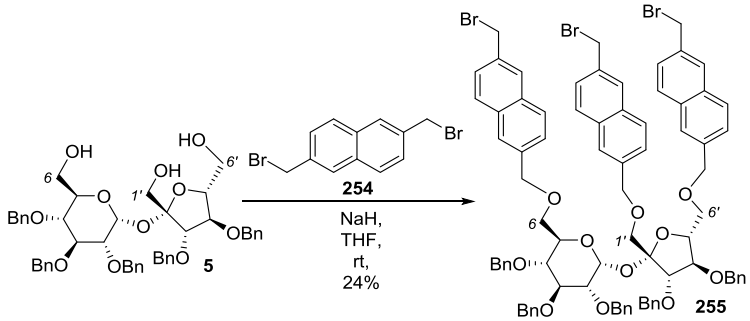

Scheme 8.15. Synthesis of sucrose-based tribromide **255**.

The Cs_2CO_3 catalyzed [1+1] coupling of (±)-CTG and sucrose-based tribromide **255** in refluxing MeCN under high-dilution conditions (*c* = 0.001M) afforded four diastereoisomeric hemicryptophanes: ***P*-256a**, ***M*-256a**, ***P*-256b**, and ***M*-256b** in 13%, 13%, 6%, and 7%, respectively (39% total yield, 2:2:1:1 ratio; Scheme 8.16). These four diastereoisomers

were successfully isolated by preparative HPLC using the mixture of hexanes/DCM/EtOAc = 50:50:10 *v/v*.

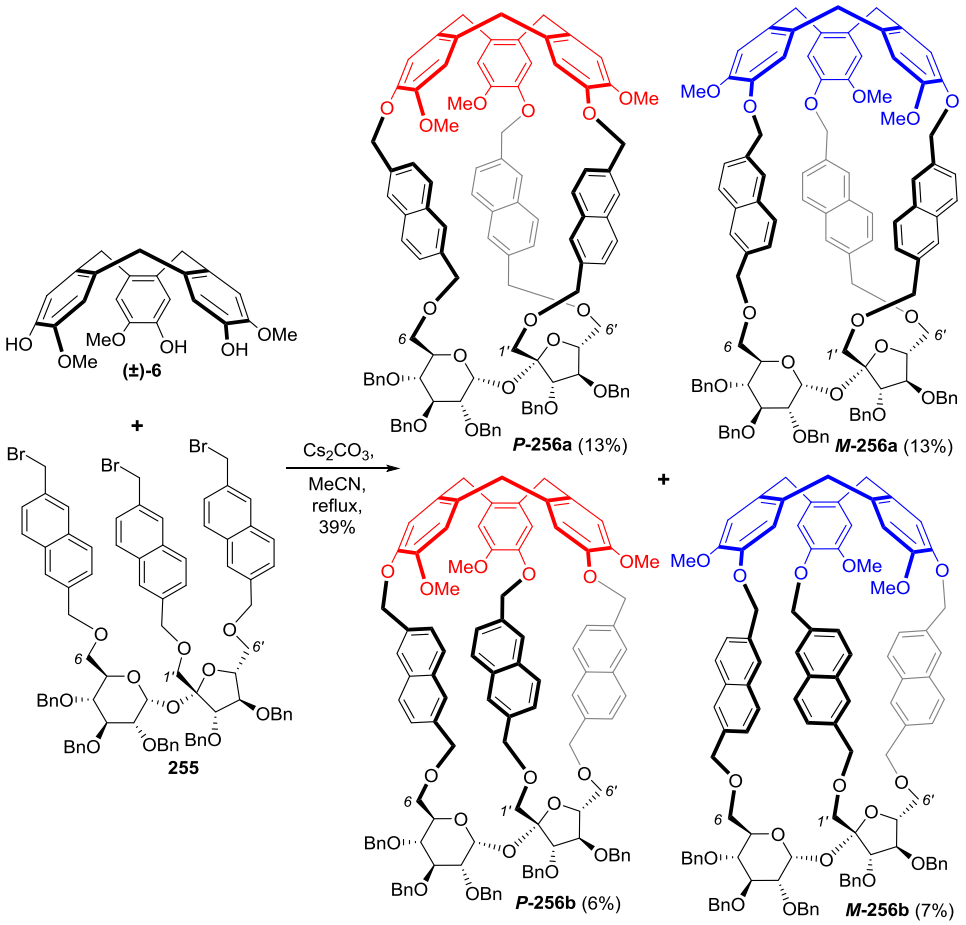

Scheme 8.16. Synthesis of four fluorescent sucrose-based hemicryptophanes.

The identification of such sophisticated C_1-symmetrical hemicryptophanes by the NMR spectroscopy was more challenging comparing to the cages described earlier, particularly due to the big crowding of the chemical shift signals. Nevertheless, the detailed analysis of all NMR spectra (^{1}H, ^{13}C, COSY, ROESY, TOCSY, HSQC, HSQC-TOCSY, and HMBC), together with the results from the ECD measurements allowed to assign unambiguously the proper structures of all four stereoisomers ***P*-256a**, ***M*-256a**, ***P*-256b**, and ***M*-256b**.

Next, I investigated the recognition properties of all four diastereoisomeric cages towards structurally related choline (**Ch**) and acetylcholine (**ACh**). The host-guest interactions were determined by the fluorescence spectroscopy titrations in MeCN due to the fluorescence properties of such prepared hemicryptophanes. Fluorescence emission spectra of four hosts ***P*-256a**, ***M*-256a**, ***P*-256b**, and ***M*-256b** strongly differed after the successive addition of each guest. While receptors ***P*-256a** and ***M*-256a** showed an increase of fluorescence intensity upon addition of **Ch** or **ACh**, cages ***P*-256b** and ***M*-256b** demonstrated

a deacrease of this parameter. This opposite behaviour might suggest the influence of the unique structure of each chiral stereoisomer, which results in the differences of the formation of the host-guest complexes. The formation of rigid host-guest complexes stabilized by intermolecular hydrogen bonds might be assigned to such fluorescence enhancement. Examples of the fluorescence titration spectra of host ***M*-256a** with **ACh** and **Ch** are shown in Figure 8.6.

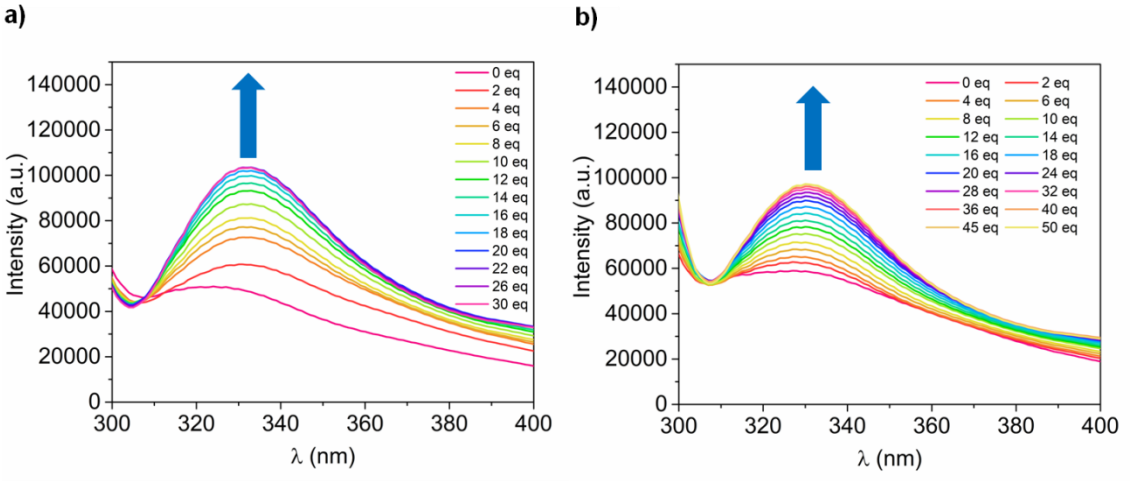

Figure 8.6. Fluorescence titration of host ***M*-256a** with a) **ACh** b) **Ch** in MeCN at 298 K excited at 280 nm (counter-ion: I^-).

The calculated association constants of hosts ***P*-256a**, ***M*-256a**, ***P*-256b**, and ***M*-256b** with **ACh** and **Ch** guests are summerized in Table 8.4. The results showed that cage ***P*-256a** is the most efficient and selective receptor for choline ($K_a = 3.8 \times 10^3\ M^{-1}$; $K_{Ch}/ K_{ACh} = 1.7$), whereas cage ***M*-256a** exhibits the best affinity and selectivity for acetylcholine ($K_a = 5.6 \times 10^3\ M^{-1}$; $K_{ACh}/ K_{Ch} = 3.1$). Therefore, hemicryptophane ***M*-256a** might efficiently recognize ACh over Ch. In the case of cages ***P*-256b** and ***M*-256b** no significant selectivty was noticed.

Table 8.4. Comparison of association constants of ***P*-256a**, ***M*-256a**, ***P*-256b**, and ***M*-256b** with imidazolium and pyridinium guests.

Guest	Host	K_a (M^{-1})[a]	K_{Ch}/ K_{ACh}
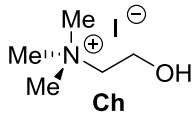 Ch	P-5a	$3.8 \times 10^3 \pm 0.9\%$	1.7
	P-5b	$2.6 \times 10^3 \pm 3.8\%$	1.1
	M-5a	$1.8 \times 10^3 \pm 1.4\%$	0.3
	M-5b	$0.5 \times 10^3 \pm 1.1\%$	0.8
Guest	**Host**	**K_a (M^{-1})[a]**	**K_{ACh}/ K_{Ch}**
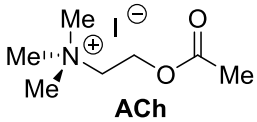 ACh	P-5a	$2.2 \times 10^3 \pm 1.6\%$	0.6
	P-5b	$2.4 \times 10^3 \pm 3.5\%$	0.9
	M-5a	$5.6 \times 10^3 \pm 1.7\%$	3.1
	M-5b	$0.6 \times 10^3 \pm 0.9\%$	1.2

[a]The K_a values were determined by fitting fluorescence titration curves using the Bindfit program.

Additional ^{1}H NMR titration studies of cages ***P*-256a** and ***M*-256a** with both ammonium guests in the mixture of $CD_3CN/CDCl_3$ (80:20) confirmed the formation of such host-guest complexes, since several upfield and downfield chemical shifts of both host and guest protons were observed. The fluorescence intensity changes along with these chemical shifts of protons strongly suggest that both guest molecules are complexed inside the cavities. The differences in the recognition of choline and acetylcholine by these diastereoisomers are probably caused by the unique shapes of their cavities, created by various connections of both sucrose and CTV units.

Moreover, the ESI-MS measurements of each host ***P*-256a** and ***M*-256a** with **Ch** and **ACh** in MeCN demonstrated the formation of stable non-covalent adducts with the 1:1 stoichiometry, which was manifested by the detection of the corresponding host-guest complexes $[M+\mathbf{Ch}]^+$ with *m/z* value of 1761.81 and $[M+\mathbf{ACh}]^+$ with *m/z* value of 1803.82.

In order to further investigate the selectivity of cage ***M*-256a** towards both structurally similar compounds (**Ch** and **ACh**) the DFT calculations were performed. The optimized structures of both ***M*-256a⊂ACh** and ***M*-256a⊂Ch** complexes demonstrated that these two guests are partially encapsulated in the host cavity (Figure 8.7).

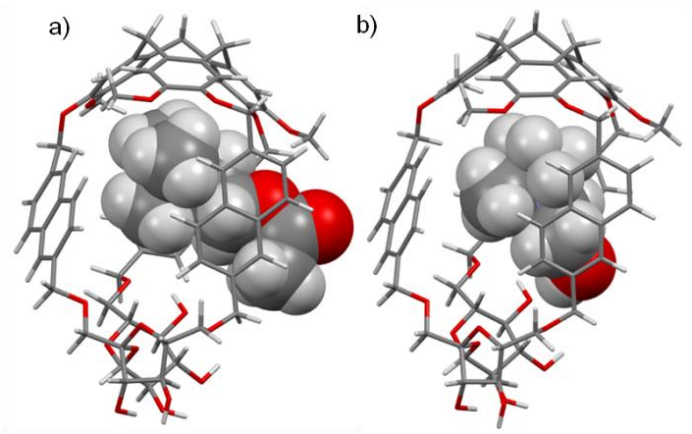

Figure 8.7. DFT calculated structures of inclusion complexes a) ***M*-256a⊂ACh** and b) ***M*-256a⊂Ch**

The ammonium part of both guests is located below electron rich CTV scaffold, whereas the rest of the molecule is situated between naphthalene linkers. Several CH-π and cation-π non-covalent interactions were found between host and each of guest molecules. However, these interactions are weaker in the case of ***M*-256a⊂Ch** inclusion complex, which is manifested by greater distances between host ***M*-256a** and choline. In the case of ***M*-256a⊂ACh** complex, several additional non-covalent interactions between the host and the ester group of acetyl-choline were observed. These DFT calculations of both inclusion complexes provided

valuable information about the molecular recognition by cage ***M*-256a** and supported its selectivity towards acetylcholine.

The additional interactions of the acetyl group with receptor ***M*-256a** as well as shorter distances between the ammonium part of **ACh** and the CTV scaffold might be responsible for such selectivity, when compared to choline.

The synthesis and recognition properties of four fluorescent diastereoisomeric sucrose-based hemicryptophanes containing naphthalene linkers have been described in the paper: "Fluorescent Molecular Cages with Sucrose and Cyclotriveratrylene Units for the Selective Recognition of Choline and Acetylcholine" Ł. Szyszka, M. Górecki, P. Cmoch, S. Jarosz, *J. Org. Chem.* **2021**, *86*, 5129–5141.

8.4. Other attempts to obtain chiral CTV-sucrose-based molecular cages containing various linkers

In this chapter, I have collected my other attempts to obtain sucrose-based hemicryptophanes. The designed molecular cages contain various linkers, and thus differ in the shape and size of the cavity. Unfortunately, the key cyclization steps failed or led to the complicated and inseparable mixtures of products.

Following the previous triple alkylation macrocyclization pathway, I also decided to introduce pyridine linkers because this moiety is widely used as a ligand for various transition metal ions.[161] For this purpose, 2,6-pyridinedimethanol (**257**) was firstly brominated to 2,6-bis(bromomethyl)pyridine, which was then reacted with triol **5** under the basic conditions (Scheme 8.17). However, I did not observe the formation of target product **259** or even its di- or monosubstituted derivatives during the ESI-MS analysis of crude reaction mixture.

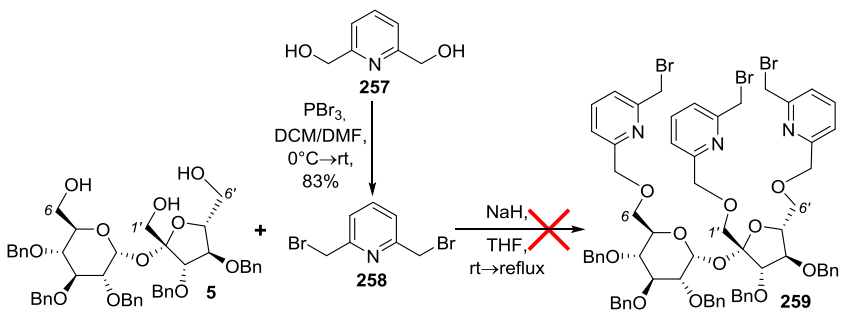

Scheme 8.17. Attempt to obtain tribromide **259**.

I also tried to enlarge the hemicryptophane cavity by the reaction of the previously synthesized triiodide **239** with proper trisphenolic CTV derivative. The nucleophilic aromatic substitution of (±)-CTG with 4-fluorobenzaldehyde afforded trialdehyde **(±)-113** in 78% yield. The one-pot sequence of the Baeyer-Villiger oxidation and the basic hydrolysis of the *in-situ* generated ester gave the target trisphenolic compound **(±)-260** in 67% yield after two steps (Scheme 8.18).

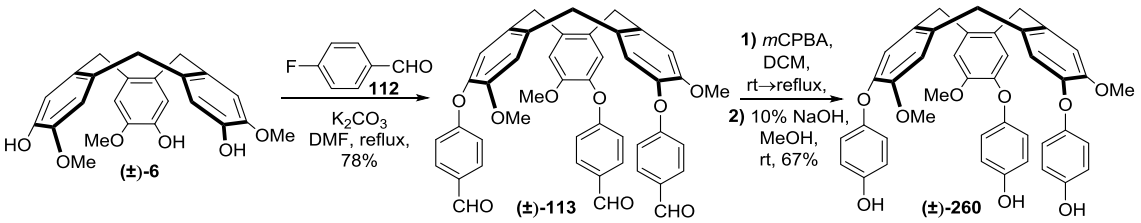

Scheme 8.18. Synthesis of trisphenolic CTV derivative **(±)-260**.

Nevertheless, the triple alkylation between **(±)-260** and **239** in the presence of Cs_2CO_3 provided the inseparable mixture of products with similar polarity, consisting of variously combined substrates (Scheme 8.19). I suppose that flexible and generally long linkers might be responsible for the formation of such complicated mixture instead of desired cages ***M*-261** and ***P*-261**. Therefore, rigid linkers, such as only phenylene or naphthalene, are preferable for the synthesis of such cages.

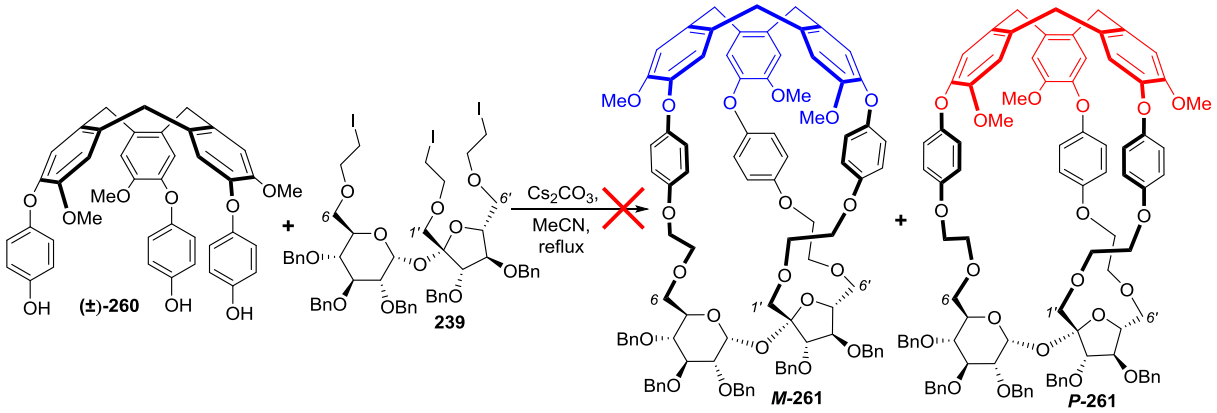

Scheme 8.19. Attempt to synthesize sucrose-based hemicryptophanes ***M*-261** and ***P*-261**.

Next, I tried to prepare more rigid cages, but structurally similar to the previous ones ***M*-261** and ***P*-261,** by attaching the phenolic units directly to the CTV aromatic rings. Treatment of (±)-CTG with trifluoromethanesulfonic anhydride in the presence of pyridine afforded CTV-based triflate **(±)-262**, which was further reacted with 4-hydroxyphenylboronic

acid (**263**) under Suzuki-Myiaura reaction conditions giving the rigid CTV derivative **(±)-264** in 92% yield (Scheme 8.20).

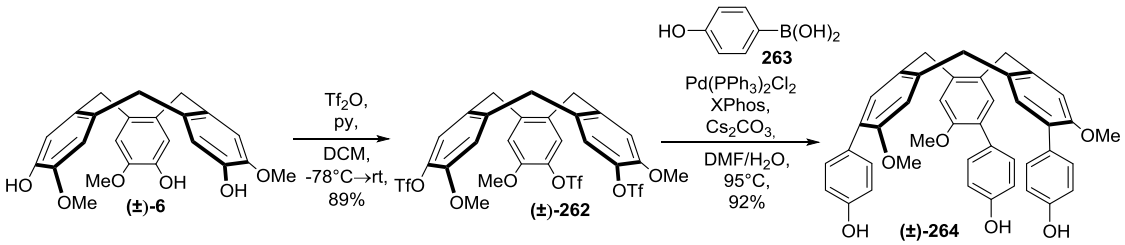

Scheme 8.20. Synthesis of rigid CTV derivative **(±)-264**.

Subsequent [1+1] coupling reaction between CTV derivative **(±)-264** and triiodide **239** in the presence of cesium carbonate as a base, unfortunately, did not lead to the expected cages ***M*-265** and ***P*-265** (Scheme 8.21). I suspect that the rigidity of the CTV scaffold might have the opposite effect than I assumed, namely the CTV moiety might have been too rigid, and thus prevent forming cage-like structure. In addition, these long linkers may also influence on the formation of differently linked compounds.

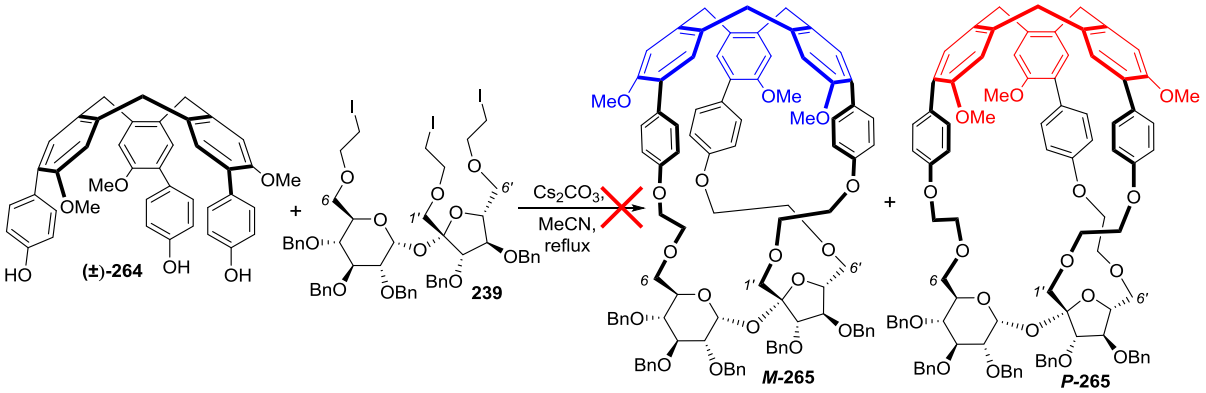

Scheme 8.21. Attempt to synthesize sucrose-based hemicryptophanes ***M*-265** and ***P*-265**.

My another approach to C_1-symmetrical sucrose-based hemicryptophanes involved the introduction of the 1,2,3-triazole rings in the linkers *via* the Huisgen 1,3-dipolar cycloaddition. This heterocyclic ring is capable of complexing anions through hydrogen bonds as well as coordinating metals by nitrogen donors.[162] Therefore, the preparation of the CTV-based molecular cages containing the 1,2,3-triazole motifs could provide heteroditopic receptors able to bind both cations and anions. For this purpose, I decided to prepare tripropargyl sucrose derivative **266** under the PTC conditions (Scheme 8.22a) and triazido CTV derivative **(±)-137** according to the literature procedure[127] (Scheme 8.22b).

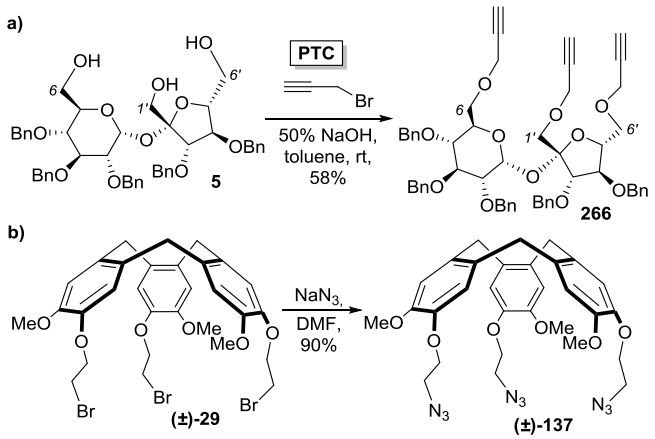

Scheme 8.22. Synthesis of a) tripropargyl sucrose derivative **266**, and b) triazido CTV derivative **(±)-137**.

The copper(I)-catalyzed alkyne-azide cycloaddition (CuAAC) between CTV derivative **(±)-137** and propargylated sucrose **266** was carried out under two different conditions, namely using CuI and DIPEA in the mixture of MeCN/$CHCl_3$ or toluene, or using $CuSO_4$ and (+)-sodium L-ascorbate in the mixture of THF, EtOH, or DMF/*i*PrOH and water (Table 8.5).

Table 8.5. Conditions for CuAAC reaction between trisazide **(±)-137** and trisalkyne **266**.

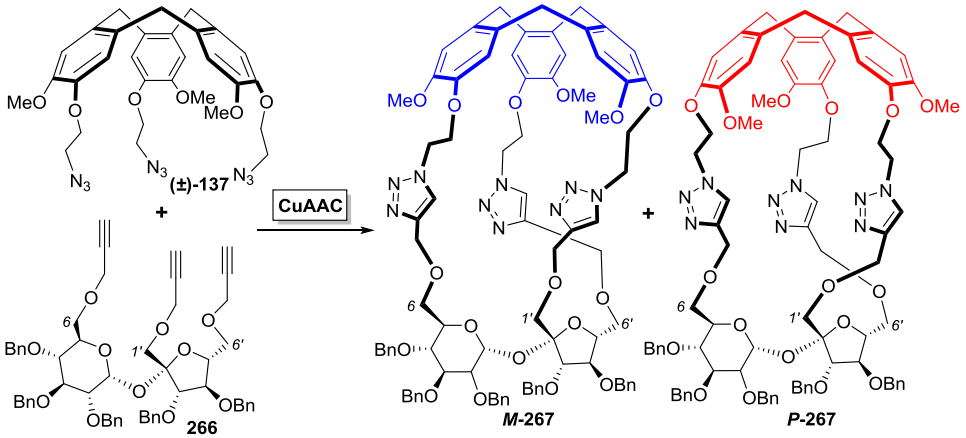

Entry	Conditions	Solvent	Temp. [°C]	Yield[a] [%]
1.	CuI, DIPEA	MeCN/$CHCl_3$	80	mixture
2.	CuI, DIPEA	toluene	80	mixture
3.	$CuSO_4$, NaAsc	THF/H_2O	60	–
4.	$CuSO_4$, NaAsc	EtOH/H_2O	60	–
5.	$CuSO_4$, NaAsc	DMF/*i*PrOH/H_2O	80	–

[a] "–" no reaction

Conducting the cyclization in the presence of CuI and DIPEA in both solvents led to a complicated and inseparable mixture of products (Table 8.5, Entries 1 and 2). On the other hand, no reaction was observed using $CuSO_4$ and NaAsc catalytic system (Table 8.5, Entries

3–5). The ^{1}H NMR analysis of the main product of the CuAAC, when using CuI and DIPEA reagents, demonstrated at least three CTV-sucrose-based compounds with the same polarity. In addition, the structure of these compounds could not be determined by ESI-MS analysis because both mono- and disubstituted products as well as triple linked cages **(±)-267** have the same exact mass. I presume that also in this case the linkers may be still too flexible for both form and provide differently linked diastereoisomers.

Then, with the CTV-based triflate **(±)-262** and tripropargyl sucrose derivative **266** in hand, I decided to test the Sonogashira coupling reaction towards sucrose-based hemicryptophanes ***M*-268** and ***P*-268** (Scheme 8.23).

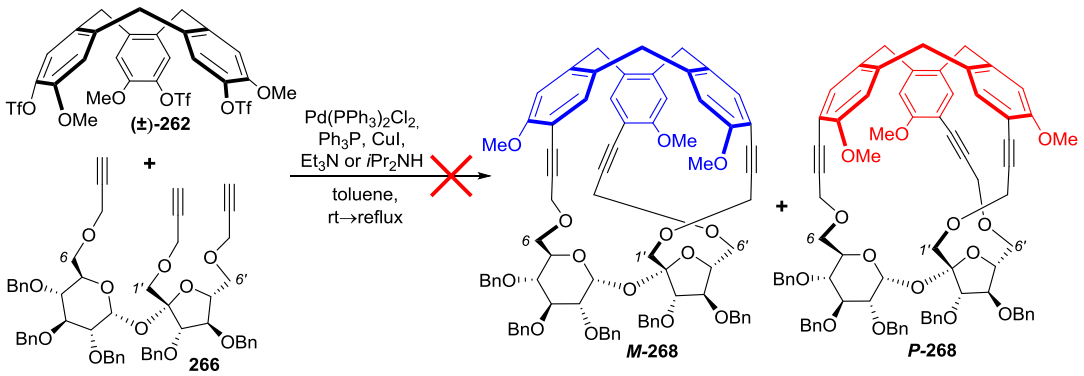

Scheme 8.23. Attempt to synthesize sucrose-based hemicryptophanes ***M*-268** and ***P*-268** *via* Sonogashira coupling.

This reaction, unfortunately, did not lead to the desired cages even with the use of additional phosphine ligand or the replacement of triethylamine with freshly distilled stronger base *i*Pr$_2$NH. During the reaction, I observed only the disappearance of the sucrose-based substrate **266** and the formation of very polar products. The ESI-MS analysis suggested that the carbohydrate substrate **266** decomposed, but the CTV-based triflate **(±)-262** remained unchanged.

In the last attempt to the C_1-symmetrical sucrose-based cages, I also applied the Sonogashira coupling reaction. However, these hemicryptophanes were characterized by much larger and rigid cavity due to the alkyne bond and additional aromatic rings. For this purpose, I firstly prepared CTV-based tribromide **(±)-116** according to the literature procedure[116] (Scheme 8.24).

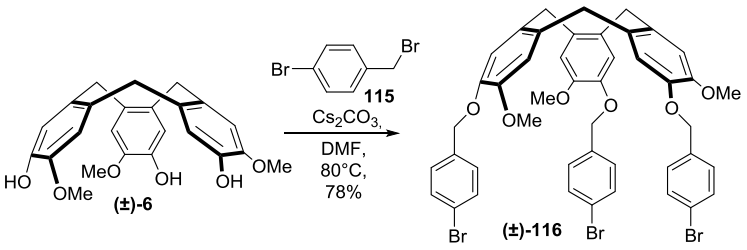

Scheme 8.24. Synthesis of tribromide CTV derivative **(±)-116**.

The Sonogashira coupling between tribromide **(±)-116** with tripropargyl sucrose derivative **266** did not, however, afford target molecular cages ***M*-269** and ***P*-269** (Scheme 8.25). Similarly to the previously described reaction in Scheme 8.23, the sucrose substrate **266** decomposed, whereas tribromide **(±)-116** remained unreacted. These results demonstrate that such coupling reaction conditions are not suitable for this sucrose derivative.

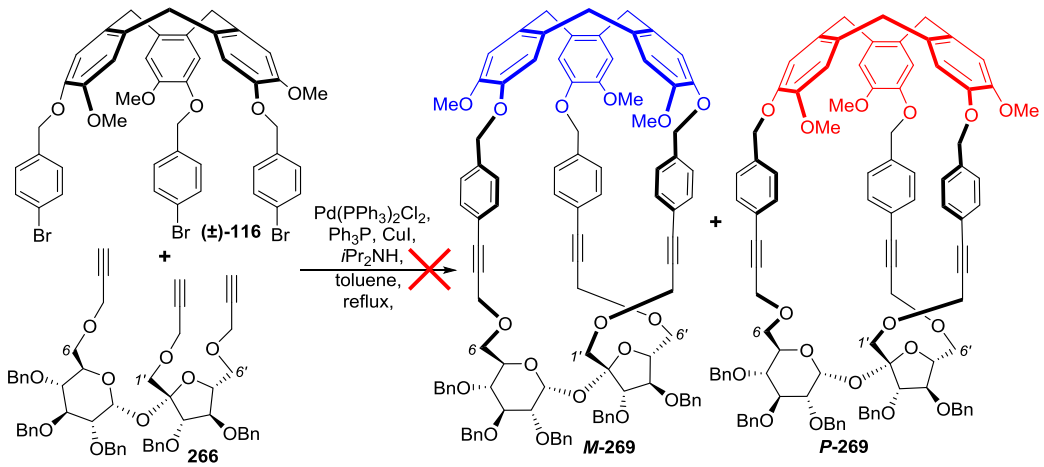

Scheme 8.25. Attempt to synthesize sucrose-based hemicryptophanes ***M*-269** and ***P*-269** *via* Sonogashira coupling.

8.5. Comment on the review paper

The review paper "*Synthesis of fine chemicals with high added value from sucrose: Towards sucrose-based macrocycles*" of which I am co-author concerns the application of sucrose as a building block for the synthesis of fine chemicals.[27] In the introduction, the basic information on sucrose, its physico-chemical properties, and methods of the selective protection of its hydroxyl groups are described. Examples of the synthesis of sucrose-based compounds modified at the terminal positions (C-6, C-1', and C-6') are presented. These transformations included, in particular, the selective functionalization of sucrose diols and triols. Special attention was paid to the preparation of sucrose-based macrocyclic receptors.

A number of different macrocyclic compounds bearing sucrose moiety obtained in our group are reviewed. These compounds differ in linkers, shape, gap size, as well as functional groups and heteroatoms in their structure. There are macrocyclic receptors, in which both terminal positions of sucrose (C-6 and C-6') are linked *via* a long carbon chain, crown and aza-crown analogues, macrocyclic sucrose dimers, cryptands, or more complex structures such as cages. Finally, the binding abilities of the selected sucrose-based macrocyclic hosts are summarized. This review paper ends with the conclusions and further perspectives on the use of sucrose as a useful framework for novel chiral, artificial receptors with particular emphasis on sucrose-based cages.

More information on sucrose-based macrocycles can be found in the paper: "Synthesis of fine chemicals with high added value from sucrose: Towards sucrose-based macrocycles" Sławomir Jarosz, Patrycja Sokołowska, and Łukasz Szyszka *Tetrahedron Lett.* **2020**, *61*, 151888.

9. Conclusions

The aim of this doctoral research was the synthesis of novel sucrose-based hemi-cryptophanes and to investigate their host-guest properties. The results presented in the above chapters, as well as in the attached below publications, confirm the realisation of the objectives both in terms of the synthesis of unprecedented C_1-symmetrical molecular cages and the study of their complexing properties. As a result of my research, I obtained and fully characterized – for the first time – twelve different sucrose-based hemicryptophanes (including two water-soluble ones) and examined their recognition abilities towards various cationic organic guests. It is worth noting that the separable C_1-symmetrical hemicrypto-phanes have not been previously described in the literature. Overall, these hemicryptophanes are still not explored.

The CTV scaffold is a valuable building block for the preparation of novel C_1-symmetrical hemicryptophanes due to its inherent chirality. During the study, I have demonstrated that the combination of the CTV unit with chiral sucrose platform leads to the pair of two (in the case of short ethylene linkers), or four diastereoisomers (in the case of phenyl or naphthyl linkers) of hemicryptophanes that vary in the size and shape of their cavity. The molecular cages I prepared are easily separable by classical silica gel chromatography or preparative HPLC without using expensive chiral columns. In addition,

introducing sucrose fragment provided water-soluble receptors ***M*-240** and ***P*-240**, which is important in the case of recognition studies in competitive aqueous media. Sucrose-based hemicryptophanes containing *p*-phenylene linkers ***M*-251a** and ***P*-251a** are capable of binding 1-methylpyridinium and 1,3-dimethylimidazolium cations (important building units of numerous pharmaceuticals, phase transfer catalysts, or ionic liquids) with moderate association constants. On the other hand, hemicryptophanes ***M*-256a** and ***P*-256a** have proved to be efficient fluorescent chemosensors for detection of choline or acetylcholine – compounds of biological significance. I assume that the introduction of chiral sucrose platform to the host's structure, together with the inherent chirality of the CTV moiety, might be responsible for the original shape of the cavity, and thus resulting in the selective recognition of these structurally related compounds.

In summary, I have successfully achieved the following objectives:

- I prepared and characterized two unprecendent water-soluble C_1-symmetrical hemicryptophanes containing sucrose unit (***M*-240** and ***P*-240**),
- I obtained and characterized four diastereoisomeric sucrose-based hemicryptophanes with *p*-phenylene linkers and investigated their binding abilities (***M*-251a, *P*-251a, *M*-251b,** and ***P*-251b**),
- For cage ***P*-251b** I obtained the X-Ray crystal structure, which gave an insight into its original structure,
- I obtained and characterized four diastereoisomeric sucrose-based hemicryptophanes with naphthalene linkers (cages ***M*-256a** and ***P*-256a** exhibit selective recognition properties towards acetylcholine and choline),
- I demonstrated that short linkers (ethylene) provide one pair of *M/P* diastereoisomers, whereas longer linkers (phenyl or naphthyl) lead to two pairs of *M/P* diastereoisomers,
- I demonstrated that it is possible to obtain and separate molecular cages with such sophisticated structure,
- I shown that the shape of the cavity plays a significant role in the selective molecular recognition process.

This research work is an important contribution to the development of the unprecedented C_1-symmetrical hemicryptophanes. I believe that the results I have achieved may provide a starting point for further study of such CTV-based molecular cages, in particular investigating their selective recognition ability.

10. References

1. Lehn J.-M. *Science*, **2002**, *295*, 2400–2403.
2. Steed, J. W.; Atwood, J. L. *Supramolecular Chemistry*, 2nd ed.;Wiley-VCH: Weinheim, **2009**.
3. Gogoi A.; Mazumder N.; Konwer S.; Ranawat H.; Chen N.-T.; Zhuo G.-Y. *Molecules*, **2019**, *24*, 1007.
4. Biros S. M.; Rebek J. Jr. *Chem. Soc. Rev.*, **2007**, *36*, 93–104.
5. Pattillo C.; Moore J.S. *Chem. Sci.*, **2019**, *10*, 7043−7048.
6. Zhang K.-D.; Ajami D.; Rebek J. *J. Am. Chem. Soc.*, **2013**, *135*, 18064−18066.
7. Sun W.; Wang Y.; Ma L.; Zheng L.; Fang W.; Chen X.; Jiang H. *J. Org. Chem.*, **2018**, *83*, 14667−14675.
8. Gidron O.; Jirasek M.; Trapp N.; Ebert M.-O.; Zhang X.; Diederich F. *J. Am. Chem. Soc.*, **2015**, *137*, 12502−12505.
9. Cirulli M.; Kaur A.; Lewis J. E. M.; Zhang Z.; Kitchen J. A.; Goldup S. M.; Roessler M. M. *J. Am. Chem. Soc.*, **2019**, *141*, 879−889.
10. Bravin C.; Guidetti A.; Licini G.; Zonta C. *Chem. Sci.*, **2019**, *10*, 3523−3528.
11. Fang Y.; Powell J. A.; Li E.; Wang Q.; Perry Z.; Kirchon A.; Yang X.; Xiao Z.; Zhu C.; Zhang L.; Huang F.; Zhou H.-C. *Chem. Soc. Rev.*, **2019**, *48*, 4707−4730.
12. Davis J. T.; Gale P. A.; Quesada R. *Chem. Soc. Rev.*, **2020**, *49*, 6056–6086.
13. Zhang D.; Ronson T. K.; Lavendomme R.; Nitschke J. R. *J. Am. Chem. Soc.*, **2019**, *141*, 18949–18953.
14. Vriezema D. M.; Aragonès M. C.; Elemans J. A. A. W.; Cornelissen J. J. L. M.; Rowan A. E.; Nolte R. J. M. *Chem. Rev.*, **2005**, *105*, 1445–1490.
15. Mena-Hernando S.; Pérez E. M. *Chem. Soc. Rev.*, **2019**, *48*, 5016–5032.
16. Su K.; Wang W.; Du S.; Ji C.; Zhou M.; Yuan D. *J. Am. Chem. Soc.*, **2020**, *142*, 18060–18072.
17. Barboiu M.; Stadler A.-M.; Lehn J.-M. *Angew. Chem. Int. Ed.*, **2016**, *55*, 4130−4154.
18. Biedermann F.; Schneider H.-J. *Chem. Rev.*, **2016**, *116*, 5216−5300.
19. Erbas-Cakmak S.; Leigh D. A.; McTernan C. T.; Nussbaumer A. L. *Chem. Rev.*, **2015**, *115*, 10081−10206.
20. Izatt R. M.; Pawlak K.; Bradshaw J. S. *Chem. Rev.*, **1995**, *95*, 2529−2586.
21. Molina P.; Zapata F.; Caballero A. *Chem. Rev.*, **2017**, *117*, 9907−9972.
22. He Q.; Vargas-Zúñiga G. I.; Kim S. H.; Kim S. K.; Sessler J. L. *Chem. Rev.*, **2019**, *119*, 9753–9835.
23. Hardie M. J. *Chem. Soc. Rev.*, **2010**, *39*, 516−527.
24. Brotin T.; Dutasta J.-P. *Chem. Rev.*, **2009**, *109*, 88−130.
25. Zhang D.; Martinez A.; Dutasta J.-P. *Chem. Rev.*, **2017**, *117*, 4900−4942.
26. Colomban C.; Châtelet B.; Martinez A. *Synthesis*, **2019**, *51*, 2081−2099.
27. Jarosz S.; Sokołowska P.; Szyszka Ł. *Tetrahedron Lett.*, **2020**, *61*, 151888.
28. Sokołowska P.; Kowalski M.; Jarosz S. *Beilstein J. Org. Chem.*, **2019**, *15*, 210−217.
29. Sokołowska P.; Dąbrowa K.; Jarosz S. *Org. Lett.*, **2021**, *23*, 2687−2692.
30. Smeets J. W. H.; Coolen H. K. A. C.; Zwikker J. W.; Nolte R. J. M. *Recl. Trav. Chim. Pays-Bas*, **1989**, *108*, 215−218.
31. Collet A.; Dutasta J.-P.; Lozach B.; Canceill J. *Cyclotriveratrylenes and cryptophanes: Their synthesis and applications to host-guest chemistry and to the design of new materials.* In: *Supramolecular Chemistry I – Directed Synthesis and Molecular Recognition. Topics in Current Chemistry*, *165*, Springer, Berlin, **1993**.
32. Henkelis J. J.; Hardie M. J. *Chem. Commun.*, **2015**, *51*, 11929−11943.
33. Hardie M. J. *Chem. Lett.*, **2016**, *45*, 1336−1346.
34. Zimmermann H.; Tolstoy P.; Limbach H.-H.; Poupko R.; Luz Z. *J. Phys. Chem. B*, **2004**, *108*, 18772−18778.
35. Collet A.; Gabard J. *J. Org. Chem.*, **1980**, *45*, 5400−5401.
36. Lafon O.; Lesot P.; Zimmermann H.; Poupko R.; Luz Z. *J. Phys. Chem. B*, **2007**, *111*, 9453−9467.
37. Collet A.; Gabard J.; Jacques J.; Cesario M.; Guilhem J.; Pascard C. *J. Chem. Soc., Perkin Trans. 1*, **1981**, 1630−1638.

38. Canceill J.; Collet A.; Gabard J.; Gottarelli G.; Spada G. P. *J. Am. Chem. Soc.*, **1985**, *107*, 1299−1308.
39. Barger G.; Ewins A. J. *J. Chem. Soc., Trans.*, **1909**, *95*, 552−560.
40. Robinson G. M. *J. Chem. Soc., Trans.*, **1915**, *107*, 267−276.
41. Erdtman H.; Haglid F.; Ryhage R. *Acta Chem. Scand.*, **1964**, *18*, 1249−1254.
42. Lindsey A. S. *J. Chem. Soc.*, **1965**, 1685−1692.
43. Goldup A.; Morrison A. B.; Smith G. W. *J. Chem. Soc.*, **1965**, 3864−3865.
44. Umezawa B.; Hoshino O.; Hara H.; Ohyama K.; Mitsubayashi S.; Sakakibara J. *Chem. Pharm. Bull.*, **1969**, *17*, 2240−2244.
45. Roche C.; Sun H.-J.; Prendergast M. E.; Leowanawat P.; Partridge B. E.; Heiney P. A.; Araoka F.; Graf R.; Spiess H. W.; Zeng X.; Ungar G.; Percec V. *J. Am. Chem. Soc.*, **2014**, *136*, 7169−7185.
46. Al-Farhan E.; Keehn P. M.; Stevenson R. *Tetrahedron Lett.*, **1992**, *33*, 3591−3594.
47. Brotin T.; Roy V.; Dutasta J.-P. *J. Org. Chem.*, **2005**, *70*, 6187−6195.
48. Scott J. L.; MacFarlane D. R.; Raston C. L.; Teoh C. M. *Green Chemistry*, **2000**, *2*, 123−126.
49. Ogoshi T.; Kitajima K.; Umeda K.; Hiramitsu S.; Kanai S.; Fujinami S.; Yamagishi T.; Nakamoto Y. *Tetrahedron*, **2009**, *65*, 10644−10649.
50. Wang D.; Ivanov M. V.; Mirzaei S.; Lindeman S. V.; Rathore R. *Org. Biomol. Chem.*, **2018**, *16*, 5712−5717.
51. Cram D. J.; Tanner M. E.; Keipert S. J.; Knobler C. B. *J. Am. Chem. Soc.* **1991**, *113*, 8909−8916.
52. Bissegger F. R.; Neuburger M.; Tiefenbacher K. *Supramol. Chem.*, **2020**, *32*, 320−324.
53. Peyrard L.; Chierici S.; Pinet S.; Batat P.; Jonusauskas G.; Pinaud N.; Meyrand P.; Gosse I. *Org. Biomol. Chem.*, **2011**, *9*, 8489−8494.
54. Rao M. L. N.; Talode J. B. *Asian J. Org. Chem.*, **2016**, *5*, 98−106.
55. Peyrard L.; Dumartin M.-L.; Chierici S.; Pinet S.; Jonusauskas G.; Meyrand P.; Gosse I. *J. Org. Chem.*, **2012**, *77*, 7023−7027.
56. Yu J.-T.; Huang Z.-T.; Zheng Q.-Y. *Org. Biomol. Chem.*, **2012**, *10*, 1359−1364.
57. Ahmad R.; Hardie M. J. *Supramol. Chem.*, **2006**, *18*, 29−38.
58. Gabard J.; Collet A. *J. Chem. Soc. Chem. Comm.*, **1981**, 1137−1139.
59. Riggle B. A.; Wang Y.; Dmochowski I. J. *J. Am. Chem. Soc.*, **2015**, *137*, 5542−5548.
60. Garcia C.; Andraud C.; Collet A. *Supramol. Chem.*, **1992**, *1*, 31−45.
61. Peterca M.; Percec V.; Imam M. R.; Leowanawat P.; Morimitsu K.; Heiney P. A. *J. Am. Chem. Soc.*, **2008**, *130*, 14840−14852.
62. Chary K. P.; Mohan G. H.; Iyengar D. S. *Chem. Lett.*, **1999**, *11*, 1223−1224.
63. Thomas R. M.; Mohan G. H.; Iyengar D. S. *Tetrahedron Lett.*, **1997**, *38*, 4721−4724.
64. Brotin T.; Devic T.; Lesage A.; Emsley L.; Collet A. *Chem. Eur. J.*, **2001**, *7*, 1561−1573.
65. Canceill J.; Collet A.; Gottarelli G. *J. Am. Chem. Soc.*, **1984**, *106*, 5997−6003.
66. Garcia C.; Malthête J.; Collet A. *Bull. Soc. Chim. Fr.*, **1993**, *130*, 93−95.
67. Sanseverino J.; Chambron J.-C.; Aubert E.; Espinosa E. *J. Org. Chem.*, **2011**, *76*, 1914−1917.
68. Chakrabarti A.; Chawla H. M.; Hundal G.; Pant N. *Tetrahedron*, **2005**, *61*, 12323−12329.
69. Milanole G.; Gao B.; Mari E.; Berthault P.; Pieters G.; Rousseau B. *Eur. J. Org. Chem.*, **2017**, 7091−7100.
70. Long A.; Colomban C.; Jean M.; Albalat M.; Vanthuyne N.; Giorgi M.; Di Bari L.; Górecki M.; Dutasta J.-P.; Martinez A. *Org. Lett.*, **2019**, *21*, 160−165.
71. Zhang S.; Echegoyen L. *J. Am. Chem. Soc.*, **2005**, *127*, 2006−2011.
72. Gawenis J. A.; Holman K. T.; Atwood J. L.; Jurisson S. S. *Inorg. Chem.*, **2002**, *41*, 6028−6031.
73. Holman K. T.; Halihan M. M.; Jurisson S. S.; Atwood J. L.; Burkhalter R. S.; Mitchell A. R.; Steed J. W. *J. Am. Chem. Soc.*, **1996**, *118*, 9567−9576.
74. Nuriman, Kuswandi B.; Verboom W. *Analytica Chimica Acta*, **2009**, *655*, 75−79.
75. Moriuchi-Kawakami T.; Mizuno Y.; Inoue T.; Matsubara S.; Moriuchi T. *Analyst*, **2019**, *144*, 1140−1146.
76. Huerta E.; Metselaar G. A.; Fragoso A.; Santos E.; Bo C.; de Mendoza J. *Angew. Chem. Int. Ed.*, **2007**, *46*, 202−205.
77. Huerta E.; Isla H.; Pérez E. M.; Bo C.; Martín N.; de Mendoza J. *J. Am. Chem. Soc.*, **2010**, *132*, 5351−5353.

78. Blanch R. J.; Williams M.; Fallon G. D.; Gardiner M. G.; Kaddour R.; Raston C. L. *Angew. Chem. Int. Ed. Engl.*, **1997**, *36*, 504−506.
79. Hardie M. J.; Godfrey P. D.; Raston C. L. *Chem. Eur. J.*, **1999**, *5*, 1828−1833.
80. Lefevre S.; Héloin A.; Pitrat D.; Mulatier J.-C.; Vanthuyne N.; Jean M.; Dutasta J.-P.; Guy L.; Martinez A. *J. Org. Chem.*, **2016**, *81*, 3199−3205.
81. Dumartin M.-L.; Givelet C.; Meyrand P.; Bibal B.; Gosse I. *Org. Biomol. Chem.*, **2009**, *7*, 2725−2728.
82. Erieau-Peyrard L.; Coiffier C.; Bordat P.; Bégué D.; Chierici S.; Pinet S.; Gosse I.; Baraille I.; Brown R. *Phys. Chem. Chem. Phys.*, **2015**, *17*, 4168−4174.
83. Xia D.; Li Y.; Jie K.; Shi B.; Yao Y. *Org. Lett.*, **2016**, *18*, 2910−2913.
84. Thorp-Greenwood F. L.; Kulak A. N.; Hardie M. J. *Nat. Chem.*, **2015**, *7*, 526−531.
85. Thorp-Greenwood F. L.; Ronson T. K.; Hardie M. J. *Chem. Sci.*, **2015**, *6*, 5779−5792.
86. Hardie M. J.; Ahmad R.; Sumby C. J. *New J. Chem.*, **2005**, *29*, 1231−1240.
87. Roche C.; Sun H.-J.; Prendergast M. E.; Leowanawat P.; Partridge B. E.; Heiney P. A.; Araoka F.; Graf R.; Spiess H. W.; Zeng X.; Ungar G.; Percec V. *J. Am. Chem. Soc.*, **2014**, *136*, 7169−7185.
88. Percec V.; Imam M. R.; Peterca M.; Wilson D. A.; Heiney P. A. *J. Am. Chem. Soc.*, **2009**, *131*, 1294−1304.
89. Bardelang D.; Camerel F.; Ziessel R.; Schmutz M.; Hannon M. J. *J. Mater. Chem.*, **2008**, *18*, 489−494.
90. Cai F.; Shen J.-S.; Wang J.-H.; Zhang H.; Zhao J.-S.; Zeng E.-M.; Jiang Y.-B. *Org. Biomol. Chem.*, **2012**, *10*, 1418−1423.
91. Yu J.-T.; Chen Z.; Sun J.; Huang Z.-T.; Zheng Q.-Y. *J. Mater. Chem.*, **2012**, *22*, 5369−5373.
92. Martin A. D.; Easun T. L.; Argent S. P.; Lewis W.; Blake A. J.; Schröder M. *CrystEngComm*, **2017**, *19*, 603−607.
93. Lunkwitz R.; Tschierske C.; Diele S. *J. Mater. Chem.*, **1997**, *7*, 2001−2011.
94. Felder D.; Heinrich B.; Guillon D.; Nicoud J.-F.; Nierengarten J.-F. *Chem. Eur. J.*, **2000**, *6*, 3501−3507.
95. Kang D.-W.; Han X.; Ma X.-J.; Liu Y.-Y.; Ma J.-F. *Dalton Trans.*, **2018**, *47*, 16197−16204.
96. Song J.-R.; Huang Z.-T.; Zheng Q.-Y. *Tetrahedron*, **2013**, *69*, 7308−7313.
97. Fowler J. M.; Britton E.; Pask C. M.; Willans C. E.; Hardie M. J. *Dalton Trans.*, **2019**, *48*, 14687−14695.
98. Thomas R. M.; Iyengar D. S. *Synth. Commun.*, **1999**, *29*, 2507−2513.
99. van Ameijde J.; Liskamp R. M. J. *Org. Biomol. Chem.*, **2003**, *1*, 2661−2669.
100. Yang F.; Chen Q.; Cheng Q.-Y.; Yan C.-G.; Han B.-H. *J. Org. Chem.*, **2012**, *77*, 971−976.
101. Feng L.-J.; Li H.; Chen Q.; Han B.-H. *RSC Adv.*, **2013**, *3*, 6985−6990.
102. Galanos N.; Chen Y.; Michael Z. P.; Gillon E.; Dutasta J.-P.; Star A.; Imberty A.; Martinez A.; Vidal S. *ChemistrySelect*, **2016**, *1*, 5863−5868.
103. Canceill J.; Collet A., Gabard J.; Kotzyba-Hibert F.; Lehn J. M. *Helv. Chim. Acta*, **1982**, *65*, 1894−1897.
104. Gosse I.; Dutasta J.-P.; Perrin M.; Thozet A. *New J. Chem.*, **1999**, *23*, 545−548.
105. Gautier A.; Mulatier J.-C.; Crassous J.; Dutasta J.-P. *Org. Lett.*, **2005**, *7*, 1207−1210.
106. Zhang D.; Mulatier J.-C.; Cochrane J. R.; Guy L.; Gao G.; Dutasta J.-P.; Martinez A. *Chem. Eur. J.*, **2016**, *22*, 8038−8042.
107. Dimitrov-Raytchev P.; Perraud O.; Aronica C.; Martinez A.; Dutasta J.-P. *J. Org. Chem.*, **2010**, *75*, 2099−2102.
108. Schmitt A.; Perraud O.; Payet E.; Chatelet B.; Bousquet B.; Valls M.; Padula D.; Di Bari L.; Dutasta J.-P.; Martinez A. *Org. Biomol. Chem.*, **2014**, *12*, 4211−4217.
109. Zhang D.; Chatelet B.; Serrano E.; Perraud O.; Dutasta J.-P.; Robert V.; Martinez A. *ChemPhysChem*, **2015**, *16*, 2931−2935.
110. Makita Y.; Katayama N.; Lee H.-H.; Abe T.; Sogawa K.; Nomoto A.; Fujiwara S.; Ogawa A. *Tetrahedron Lett.*, **2016**, *57*, 5112−5115.
111. Chatelet B.; Payet E.; Perraud O.; Dimitrov-Raytchev P.; Chapellet L.-L.; Dufaud V.; Martinez A.; Dutasta J.-P. *Org. Lett.*, **2011**, *13*, 3706−3709.

112. Perraud O.; Tommasino J.-B.; Robert V.; Albela B.; Khrouz L.; Bonneviot L.; Dutasta J.-P.; Martinez A. *Dalton Trans.*, **2013**, *42*, 1530−1535.
113. Lefevre S.; Zhang D.; Godart E.; Jean M.; Vanthuyne N.; Mulatier J.-C.; Dutasta J.-P.; Guy L.; Martinez A. *Chem. Eur. J.*, **2016**, *22*, 2068−2074.
114. Chatelet B.; Joucla L.; Padula D.; Di Bari L.; Pilet G.; Robert V.; Dufaud V.; Dutasta J.-P.; Martinez A. *Org. Lett.*, **2015**, *17*, 500−503.
115. Makita Y.; Sugimoto K.; Furuyoshi K.; Ikeda K.; Fujiwara S.; Shin-ike T.; Ogawa A. Inorg. *Chem.*, **2010**, *49*, 7220−7222.
116. Makita Y.; Danno T.; Ikeda K.; Lee H.-H.; Abe T.; Sogawa K.; Nomoto A.; Fujiwara S.; Ogawa A. *Tetrahedron Lett.*, **2017**, *58*, 4507−4509.
117. Rivera D. G.; Wessjohann L. A. *J. Am. Chem. Soc.*, **2006**, *128*, 7122−7123.
118. Godart E.; Long A.; Rosas R.; Lemercier G.; Jean M.; Leclerc S.; Bouguet-Bonnet S.; Godfrin C.; Chapellet L.-L.; Dutasta J.-P.; Martinez A. *Org. Lett.*, **2019**, *21*, 1999−2003.
119. Delecluse M.; Colomban C.; Moraleda D.; de Riggi I.; Duprat F.; Michaud-Chevallier S.; Dutasta J.-P.; Robert V.; Chatelet B.; Martinez A. *Chem. Eur. J.*, **2019**, *25*, 3337−3342.
120. Delecluse M.; Colomban C.; Chatelet B.; Chevallier-Michaud S.; Moraleda D.; Dutasta J.-P.; Martinez A. *J. Org. Chem.*, **2020**, *85*, 4706−4711.
121. Fantozzi N.; Pétuya R.; Insuasty A.; Long A.; Lefevre S.; Schmitt A.; Robert V.; Dutasta J.-P.; Baraille I.; Guy L.; Genin E.; Bégué D.; Martinez A.; Pinet S.; Gosse I. *New J. Chem.*, **2020**, *44*, 11853−11860.
122. Schmitt A.; Chatelet B.; Padula D.; Di Bari L.; Dutasta J.-P.; Martinez A. *New J. Chem.*, **2015**, *39*, 1749−1753.
123. Zhang D.; Bousquet B.; Mulatier J.-C.; Pitrat D.; Jean M.; Vanthuyne N.; Guy L.; Dutasta J.-P.; Martinez A. *J. Org. Chem.*, **2017**, *82*, 6082−6088.
124. Qiu G.; Colomban C.; Vanthuyne N.; Giorgi M.; Martinez A. *Chem. Commun.*, **2019**, *55*, 14158−14161.
125. Perraud O.; Robert V.; Gornitzka H.; Martinez A., Dutasta J.-P. *Angew. Chem. Int. Ed.*, **2012**, *51*, 504−508.
126. Lefevre S.; Simonet R.; Pitrat D.; Mulatier J.-C.; Vanthuyne N.; Jean M.; Dutasta J.-P.; Guy L.; Martinez A. *ChemistrySelect*, **2016**, *1*, 6316−6320.
127. Long A.; Perraud O.; Albalat M.; Robert V.; Dutasta J.-P.; Martinez A. *J. Org. Chem.*, **2018**, *83*, 6301−6306.
128. Long A.; Fantozzi N.; Pinet S.; Genin E.; Pétuya R.; Bégué D.; Robert V.; Dutasta J.-P.; Gosse I.; Martinez A. *Org. Biomol. Chem.*, **2019**, *17*, 5253−5257.
129. Long A.; Antonetti E.; Insuasty A.; Pinet S.; Gosse I.; Robert V.; Dutasta J.-P.; Martinez A. *J. Org. Chem.*, **2020**, *85*, 6400−6407.
130. Long A.; Perraud O.; Jeanneau E.; Aronica C.; Dutasta J.-P.; Martinez A. *Beilstein J. Org.*, **2018**, *14*, 1885−1889.
131. Le Gac S.; Jabin I. *Chem. Eur. J.*, **2008**, *14*, 548−557.
132. Wang L.; Wang G.-T.; Zhao X.; Jiang X.-K.; Li Z.-T. *J. Org. Chem.*, **2011**, *76*, 3531−3535.
133. Cochrane J. R.; Schmitt A.; Wille U.; Hutton C. A. *Chem. Commun.*, **2013**, *49*, 8504−8506.
134. Brégier F.; Karuppannan S.; Chambron J.-C. *Eur. J. Org. Chem.*, **2012**, 1920−1925.
135. Brégier F.; Lavalle J.; Chambron J.-C. *Eur. J. Org. Chem.*, **2013**, 2666−2671.
136. Gosse I.; Robeyns K.; Bougault C.; Martinez A.; Tinant B.; Dutasta J.-P. *Inorg. Chem.*, **2016**, *55*, 1011−1013.
137. Khan N. S.; Perez-Aguilar J. M.; Kaufmann T.; Aru Hill P.; Taratula O.; Lee O-S.; Carroll P. J.; Saven J. G.; Dmochowski I. J. *J. Org. Chem.*, **2011**, *76*, 1418−1424.
138. Qiu G.; Nava P.; Martinez A.; Colomban C. *Chem. Commun.*, **2021**, *57*, 2281−2284.
139. Ernst B.; Hart G. W.; Sinaý P. *Carbohydrates in Chemistry and Biology*; Wiley-VCH: Weinheim, **2000**.
140. Perraud O.; Martinez A.; Dutasta J.-P. *Chem. Commun.*, **2011**, *47*, 5861−5863.
141. Hasselmo M. E.; Sarter M. *Neuropsychopharmacology*, **2011**, *36*, 52−73.
142. Perraud O.; Lefevre S.; Robert V.; Martinez A.; Dutasta J.-P. *Org. Biomol. Chem.*, **2012**, *10*, 1056−1059.

143. Schmitt A.; Robert V.; Dutasta J.-P.; Martinez A. *Org. Lett.*, **2014**, *16*, 2374−2377.
144. Schmitt A.; Chatelet B.; Collin S.; Dutasta J.-P.; Martinez A. *Chirality*, **2013**, *25*, 475−479.
145. Perraud O.; Robert V.; Martinez A.; Dutasta J.-P. *Chem. Eur. J.*, **2011**, *17*, 13405−13408.
146. Kruk Z. L.; Pycock C. J. *Neurotransmitters and Drugs, 3rd Ed.*; Springer, **1991**.
147. Sohlenkamp C.; López-Lara I. M.; Geiger O. *Prog. Lipid Res.*, **2003**, *42*, 115−162.
148. Longo N.; Frigeni M.; Pasquali M. *Biochim. Biophys. Acta*, **2016**, *1863*, 2422−2435.
149. Perraud O.; Robert V.; Gornitzka H.; Martinez A., Dutasta J.-P. *Angew. Chem. Int. Ed.*, **2012**, *51*, 504−508.
150. Zhang D.; Gao G.; Guy L.; Robert V.; Dutasta J.-P.; Martinez A. *Chem. Commun.*, **2015**, *51*, 2679−2682.
151. Molina P.; Zapata F.; Caballero A. *Chem. Rev.*, **2017**, *117*, 9907−9972.
152. Busschaert N.; Caltagirone C.; van Rossom W.; Gale P. A. *Chem. Rev.*, **2015**, *115*, 8038−8155.
153. Perraud O.; Robert V.; Martinez A.; Dutasta J.-P. *Chem. Eur. J.*, **2011**, *17*, 4177−4182.
154. Zhang D.; Chatelet B.; Serrano E.; Perraud O.; Dutasta J.-P.; Robert V.; Martinez A. *ChemPhysChem*, **2015**, *16*, 2931−2935.
155. Li Z.; Liu Z.; Sun H.; Gao C. *Chem. Rev.*, **2015**, *115*, 7046−7117.
156. Ranguin R.; Jean-Marius C.; Yacou C.; Gaspard S.; Feidt C.; Rychen G.; Delannoy M. Environ. *Sci. Pollut. Res.*, **2020**, *27*, 41093−41104.
157. Long A.; Lefevre S.; Guy L.; Robert V.; Dutasta J.-P.; Chevallier M. L.; Della-Negra O.; Saaidi P.-L.; Martinez A. *New J. Chem.*, **2019**, *43*, 10222−10226.
158. Jarosz S. *J. Carbohydr. Chem.*, **2015**, *34*, 365−387.
159. Arduini A.; Calzavacca F.; Demuru D.; Pochini A.; Secchi A. *J. Org. Chem.*, **2004**, *69*, 1386−1388.
160. Łukasik B.; Milczarek J.; Pawlowska R.; Żurawiński R.; Chworos A. *New. J. Chem.*, **2017**, *41*, 6977−6980.
161. Hancock R. D.; Martell A. E. *Chem. Rev.*, **1989**, *89*, 1875−1914.
162. Schulze B.; Schubert U. S. *Chem. Soc. Rev.*, **2014**, *43*, 2522−2571.

OL | Organic Letters

Letter

Cite This: *Org. Lett.* 2019, 21, 6523−6528

pubs.acs.org/OrgLett

Synthesis of Cyclotriveratrylene-Sucrose-Based Capsules

Łukasz Szyszka, Piotr Cmoch, Aleksandra Butkiewicz, Mykhaylo A. Potopnyk,* and Sławomir Jarosz*

Institute of Organic Chemistry, Polish Academy of Sciences, Kasprzaka 44/52, 01-224 Warsaw, Poland

Supporting Information

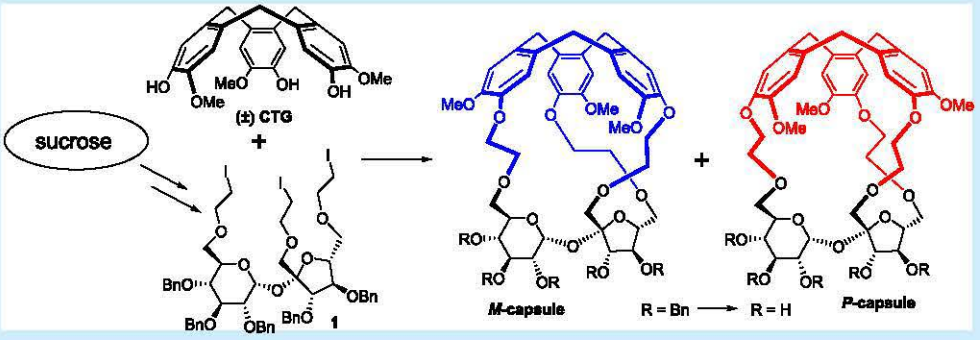

ABSTRACT: Cyclotriveratrylene (CTV) is a C_3-symmetrical macrocycle, which can be used as a chiral building block in the construction of supramolecular containers. Coupling of the CTV unit with a sucrose molecule gave enantiopure water-soluble (after deprotection) containers. The absolute configuration of the synthesized capsules was determined by NMR and ECD spectroscopies and DFT calculations.

DOI: 10.1021/acs.orglett.9b02451
Org. Lett. 2019, 21, 6523−6528

DOI: 10.1021/acs.orglett.9b02451
Org. Lett. 2019, 21, 6523−6528

DOI: 10.1021/acs.orglett.9b02451
Org. Lett. 2019, 21, 6523−6528

DOI: 10.1021/acs.orglett.9b02451
Org. Lett. 2019, 21, 6523−6528

DOI: 10.1021/acs.orglett.9b02451
Org. Lett. 2019, 21, 6523−6528

DOI: 10.1021/acs.orglett.9b02451
Org. Lett. 2019, 21, 6523−6528

Supporting Information for

Synthesis of Cyclotriveratrylene-Sucrose-Based Capsules

Łukasz Szyszka, Piotr Cmoch, Aleksandra Butkiewicz, Mykhaylo A. Potopnyk and Sławomir Jarosz

Institute of Organic Chemistry, Polish Academy of Sciences, ul. Kasprzaka 44/52, 01-224 Warsaw, Poland

Contents

1. General

Commercially available reagents and solvents were used as received. TLC was performed on Merck silica gel 60 F_{254} plates. Compounds were purified using automatic flash chromatography system Knauer with UV and ELSD detection and Grace Resolv or Reveleris cartridges. The NMR spectra were recorded with Bruker Avance II 400 MHz (at 400 MHz and 100 MHz for ^{1}H and ^{13}C NMR spectra, respectively), Varian VNMRS 500 MHz (at 500 MHz and 125 MHz for ^{1}H and ^{13}C NMR spectra, respectively) or Varian VNMRS 600 MHz (at 600 MHz and 150 MHz for ^{1}H and ^{13}C NMR spectra, respectively) spectrometers for solutions in $CDCl_3$, acetone-d_6, CD_3OD or CD_3CN, and TMS as the internal standard at 298 K. All significant resonances were assigned by COSY (^{1}H-^{1}H), HSQC (^{1}H-^{13}C) and HMBC (^{1}H-^{13}C) correlations. Mass spectra were measured with Synapt G2-S HDMS (*Waters Inc*) mass spectrometer equipped with an electrospray ion source and q-TOF type mass analyzer. Optical rotations were measured with a Jasco P 2000 apparatus in $CHCl_3$ or MeOH with a sodium lamp at r.t. (c~1). Elemental analyses were obtained with a Perkin–Elmer 2400 CHN analyzer. The ECD and UV spectra of ***P*-8** and ***M*-8** were recorded at room temperature in MeCN (for UV-spectroscopy, Fluka) on a Jasco J-715 spectropolarimeter with concentrations of 7.0×10^{-5} M in 0.1 cm quartz cell. All spectra were recorded using a 100 nm/min scanning speed, a step size of 0.2 nm, a bandwidth of 1 nm, a response time of 0.5 s, and an accumulation of 5 scans. The baseline of the spectra was corrected by subtracting the spectrum of the pure solvent recorded under the same conditions.

2. Computational details

First, the conformational analysis of ***M*-8** and ***P*-8** was performed by using Conflex 7 program[1] with the MMFF94s force field and 5 kcal/mol energy window. Next, ten most stable conformers for each ***P*-8** and ***M*-8** molecules were optimized at the CAM-B3LYP/SVP/PCM (MeCN) level.[2] The stable structures were found by ascertaining that all the harmonic frequencies were real and the relative abundances were calculated on the ΔG values relative to the most stable conformer. The Electronic Absorption EA and ECD spectra were calculated for all conformers with a population higher than 1% taking into account the lowest 150 singlet states. Finally, the EA and ECD spectra were averaged taking into account the ΔG values at room temperature and plotted with Gaussian bandshape and 0.20 eV half-height width. All calculations were performed using the Gaussian 16 package of programs.[3]

3. Synthesis

3.1. Synthesis of 1-*O*-allyl-vanillyl alcohol (S1)

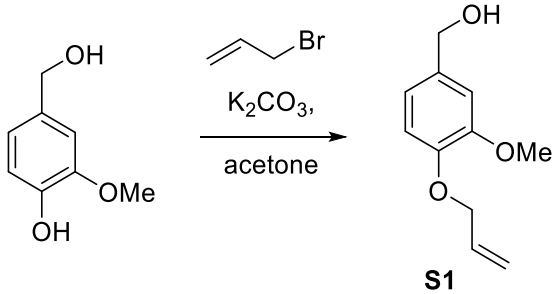

S1

1-*O*-allyl-vanillyl alcohol (**S1**) was prepared according to the literature procedure.[4] To the solution of vanillyl alcohol (5 g, 0.032 mol) in acetone (25 mL), K_2CO_3 (4.5 g, 0.032 mol)

and allyl bromide (3.3 mL, 0.038 mol) were added. The mixture was stirred under reflux overnight. Afterwards, acetone was removed under vacuum and the residue was partitioned between CH_2Cl_2 (50 mL) and water (30 mL). The organic phase was then dried over Na_2SO_4 and concentrated. The crude product was purified by crystallization from methyl *tert*-butyl ether/hexanes obtaining **S1** (6 g, 0.031 mol, 95%) as white crystals. ^{1}H NMR (400 MHz, $CDCl_3$) δ: 6.93 (s, 1H), 6.85 (s, 2H), 6.02–6.13 (m, 1H), 5.39 (dd, *J* = 1.5 Hz, 17.3 Hz, 1H), 5.28 (dd, *J* = 1.4 Hz, 10.5 Hz, 1H), 4.58–4.62 (m, 4H), 3.88 (s, 3H), 1.76 (s, OH) ppm. ^{13}C{H} NMR (100 MHz, $CDCl_3$) δ: 149.62, 147.54, 134.01, 133.31, 119.26, 117.89, 113.44, 110.88, 69.95, 65.24, 55.88 ppm. HRMS (ESI-TOF) calcd for $C_{11}H_{14}O_3Na$ $[M + Na]^+$: 217.0841, found: 217.0836. ^{1}H and ^{13}C NMR spectra were consistent with those previously reported in the literature.[4]

3.2. Synthesis of cyclotri-1-*O*-allyl-vanillyl alcohol (S2)

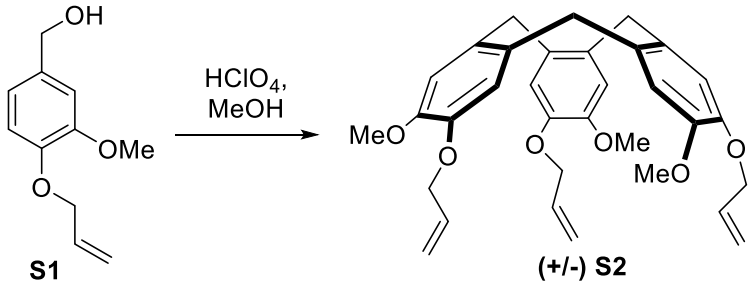

Racemic compound **S2** was prepared according to a modified literature procedure.[4] To the cooled to 0 °C solution of **S1** (11.1 g, 0.057 mol) in MeOH (66.6 mL), 65% aqueous $HClO_4$ (33.3 mL) was added dropwise, the reaction mixture was allowed to reach room temperature, and stirred for 20 h. Then it was diluted with CH_2Cl_2 (60 mL), cooled to 0 °C, and 50% aq. NaOH was carefully added dropwise as its color changed from pink to yellow. The layers were separated and the aqueous one was washed with CH_2Cl_2 (3× 30 mL). Combined organic phases were washed with water (80 mL), then brine (50 mL), dried over Na_2SO_4, and concentrated under reduced pressure. The resulting residue was suspended in Et_2O (50 mL) and stirred for 4h before being filtered off. The solid was washed with Et_2O (3 × 10 mL) and dried in high vacuum. Pure racemic compound **12** (5.22 g, 0.01 mol, 52 %) was obtained as a white solid. ^{1}H NMR (400 MHz, $CDCl_3$) δ: 6.85 (s, 3H), 6.79 (s, 3H), 6.01–6.11 (m, 3H), 5.37 (d, *J* = 17.2 Hz, 3H), 5.25 (d, *J* = 10.7 Hz, 3H), 4.74 (d, *J* = 13.7 Hz, 3H), 4.53–4.64 (m, 6H) 3.83 (s, 9H), 3.51 (d, *J* = 13.8 Hz, 3H) ppm. ^{13}C{H} NMR (100 MHz, $CDCl_3$) δ: 148.24, 146.79, 133.77, 132.36, 131.77, 117.47, 115.66, 113.69, 70.23, 56.13, 36.52 ppm. HRMS (ESI-TOF) calcd for $C_{33}H_{36}O_6Na$ $[M + Na]^+$: 551.2410, found: 551.2407. ^{1}H and ^{13}C NMR spectra were consistent with those previously reported in the literature.[4]

3.3. Cyclotriguaiacylene (7)

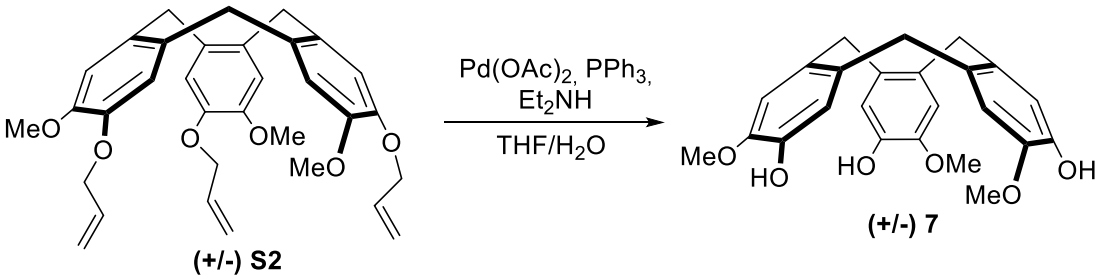

Racemic compound **7** was prepared according to a modified literature procedure.[5] This reaction was conducted under an argon atmosphere. To a solution of **S2** (9.0 g, 0.017 mol) in THF (225 mL) and H_2O (45 mL), $Pd(OAc)_2$ (572.5 mg, 2.55 mmol), PPh_3 (2.0 g, 7.65 mmol), and diethylamine (90 mL) were added, and the mixture was stirred for 4 h at 80 °C. After removal of solvents under vacuum, ethyl acetate (100 mL) was added, the dark insoluble residue was filtered and washed with ethyl acetate. The resulting filtrate was washed with water (100 mL) and then with brine (100 mL). Combined organic phases were dried over Na_2SO_4 and concentrated. The resulting yellow solid was washed with ether (3 × 50 mL) and recrystallized from dichloromethane/hexanes giving the desired product **7** (4.52 g, 0.011 mol, 65%) as off-white powder. ^{1}H NMR (500 MHz, acetone-d_6): δ = 6.99 (s, 3H), 6.93 (s, 3H), 4.74 (d, J = 13.6 Hz, 3H), 3.80 (s, 9H), 3.50 (d, J = 13.6 Hz, 3H) ppm. ^{13}C{H} NMR (125 MHz, acetone-d_6): δ = 146.81, 145.83, 133.86, 132.00, 117.15, 114.24, 56.54, 36.47 ppm. HRMS (ESI-TOF) calcd for $C_{24}H_{24}O_6Na$ $[M + Na]^+$: 431.1471, found: 431.1472. ^{1}H and ^{13}C NMR spectra were consistent with those previously reported in the literature.[5]

3.4. 1',6,6'-Tri-*O*-*tert*-butyldimethylsilylsucrose (S3)

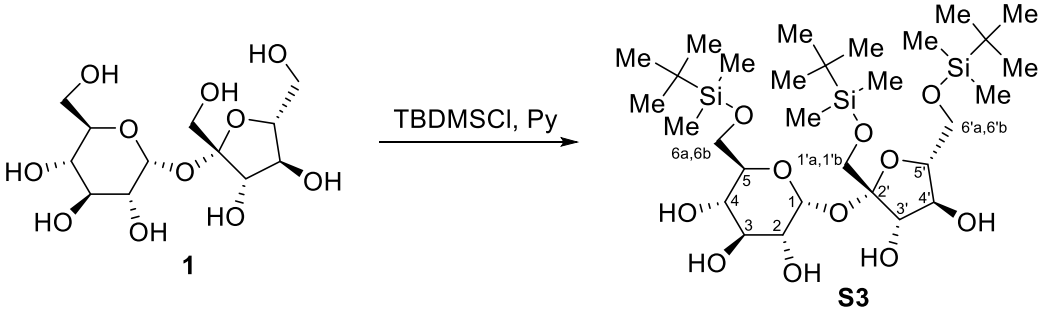

Sucrose (**1**, 10 g, 0.029 mol) was dissolved in boiling pyridine (200 mL). After cooling to room temperature, a solution of *tert*-butyldimethylsilyl chloride (16.5 g, 0.109 mol) in pyridine (100 mL) was added dropwise during 30 min and the mixture was stirred for 24 h at 60 °C. Pyridine was evaporated and the products were isolated by column chromatography (hexanes/ethyl acetate = 1:2 to 100% ethyl acetate) to afford compound **S3** (13.0 g, 0.019 mol, 65 %) as a white solid. $[\alpha]_D$ = +50.4 (MeOH). ^{1}H NMR (600 MHz, CD_3OD): δ = 5.39 (d, $J_{1,2}$ = 3.9 Hz, 1H, H-1), 4.17 (d, $J_{3',4'}$ = 8.7 Hz, 1H, H-3'), 3.87–3.92 (m, 2H, H-4', H-6'a), 3.81–3.86 (m, 3H, H-6'b, H-6a, H-6b), 3.78 (m, 1H, H-5), 3.70 (d, $J_{1'a,1'b}$ = 11.2 Hz, 1H, H-1'a), 3.68 (m, 1H, H-5'), 3.66 (d, 1H, H-1'b), 3.61 (dd, $J_{3,2}$ = 9.8 Hz, $J_{3,4}$ = 9.0 Hz, 1H, H-3), 3.54 (dd, $J_{4,5}$ = 9.8 Hz, 1H, H-4), 3.32 (dd, 1H, H-2), 0.912 (s, 9H, ^{t}Bu), 0.909 (s, 9H, ^{t}Bu), 0.900 (s, 9H, ^{t}Bu), 0.81–0.95 (m, 18H, 6 × SiCH_3) ppm. ^{13}C{H} NMR (150 MHz, CD_3OD): δ

= 105.55 (C-2'), 93.25 (C-1), 83.86 (C-5'), 77.47 (C-3'), 75.80 (C-4'), 74.98 (C-3), 74.26 (C-5), 73.21 (C-2), 71.34 (C-4), 65.86 (C-6'), 64.27 (C-1'), 64.00 (C-6), 26.61 (triple intensity, 3C-^{t}Bu), 26.50 (triple intensity, 3C-^{t}Bu), 26.44 (triple intensity, 3C-^{t}Bu), 19.44 (C_{quat}, ^{t}Bu), 19.21 (C_{quat}, ^{t}Bu), 19.18 (C_{quat}, ^{t}Bu), -4.84, -4.84, -4.93, -4.97, -5.05, -5.22 (6 × *C*H$_3$-Si) ppm. HRMS (ESI-TOF) calcd for $C_{30}H_{64}O_{11}Si_3Na$ $[M + Na]^+$: 707.3654, found: 707.3632. Anal. calcd for $C_{30}H_{64}O_{11}Si_3$: C, 52.60; H, 9.42; found: C, 52.59; H, 9.27.

3.5. 1',6,6'-Tri-*O*-*tert*-butyldimethylsilyl-2,3,3',4,4'-penta-*O*-benzylsucrose (2)

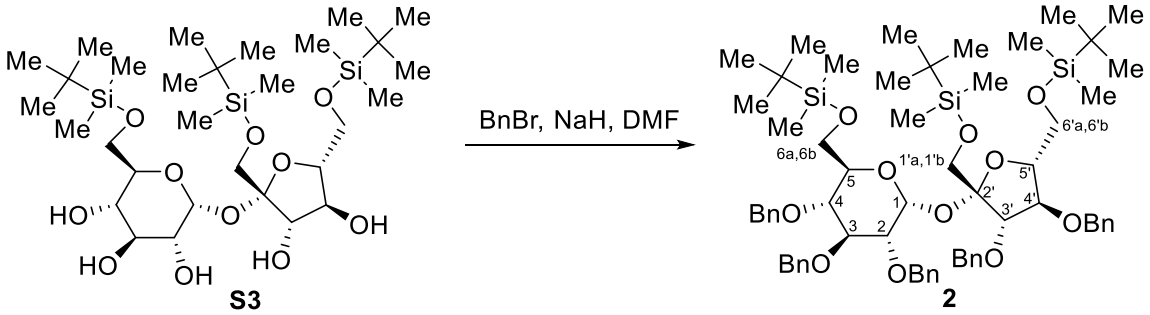

Sodium hydride (60% dispersion in mineral oil, 6.47 g, 161.7 mmol) was added portionwise at 0–5 °C to a stirred solution of compound **S3** (10.55 g, 15.4 mmol) in DMF (385 mL) and the mixture was stirred at room temperature for 30 min. Benzyl bromide (19.2 mL, 161.7 mmol) was added dropwise during 20 min and the mixture was stirred overnight. Excess of hydride was decomposed by careful addition of methanol (20 mL) and the mixture was partitioned between saturated aq. NH_4Cl (200 mL) and diethyl ether (300 mL). The layers were separated and the aqueous one was extracted with diethyl ether (3 × 200 mL). Combined organic solutions were dried over Na_2SO_4, concentrated, and the resulting residue was purified by column chromatography (hexanes/CH_2Cl_2 = 4:1 to 1:1) to afford pure product **2** (9.6 g, 55 %) as a colorless oil. $[\alpha]_D$ = +30.3 ($CHCl_3$). ^{1}H NMR (600 MHz, $CDCl_3$): δ = 7.37–7.53 (m, 25H, 25 × H-Ph), 6.06 (d, $J_{1,2}$ = 3.7 Hz, 1H, H-1), 5.07 (d, *J* = 10.7 Hz, 1H, benzylic H), 5.01 (d, *J* = 11.0 Hz, 1H, benzylic H), 4.93 (d, *J* = 10.7 Hz, 1H, benzylic H), 4.91 (d, *J* = 11.8 Hz, 1H, benzylic H), 4.90 (d, *J* = 11.1 Hz, 1H, benzylic H), 4.90 (d, *J* = 11.0 Hz, 1H, benzylic H), 4.84 (d, *J* = 11.0 Hz, 1H, benzylic H), 4.79 (d, *J* = 11.7 Hz, 1H, benzylic H), 4.74 (d, *J* = 11.0 Hz, 1H, benzylic H), 4.69 (d, *J* = 11.0 Hz, 1H, benzylic H), 4.65 (d, $J_{3',4'}$ = 8.2 Hz, 1H, H-3'), 4.46 (dd, $J_{4',3'}$ = 8.2 Hz, $J_{4',5'}$ = 8.0 Hz, 1H, H-4'), 4.10 (dd, $J_{3,2}$ = 9.6 Hz, $J_{3,4}$ = 9.1 Hz, 1H, H-3), 4.04–4.07 (m, 2H, H-5, H-6'a), 3.97–4.01 (m, 2H, H-5', H-6'b), 3.91 (d, $J_{1'a,1'b}$ = 11.1 Hz, 1H, H-1'a), 3.86 (dd, $J_{4,5}$ = 10.0 Hz, $J_{4,3}$ = 9.1 Hz, 1H, H-4), 3.78 (d, $J_{1'b,1'a}$ = 11.1 Hz, 1H, H-1'b), 3.73 (dd, $J_{6a,6b}$ = 11.7 Hz, $J_{6a,5}$ = 2.2 Hz, 1H, H-6a), 3.65 (dd, $J_{2,1}$ = 3.7 Hz, $J_{2,3}$ = 9.6 Hz, 1H, H-2), 3.59 (dd, $J_{6b,6a}$ = 10.7 Hz, 1H, H-6b), 1.05 (s, 9H, ^{t}Bu), 1.05 (s, 9H, ^{t}Bu), 1.02 (s, 9H, ^{t}Bu), 0.23 (s, 3H, SiC*H*$_3$), 0.21 (s, 3H, SiC*H*$_3$), 0.21 (s, 3H, SiC*H*$_3$), 0.20 (s, 3H, SiC*H*$_3$), 0.15 (s, 3H, SiC*H*$_3$), 0.14 (s, 3H, SiC*H*$_3$) ppm. ^{13}C{H} NMR (150 MHz, $CDCl_3$): δ = 139.26, 139.22, 138.83, 138.72, 138.30 (C_{quat}, 5 × C-Ph), 127.50–128.46 (m, 25 × C-Ph), 104.53 (C-2'), 88.94 (C-1), 83.17 (C-3'), 82.32 (C-3), 81.11 (C-4'), 80.72 (C-5'), 80.60 (C-2), 77.41 (C-4), 75.83, 74.86, 73.27, 72.79, 72.08 (5 × O*C*H$_2$Ph), 71.53 (C-5), 65.96 (C-1'), 63.57 (C-6'), 61.66 (C-6), 26.14 (triple intensity, 3C-^{t}Bu), 26.13 (triple intensity, 3C-^{t}Bu), 26.07 (triple intensity, 3C-^{t}Bu),18.52, 18.45, 18.43 (3 × C_{quat}, ^{t}Bu), -4.91, -5.04, -5.10, -5.24, -5.24, -5.28 (6 × Si*C*H$_3$) ppm. HRMS (ESI-TOF) calcd for $C_{65}H_{94}O_{11}Si_3Na$ $[M + Na]^+$:

1157.6002, found: 1157.6008. Anal. calcd for $C_{67}H_{94}O_{12}Si_3$ ($C_{65}H_{94}O_{11}Si_3$+ H_2O): C, 67.83; H, 8.54; found: C, 67.89; H, 8.42.

3.6. 2,3,3',4,4'-Penta-*O*-benzylsucrose (3)

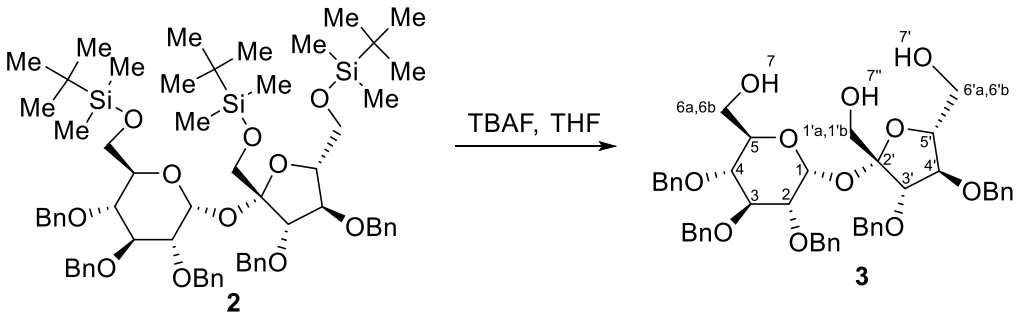

To a solution of **2** (7 g, 6.16 mmol) in THF (30 mL), a 1M TBAF solution in THF (27.7 mL) was added and the mixture was stirred for 24 h at 60 °C. The solvent was evaporated *in vacuo* and the residue was purified by column chromatography (hexanes/ethyl acetate = 4:1 to 1:2) to give pure triol **3** (3.8 g, 78 %) as a colorless oil. $[\alpha]_D$ = +18.8 ($CHCl_3$). ^{1}H NMR (600 MHz, $CDCl_3$): δ = 7.22–7.42 (m, 25H, 25 × H-Ph), 5.25 (d, $J_{1,2}$ = 3.5 Hz, 1H, H-1), 4.92 (d, *J* = 11.7 Hz, 1H, benzylic H), 4.87 (d, *J* = 11.0 Hz, 1H, benzylic H), 4.83 (d, *J* = 11.5 Hz, 1H, benzylic H), 4.80 (s, 2H, benzylic H), 4.69 (d, *J* = 11.6 Hz, 1H, benzylic H), 4.64 (d, *J* = 11.1 Hz, 1H, benzylic H), 4.62 (d, *J* = 11.7 Hz, 1H, benzylic H), 4.56 (d, *J* = 11.7 Hz, 1H, benzylic H), 4.49 (d, *J* = 11.6 Hz, 1H, benzylic H), 4.11 (m, 1H, H-3'), 4.09 (m, 1H, H-4'), 4.07 (m, 1H, H-5), 4.02 (dd, $J_{3,2}$ = 9.4 Hz, $J_{3,4}$ = 9.4 Hz, 1H, H-3), 3.98 (dd, $J_{5',4'}$ = 9.2 Hz, $J_{5',6'a}$ = 4.5 Hz, 1H, H-5'), 3.89 (dd, $J_{7',6'a}$ = 10.9 Hz, $J_{7',6'b}$ = 3.3 Hz, 1H, H-7'), 3.83 (d, $J_{6'a,6'b}$ = 11.8 Hz, 1H, H-6a), 3.68 (dd, $J_{6b,6a}$ = 12.0 Hz, $J_{6b,5}$ = 3.5 Hz, 1H, H-6b), 3.61 (s, 2H, H-1'a, H-1'b), 3.55–3.59 (m, 2H, H-2, H-6'a), 3.49 (dd, $J_{4,5}$ = 9.6 Hz, $J_{4,3}$ = 9.4 Hz, 1H, H-4), 3.39 (dd, $J_{6'b,7'}$ = 10.9 Hz, $J_{6'b,6'a}$ = 11.3 Hz, 1H, H-6'b), 3.25 (s, 1H, H-7''), 2.63 (s, 1H, H-7) ppm. ^{13}C{H} NMR (150 MHz, $CDCl_3$): δ = 138.37, 138.35, 138.19, 137.81, 136.74 (C_{quat}, 5 × C-Ph), 127.72–128.91 (m, 25 × C-Ph), 106.05 (C-2'), 91.09 (C-1), 86.35 (C-3'), 82.33 (C-5'), 82.23 (C-4'), 81.99 (C-3), 78.83 (C-2), 77.77 (C-4), 75.69, 75.11, 75.11 (3 × O<u>*C*</u>H_2Ph), 73.87 (C-5), 72.89, 72.50 (2 × O<u>*C*</u>H_2Ph), 64.83 (C-6'), 61.71 (C-6), 60.94 (C-1') ppm. HRMS (ESI-TOF) calcd for $C_{47}H_{52}O_{11}Na$ $[M + Na]^+$: 815.3407, found: 815.3391. Anal. calcd for $C_{47}H_{52}O_{11}$: C, 71.19; H, 6.61; found: C, 70.98; H, 6.68.

3.7. 2,3,3',4,4'-Penta-*O*-benzyl-1',6,6'-tri-*O*-(2-*tert*-butoxy-2-oxoethyl)-sucrose (4)

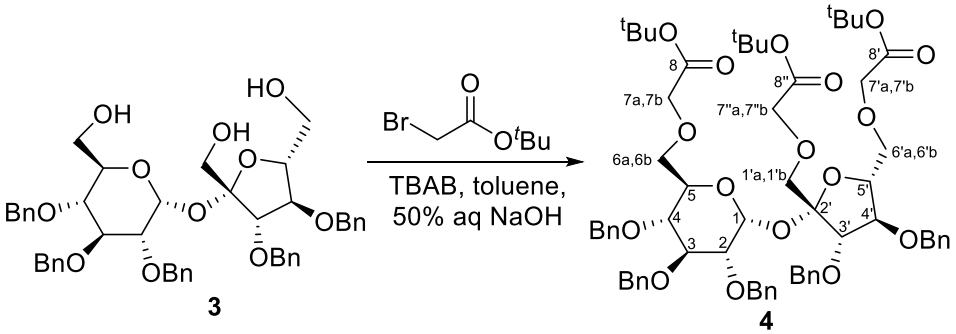

To a solution of triol **3** (280 mg, 0.35 mmol) in toluene (8 mL), Bu_4NBr (22.8 mg, 0.07 mmol) was added followed by 50% aqueous NaOH (8 mL). Next, *tert*-butyl bromoacetate (0.31 mL, 2.12 mmol) was added and the mixture was vigorously stirred at room temperature for 24 h. The layers were separated and the aqueous one extracted with ether (3 × 15 mL). Combined organic solutions were washed with water (2 × 10 mL) and brine (10 mL), dried over Na_2SO_4, concentrated, and the residue was purified by flash chromatography (hexanes/ethyl acetate = 90:10) to afford pure product **4** (224 mg, 0.2 mmol, 56%) as a yellowish oil. $[\alpha]_D$ = +33.7 ($CHCl_3$). ^{1}H NMR (600 MHz, $CDCl_3$): δ = 7.21–7.37 (m, 25H, 25 × H-Ph), 5.69 (d, $J_{1,2}$ = 3.6 Hz, 1H, H-1), 4.91 (d, J = 11.0 Hz, 1H, benzylic H), 4.86 (d, J = 10.8 Hz, 1H, benzylic H), 4.84 (d, J = 11.0 Hz, 1H, benzylic H), 4.77 (d, J = 11.0 Hz, 1H, benzylic H), 4.72 (d, J = 11.5 Hz, 1H, benzylic H), 4.70 (d, J = 12.2 Hz, 1H, benzylic H), 4.67 (d, J = 11.3 Hz, 1H, benzylic H), 4.62 (d, J = 11.8 Hz, 1H, benzylic H), 4.59 (d, J = 11.7 Hz, 1H, benzylic H), 4.58 (d, J = 11.7 Hz, 1H, benzylic H), 4.50 (d, $J_{3',4'}$ = 7.4 Hz, 1H, H-3'), 4.10–4.14 (m, 2H, H-4', H-5'), 4.06 (m, 1H, H-5), 4.04 (d, $J_{7''a,7''b}$ = 16.5 Hz, 1H, H-7''a), 4.03 (d, $J_{7'a,7'b}$ = 16.5 Hz, 1H, H-7'a), 3.96 (d, $J_{7'b,7'a}$ = 16.5 Hz, 1H, H-7'b), 3.94 (dd, $J_{3,4}$ = 9.8 Hz, $J_{3,2}$ = 9.7 Hz, 1H, H-3), 3.92 (d, $J_{7''b,7''a}$ = 16.5 Hz, 1H, H-7''b), 3.90 (d, $J_{1'a,1'b}$ = 11.1 Hz, 1H, H-1'a), 3.89 (d, $J_{7a,7b}$ = 16.4 Hz, 1H, H-7a), 3.85 (d, $J_{7b,7a}$ = 16.4 Hz, 1H, H-7b), 3.79 (dd, $J_{6'a,6'b}$ = 10.4 Hz, $J_{6'a,5'}$ = 6.1 Hz, 1H, H-6'a), 3.76 (dd, $J_{6'b,6'a}$ = 10.4 Hz, $J_{6'b,5'}$ = 3.6 Hz, 1H, H-6'b), 3.65 (dd, $J_{4,3}$ = 9.8 Hz, $J_{4,5}$ = 9.3 Hz, 1H, H-4), 3.61 (dd, $J_{6a,6b}$ = 10.8 Hz, $J_{6a,5}$ = 3.2 Hz, 1H, H-6a), 3.54 (dd, $J_{2,3}$ = 9.7 Hz, $J_{2,1}$ = 3.6 Hz, 1H, H-2), 3.52 (d, $J_{1'b,1'a}$ = 11.1 Hz, 1H, H-1'b), 3.47 (dd, $J_{6b,6a}$ = 10.8 Hz, $J_{6b,5}$ = 1.7 Hz, 1H, H-6b), 1.45 (s, 9H, 9 × -$CO_2C(C\underline{H}_3)_3$), 1.44 (s, 9H, 9 × -$CO_2C(C\underline{H}_3)_3$), 1.43 (s, 9H, 9 ×-$CO_2C(C\underline{H}_3)_3$) ppm. ^{13}C{H} NMR (150 MHz, $CDCl_3$): δ = 169.33, 169.29, 169.19 (C-8, C-8', C-8"), 138.96, 138.81, 138.39, 138.39, 138.32 (C_{quat}, 5 × C-Ph), 127.36–128.23 (m, 25 × C-Ph), 104.46 (C-2'), 89.96 (C-1), 83.85 (C-3'), 82.16 (C-5'), 81.91 (C-3), 81.42, 81.31, 81.19 (3 ×C_{quat}, $CO_2\underline{C}(CH_3)_3$), 79.59 (C-4'), 79.53 (C-2), 77.29 (C-4), 75.40, 74.70, 73.06 (3 × O$\underline{C}H_2$Ph), 72.62 (C-6'), 72.41 (C-1'), 72.40, 72.26 (2 × O$\underline{C}H_2$Ph), 70.54 (C-5), 69.72 (C-6), 69.09 (C-7''), 69.04 (C-7), 68.97 (C-7'), 28.10, 28.08, 28.08 (triple intensity, 9 × -$CO_2C(\underline{C}H_3)_3$) ppm. HRMS (ESI-TOF) calcd for $C_{65}H_{82}O_{17}Na$ $[M + Na]^+$: 1157.5450, found: 1157.5457. Anal. calcd for $C_{65}H_{82}O_{17}$: C, 68.76; H, 7.28; found: C, 68.76; H, 7.20.

3.8. 2,3,3',4,4'-Penta-*O*-benzyl-1',6,6'-tri-O-(2-hydroxyethyl)-sucrose (5)

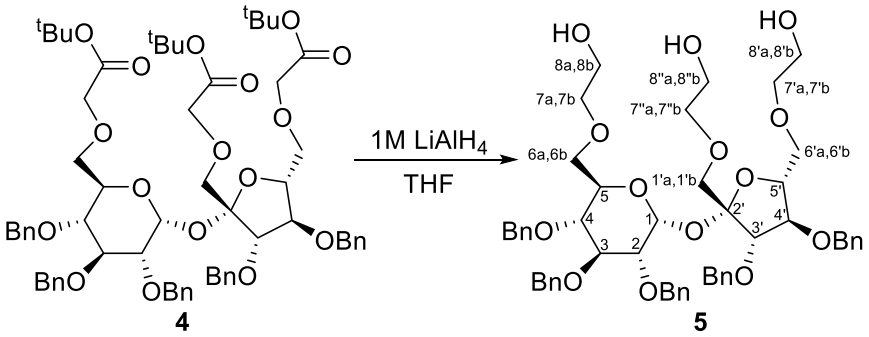

4 **5**

To the cooled to -78 °C solution of compound **4** (559 mg, 0.49 mmol) in dry THF (16 mL), 1M $LiAlH_4$ in THF (2.95 mL, 2.95 mmol) was added dropwise, the mixture was allowed to reach room temperature, and stirred additional 20 min at rt. Excess of hydride was carefully

decomposed with aqueous saturated Na_2SO_4 (5 mL) and then Celite was added. Next, the resulting residue was filtered and washed with ethyl acetate (3 × 10 mL). The organic solution was dried over Na_2SO_4, concentrated, and purified by flash chromatography (hexanes/ethyl acetate = 1:1 to 1:4) to give pure product **5** (408 mg, 0.44 mmol, 90%) as a yellowish oil. $[\alpha]_D$= +37.9 ($CHCl_3$). ^{1}H NMR (600 MHz, $CDCl_3$): δ = 7.21–7.38 (m, 25H, 25 × H-Ph), 6.12 (d, $J_{1,2}$ = 3.9 Hz, 1H, H-1), 4.98 (d, J = 11.0 Hz, 1H, benzylic H), 4.82 (d, J = 11.1 Hz, 2H, 2 × benzylic H), 4.74 (d, J = 11.2 Hz, 2H, 2 × benzylic H), 4.69 (dd, $J_{4',5'}$ = 8.6 Hz, $J_{4',3'}$ = 8.5 Hz, 1H, H-4'), 4.66 (s, 2H, 2 × benzylic H), 4.61 (d, J = 11.8 Hz, 1H, benzylic H), 4.59 (d, J = 11.1 Hz, 1H, benzylic H), 4.52 (d, J = 11.2 Hz, 1H, benzylic H), 4.30 (d, $J_{3',4'}$ = 8.5 Hz, 1H, H-3'), 4.15 (m, 1H, H-5), 3.92 (dd, $J_{3,2}$ = 9.3 Hz, $J_{3,4}$ = 9.2 Hz, 1H, H-3), 3.84–3.94 (m, 2H, H-5', H-6'a), 3.62–3.71 (m, 5H, H-4, H-1'a, H-8''a, H-8''b, H-8a), 3.61 (m, 2H, H-7''a, H-7''b), 3.55 (d, $J_{1'b,1'a}$ = 10.8 Hz, 1H, H-1'b), 3.52 (m, 1H, H-8b), 3.46 (dd, $J_{2,3}$ = 9.6 Hz, $J_{2,1}$ = 3.9 Hz, 1H, H-2), 3.42 (m, 1H, H-8'b), 3.38 (m, 1H, H-6'b), 3.24–3.35 (m, 7H, H-8'b, H-6a, H-6b, H-7a, H-7b, H-7'a, H-7'b) ppm. ^{13}C{H} NMR (150 MHz, $CDCl_3$): δ = 139.08, 138.68, 138.02, 137.95, 137.65 (C_{quat}, 5 × C-Ph), 127.34–128.54 (m, 25 × C-Ph), 103.57 (C-2'), 88.05 (C-1), 83.74 (C-3'), 81.92 (C-3), 79.01 (C-5'), 78.92 (C-4'), 78.76 (C-2), 77.03 (C-4), 75.27, 74.69 (2 × O<u>*C*</u>H_2Ph), 74.52 (C-1'), 73.16, 73.08 (2 × O<u>*C*</u>H_2Ph), 73.04 (C-7''), 72.94 (C-7), 72.25 (C-7'), 72.02 (O<u>*C*</u>H_2Ph), 70.61 (C-5), 68.44 (C-6'), 68.40 (C-6), 61.62, 61.61, 61.57 (C-8, C-8', C-8'') ppm. HRMS (ESI-TOF) calcd for $C_{53}H_{64}O_{14}Na$ [M + Na]$^+$: 947.4194, found: 947.4183. Anal. calcd for $C_{53}H_{64}O_{14}$: C, 68.81; H, 6.97; found: C, 68.75; H, 6.95.

3.9. 2,3,3',4,4'-Penta-*O*-benzyl-1',6,6'-tri-O-(2-iodoethyl)-sucrose (6)

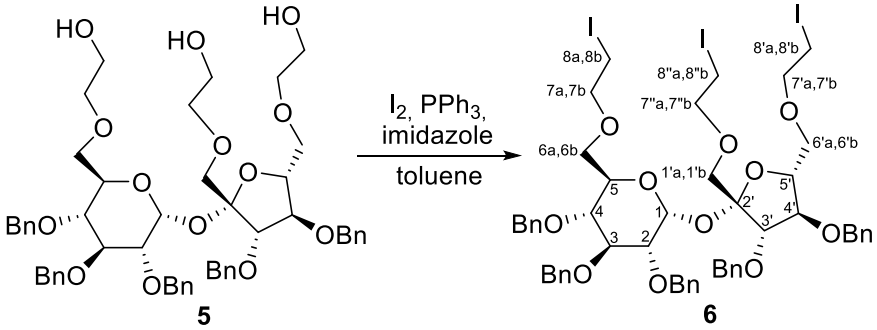

To a solution of triol **5** (702 mg, 0.759 mmol) in toluene (25 mL), PPh_3 (716 mg, 2.73 mmol) was added, the mixture was boiled under reflux for 15 min, and then cooled to 50 °C. Imidazole (310 mg, 4.55 mmol) was added, the mixture was allowed to reach room temperature, and the solution of iodine (693 mg, 2.73 mmol) in toluene (20 mL) was added dropwise during 20 min. After another 20 min, the excess of iodine was decomposed with saturated $Na_2S_2O_3$ (5 mL). Water (20 mL) was added, the phases were separated, the aqueous one was extracted with ethyl acetate (2 × 20 mL) and combined organic phases were washed with water (30 mL), brine (30 mL), dried over Na_2SO_4 and concentrated. The resulting residue was purified by flash chromatography (hexanes/ethyl acetate = 9:1) to afford compound **6** (810 mg, 0.64 mmol, 85%) as a colorless oil. $[\alpha]_D$ = +33.8 ($CHCl_3$). ^{1}H NMR (600 MHz, $CDCl_3$): δ = 7.24–7.37 (m, 25H, 25 × H-Ph), 5.65 (d, $J_{1,2}$ = 3.5 Hz, 1H, H-1), 4.94 (d, J = 10.9 Hz, 1H, benzylic H), 4.90 (d, J = 11.1 Hz, 1H, benzylic H), 4.80 (d, J = 10.9 Hz, 1H, benzylic H), 4.79 (d, J = 11.4 Hz, 1H, benzylic H), 4.68 (d, J = 11.7Hz, 1H, benzylic H), 4.67 (d, J = 11.5 Hz, 1H, benzylic H), 4.66 (d, J = 11.8 Hz, 1H, benzylic H), 4.64 (d, J = 11.5

Hz, 1H, benzylic H), 4.63 (d, J = 11.8 Hz, 1H, benzylic H), 4.59 (d, J = 11.8 Hz, 1H, benzylic H), 4.45 (d, $J_{3',4'}$ = 7.3 Hz, 1H, H-3'), 4.12 (dd, $J_{4',3'}$ = 7.3 Hz, $J_{4',5'}$ = 7.3 Hz, 1H, H-4'), 4.07 (m, 1H, H-5'), 4.04 (m, 1H, H-5), 3.95 (dd, $J_{3,2}$ = 9.4 Hz, $J_{3,4}$ = 9.3 Hz, 1H, H-3), 3.65–3.73 (m, 7H, H-7a, H-7'a, H-7''a, H-7''b, H-6'a, H-6'b, H-1'a), 3.64 (m, 1H, H-4), 3.57 (m, 1H, H-6a), 3.51–3.56 (m, 3H, H-7b, H-7'b, H-2), 3.46 (d, $J_{1'b,1'a}$ = 11.0 Hz, 1H, H-1'b), 3.39 (dd, $J_{6b,6a}$ = 10.7 Hz, $J_{6b,5}$ = 1.4 Hz, 1H, H-6b), 3.08–3.22 (m, 6H, H-8a, H-8b, H-8'a, H-8'b, H-8''a, H-8''b) ppm. $^{13}C\{H\}$ NMR (150 MHz, $CDCl_3$): δ = 138.76, 138.59, 138.23, 138.16, 138.13 (C_{quat}, 5 × C-Ph), 127.53–128.38 (m, 25 × C-Ph), 104.38 (C-2'), 90.10 (C-1), 83.67 (C-3'), 82.18 (C-4'), 81.95 (C-3), 79.83 (C-2), 79.59 (C-5'), 77.39 (C-4), 75.54, 74.94, 73.13, 72.67, 72.53 (5 × O<u>C</u>H_2Ph), 72.16 (C-7'), 72.06 (C-7), 71.95 (C-7"), 71.81 (C-6'), 71.67 (C-1'), 70.63 (C-5), 69.25 (C-6), 2.82, 2.80, 2.73 (C-8, C-8', C-8'') ppm. HRMS (ESI-TOF) calcd for $C_{53}H_{61}O_{11}I_3Na$ $[M + Na]^+$: 1277.1246, found: 1277.1244. Anal. calcd for $C_{53}H_{61}O_{11}I_3$: C, 50.73; H, 4.90; found: C, 50.72; H, 5.01.

3.10. General procedure for the synthesis of compounds *M*-8 and *P*-8

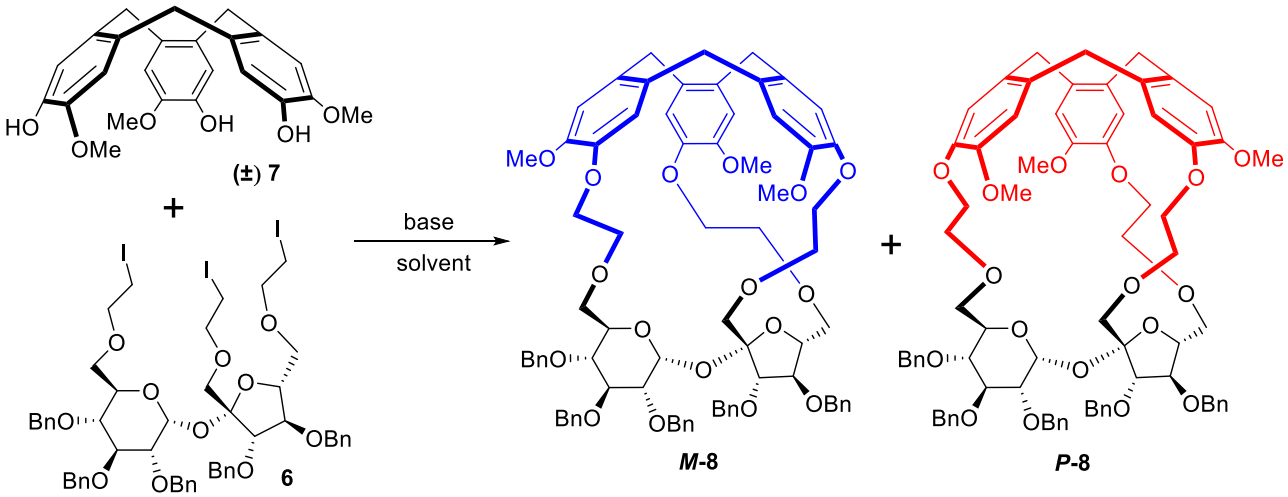

To a solution (0.002 M, 160 mL or 0.001 M, 320 mL) of ***rac*-7** (130 mg, 0.319 mmol) in dry solvent (acetone/acetonitrile/propionitrile/DMF), cesium carbonate (623 mg, 1.91 mmol) was added and the mixture was stirred at room temperature for 30 min under an argon atmosphere. The solution of compound **6** (400 mg, 0.319 mmol) in appropriate dry solvent (10 mL) was added dropwise during 40 min, the mixture was stirred at required temperature for 48-96 h (for details see Table 1 of the main text). After cooling to rt., the mixture was filtered through Celite and the solvents were removed under vacuum. The residue was dissolved in CH_2Cl_2 (20 mL) and washed with water (2 × 10 mL). The aqueous phases were extracted with CH_2Cl_2 (2 × 20 mL) and the combined organic solutions were washed with brine (20 mL), dried over Na_2SO_4, and concentrated. The resulting residue was purified by flash chromatography (hexanes/ethyl acetate = 4:1 to 3:1) to afford pure compounds ***M*-8** and ***P*-8** as colorless solids.

3.10.1. Characterization of compound *M*-8

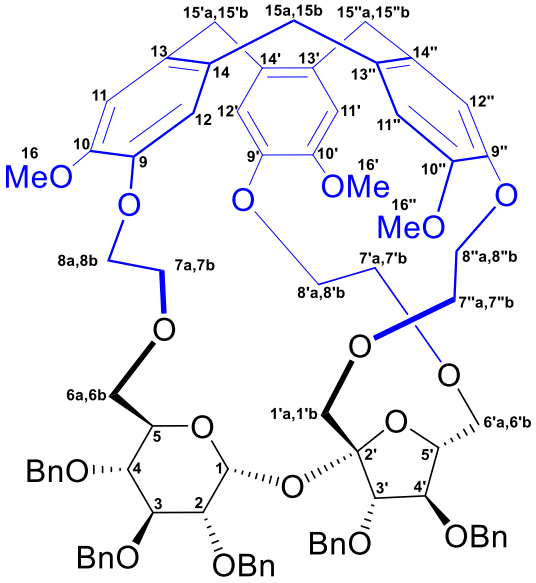

***M*-8**

$[\alpha]_D$= -60.7 ($CHCl_3$). ^{1}H NMR (600 MHz, CD_3CN): δ = 7.16–7.43 (m, 25H, 25 × H-Ph), 7.024 (s, 1H, H-12'), 7.009 (s, 1H, H-11), 6.972 (s, 1H, H-12), 6.963 (s, 1H, H-11'), 6.910 (s, 1H, H-11"), 6.837 (s, 1H, H-12"), 5.26 (d, $J_{1,2}$ = 3.1 Hz, 1H, H-1), 4.90 (d, *J*= 11.3 Hz, 1H, benzylic H), 4.75 (d, $J_{15"b,15"a}$ = 13.3 Hz, 1H, H-15"b), 4.74 (d, *J* = 11.3 Hz, 1H, benzylic H), 4.72 (d, *J* = 11.0 Hz, 1H, benzylic H), 4.72 (d, 1H, H-15'b), 4.69 (d, *J* = 11.2 Hz, 1H, benzylic H), 4.68 (d, $J_{15b,15a}$ = 13.7 Hz, 1H, H-15b), 4.65 (d, *J* = 11.8 Hz, 1H, benzylic H), 4.62 (d, *J* = 11.6 Hz, 1H, benzylic H), 4.59 (d, *J* = 11.0 Hz, 1H, benzylic H), 4.54 (d, *J* = 11.2 Hz, 1H, benzylic H), 4.49 (d, *J* = 11.8 Hz, 1H, benzylic H), 4.45 (d, *J* = 11.6 Hz, 1H, benzylic H), 4.37 (dt, $J_{8b,8a}$ = 13.0 Hz, $J_{8b,7}$ = 2.8 Hz, 1H, H-8b), 4.28 (dd, $J_{8"b,8"a}$ = 11.6 Hz, $J_{8"b,7"}$ = 7.0 Hz, 1H, H-8"b), 4.23 (m, 1H, H-8'b), 4.19 (m, 1H, H-8'a), 4.16 (m, 1H, H-8"a), 4.12 (m, 1H, H-8a), 3.97 (d, $J_{3',4'}$ = 6.6 Hz, 1H, H-3'), 3.97 (d, $J_{1'b,1'a}$ = 11.9 Hz, 1H, H-1'b), 3.94 (m, 1H, H-7"b), 3.79 (s, 3H, 3 × H-16"), 3.77 (dd, $J_{6a,6b}$ = 13.0 Hz, $J_{6a,5}$ = 2.4 Hz, 1H, H-6b), 3.74 (s, 3H, 3 × H-16), 3.74 (dd, $J_{7b,7a}$ = 13.3 Hz, $J_{7b,8}$ = 2.4 Hz, 1H, H-7b), 3.72 (s, 3H, 3 × H-16'), 3.72 (m, 1H, H-7"a), 3.65 (m, 1H, H-4'), 3.65 (m, 1H, H-3), 3.56 (m, 1H, H-7a), 3.53 (m, 1H, H-4), 3.52 (d, $J_{15"a,15"b}$ = 13.3 Hz, 1H, H-15"a), 3.50 (d, $J_{15'a,15'b}$ = 13.7 Hz ,1H, H-15'a), 3.49 (d, $J_{15a,15b}$ = 13.7 Hz, 1H, H-15a), 3.42 (d, $J_{1'a,1'b}$ = 11.9 Hz, 1H, H-1'a), 3.37 (dd, $J_{2,3}$ = 9.7 Hz, $J_{2,1}$ = 3.1 Hz, 1H, H-2), 3.36 (m, 1H, H-5'), 3.34 (m, 1H, H-5), 3.28 (m, 1H, H-7'b), 2.96 (dt, $J_{7'a,7'b}$ = 10.8 Hz, $J_{7'a,8}$ = 3.5 Hz, 1H, H-7'a), 2.89 (dd, $J_{6a,6b}$ = 13.0 Hz, $J_{6a,5}$ = 0.8 Hz, 1H, H-6a), 2.61 (dd, $J_{6'b,6'a}$ = 8.9 Hz, $J_{6'b,5'}$= 8.7 Hz, 1H, H-6'b), 1.59 (dd, $J_{6'a,6'b}$ = 8.9 Hz, $J_{6'a,5'}$ = 5.0 Hz, 1H, H-6'a) ppm. ^{13}C{H} NMR (150 MHz, CD_3CN): δ = 150.55 (C-10'), 149.75 (C-10), 148.06 (C-10"), 146.77 (C-9"), 145.60 (C-9), 145.03 (C-9'), 140.15, 140.00, 140.01, 139.87, 139.81 (C_{quat}, 5 × C-Ph), 135.15 (C-13'), 134.06 (C-13), 133.30 (C-14), 132.95 (C-14"), 131.91 (C-13"), 131.74 (C-14'), 128.21–129.33 (m, 25 ×C-Ph), 121.82 (C-12'), 117.41 (C-12), 114.96 (C-11), 114.14 (C-11'), 113.62 (C-12"), 113.04 (C-11"), 105.34 (C-2'), 91.64 (C-1), 86.59 (C-4'), 85.06 (C-3'), 82.22 (C-3), 81.81 (C-2), 80.54 (C-5'), 78.08 (C-4), 75.93, 75.34, 73.83 (3 × O<u>C</u>H_2Ph), 73.67 (C-6'), 73.22 (C-5), 72.47, 72.39 (2 × O<u>C</u>H_2Ph), 70.83 (C-1'), 70.76 (C-6), 70.65 (C-8"), 69.91 (C-7), 69.69 (C-8'), 69.21 (C-7"), 68.94 (C-8), 67.57 (C-7'), 56.89 (C-16), 56.39 (C-16'), 56.24 (C-16"), 36.32 (C-15"), 36.18 (C-15), 35.87 (C-15')

ppm. HRMS (ESI-TOF) calcd for $C_{77}H_{82}O_{17}Na$ $[M + Na]^+$: 1301.5450, found: 1301.5447. Anal. calcd for $C_{77}H_{82}O_{17}$: C, 72.28; H, 6.46; found: C, 72.26; H, 6.67.

3.10.2. Characterization of compound *P*-8

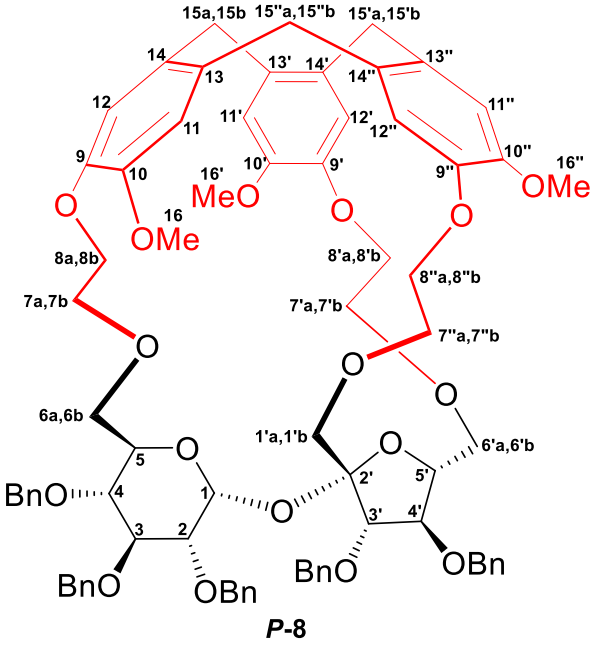

***P*-8**

$[\alpha]_D$= +101.4 ($CHCl_3$). ^1H NMR (600 MHz, CD_3CN): δ = 7.20–7.35 (m, 25H, 25 × H-Ph), 7.004 (s, 1H, H-11), 6.971 (s, 1H, H-12'), 6.919 (s, 1H, H-11''), 6.915 (s, 1H, H-11'), 6.902 (s, 1H, H-12), 6.896 (s, 1H, H-12''), 4.93 (d, $J_{1,2}$ = 3.5 Hz, 1H, H-1), 4.75 (d, $J_{15b,15a}$ = 13.3 Hz, 1H, H-15b), 4.74 (d, *J* = 11.3 Hz, 1H, benzylic H), 4.72 (d, *J* = 11.3 Hz, 1H, benzylic H), 4.70 (m, 1H, H-15'b), 4.66 (m, 2H, 2 × benzylic H), 4.65 (m, 1H, benzylic H), 4.65 (d, *J* = 11.3 Hz, 1H, benzylic H), 4.65 (d, $J_{15''b,15''a}$ = 13.5 Hz, 1H, H-15''b), 4.62 (d, *J*= 11.7 Hz, 1H, benzylic H), 4.55 (d, *J* = 11.3 Hz, 1H, benzylic H), 4.52 (d, *J*= 11.7 Hz, 1H, benzylic H), 4.47 (d, *J* = 11.3 Hz, 1H, benzylic H), 4.28 (ddd, $J_{8''b,8''a}$ = 12.3 Hz, $J_{8''b,7''a}$ = 6.1 Hz, $J_{8''b,7''b}$ = 1.5 Hz, 1H, H-8''b), 4.22 (m, 2H, H-8a, H-8b), 4.12 (d, $J_{3',4'}$ = 7.5 Hz, 1H, H-3'), 4.09 (ddd, $J_{8''a,8''b}$ = 12.3 Hz, $J_{8''a,7''a}$ = 6.2 Hz, $J_{8''a,7''b}$ = 2.0 Hz, 1H, H-8''a), 4.05 (m, 2H, H-8'a, H-8'b), 3.772 (s, 3H, 3 × H-16), 3.75 (m, 1H, H-7''b), 3.71 (dd, $J_{4'5'}$ = 7.6 Hz, $J_{4'3'}$ = 7.5 Hz, 1H, H-4'), 3.678 (s, 3H, 3 × H-16'), 3.653 (s, 3H, 3 × H-16''), 3.646 (m, 1H, H-3), 3.62 (m, 1H, H-7''a), 3.56 (m, 1H, H-7b), 3.49 (d, $J_{15a,15b}$ = 13.3 Hz, 1H, H-15a), 3.48 (d, $J_{15''a,15''b}$ = 13.5 Hz, 1H, H-15''a), 3.47 (m, 1H, H-7a), 3.47 (d, $J_{1'b,1'a}$ = 11.6 Hz, 1H, H-1'b), 3.46 (m, 1H, H-15'a), 3.456 (m, 1H, H-4), 3.436 (m, 1H, H-5), 3.42 (m, 1H, H-6b), 3.354 (dd, $J_{2,3}$ = 9.6 Hz, $J_{2,1}$ = 3.5 Hz, 1H, H-2), 3.32 (m, 1H, H-7'b), 3.21 (d, $J_{1'a,1'b}$ = 11.6 Hz, 1H, H-1'a), 3.20 (m, 1H, H-7'a), 3.14 (ddd, $J_{5',4'}$ = 7.6 Hz, $J_{5',6'a}$ = 6.6 Hz, $J_{5',6'b}$ = 4.5 Hz, 1H, H-5'), 2.47 (dd, $J_{6a,6b}$ = 11.6 Hz, $J_{6a,5}$ = 1.6 Hz, 1H, H-6a), 2.29 (dd, $J_{6'a,6'b}$ = 11.5 Hz, $J_{6'a,5'}$ = 6.6 Hz, 1H, H-6'a), 2.02 (dd, $J_{6'b,6'a}$ = 11.5 Hz, $J_{6'b,5'}$ = 4.5 Hz, 1H, H-6'b) ppm. $^{13}C\{H\}$ NMR (150 MHz, CD_3CN): δ = 150.39 (C-10'), 150.23 (C-10), 148.33 (C-10''), 146.47 (C-9''), 145.75 (C-9), 145.45 (C-9'), 140.15, 139.99, 139.92, 139.75, 139.68 (C_{quat}, 5 × C-Ph), 135.48 (C-13'), 134.01 (C-14), 133.88 (C-14''), 133.40 (C-13''), 132.47, 132.42 (C-13, C-14'), 128.31–129.29 (m, 25 × C-Ph), 122.32 (C-12'), 119.49 (C-12), 115.98 (C-11), 115.41 (C-12''), 113.92 (C-11'), 113.85 (C-11''), 104.22 (C-2'), 92.04 (C-1), 84.90 (C-3'), 84.61 (C-4'), 82.51 (C-3), 81.19 (C-2), 78.62 (C-5'), 78.17 (C-4), 75.83, 75.16, 73.90, 72.87 (4 × O<u>*C*</u>H_2Ph), 72.74 (C-

6'), 72.71 (O<u>*C*</u>H$_2$Ph), 71.83 (C-5), 70.63 (C-7'), 70.39 (C-1'), 70.17 (C-6), 69.96 (C-8'), 69.89 (C-7"), 69.46 (C-7), 68.09 (C-8), 66.94 (C-8"), 57.59 (C-16), 56.40 (C-16'), 56.11 (C-16"), 36.33 (C-15"), 36.20 (C-15), 35.95 (C-15') ppm. HRMS (ESI-TOF) calcd for $C_{77}H_{82}O_{17}Na$ $[M + Na]^+$: 1301.5450, found: 1301.5426. Anal. calcd for $C_{77}H_{82}O_{17}$: C, 72.28; H, 6.46; found: C, 72.30; H, 6.53.

3.11. Compound *M*-9

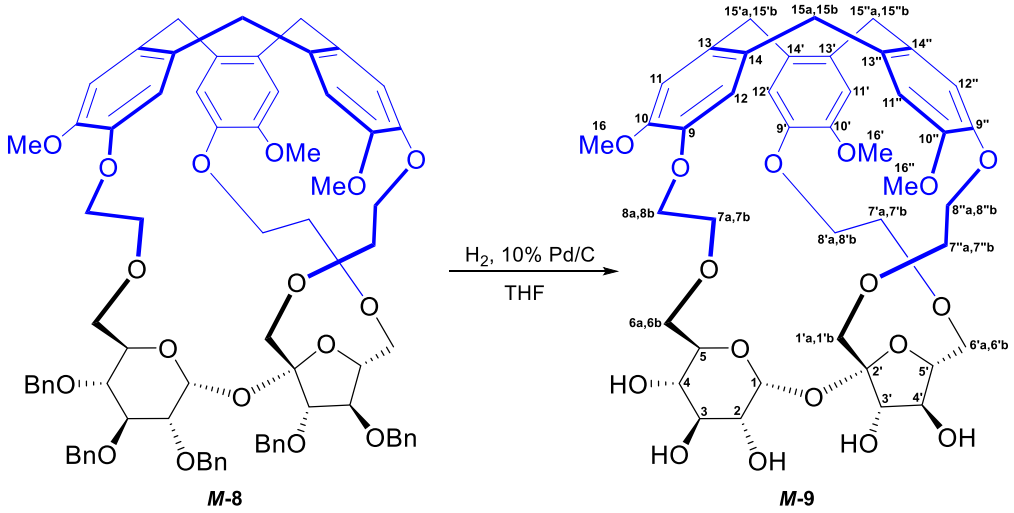

To a solution of compound ***M*-8** (51 mg, 0.04 mmol) in THF (4 mL), 10% Pd/C (10.6 mg, 0.01 mmol) was added and the mixture was stirred under a hydrogen atmosphere in an autoclave for 24 h at room temperature. The mixture was filtered through Celite, washed with THF (20 mL), and concentrated under reduced pressure. The pure product ***M*-9** (32.5 mg, 98%) was obtained as a white solid without further purification. $[\alpha]_D$ = –43.7 ($CHCl_3$). ^{1}H NMR (500 MHz, CD_3OD): δ = 7.07 (s, 1H, H-11'), 7.04 (s, 1H, H-12), 7.03 (s, 1H, H-11), 7.01 (s, 1H, H-12'), 6.91 (s, 1H, H-11''), 6.89 (s, 1H, H-12''), 5.00 (d, $J_{1,2}$ = 3.6 Hz, 1H, H-1), 4.79 (d, $J_{15'b,15'a}$ = 13.3 Hz, 1H, H-15'b), 4.75 (d, $J_{15''b,15''a}$ = 13.5 Hz, 1H, H-15''b), 4.71 (d, $J_{15b,15a}$ = 13.3 Hz, 1H, H-15b), 4.40 (m, 1H, H-7a), 4.29 (m, 1H, H-8''a), 4.19–4.23 (m, 2H, H-8'a, H-8'b), 4.11–4.18 (m, 2H, H-7b, H-8''b), 3.96 (d, $J_{3',4'}$ = 8.3 Hz, 1H, H-3'), 3.92 (m, 1H, H-7"a), 3.82 (s, 3H, 3 × H-16'), 3.77 (s, 3H, 3 × H-16), 3.77 (s, 3H, 3 × H-16''), 3.70–3.78 (m, 3H, H-7"b, H-1'a, H-6a), 3.62–3.68 (m, 2H, H-4', H-8a), 3.46–3.60 (m, 6H, H-3, H-1'b, H-8b, H-15a, H-15'a, H-15"a), 3.30–3.38 (m, 2H, H-4, H-5'), 3.20–3.27 (m, 3H, H-2, H-5, H-7'a), 3.01 (m, 1H, H-7'b), 2.74–2.80 (m, 2H, H-6'a, H-6b), 1.73 (dd, $J_{6'b,6'a}$ = 9.2 Hz, $J_{6'b,5'}$ = 5.9 Hz, 1H, H-6') ppm. ^{13}C{H} NMR (125 MHz, CD_3OD): δ = 150.56 (C-10'), 149.84 (C-10), 148.70 (C-10"), 147.10 (C-9''), 145.99 (C-9), 144.97 (C-9'), 136.03 (C-13'), 134.87 (C-13), 134.10 (C-14), 133.48 (C-13''), 132.69 (C-14''), 132.63 (C-14'), 121.85 (C-11'), 117.96 (C-12), 115.12 (C-11), 114.44 (C-12''), 114.04 (C-12'), 113.51 (C-11"), 105.89 (C-2'), 94.33 (C-1), 80.69 (C-5'), 79.68 (C-4'), 78.15 (C-3'), 75.02 (C-6'), 74.51 (C-3), 73.75 (C-5), 73.45 (C-2), 71.38 (C-6), 71.23 (C-8''), 70.96 (C-8), 70.71 (C-4), 70.40 (C-8'), 70.22 (C-7''), 69.86 (C-1'), 69.45 (C-7), 67.96 (C-7'), 57.00 (C-16), 56.33 (C-16'), 56.06 (C-16''), 36.60 (C-15'), 36.50 (C-15), 36.14 (C-15'') ppm. HRMS (ESI-TOF) calcd for $C_{42}H_{52}O_{17}K$ $[M + K]^+$: 867.2842, found: 867.2832.

3.12. Compound *P*-9

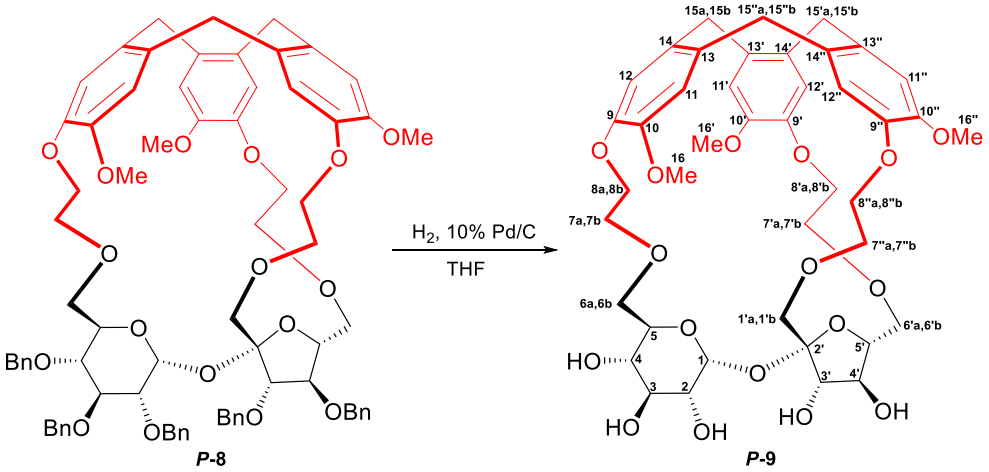

Compound ***P*-9** was synthesized according to previously described procedure for compound ***M*-9**. Compound ***P*-8** (48 mg, 0.038 mmol), 10% Pd/C (10 mg, 0.009 mmol) in THF (4 mL) gave unprotected ***P*-9** (31 mg, 99%) as a white solid. $[\alpha]_D$ = +120.5 ($CHCl_3$). ^{1}H NMR (500 MHz, CD_3OD): δ = 7.05 (s, 1H, H-11'), 7.02 (s, 1H, H-12), 7.00 (s, 1H, H-12''), 6.98 (s, 2H, H-11, H-12'), 6.95 (s, 1H, H-11''), 4.80 (d, $J_{15b,15a}$ = 13.2 Hz, 1H, H-15b), 4.78 (d, $J_{15'b,15'a}$ = 13.4 Hz, 1H, H-15'b), 4.77 (d, $J_{1,2}$ = 3.6 Hz, 1H, H-1), 4.72 (d, $J_{15''b,15''a}$ = 13.4 Hz, 1H, H-15''b), 4.40 (m, 1H, H-8''a), 4.31 (m, 1H, H-8a), 4.22–4.28 (m, 2H, H-8b, H-8'a), 4.16–4.21 (m, 2H, H-8'b, H-8''b), 4.03 (d, $J_{3',4'}$ = 8.8 Hz, 1H, H-3'), 3.85 (s, 3H, 3 × H-16''), 3.832 (s, 3H, 3 × H-16), 3.828 (s, 3H, 3 × H-16'), 3.80 (m, 1H, H-7''a), 3.73 (m, 1H, H-7''b), 3.68 (dd, $J_{4',3'}$ = 8.8 Hz, $J_{4',5'}$ = 8.2 Hz, 1H, H-4'), 3.51–3.61 (m, 7H, H-15a, H-15'a, H-15"a, H-7'a, H-7a, H-7b, H-1'a), 3.49 (dd, $J_{6a,6b}$ = 12.2 Hz, $J_{6a,5}$ = 1.5 Hz, 1H, H-6a), 3.45 (dd, $J_{3,2}$ = 9.7 Hz, $J_{3,4}$ = 8.7 Hz, 1H, H-3), 3.37–3.41 (m, 2H, H-4, H-7'b), 3.35 (m, 1H, H-5), 3.27 (dd, $J_{2,3}$ = 9.7 Hz, $J_{2,1}$ = 3.6 Hz, 1H, H-2), 3.23 (d, $J_{1'b,1'a}$ = 12.0 Hz, 1H, H-1'b), 3.11 (ddd, $J_{5',4'}$ = 8.2 Hz, $J_{5',6'a}$ = 6.9 Hz, $J_{5',6'b}$ = 4.5 Hz, 1H, H-5'), 2.50 (dd, $J_{6'a,6'b}$ = 11.4 Hz, $J_{6'a,5'}$ = 6.9 Hz, 1H, H-6'a), 2.44 (dd, $J_{6b,6a}$ = 12.2 Hz, $J_{6b,5}$ = 1.8 Hz, 1H, H-6b), 2.15 (dd, $J_{6'b,6'a}$ = 11.4 Hz, $J_{6'b,5'}$ = 4.4 Hz, 1H, H-6'b) ppm. ^{13}C{H} NMR (125 MHz, CD_3OD): δ = 150.69 (C-10), 150.40 (C-10'), 148.66 (C-10"), 146.30 (C-9''), 145.93 (C-9'), 145.55 (C-9), 135.51 (C-13'), 134.98 (C-13), 134.46 (C-14), 134.11 (C-13''), 133.20 (C-14'), 132.96 (C-14"), 121.83 (C-11'), 120.69 (C-12'), 115.94 (C-11''), 115.22 (C-12), 114.42 (C-11), 114.22 (C-12"), 104.60 (C-2'), 94.63 (C-1), 79.65 (C-5'), 78.11 (C-3'), 77.54 (C-4'), 74.69(C-3), 73.63 (C-5), 73.35 (C-2), 73.17(C-6'), 71.28 (C-7), 71.17 (C-7'), 70.59 (C-4), 70.44 (C-7''), 70.44 (C-6), 70.41 (C-8'), 69.21 (C-8), 68.61 (C-1'), 67.58 (C-8''), 56.93 (C-16), 56.53 (C-16'), 56.25 (C-16''), 36.69 (C-15"), 36.53 (C-15), 36.37 (C-15') ppm. HRMS (ESI-TOF) calcd for $C_{42}H_{52}O_{17}K$ $[M + K]^+$: 867.2842, found: 867.2838.

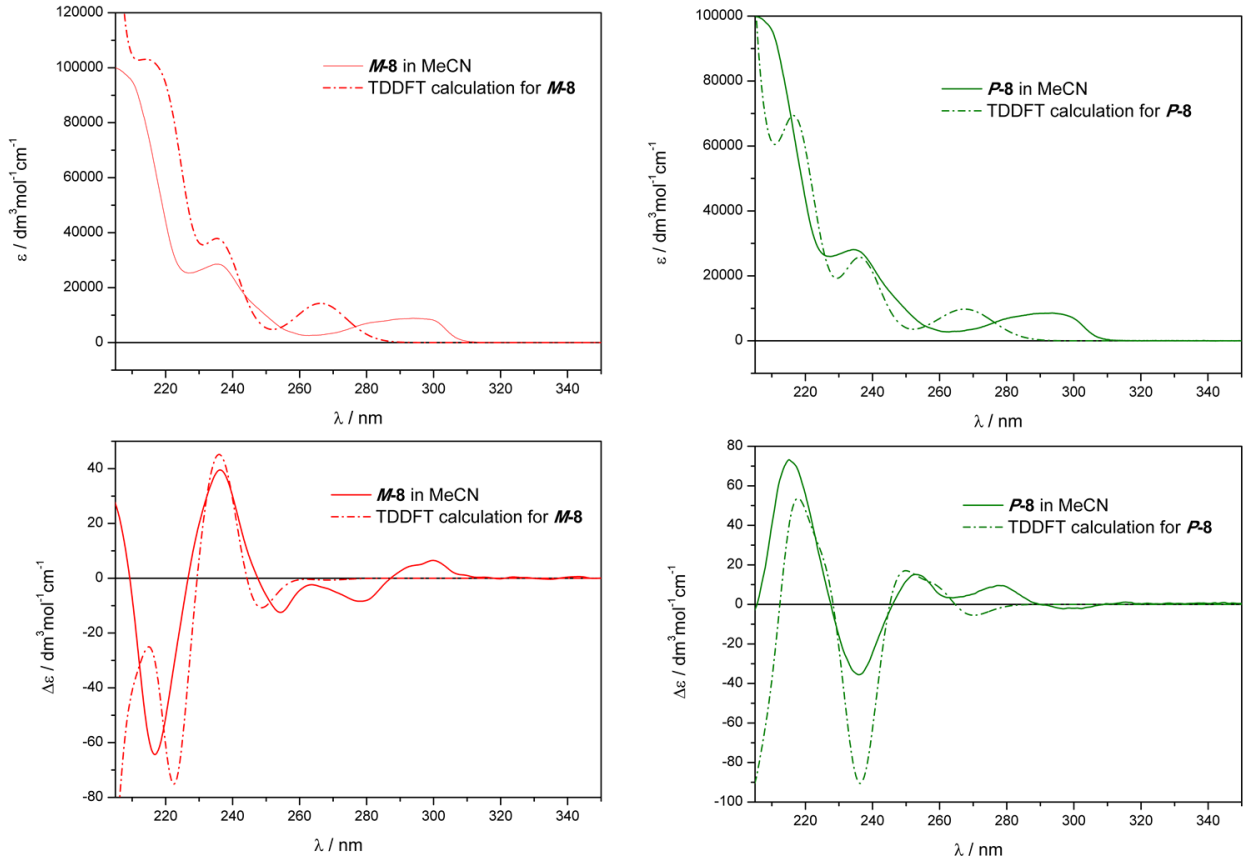

Figure S1. Comparison of experimental UV (top) and ECD (bottom) spectra of compounds ***M*-8** and ***P*-8** in MeCN solution with the simulated curves calculated at CAM-B3LYP/SVP/PCM(MeCN) level of theory.

Table S1. Calculated at CAM-B3LYP/SVP/PCM(CH_3CN) level of theory relative energies and conformer distribution at 25° C for *M*-8.

Conformer.	ΔG [kcal mol^{-1}]	Pop. [%]
***M*-8**(1)	0.00	43.7
***M*-8**(2)	0.46	20.2
***M*-8**(3)	0.60	15.8
***M*-8**(4)	0.99	8.2
***M*-8**(5)	1.13	6.4
***M*-8**(6)	1.21	5.7

Cartesian coordinates for individual conformers of compound *M*-8.

Compound ***M*-8**,conformer 1

Center Number	Atomic Number	Atomic Type	Coordinates (Angstroms) X	Y	Z
1	6	0	-4.595787	-1.927003	2.696787
2	6	0	-5.340892	-0.780099	2.396877
3	6	0	-4.904630	0.452196	2.911562
4	6	0	-3.731207	0.487324	3.676380
5	6	0	-2.970757	-0.651411	3.930932
6	6	0	-3.427503	-1.887920	3.445321
7	1	0	-4.923842	-2.905747	2.340691
8	1	0	-3.406022	1.437411	4.103947
9	6	0	-5.658107	1.756041	2.702008
10	1	0	-5.495160	2.383434	3.589458
11	1	0	-6.736388	1.564441	2.666166
12	6	0	-6.591441	-0.937961	1.551553
13	1	0	-7.364920	-0.238196	1.887228
14	1	0	-6.997691	-1.941890	1.739563
15	6	0	-5.222826	2.552703	1.483372
16	6	0	-5.901554	2.521284	0.253559
17	6	0	-4.083575	3.359474	1.598887
18	6	0	-5.393590	3.275126	-0.810570
19	6	0	-3.574474	4.091631	0.532995
20	1	0	-3.549300	3.425873	2.548824
21	6	0	-4.237010	4.034922	-0.701602
22	1	0	-5.904703	3.272759	-1.775505
23	6	0	-6.387888	-0.803912	0.050294
24	6	0	-5.834494	-1.885867	-0.643002
25	6	0	-6.723622	0.352012	-0.674026
26	6	0	-5.622683	-1.862440	-2.015862
27	1	0	-5.522431	-2.784413	-0.106766
28	6	0	-6.592837	0.333935	-2.066988
29	6	0	-6.064167	-0.752192	-2.751361
30	1	0	-6.895899	1.197165	-2.662738

31	6	0	-7.123982	1.658306	-0.016217
32	1	0	-7.792480	2.205657	-0.694985
33	1	0	-7.694240	1.485615	0.902511
34	8	0	-2.733233	-3.043992	3.661797
35	8	0	-1.831497	-0.637619	4.669046
36	8	0	-2.428254	4.812337	0.698880
37	8	0	-3.771491	4.745635	-1.774989
38	8	0	-5.940989	-0.687846	-4.109480
39	8	0	-4.999038	-2.925827	-2.608948
40	6	0	-6.719545	-1.619707	-4.843453
41	1	0	-6.528945	-1.430374	-5.907331
42	1	0	-6.442054	-2.657485	-4.602968
43	1	0	-7.793741	-1.477205	-4.640030
44	6	0	-2.685816	-3.501769	5.003909
45	1	0	-2.182937	-2.774868	5.657390
46	1	0	-3.701575	-3.697908	5.386444
47	1	0	-2.117945	-4.440655	5.000954
48	6	0	-2.562332	6.222865	0.612599
49	1	0	-1.560822	6.648660	0.750346
50	1	0	-2.955912	6.527938	-0.367627
51	1	0	-3.226633	6.601049	1.407738
52	6	0	-3.773963	-2.644644	-3.277799
53	1	0	-3.941833	-2.013886	-4.163876
54	1	0	-3.383396	-3.616221	-3.609182
55	6	0	-2.759502	-1.981666	-2.360345
56	1	0	-3.089083	-0.968617	-2.076300
57	1	0	-2.661473	-2.564966	-1.428609
58	6	0	-0.891744	0.410707	4.496744
59	1	0	-1.243308	1.114107	3.728633
60	1	0	-0.786275	0.975675	5.436860
61	6	0	0.454419	-0.184391	4.117059
62	1	0	1.173055	0.640563	3.949968
63	1	0	0.831685	-0.796270	4.948925
64	6	0	-3.021139	4.027410	-2.743641
65	1	0	-3.394905	2.994767	-2.837435
66	1	0	-3.169279	4.532024	-3.709045
67	6	0	-1.543487	4.021006	-2.397319
68	1	0	-1.387991	3.571241	-1.400678
69	1	0	-1.178044	5.063633	-2.341123
70	8	0	-1.540656	-1.922011	-3.066295
71	8	0	0.386171	-1.042825	3.007154
72	8	0	-0.865333	3.313126	-3.405702
73	6	0	2.438100	3.065281	-1.704466
74	6	0	1.181876	2.480954	-2.349716
75	6	0	1.994826	0.245623	-2.211756
76	6	0	3.296167	0.703345	-1.532449
77	6	0	3.099524	2.028066	-0.804079
78	1	0	0.461815	2.268631	-1.542223
79	1	0	3.150149	3.353944	-2.499335
80	1	0	2.189879	-0.604526	-2.876544

81	1	0	4.035405	0.871294	-2.335896
82	1	0	2.428171	1.862329	0.055197
83	8	0	1.502146	1.274018	-3.030624
84	8	0	1.077587	-0.096634	-1.215909
85	8	0	3.783775	-0.233290	-0.610144
86	8	0	4.339188	2.534617	-0.362491
87	8	0	2.053184	4.191087	-0.951552
88	6	0	4.621645	2.363460	1.008061
89	1	0	3.891824	2.920943	1.623578
90	1	0	4.531497	1.296733	1.277282
91	6	0	2.947936	5.278871	-0.961707
92	1	0	2.967229	5.747570	-1.964776
93	1	0	3.971056	4.928698	-0.748328
94	6	0	6.016263	2.843502	1.314180
95	6	0	6.336244	3.285161	2.601254
96	6	0	7.018001	2.818137	0.340971
97	6	0	7.633537	3.683622	2.913590
98	1	0	5.558688	3.320417	3.369118
99	6	0	8.315062	3.223025	0.650437
100	1	0	6.768709	2.485053	-0.667148
101	6	0	8.628374	3.654336	1.937640
102	1	0	7.867149	4.026684	3.924011
103	1	0	9.087684	3.200997	-0.121671
104	1	0	9.645091	3.971647	2.179538
105	6	0	2.545171	6.305785	0.065543
106	6	0	1.489658	6.088314	0.951592
107	6	0	3.262555	7.504386	0.148270
108	6	0	1.161968	7.050849	1.908036
109	1	0	0.921309	5.160552	0.884508
110	6	0	2.934798	8.464196	1.100087
111	1	0	4.090590	7.686464	-0.542552
112	6	0	1.881067	8.239832	1.986651
113	1	0	0.336086	6.865657	2.598938
114	1	0	3.505195	9.394370	1.151454
115	1	0	1.623083	8.991579	2.735707
116	6	0	0.535468	3.429266	-3.349047
117	1	0	0.816112	4.466900	-3.101060
118	1	0	0.926832	3.189888	-4.348714
119	6	0	0.066920	-1.074664	-1.430064
120	8	0	-0.837188	-0.915502	-0.384568
121	6	0	-0.329443	-1.536381	0.802050
122	6	0	0.760289	-2.525807	0.331421
123	6	0	0.614694	-2.481813	-1.188479
124	1	0	-1.151226	-2.102157	1.267048
125	1	0	1.765467	-2.166836	0.611480
126	1	0	-0.180343	-3.198105	-1.460792
127	6	0	-0.666274	-0.873287	-2.755976
128	1	0	-1.188319	0.099645	-2.713310
129	1	0	0.064195	-0.824125	-3.572838
130	8	0	1.763901	-2.733123	-1.938438

131	8	0	0.564892	-3.847196	0.764567
132	6	0	0.953712	-4.100915	2.105296
133	1	0	0.443765	-3.395124	2.780668
134	1	0	2.041184	-3.938771	2.216185
135	6	0	0.591848	-5.519325	2.447410
136	6	0	1.562366	-6.521062	2.500940
137	6	0	-0.745595	-5.858420	2.681319
138	6	0	1.208624	-7.839247	2.787698
139	1	0	2.609338	-6.265423	2.318022
140	6	0	-1.102414	-7.174155	2.962888
141	1	0	-1.509063	-5.076267	2.650585
142	6	0	-0.124852	-8.168224	3.017098
143	1	0	1.978894	-8.612564	2.829912
144	1	0	-2.149251	-7.427121	3.146073
145	1	0	-0.404399	-9.200111	3.241158
146	6	0	4.643339	-1.214633	-1.134316
147	1	0	4.137019	-1.792420	-1.926817
148	1	0	5.528645	-0.734401	-1.593608
149	6	0	5.091482	-2.160848	-0.049521
150	6	0	4.656335	-2.035110	1.270194
151	6	0	5.970364	-3.200606	-0.374468
152	6	0	5.089527	-2.933411	2.247030
153	1	0	3.971646	-1.228080	1.531012
154	6	0	6.402136	-4.096366	0.598258
155	1	0	6.318080	-3.310948	-1.405047
156	6	0	5.961597	-3.966317	1.916050
157	1	0	4.740480	-2.820981	3.276125
158	1	0	7.088173	-4.902094	0.327378
159	1	0	6.300995	-4.667969	2.681062
160	6	0	3.100393	-4.309300	-3.143479
161	6	0	2.851845	-3.695551	-4.374915
162	6	0	4.194878	-5.168678	-3.025913
163	6	0	3.681906	-3.937656	-5.466158
164	1	0	1.999238	-3.020939	-4.471852
165	6	0	5.022241	-5.419006	-4.119579
166	1	0	4.405748	-5.644655	-2.065075
167	6	0	4.768994	-4.802211	-5.342491
168	1	0	3.477501	-3.449926	-6.422000
169	1	0	5.874125	-6.094146	-4.012184
170	1	0	5.419497	-4.992692	-6.198902
171	6	0	2.178482	-4.083960	-1.973649
172	1	0	1.288348	-4.734663	-2.066236
173	1	0	2.678941	-4.364959	-1.031912
174	6	0	0.114633	-0.447517	1.765355
175	1	0	-0.706720	0.285767	1.828850
176	1	0	1.002868	0.076290	1.369605

Compound ***M*-8**, conformer 2

Center Number	Atomic Number	Atomic Type	Coordinates (Angstroms) X	Y	Z
1	6	0	-4.652068	-1.541195	3.282535
2	6	0	-5.566789	-0.686133	2.664773
3	6	0	-5.353962	0.701301	2.754023
4	6	0	-4.246448	1.155975	3.477561
5	6	0	-3.325255	0.296730	4.074612
6	6	0	-3.526868	-1.088878	3.968019
7	1	0	-4.797646	-2.622563	3.246479
8	1	0	-4.087870	2.230251	3.595147
9	6	0	-6.266730	1.730191	2.107133
10	1	0	-6.234800	2.643896	2.716810
11	1	0	-7.307130	1.386696	2.136394
12	6	0	-6.760753	-1.309600	1.963385
13	1	0	-7.629344	-0.646291	2.039238
14	1	0	-7.032285	-2.219048	2.517689
15	6	0	-5.871411	2.100680	0.686308
16	6	0	-6.453165	1.526213	-0.456687
17	6	0	-4.865321	3.060603	0.514129
18	6	0	-5.978271	1.911611	-1.715275
19	6	0	-4.389828	3.429574	-0.738663
20	1	0	-4.413170	3.545636	1.381744
21	6	0	-4.946789	2.825924	-1.875384
22	1	0	-6.416111	1.483151	-2.619208
23	6	0	-6.536351	-1.708791	0.514786
24	6	0	-5.868729	-2.909814	0.253333
25	6	0	-6.961108	-0.928373	-0.573142
26	6	0	-5.617534	-3.357858	-1.037356
27	1	0	-5.499042	-3.526989	1.074510
28	6	0	-6.776176	-1.424206	-1.868324
29	6	0	-6.123623	-2.624220	-2.120729
30	1	0	-7.139548	-0.864628	-2.732562
31	6	0	-7.540065	0.464170	-0.415514
32	1	0	-8.235159	0.650881	-1.245800
33	1	0	-8.132163	0.545253	0.502064
34	8	0	-2.686973	-2.039326	4.449503
35	8	0	-2.267978	0.771907	4.793321
36	8	0	-3.374519	4.336197	-0.834659
37	8	0	-4.505674	3.162525	-3.126865
38	8	0	-5.954446	-3.031698	-3.412679
39	8	0	-4.896629	-4.507760	-1.212587
40	6	0	-6.623426	-4.229547	-3.774692
41	1	0	-6.404532	-4.412205	-4.834297
42	1	0	-6.272873	-5.085108	-3.177503
43	1	0	-7.713268	-4.122220	-3.646535
44	6	0	-2.051204	-1.880680	5.705970
45	1	0	-1.133506	-1.286710	5.619180
46	1	0	-2.723797	-1.403415	6.435256
47	1	0	-1.803971	-2.891738	6.057637

48	6	0	-3.702844	5.568780	-1.459473
49	1	0	-4.049068	5.413324	-2.490937
50	1	0	-4.481510	6.099872	-0.886790
51	1	0	-2.789180	6.175100	-1.468353
52	6	0	-3.658233	-4.371099	-1.901384
53	1	0	-3.817982	-4.036622	-2.937839
54	1	0	-3.212971	-5.374946	-1.923157
55	6	0	-2.715143	-3.413651	-1.191432
56	1	0	-3.115340	-2.387145	-1.210012
57	1	0	-2.613379	-3.703306	-0.131368
58	6	0	-1.357746	1.668720	4.178387
59	1	0	-1.715651	1.945154	3.175530
60	1	0	-1.300006	2.594907	4.772440
61	6	0	0.025754	1.040924	4.122884
62	1	0	0.715999	1.746671	3.622119
63	1	0	0.393425	0.877155	5.145908
64	6	0	-3.630148	2.244553	-3.764083
65	1	0	-3.927154	1.205710	-3.544939
66	1	0	-3.727806	2.405600	-4.846882
67	6	0	-2.190339	2.476474	-3.344825
68	1	0	-1.900385	3.514453	-3.593557
69	1	0	-2.089493	2.366283	-2.250114
70	8	0	-1.475364	-3.472205	-1.861225
71	8	0	0.044534	-0.220152	3.498606
72	8	0	-1.384669	1.556948	-4.038827
73	6	0	1.742110	2.209664	-2.156140
74	6	0	0.637263	1.287317	-2.674140
75	6	0	1.731980	-0.666002	-1.852447
76	6	0	2.938529	0.150478	-1.357928
77	6	0	2.490445	1.561636	-0.996829
78	1	0	-0.129558	1.221489	-1.884665
79	1	0	2.459621	2.411863	-2.972695
80	1	0	2.053118	-1.647779	-2.221095
81	1	0	3.645394	0.217619	-2.203488
82	1	0	1.789697	1.498435	-0.148367
83	8	0	1.148610	-0.011205	-2.949219
84	8	0	0.825467	-0.794847	-0.796604
85	8	0	3.568855	-0.408762	-0.235597
86	8	0	3.590068	2.373446	-0.651840
87	8	0	1.123249	3.401201	-1.730698
88	6	0	3.757365	2.609081	0.725029
89	1	0	2.859879	3.108949	1.136632
90	1	0	3.869093	1.650524	1.261654
91	6	0	1.835426	4.596029	-1.959069
92	1	0	1.787727	4.863283	-3.033552
93	1	0	2.897779	4.464132	-1.703052
94	6	0	4.967167	3.473351	0.973763
95	6	0	5.234018	3.915408	2.274544
96	6	0	5.838737	3.836546	-0.053700
97	6	0	6.349900	4.701425	2.542425

98	1	0	4.556155	3.641203	3.087821
99	6	0	6.957414	4.627050	0.214279
100	1	0	5.634808	3.492120	-1.067466
101	6	0	7.217707	5.061130	1.510609
102	1	0	6.543628	5.038520	3.563227
103	1	0	7.629817	4.904674	-0.600843
104	1	0	8.093285	5.679608	1.719495
105	6	0	1.261479	5.718356	-1.131935
106	6	0	0.024829	5.605962	-0.494578
107	6	0	1.983987	6.909368	-1.001569
108	6	0	-0.475834	6.664913	0.263773
109	1	0	-0.550247	4.684976	-0.592082
110	6	0	1.480719	7.968132	-0.252036
111	1	0	2.957585	7.005957	-1.490158
112	6	0	0.246836	7.848336	0.387354
113	1	0	-1.442133	6.558217	0.762207
114	1	0	2.058612	8.890480	-0.159555
115	1	0	-0.147099	8.675394	0.982045
116	6	0	-0.005954	1.817068	-3.949657
117	1	0	0.174852	2.902781	-4.028913
118	1	0	0.479111	1.320561	-4.802850
119	6	0	-0.025031	-1.927302	-0.646595
120	8	0	-0.967859	-1.563269	0.309330
121	6	0	-0.383276	-1.638168	1.619559
122	6	0	0.900291	-2.486572	1.453055
123	6	0	0.721154	-3.063981	0.049733
124	1	0	-1.085237	-2.165109	2.284183
125	1	0	1.792690	-1.840702	1.448980
126	1	0	0.033317	-3.925575	0.118031
127	6	0	-0.736134	-2.287139	-1.947709
128	1	0	-1.366946	-1.428706	-2.240803
129	1	0	0.011092	-2.438458	-2.737161
130	8	0	1.880470	-3.425808	-0.636211
131	8	0	1.034835	-3.530636	2.382491
132	6	0	1.552327	-3.155988	3.652542
133	1	0	1.426292	-4.044691	4.286888
134	1	0	0.955425	-2.334353	4.078412
135	6	0	3.010024	-2.758936	3.599867
136	6	0	3.392747	-1.419965	3.711328
137	6	0	3.999380	-3.727537	3.396292
138	6	0	4.735465	-1.052953	3.619683
139	1	0	2.622452	-0.660258	3.863016
140	6	0	5.340380	-3.365807	3.304135
141	1	0	3.713196	-4.779651	3.316026
142	6	0	5.711287	-2.024941	3.413810
143	1	0	5.019230	-0.001620	3.706678
144	1	0	6.102561	-4.133027	3.150334
145	1	0	6.763182	-1.740001	3.341535
146	6	0	4.469147	-1.471459	-0.487459
147	1	0	4.707638	-1.881305	0.506653

148	1	0	3.976230	-2.276808	-1.050439
149	6	0	5.746949	-1.059637	-1.183823
150	6	0	6.347847	-1.920791	-2.105805
151	6	0	6.371669	0.155279	-0.888862
152	6	0	7.557102	-1.581851	-2.711175
153	1	0	5.864640	-2.870187	-2.352269
154	6	0	7.574369	0.500175	-1.499824
155	1	0	5.899796	0.842233	-0.185700
156	6	0	8.173703	-0.369422	-2.410493
157	1	0	8.015132	-2.266911	-3.428299
158	1	0	8.046906	1.456012	-1.261457
159	1	0	9.118072	-0.099581	-2.888446
160	6	0	3.511157	-5.060161	-1.246263
161	6	0	3.280961	-4.937160	-2.620280
162	6	0	4.733467	-5.574427	-0.809653
163	6	0	4.254801	-5.321415	-3.537581
164	1	0	2.329123	-4.530944	-2.968329
165	6	0	5.707156	-5.968270	-1.726639
166	1	0	4.929088	-5.662092	0.262062
167	6	0	5.471033	-5.840673	-3.093119
168	1	0	4.063393	-5.218095	-4.608033
169	1	0	6.658678	-6.368392	-1.369710
170	1	0	6.234419	-6.143462	-3.813100
171	6	0	2.450124	-4.663563	-0.254277
172	1	0	1.653944	-5.432134	-0.221888
173	1	0	2.876349	-4.600415	0.758861
174	6	0	-0.220311	-0.212179	2.119448
175	1	0	-1.164986	0.309120	1.891703
176	1	0	0.586035	0.299923	1.564679

Compound ***M*-8**, conformer 3

Center Number	Atomic Number	Atomic Type	Coordinates (Angstroms) X	Y	Z
1	6	0	-3.790290	2.492733	3.347959
2	1	0	-3.941692	1.830806	4.214046
3	1	0	-3.411525	3.458645	3.708333
4	6	0	-2.771663	1.876471	2.402636
5	1	0	-3.082731	0.865071	2.092822
6	1	0	-2.693933	2.487837	1.487054
7	6	0	-0.927831	-0.250745	-4.535584
8	1	0	-1.266592	-0.983089	-3.789065
9	1	0	-0.827357	-0.782029	-5.495732
10	6	0	0.417667	0.340682	-4.148043
11	1	0	1.143884	-0.484330	-4.018514
12	1	0	0.781931	0.985052	-4.960984
13	6	0	-2.933370	-4.090642	2.591201
14	1	0	-3.303455	-3.056255	2.676874

15	1	0	-3.110127	-4.595542	3.551918
16	6	0	-1.446874	-4.090502	2.285171
17	1	0	-1.263346	-3.652859	1.287827
18	1	0	-1.081225	-5.134271	2.250198
19	8	0	-1.545798	1.823146	3.096807
20	8	0	0.355033	1.158039	-3.007122
21	8	0	-0.797067	-3.373572	3.305786
22	6	0	2.528041	-3.063038	1.655851
23	6	0	1.253908	-2.506441	2.290062
24	6	0	2.024218	-0.253560	2.176158
25	6	0	3.330279	-0.681938	1.485501
26	6	0	3.159859	-2.008493	0.754306
27	1	0	0.539727	-2.298423	1.476162
28	1	0	3.243794	-3.323795	2.457561
29	1	0	2.210336	0.589443	2.852386
30	1	0	4.077761	-0.837209	2.283917
31	1	0	2.478839	-1.857026	-0.100105
32	8	0	1.549261	-1.299367	2.983033
33	8	0	1.096763	0.092186	1.190379
34	8	0	3.792928	0.268719	0.564667
35	8	0	4.408143	-2.483022	0.301925
36	8	0	2.184466	-4.204177	0.906396
37	6	0	4.664526	-2.319582	-1.074554
38	1	0	3.915444	-2.869319	-1.673394
39	1	0	4.581700	-1.252334	-1.345605
40	6	0	3.120441	-5.270842	0.949698
41	1	0	3.189878	-5.657428	1.983702
42	1	0	4.116468	-4.909893	0.654159
43	6	0	6.045748	-2.820521	-1.405997
44	6	0	6.322433	-3.319181	-2.682235
45	6	0	7.078159	-2.760559	-0.466452
46	6	0	7.607509	-3.739427	-3.017798
47	1	0	5.520801	-3.381258	-3.423136
48	6	0	8.362319	-3.186816	-0.798740
49	1	0	6.862991	-2.383497	0.534130
50	6	0	8.632520	-3.674778	-2.075797
51	1	0	7.807272	-4.126933	-4.019349
52	1	0	9.159191	-3.137020	-0.053048
53	1	0	9.639432	-4.008806	-2.335485
54	6	0	2.659209	-6.359025	0.020021
55	6	0	3.261084	-6.535776	-1.227652
56	6	0	1.593119	-7.190141	0.378250
57	6	0	2.811232	-7.524842	-2.101171
58	1	0	4.095485	-5.892122	-1.518136
59	6	0	1.138499	-8.177169	-0.491944
60	1	0	1.117263	-7.063957	1.354146
61	6	0	1.747783	-8.346253	-1.735474
62	1	0	3.294171	-7.653652	-3.072302
63	1	0	0.308177	-8.822821	-0.197357
64	1	0	1.394505	-9.122677	-2.417615

65	6	0	0.606468	-3.468810	3.274697
66	1	0	0.907477	-4.501024	3.028942
67	1	0	0.975528	-3.226728	4.282134
68	6	0	0.070296	1.046878	1.433545
69	8	0	-0.836567	0.899467	0.388617
70	6	0	-0.351685	1.566248	-0.782398
71	6	0	0.724846	2.559880	-0.291475
72	6	0	0.591328	2.470084	1.227348
73	1	0	-1.187827	2.131689	-1.221640
74	1	0	1.733700	2.225799	-0.589087
75	1	0	-0.214428	3.163678	1.525665
76	6	0	-0.653683	0.798716	2.756912
77	1	0	-1.157733	-0.182405	2.692161
78	1	0	0.080884	0.742525	3.569551
79	8	0	1.742033	2.721990	1.975117
80	8	0	0.504923	3.889854	-0.684763
81	6	0	0.876799	4.189100	-2.020804
82	1	0	0.362849	3.502669	-2.712888
83	1	0	1.963694	4.036741	-2.149632
84	6	0	0.503359	5.615809	-2.312343
85	6	0	1.468908	6.622847	-2.354694
86	6	0	-0.839554	5.955967	-2.510708
87	6	0	1.104833	7.947342	-2.595984
88	1	0	2.520135	6.366460	-2.199283
89	6	0	-1.206628	7.277801	-2.746725
90	1	0	-1.599117	5.169779	-2.488709
91	6	0	-0.233968	8.277204	-2.790345
92	1	0	1.871283	8.724848	-2.630051
93	1	0	-2.257708	7.531515	-2.902530
94	1	0	-0.521555	9.313993	-2.978768
95	6	0	4.635488	1.264601	1.088822
96	1	0	4.125245	1.822704	1.892756
97	1	0	5.537032	0.800685	1.533241
98	6	0	5.048785	2.231751	0.008719
99	6	0	4.605600	2.105406	-1.308260
100	6	0	5.902353	3.291938	0.335185
101	6	0	5.006177	3.023083	-2.280972
102	1	0	3.940082	1.282704	-1.569714
103	6	0	6.301670	4.206945	-0.633474
104	1	0	6.255799	3.402958	1.363733
105	6	0	5.853355	4.076082	-1.948590
106	1	0	4.651107	2.910099	-3.307942
107	1	0	6.968233	5.028512	-0.361538
108	1	0	6.167274	4.792892	-2.710430
109	6	0	3.076261	4.281710	3.202564
110	6	0	2.870972	3.621693	4.417984
111	6	0	4.153592	5.162594	3.086028
112	6	0	3.726882	3.839122	5.494304
113	1	0	2.031898	2.930172	4.514086
114	6	0	5.006806	5.388170	4.165177

115	1	0	4.330609	5.675151	2.137237
116	6	0	4.796885	4.724966	5.371874
117	1	0	3.556372	3.315155	6.437529
118	1	0	5.844903	6.080498	4.058756
119	1	0	5.467742	4.896014	6.216603
120	6	0	2.127642	4.079839	2.050057
121	1	0	1.226086	4.705902	2.190878
122	1	0	2.595656	4.407159	1.106716
123	6	0	0.102609	0.516932	-1.783963
124	1	0	-0.706893	-0.227528	-1.866265
125	1	0	1.002352	-0.004759	-1.411811
126	6	0	-4.034005	-3.312406	-1.724911
127	6	0	-5.197104	-2.546392	-1.577272
128	6	0	-5.867453	-2.574532	-0.342991
129	6	0	-5.332593	-3.351296	0.691355
130	6	0	-4.153862	-4.071171	0.551364
131	6	0	-3.494318	-4.060888	-0.685973
132	1	0	-3.501076	-3.328027	-2.677739
133	1	0	-5.837609	-3.396246	1.658476
134	6	0	-7.104351	-1.745922	-0.034046
135	1	0	-7.756730	-2.328358	0.631084
136	1	0	-7.685590	-1.551922	-0.941553
137	6	0	-5.660086	-1.720519	-2.765830
138	1	0	-6.741014	-1.549013	-2.713862
139	1	0	-5.494780	-2.316110	-3.674557
140	6	0	-6.720146	-0.456091	0.665297
141	6	0	-6.407818	0.729453	-0.020855
142	6	0	-6.577128	-0.484281	2.056961
143	6	0	-5.863613	1.794418	0.705242
144	6	0	-6.057535	0.584815	2.774380
145	1	0	-6.862224	-1.372131	2.624770
146	6	0	-5.638326	1.726208	2.074383
147	1	0	-5.569438	2.715614	0.198160
148	6	0	-4.929214	-0.398687	-2.937004
149	6	0	-3.759868	-0.389640	-3.708682
150	6	0	-5.378906	0.807094	-2.373906
151	6	0	-3.014912	0.767397	-3.922299
152	1	0	-3.424297	-1.318569	-4.172847
153	6	0	-4.650921	1.974525	-2.634529
154	6	0	-3.485574	1.978655	-3.388622
155	1	0	-4.989540	2.934813	-2.240060
156	6	0	-6.625569	0.914152	-1.514862
157	1	0	-7.049282	1.917510	-1.663497
158	1	0	-7.390240	0.214387	-1.870106
159	8	0	-2.318215	-4.723075	-0.878343
160	8	0	-3.658960	-4.801420	1.598045
161	8	0	-5.921279	0.475246	4.128374
162	8	0	-5.024714	2.777578	2.698370
163	8	0	-2.806009	3.150340	-3.564022
164	8	0	-1.876840	0.795955	-4.661583

165	6	0	-2.773064	3.659661	-4.887867
166	1	0	-2.215211	4.603873	-4.852890
167	1	0	-2.267077	2.963841	-5.572146
168	1	0	-3.793576	3.859049	-5.255794
169	6	0	-2.381836	-6.139968	-0.847546
170	1	0	-2.763295	-6.502706	0.118013
171	1	0	-3.023594	-6.520162	-1.660185
172	1	0	-1.359554	-6.510727	-0.995212
173	6	0	-6.706475	1.369952	4.900514
174	1	0	-6.446885	2.419315	4.692448
175	1	0	-7.780364	1.217953	4.702383
176	1	0	-6.502677	1.148065	5.955621

Compound ***M*-8**, conformer 4

Center Number	Atomic Number	Atomic Type	Coordinates (Angstroms) X	Y	Z
1	6	0	4.038976	1.813632	-3.489743
2	1	0	4.078171	1.127670	-4.349209
3	1	0	3.826878	2.825872	-3.859518
4	6	0	2.933685	1.385657	-2.538146
5	1	0	3.069963	0.338548	-2.221806
6	1	0	2.968440	2.007067	-1.627212
7	6	0	0.935346	-0.101158	4.570199
8	1	0	1.162010	-0.926837	3.880827
9	1	0	0.717723	-0.543979	5.555210
10	6	0	-0.277032	0.682372	4.096888
11	1	0	-1.133265	-0.012212	4.001616
12	1	0	-0.539763	1.439326	4.849918
13	6	0	1.281189	-3.884915	-1.808525
14	1	0	0.377989	-4.071576	-1.205396
15	1	0	1.592235	-2.839871	-1.644056
16	6	0	1.017912	-4.098182	-3.291224
17	1	0	1.968500	-3.992519	-3.833811
18	1	0	0.645293	-5.125541	-3.461390
19	8	0	1.709852	1.537821	-3.222811
20	8	0	-0.050831	1.388142	2.903813
21	8	0	0.132166	-3.147275	-3.828497
22	6	0	-2.900044	-2.725738	-1.645816
23	6	0	-1.642496	-2.287363	-2.394952
24	6	0	-2.140660	0.029079	-2.153875
25	6	0	-3.428307	-0.277602	-1.369654
26	6	0	-3.338783	-1.633727	-0.675877
27	1	0	-0.833458	-2.187845	-1.655011
28	1	0	-3.713227	-2.900007	-2.374236
29	1	0	-2.275637	0.911964	-2.789533
30	1	0	-4.247691	-0.334008	-2.108802
31	1	0	-2.577274	-1.573999	0.119997

32	8	0	-1.858793	-1.033472	-3.026579
33	8	0	-1.111276	0.230802	-1.229728
34	8	0	-3.715887	0.691751	-0.398269
35	8	0	-4.585809	-1.997426	-0.128212
36	8	0	-2.598000	-3.912237	-0.947259
37	6	0	-4.740468	-1.775038	1.255114
38	1	0	-3.991006	-2.356101	1.823777
39	1	0	-4.568773	-0.709136	1.484236
40	6	0	-3.623966	-4.894671	-0.931112
41	1	0	-3.839837	-5.224693	-1.963339
42	1	0	-4.544116	-4.460033	-0.512143
43	6	0	-6.126995	-2.170587	1.691265
44	6	0	-7.203477	-2.127653	0.802051
45	6	0	-6.360575	-2.550544	3.016308
46	6	0	-8.488542	-2.454535	1.230899
47	1	0	-7.022852	-1.841802	-0.234757
48	6	0	-7.645361	-2.871111	3.447573
49	1	0	-5.525059	-2.598056	3.720000
50	6	0	-8.714910	-2.824625	2.554838
51	1	0	-9.320391	-2.419412	0.523524
52	1	0	-7.810977	-3.166506	4.486093
53	1	0	-9.722260	-3.080829	2.890234
54	6	0	-3.167439	-6.062565	-0.101638
55	6	0	-2.549344	-7.165051	-0.696501
56	6	0	-3.320252	-6.043885	1.288053
57	6	0	-2.098236	-8.232027	0.078323
58	1	0	-2.425299	-7.190450	-1.782239
59	6	0	-2.868887	-7.106368	2.066777
60	1	0	-3.807081	-5.188466	1.763359
61	6	0	-2.257111	-8.204027	1.462192
62	1	0	-1.622089	-9.090087	-0.401140
63	1	0	-2.999087	-7.080930	3.150883
64	1	0	-1.906604	-9.040125	2.071300
65	6	0	-1.221813	-3.282504	-3.461888
66	1	0	-1.427643	-4.303004	-3.101332
67	1	0	-1.837901	-3.101389	-4.357387
68	6	0	0.023762	1.035660	-1.523719
69	8	0	0.941132	0.771776	-0.510785
70	6	0	0.643009	1.547472	0.653950
71	6	0	-0.282092	2.690728	0.184736
72	6	0	-0.280359	2.524039	-1.332968
73	1	0	1.586611	1.978839	1.021985
74	1	0	-1.306387	2.550688	0.571325
75	1	0	0.588621	3.086405	-1.717722
76	6	0	0.659836	0.679864	-2.868616
77	1	0	0.986597	-0.374452	-2.831787
78	1	0	-0.095314	0.764567	-3.660316
79	8	0	-1.439978	2.913594	-2.005292
80	8	0	0.190334	3.978160	0.489255
81	6	0	0.000222	4.391404	1.833578

82	1	0	0.476109	3.671582	2.517811
83	1	0	-1.079639	4.409260	2.068363
84	6	0	0.603660	5.758447	1.997188
85	6	0	-0.182648	6.909330	1.914545
86	6	0	1.983143	5.892364	2.187660
87	6	0	0.394431	8.173643	2.023956
88	1	0	-1.261495	6.813707	1.766077
89	6	0	2.563003	7.153993	2.294067
90	1	0	2.601063	4.993351	2.262347
91	6	0	1.769085	8.297852	2.212160
92	1	0	-0.232652	9.065825	1.961407
93	1	0	3.640867	7.246911	2.445602
94	1	0	2.223203	9.287541	2.298517
95	6	0	-4.433506	1.813050	-0.851179
96	1	0	-3.887604	2.319899	-1.665813
97	1	0	-5.412470	1.497148	-1.259645
98	6	0	-4.648113	2.794010	0.273277
99	6	0	-4.078013	2.611668	1.533815
100	6	0	-5.431000	3.931423	0.044327
101	6	0	-4.284336	3.550267	2.546352
102	1	0	-3.468320	1.727552	1.720117
103	6	0	-5.635906	4.867709	1.052559
104	1	0	-5.883690	4.085769	-0.938775
105	6	0	-5.061242	4.680561	2.310394
106	1	0	-3.831852	3.392619	3.528140
107	1	0	-6.250068	5.749635	0.857026
108	1	0	-5.222822	5.413977	3.103319
109	6	0	-2.688297	4.602506	-3.142574
110	6	0	-2.673098	3.937747	-4.373117
111	6	0	-3.674941	5.561277	-2.905313
112	6	0	-3.625523	4.227854	-5.345621
113	1	0	-1.906053	3.184474	-4.563903
114	6	0	-4.625505	5.859246	-3.881176
115	1	0	-3.703881	6.078368	-1.943067
116	6	0	-4.604259	5.191674	-5.102998
117	1	0	-3.603277	3.700223	-6.301828
118	1	0	-5.390966	6.612271	-3.681096
119	1	0	-5.351009	5.419898	-5.866643
120	6	0	-1.636744	4.310691	-2.105086
121	1	0	-0.680984	4.791557	-2.387789
122	1	0	-1.929981	4.735810	-1.130961
123	6	0	0.073530	0.633451	1.726593
124	1	0	0.767078	-0.216114	1.848002
125	1	0	-0.903055	0.229726	1.403694
126	6	0	3.300489	-3.644439	1.933943
127	6	0	4.600680	-3.174120	1.707591
128	6	0	5.167624	-3.348786	0.435672
129	6	0	4.385540	-3.932308	-0.568976
130	6	0	3.072246	-4.322433	-0.357223
131	6	0	2.524431	-4.206607	0.929522

132	1	0	2.843427	-3.552942	2.921049
133	1	0	4.780749	-4.047350	-1.579771
134	6	0	6.543958	-2.830817	0.044739
135	1	0	7.021544	-3.569249	-0.614172
136	1	0	7.192954	-2.735297	0.921473
137	6	0	5.292074	-2.438778	2.841966
138	1	0	6.380667	-2.479175	2.728120
139	1	0	5.065698	-2.961191	3.782024
140	6	0	6.417977	-1.517088	-0.702448
141	6	0	6.350517	-0.268457	-0.059967
142	6	0	6.250429	-1.567945	-2.090291
143	6	0	5.994753	0.850879	-0.820580
144	6	0	5.925411	-0.447576	-2.843297
145	1	0	6.356137	-2.513396	-2.625991
146	6	0	5.730470	0.774796	-2.183438
147	1	0	5.887183	1.829132	-0.347370
148	6	0	4.823944	-0.998858	2.977702
149	6	0	3.700764	-0.749734	3.776022
150	6	0	5.446290	0.080236	2.328559
151	6	0	3.160860	0.523879	3.932483
152	1	0	3.227712	-1.582231	4.299295
153	6	0	4.938803	1.367191	2.547247
154	6	0	3.816413	1.609571	3.328394
155	1	0	5.422497	2.234116	2.092352
156	6	0	6.652437	-0.073698	1.419501
157	1	0	7.257701	0.839460	1.510775
158	1	0	7.291810	-0.888935	1.776702
159	8	0	1.238220	-4.565357	1.202111
160	8	0	2.325926	-4.767329	-1.414227
161	8	0	5.752108	-0.578598	-4.191248
162	8	0	5.303996	1.896533	-2.839878
163	8	0	3.357269	2.889168	3.458657
164	8	0	2.051256	0.770301	4.676496
165	6	0	3.426031	3.446986	4.761423
166	1	0	3.046598	4.474032	4.688739
167	1	0	2.808196	2.880421	5.472535
168	1	0	4.468422	3.473868	5.120838
169	6	0	0.912200	-5.936368	1.033499
170	1	0	1.521403	-6.567132	1.702242
171	1	0	-0.146174	-6.049818	1.298361
172	1	0	1.062844	-6.262776	-0.006299
173	6	0	6.678588	0.127712	-5.001010
174	1	0	6.620106	1.213711	-4.830040
175	1	0	7.708534	-0.213102	-4.804473
176	1	0	6.423337	-0.089203	-6.045917

Compound ***M*-8**, conformer 5

Center	Atomic	Atomic	Coordinates (Angstroms)		

Number	Number	Type	X	Y	Z
1	6	0	-4.660058	-1.273441	2.852401
2	6	0	-5.292521	-0.070090	2.515628
3	6	0	-4.728086	1.130521	2.978046
4	6	0	-3.539810	1.076030	3.717330
5	6	0	-2.883827	-0.120428	3.994379
6	6	0	-3.475624	-1.323623	3.575376
7	1	0	-5.091943	-2.227503	2.543075
8	1	0	-3.109838	2.004027	4.097796
9	6	0	-5.333571	2.499731	2.709167
10	1	0	-5.098355	3.149297	3.563862
11	1	0	-6.426346	2.433349	2.671811
12	6	0	-6.564521	-0.135548	1.689315
13	1	0	-7.249906	0.665575	1.988455
14	1	0	-7.078055	-1.074050	1.942003
15	6	0	-4.788328	3.150028	1.450087
16	6	0	-5.437349	3.094346	0.206698
17	6	0	-3.543702	3.789668	1.530398
18	6	0	-4.775462	3.607876	-0.915328
19	6	0	-2.893925	4.297646	0.413751
20	1	0	-3.034450	3.888894	2.491047
21	6	0	-3.507908	4.163505	-0.840869
22	1	0	-5.230835	3.539674	-1.904828
23	6	0	-6.378349	-0.115213	0.178647
24	6	0	-5.984148	-1.294931	-0.462255
25	6	0	-6.588632	1.031634	-0.606387
26	6	0	-5.816233	-1.375716	-1.840128
27	1	0	-5.766901	-2.193796	0.118568
28	6	0	-6.516764	0.915891	-1.998455
29	6	0	-6.151796	-0.265826	-2.629526
30	1	0	-6.734392	1.774250	-2.637175
31	6	0	-6.780285	2.415401	-0.018128
32	1	0	-7.362118	3.023091	-0.725056
33	1	0	-7.362260	2.381239	0.908636
34	8	0	-2.898801	-2.535658	3.826679
35	8	0	-1.718150	-0.180797	4.689588
36	8	0	-1.661393	4.868001	0.553103
37	8	0	-2.866811	4.531213	-1.992688
38	8	0	-6.077099	-0.296813	-3.992350
39	8	0	-5.340339	-2.537238	-2.384132
40	6	0	-6.989815	-1.169983	-4.638623
41	1	0	-6.822064	-1.068678	-5.718252
42	1	0	-6.827351	-2.217579	-4.341807
43	1	0	-8.030369	-0.887357	-4.408573
44	6	0	-2.837065	-2.927959	5.188851
45	1	0	-2.228919	-2.228473	5.779699
46	1	0	-3.848764	-2.992445	5.623398
47	1	0	-2.373835	-3.922365	5.213296
48	6	0	-1.574594	6.240809	0.198587

49	1	0	-2.261768	6.845066	0.813464
50	1	0	-0.543320	6.556470	0.397112
51	1	0	-1.807691	6.396444	-0.865231
52	6	0	-4.127238	-2.440574	-3.125358
53	1	0	-4.273907	-1.869144	-4.054195
54	1	0	-3.854816	-3.471644	-3.388047
55	6	0	-3.009404	-1.816049	-2.306855
56	1	0	-3.223878	-0.755746	-2.094943
57	1	0	-2.929809	-2.331195	-1.334595
58	6	0	-0.683446	0.745904	4.396510
59	1	0	-1.014925	1.453394	3.623261
60	1	0	-0.445862	1.331445	5.298944
61	6	0	0.559212	-0.005880	3.949482
62	1	0	1.347706	0.729774	3.700385
63	1	0	0.928282	-0.627156	4.778172
64	6	0	-1.763972	3.695760	-2.326106
65	1	0	-0.876988	3.988705	-1.741798
66	1	0	-2.004807	2.647106	-2.083738
67	6	0	-1.506575	3.809828	-3.819704
68	1	0	-1.196799	4.841250	-4.071417
69	1	0	-2.444036	3.601213	-4.355446
70	8	0	-1.820110	-1.935792	-3.055776
71	8	0	0.322266	-0.888213	2.882650
72	8	0	-0.558390	2.874840	-4.272191
73	6	0	2.493758	2.821993	-2.079259
74	6	0	1.266568	2.240029	-2.781483
75	6	0	1.943924	-0.007167	-2.381103
76	6	0	3.236096	0.446870	-1.684379
77	6	0	3.056542	1.829480	-1.064591
78	1	0	0.469651	2.145384	-2.027956
79	1	0	3.275769	3.034884	-2.831881
80	1	0	2.109695	-0.931827	-2.946218
81	1	0	4.014814	0.524571	-2.464114
82	1	0	2.331609	1.753174	-0.236999
83	8	0	1.557324	0.959665	-3.322368
84	8	0	0.972077	-0.187351	-1.393152
85	8	0	3.644211	-0.437220	-0.675058
86	8	0	4.287280	2.327797	-0.590895
87	8	0	2.076128	4.010716	-1.450666
88	6	0	4.525496	2.180345	0.792454
89	1	0	3.781122	2.755401	1.372161
90	1	0	4.421117	1.119696	1.077378
91	6	0	3.039673	5.018264	-1.226560
92	1	0	2.837546	5.860888	-1.914134
93	1	0	4.048849	4.644616	-1.449211
94	6	0	5.912711	2.659280	1.131226
95	6	0	6.951683	2.577223	0.200893
96	6	0	6.188180	3.157870	2.407758
97	6	0	8.240715	2.982019	0.542002
98	1	0	6.738439	2.199455	-0.799801

99	6	0	7.477563	3.555856	2.752559
100	1	0	5.381127	3.240401	3.140659
101	6	0	8.509290	3.469680	1.819317
102	1	0	9.042515	2.915197	-0.197095
103	1	0	7.675881	3.943774	3.754276
104	1	0	9.519842	3.786684	2.086203
105	6	0	3.003917	5.521751	0.197355
106	6	0	1.944081	5.222703	1.055168
107	6	0	4.045187	6.329554	0.666069
108	6	0	1.927634	5.721599	2.358311
109	1	0	1.124694	4.597790	0.698634
110	6	0	4.028982	6.827924	1.965413
111	1	0	4.883548	6.567524	0.005436
112	6	0	2.968017	6.524277	2.818671
113	1	0	1.089436	5.480097	3.016248
114	1	0	4.852591	7.453605	2.316757
115	1	0	2.954463	6.912984	3.839255
116	6	0	0.781689	3.126482	-3.916184
117	1	0	0.918803	4.181205	-3.629365
118	1	0	1.413095	2.923157	-4.796351
119	6	0	-0.098083	-1.112670	-1.525957
120	8	0	-0.974315	-0.815721	-0.486232
121	6	0	-0.514775	-1.405969	0.734137
122	6	0	0.474873	-2.518729	0.325949
123	6	0	0.350617	-2.538288	-1.196055
124	1	0	-1.382449	-1.862398	1.234278
125	1	0	1.507469	-2.249395	0.607205
126	1	0	-0.489668	-3.210868	-1.443289
127	6	0	-0.835282	-0.959423	-2.856130
128	1	0	-1.254754	0.061470	-2.903561
129	1	0	-0.117864	-1.062540	-3.680425
130	8	0	1.489202	-2.910147	-1.912385
131	8	0	0.142727	-3.792791	0.815755
132	6	0	0.456673	-4.013689	2.181980
133	1	0	-0.029459	-3.247543	2.806501
134	1	0	1.547643	-3.922521	2.333051
135	6	0	-0.020348	-5.387960	2.560802
136	6	0	0.854227	-6.476151	2.579925
137	6	0	-1.371709	-5.599394	2.854918
138	6	0	0.391902	-7.754150	2.890838
139	1	0	1.911784	-6.319795	2.351477
140	6	0	-1.837204	-6.875244	3.162344
141	1	0	-2.058396	-4.748410	2.850521
142	6	0	-0.955521	-7.955947	3.180650
143	1	0	1.087519	-8.596188	2.905939
144	1	0	-2.893915	-7.028492	3.393118
145	1	0	-1.319867	-8.956393	3.424610
146	6	0	4.453999	-1.507155	-1.094935
147	1	0	3.931075	-2.116716	-1.852310
148	1	0	5.377179	-1.119869	-1.567138

149	6	0	4.817795	-2.387493	0.073725
150	6	0	4.328932	-2.152820	1.359402
151	6	0	5.667177	-3.479980	-0.136531
152	6	0	4.680453	-2.995838	2.415139
153	1	0	3.666448	-1.304619	1.531763
154	6	0	6.017369	-4.320725	0.914894
155	1	0	6.056567	-3.675552	-1.139195
156	6	0	5.523553	-4.081562	2.198022
157	1	0	4.289865	-2.798161	3.416070
158	1	0	6.681557	-5.168677	0.733116
159	1	0	5.798860	-4.739928	3.024756
160	6	0	2.779875	-4.626038	-2.962614
161	6	0	2.627610	-4.081892	-4.241796
162	6	0	3.828921	-5.517369	-2.728604
163	6	0	3.507033	-4.423955	-5.265255
164	1	0	1.811390	-3.381958	-4.430503
165	6	0	4.705902	-5.867658	-3.754308
166	1	0	3.965116	-5.939497	-1.729891
167	6	0	4.548289	-5.320110	-5.025100
168	1	0	3.377792	-3.990065	-6.259385
169	1	0	5.521345	-6.566728	-3.555847
170	1	0	5.237569	-5.589004	-5.828507
171	6	0	1.805449	-4.287243	-1.865396
172	1	0	0.877006	-4.876624	-1.989241
173	1	0	2.224604	-4.559849	-0.882525
174	6	0	0.046990	-0.314619	1.631123
175	1	0	-0.709927	0.485356	1.697824
176	1	0	0.957998	0.117558	1.180351

Compound ***M*-8**, conformer 6

Center Number	Atomic Number	Atomic Type	Coordinates (Angstroms) X	Y	Z
1	6	0	0.134797	-4.404015	3.341042
2	1	0	0.678850	-4.144646	4.261765
3	1	0	-0.883885	-4.712379	3.612071
4	6	0	0.064351	-3.191007	2.427700
5	1	0	1.072848	-2.802414	2.208208
6	1	0	-0.391275	-3.476738	1.463905
7	6	0	0.933055	-0.340542	-4.465530
8	1	0	1.667209	-0.146576	-3.670613
9	1	0	1.322597	0.112520	-5.391263
10	6	0	-0.410913	0.285102	-4.131918
11	1	0	-0.266197	1.370656	-3.974375
12	1	0	-1.094823	0.157012	-4.983123
13	6	0	4.701709	0.456170	2.943033
14	1	0	4.143382	-0.491294	3.017575
15	1	0	5.125396	0.680221	3.932453

16	6	0	3.774285	1.583897	2.527085
17	1	0	3.368195	1.393672	1.517983
18	1	0	4.352146	2.525529	2.471253
19	8	0	-0.701739	-2.216465	3.098266
20	8	0	-1.045784	-0.314928	-3.031807
21	8	0	2.756941	1.685214	3.493090
22	6	0	0.448397	4.070735	1.764199
23	6	0	0.843892	2.724477	2.371650
24	6	0	-1.358318	1.844208	2.191618
25	6	0	-1.873629	3.130616	1.525012
26	6	0	-0.753724	3.911662	0.837540
27	1	0	1.171028	2.066650	1.549370
28	1	0	0.167288	4.759894	2.581568
29	1	0	-2.135598	1.422176	2.840548
30	1	0	-2.261765	3.772028	2.336276
31	1	0	-0.417826	3.353139	-0.052813
32	8	0	-0.275301	2.145764	3.030122
33	8	0	-0.993697	0.934376	1.196582
34	8	0	-2.883128	2.874788	0.584798
35	8	0	-1.197049	5.202799	0.480015
36	8	0	1.556483	4.572496	1.056520
37	6	0	-1.756726	5.365465	-0.816583
38	1	0	-2.439842	4.535626	-1.041364
39	1	0	-2.353423	6.287538	-0.757470
40	6	0	1.807340	5.949484	1.202741
41	1	0	2.015778	6.187924	2.263986
42	1	0	0.916036	6.528394	0.910396
43	6	0	-0.720492	5.503633	-1.906577
44	6	0	-0.491034	4.469006	-2.816557
45	6	0	0.032371	6.677454	-2.022771
46	6	0	0.470372	4.599119	-3.818663
47	1	0	-1.080776	3.551275	-2.745521
48	6	0	0.992239	6.812558	-3.020663
49	1	0	-0.143928	7.499621	-1.324275
50	6	0	1.214893	5.770831	-3.921526
51	1	0	0.636199	3.782030	-4.524510
52	1	0	1.570688	7.735747	-3.098589
53	1	0	1.967041	5.876178	-4.706431
54	6	0	2.982973	6.367351	0.358194
55	6	0	3.658121	5.466259	-0.465142
56	6	0	3.401254	7.702251	0.387518
57	6	0	4.728569	5.895249	-1.251292
58	1	0	3.336676	4.424909	-0.488920
59	6	0	4.470159	8.129342	-0.393704
60	1	0	2.879824	8.417449	1.030026
61	6	0	5.138609	7.224988	-1.219508
62	1	0	5.243556	5.181797	-1.899018
63	1	0	4.783947	9.175104	-0.359336
64	1	0	5.976298	7.558399	-1.835870
65	6	0	1.969799	2.846421	3.386212

66	1	0	2.604669	3.707833	3.119869
67	1	0	1.521016	3.032497	4.373330
68	6	0	-1.046266	-0.470114	1.421865
69	8	0	-0.276562	-1.045141	0.415144
70	6	0	-1.027507	-1.118591	-0.801784
71	6	0	-2.510465	-0.954943	-0.398681
72	6	0	-2.446203	-1.009202	1.126288
73	1	0	-0.881902	-2.122266	-1.230435
74	1	0	-2.897605	0.029067	-0.714733
75	1	0	-2.459664	-2.075228	1.412722
76	6	0	-0.463847	-0.873870	2.777400
77	1	0	0.615162	-0.636769	2.770572
78	1	0	-0.930491	-0.278525	3.571151
79	8	0	-3.431760	-0.313888	1.826696
80	8	0	-3.349180	-1.987236	-0.847655
81	6	0	-3.721744	-1.908528	-2.214551
82	1	0	-2.819681	-1.873746	-2.845929
83	1	0	-4.289184	-0.976963	-2.392824
84	6	0	-4.558126	-3.112117	-2.548520
85	6	0	-5.951988	-3.037090	-2.577922
86	6	0	-3.940169	-4.343974	-2.789821
87	6	0	-6.719054	-4.169529	-2.848251
88	1	0	-6.442817	-2.078568	-2.389730
89	6	0	-4.703803	-5.477443	-3.056361
90	1	0	-2.848483	-4.405987	-2.775969
91	6	0	-6.095798	-5.392259	-3.086175
92	1	0	-7.808637	-4.096241	-2.872070
93	1	0	-4.210998	-6.433773	-3.246059
94	1	0	-6.694826	-6.280717	-3.298234
95	6	0	-4.194729	2.838639	1.090454
96	1	0	-4.291126	2.057268	1.863837
97	1	0	-4.443276	3.805685	1.567985
98	6	0	-5.179361	2.554872	-0.015426
99	6	0	-4.768128	2.282928	-1.320894
100	6	0	-6.548543	2.553715	0.274878
101	6	0	-5.707334	2.011378	-2.317305
102	1	0	-3.703475	2.285776	-1.554701
103	6	0	-7.485090	2.282136	-0.717222
104	1	0	-6.884470	2.765615	1.293401
105	6	0	-7.067002	2.008112	-2.020152
106	1	0	-5.369266	1.802113	-3.334888
107	1	0	-8.549857	2.285487	-0.473328
108	1	0	-7.801469	1.796607	-2.800261
109	6	0	-5.522965	-0.390965	2.984909
110	6	0	-4.931014	-0.202025	4.237609
111	6	0	-6.885842	-0.126717	2.835270
112	6	0	-5.688230	0.241884	5.318125
113	1	0	-3.865330	-0.404728	4.359275
114	6	0	-7.647796	0.310109	3.918051
115	1	0	-7.356517	-0.258918	1.857990

116	6	0	-7.050273	0.497695	5.162044
117	1	0	-5.212816	0.387127	6.290837
118	1	0	-8.712975	0.512324	3.785509
119	1	0	-7.644408	0.845286	6.010026
120	6	0	-4.712576	-0.912310	1.826870
121	1	0	-4.600732	-2.009621	1.911219
122	1	0	-5.235210	-0.719483	0.875016
123	6	0	-0.470676	-0.089418	-1.771405
124	1	0	0.624960	-0.215508	-1.788078
125	1	0	-0.685115	0.932060	-1.408992
126	6	0	5.104844	-0.838981	-1.361355
127	6	0	5.226513	-2.228183	-1.228904
128	6	0	5.585958	-2.755094	0.022901
129	6	0	5.777223	-1.871133	1.091282
130	6	0	5.607188	-0.499493	0.963527
131	6	0	5.280211	0.031345	-0.292554
132	1	0	4.852509	-0.396935	-2.327345
133	1	0	6.060156	-2.253032	2.074353
134	6	0	5.709319	-4.243457	0.309133
135	1	0	6.529096	-4.393704	1.025086
136	1	0	5.986106	-4.796692	-0.594407
137	6	0	4.959750	-3.086497	-2.454045
138	1	0	5.507575	-4.032618	-2.382294
139	1	0	5.376192	-2.565456	-3.327474
140	6	0	4.425966	-4.776554	0.915752
141	6	0	3.355881	-5.265425	0.147804
142	6	0	4.269173	-4.679827	2.302702
143	6	0	2.140930	-5.526181	0.790987
144	6	0	3.068190	-4.964924	2.937922
145	1	0	5.100000	-4.356067	2.932651
146	6	0	1.964441	-5.337910	2.156251
147	1	0	1.274168	-5.864228	0.219207
148	6	0	3.489834	-3.356478	-2.733403
149	6	0	2.797811	-2.447604	-3.544113
150	6	0	2.806123	-4.480256	-2.239360
151	6	0	1.452387	-2.607733	-3.866658
152	1	0	3.333010	-1.589332	-3.954312
153	6	0	1.467326	-4.658936	-2.608387
154	6	0	0.781432	-3.752065	-3.405081
155	1	0	0.916118	-5.539236	-2.271157
156	6	0	3.451135	-5.525604	-1.348022
157	1	0	2.954098	-6.485836	-1.545888
158	1	0	4.498767	-5.670751	-1.634741
159	8	0	5.092968	1.369855	-0.476365
160	8	0	5.790995	0.324767	2.040986
161	8	0	2.980997	-4.822010	4.292789
162	8	0	0.722614	-5.529466	2.696852
163	8	0	-0.534648	-3.976649	-3.693322
164	8	0	0.766966	-1.737041	-4.651457
165	6	0	-0.838289	-4.249570	-5.052113

166	1	0	-1.918993	-4.431841	-5.106913
167	1	0	-0.579659	-3.399052	-5.698664
168	1	0	-0.304467	-5.150201	-5.399113
169	6	0	6.249442	2.181983	-0.346857
170	1	0	6.709374	2.067882	0.645280
171	1	0	6.990524	1.933800	-1.125163
172	1	0	5.927569	3.222499	-0.477255
173	6	0	2.727216	-6.012147	5.022416
174	1	0	1.761840	-6.460876	4.742113
175	1	0	3.529415	-6.750219	4.857229
176	1	0	2.705624	-5.739315	6.085004

Table S2. Calculated at CAM-B3LYP/SVP/PCM(CH_3CN) level of theory relative energies and conformer distribution at 25° C for *P*-8.

Conformer	ΔG [kcal mol^{-1}]	Pop. [%]
***P*-8**(1)	0.00	52.7
***P*-8**(2)	0.38	28.0
***P*-8**(3)	1.17	7.3
***P*-8**(4)	1.27	6.2
***P*-8**(5)	1.69	3.1
***P*-8**(6)	1.73	2.7

Cartesian coordinates for individual conformers of compound *P*-8.

Compound ***P*-8**, conformer 1

Center Number	Atomic Number	Atomic Type	Coordinates (Angstroms) X	Y	Z
1	8	0	-3.775853	-0.352682	4.666314
2	6	0	1.271063	4.526839	2.002037
3	1	0	2.320184	4.816751	2.149278
4	1	0	0.773500	4.555417	2.986014
5	6	0	1.206385	3.126222	1.417288
6	1	0	0.162404	2.776913	1.363632
7	1	0	1.591161	3.149010	0.382966
8	6	0	-2.548915	-1.070968	4.651204
9	1	0	-2.255197	-1.306527	5.686447
10	1	0	-1.747803	-0.456058	4.216946
11	6	0	-2.717988	-2.362020	3.878419
12	1	0	-1.792720	-2.960520	3.989249
13	1	0	-3.547698	-2.938246	4.313787
14	6	0	-2.847029	0.530449	-3.810268
15	1	0	-2.582311	0.693196	-4.864837
16	1	0	-2.250198	1.223848	-3.195488
17	6	0	-2.555989	-0.897364	-3.387874
18	1	0	-3.025305	-1.087945	-2.414779
19	1	0	-2.992413	-1.605884	-4.117115
20	8	0	1.970797	2.276419	2.239702
21	8	0	-3.033585	-2.179637	2.520873
22	8	0	-1.156781	-1.067978	-3.316952
23	6	0	3.237587	0.267923	0.537699
24	6	0	1.804149	0.121088	1.051885
25	6	0	0.943578	-0.148346	-1.150854
26	6	0	2.316506	0.117693	-1.784044
27	6	0	3.418615	-0.352429	-0.842234
28	1	0	1.630659	-0.940624	1.297178
29	1	0	3.470664	1.342691	0.459083
30	1	0	0.133929	0.253694	-1.770129

31	1	0	2.406808	1.212600	-1.888422
32	1	0	3.353616	-1.448778	-0.744828
33	8	0	0.867214	0.534274	0.069655
34	8	0	0.787987	-1.534329	-0.977389
35	8	0	2.490714	-0.508048	-3.028192
36	8	0	4.696507	0.014077	-1.312924
37	8	0	4.095061	-0.349985	1.471472
38	6	0	1.850032	0.103482	-4.141024
39	1	0	2.124407	-0.527614	-4.998993
40	6	0	5.403643	-0.991635	-1.999151
41	1	0	5.590231	-1.853151	-1.330718
42	1	0	4.799782	-1.362472	-2.845349
43	6	0	5.249745	0.390779	1.835073
44	1	0	4.942997	1.358076	2.270834
45	1	0	5.859905	0.592272	0.940650
46	6	0	6.716798	-0.455622	-2.507750
47	6	0	7.746942	-1.343067	-2.835674
48	6	0	6.921486	0.913200	-2.694473
49	6	0	8.952717	-0.873826	-3.349189
50	1	0	7.603223	-2.416528	-2.684819
51	6	0	8.131264	1.384572	-3.203383
52	1	0	6.123466	1.608174	-2.432390
53	6	0	9.149441	0.494205	-3.534901
54	1	0	9.747122	-1.580431	-3.599940
55	1	0	8.278054	2.458458	-3.340841
56	1	0	10.096706	0.864190	-3.933247
57	6	0	6.032029	-0.409198	2.839313
58	6	0	5.757140	-0.300215	4.205107
59	6	0	7.003542	-1.320762	2.417430
60	6	0	6.440493	-1.083698	5.132413
61	1	0	4.999223	0.410187	4.545479
62	6	0	7.689271	-2.106664	3.340722
63	1	0	7.226441	-1.412587	1.351173
64	6	0	7.407826	-1.989942	4.700906
65	1	0	6.218616	-0.985569	6.197347
66	1	0	8.448490	-2.812882	2.997549
67	1	0	7.946176	-2.603677	5.426494
68	6	0	1.559848	0.933053	2.313417
69	1	0	2.138143	0.478792	3.129054
70	1	0	0.485645	0.866689	2.566865
71	6	0	-0.475506	-2.102877	-1.197153
72	8	0	-1.480740	-1.304749	-0.614516
73	6	0	-2.304548	-2.033540	0.286776
74	6	0	-2.010525	-3.508317	0.000663
75	6	0	-0.553714	-3.474280	-0.471296
76	1	0	-3.354108	-1.787692	0.065574
77	1	0	-2.107827	-4.125530	0.908610
78	1	0	-0.355949	-4.307441	-1.166126
79	6	0	-0.750635	-2.265551	-2.701985
80	1	0	0.183644	-2.598227	-3.177819

81	1	0	-1.514848	-3.046001	-2.840049
82	8	0	0.271141	-3.559465	0.655279
83	8	0	-2.793773	-4.033875	-1.043314
84	6	0	-2.016643	-1.626046	1.722674
85	1	0	-2.002889	-0.522837	1.775830
86	1	0	-1.023792	-1.999381	2.027845
87	6	0	-4.150741	-4.252998	-0.731234
88	1	0	-4.716469	-3.304822	-0.738911
89	1	0	-4.230447	-4.669031	0.291986
90	1	0	0.755059	0.054109	-4.034093
91	6	0	2.286229	1.528256	-4.390710
92	6	0	3.629217	1.823787	-4.650713
93	6	0	1.363072	2.574574	-4.352596
94	6	0	4.036729	3.135771	-4.870015
95	1	0	4.362853	1.014390	-4.676688
96	6	0	1.766567	3.891443	-4.573737
97	1	0	0.313206	2.358232	-4.138839
98	6	0	3.104620	4.174292	-4.833156
99	1	0	5.088242	3.351632	-5.072654
100	1	0	1.030492	4.696826	-4.530961
101	1	0	3.424812	5.204324	-5.005305
102	6	0	2.201101	-4.391430	1.770874
103	6	0	3.225034	-3.588675	2.277980
104	6	0	1.746290	-5.471857	2.534879
105	6	0	3.792733	-3.865700	3.522259
106	1	0	3.581598	-2.726623	1.709718
107	6	0	2.307386	-5.748099	3.777752
108	1	0	0.944108	-6.104706	2.146459
109	6	0	3.335418	-4.945075	4.273416
110	1	0	4.593835	-3.228206	3.903944
111	1	0	1.945561	-6.596799	4.362590
112	1	0	3.779244	-5.163277	5.247405
113	6	0	1.567402	-4.094693	0.438829
114	1	0	2.182716	-3.387002	-0.135823
115	1	0	1.477028	-5.023784	-0.153353
116	6	0	-4.767182	-5.214178	-1.716337
117	6	0	-3.987685	-6.131559	-2.423241
118	6	0	-6.152962	-5.218736	-1.903211
119	6	0	-4.582855	-7.036136	-3.301070
120	1	0	-2.906192	-6.127323	-2.283720
121	6	0	-6.749322	-6.126653	-2.774572
122	1	0	-6.773882	-4.502614	-1.358102
123	6	0	-5.964478	-7.038579	-3.478660
124	1	0	-3.960245	-7.746063	-3.850479
125	1	0	-7.833235	-6.117672	-2.909164
126	1	0	-6.429756	-7.747703	-4.166738
127	6	0	-1.613296	5.240706	1.672895
128	6	0	-2.943792	5.013337	1.300696
129	6	0	-3.250185	4.894995	-0.064635
130	6	0	-2.215873	5.041764	-0.997088

131	6	0	-0.892657	5.238106	-0.622910
132	6	0	-0.584371	5.321356	0.743461
133	1	0	-1.361554	5.341274	2.730029
134	1	0	-2.424710	4.979020	-2.066889
135	6	0	-4.642317	4.585958	-0.587040
136	1	0	-4.779741	5.129489	-1.532204
137	1	0	-5.405443	4.973989	0.096348
138	6	0	-3.973210	4.865178	2.408675
139	1	0	-4.967837	5.153579	2.052167
140	1	0	-3.720176	5.576807	3.207145
141	6	0	-4.877958	3.109279	-0.859571
142	6	0	-5.456084	2.229089	0.072911
143	6	0	-4.489785	2.601161	-2.103450
144	6	0	-5.641959	0.891906	-0.294414
145	6	0	-4.639190	1.262300	-2.446276
146	1	0	-4.050561	3.263667	-2.852448
147	6	0	-5.241214	0.391062	-1.528018
148	1	0	-6.115758	0.192223	0.397009
149	6	0	-3.999433	3.469030	3.004784
150	6	0	-3.090672	3.190200	4.038942
151	6	0	-4.847191	2.452377	2.547633
152	6	0	-2.985149	1.927768	4.609841
153	1	0	-2.463295	3.998357	4.412914
154	6	0	-4.722784	1.177432	3.120280
155	6	0	-3.806994	0.893296	4.119172
156	1	0	-5.355642	0.354012	2.783982
157	6	0	-5.893736	2.653689	1.463416
158	1	0	-6.775853	2.056824	1.734809
159	1	0	-6.231084	3.696120	1.452919
160	8	0	0.722056	5.485415	1.111031
161	8	0	0.071580	5.284443	-1.585060
162	6	0	0.795573	6.497750	-1.703693
163	1	0	1.505537	6.365203	-2.529931
164	1	0	0.119938	7.336089	-1.944033
165	1	0	1.349109	6.728126	-0.782512
166	8	0	-4.233081	0.819756	-3.678103
167	8	0	-5.407455	-0.938989	-1.789489
168	6	0	-6.310215	-1.266248	-2.835719
169	1	0	-6.321732	-2.360314	-2.917055
170	1	0	-7.327163	-0.912776	-2.597232
171	1	0	-5.986270	-0.831738	-3.791982
172	8	0	-2.151919	1.605210	5.625170
173	6	0	-1.260882	2.580190	6.114450
174	1	0	-0.672868	2.100450	6.905883
175	1	0	-0.578177	2.937261	5.325430
176	1	0	-1.797173	3.443795	6.540805

Compound ***P*-8**, conformer 2

Center Number	Atomic Number	Atomic Type	Coordinates (Angstroms) X	Y	Z
1	6	0	-4.477254	-2.852515	-2.202090
2	6	0	-4.900208	-3.399695	-0.981080
3	6	0	-4.242477	-4.540171	-0.503601
4	6	0	-3.219373	-5.116022	-1.275053
5	6	0	-2.816639	-4.573774	-2.489294
6	6	0	-3.449158	-3.401344	-2.948516
7	1	0	-4.953249	-1.955957	-2.603354
8	1	0	-2.740872	-6.024138	-0.910386
9	6	0	-4.538628	-5.171746	0.845168
10	1	0	-4.372536	-6.255104	0.764307
11	1	0	-5.594040	-5.047022	1.109783
12	6	0	-6.047466	-2.720244	-0.251044
13	1	0	-6.584082	-3.447253	0.368664
14	1	0	-6.769889	-2.381398	-1.006934
15	6	0	-3.641759	-4.635132	1.948183
16	6	0	-4.014299	-3.591117	2.810931
17	6	0	-2.360736	-5.186932	2.075807
18	6	0	-3.095113	-3.158359	3.774340
19	6	0	-1.438371	-4.716214	3.000940
20	1	0	-2.058507	-6.008074	1.422914
21	6	0	-1.814457	-3.686114	3.875040
22	1	0	-3.359853	-2.360588	4.471031
23	6	0	-5.649198	-1.514696	0.581628
24	6	0	-5.604027	-0.265772	-0.047064
25	6	0	-5.332361	-1.591006	1.949926
26	6	0	-5.224330	0.894780	0.618276
27	1	0	-5.872978	-0.170351	-1.100917
28	6	0	-4.967354	-0.416857	2.616399
29	6	0	-4.889179	0.815184	1.976889
30	1	0	-4.733783	-0.442833	3.683014
31	6	0	-5.358165	-2.885814	2.744552
32	1	0	-5.665643	-2.644991	3.771692
33	1	0	-6.127362	-3.559279	2.351232
34	8	0	-3.115863	-2.850998	-4.148543
35	8	0	-1.856014	-5.090205	-3.288439
36	6	0	-1.151444	-6.231822	-2.859192
37	1	0	-0.416463	-6.460496	-3.640068
38	1	0	-0.621835	-6.048079	-1.909543
39	1	0	-1.820777	-7.098535	-2.732529
40	8	0	-0.175480	-5.234162	3.094766
41	8	0	-0.941386	-3.154305	4.776251
42	6	0	-0.524176	-4.003826	5.831649
43	1	0	-1.387182	-4.335538	6.433434
44	1	0	0.013995	-4.883782	5.450822
45	1	0	0.147811	-3.415587	6.469757
46	8	0	-4.526122	1.932056	2.682951
47	8	0	-5.152798	2.066101	-0.080872

48	6	0	-6.072094	3.080762	0.296737
49	1	0	-5.879270	3.943995	-0.352449
50	1	0	-7.110183	2.741288	0.144935
51	1	0	-5.932323	3.373771	1.346947
52	6	0	0.669927	-5.071269	1.966644
53	1	0	1.617585	-5.564127	2.222932
54	1	0	0.255675	-5.576540	1.077353
55	6	0	0.919171	-3.603942	1.660042
56	1	0	-0.010017	-3.118048	1.324091
57	1	0	1.238420	-3.085928	2.581083
58	6	0	-1.786917	-2.375954	-4.320830
59	1	0	-1.330881	-2.887670	-5.183256
60	1	0	-1.175575	-2.614395	-3.438194
61	6	0	-1.800706	-0.884400	-4.581427
62	1	0	-0.772398	-0.562385	-4.836973
63	1	0	-2.445398	-0.675964	-5.448082
64	6	0	-3.129412	2.137277	2.858356
65	1	0	-2.994793	2.645112	3.824372
66	1	0	-2.603413	1.170149	2.902677
67	6	0	-2.564007	2.966482	1.720139
68	1	0	-2.902020	2.541018	0.767720
69	1	0	-2.939724	4.005236	1.780024
70	8	0	1.909158	-3.526515	0.659335
71	8	0	-2.311527	-0.121462	-3.516885
72	8	0	-1.153898	2.950457	1.809692
73	6	0	3.250664	-0.949616	0.881956
74	6	0	1.949722	-1.125173	0.094590
75	6	0	0.884786	0.632983	1.272842
76	6	0	2.106811	0.857508	2.172113
77	6	0	3.386651	0.466689	1.435886
78	1	0	2.002696	-0.506735	-0.817104
79	1	0	3.234364	-1.645819	1.738592
80	1	0	-0.046524	0.824154	1.816901
81	1	0	2.002488	0.182216	3.040032
82	1	0	3.534729	1.158734	0.591169
83	8	0	0.839005	-0.708164	0.873948
84	8	0	0.993515	1.488630	0.163454
85	8	0	2.198755	2.190673	2.606907
86	8	0	4.501778	0.491414	2.298888
87	8	0	4.307859	-1.281619	0.017850
88	6	0	1.539112	2.466264	3.833586
89	1	0	0.460126	2.264780	3.738357
90	6	0	5.230115	1.711378	2.362283
91	1	0	4.535615	2.561080	2.410366
92	1	0	5.783315	1.670913	3.312035
93	6	0	5.423334	-1.963755	0.565746
94	1	0	5.114945	-2.486198	1.486516
95	1	0	6.210750	-1.245827	0.838591
96	6	0	6.199990	1.884276	1.216879
97	6	0	7.412275	1.185178	1.205283

98	6	0	5.903318	2.724866	0.140767
99	6	0	8.299892	1.313055	0.140763
100	1	0	7.665749	0.537678	2.048814
101	6	0	6.788112	2.855360	-0.929610
102	1	0	4.970356	3.294465	0.142899
103	6	0	7.986705	2.147006	-0.933109
104	1	0	9.244586	0.764601	0.150064
105	1	0	6.539868	3.516451	-1.762806
106	1	0	8.682500	2.249511	-1.768717
107	6	0	5.941644	-2.959874	-0.438154
108	6	0	5.210966	-4.122540	-0.711173
109	6	0	7.133157	-2.732632	-1.128054
110	6	0	5.667500	-5.038805	-1.653450
111	1	0	4.273521	-4.302327	-0.177190
112	6	0	7.594466	-3.650623	-2.072402
113	1	0	7.707367	-1.825265	-0.923402
114	6	0	6.862024	-4.804690	-2.336558
115	1	0	5.091267	-5.944408	-1.856486
116	1	0	8.529909	-3.461433	-2.603688
117	1	0	7.221255	-5.525259	-3.074694
118	6	0	1.723172	-2.560639	-0.347137
119	1	0	2.452218	-2.794656	-1.133156
120	1	0	0.708018	-2.634684	-0.777895
121	6	0	-0.148090	2.161404	-0.289356
122	8	0	-1.242559	1.274061	-0.362696
123	6	0	-1.835747	1.244630	-1.655834
124	6	0	-1.285358	2.475631	-2.380598
125	6	0	0.096630	2.648372	-1.744264
126	1	0	-2.927089	1.312696	-1.532399
127	1	0	-1.191965	2.301399	-3.464771
128	1	0	0.402491	3.707512	-1.767803
129	6	0	-0.493732	3.344469	0.630878
130	1	0	0.450032	3.829548	0.917963
131	1	0	-1.108037	4.064487	0.068321
132	8	0	1.002084	1.850904	-2.453054
133	8	0	-2.031709	3.641255	-2.127960
134	6	0	-1.513917	-0.064505	-2.359296
135	1	0	-1.732388	-0.896922	-1.667114
136	1	0	-0.441041	-0.097427	-2.613629
137	6	0	-3.275345	3.716072	-2.786349
138	1	0	-4.016127	3.049981	-2.310268
139	1	0	-3.158101	3.373648	-3.833143
140	1	0	1.946308	1.808835	4.622756
141	6	0	1.758331	3.909754	4.195920
142	6	0	2.933798	4.309212	4.838659
143	6	0	0.805612	4.876877	3.864203
144	6	0	3.154089	5.649409	5.146165
145	1	0	3.683014	3.558972	5.104721
146	6	0	1.022576	6.218766	4.172450
147	1	0	-0.109979	4.562897	3.356811

148	6	0	2.197242	6.607421	4.813238
149	1	0	4.075056	5.948346	5.651692
150	1	0	0.269431	6.965603	3.911165
151	1	0	2.367213	7.658622	5.056678
152	6	0	3.136794	1.451753	-3.419246
153	6	0	2.931241	1.660931	-4.787536
154	6	0	4.045610	0.471494	-3.014600
155	6	0	3.622616	0.909572	-5.732527
156	1	0	2.220559	2.425023	-5.112851
157	6	0	4.743098	-0.280475	-3.960785
158	1	0	4.209215	0.275163	-1.952419
159	6	0	4.533658	-0.063557	-5.319732
160	1	0	3.454662	1.085276	-6.797475
161	1	0	5.450820	-1.043416	-3.628092
162	1	0	5.079441	-0.652227	-6.060497
163	6	0	2.360259	2.258687	-2.413953
164	1	0	2.773291	2.122197	-1.404033
165	1	0	2.419131	3.334450	-2.662382
166	6	0	-3.790487	5.133226	-2.773274
167	6	0	-2.923433	6.220971	-2.653635
168	6	0	-5.159864	5.373412	-2.922798
169	6	0	-3.416663	7.524334	-2.682250
170	1	0	-1.855450	6.037224	-2.531843
171	6	0	-5.652888	6.675357	-2.958813
172	1	0	-5.849768	4.530003	-3.013331
173	6	0	-4.781473	7.756544	-2.836871
174	1	0	-2.727042	8.365885	-2.583815
175	1	0	-6.725247	6.846258	-3.076701
176	1	0	-5.166939	8.778160	-2.859367

Compound ***P*-8**, conformer 3

Center Number	Atomic Number	Atomic Type	Coordinates (Angstroms) X	Y	Z
1	6	0	4.986901	-0.726446	2.492356
2	6	0	4.862443	-2.123736	2.462103
3	6	0	3.988988	-2.731129	3.372698
4	6	0	3.298526	-1.930941	4.298207
5	6	0	3.435143	-0.548258	4.325677
6	6	0	4.286354	0.065627	3.385203
7	1	0	5.649467	-0.212659	1.793611
8	1	0	2.648635	-2.417259	5.024659
9	6	0	3.707759	-4.223422	3.389757
10	1	0	3.517044	-4.526608	4.428870
11	1	0	4.589971	-4.787183	3.068295
12	6	0	5.675765	-2.893634	1.434703
13	1	0	5.886728	-3.905414	1.798265
14	1	0	6.653041	-2.399464	1.341099

15	6	0	2.495785	-4.604458	2.556225
16	6	0	2.576467	-5.059119	1.229814
17	6	0	1.231335	-4.450679	3.137359
18	6	0	1.388173	-5.362694	0.554057
19	6	0	0.056496	-4.696167	2.438729
20	1	0	1.153577	-4.106752	4.170159
21	6	0	0.134399	-5.176300	1.122717
22	1	0	1.416479	-5.736651	-0.471331
23	6	0	5.050410	-2.950780	0.052208
24	6	0	5.302198	-1.891479	-0.825957
25	6	0	4.233712	-4.008524	-0.386171
26	6	0	4.748822	-1.825740	-2.099637
27	1	0	5.951949	-1.068076	-0.523109
28	6	0	3.699278	-3.946656	-1.677236
29	6	0	3.924048	-2.873453	-2.531988
30	1	0	3.077003	-4.762571	-2.051236
31	6	0	3.885435	-5.212011	0.474057
32	1	0	3.797399	-6.085971	-0.186293
33	1	0	4.705040	-5.438279	1.164797
34	8	0	4.490322	1.411960	3.396760
35	8	0	2.816686	0.273876	5.203352
36	6	0	1.900612	-0.272970	6.123059
37	1	0	1.506351	0.564656	6.710606
38	1	0	1.064721	-0.777534	5.610363
39	1	0	2.387224	-0.990052	6.804374
40	8	0	-1.177348	-4.487754	2.990500
41	8	0	-0.978513	-5.404288	0.370104
42	6	0	-1.846897	-6.434869	0.810186
43	1	0	-2.669166	-6.488752	0.085297
44	1	0	-1.324505	-7.406364	0.830982
45	1	0	-2.255018	-6.219199	1.807770
46	8	0	3.370635	-2.868457	-3.785640
47	8	0	4.989895	-0.722350	-2.867980
48	6	0	5.743592	-0.929216	-4.052816
49	1	0	5.847957	0.048784	-4.539490
50	1	0	6.746663	-1.319849	-3.813704
51	1	0	5.232949	-1.624866	-4.734008
52	6	0	-1.457260	-3.181045	3.469489
53	1	0	-2.480400	-3.216866	3.867425
54	1	0	-0.784119	-2.899198	4.296484
55	6	0	-1.369795	-2.158453	2.350299
56	1	0	-0.333168	-2.079040	1.985453
57	1	0	-1.983790	-2.498712	1.498656
58	6	0	3.375683	2.263856	3.166489
59	1	0	3.283051	2.965716	4.010461
60	1	0	2.445517	1.679048	3.124734
61	6	0	3.575678	3.052994	1.889690
62	1	0	2.762874	3.801003	1.809512
63	1	0	4.530358	3.596522	1.944802
64	6	0	2.018874	-2.433942	-3.873333

65	1	0	1.554035	-2.981770	-4.705841
66	1	0	1.474201	-2.686516	-2.949255
67	6	0	1.958380	-0.935341	-4.101889
68	1	0	2.613359	-0.439693	-3.375088
69	1	0	2.330730	-0.689933	-5.114697
70	8	0	-1.811725	-0.916878	2.847687
71	8	0	3.639137	2.261643	0.728870
72	8	0	0.621439	-0.507030	-3.954987
73	6	0	-3.122439	0.457045	0.630718
74	6	0	-1.608647	0.515960	0.847353
75	6	0	-1.171385	-0.238085	-1.363212
76	6	0	-2.662232	-0.453321	-1.651356
77	6	0	-3.484428	0.550164	-0.848930
78	1	0	-1.258816	1.532282	0.601389
79	1	0	-3.492401	-0.513684	1.005553
80	1	0	-0.547957	-0.983575	-1.869961
81	1	0	-2.914295	-1.465091	-1.289780
82	1	0	-3.248307	1.565316	-1.209241
83	8	0	-0.945992	-0.417800	0.008223
84	8	0	-0.837639	1.058162	-1.778003
85	8	0	-2.992878	-0.323447	-3.009521
86	8	0	-4.866156	0.297325	-0.971861
87	8	0	-3.686778	1.502646	1.381920
88	6	0	-2.631893	-1.408030	-3.852898
89	1	0	-2.982836	-1.111343	-4.852396
90	6	0	-5.548209	1.080361	-1.921468
91	1	0	-5.500377	2.150003	-1.641200
92	1	0	-5.063763	0.982101	-2.907849
93	6	0	-5.003904	1.329268	1.871770
94	1	0	-5.259995	0.256779	1.868161
95	1	0	-5.729638	1.836442	1.215249
96	6	0	-6.989471	0.650696	-2.019413
97	6	0	-7.421514	-0.577197	-1.515044
98	6	0	-7.916638	1.483924	-2.654410
99	6	0	-8.754816	-0.966025	-1.645807
100	1	0	-6.702128	-1.224701	-1.013708
101	6	0	-9.245815	1.094735	-2.789413
102	1	0	-7.592812	2.451981	-3.046730
103	6	0	-9.670647	-0.134110	-2.284071
104	1	0	-9.078891	-1.928603	-1.243148
105	1	0	-9.957180	1.757383	-3.287565
106	1	0	-10.714498	-0.438966	-2.385717
107	6	0	-5.097784	1.873462	3.274430
108	6	0	-4.346528	1.286499	4.300354
109	6	0	-5.917087	2.961500	3.575309
110	6	0	-4.418273	1.780197	5.598770
111	1	0	-3.699753	0.434834	4.071478
112	6	0	-5.993427	3.456982	4.877930
113	1	0	-6.504558	3.428415	2.780419
114	6	0	-5.243434	2.867805	5.891298

115	1	0	-3.829716	1.313287	6.391902
116	1	0	-6.640158	4.309104	5.098713
117	1	0	-5.300125	3.253943	6.911478
118	6	0	-1.216995	0.229922	2.287047
119	1	0	-1.542761	1.075989	2.905180
120	1	0	-0.114984	0.159816	2.339418
121	6	0	0.430332	1.302507	-2.314947
122	8	0	1.420779	0.609614	-1.590143
123	6	0	2.480257	1.459551	-1.164707
124	6	0	2.289045	2.772516	-1.929264
125	6	0	0.771005	2.803717	-2.162963
126	1	0	3.433264	0.980301	-1.435355
127	1	0	2.616208	3.634386	-1.326952
128	1	0	0.534463	3.364093	-3.083520
129	6	0	0.476720	0.882363	-3.795325
130	1	0	-0.474539	1.185923	-4.256453
131	1	0	1.298546	1.417726	-4.294978
132	8	0	0.096529	3.341038	-1.060878
133	8	0	2.924227	2.774424	-3.187672
134	6	0	2.441195	1.630665	0.345793
135	1	0	2.335683	0.634331	0.810399
136	1	0	1.563653	2.237549	0.627414
137	6	0	4.332887	2.919746	-3.167963
138	1	0	4.643746	2.802638	-4.216604
139	1	0	4.806554	2.103961	-2.596504
140	1	0	-1.536356	-1.510954	-3.909079
141	6	0	-3.261427	-2.723771	-3.457741
142	6	0	-4.651933	-2.839098	-3.348943
143	6	0	-2.470527	-3.840974	-3.185579
144	6	0	-5.235939	-4.046368	-2.979386
145	1	0	-5.280830	-1.968541	-3.550089
146	6	0	-3.052062	-5.054641	-2.817875
147	1	0	-1.382705	-3.759601	-3.254970
148	6	0	-4.436263	-5.159441	-2.714142
149	1	0	-6.322704	-4.122004	-2.898370
150	1	0	-2.417087	-5.916806	-2.603100
151	1	0	-4.895027	-6.107408	-2.424347
152	6	0	-0.751788	5.210812	0.160569
153	6	0	-0.346794	6.367119	0.831151
154	6	0	-1.860591	4.506604	0.640173
155	6	0	-1.040521	6.818433	1.953242
156	1	0	0.524798	6.921624	0.473689
157	6	0	-2.545913	4.946859	1.768999
158	1	0	-2.188455	3.598326	0.134596
159	6	0	-2.140458	6.107464	2.427191
160	1	0	-0.711265	7.725237	2.465491
161	1	0	-3.397897	4.369860	2.135082
162	1	0	-2.678837	6.453865	3.312177
163	6	0	-0.018090	4.747733	-1.070668
164	1	0	-0.563909	5.061033	-1.982305

165	1	0	0.975530	5.228543	-1.113646
166	6	0	4.788689	4.259771	-2.638518
167	6	0	4.296885	5.441542	-3.203573
168	6	0	5.700120	4.343062	-1.585130
169	6	0	4.714947	6.680677	-2.728442
170	1	0	3.576141	5.384127	-4.022920
171	6	0	6.126606	5.583630	-1.110855
172	1	0	6.071304	3.425380	-1.122567
173	6	0	5.634679	6.754358	-1.681433
174	1	0	4.325259	7.596348	-3.178887
175	1	0	6.841737	5.633887	-0.286791
176	1	0	5.964766	7.726840	-1.309598

Compound ***P*-8**, conformer 4

Center Number	Atomic Number	Atomic Type	Coordinates (Angstroms) X	Y	Z
1	8	0	2.828283	0.592454	-5.032082
2	6	0	-1.233508	4.982686	-0.535253
3	1	0	-2.251598	5.387012	-0.454389
4	1	0	-0.881344	5.159059	-1.565714
5	6	0	-1.244145	3.494497	-0.232241
6	1	0	-0.244083	3.061894	-0.395951
7	1	0	-1.489127	3.342598	0.833271
8	6	0	1.554521	-0.032073	-4.935885
9	1	0	1.064728	-0.008101	-5.922297
10	1	0	0.908036	0.518049	-4.236993
11	6	0	1.718498	-1.472858	-4.499932
12	1	0	0.731189	-1.971304	-4.557955
13	1	0	2.397711	-1.985778	-5.196822
14	6	0	3.386207	-0.502414	3.465341
15	1	0	3.317082	-0.563437	4.560926
16	1	0	2.759608	0.339412	3.128271
17	6	0	2.900999	-1.784231	2.814527
18	1	0	3.185320	-1.778614	1.755053
19	1	0	3.384992	-2.658963	3.288890
20	8	0	-2.190454	2.879549	-1.075455
21	8	0	2.278488	-1.624341	-3.219528
22	8	0	1.499675	-1.859197	2.962978
23	6	0	-3.306554	0.648107	0.429894
24	6	0	-2.013972	0.517961	-0.379640
25	6	0	-0.814353	-0.311567	1.492111
26	6	0	-2.022908	-0.131304	2.419990
27	6	0	-3.319812	-0.295537	1.629806
28	1	0	-2.000143	-0.473326	-0.863477
29	1	0	-3.373094	1.680016	0.815889
30	1	0	0.125662	-0.118791	2.020908
31	1	0	-1.986455	0.908583	2.787462

32	1	0	-3.382944	-1.331885	1.260678
33	8	0	-0.880677	0.638077	0.465460
34	8	0	-0.832242	-1.620770	0.981548
35	8	0	-2.023038	-1.028601	3.500538
36	8	0	-4.449256	0.020608	2.412776
37	8	0	-4.374077	0.400610	-0.449937
38	6	0	-1.163582	-0.708816	4.585791
39	1	0	-1.312577	-1.525566	5.307620
40	6	0	-5.057036	-1.056252	3.114551
41	1	0	-4.286912	-1.661436	3.612030
42	1	0	-5.674496	-0.582888	3.891777
43	6	0	-5.557162	1.164891	-0.288302
44	1	0	-5.318147	2.098239	0.247647
45	1	0	-6.286156	0.609935	0.320268
46	6	0	-5.924726	-1.927748	2.236783
47	6	0	-7.193829	-1.492337	1.838780
48	6	0	-5.475451	-3.173309	1.790281
49	6	0	-7.988032	-2.275144	1.005773
50	1	0	-7.567036	-0.528981	2.196186
51	6	0	-6.266736	-3.961618	0.954843
52	1	0	-4.494901	-3.537558	2.107887
53	6	0	-7.523119	-3.512025	0.557755
54	1	0	-8.978467	-1.922868	0.708594
55	1	0	-5.899422	-4.932440	0.615005
56	1	0	-8.145600	-4.127974	-0.094918
57	6	0	-6.134974	1.486124	-1.641883
58	6	0	-5.507865	2.429660	-2.464466
59	6	0	-7.278275	0.836311	-2.108938
60	6	0	-6.018128	2.716995	-3.726629
61	1	0	-4.608109	2.937724	-2.105911
62	6	0	-7.793373	1.123532	-3.373623
63	1	0	-7.771985	0.095655	-1.474427
64	6	0	-7.163683	2.063999	-4.184292
65	1	0	-5.522622	3.457320	-4.358909
66	1	0	-8.690224	0.608996	-3.725802
67	1	0	-7.565248	2.291280	-5.174343
68	6	0	-1.908305	1.560926	-1.479423
69	1	0	-2.643305	1.316045	-2.256431
70	1	0	-0.896521	1.497236	-1.920281
71	6	0	0.383886	-2.300061	0.822654
72	8	0	1.355417	-1.444470	0.263778
73	6	0	1.942732	-1.980490	-0.915520
74	6	0	1.546031	-3.459113	-0.928842
75	6	0	0.196154	-3.449144	-0.205242
76	1	0	3.034154	-1.863094	-0.837211
77	1	0	1.430517	-3.839796	-1.956710
78	1	0	0.020619	-4.414664	0.297855
79	6	0	0.884893	-2.845110	2.170992
80	1	0	0.012498	-3.231460	2.718194
81	1	0	1.581315	-3.676599	1.981832

82	8	0	-0.800194	-3.191662	-1.153275
83	8	0	2.428283	-4.272682	-0.194414
84	6	0	1.471836	-1.215471	-2.142217
85	1	0	1.571506	-0.134587	-1.938284
86	1	0	0.407873	-1.434578	-2.336159
87	6	0	3.685325	-4.495866	-0.791765
88	1	0	4.338096	-3.612139	-0.681876
89	1	0	3.551339	-4.666074	-1.877855
90	1	0	-0.109030	-0.742684	4.270137
91	6	0	-1.472861	0.617079	5.241543
92	6	0	-0.490257	1.601671	5.357060
93	6	0	-2.752793	0.879249	5.743176
94	6	0	-0.772547	2.822948	5.969468
95	1	0	0.509574	1.413240	4.957532
96	6	0	-3.039752	2.097379	6.350584
97	1	0	-3.530454	0.117157	5.652794
98	6	0	-2.048327	3.073078	6.467058
99	1	0	0.007999	3.582642	6.049901
100	1	0	-4.042287	2.288865	6.739826
101	1	0	-2.273603	4.028864	6.945349
102	6	0	-2.956478	-3.575732	-2.077717
103	6	0	-3.958772	-2.610059	-2.194644
104	6	0	-2.732058	-4.451403	-3.145821
105	6	0	-4.728317	-2.526422	-3.355622
106	1	0	-4.140923	-1.902561	-1.382227
107	6	0	-3.496023	-4.367634	-4.305525
108	1	0	-1.948557	-5.209114	-3.063336
109	6	0	-4.499384	-3.403724	-4.411920
110	1	0	-5.508518	-1.765383	-3.431738
111	1	0	-3.312227	-5.059622	-5.130489
112	1	0	-5.101950	-3.338494	-5.320667
113	6	0	-2.100852	-3.666436	-0.843022
114	1	0	-2.538358	-3.078986	-0.022880
115	1	0	-2.028531	-4.717118	-0.506922
116	6	0	4.354616	-5.696069	-0.170759
117	6	0	3.611273	-6.707948	0.439701
118	6	0	5.745388	-5.824778	-0.236818
119	6	0	4.246848	-7.827268	0.974482
120	1	0	2.526939	-6.607894	0.497818
121	6	0	6.380877	-6.945999	0.290867
122	1	0	6.339199	-5.037291	-0.708758
123	6	0	5.632378	-7.951551	0.900624
124	1	0	3.652913	-8.609691	1.452541
125	1	0	7.468133	-7.031726	0.230957
126	1	0	6.129437	-8.828956	1.320010
127	6	0	1.737385	5.454359	-0.572881
128	6	0	3.078984	5.060897	-0.493180
129	6	0	3.570471	4.589303	0.735009
130	6	0	2.701853	4.549873	1.832523
131	6	0	1.362562	4.906457	1.739982

132	6	0	0.869445	5.359001	0.507014
133	1	0	1.343245	5.833862	-1.517384
134	1	0	3.057008	4.203944	2.805252
135	6	0	4.991805	4.091657	0.934049
136	1	0	5.319804	4.392609	1.938781
137	1	0	5.674327	4.586832	0.234832
138	6	0	3.910961	5.120303	-1.763397
139	1	0	4.971612	5.254053	-1.525530
140	1	0	3.611776	6.014470	-2.328095
141	6	0	5.131936	2.582072	0.830095
142	6	0	5.468616	1.914450	-0.361270
143	6	0	4.906516	1.819669	1.980623
144	6	0	5.582859	0.520365	-0.338337
145	6	0	4.984922	0.431639	1.987330
146	1	0	4.659864	2.311978	2.923850
147	6	0	5.341427	-0.232405	0.805587
148	1	0	5.870330	-0.023024	-1.240625
149	6	0	3.706181	3.904119	-2.649567
150	6	0	2.626439	3.933910	-3.547635
151	6	0	4.503991	2.755357	-2.577997
152	6	0	2.304152	2.847577	-4.351785
153	1	0	2.036143	4.846352	-3.621694
154	6	0	4.161133	1.658293	-3.382950
155	6	0	3.078183	1.674718	-4.245076
156	1	0	4.747927	0.738484	-3.347078
157	6	0	5.721305	2.630084	-1.676191
158	1	0	6.486678	2.063176	-2.224770
159	1	0	6.157877	3.617954	-1.491546
160	8	0	-0.452624	5.696187	0.411077
161	8	0	0.554609	4.749053	2.826093
162	6	0	-0.015037	5.925783	3.374410
163	1	0	-0.613075	5.615566	4.240818
164	1	0	0.771220	6.621383	3.713590
165	1	0	-0.663837	6.435388	2.647934
166	8	0	4.750957	-0.263013	3.145230
167	8	0	5.418947	-1.593993	0.731781
168	6	0	6.446977	-2.208176	1.495023
169	1	0	6.365358	-3.289581	1.328674
170	1	0	7.439567	-1.866356	1.157510
171	1	0	6.330387	-1.993069	2.566642
172	8	0	1.296443	2.823667	-5.253281
173	6	0	0.452716	3.945921	-5.365508
174	1	0	-0.294269	3.702996	-6.130529
175	1	0	-0.063324	4.161740	-4.415113
176	1	0	1.009777	4.843226	-5.681393

Compound ***P*-8**, conformer 5

Center	Atomic	Atomic	Coordinates (Angstroms)		

Number	Number	Type	X	Y	Z
1	8	0	-3.963527	-0.447300	4.519839
2	6	0	1.187363	4.478969	2.193778
3	1	0	2.219932	4.785307	2.409319
4	1	0	0.639951	4.442854	3.150721
5	6	0	1.189101	3.110313	1.534810
6	1	0	0.159347	2.735969	1.417858
7	1	0	1.615929	3.198047	0.520628
8	6	0	-2.711758	-1.126147	4.534810
9	1	0	-2.448241	-1.378426	5.574807
10	1	0	-1.918506	-0.473260	4.143093
11	6	0	-2.813812	-2.404461	3.730119
12	1	0	-1.876077	-2.977995	3.863738
13	1	0	-3.641539	-3.012413	4.124071
14	6	0	-2.701745	0.628491	-3.906869
15	1	0	-2.402904	0.810839	-4.949001
16	1	0	-2.129398	1.313736	-3.260489
17	6	0	-2.419066	-0.805208	-3.499729
18	1	0	-2.920108	-1.013976	-2.546277
19	1	0	-2.828731	-1.502229	-4.255142
20	8	0	1.944803	2.239326	2.343460
21	8	0	-3.085152	-2.201798	2.366568
22	8	0	-1.022700	-0.973285	-3.384845
23	6	0	3.256344	0.280788	0.617332
24	6	0	1.812236	0.117299	1.095920
25	6	0	1.000874	-0.095013	-1.130678
26	6	0	2.386535	0.186764	-1.727338
27	6	0	3.468832	-0.304151	-0.773436
28	1	0	1.634894	-0.950982	1.307534
29	1	0	3.487322	1.357915	0.571230
30	1	0	0.205055	0.321295	-1.758277
31	1	0	2.477826	1.283625	-1.806934
32	1	0	3.403292	-1.402646	-0.704959
33	8	0	0.896983	0.556928	0.104429
34	8	0	0.843494	-1.484741	-0.993372
35	8	0	2.585295	-0.412841	-2.981034
36	8	0	4.755955	0.074523	-1.208046
37	8	0	4.095559	-0.358730	1.553192
38	6	0	1.995988	0.244509	-4.093580
39	1	0	2.257230	-0.384248	-4.957914
40	6	0	5.480100	-0.915923	-1.896860
41	1	0	5.640199	-1.795669	-1.245149
42	1	0	4.903567	-1.262849	-2.771858
43	6	0	5.235427	0.378498	1.966908
44	1	0	4.911674	1.333011	2.418119
45	1	0	5.868941	0.605248	1.094875
46	6	0	6.813422	-0.377316	-2.347706
47	6	0	7.815163	-1.266898	-2.750861
48	6	0	7.068307	0.994291	-2.402287

49	6	0	9.042643	-0.795618	-3.206629
50	1	0	7.631099	-2.343897	-2.705399
51	6	0	8.300383	1.467285	-2.854316
52	1	0	6.291499	1.689606	-2.084017
53	6	0	9.290216	0.576097	-3.259665
54	1	0	9.814122	-1.503772	-3.517421
55	1	0	8.486405	2.543353	-2.888315
56	1	0	10.254635	0.947238	-3.613243
57	6	0	5.994201	-0.442750	2.972019
58	6	0	5.696616	-0.353308	4.334365
59	6	0	6.965984	-1.355151	2.552290
60	6	0	6.357979	-1.156769	5.260672
61	1	0	4.938185	0.357362	4.672986
62	6	0	7.629518	-2.161032	3.474420
63	1	0	7.206564	-1.431746	1.488684
64	6	0	7.325542	-2.063670	4.831369
65	1	0	6.118453	-1.073752	6.323064
66	1	0	8.389157	-2.867696	3.133085
67	1	0	7.846592	-2.693106	5.556142
68	6	0	1.538863	0.893127	2.373791
69	1	0	2.103631	0.419275	3.187832
70	1	0	0.460565	0.814743	2.605193
71	6	0	-0.410881	-2.050186	-1.265535
72	8	0	-1.436168	-1.264058	-0.701144
73	6	0	-2.287214	-2.009986	0.159482
74	6	0	-1.982032	-3.478940	-0.144333
75	6	0	-0.510945	-3.434915	-0.568271
76	1	0	-3.329601	-1.761529	-0.090688
77	1	0	-2.107932	-4.113135	0.748232
78	1	0	-0.289357	-4.255046	-1.271354
79	6	0	-0.635275	-2.182937	-2.781595
80	1	0	0.315008	-2.504618	-3.232511
81	1	0	-1.393149	-2.961291	-2.960830
82	8	0	0.276768	-3.539542	0.583016
83	8	0	-2.730432	-3.985449	-1.222695
84	6	0	-2.046822	-1.627651	1.611051
85	1	0	-2.041598	-0.525540	1.684196
86	1	0	-1.062080	-2.001168	1.941022
87	6	0	-4.098317	-4.204410	-0.961038
88	1	0	-4.663146	-3.256166	-0.991224
89	1	0	-4.215863	-4.618964	0.059087
90	1	0	0.897561	0.242425	-4.011914
91	6	0	2.503930	1.650977	-4.312123
92	6	0	1.615856	2.722439	-4.418272
93	6	0	3.877169	1.900443	-4.411922
94	6	0	2.085032	4.019046	-4.631091
95	1	0	0.541546	2.542066	-4.327720
96	6	0	4.349427	3.192536	-4.618253
97	1	0	4.581700	1.071167	-4.317754
98	6	0	3.453082	4.256616	-4.731144

99	1	0	1.376245	4.846223	-4.710896
100	1	0	5.424393	3.372189	-4.692895
101	1	0	3.823827	5.270928	-4.894712
102	6	0	2.169747	-4.388688	1.747314
103	6	0	3.186339	-3.602239	2.293107
104	6	0	1.681341	-5.472295	2.485687
105	6	0	3.714378	-3.898725	3.550355
106	1	0	3.567730	-2.737719	1.745104
107	6	0	2.202650	-5.767727	3.741364
108	1	0	0.884262	-6.092106	2.066962
109	6	0	3.224030	-4.981156	4.275777
110	1	0	4.510406	-3.273877	3.962416
111	1	0	1.814845	-6.618628	4.306008
112	1	0	3.636622	-5.214510	5.259934
113	6	0	1.579245	-4.071809	0.400141
114	1	0	2.212757	-3.355946	-0.143849
115	1	0	1.507932	-4.991930	-0.208506
116	6	0	-4.677777	-5.167511	-1.966574
117	6	0	-3.872933	-6.088396	-2.639722
118	6	0	-6.055257	-5.170704	-2.206967
119	6	0	-4.435111	-6.995383	-3.536564
120	1	0	-2.797598	-6.084888	-2.458713
121	6	0	-6.618933	-6.081013	-3.097411
122	1	0	-6.695701	-4.451727	-1.688905
123	6	0	-5.808888	-6.996661	-3.767255
124	1	0	-3.792829	-7.708149	-4.058993
125	1	0	-7.696825	-6.071002	-3.273802
126	1	0	-6.248315	-7.707748	-4.470147
127	6	0	-1.701583	5.211190	1.768399
128	6	0	-3.012103	4.989450	1.327009
129	6	0	-3.249389	4.884526	-0.052959
130	6	0	-2.167459	5.024763	-0.930514
131	6	0	-0.864356	5.210580	-0.487703
132	6	0	-0.627139	5.296959	0.892487
133	1	0	-1.502775	5.304566	2.837695
134	1	0	-2.320704	4.963559	-2.009712
135	6	0	-4.615860	4.596541	-0.649867
136	1	0	-4.704277	5.163780	-1.586870
137	1	0	-5.409849	4.972349	0.004532
138	6	0	-4.096296	4.828443	2.379697
139	1	0	-5.072008	5.124165	1.979345
140	1	0	-3.882206	5.525746	3.201611
141	6	0	-4.843005	3.128669	-0.969370
142	6	0	-5.456210	2.226738	-0.081311
143	6	0	-4.408455	2.651265	-2.209866
144	6	0	-5.626500	0.898609	-0.486787
145	6	0	-4.544181	1.321175	-2.590283
146	1	0	-3.942791	3.332054	-2.925785
147	6	0	-5.178775	0.427804	-1.716258
148	1	0	-6.126468	0.182597	0.168531

149	6	0	-4.150023	3.422903	2.950890
150	6	0	-3.314212	3.124229	4.033439
151	6	0	-4.963287	2.402687	2.427649
152	6	0	-3.232194	1.851802	4.581501
153	1	0	-2.700286	3.903439	4.489733
154	6	0	-4.862579	1.117655	2.974341
155	6	0	-4.000523	0.819756	4.022236
156	1	0	-5.462654	0.296698	2.577473
157	6	0	-5.955856	2.622817	1.296658
158	1	0	-6.848244	2.020195	1.515969
159	1	0	-6.293835	3.664947	1.291284
160	8	0	0.657242	5.470776	1.327966
161	8	0	0.149647	5.241582	-1.397616
162	6	0	0.876505	6.454067	-1.503977
163	1	0	1.630469	6.305105	-2.287552
164	1	0	0.213433	7.284814	-1.799487
165	1	0	1.378427	6.706972	-0.559244
166	8	0	-4.093145	0.908745	-3.816598
167	8	0	-5.333604	-0.895387	-2.016075
168	6	0	-6.195967	-1.197790	-3.103217
169	1	0	-6.203130	-2.289638	-3.210726
170	1	0	-7.221542	-0.850352	-2.894800
171	1	0	-5.836702	-0.740643	-4.036040
172	8	0	-2.393219	1.619012	5.634235
173	6	0	-3.031390	1.366666	6.875448
174	1	0	-2.240755	1.191797	7.616086
175	1	0	-3.633735	2.234776	7.190982
176	1	0	-3.681726	0.479432	6.821603

Compound ***P*-8**, conformer 6

Center Number	Atomic Number	Atomic Type	Coordinates (Angstroms) X	Y	Z
1	8	0	-3.947255	-0.497412	4.525941
2	6	0	1.178825	4.471493	2.207108
3	1	0	2.211780	4.778689	2.419474
4	1	0	0.636097	4.429728	3.166398
5	6	0	1.180356	3.105824	1.541718
6	1	0	0.150709	2.730559	1.426175
7	1	0	1.604331	3.198504	0.526783
8	6	0	-2.694045	-1.173798	4.532705
9	1	0	-2.429397	-1.436109	5.569917
10	1	0	-1.902421	-0.515287	4.147234
11	6	0	-2.793934	-2.443956	3.715037
12	1	0	-1.855057	-3.017049	3.842283
13	1	0	-3.620336	-3.057537	4.102999
14	6	0	-2.705949	0.646422	-3.892301
15	1	0	-2.407835	0.838644	-4.932874

16	1	0	-2.134650	1.326872	-3.239937
17	6	0	-2.419924	-0.790388	-3.498560
18	1	0	-2.916316	-1.008072	-2.544696
19	1	0	-2.831966	-1.481392	-4.258157
20	8	0	1.939461	2.232484	2.344522
21	8	0	-3.066270	-2.227587	2.353788
22	8	0	-1.022763	-0.957306	-3.391456
23	6	0	3.262856	0.284800	0.614572
24	6	0	1.817722	0.115460	1.087421
25	6	0	1.014513	-0.088633	-1.143166
26	6	0	2.402087	0.198162	-1.733892
27	6	0	3.481860	-0.294271	-0.777647
28	1	0	1.641915	-0.954179	1.293530
29	1	0	3.490532	1.362847	0.573217
30	1	0	0.219711	0.329585	-1.770888
31	1	0	2.491214	1.295712	-1.807376
32	1	0	3.418978	-1.393205	-0.713738
33	8	0	0.905480	0.557727	0.094431
34	8	0	0.858834	-1.479383	-1.013688
35	8	0	2.608914	-0.394879	-2.989104
36	8	0	4.769950	0.089786	-1.204712
37	8	0	4.101156	-0.355360	1.550782
38	6	0	1.997947	0.246243	-4.101225
39	1	0	2.286322	-0.367768	-4.967132
40	6	0	5.498168	-0.894177	-1.900002
41	1	0	5.670173	-1.773610	-1.251223
42	1	0	4.918082	-1.243008	-2.771811
43	6	0	5.239930	0.382666	1.966354
44	1	0	4.914298	1.333742	2.423525
45	1	0	5.870750	0.616022	1.094200
46	6	0	6.822574	-0.341340	-2.359043
47	6	0	7.033394	1.033078	-2.488376
48	6	0	7.858400	-1.218002	-2.698190
49	6	0	8.254906	1.520788	-2.952059
50	1	0	6.230654	1.719193	-2.217605
51	6	0	9.075892	-0.732273	-3.166510
52	1	0	7.709714	-2.296147	-2.592124
53	6	0	9.278781	0.641474	-3.295073
54	1	0	8.406294	2.598825	-3.044784
55	1	0	9.874527	-1.430614	-3.426803
56	1	0	10.235165	1.024231	-3.657984
57	6	0	6.003028	-0.442034	2.965312
58	6	0	5.703083	-0.366198	4.327988
59	6	0	6.981441	-1.344284	2.539142
60	6	0	6.368529	-1.173141	5.248284
61	1	0	4.939546	0.336562	4.671610
62	6	0	7.649185	-2.153545	3.455294
63	1	0	7.223920	-1.410158	1.475246
64	6	0	7.342728	-2.069866	4.812574
65	1	0	6.127069	-1.100830	6.311021

66	1	0	8.414009	-2.852154	3.108989
67	1	0	7.867002	-2.701987	5.532669
68	6	0	1.537845	0.884835	2.367767
69	1	0	2.101745	0.409207	3.181380
70	1	0	0.459122	0.802014	2.595584
71	6	0	-0.396487	-2.044853	-1.281860
72	8	0	-1.419639	-1.263670	-0.706901
73	6	0	-2.268844	-2.017573	0.148677
74	6	0	-1.960878	-3.483981	-0.164952
75	6	0	-0.491014	-3.433695	-0.592456
76	1	0	-3.311942	-1.769702	-0.099217
77	1	0	-2.082454	-4.123669	0.724273
78	1	0	-0.268911	-4.249211	-1.300703
79	6	0	-0.629804	-2.169725	-2.797274
80	1	0	0.318059	-2.487741	-3.255932
81	1	0	-1.387552	-2.948163	-2.976299
82	8	0	0.299769	-3.542411	0.556352
83	8	0	-2.711353	-3.986396	-1.243766
84	6	0	-2.028889	-1.645550	1.602997
85	1	0	-2.025650	-0.544046	1.684927
86	1	0	-1.043481	-2.019965	1.929983
87	6	0	-4.077773	-4.210584	-0.978759
88	1	0	-4.645209	-3.263694	-1.001647
89	1	0	-4.190726	-4.631167	0.039403
90	1	0	0.900391	0.203058	-4.020933
91	6	0	2.451351	1.672333	-4.310063
92	6	0	3.806617	1.964176	-4.500999
93	6	0	1.531454	2.722138	-4.307362
94	6	0	4.229759	3.276142	-4.687962
95	1	0	4.537172	1.151742	-4.497371
96	6	0	1.950722	4.038993	-4.498168
97	1	0	0.471613	2.508278	-4.146752
98	6	0	3.301083	4.318328	-4.688708
99	1	0	5.290946	3.489002	-4.836026
100	1	0	1.217184	4.848006	-4.488084
101	1	0	3.633228	5.348342	-4.836405
102	6	0	2.195759	-4.396809	1.711959
103	6	0	3.208386	-3.609424	2.263790
104	6	0	1.713548	-5.489066	2.441578
105	6	0	3.738636	-3.913461	3.518281
106	1	0	3.584844	-2.738357	1.722785
107	6	0	2.237064	-5.792081	3.694539
108	1	0	0.919638	-6.109727	2.018110
109	6	0	3.254469	-5.004488	4.234951
110	1	0	4.531518	-3.287806	3.935144
111	1	0	1.854126	-6.649704	4.252290
112	1	0	3.668837	-5.243786	5.216933
113	6	0	1.602686	-4.071765	0.367864
114	1	0	2.234314	-3.351475	-0.172461
115	1	0	1.531609	-4.987929	-0.246711

116	6	0	-4.658047	-5.169529	-1.987779
117	6	0	-3.853036	-6.084276	-2.669039
118	6	0	-6.036360	-5.175176	-2.223346
119	6	0	-4.415862	-6.987650	-3.569126
120	1	0	-2.777080	-6.078827	-2.491788
121	6	0	-6.600639	-6.081909	-3.117039
122	1	0	-6.676951	-4.460987	-1.698882
123	6	0	-5.790428	-6.991422	-3.795004
124	1	0	-3.773449	-7.695597	-4.097908
125	1	0	-7.679169	-6.073894	-3.289597
126	1	0	-6.230372	-7.699659	-4.500445
127	6	0	-1.711467	5.189064	1.800654
128	6	0	-3.023665	4.967682	1.364427
129	6	0	-3.269182	4.880978	-0.015371
130	6	0	-2.194533	5.045365	-0.897741
131	6	0	-0.889889	5.234819	-0.460815
132	6	0	-0.643326	5.295305	0.919222
133	1	0	-1.506386	5.265985	2.870042
134	1	0	-2.355103	5.002358	-1.976772
135	6	0	-4.636700	4.587296	-0.606871
136	1	0	-4.734580	5.159990	-1.539588
137	1	0	-5.429912	4.952651	0.054377
138	6	0	-4.101200	4.791996	2.421659
139	1	0	-5.080117	5.087430	2.028987
140	1	0	-3.885426	5.483635	3.247928
141	6	0	-4.854864	3.119732	-0.935050
142	6	0	-5.460854	2.207996	-0.052033
143	6	0	-4.419571	2.653136	-2.179494
144	6	0	-5.624888	0.881855	-0.466601
145	6	0	-4.548841	1.325030	-2.568937
146	1	0	-3.958558	3.341292	-2.891376
147	6	0	-5.177418	0.422215	-1.700257
148	1	0	-6.119552	0.158569	0.184723
149	6	0	-4.147629	3.382297	2.982626
150	6	0	-3.306458	3.078280	4.059475
151	6	0	-4.961172	2.363968	2.456241
152	6	0	-3.219646	1.802482	4.598882
153	1	0	-2.692339	3.855775	4.518440
154	6	0	-4.855768	1.075618	2.994139
155	6	0	-3.988495	0.772607	4.036326
156	1	0	-5.456248	0.256147	2.594834
157	6	0	-5.958441	2.590116	1.330603
158	1	0	-6.847644	1.981872	1.547270
159	1	0	-6.300648	3.630867	1.335520
160	8	0	0.643385	5.466530	1.348379
161	8	0	0.116822	5.295302	-1.377411
162	6	0	0.836842	6.514130	-1.455882
163	1	0	1.586046	6.390378	-2.248230
164	1	0	0.167419	7.348965	-1.724246
165	1	0	1.344155	6.743876	-0.508237

166	8	0	-4.097708	0.923445	-3.798842
167	8	0	-5.326466	-0.899479	-2.009520
168	6	0	-6.189987	-1.197888	-3.096869
169	1	0	-6.192241	-2.288927	-3.212502
170	1	0	-7.216684	-0.856877	-2.883452
171	1	0	-5.835095	-0.732097	-4.027095
172	8	0	-2.375882	1.564630	5.646672
173	6	0	-3.008481	1.303831	6.888997
174	1	0	-2.214505	1.125457	7.625212
175	1	0	-3.610612	2.169192	7.212386
176	1	0	-3.657888	0.416085	6.832440

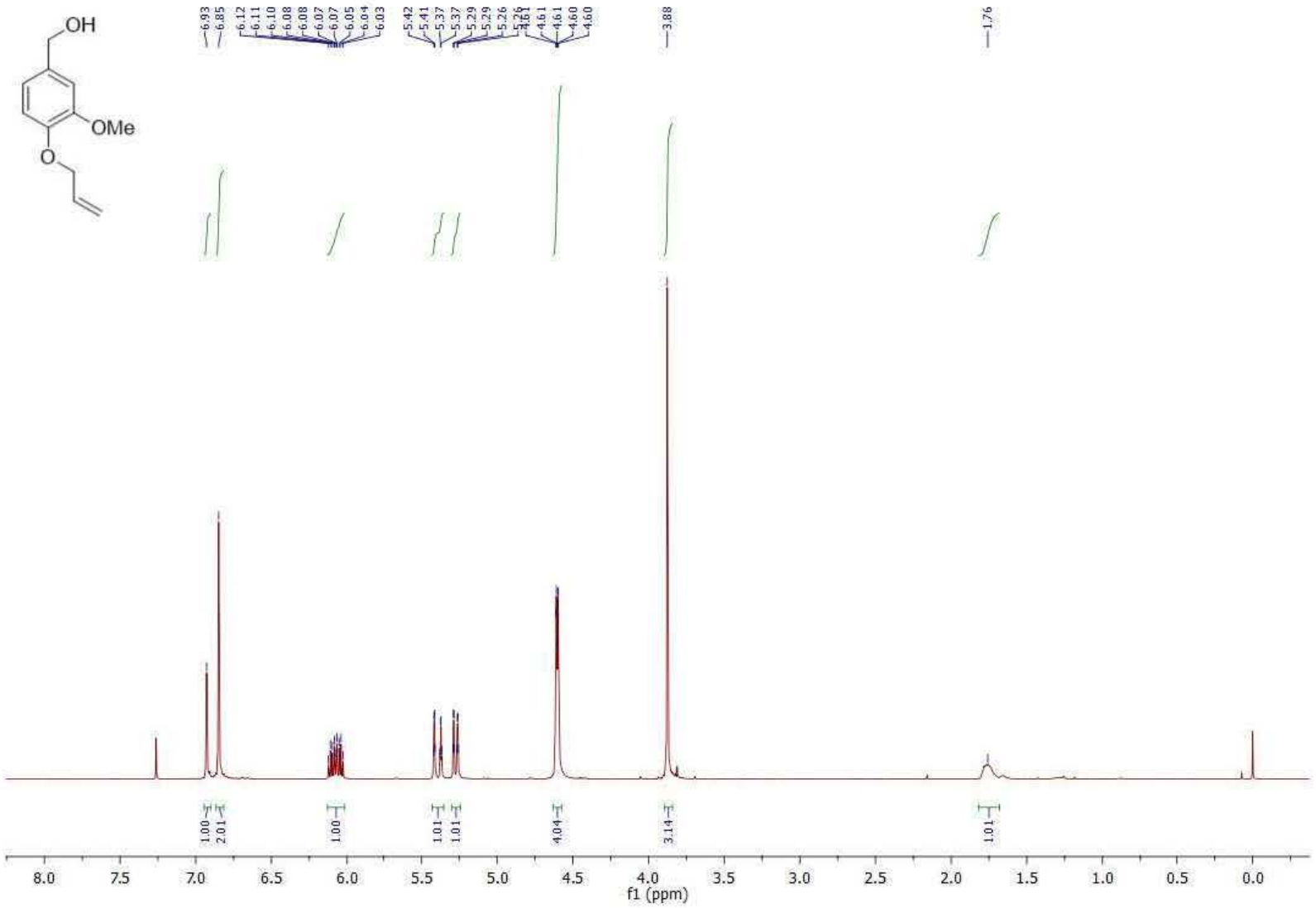

Figure S2. ^{1}H NMR spectrum of compound **S1.**

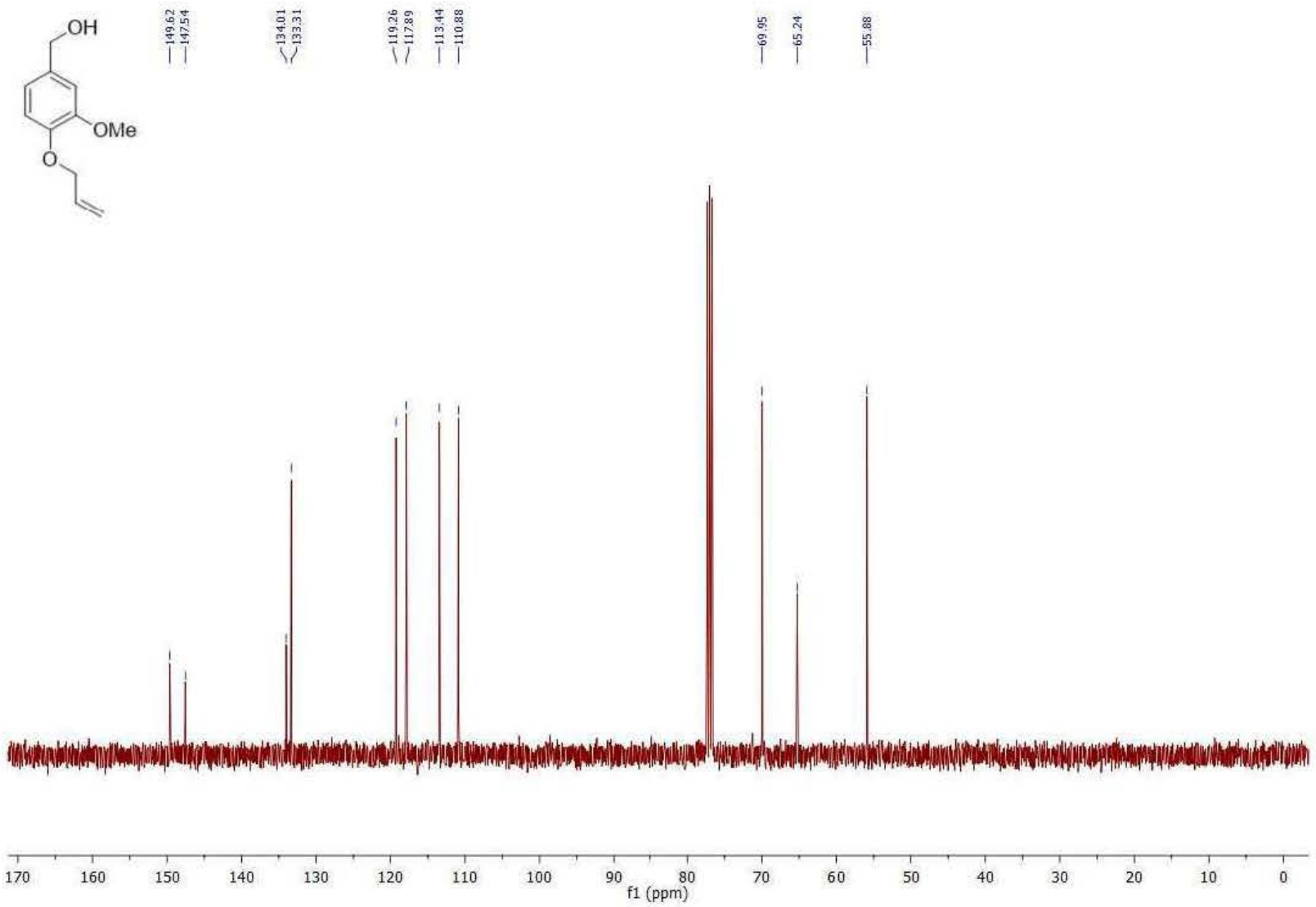

Figure S3. ^{13}C NMR spectrum of compound **S1**.

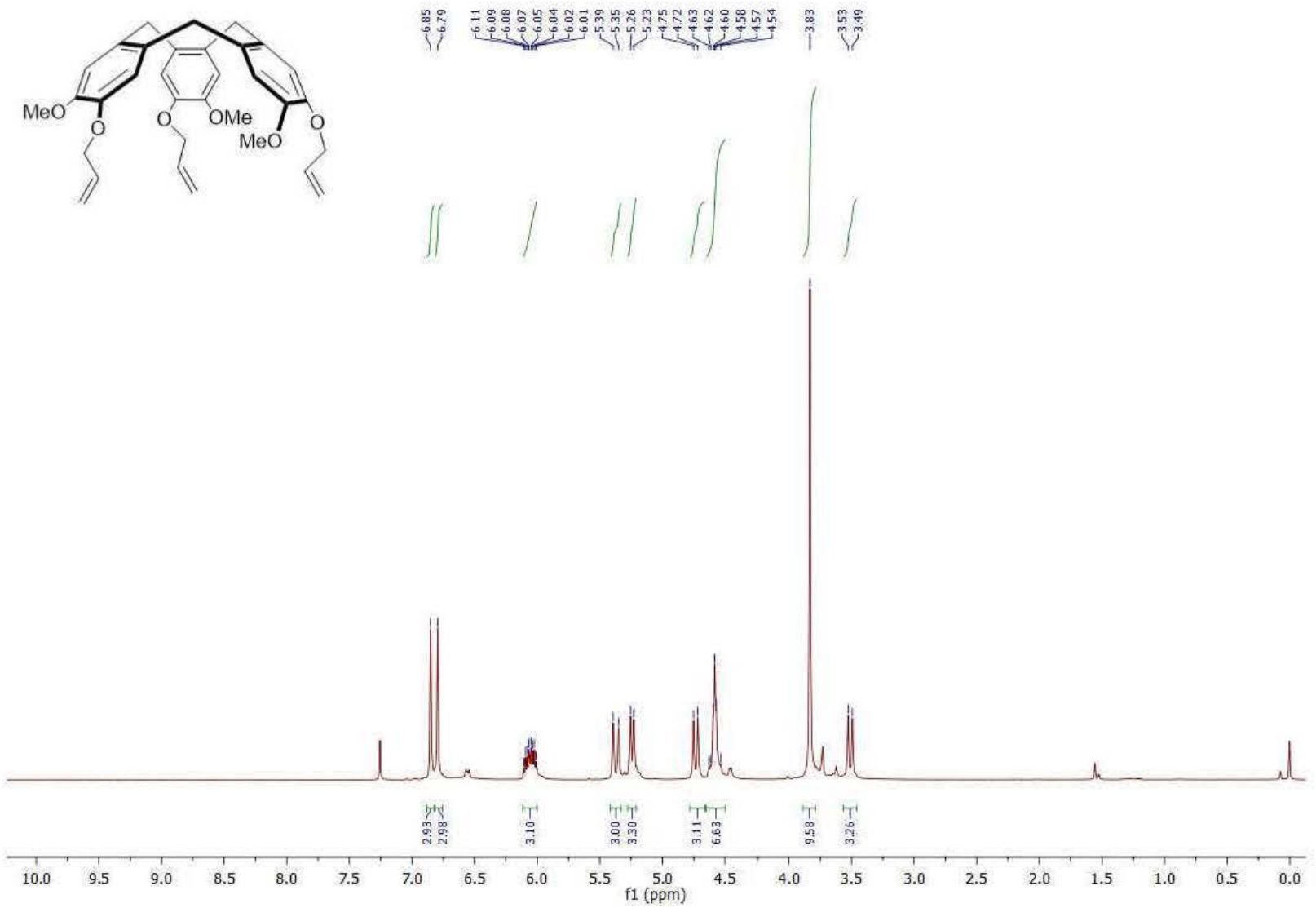

Figure S4. ^{1}H NMR spectrum of compound ***rac*-S2.**

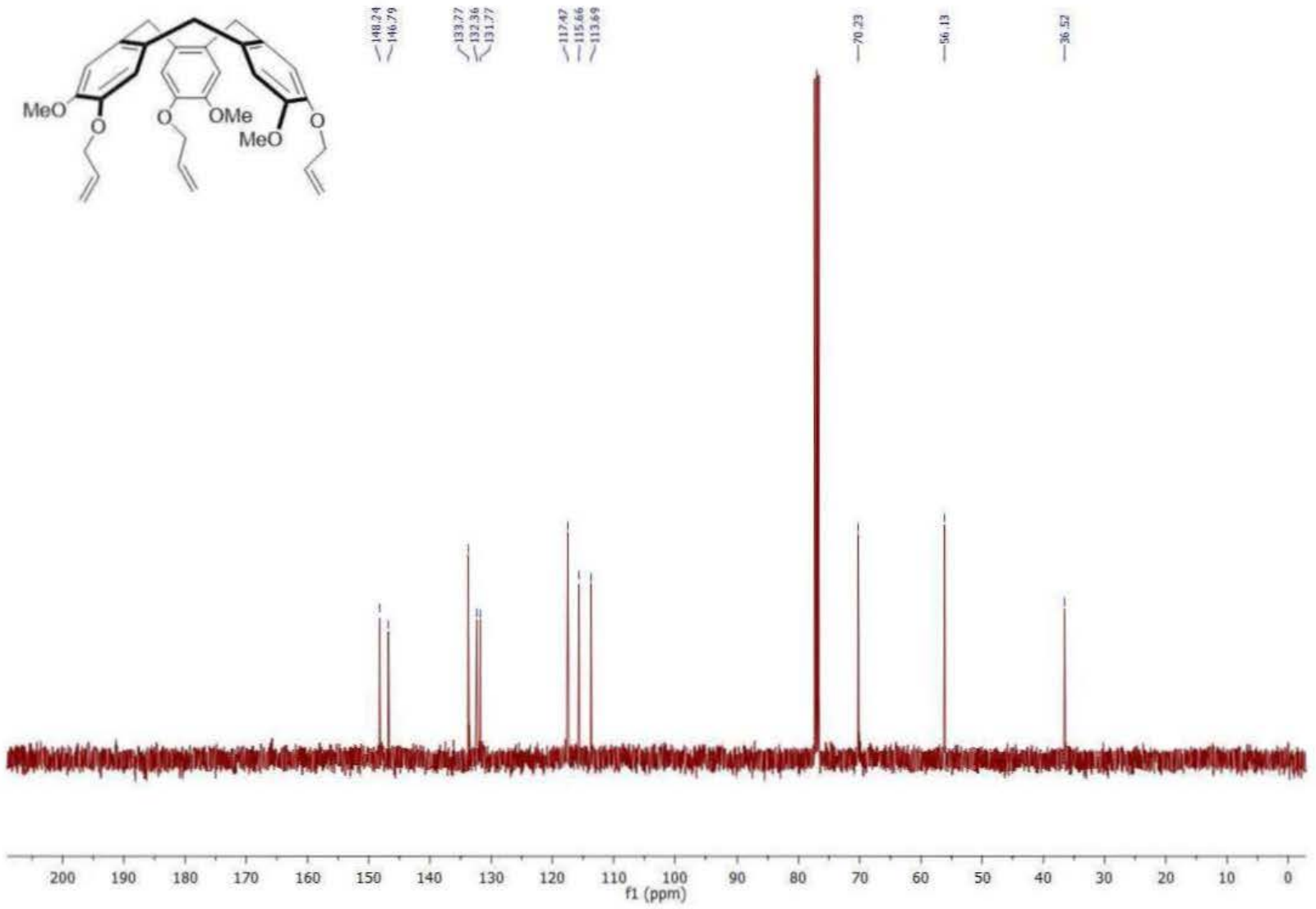

Figure S5. ^{13}C NMR spectrum of compound ***rac*-S2**.

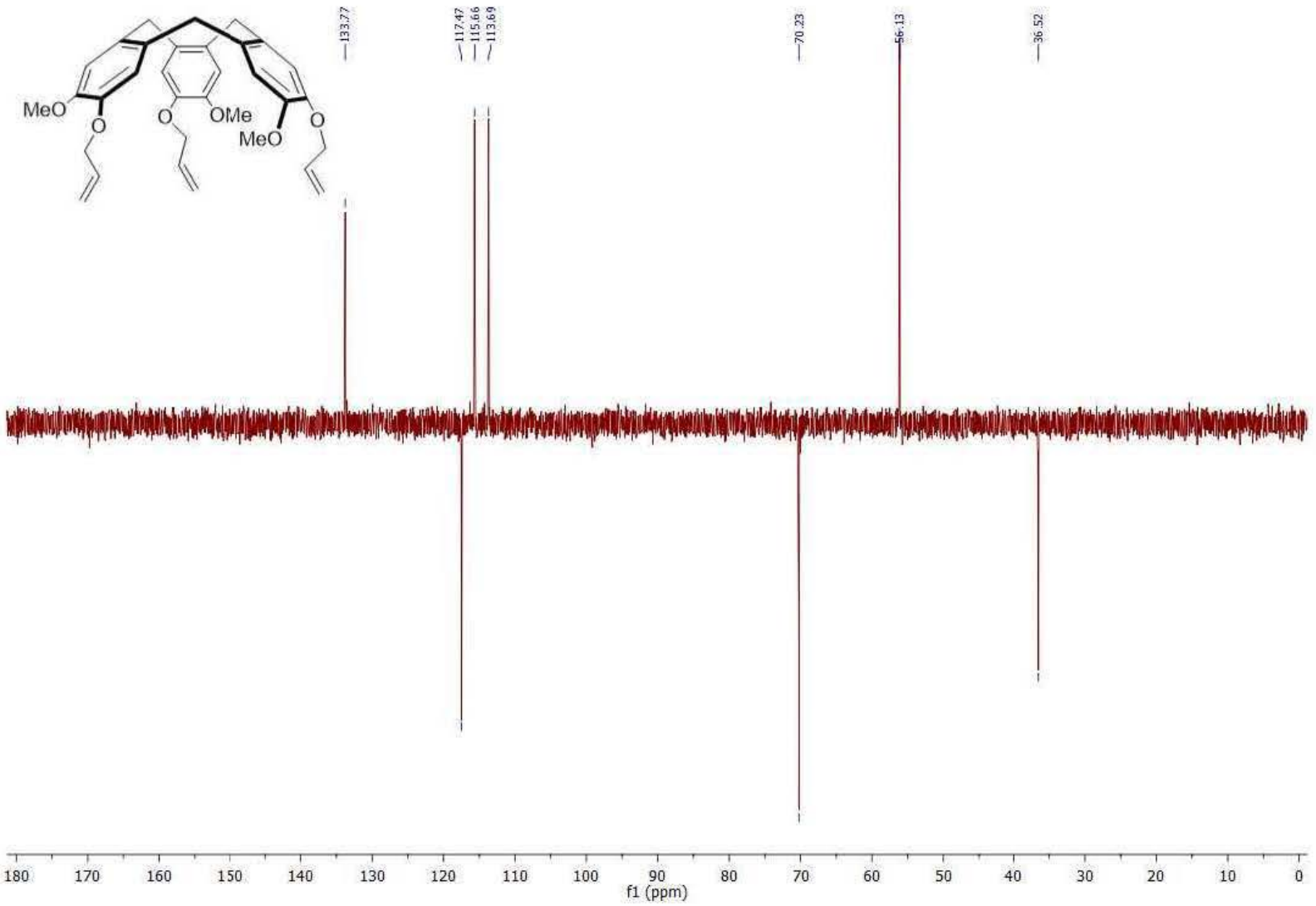

Figure S6. DEPT ^{13}C NMR spectrum of compound ***rac*-S2**.

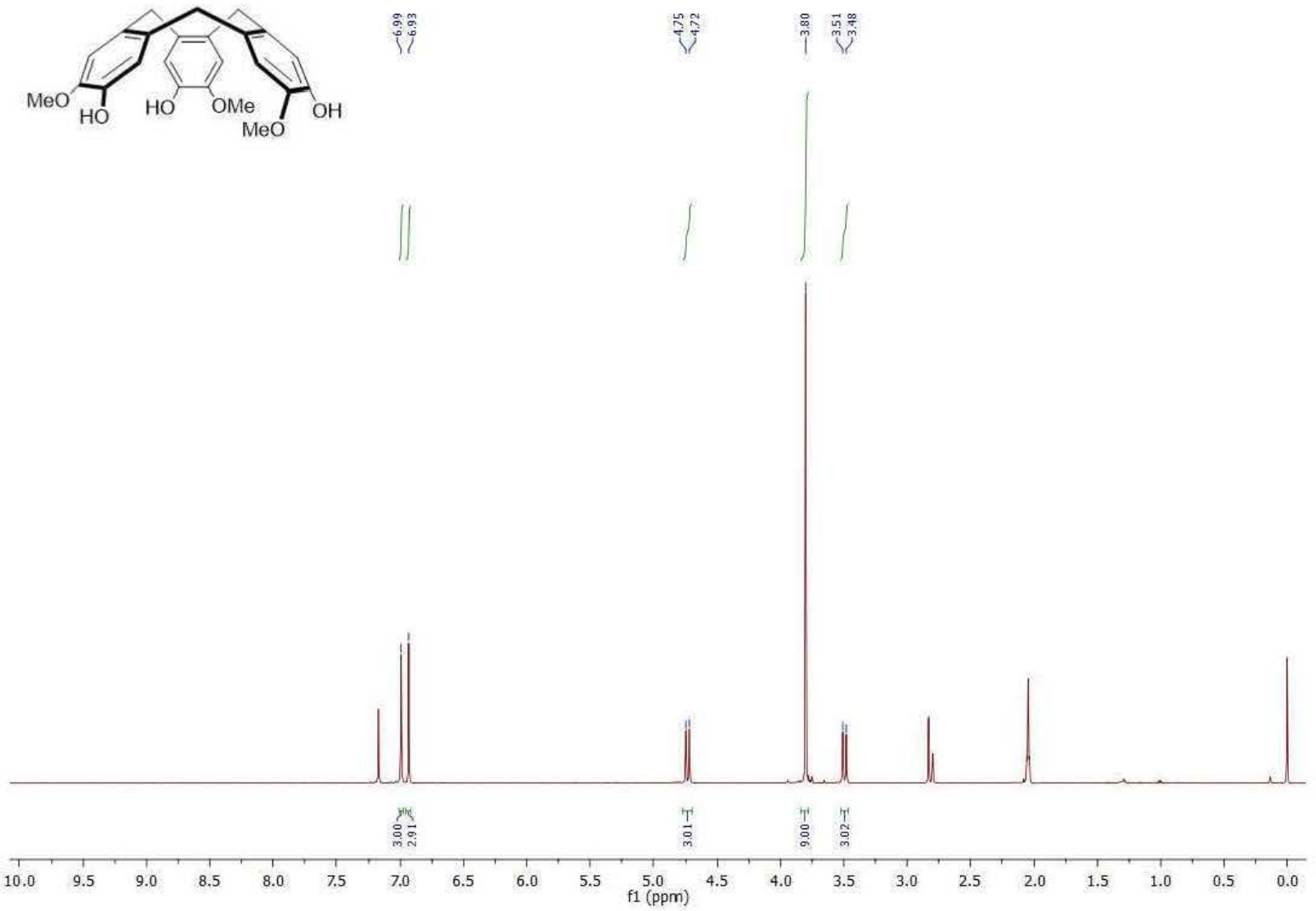

Figure S7. ^{1}H NMR spectrum of compound ***rac*-7.**

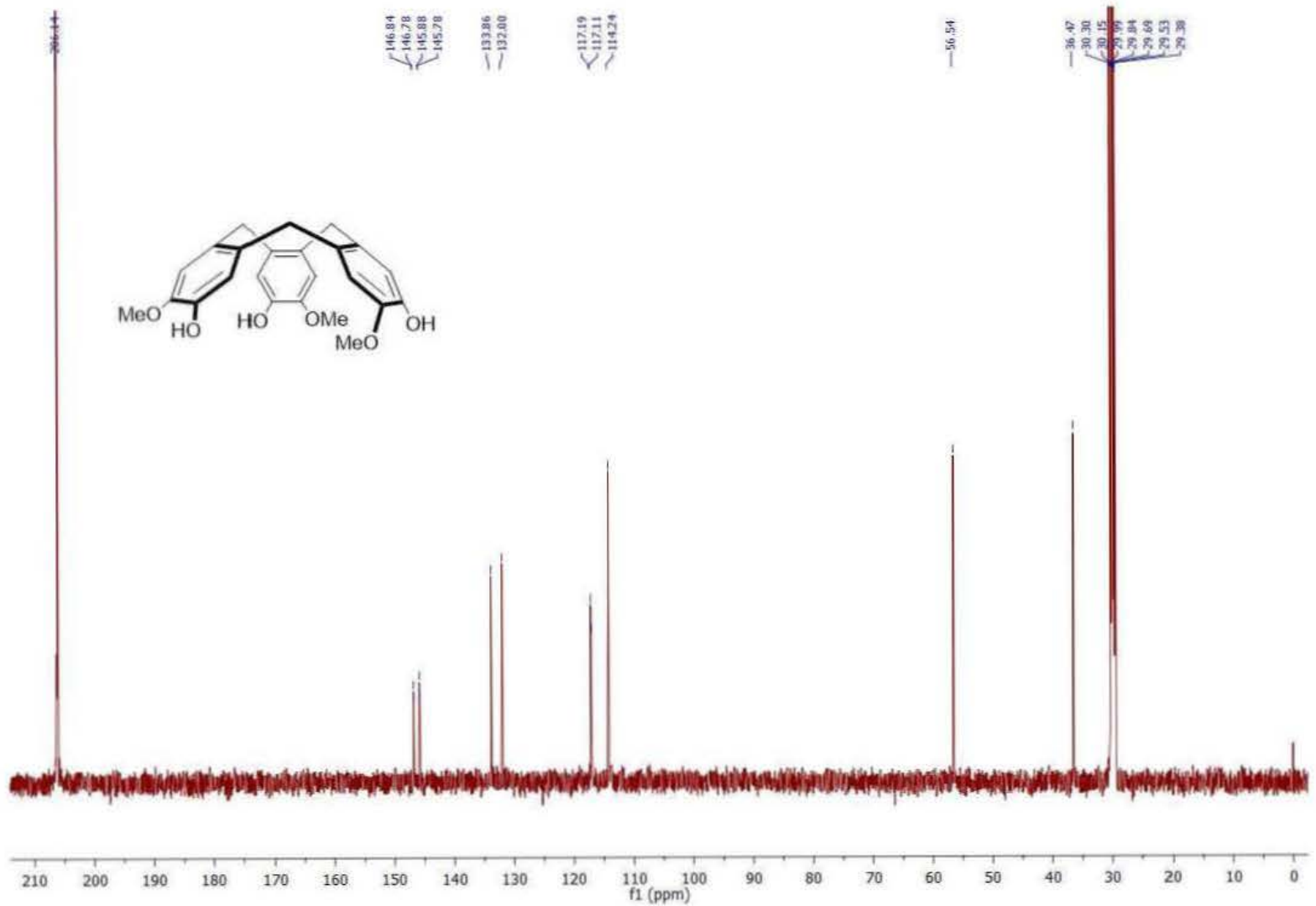

Figure S8. ^{13}C NMR spectrum of compound ***rac*-7**.

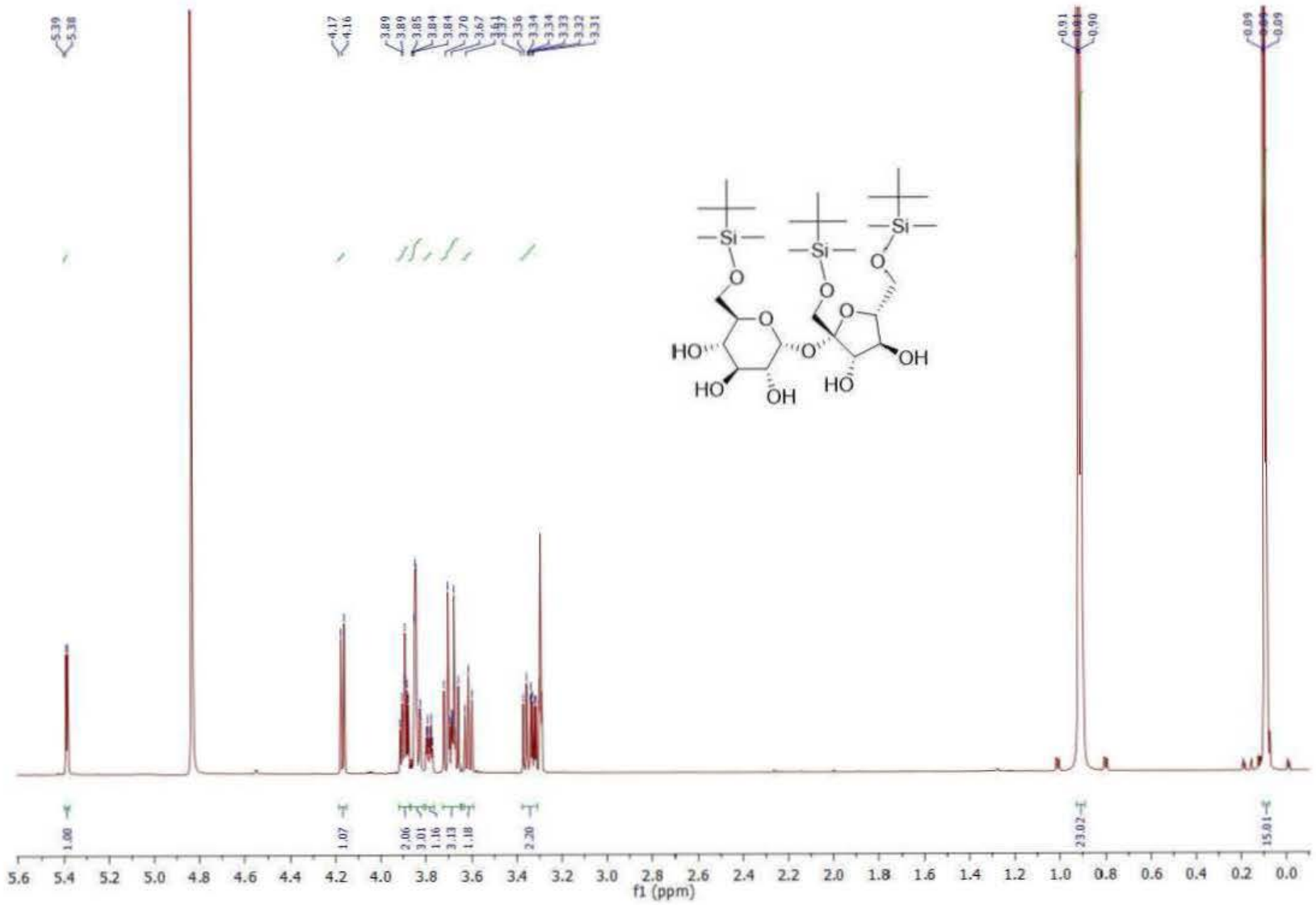

Figure S9. ^{1}H NMR spectrum of compound **S3.**

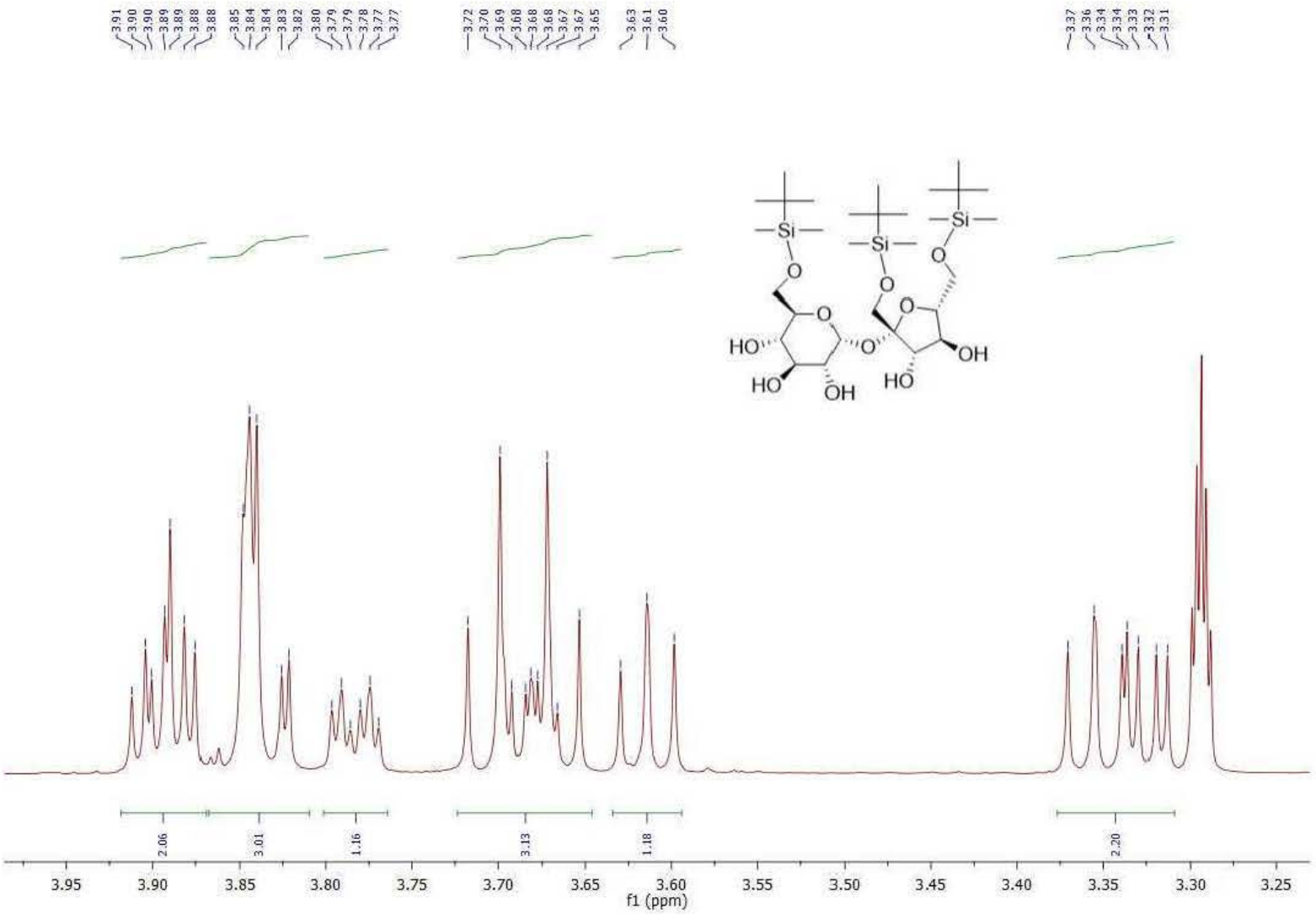

Figure S10. ^{1}H NMR spectrum of compound **S3** (aliphatic part).

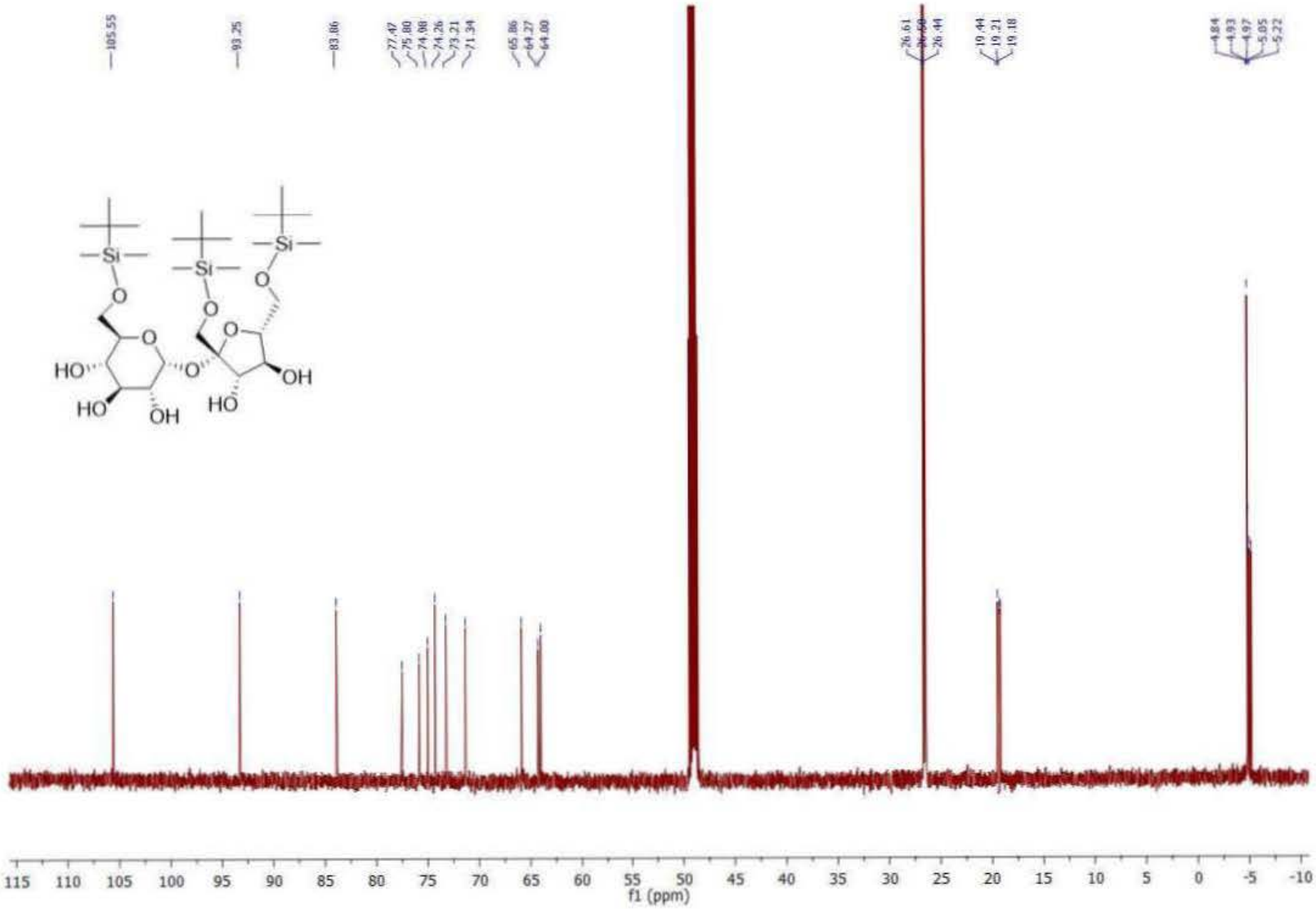

Figure S11. ^{13}C NMR spectrum of compound **S3.**

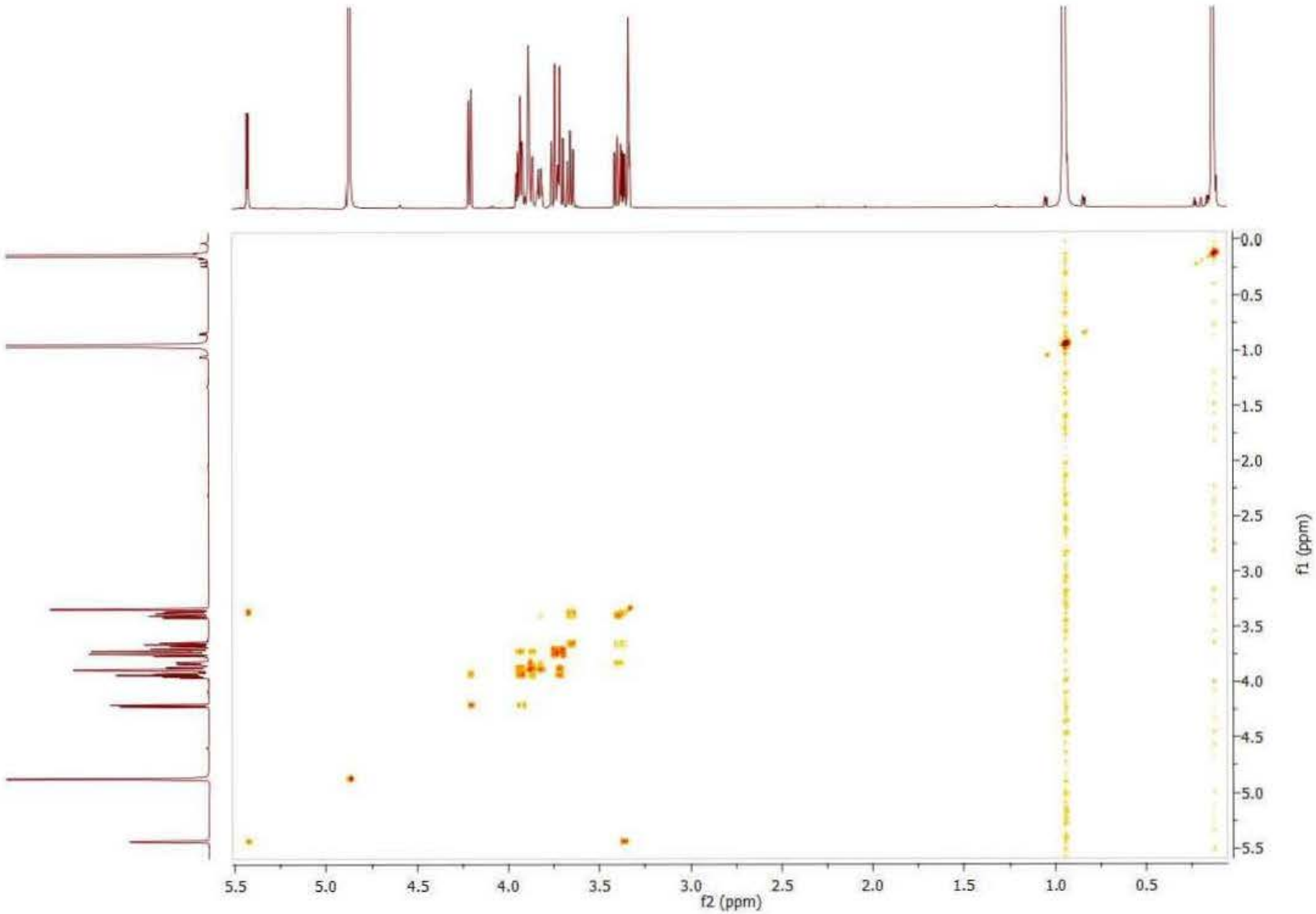

Figure S12. ^{1}H–^{1}H COSY spectrum of compound **S3**.

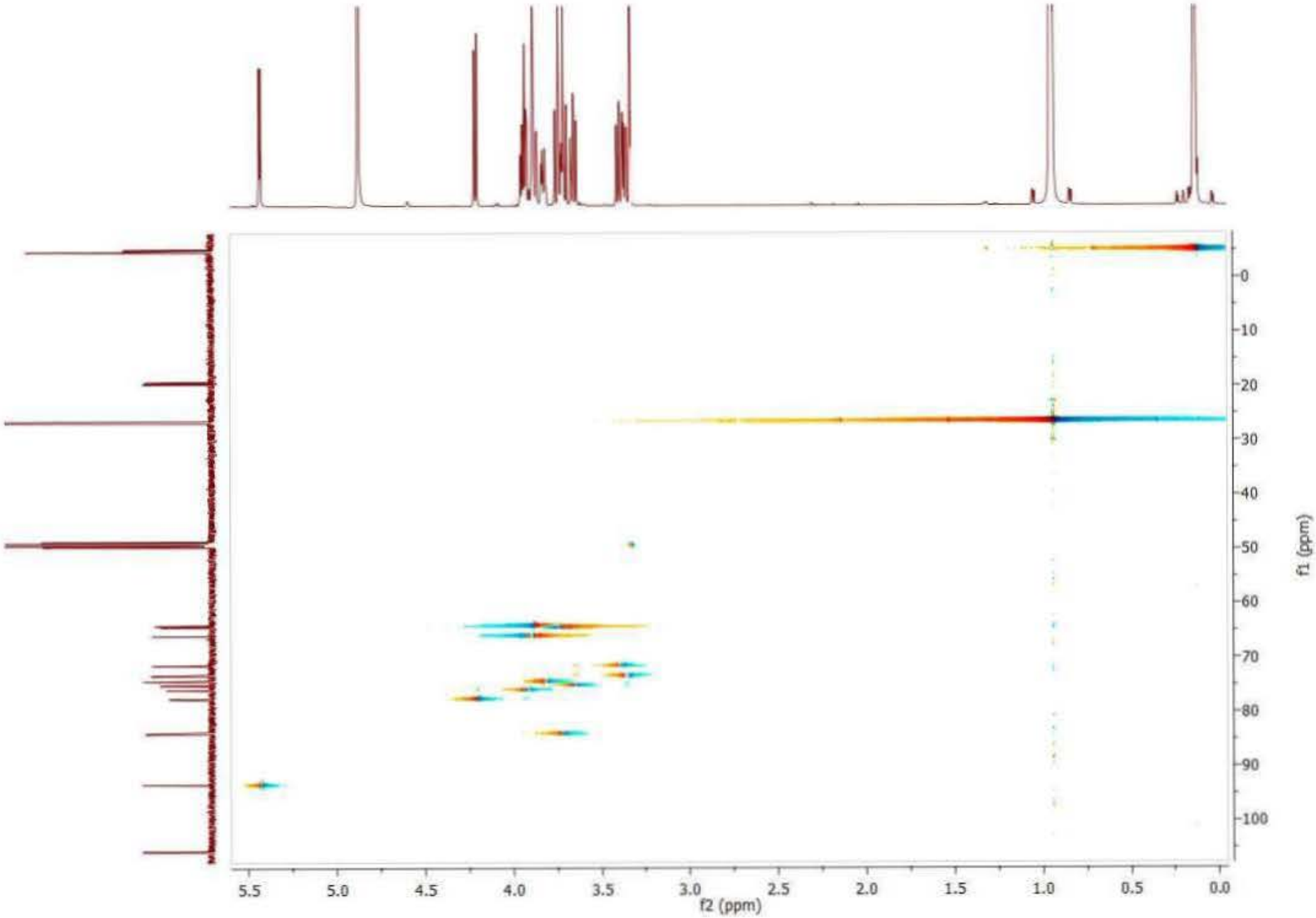

Figure S13. ^{1}H–^{13}C HSQC spectrum of compound **S3**.

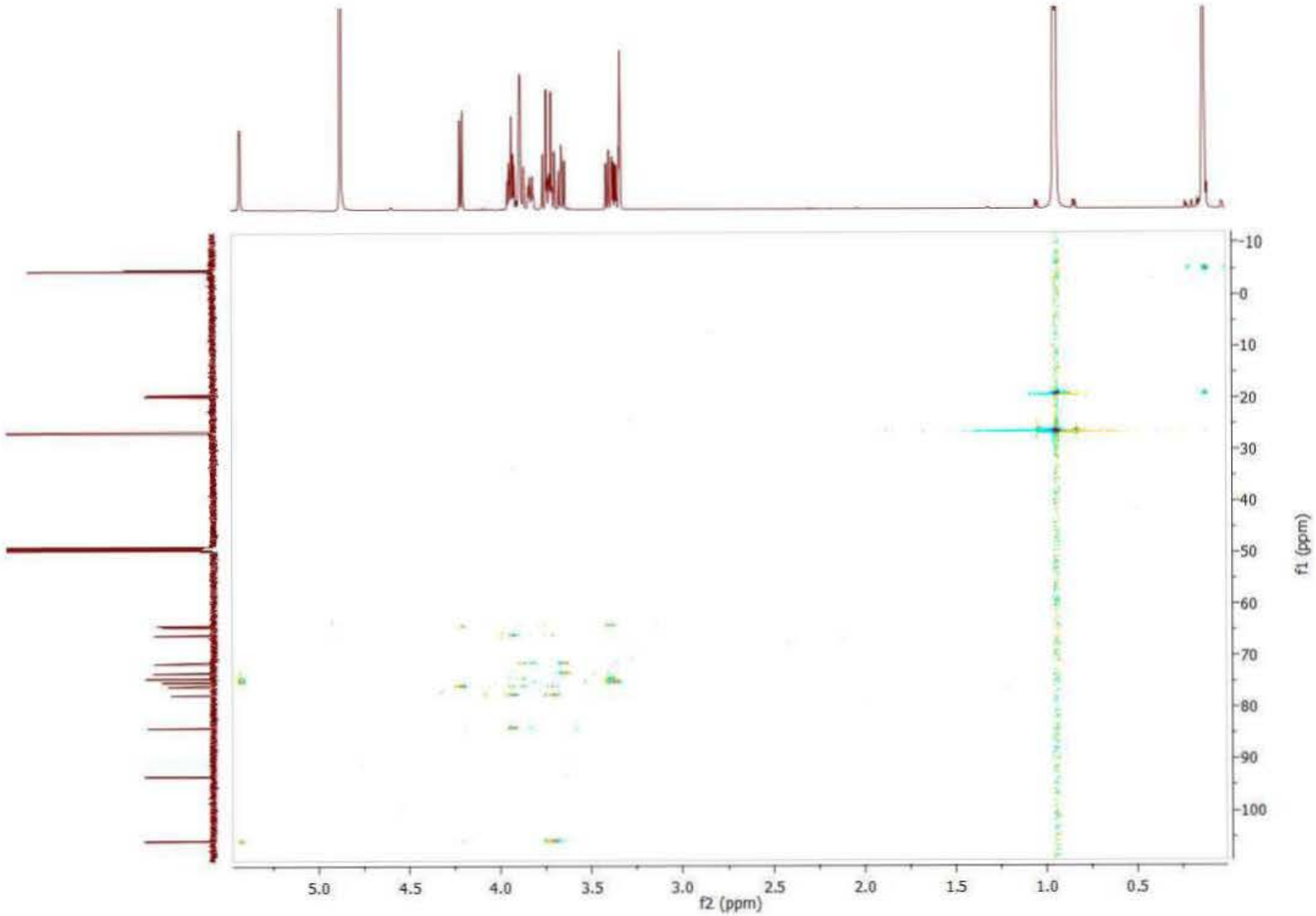

Figure S14. $^{1}H–^{13}C$ HMBC spectrum of compound **S3**.

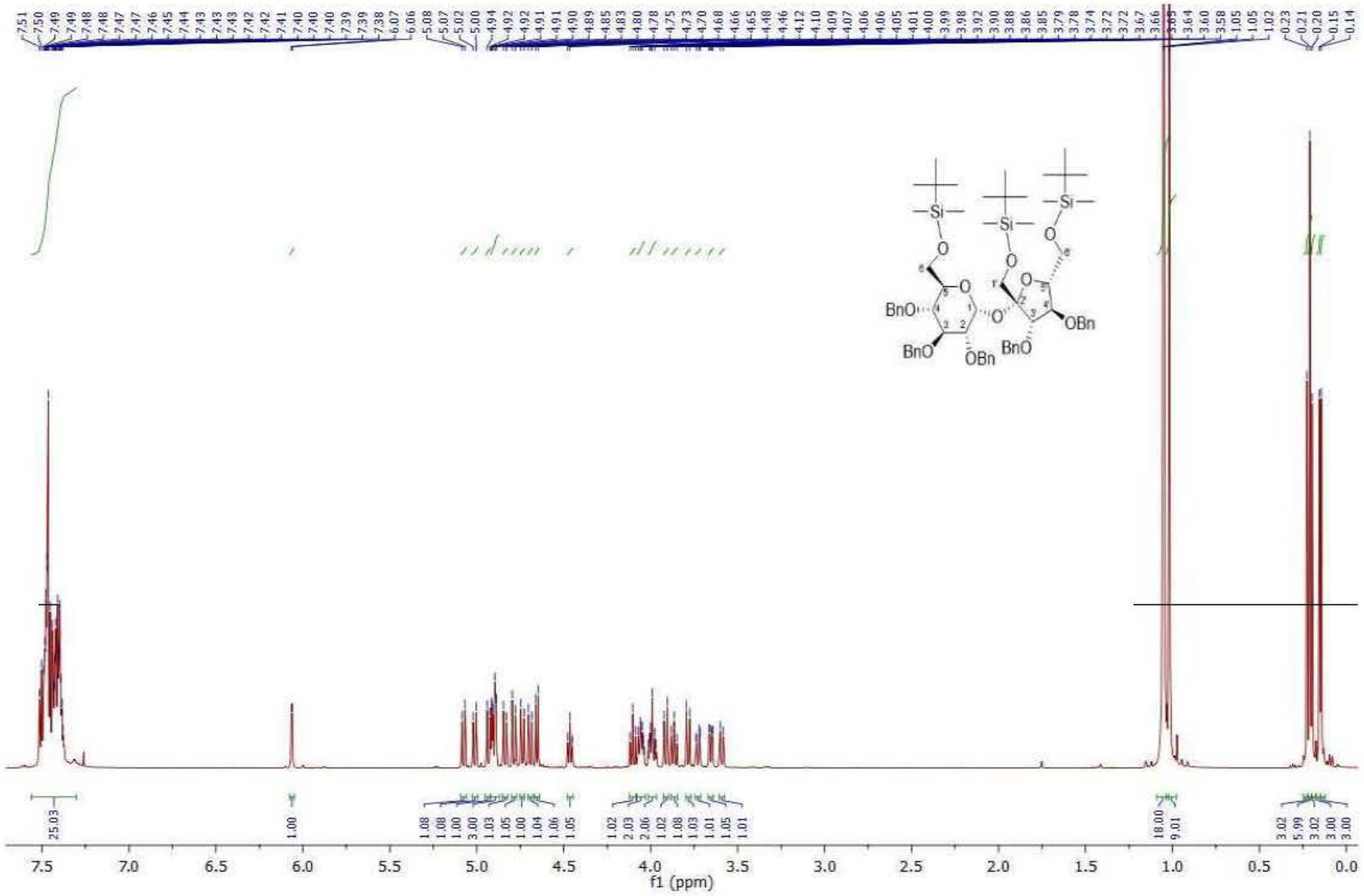

Figure S15. ^{1}H NMR spectrum of compound **2.**

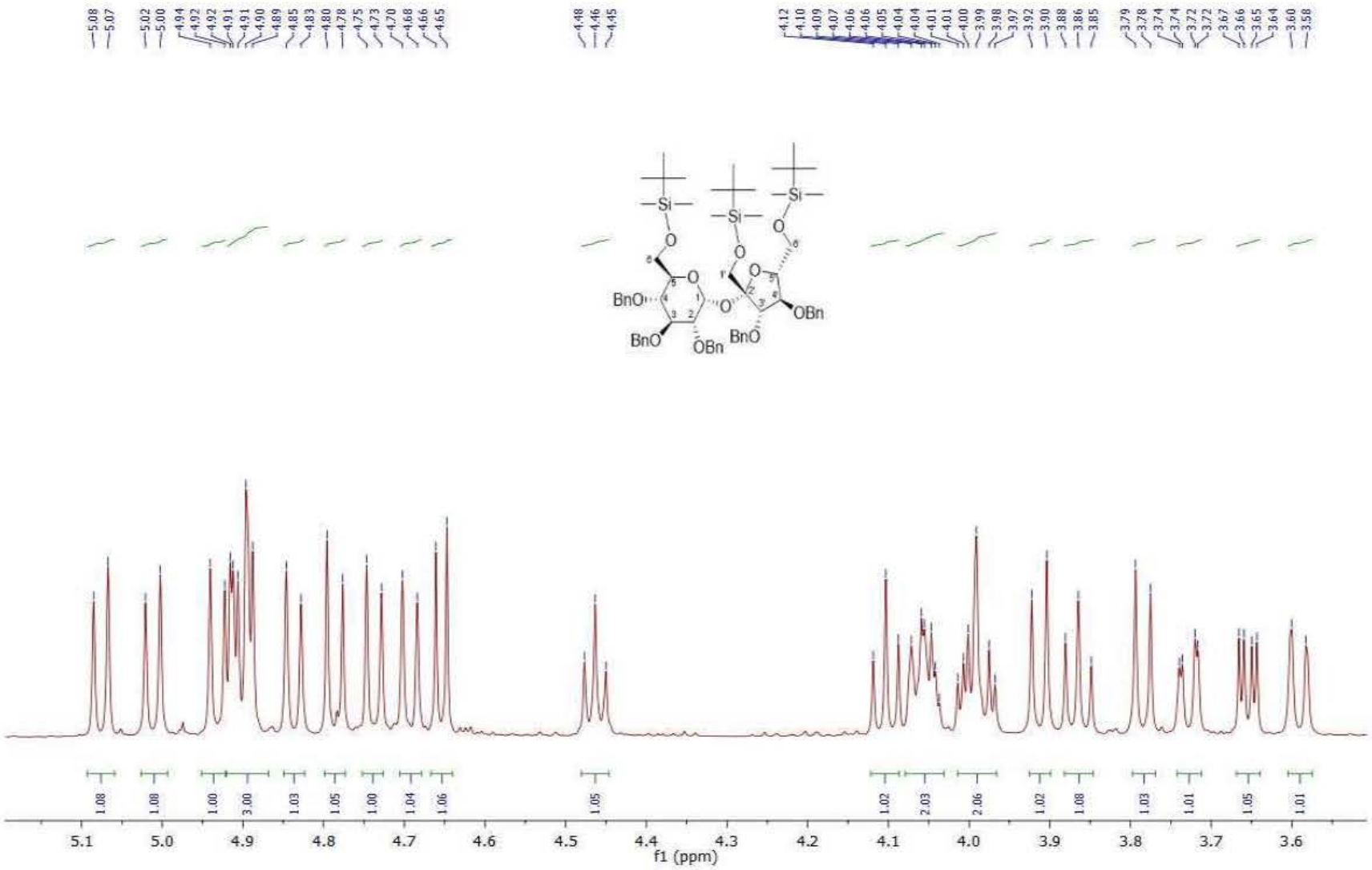

Figure S16. ^{1}H NMR spectrum of compound **2** (aliphatic part).

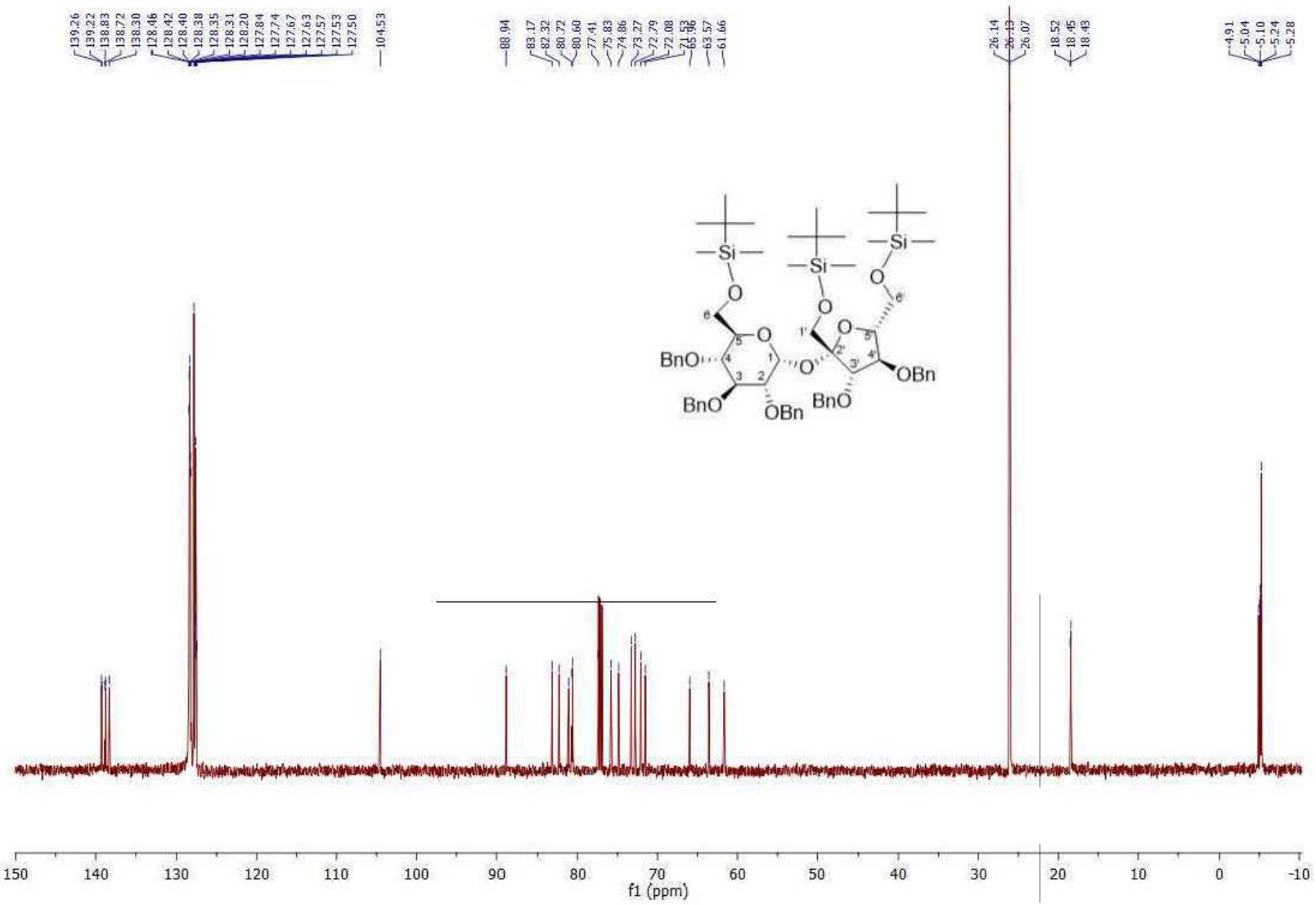

Figure S17. ^{13}C NMR spectrum of compound **2**.

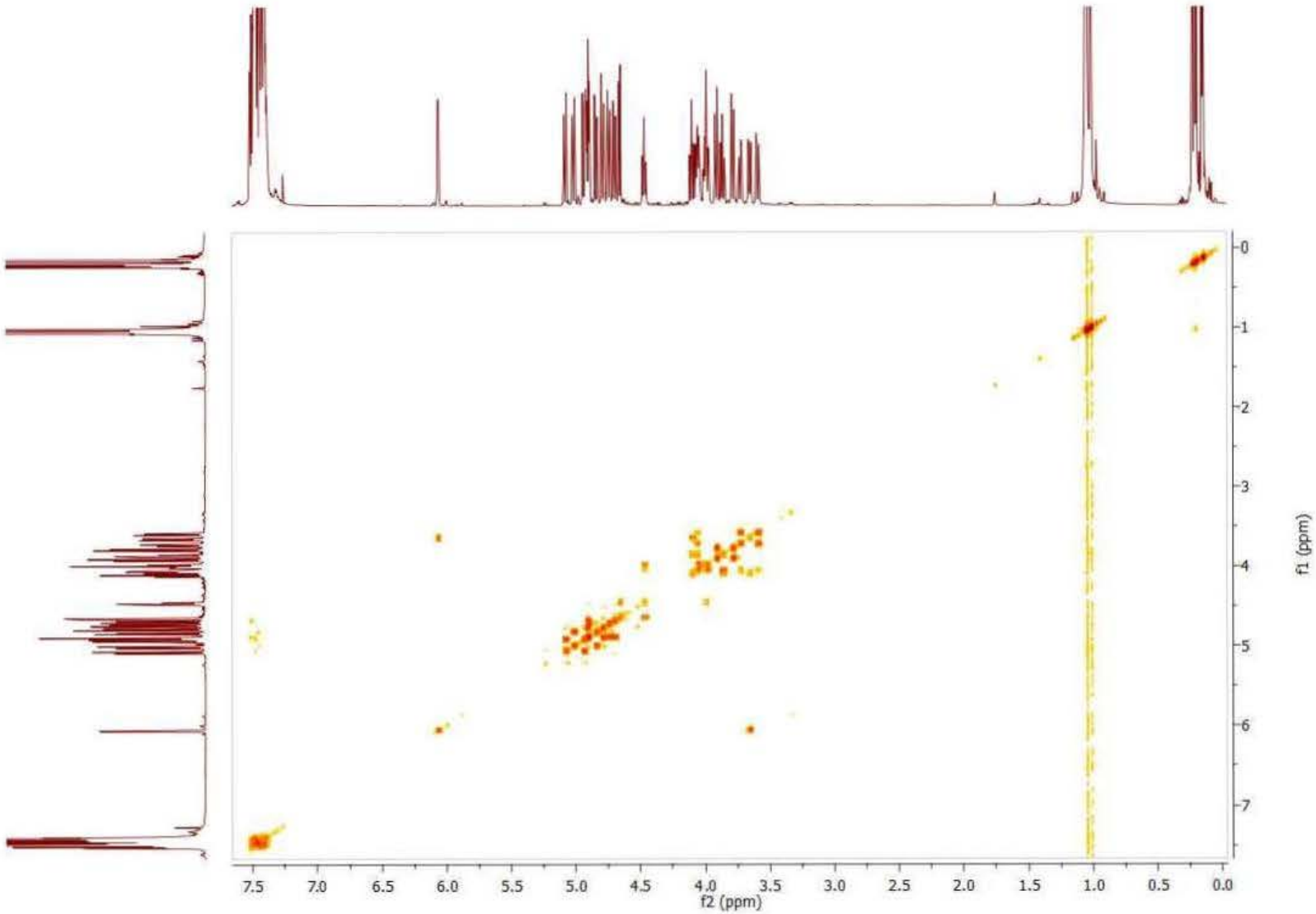

Figure S18. $^{1}H–^{1}H$ COSY spectrum of compound **2**.

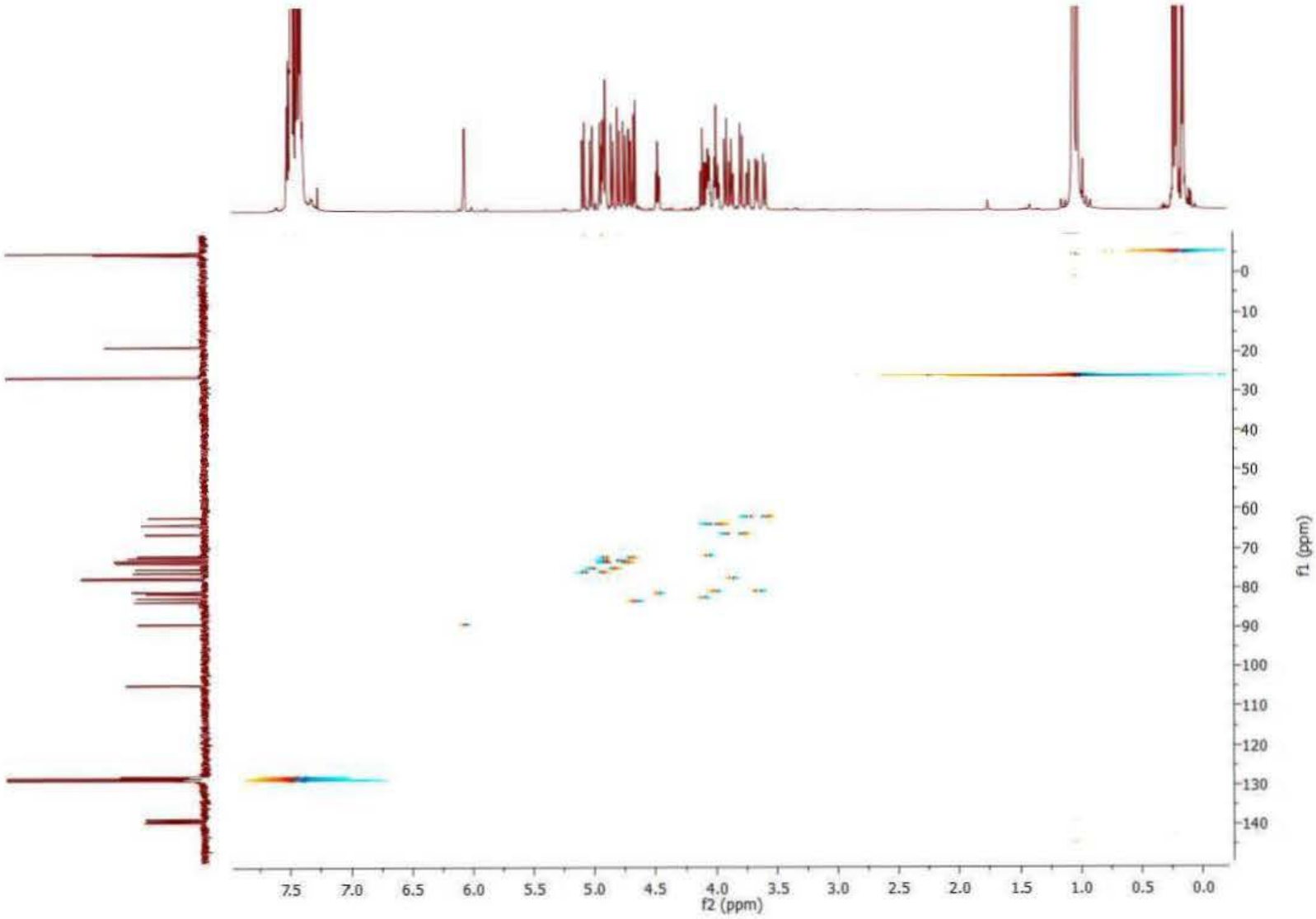

Figure S19. ^{1}H–^{13}C HSQC spectrum of compound **2**.

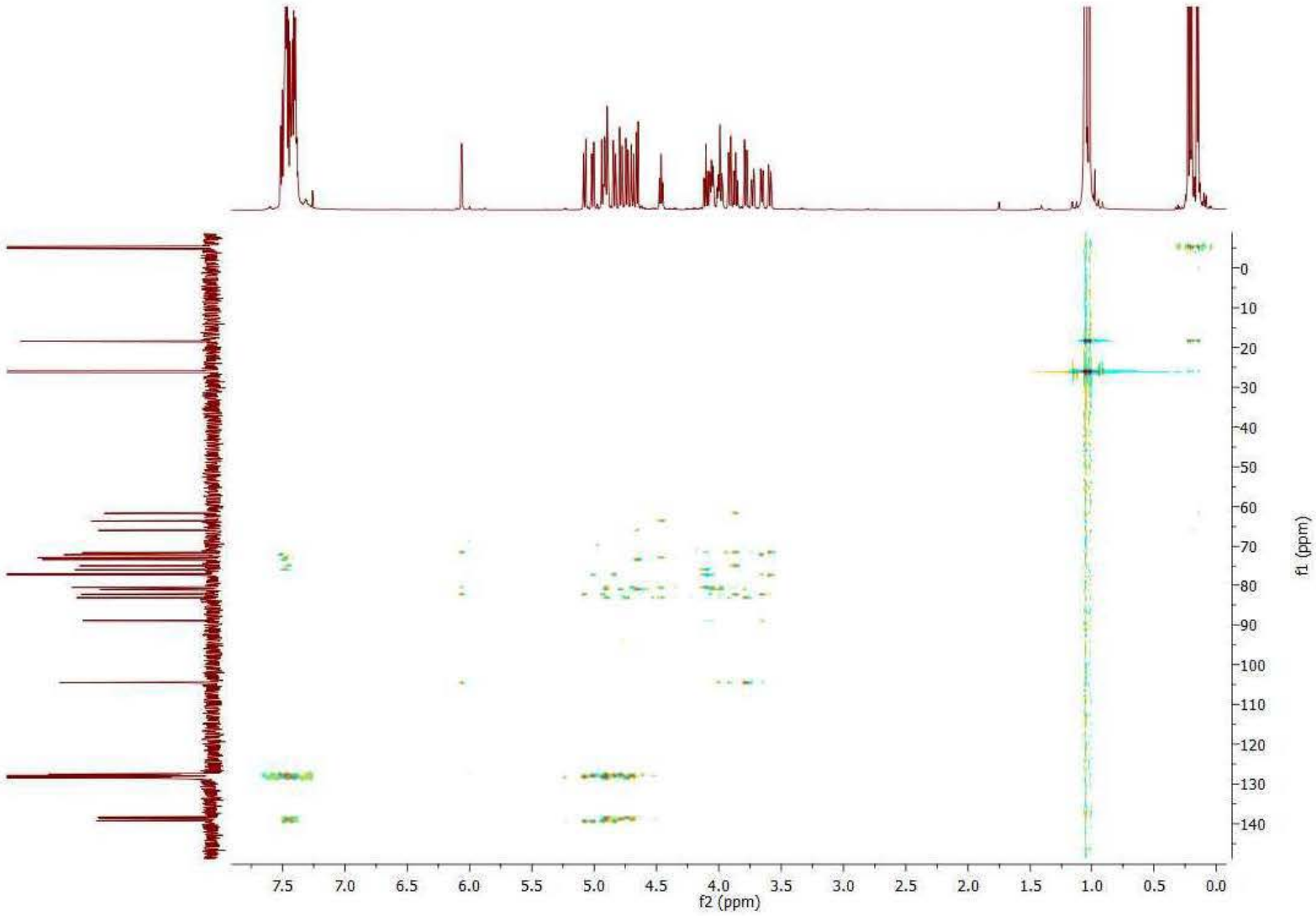

Figure S20. ^{1}H–^{13}C HMBC spectrum of compound **2**.

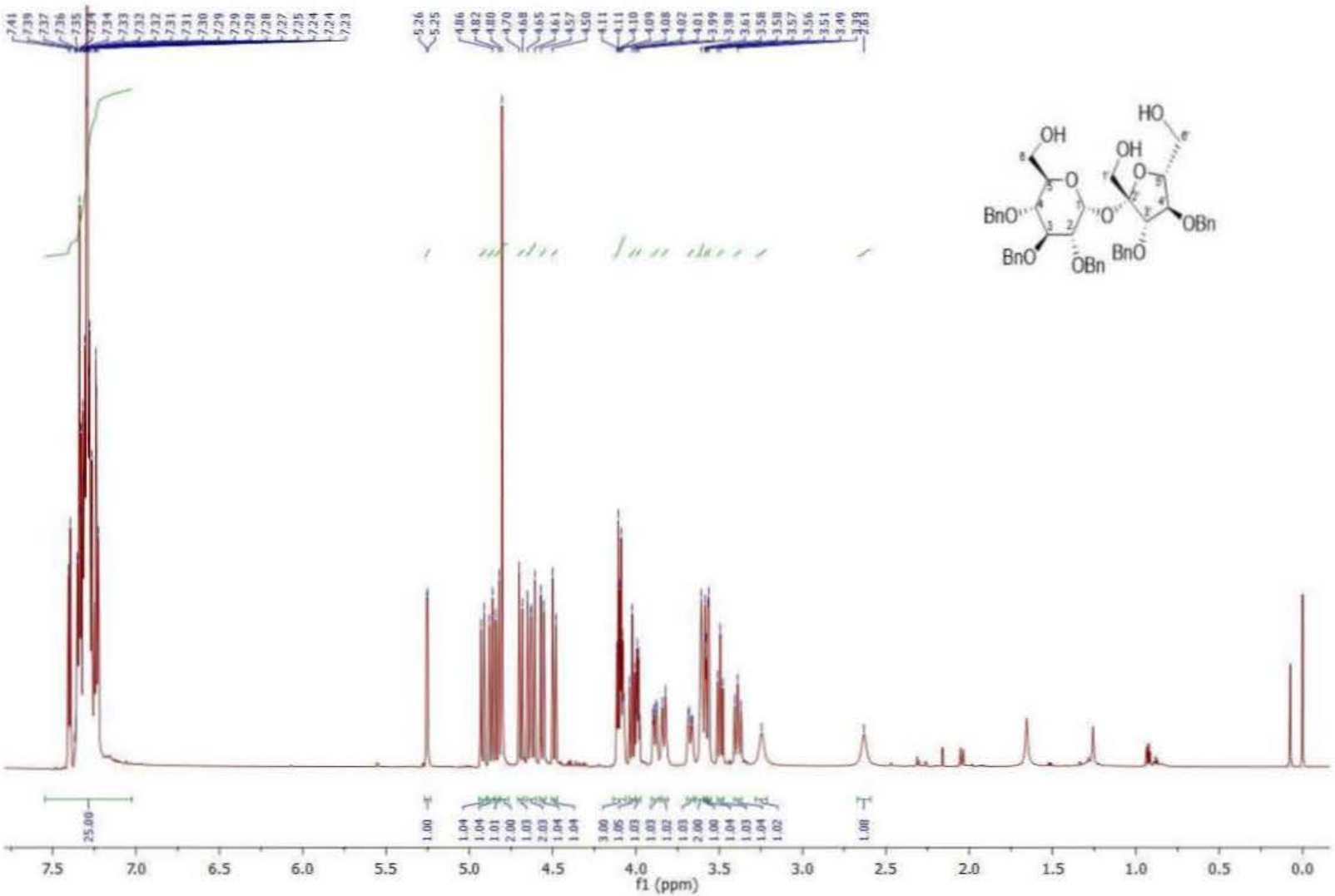

Figure S21. ^{1}H NMR spectrum of compound **3.**

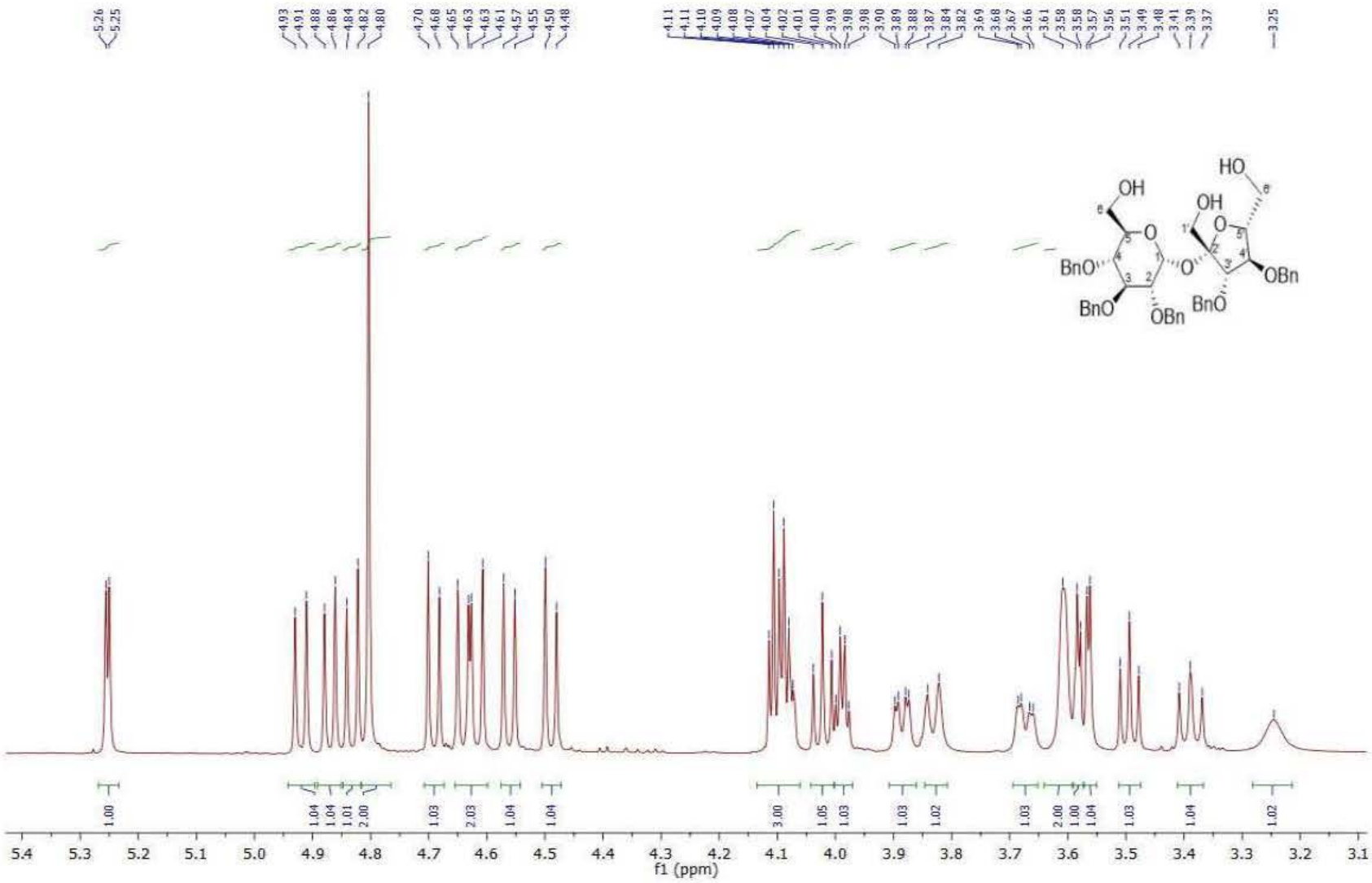

Figure S22. ^{1}H NMR spectrum of compound **3** (aliphatic part).

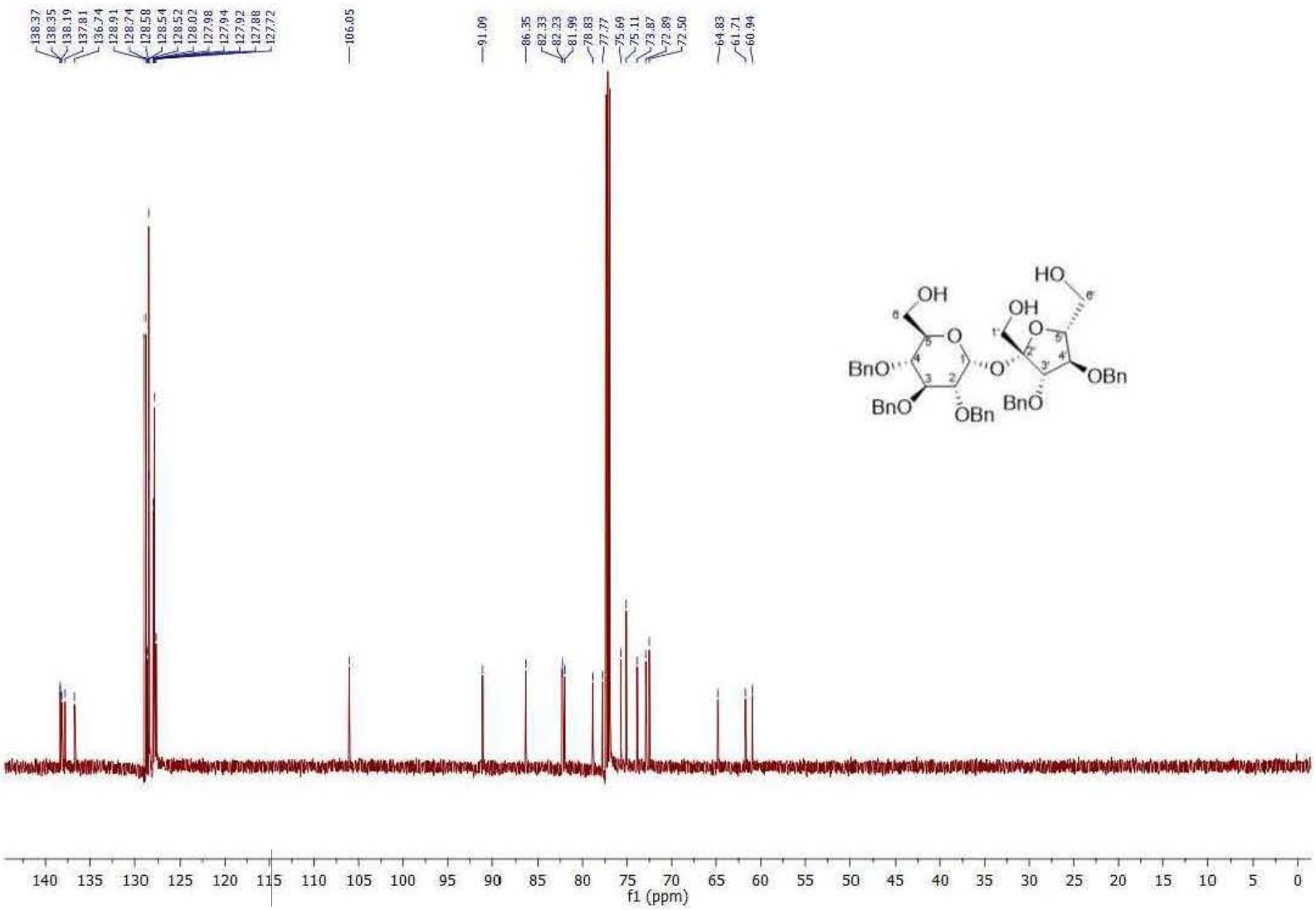

Figure S23. ^{13}C NMR spectrum of compound **3**.

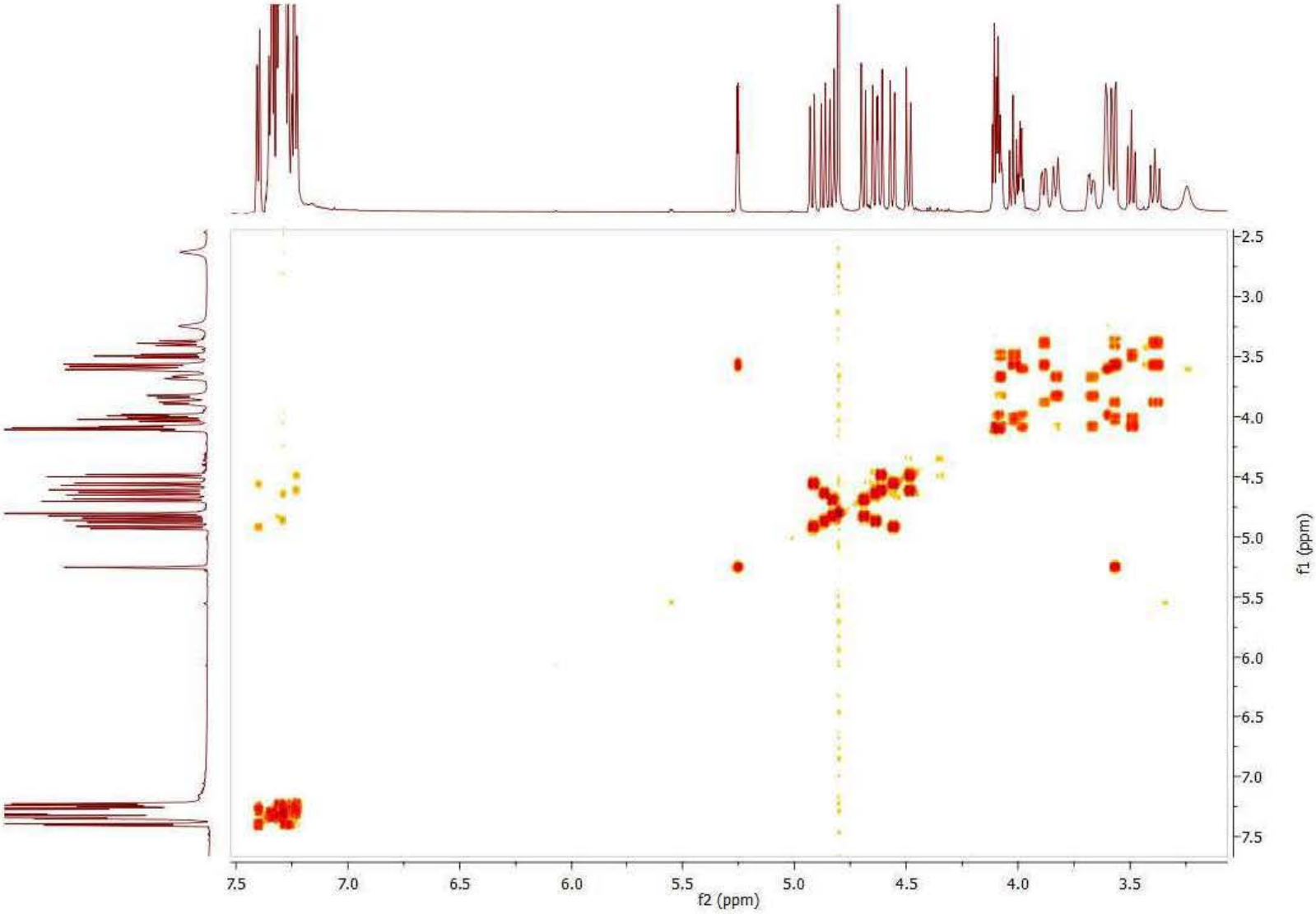

Figure S24. ^{1}H–^{1}H COSY spectrum of compound **3**.

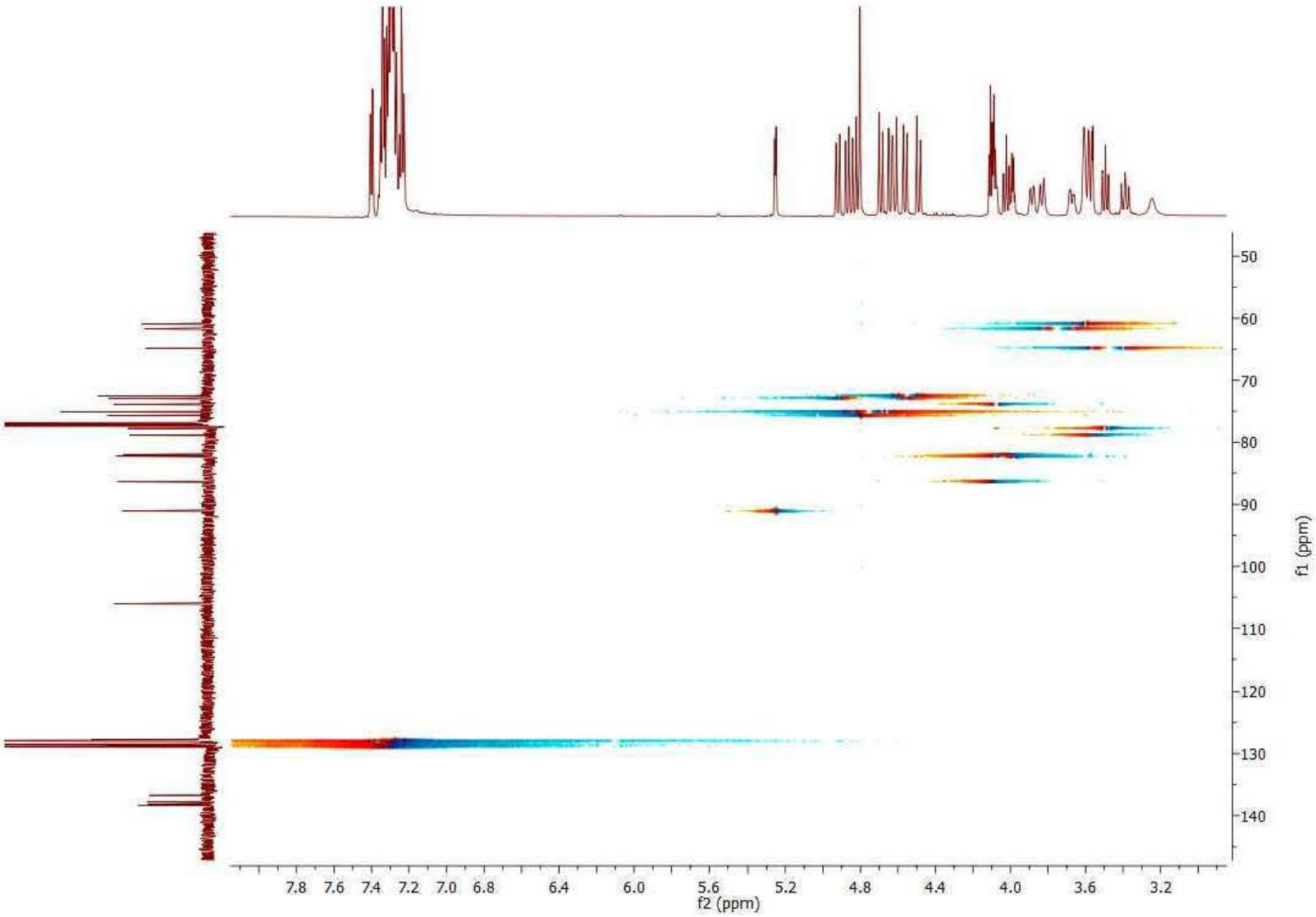

Figure S25. $^{1}H–^{13}C$ HSQC spectrum of compound **3**.

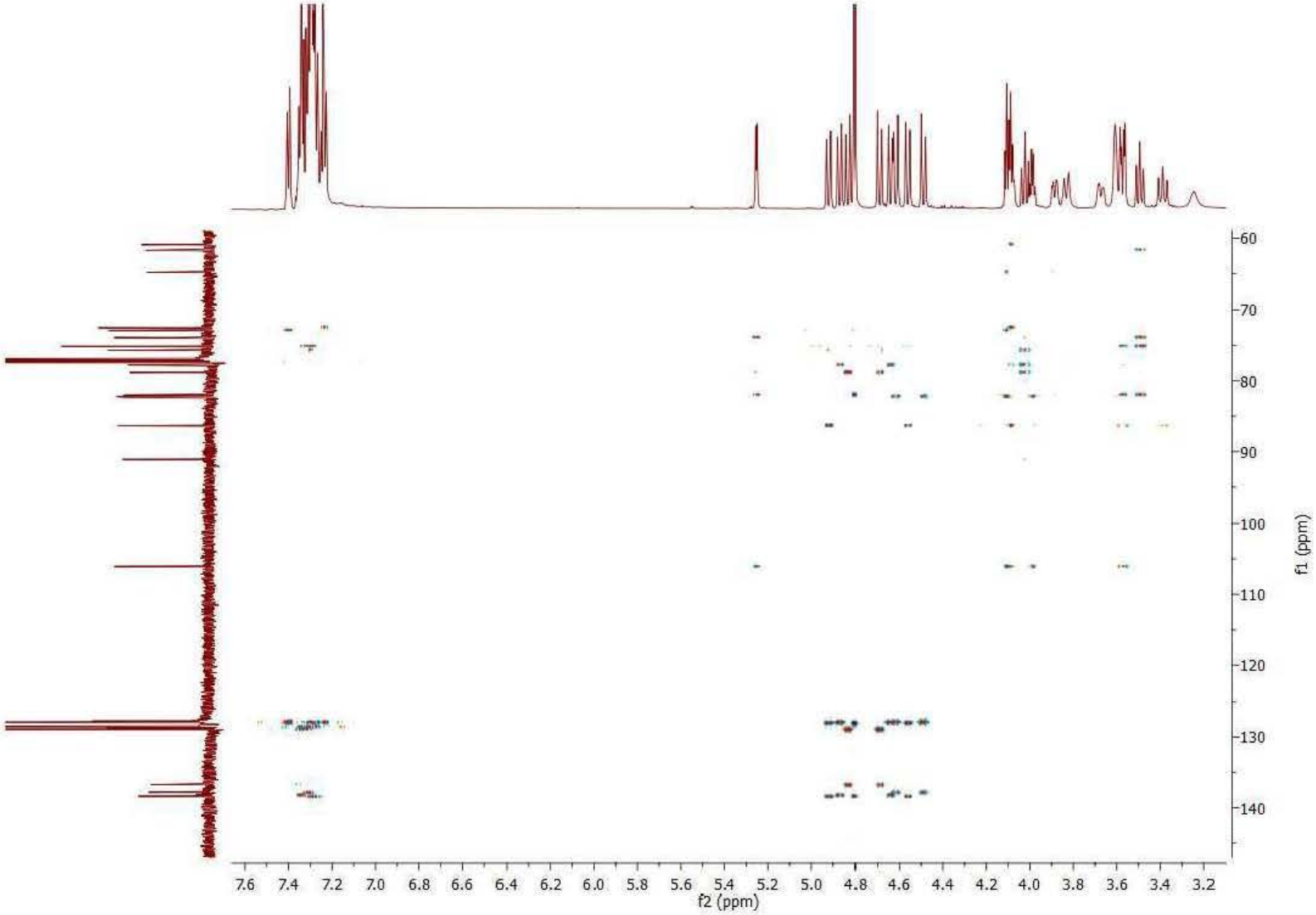

Figure S26. $^{1}H–^{13}C$ HMBC spectrum of compound **3**.

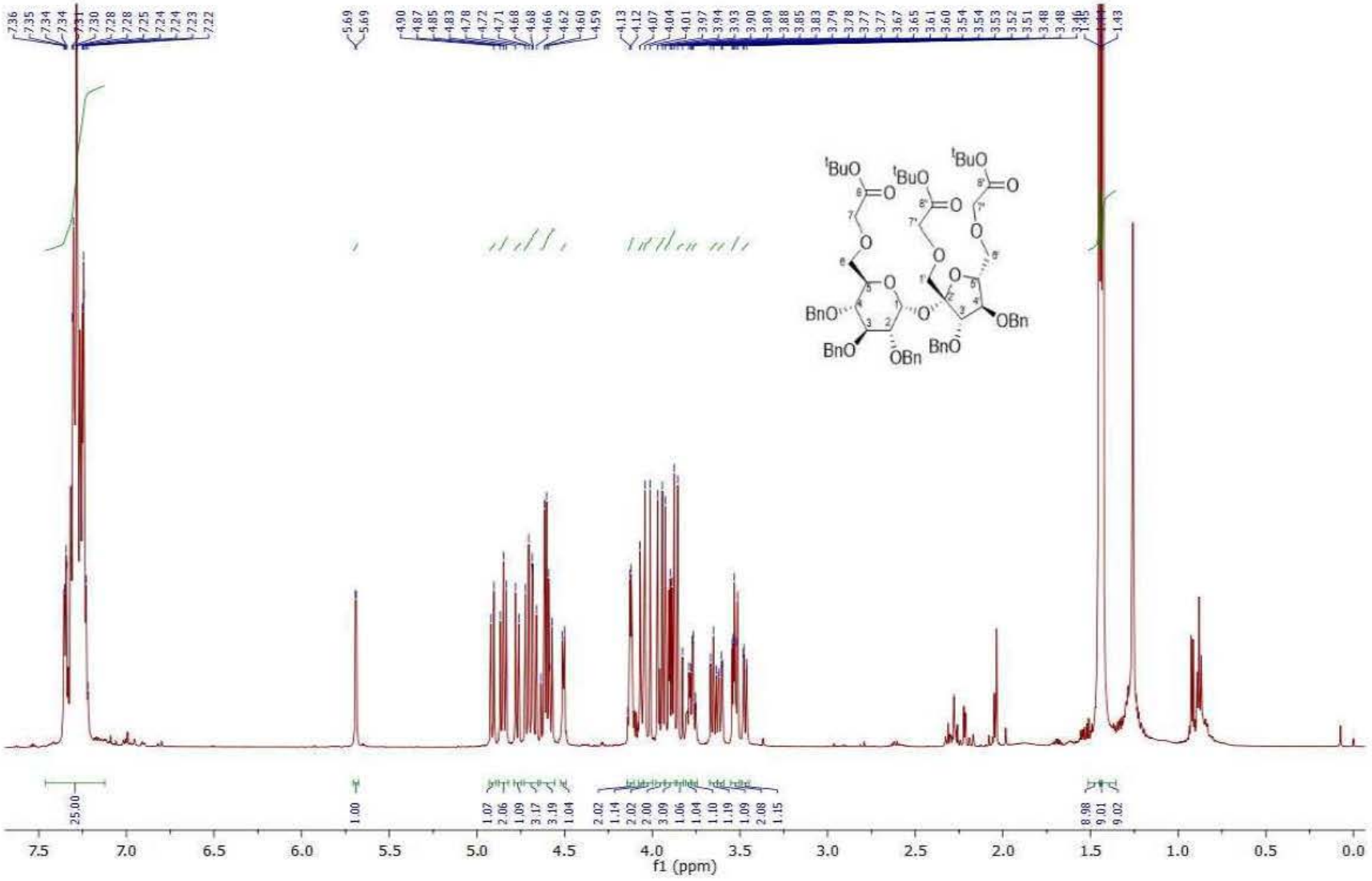

Figure S27. ^{1}H NMR spectrum of compound **4.**

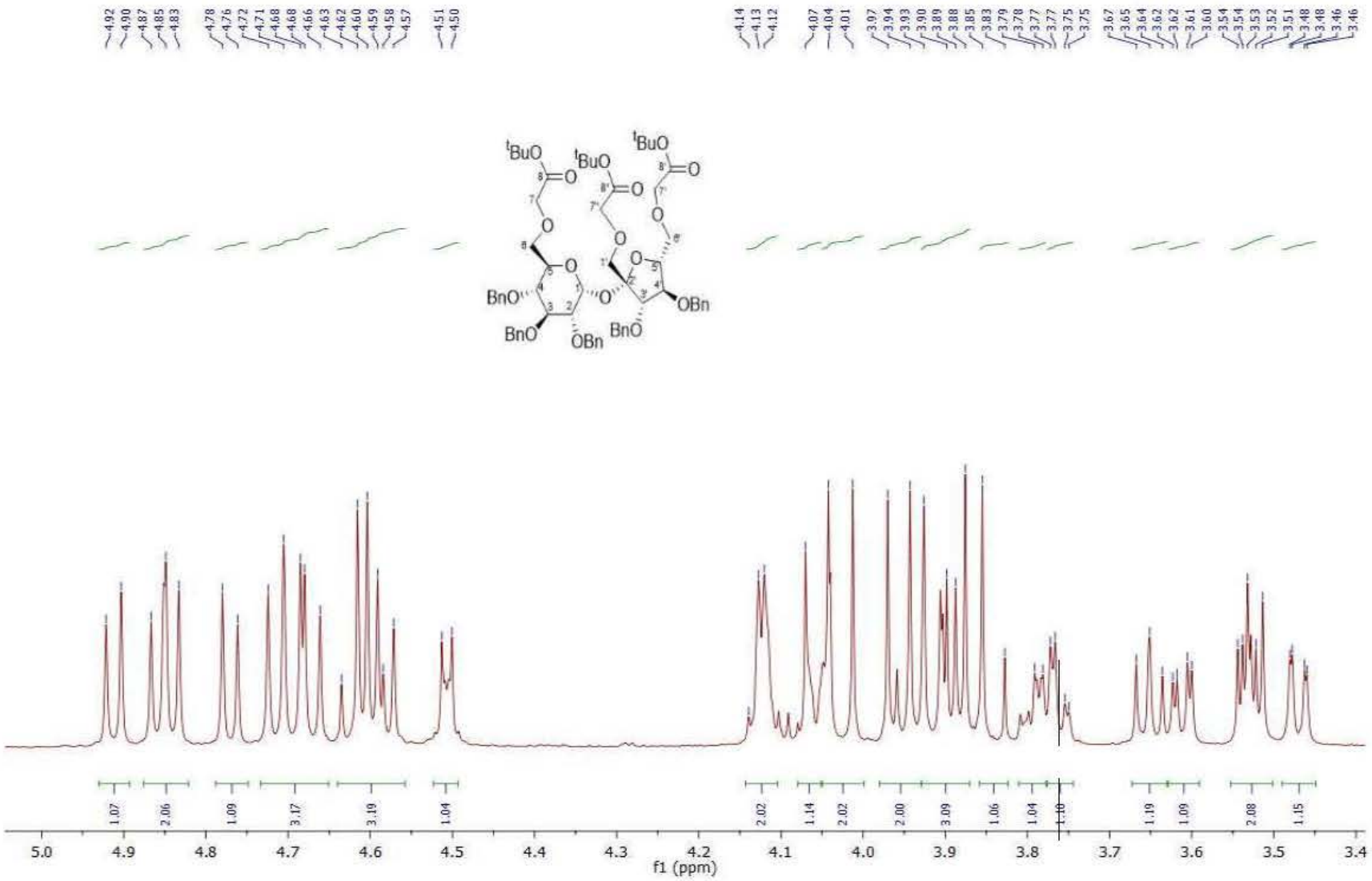

Figure S28. ^{1}H NMR spectrum of compound **4** (aliphatic part).

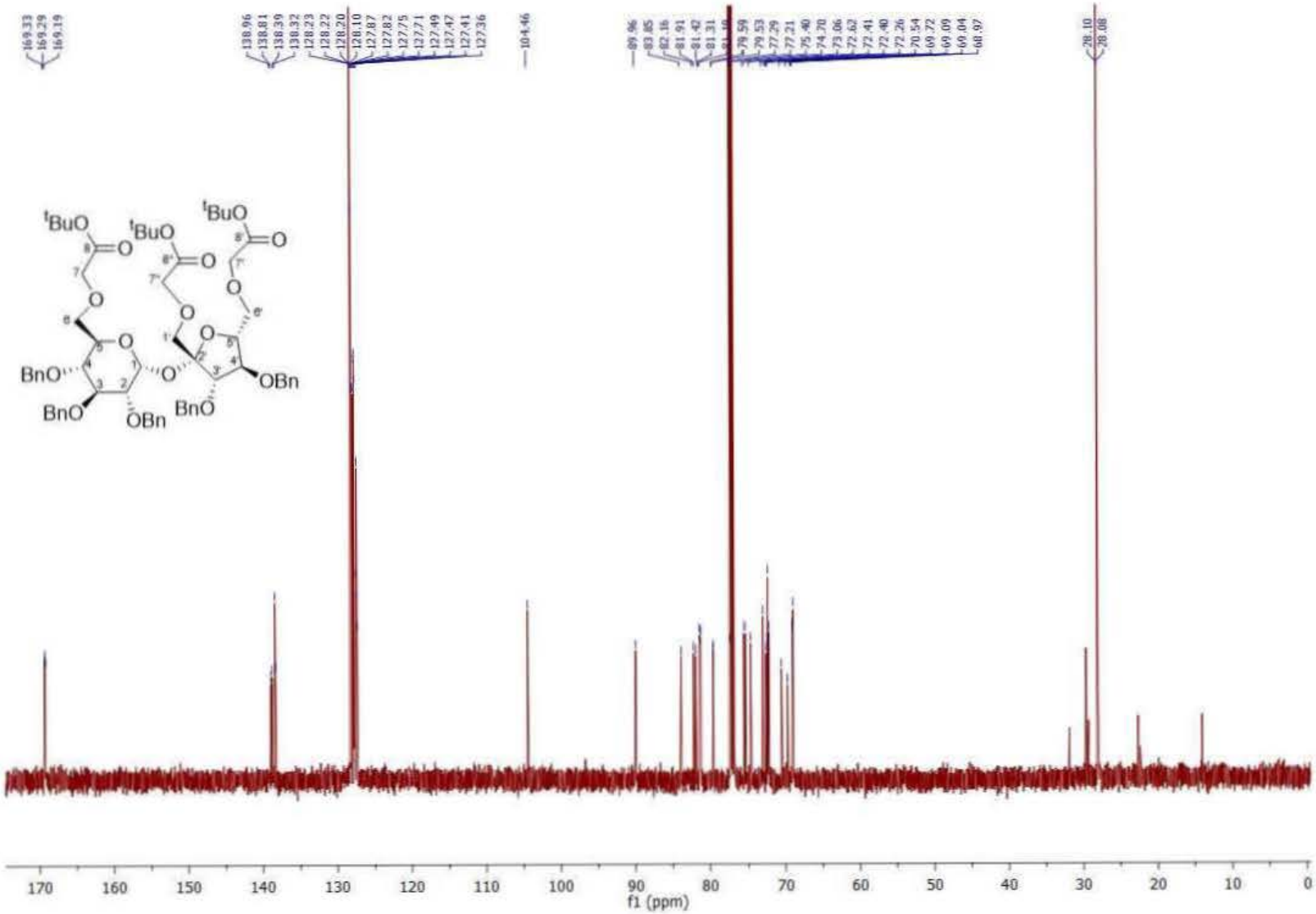

Figure S29. ^{13}C NMR spectrum of compound **4**.

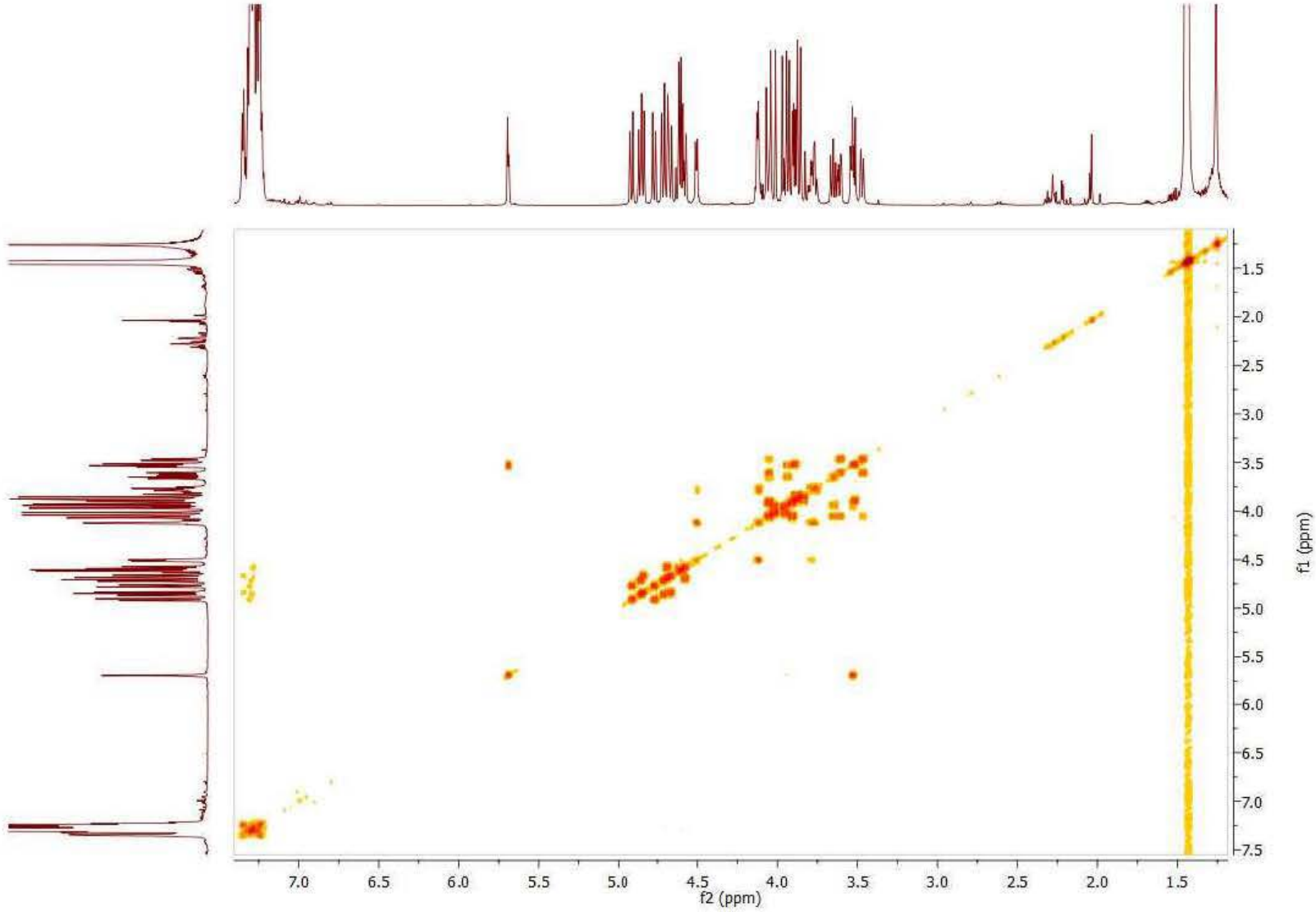

Figure S30. ^{1}H–^{1}H COSY spectrum of compound **4**.

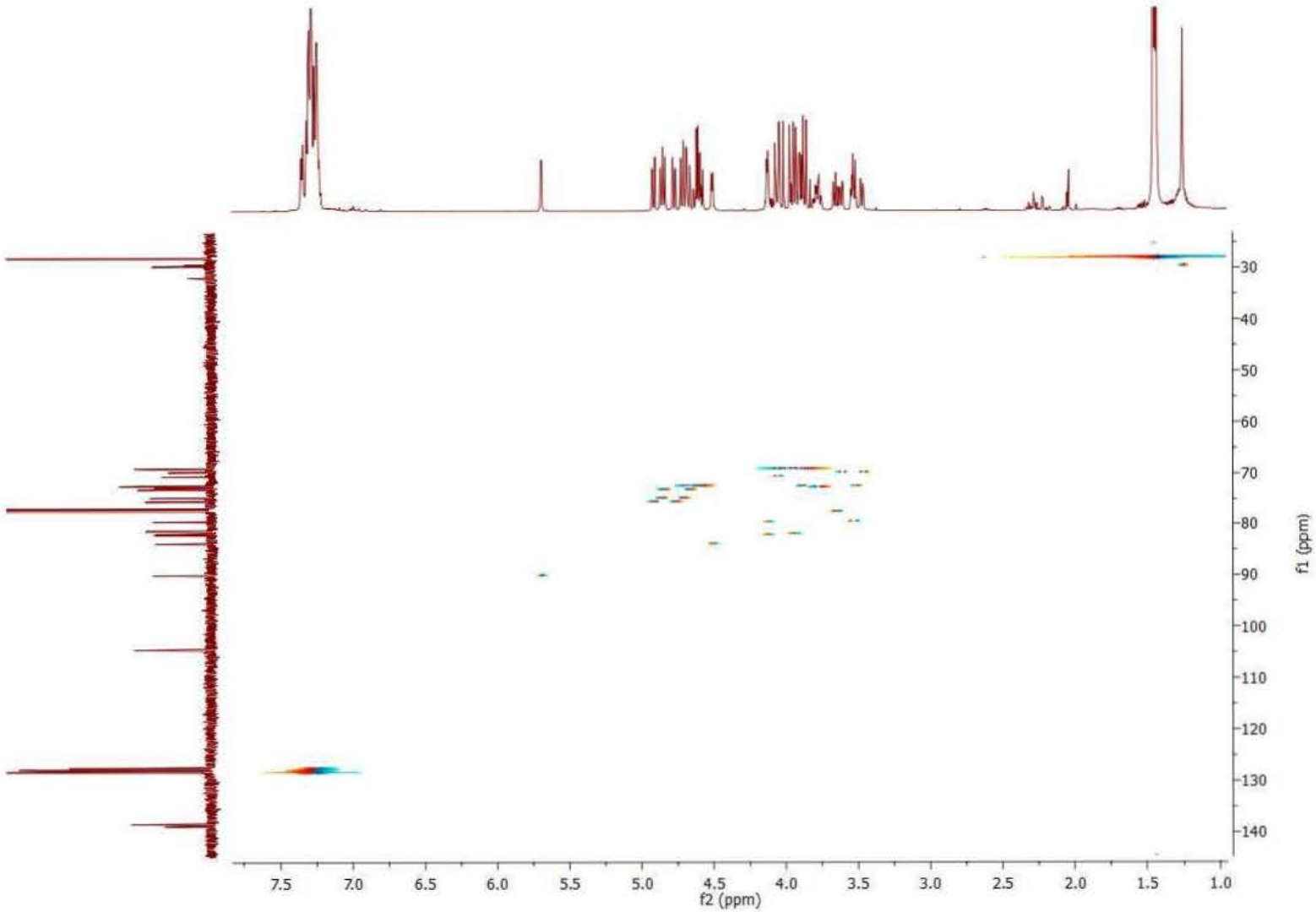

Figure S31. $^{1}H–^{13}C$ HSQC spectrum of compound **4**.

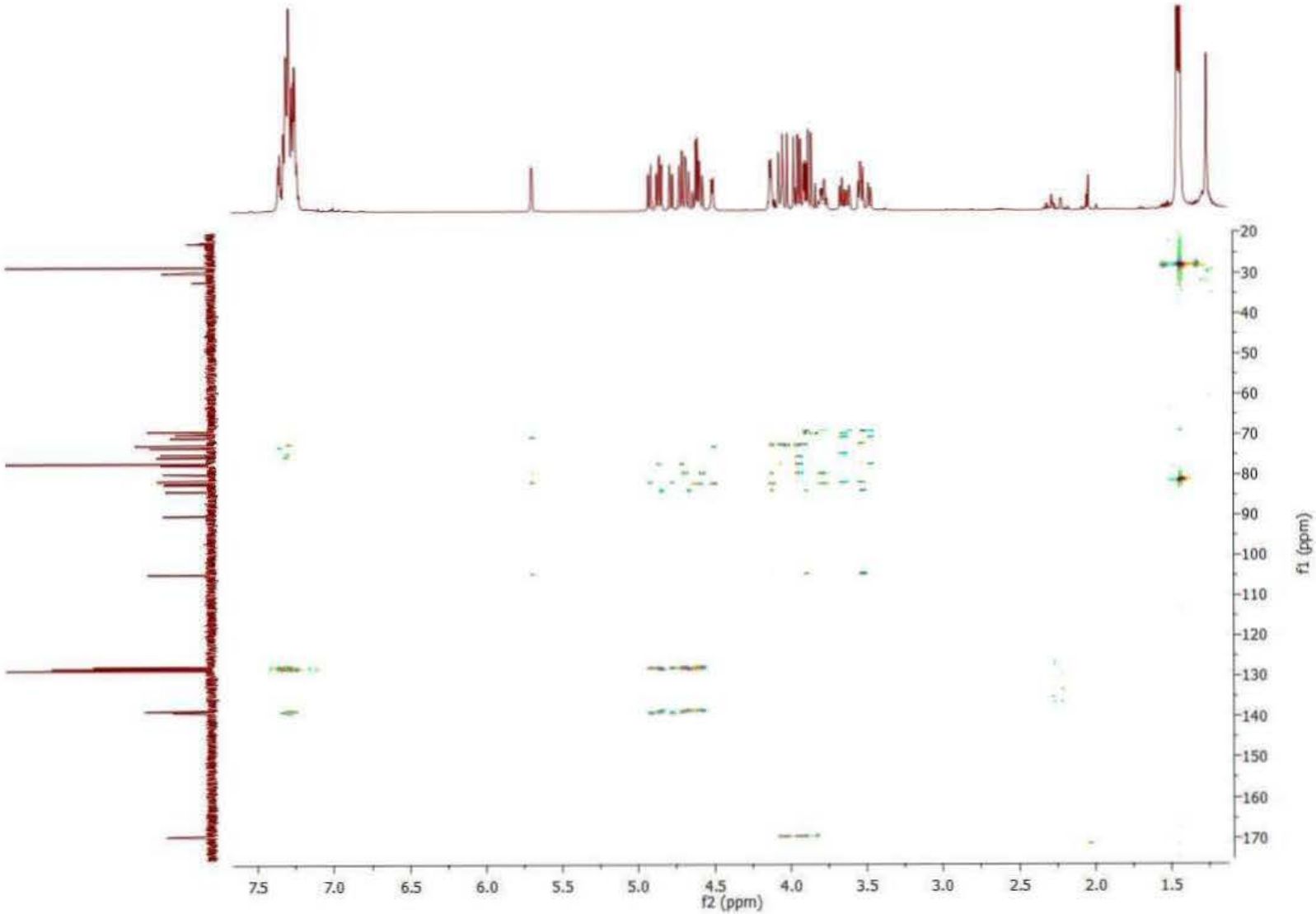

Figure S32. $^{1}H–^{13}C$ HMBC spectrum of compound **4**.

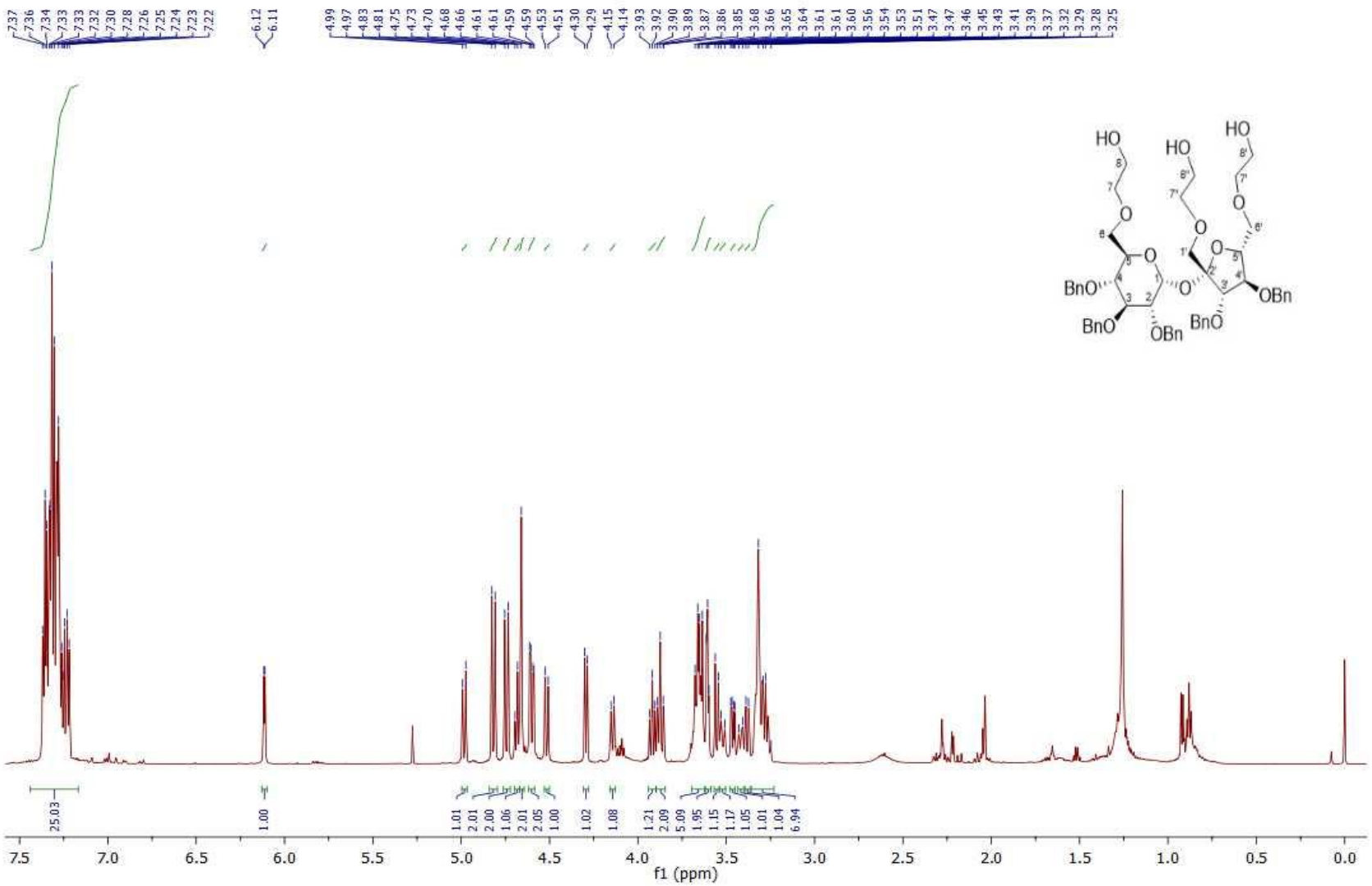

Figure S33. ^{1}H NMR spectrum of compound **5**.

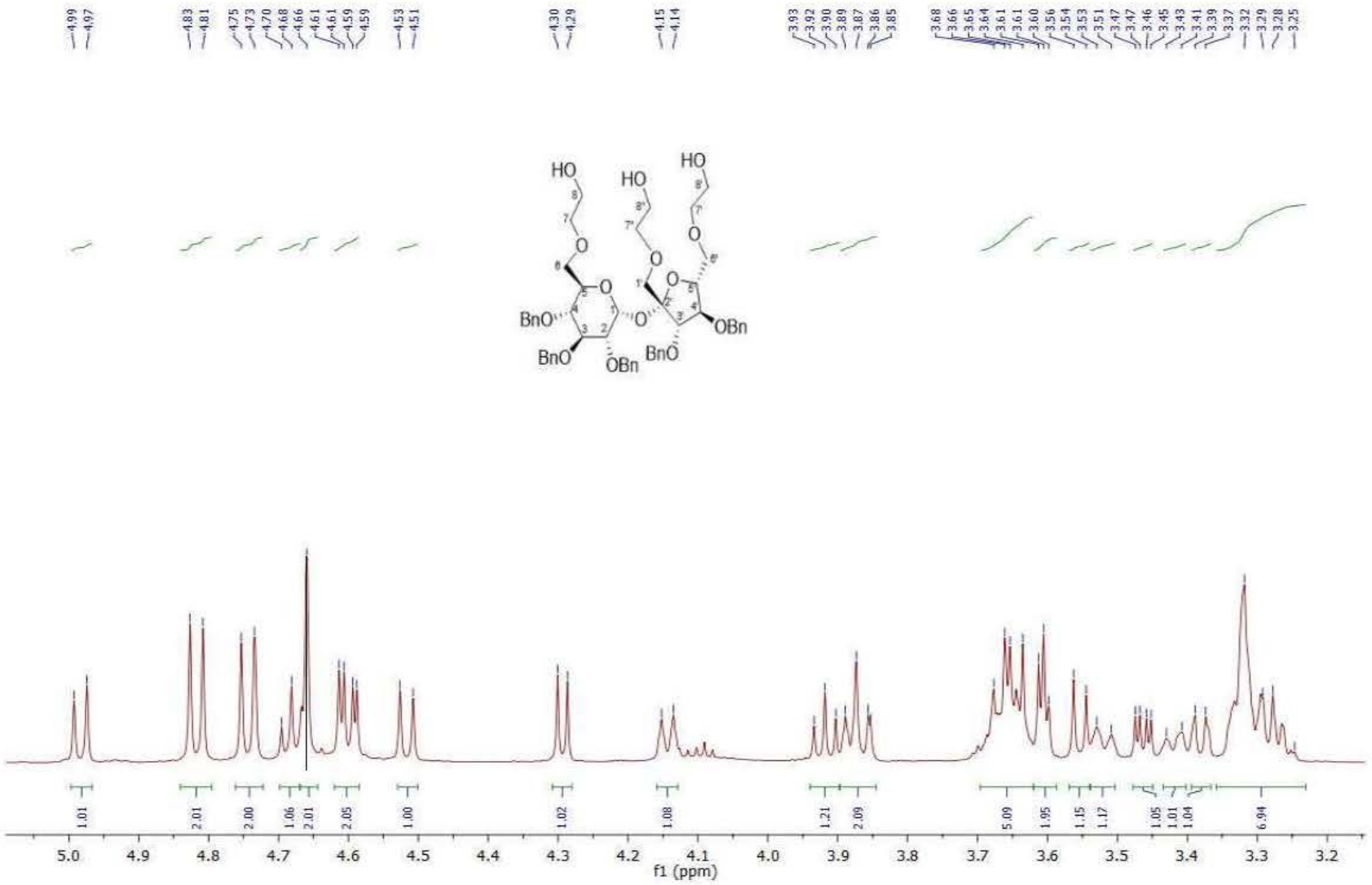

Figure S34. ^{1}H NMR spectrum of compound **5** (aliphatic part).

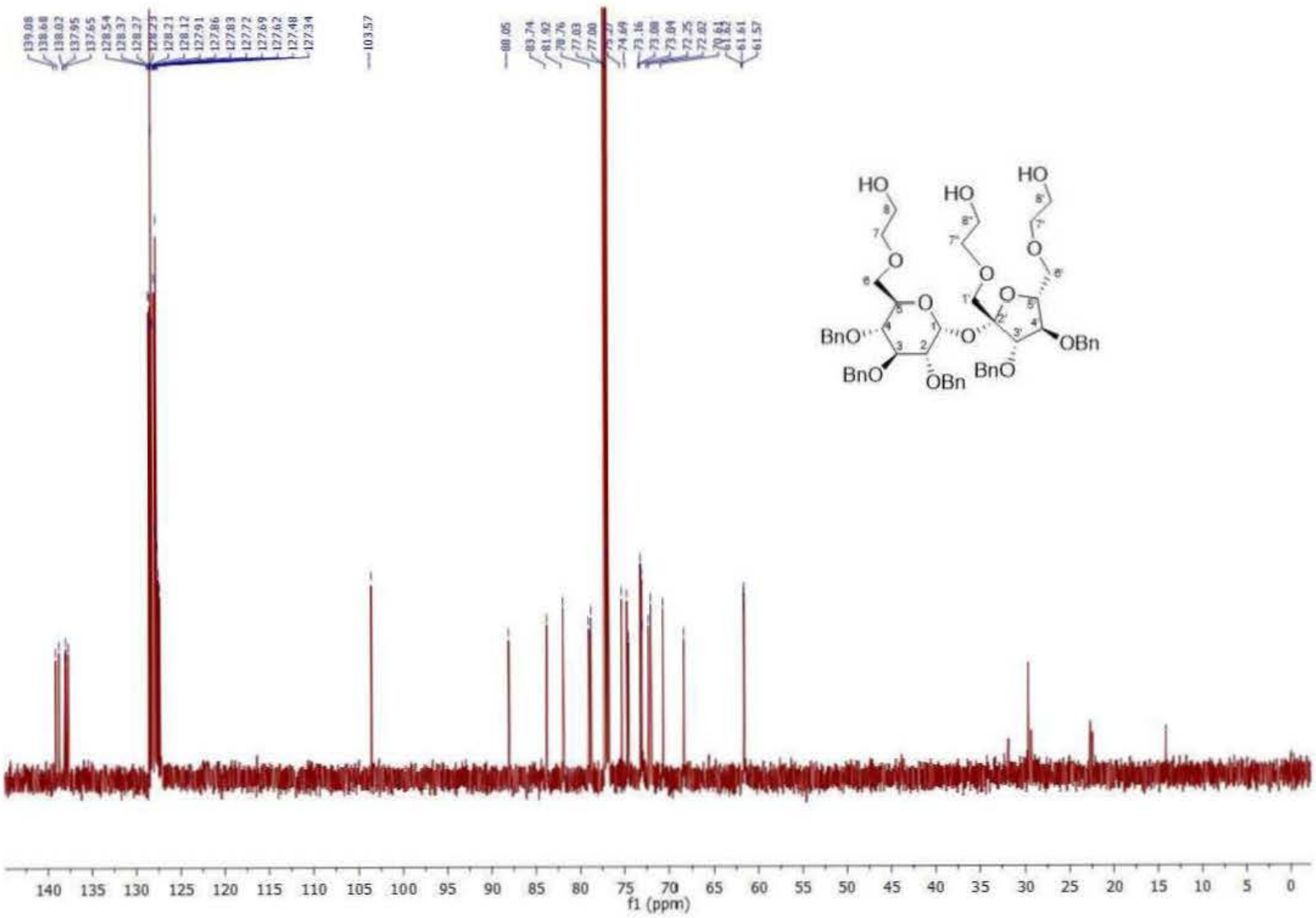

Figure S35. ^{13}C NMR spectrum of compound **5**.

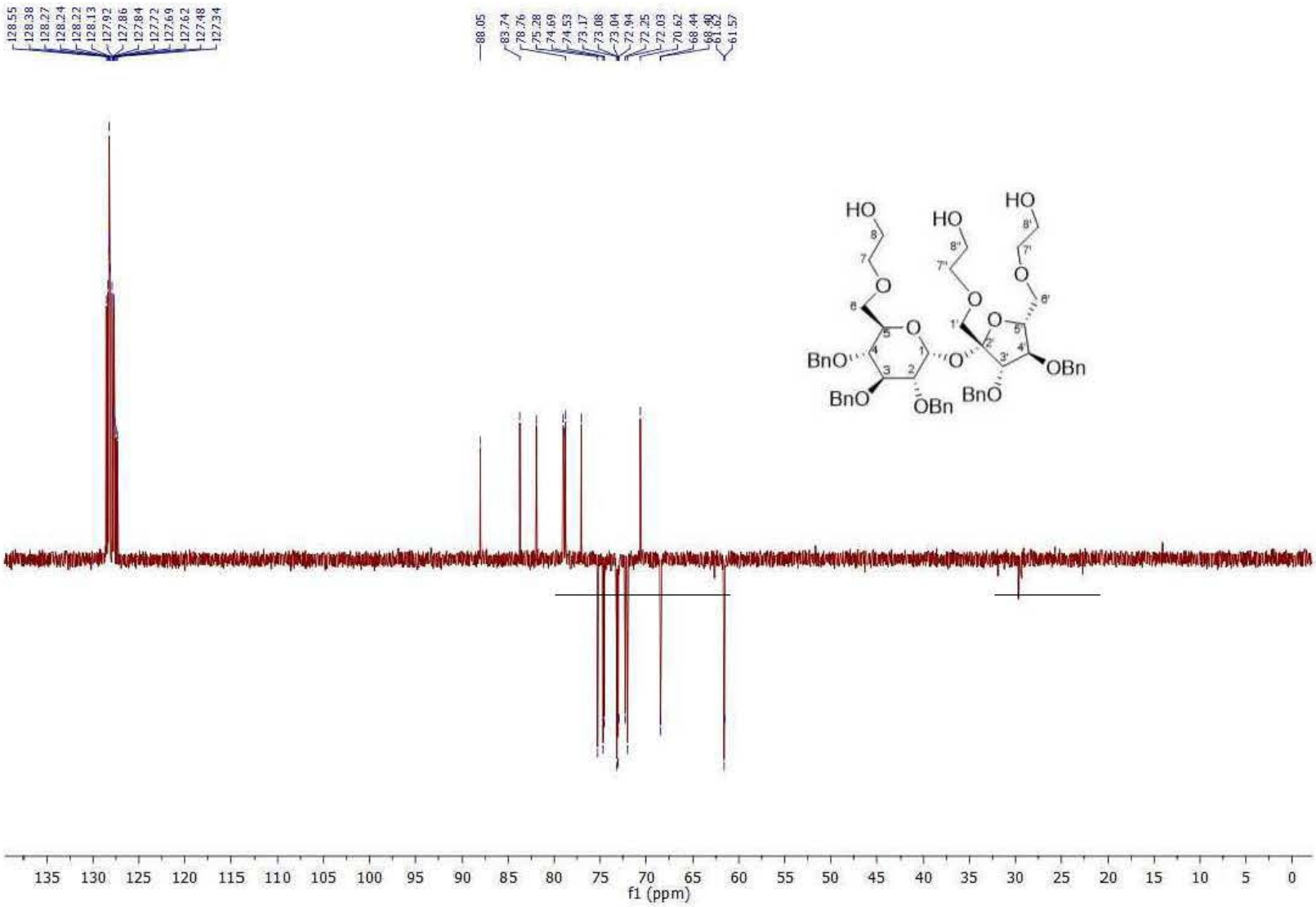

Figure S36. DEPT^{13}C NMR spectrum of compound **5**.

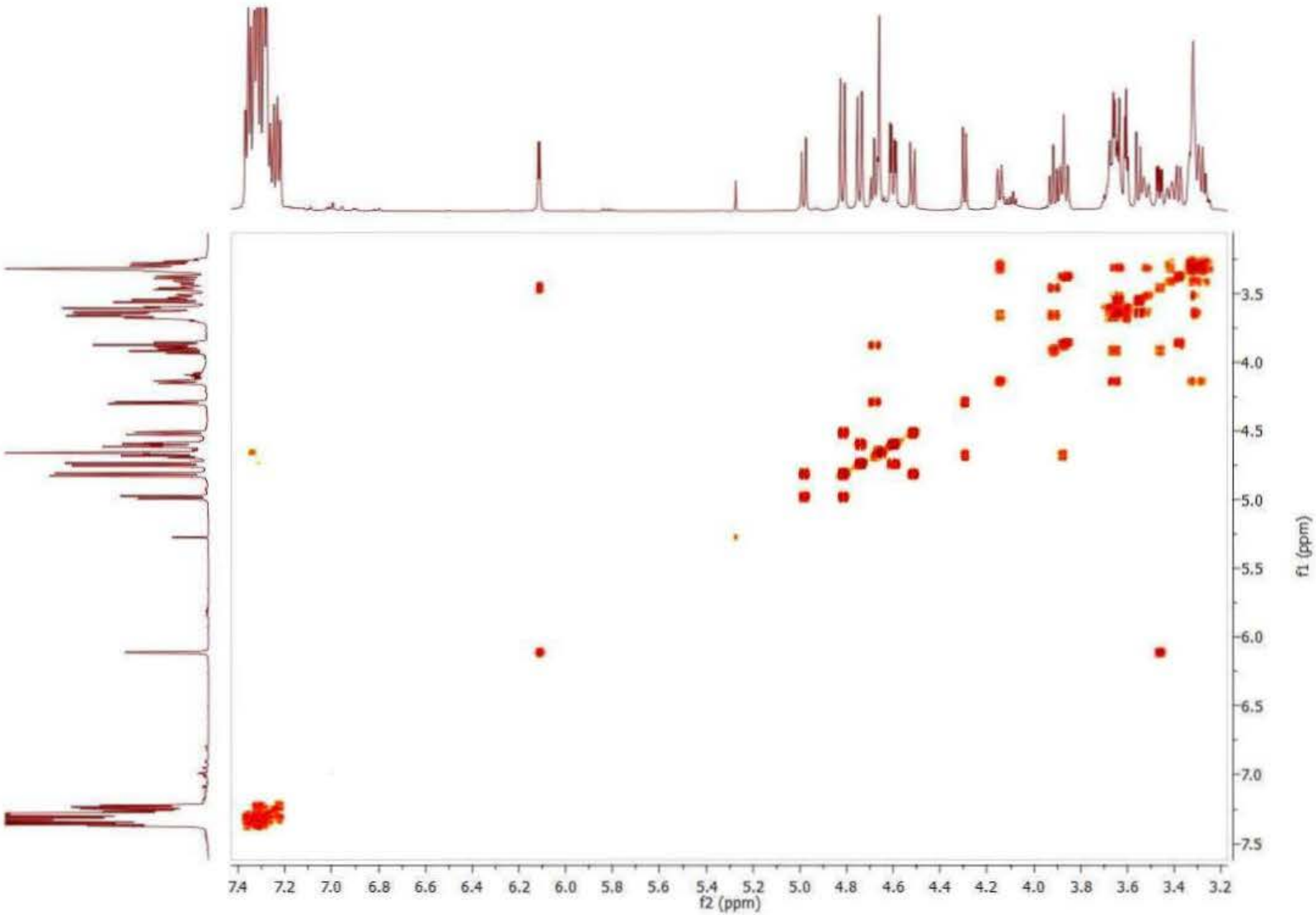

Figure S37. ^{1}H–^{1}H COSY spectrum of compound **5**.

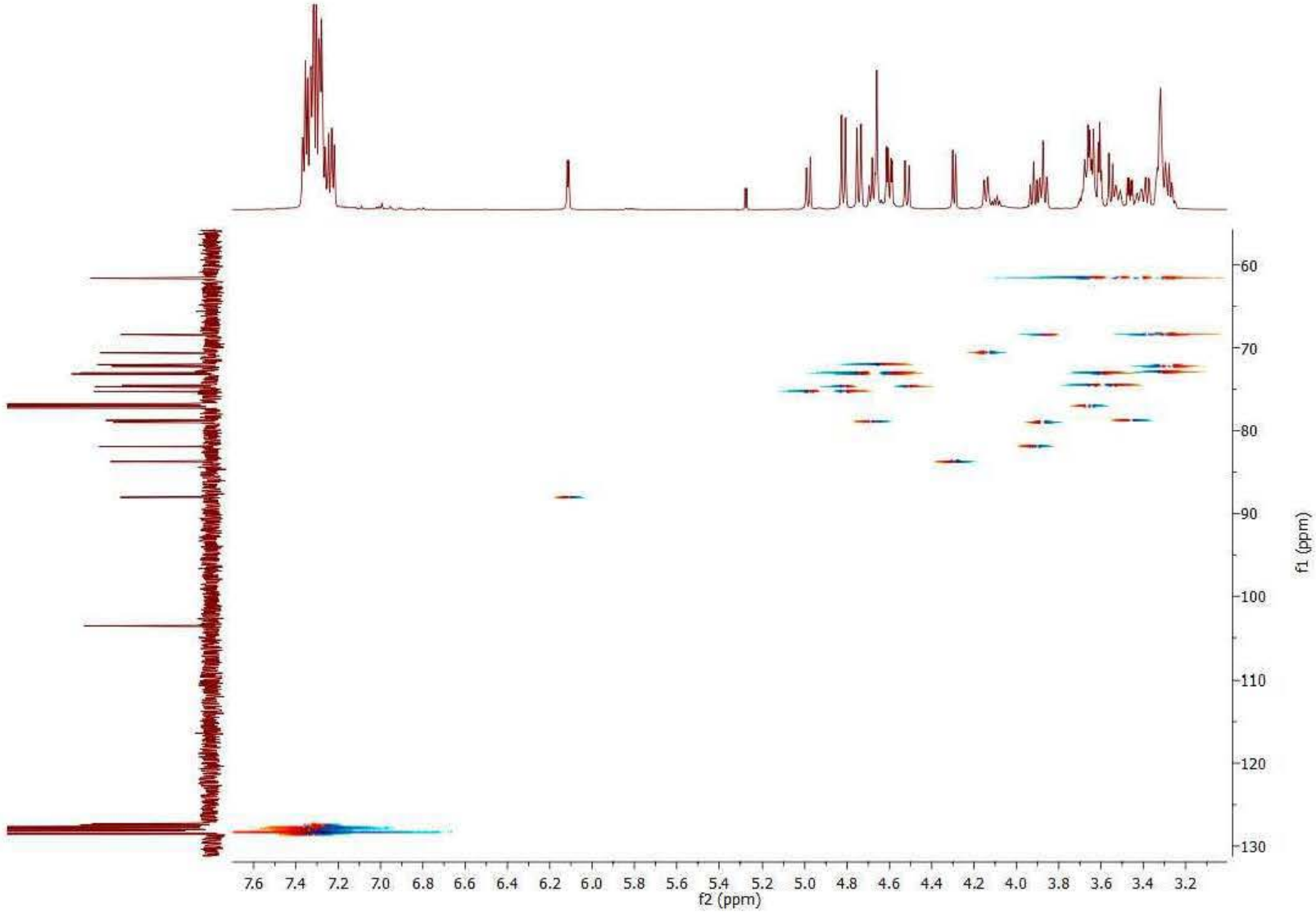

Figure S38. $^{1}H–^{13}C$ HSQC spectrum of compound **5**.

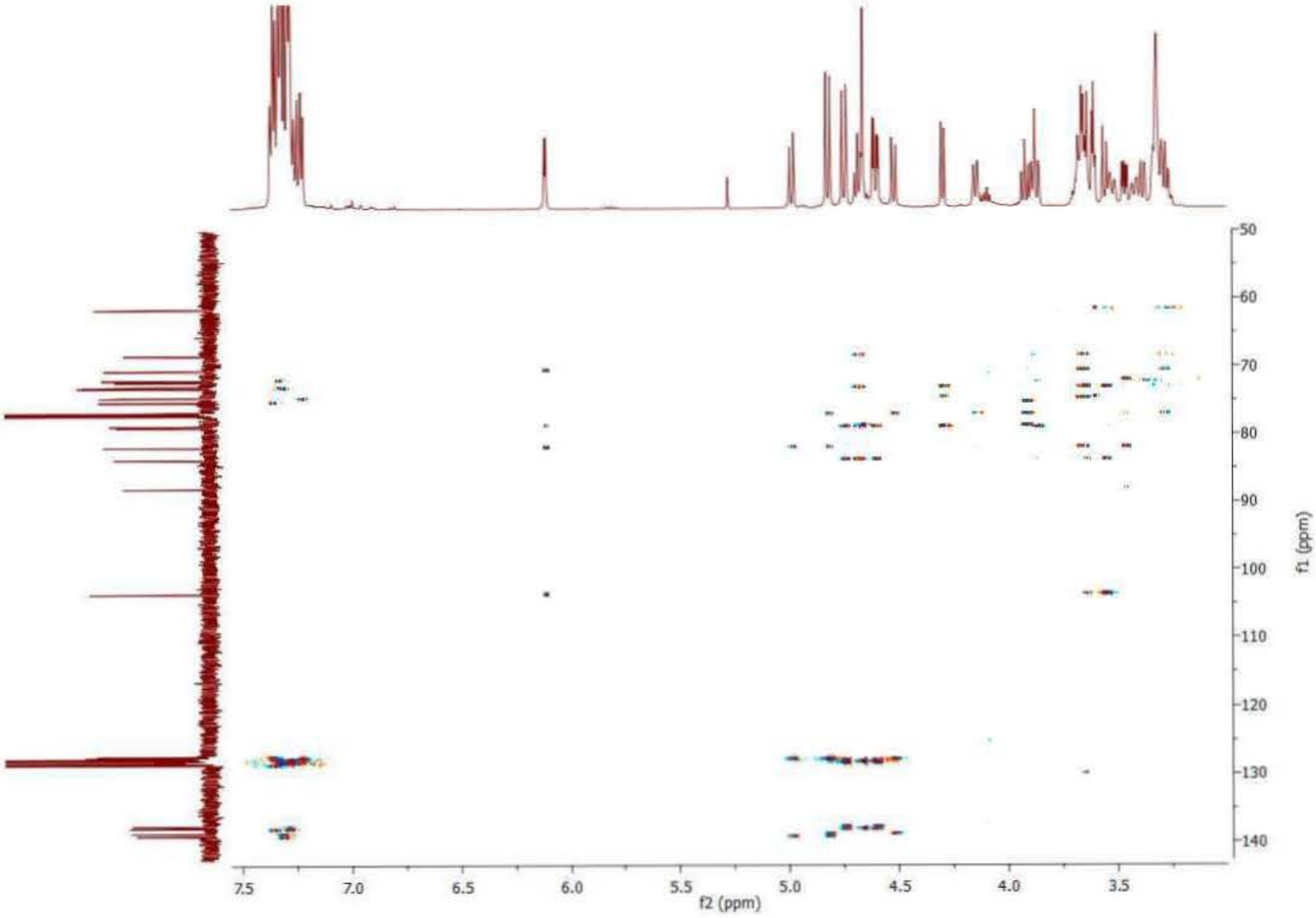

Figure S39. ^{1}H–^{13}C HMBC spectrum of compound **5**.

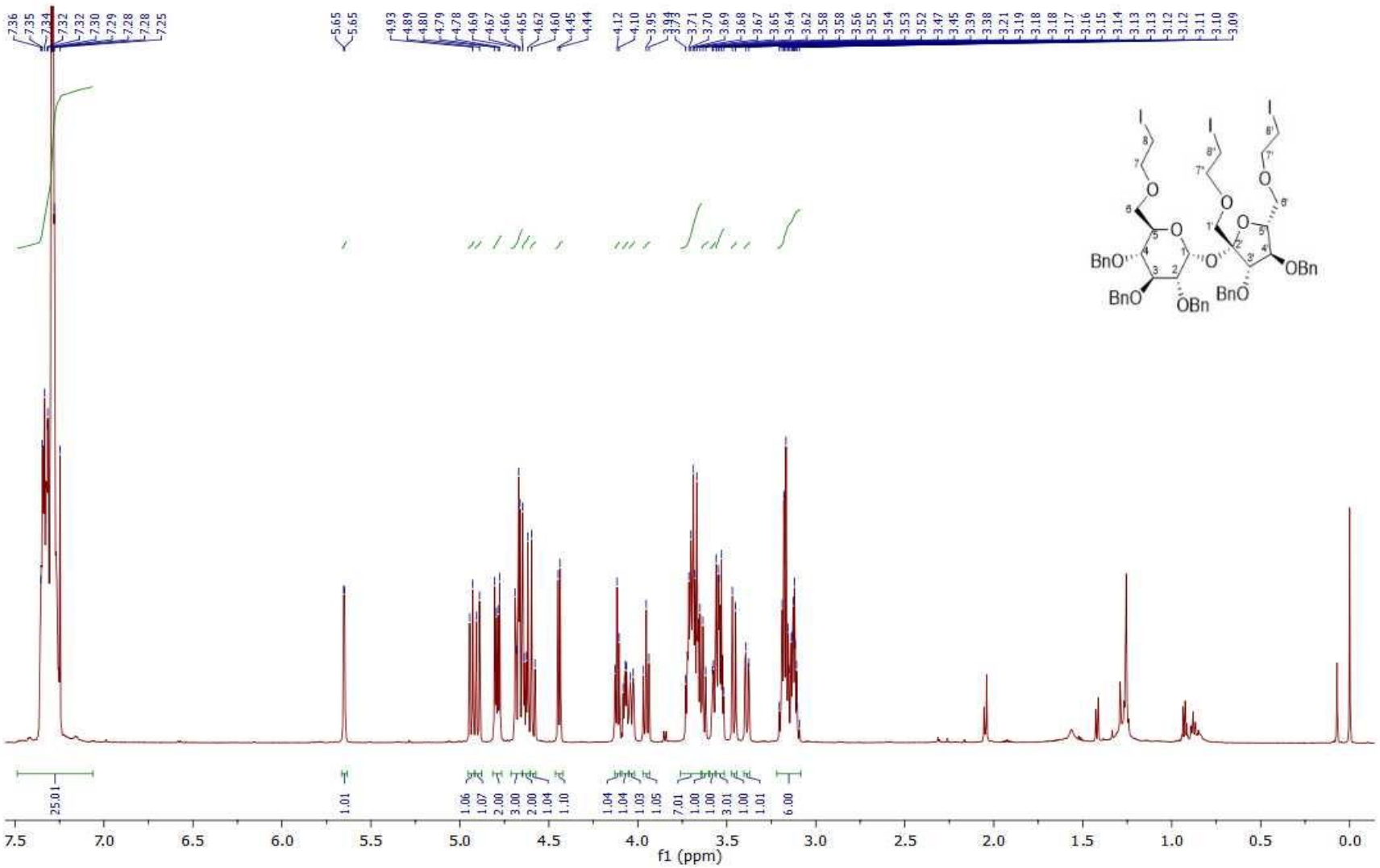

Figure S40. ^{1}H NMR spectrum of compound **6**.

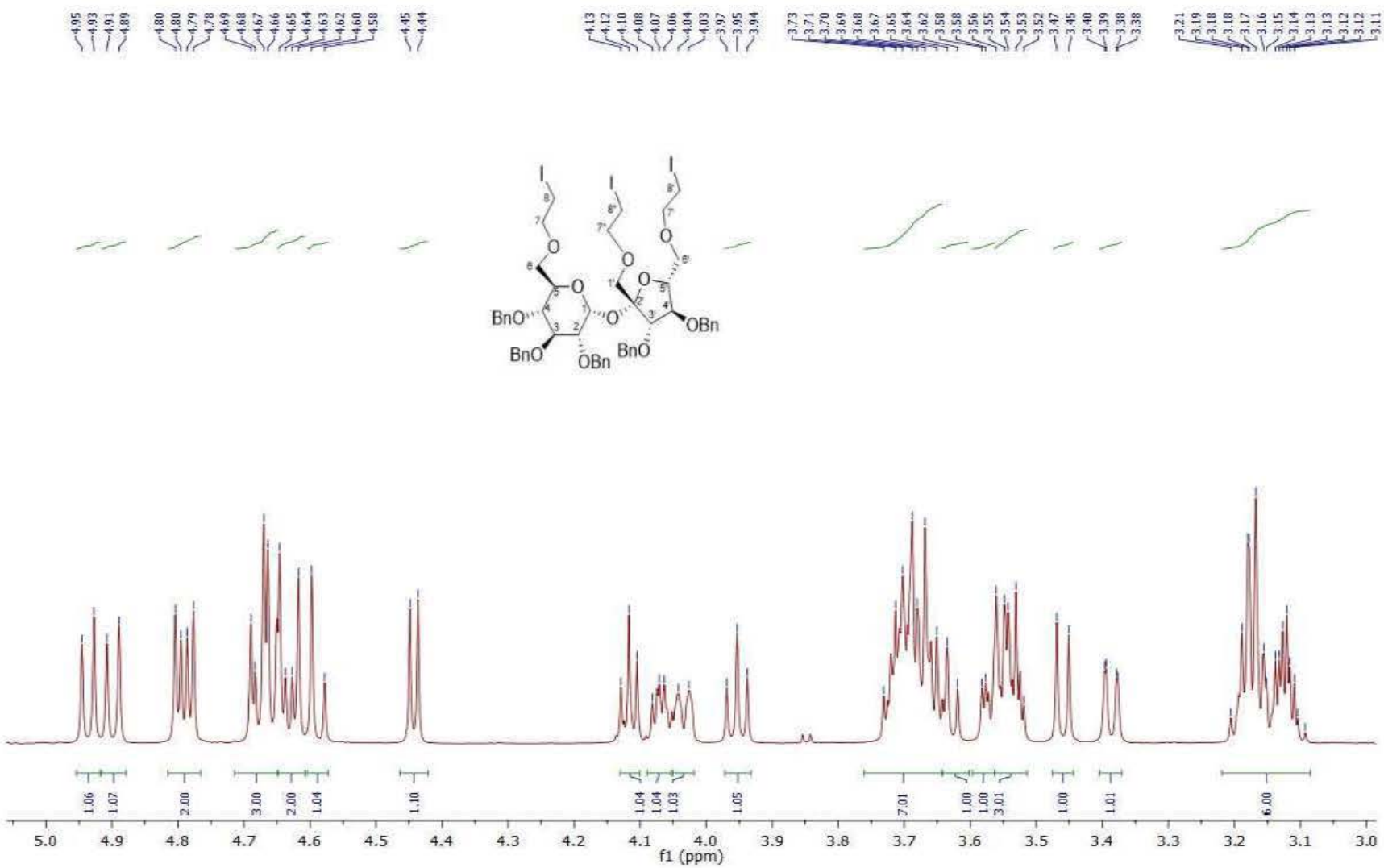

Figure S41. ^{1}H NMR spectrum of compound **6** (aliphatic part).

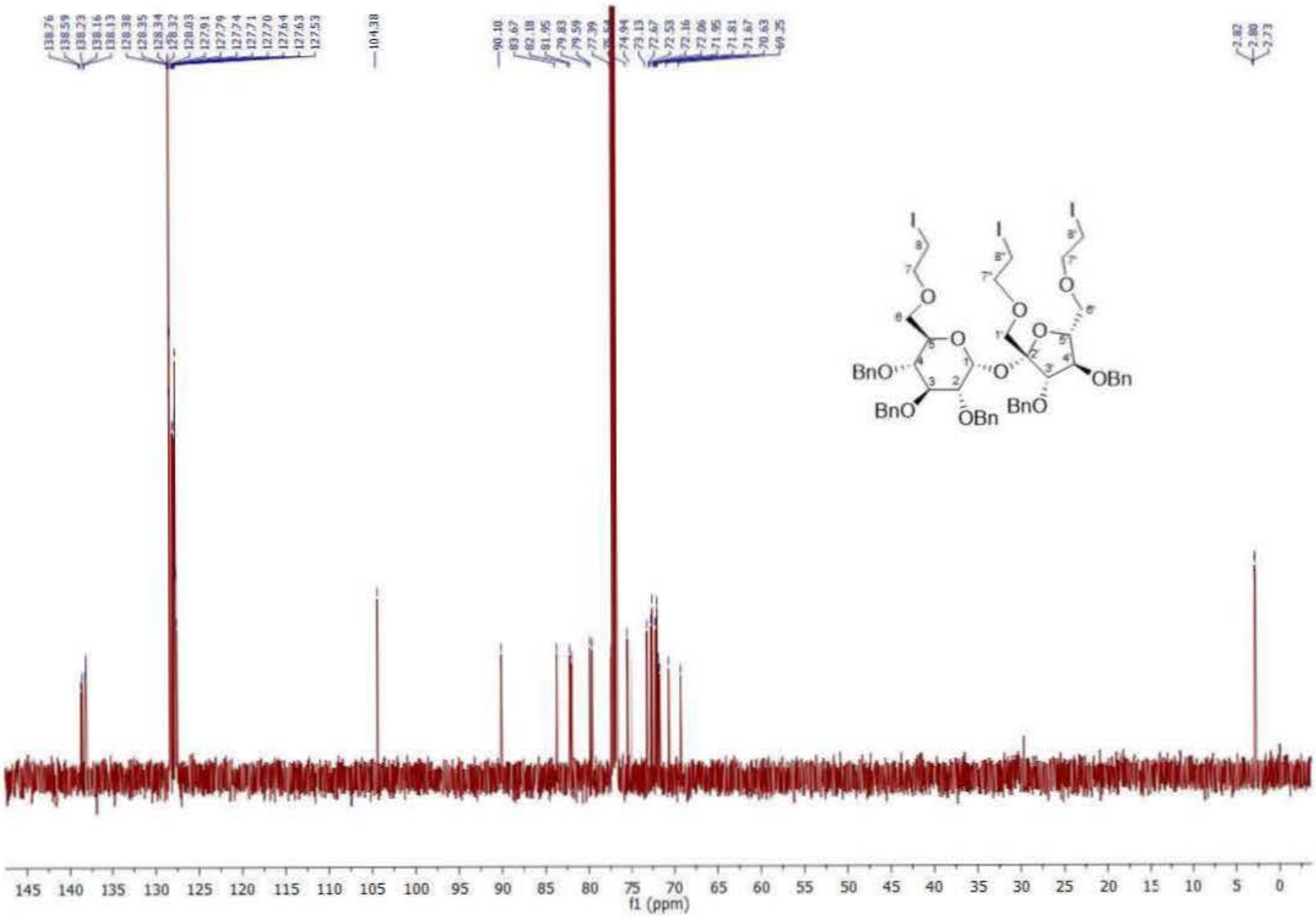

Figure S42. ^{13}C NMR spectrum of compound **6**.

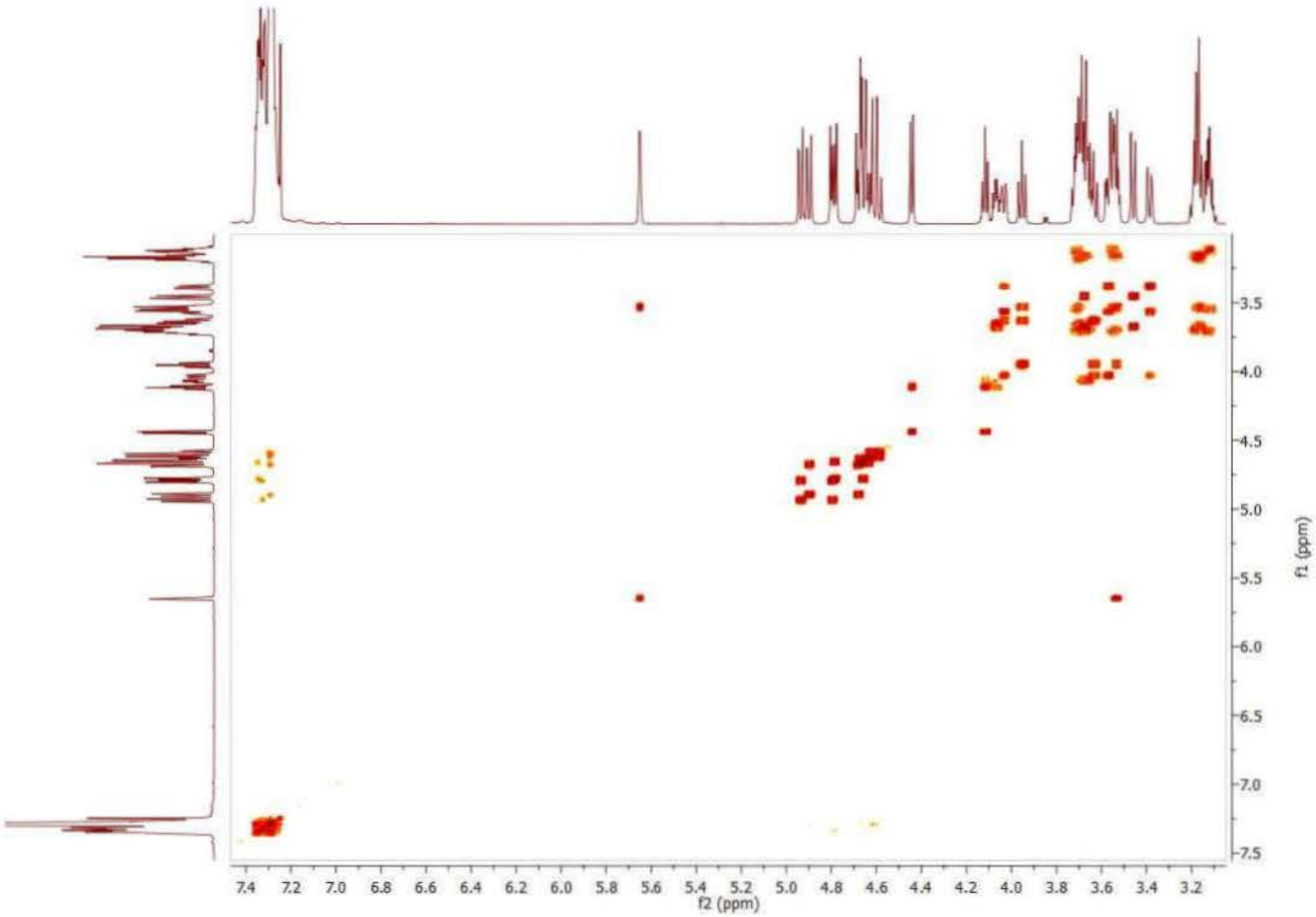

Figure S43. ^{1}H–^{1}H COSY spectrum of compound **6**.

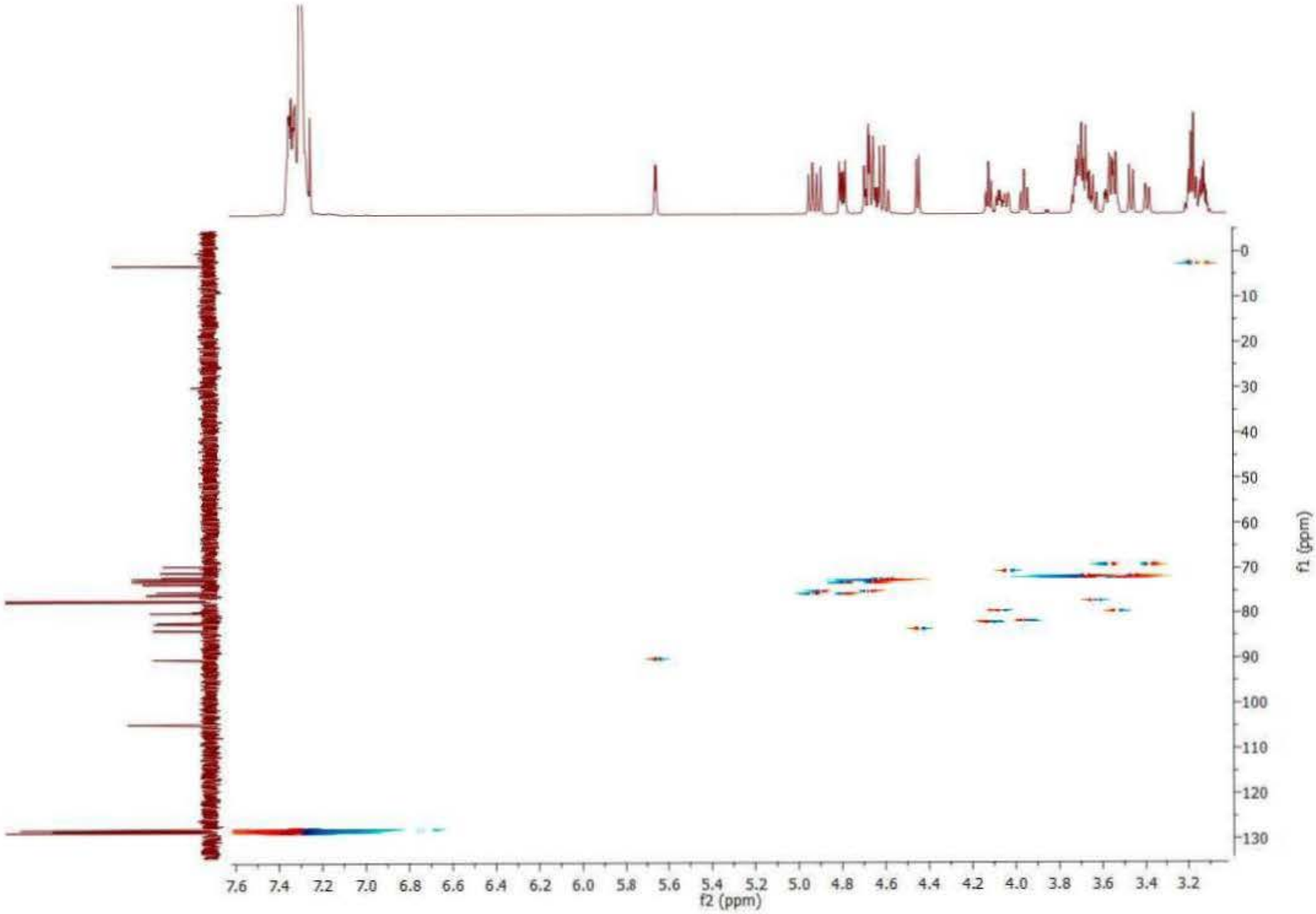

Figure S44. $^{1}H–^{13}C$ HSQC spectrum of compound **6**.

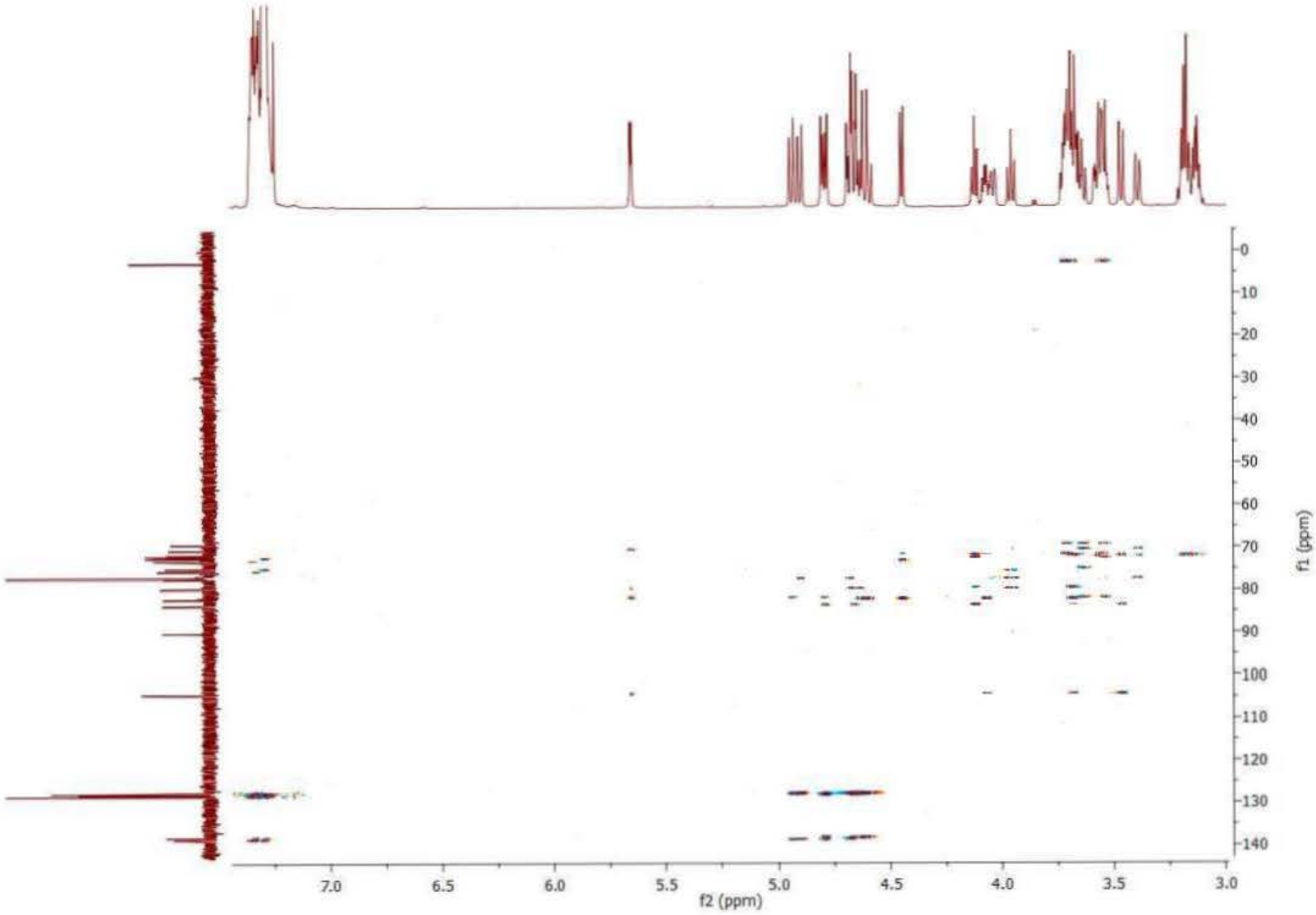

Figure S45. ^{1}H–^{13}C HMBC spectrum of compound **6**.

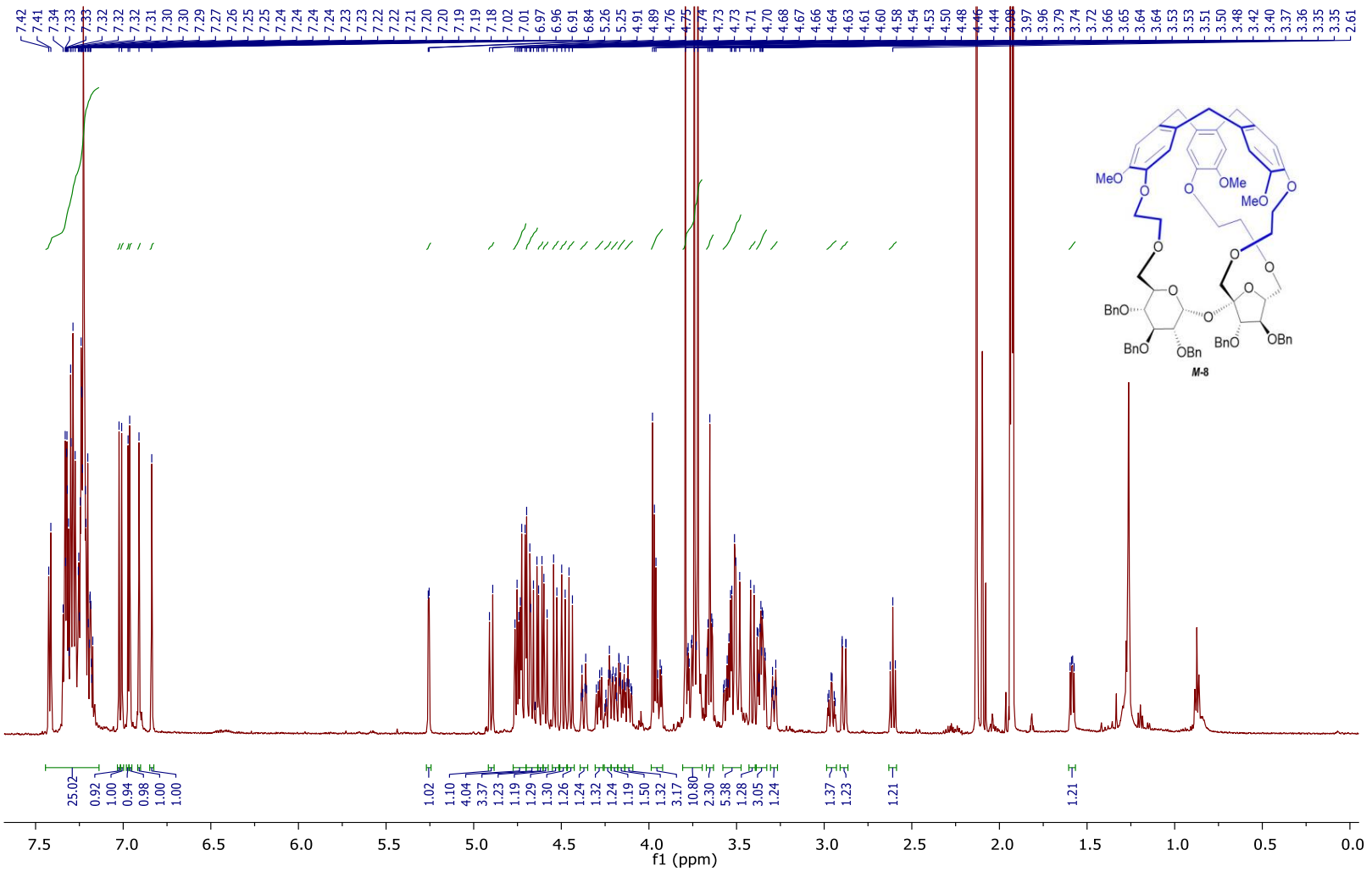

Figure S46. ^{1}H NMR spectrum of compound ***M*-8.**

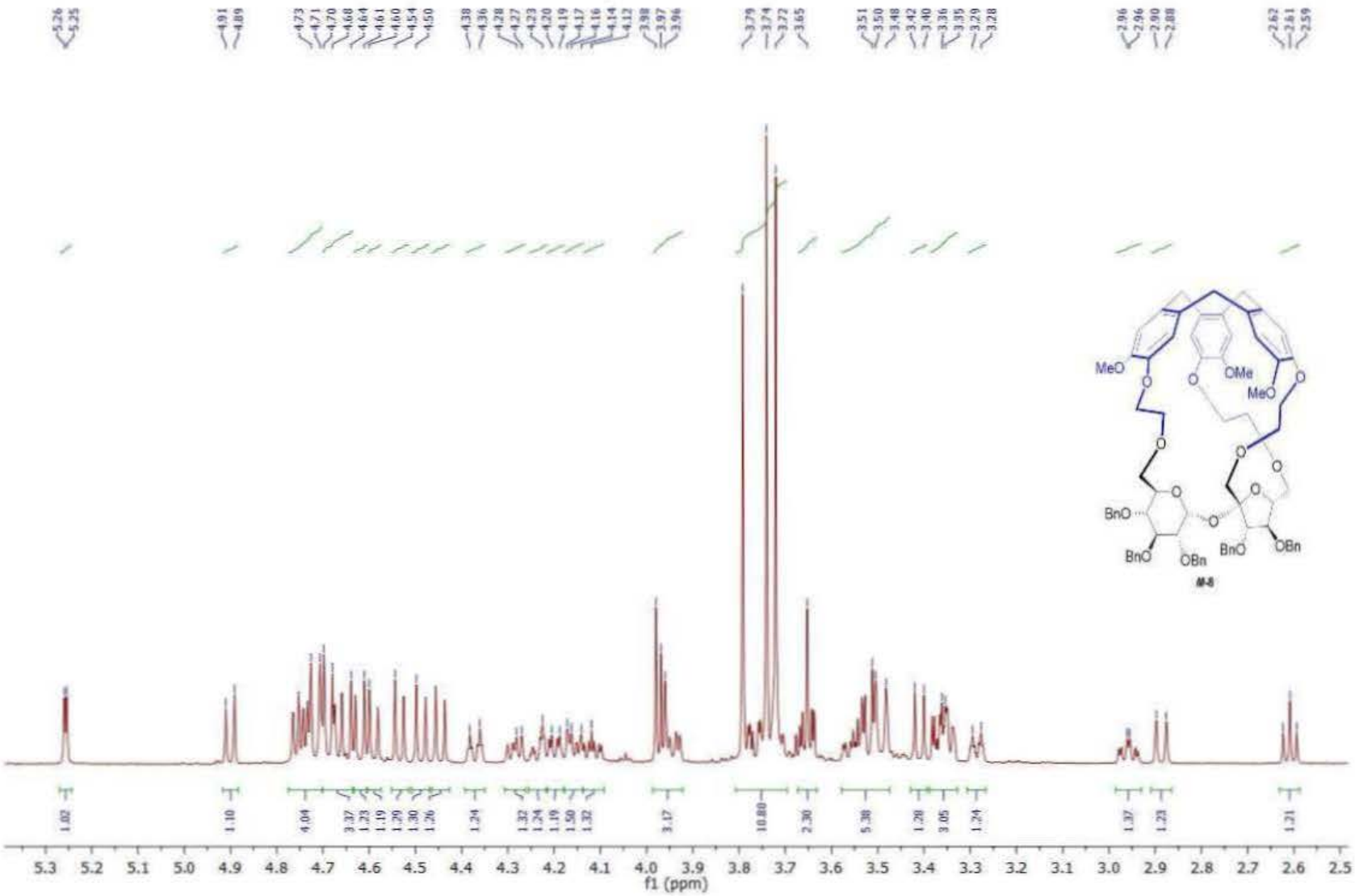

Figure S47. ^{1}H NMR spectrum of compound ***M*-8** (aliphatic part).

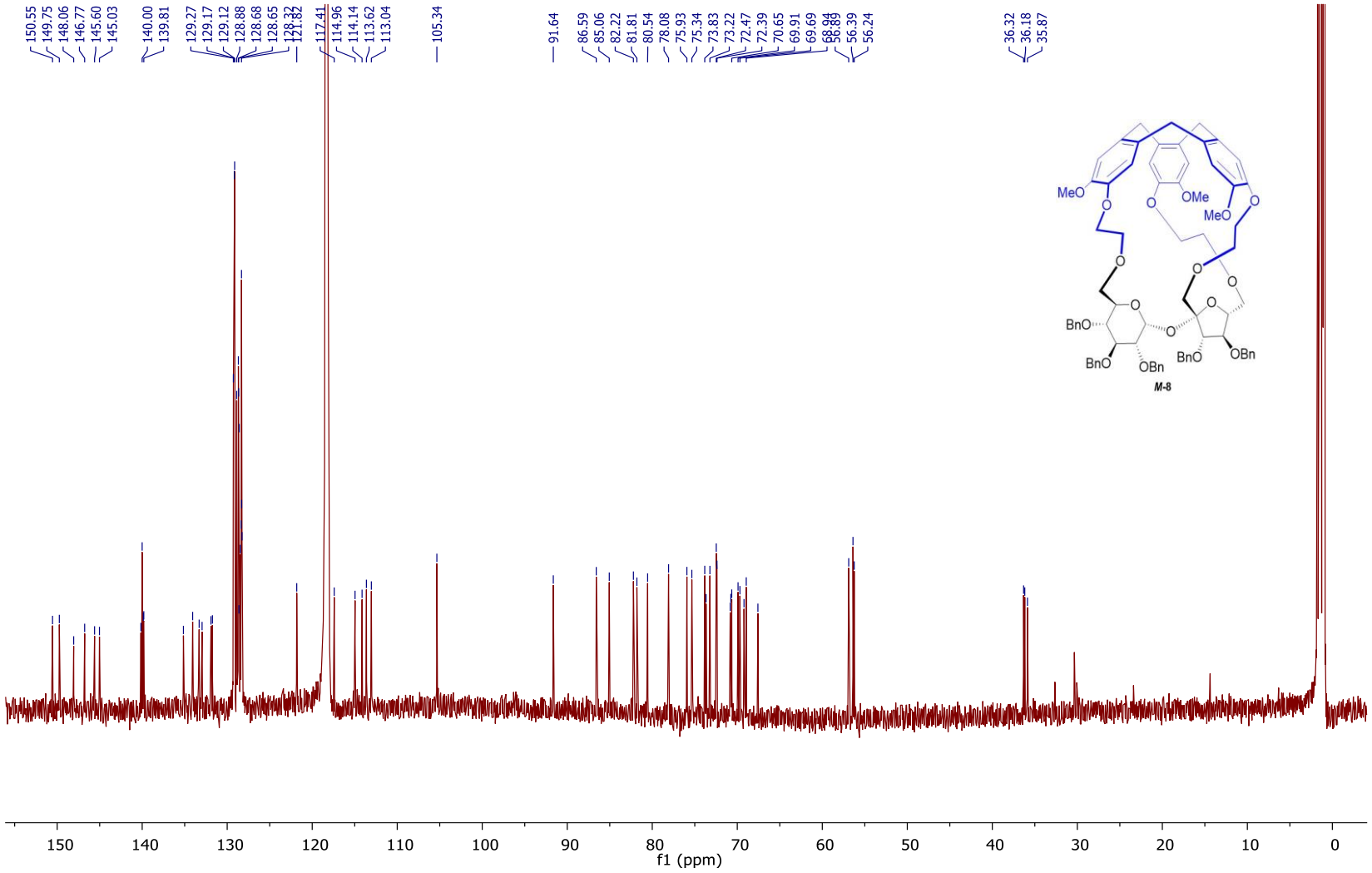

Figure S48. ^{13}C NMR spectrum of compound ***M*-8**.

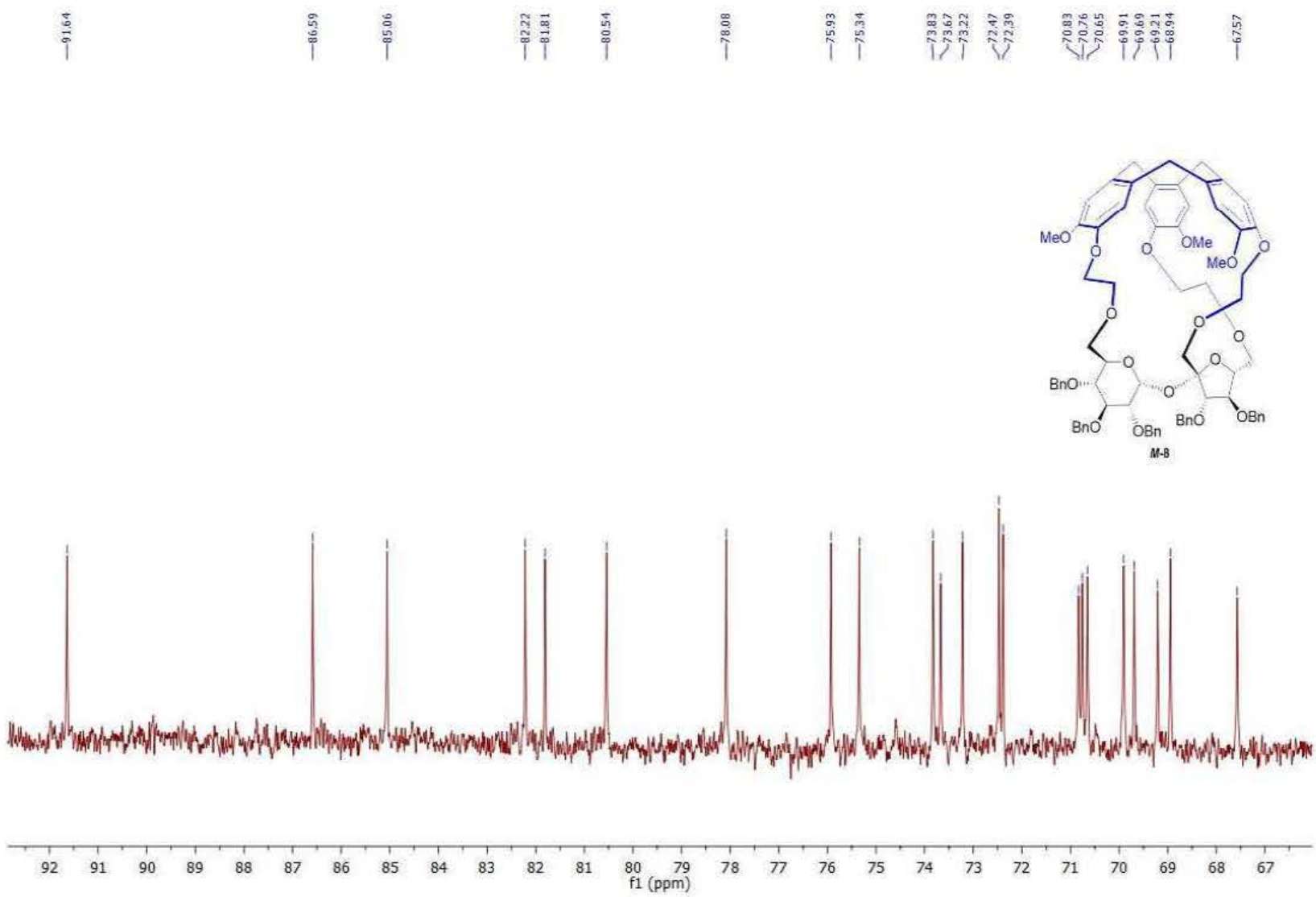

Figure S49. ^{13}C NMR spectrum of compound ***M*-8** (aliphatic part).

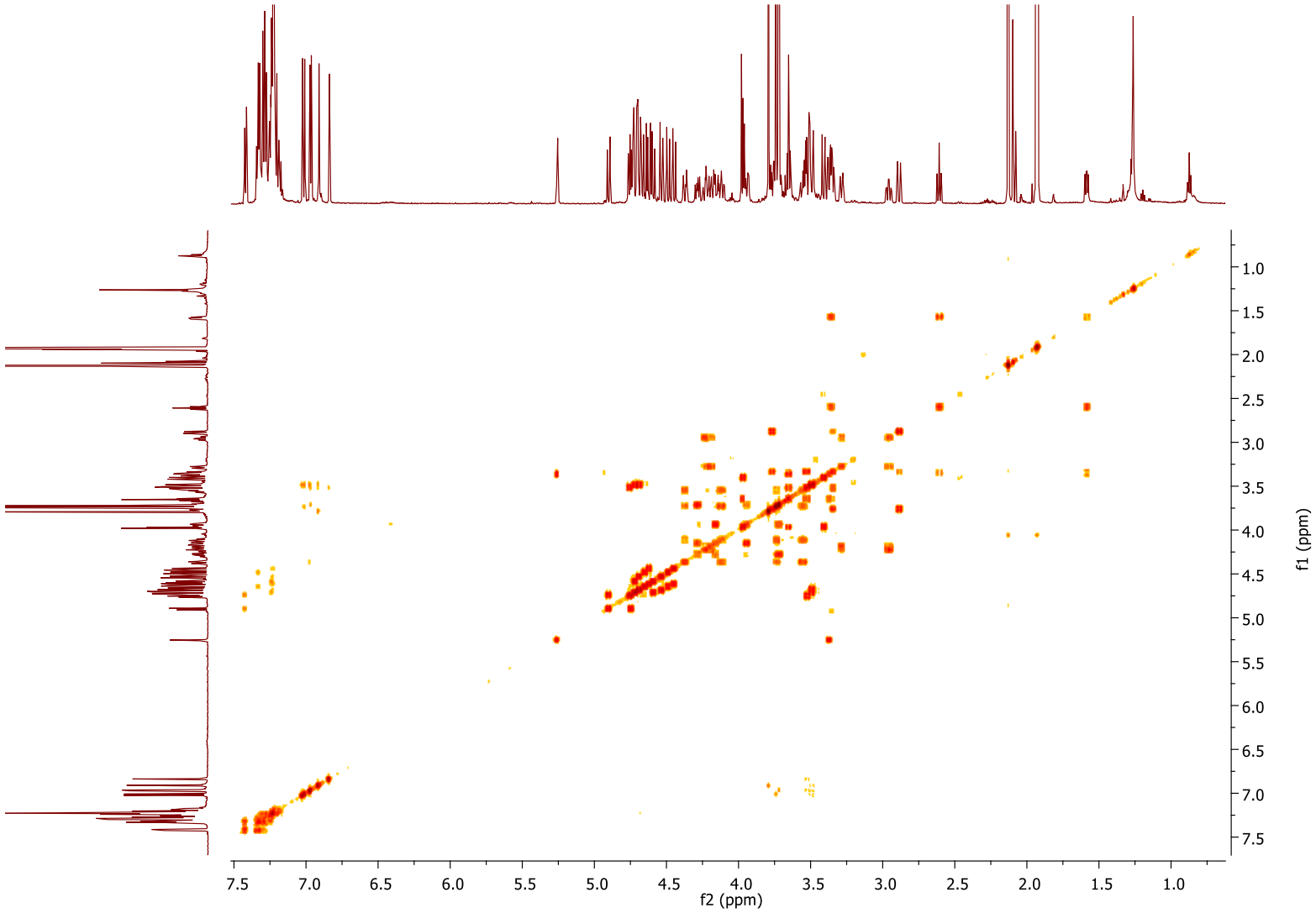

Figure S50. ^{1}H–^{1}H COSY spectrum of compound ***M*-8**.

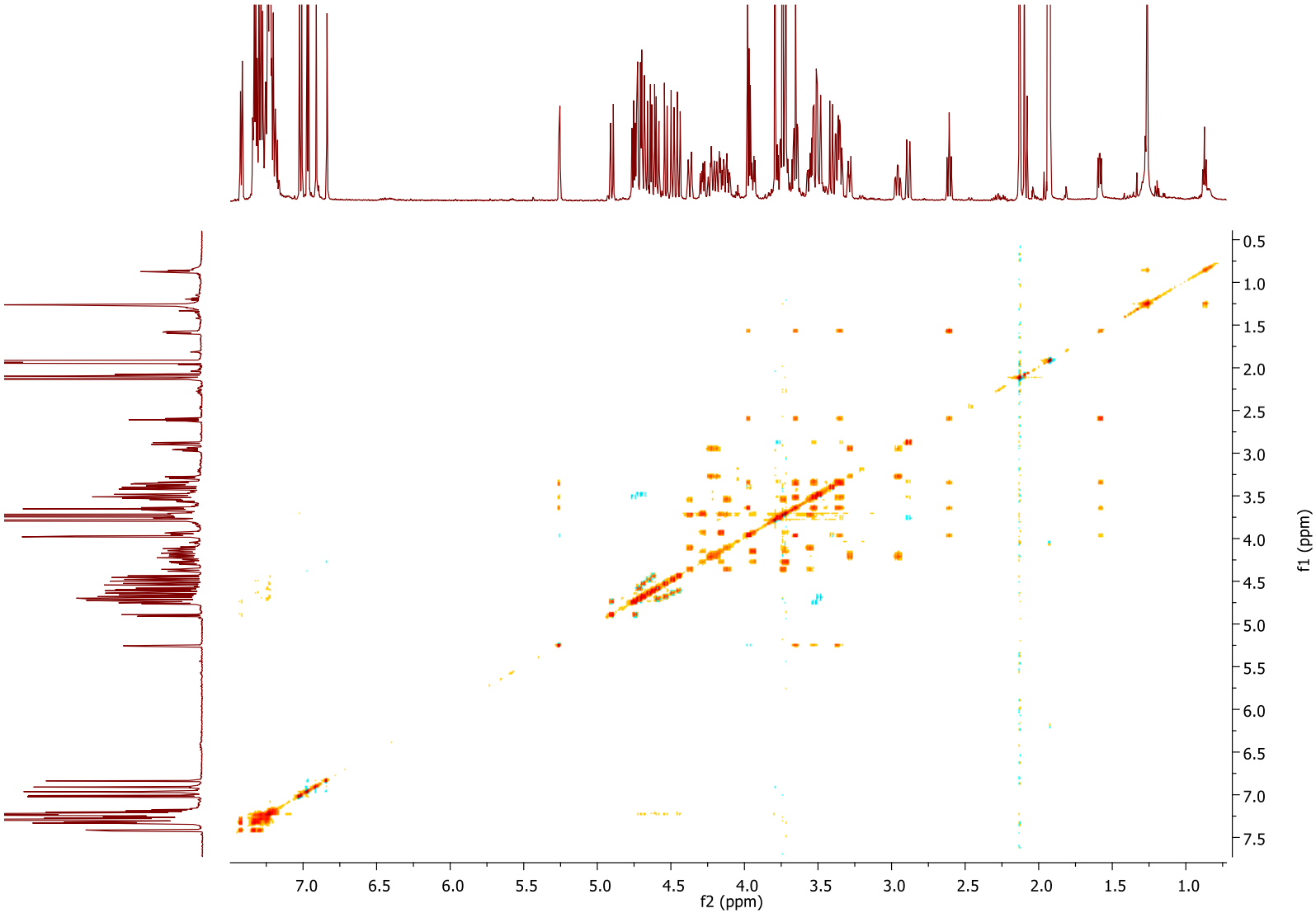

Figure S51. ^{1}H–^{1}H TOCSY spectrum of compound ***M*-8**.

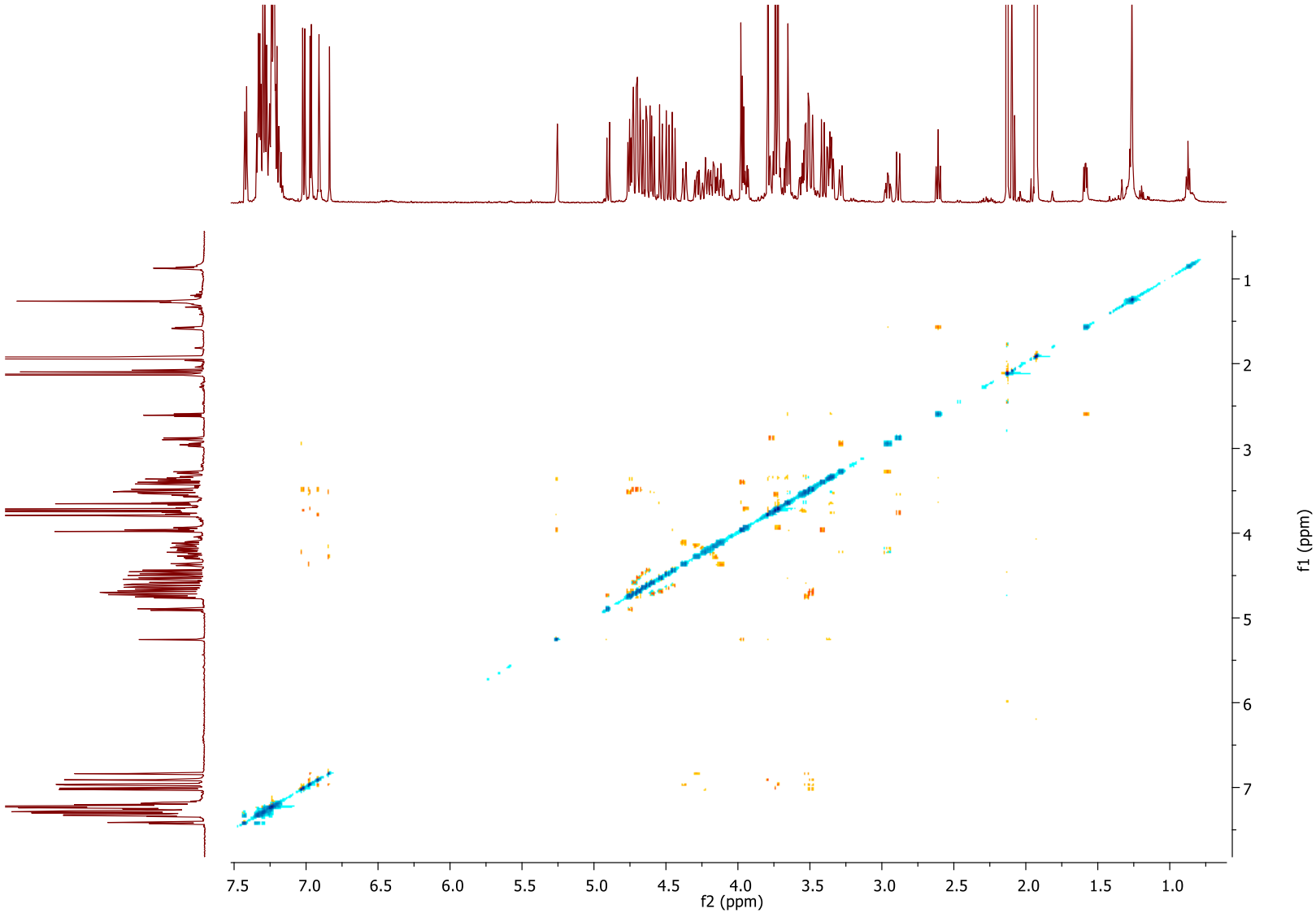

Figure S52. ^{1}H–^{1}H ROESY spectrum of compound ***M*-8**.

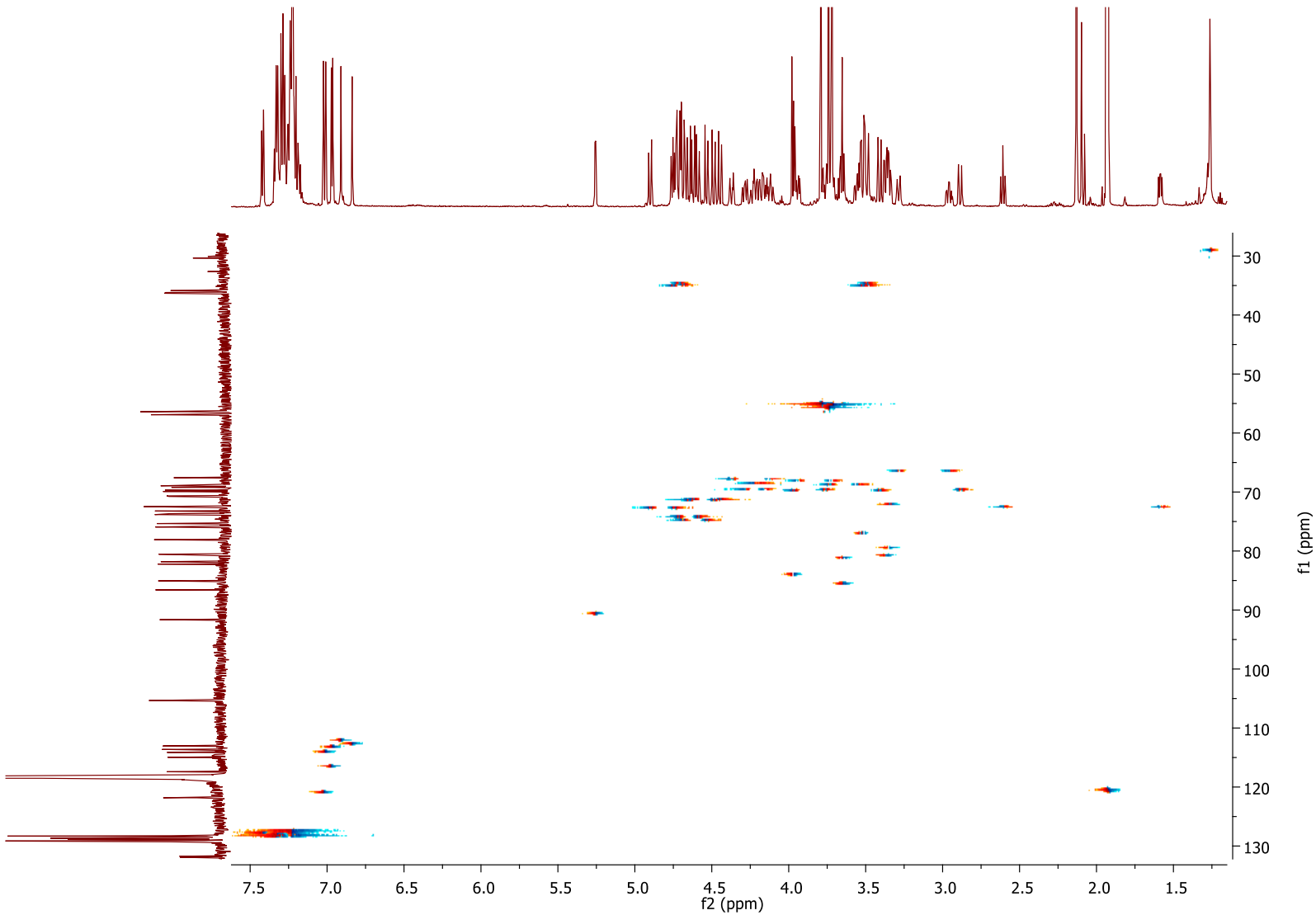

Figure S53. ^{1}H–^{13}C HSQC spectrum of compound ***M*-8**.

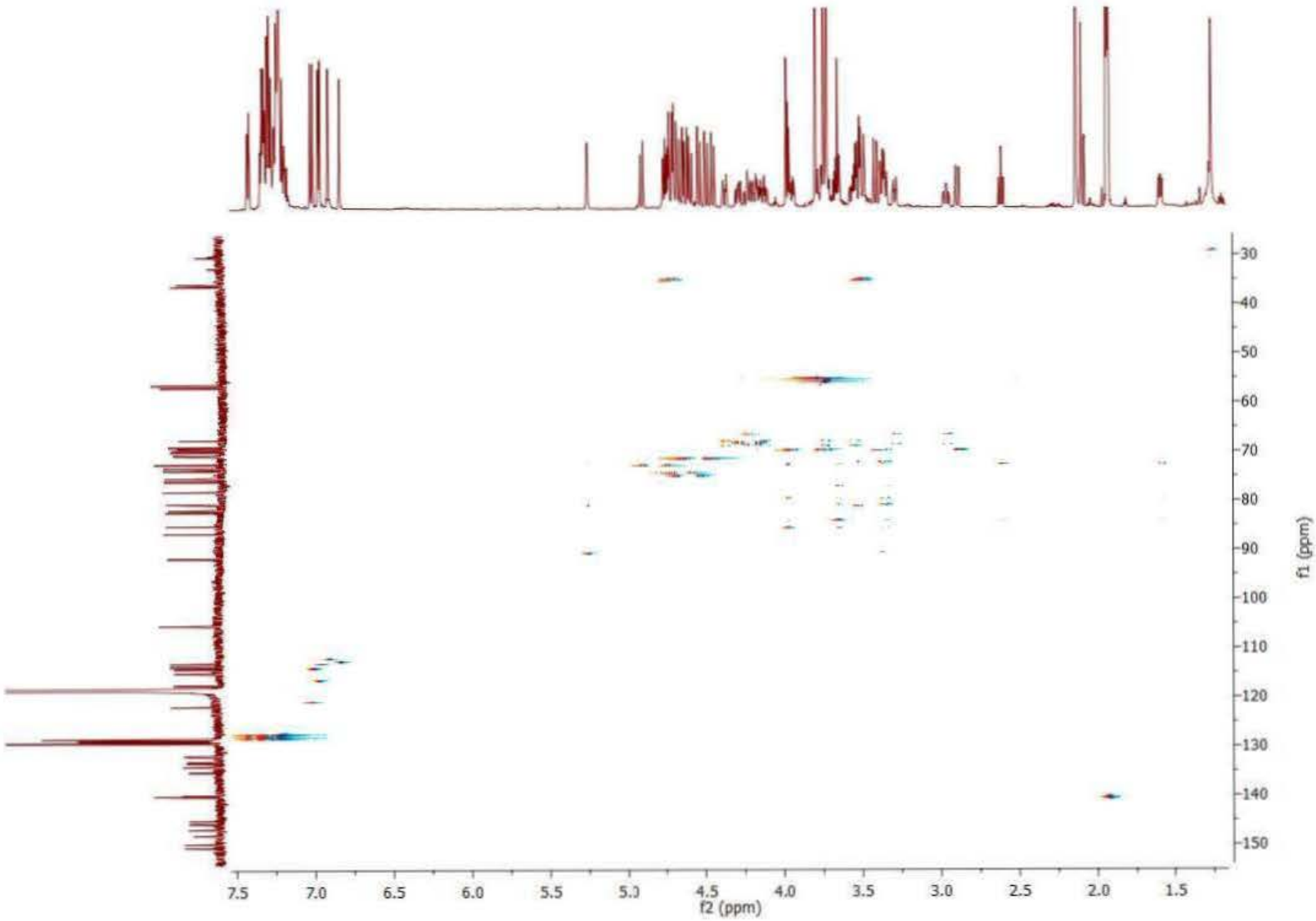

Figure S54. ^{1}H–^{13}C HSQCTOCSY spectrum of compound ***M*-8**.

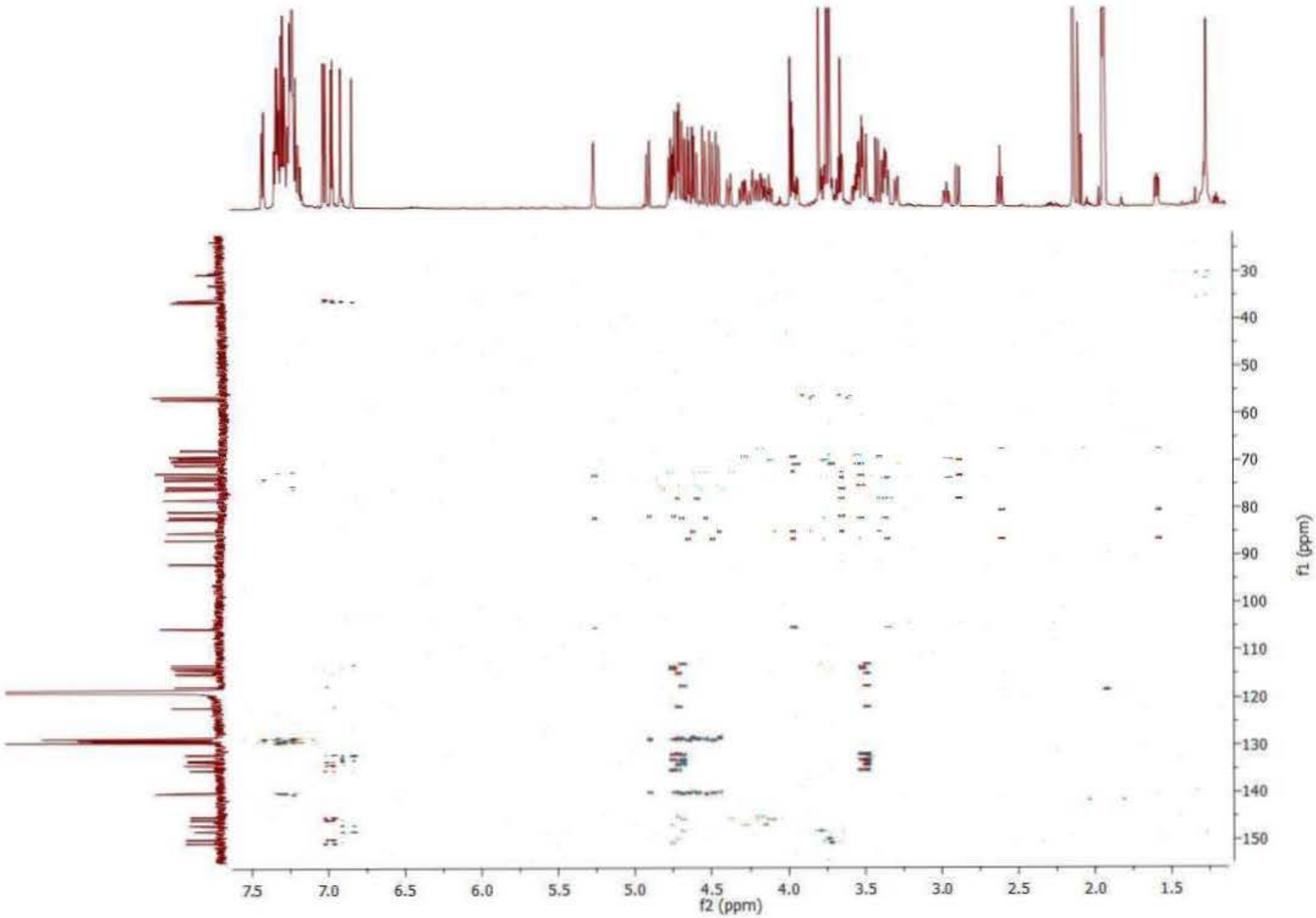

Figure S55. $^{1}H–^{13}C$ HMBC spectrum of compound ***M*-8**.

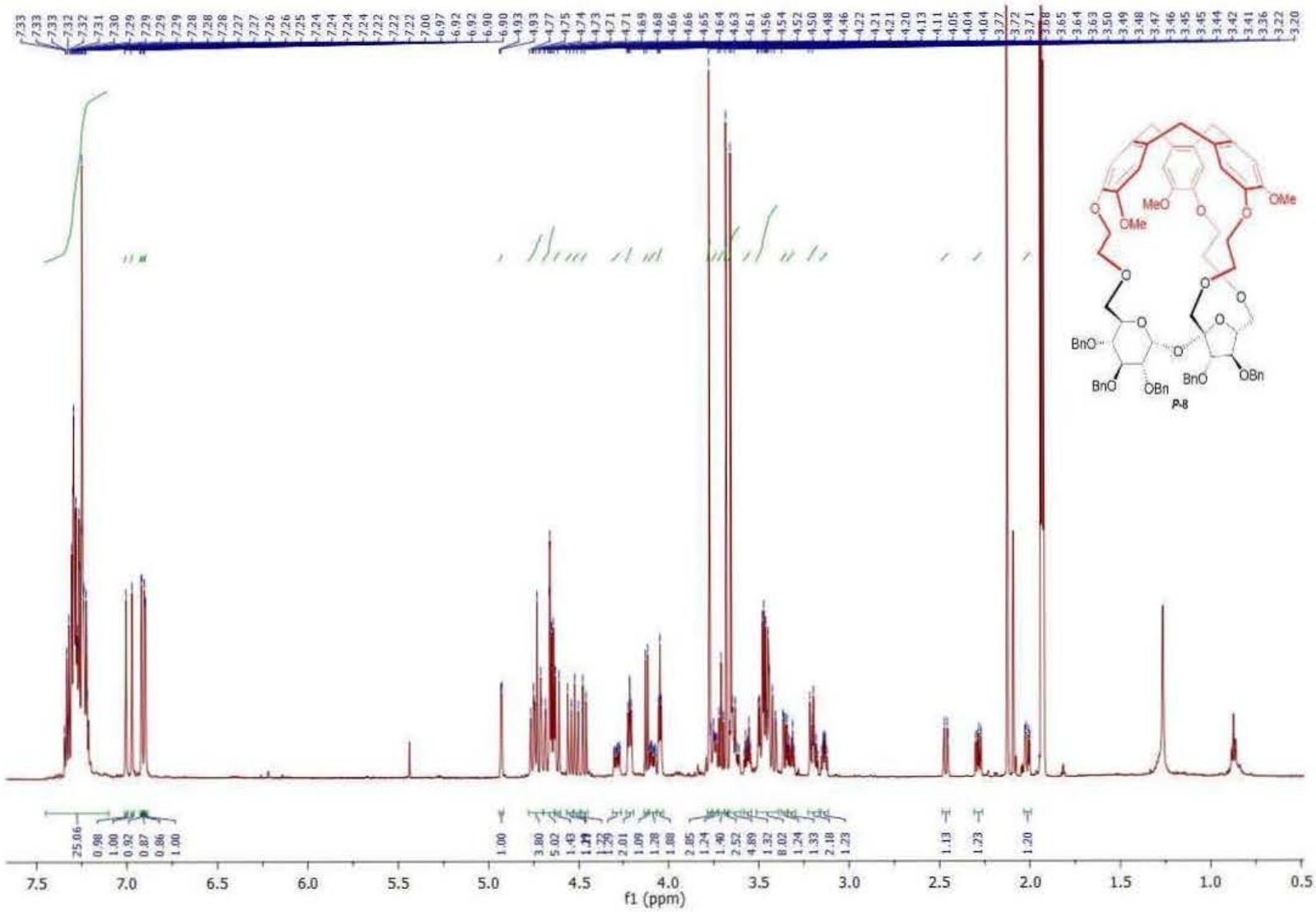

Figure S56. ^{1}H NMR spectrum of compound ***P*-8.**

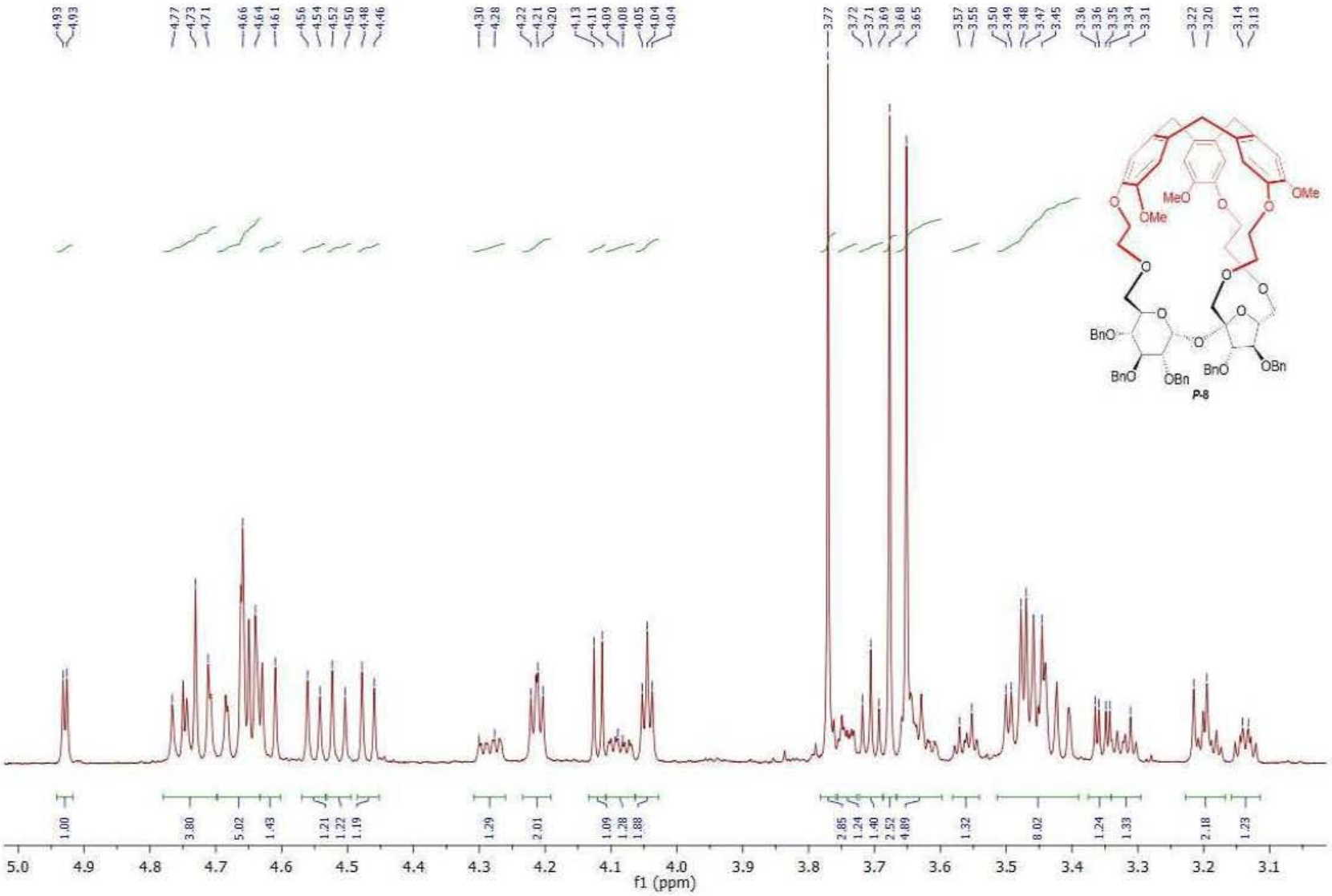

Figure S57. ^{1}H NMR spectrum of compound ***P*-8** (aliphatic part).

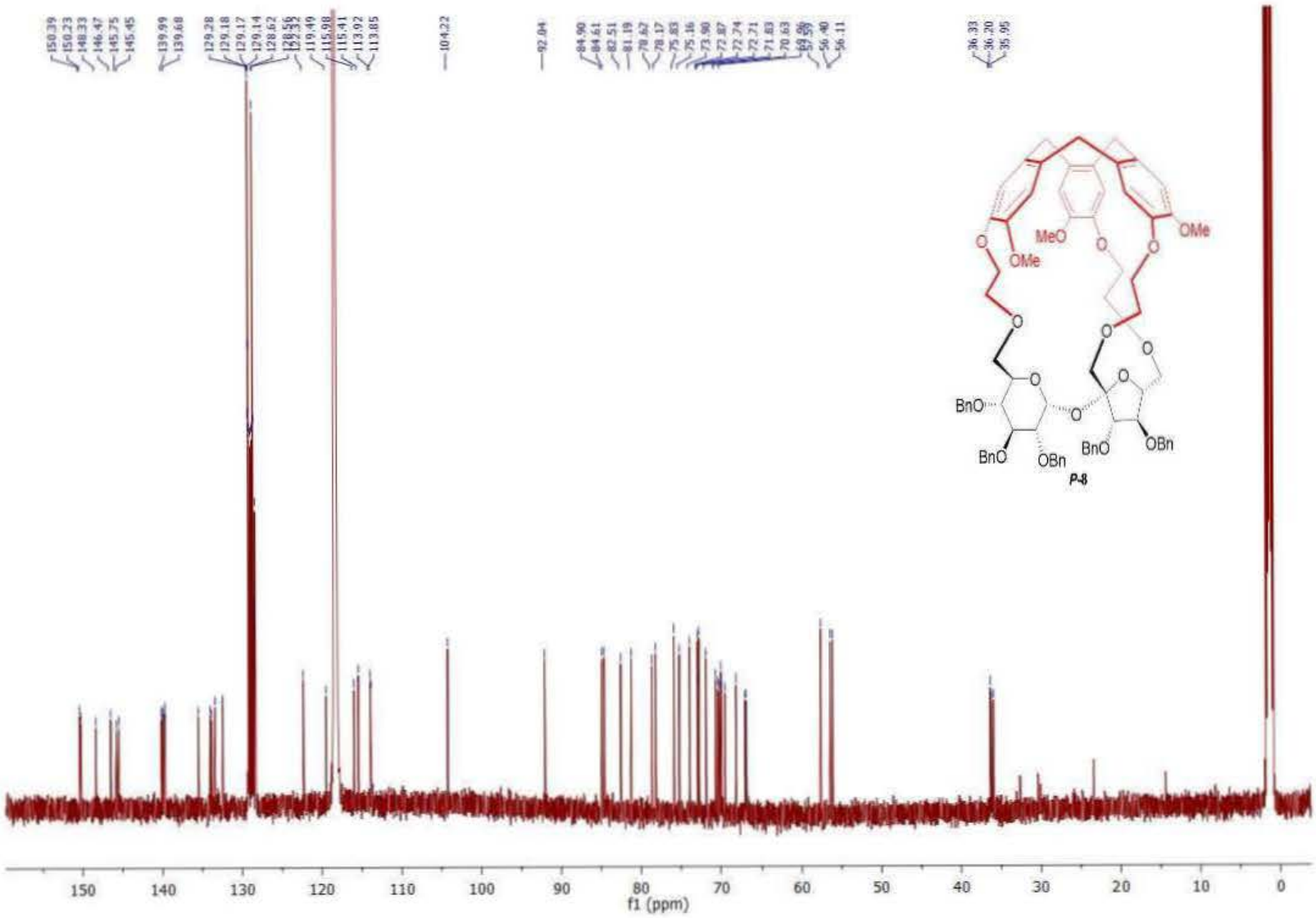

Figure S58. ^{13}C NMR spectrum of compound ***P*-8**.

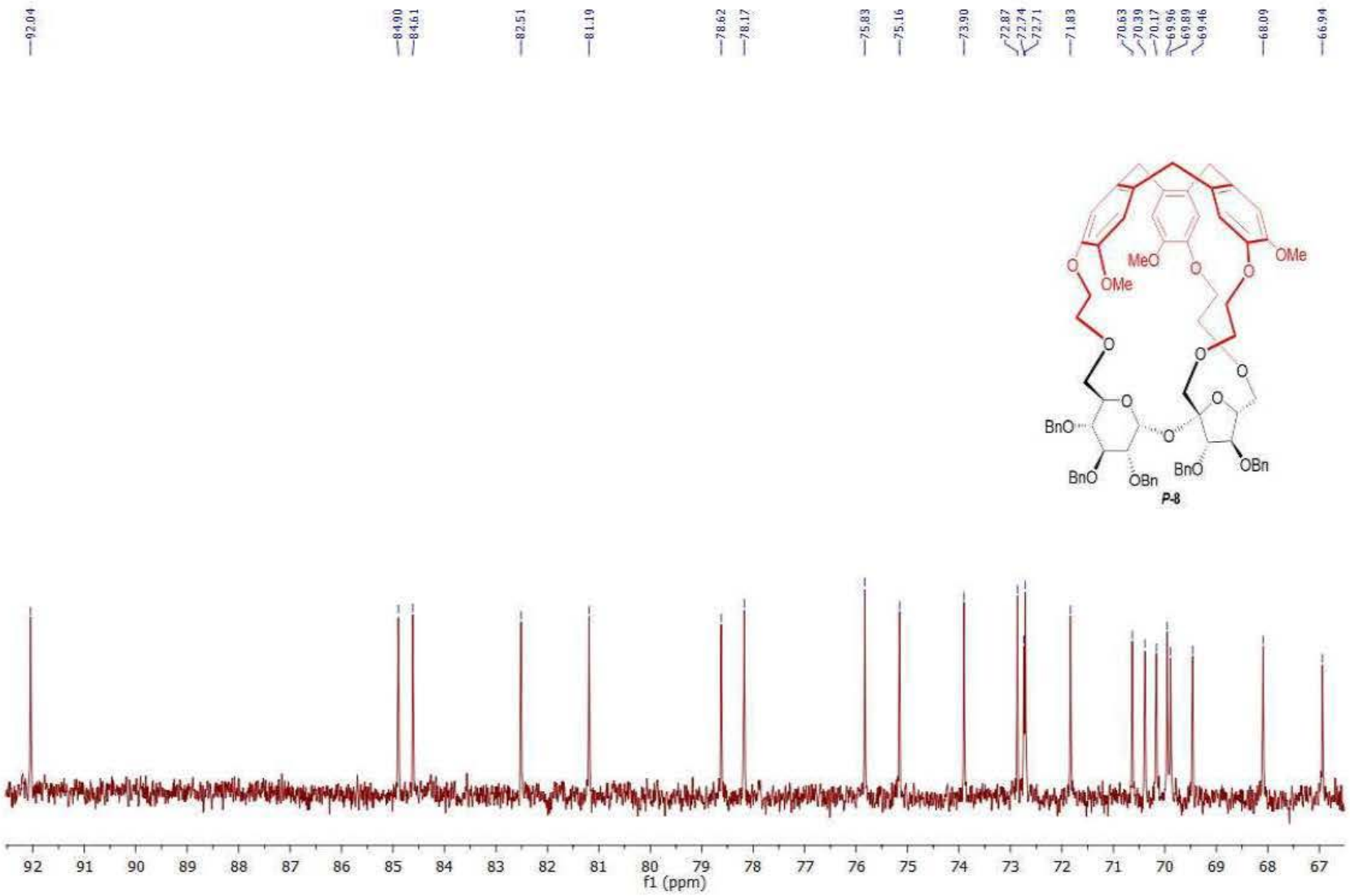

Figure S59. ^{13}C NMR spectrum of compound ***P*-8** (aliphatic part).

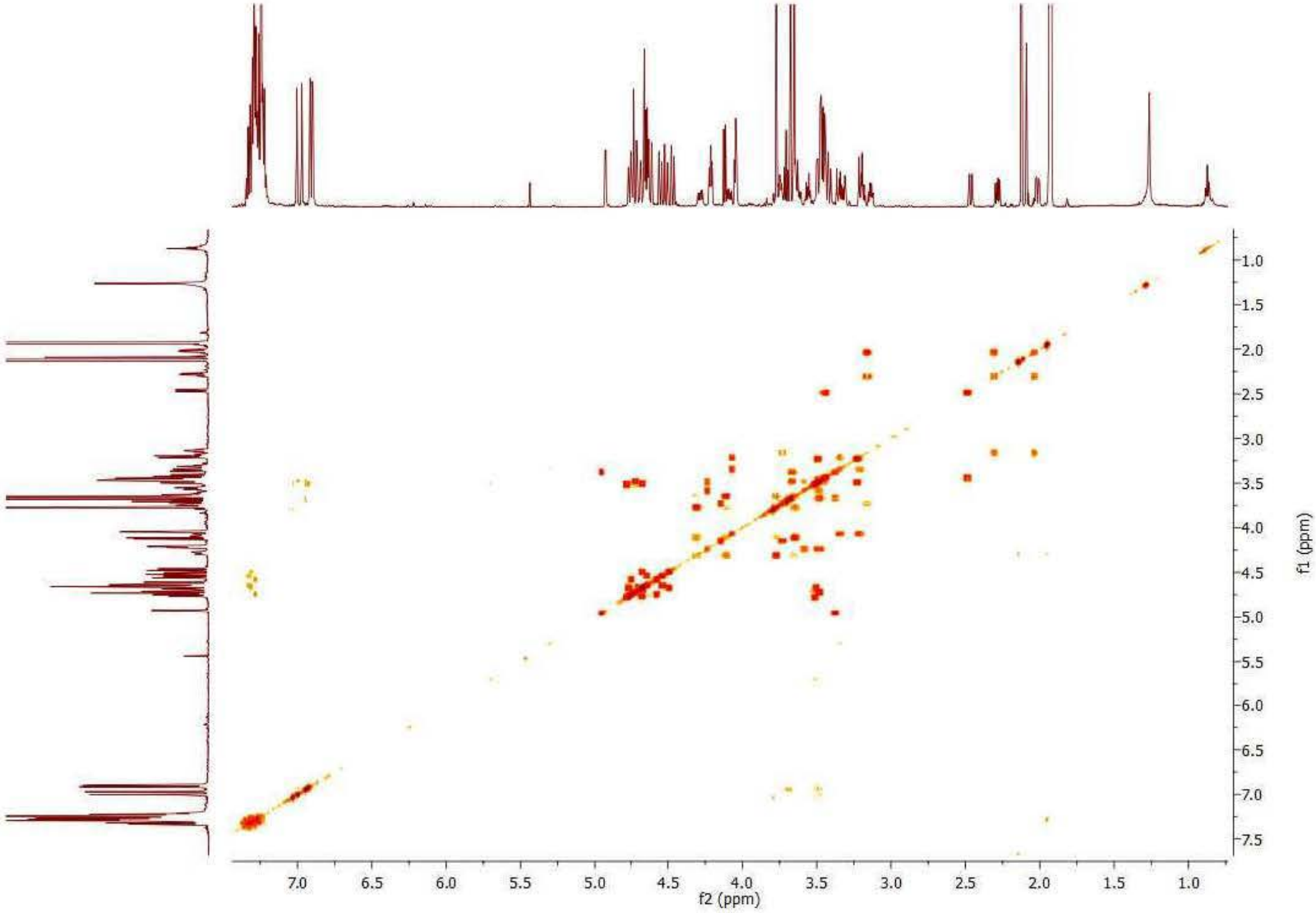

Figure S60. $^{1}H–^{1}H$ COSY spectrum of compound ***P*-8**.

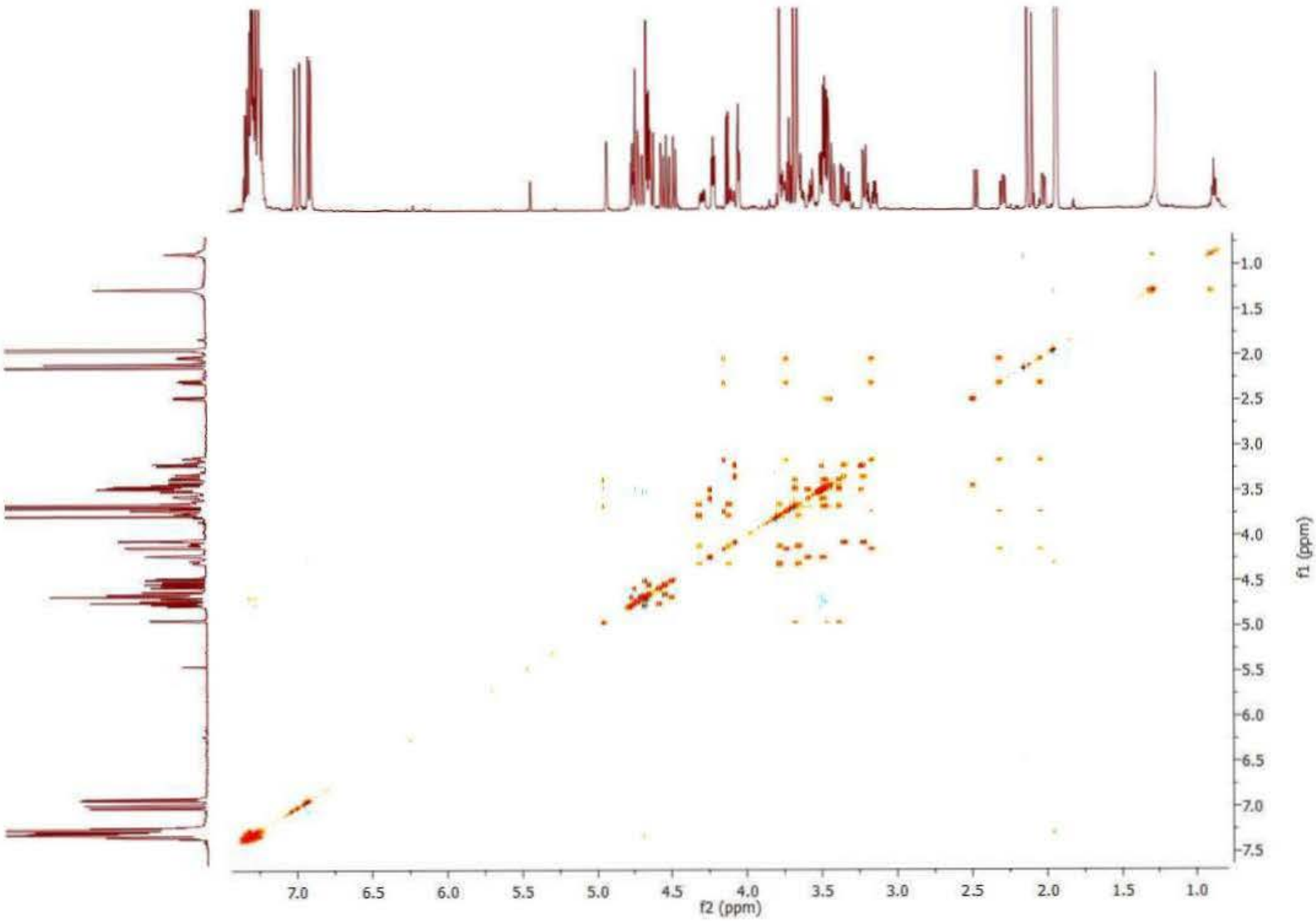

Figure S61. ^{1}H–^{1}H TOCSY spectrum of compound ***P*-8**.

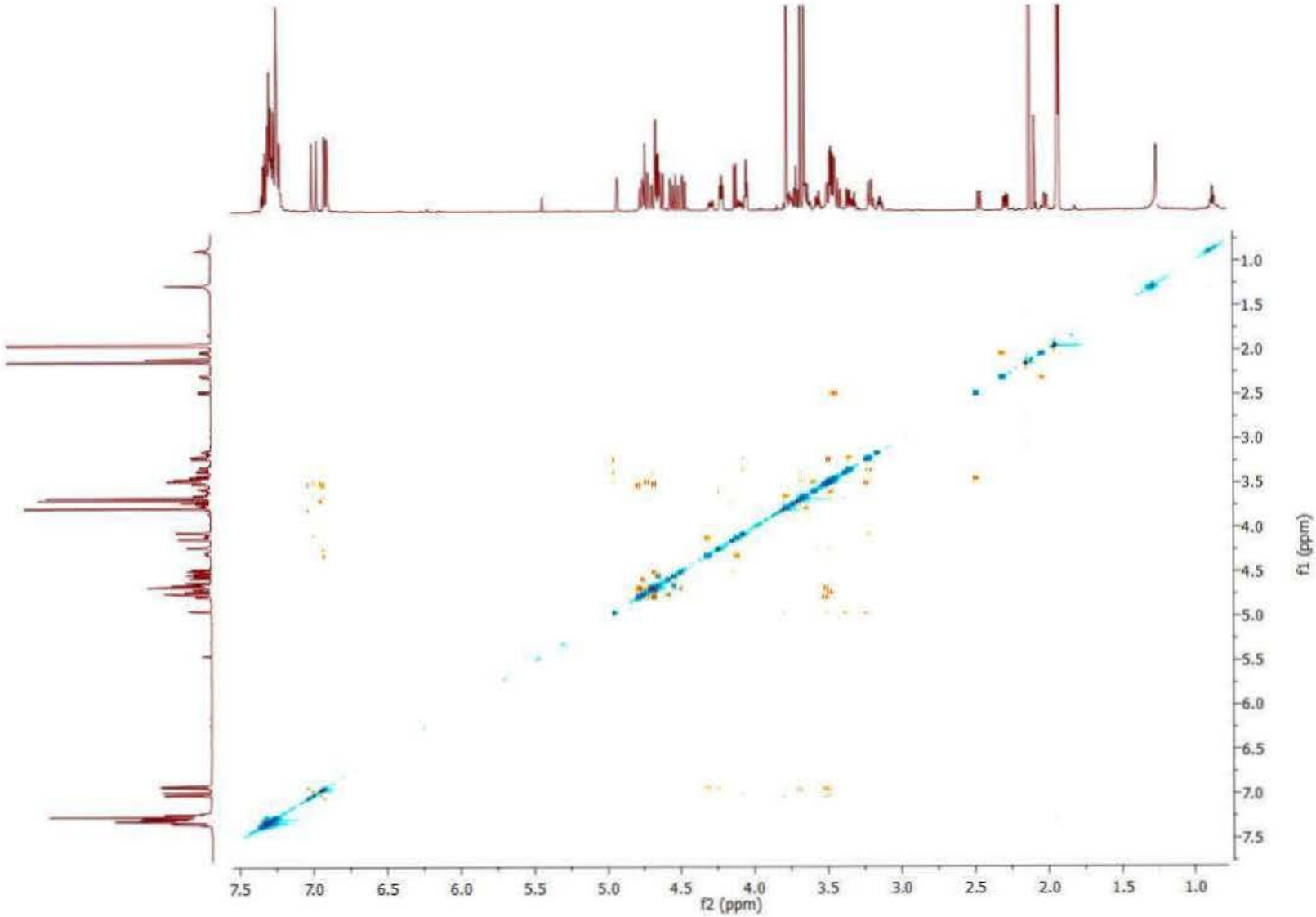

Figure S62. ^{1}H–^{1}H ROESY spectrum of compound ***P*-8**.

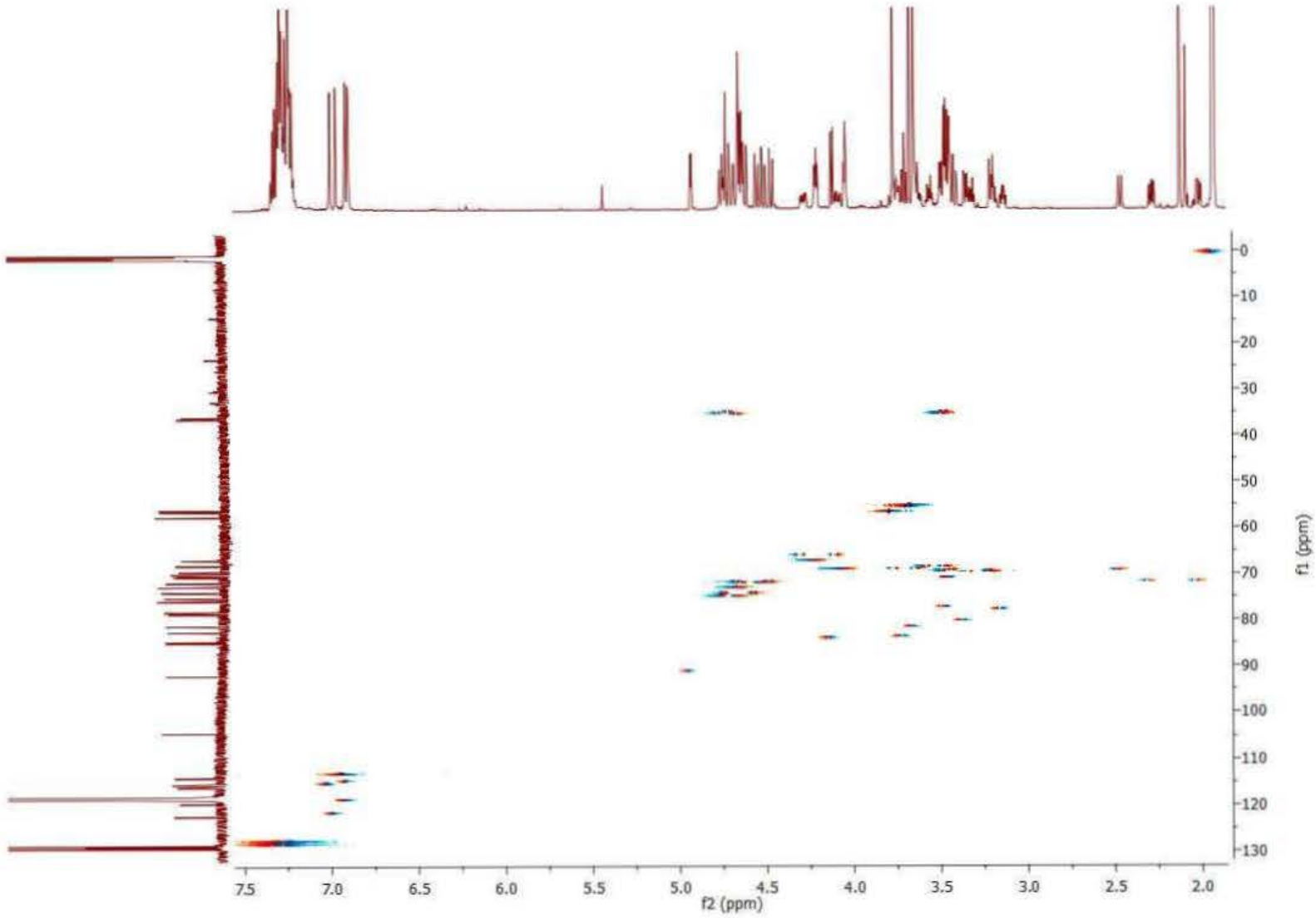

Figure S63. ^{1}H–^{13}C HSQC spectrum of compound ***P*-8**.

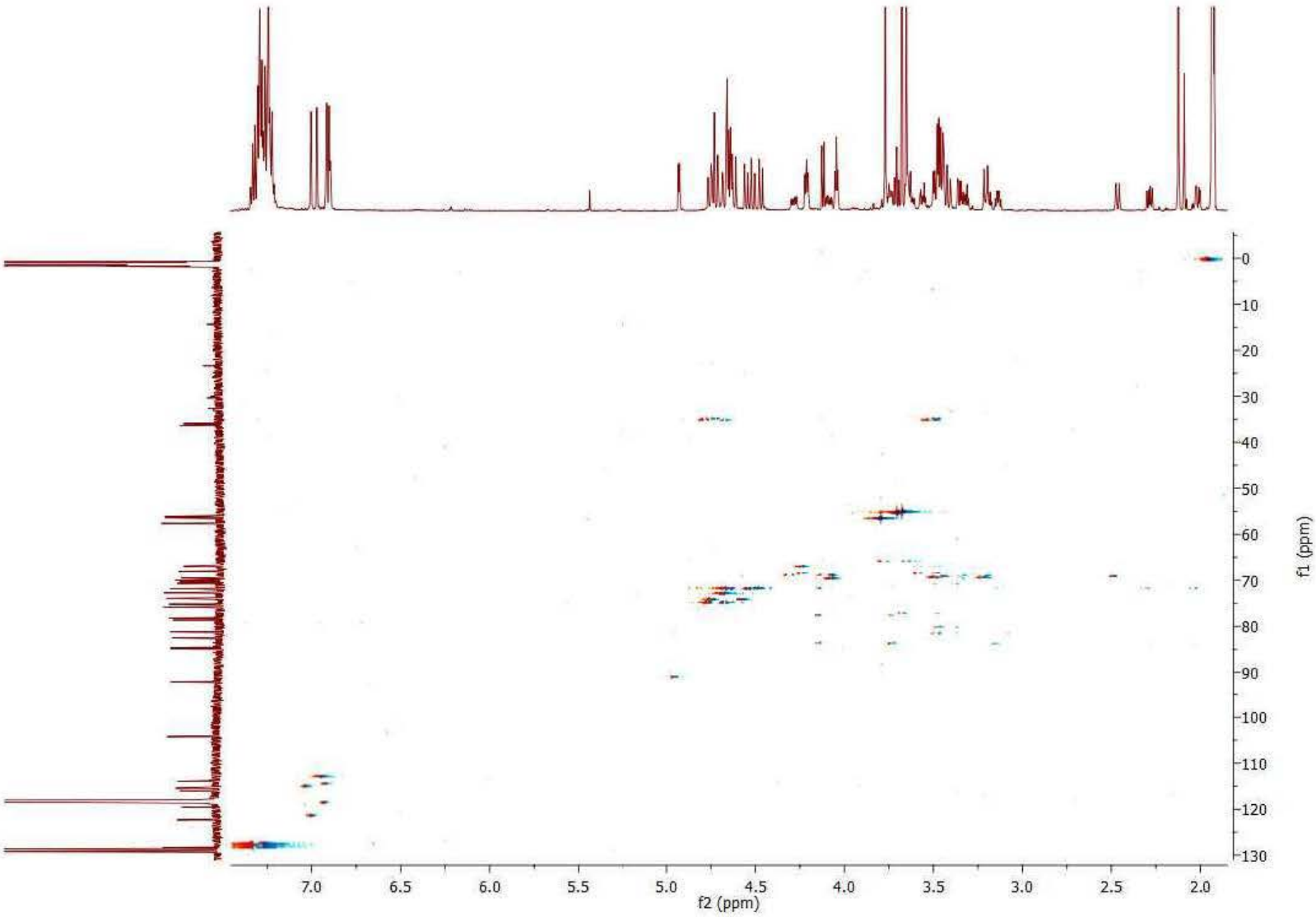

Figure S64. $^{1}H–^{13}C$ HSQC TOCSY spectrum of compound ***P*-8**.

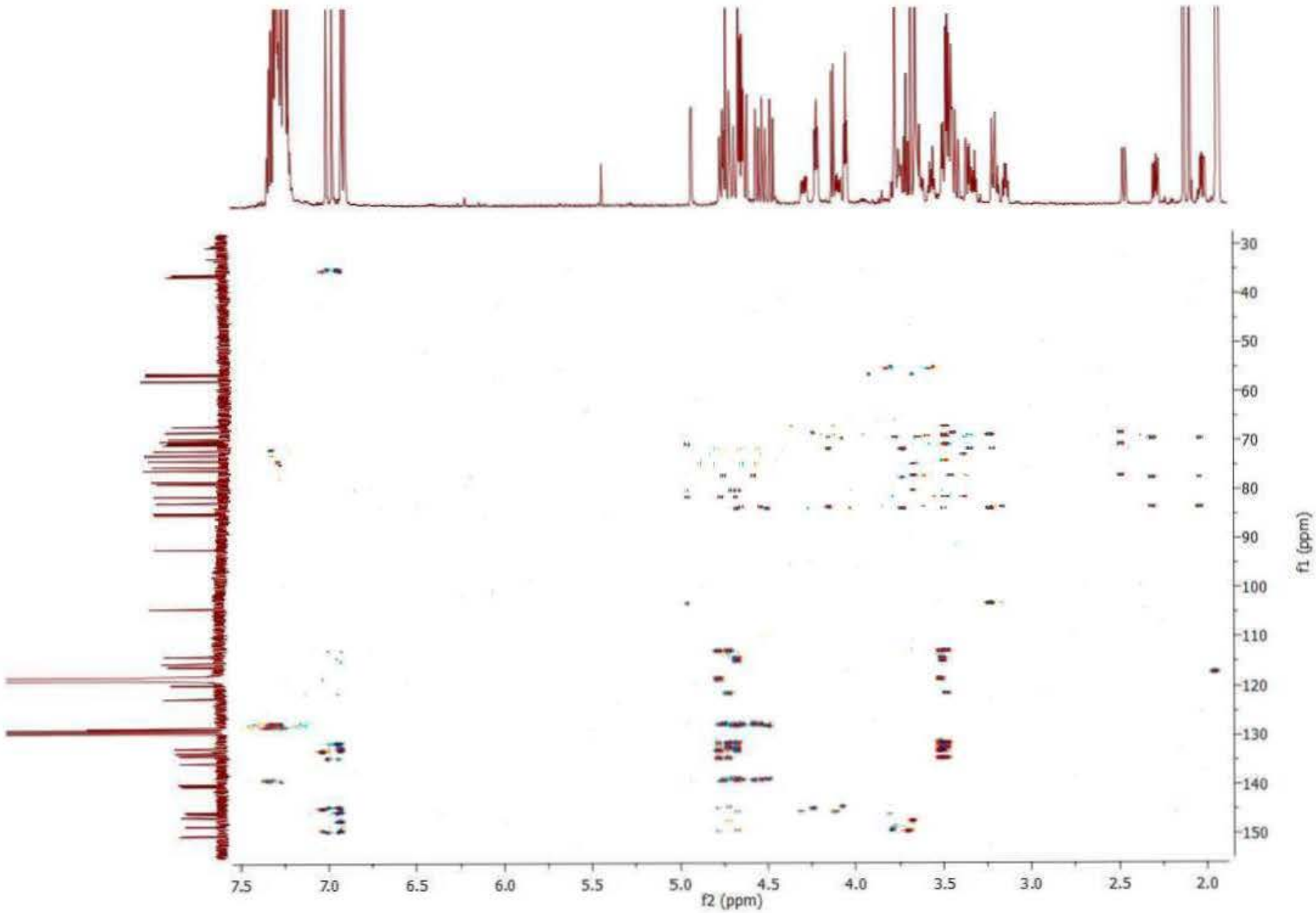

Figure S65. ^{1}H–^{13}C HMBC spectrum of compound ***P*-8**.

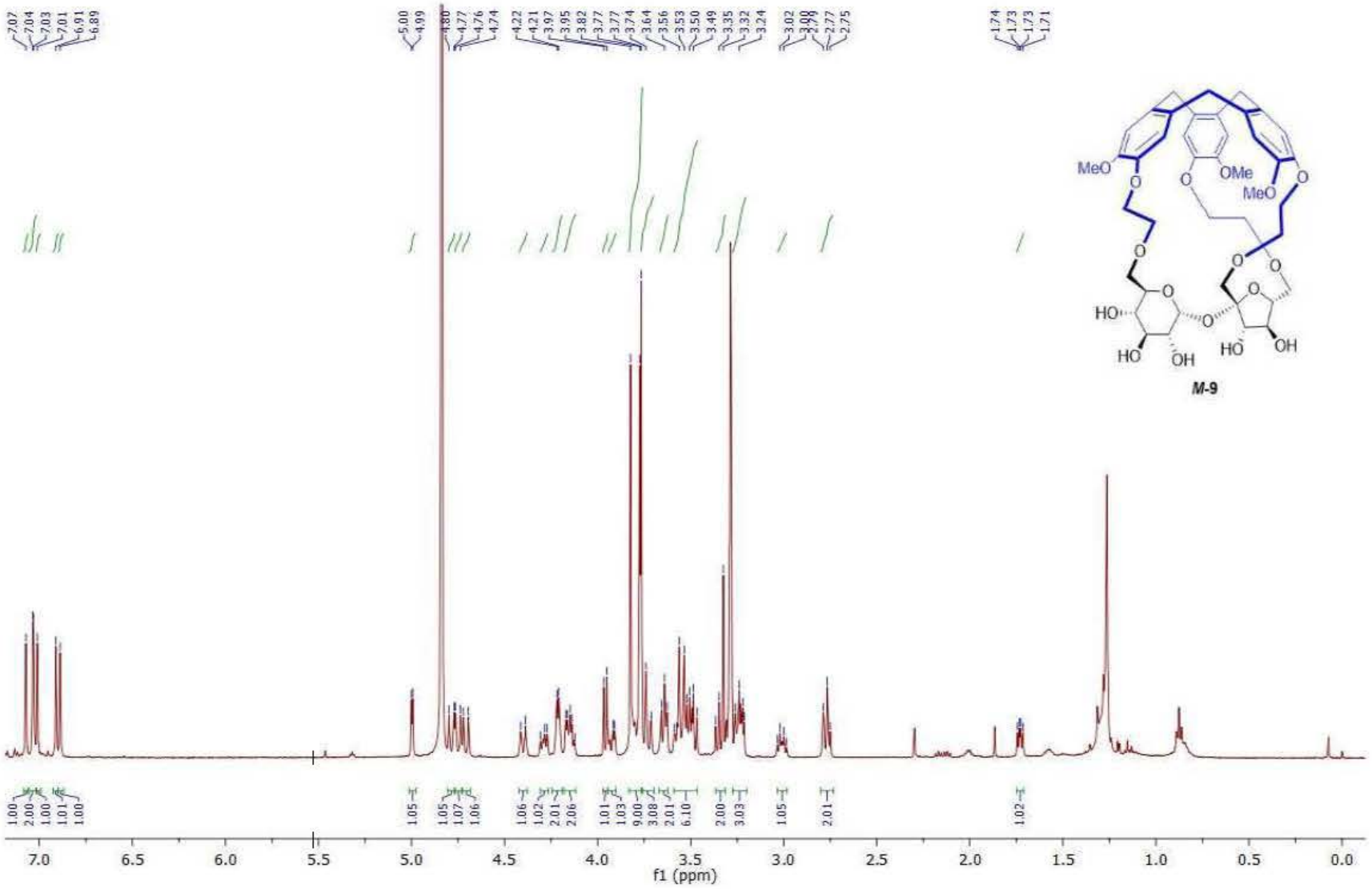

Figure S66. ^{1}H NMR spectrum of compound ***M*-9.**

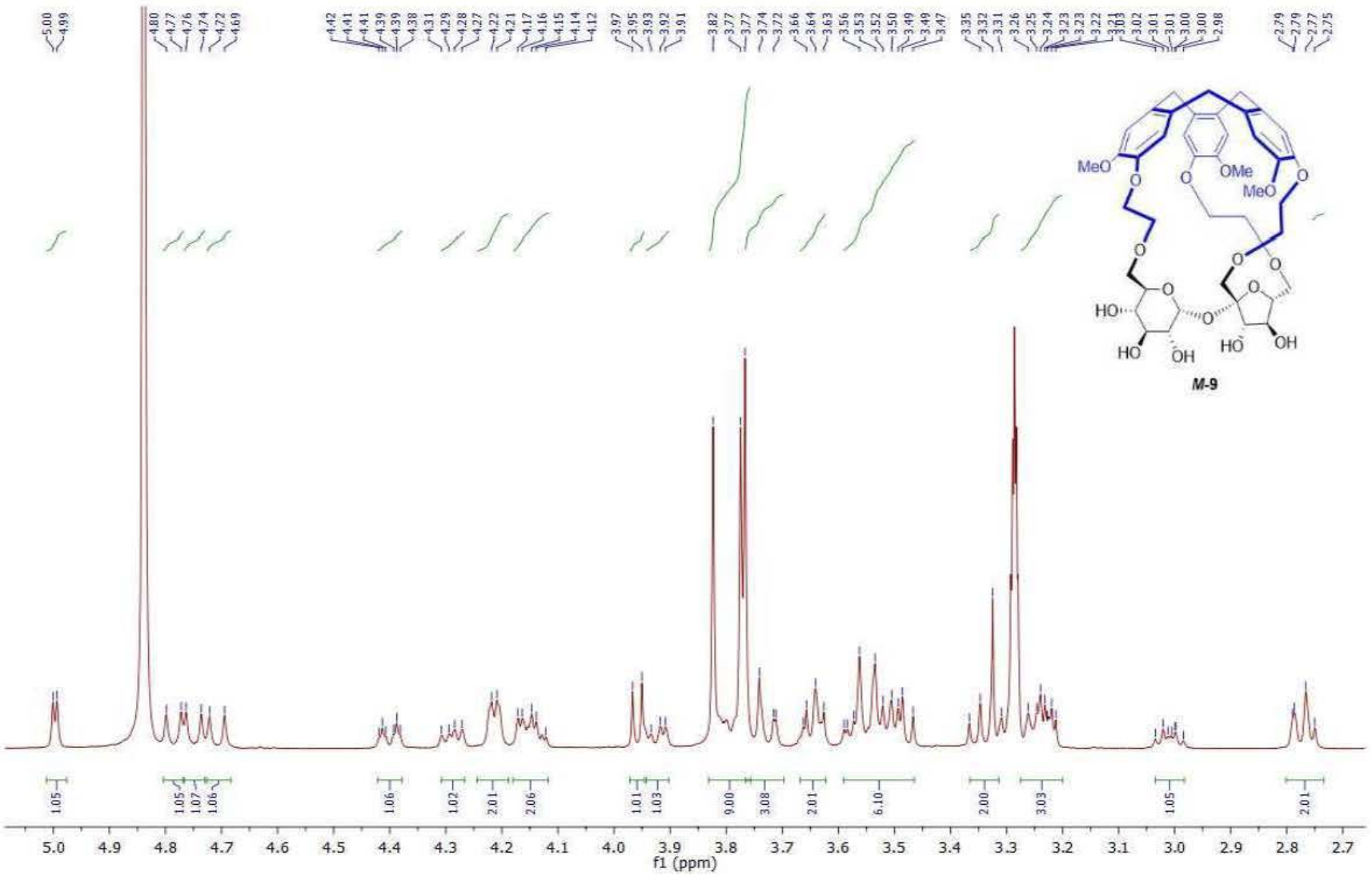

Figure S67. ^{1}H NMR spectrum of compound ***M*-9** (aliphatic part).

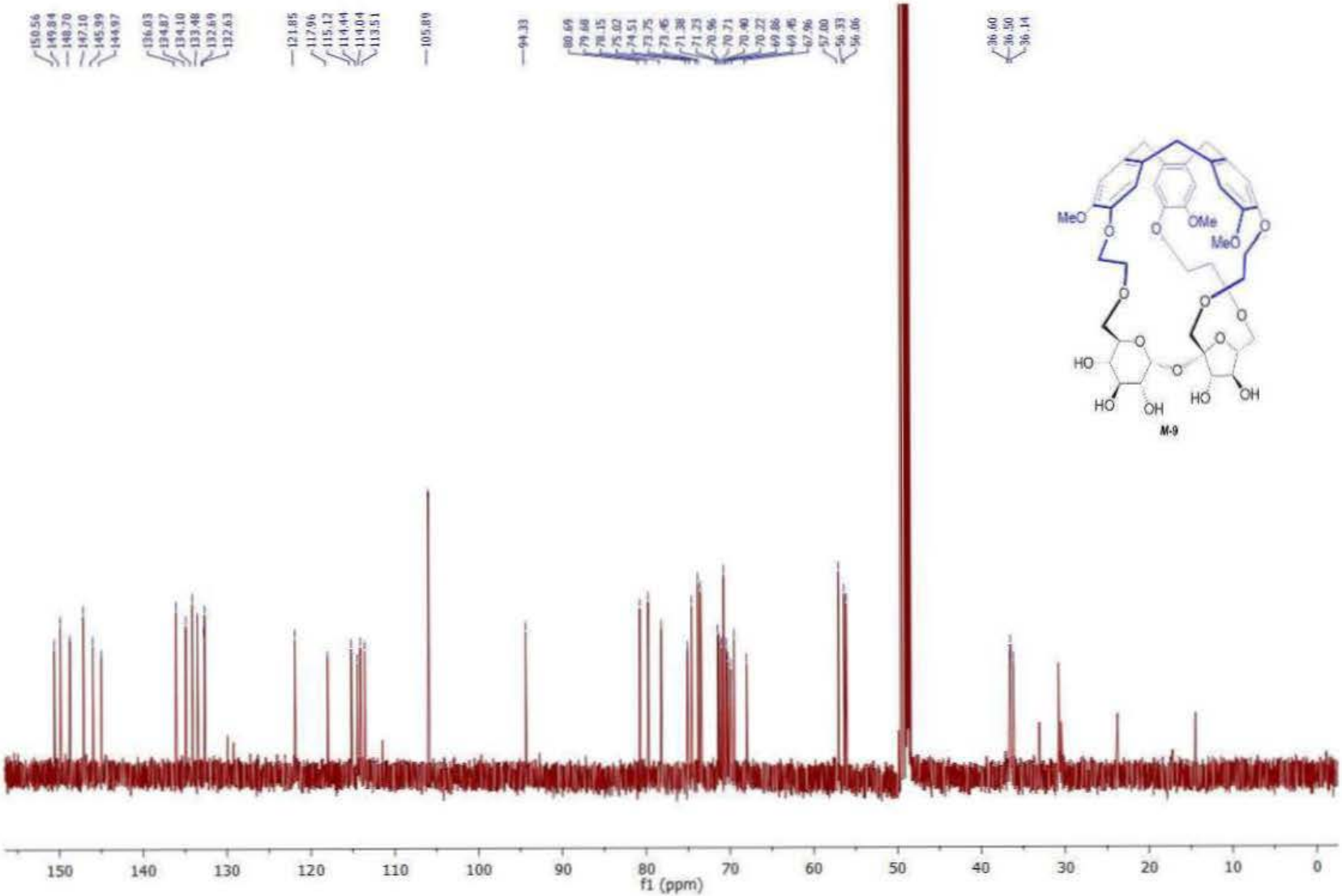

Figure S68. ^{13}C NMR spectrum of compound ***M*-9**.

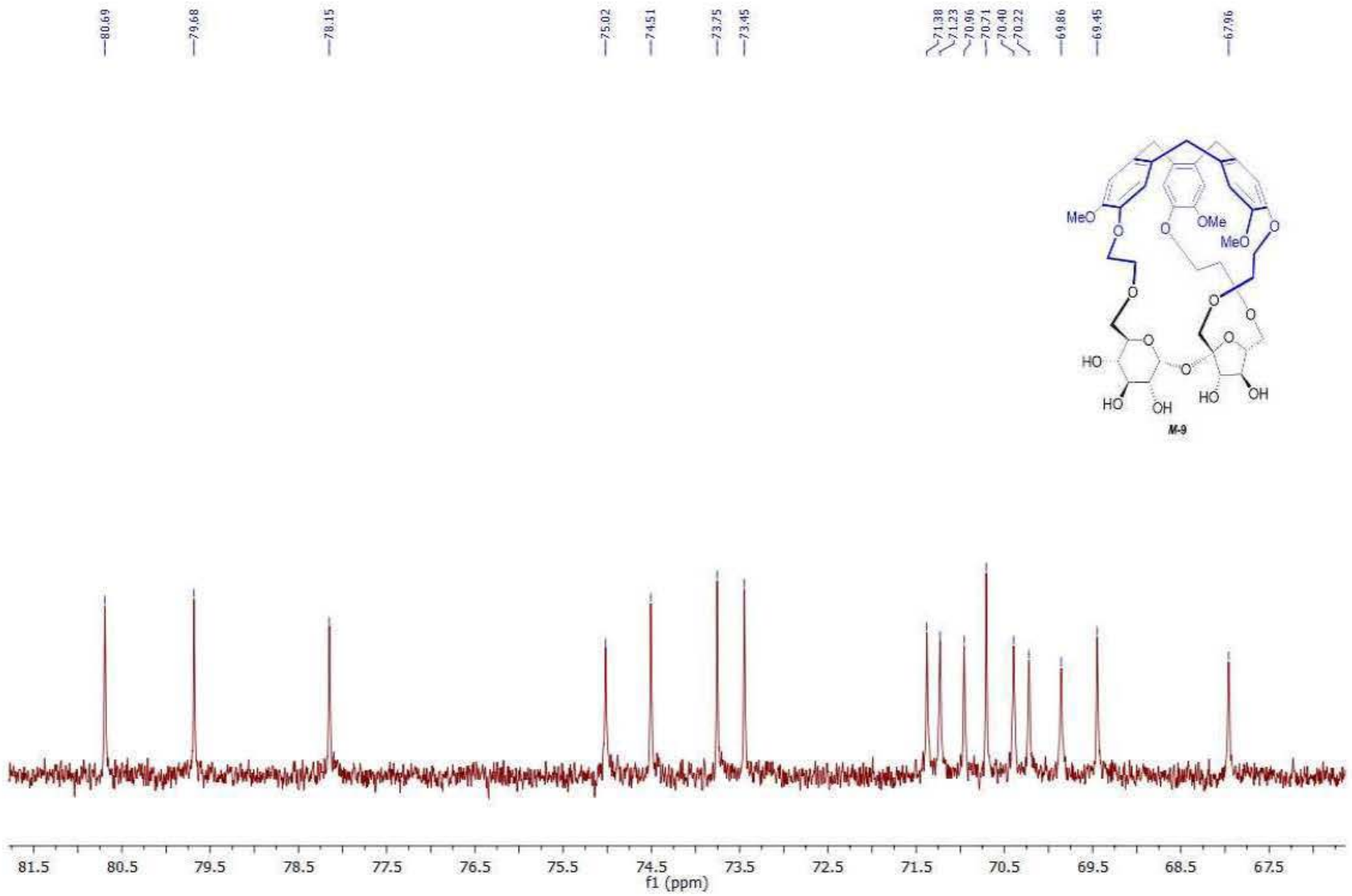

Figure S69. ^{13}C NMR spectrum of compound ***M*-9** (aliphatic part).

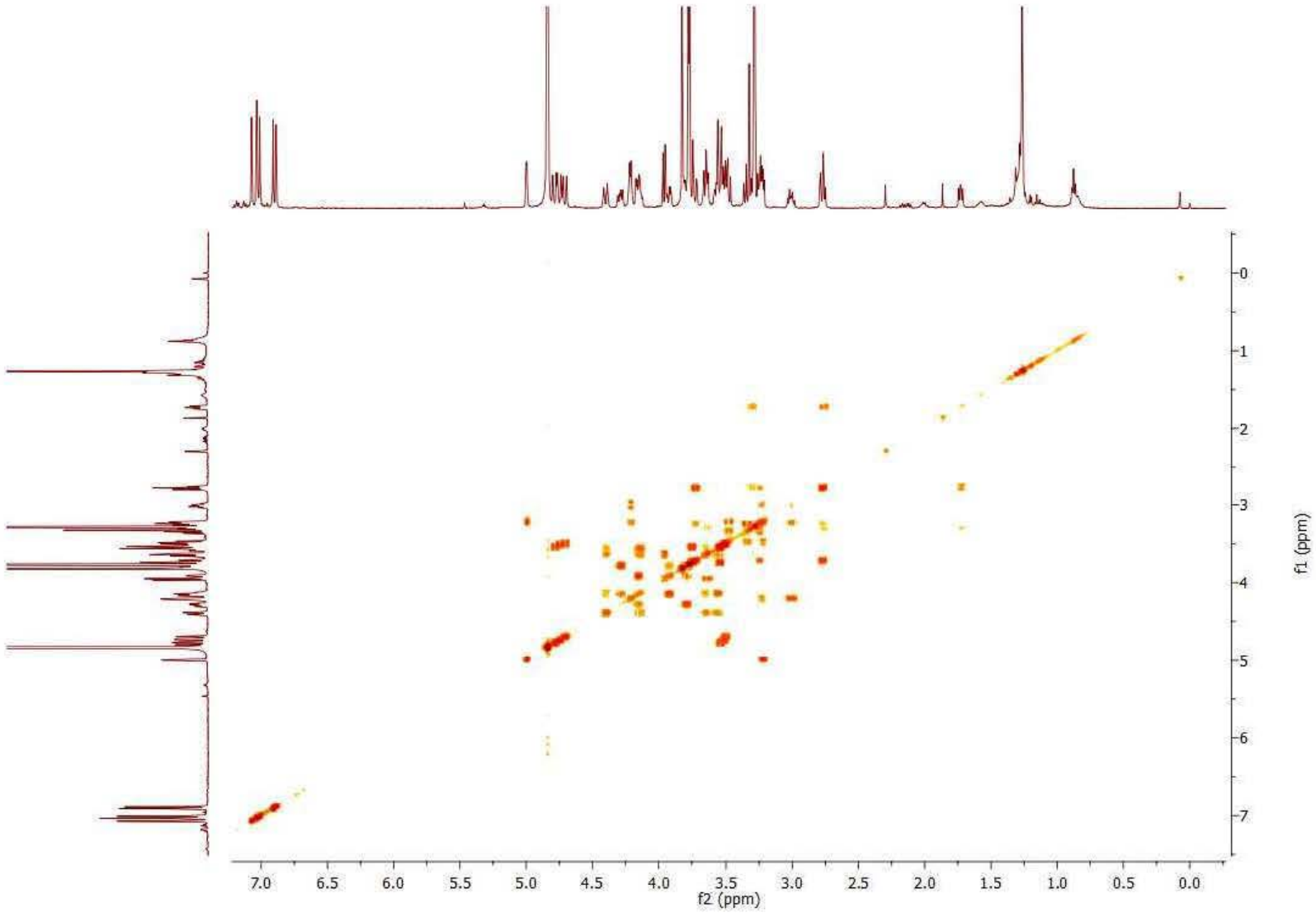

Figure S70. ^{1}H–^{1}H COSY spectrum of compound ***M*-9**.

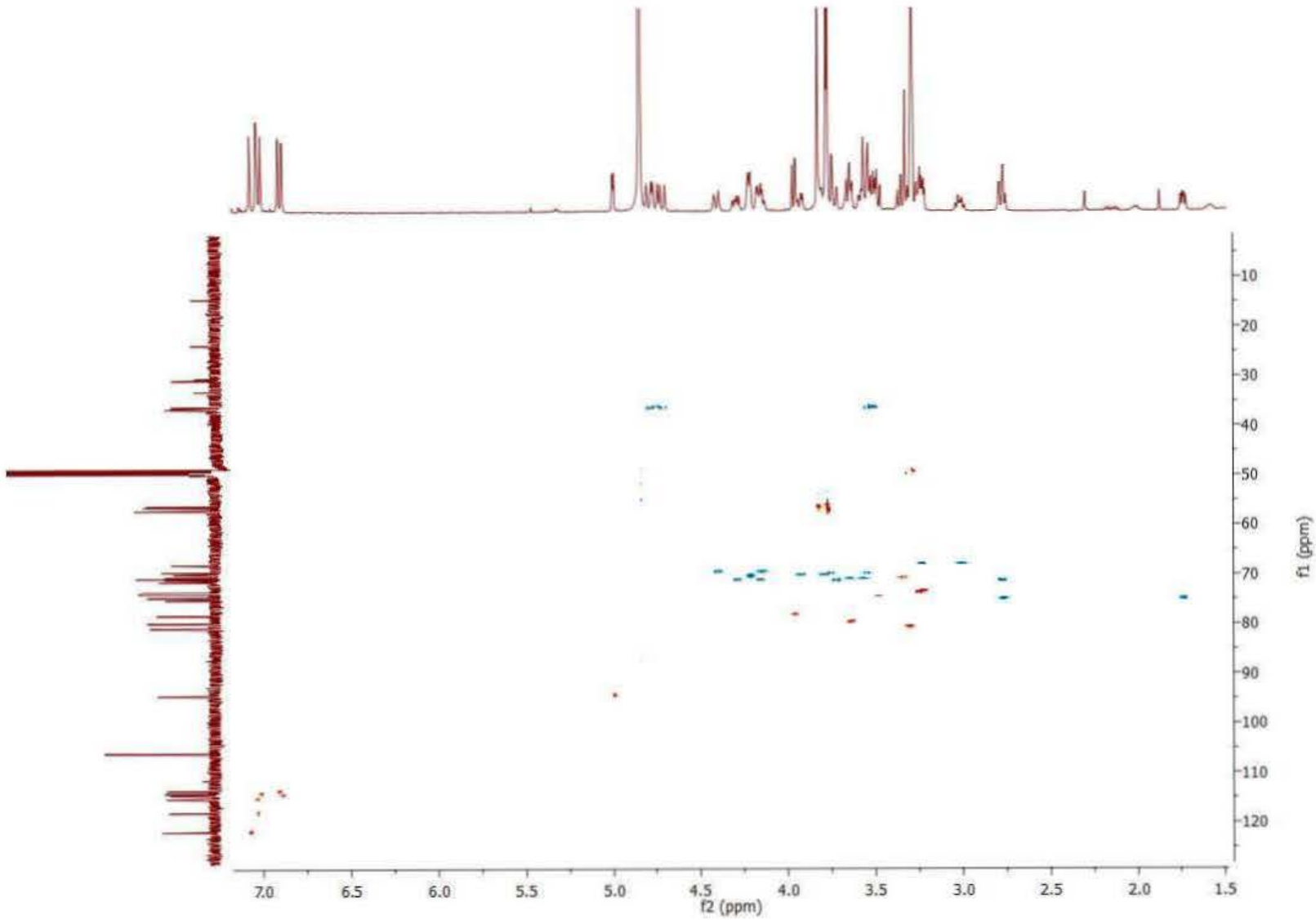

Figure S71. ^{1}H–^{13}C HSQC spectrum of compound ***M*-9**.

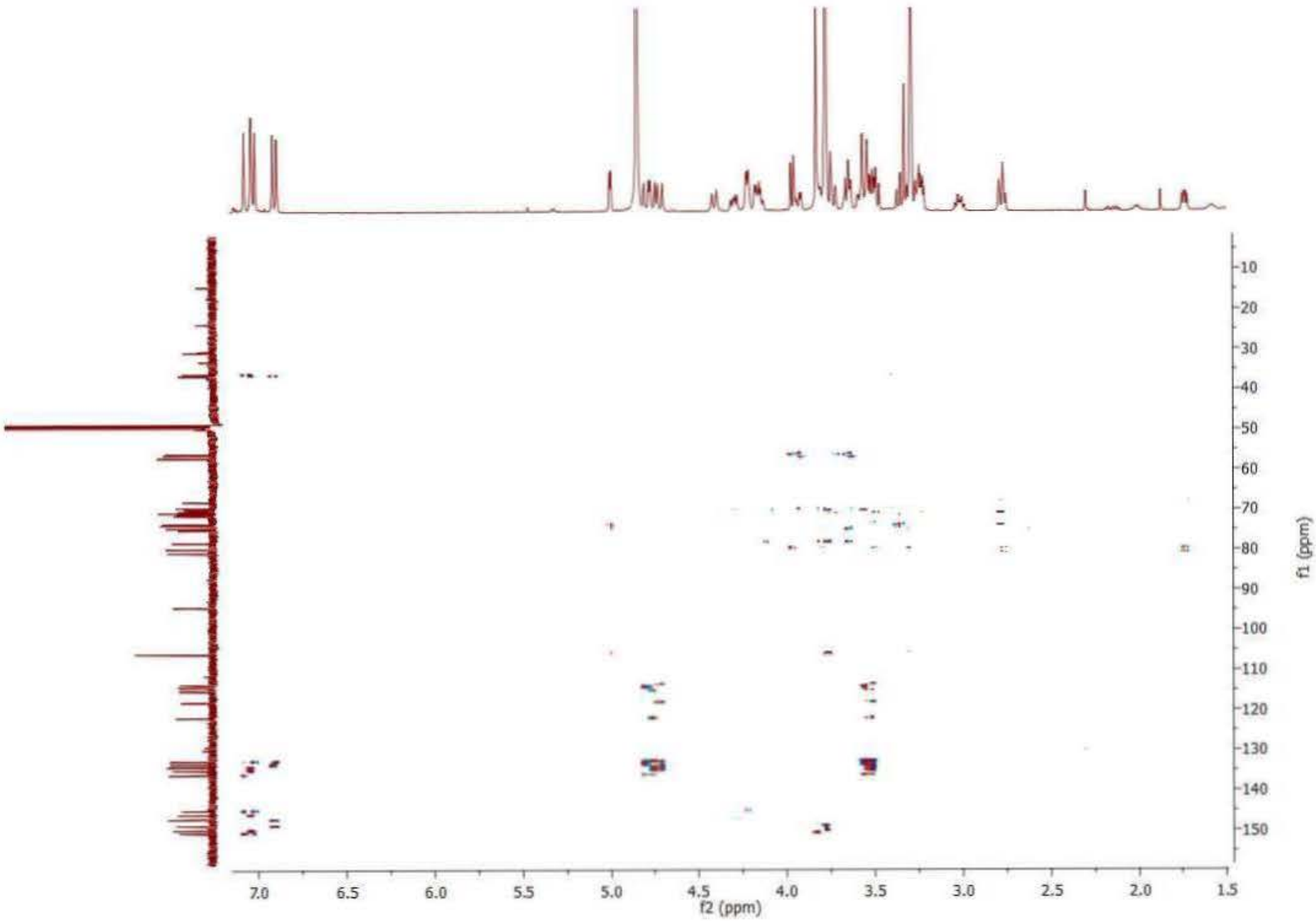

Figure S72. ^{1}H–^{13}C HMBC spectrum of compound ***M*-9**.

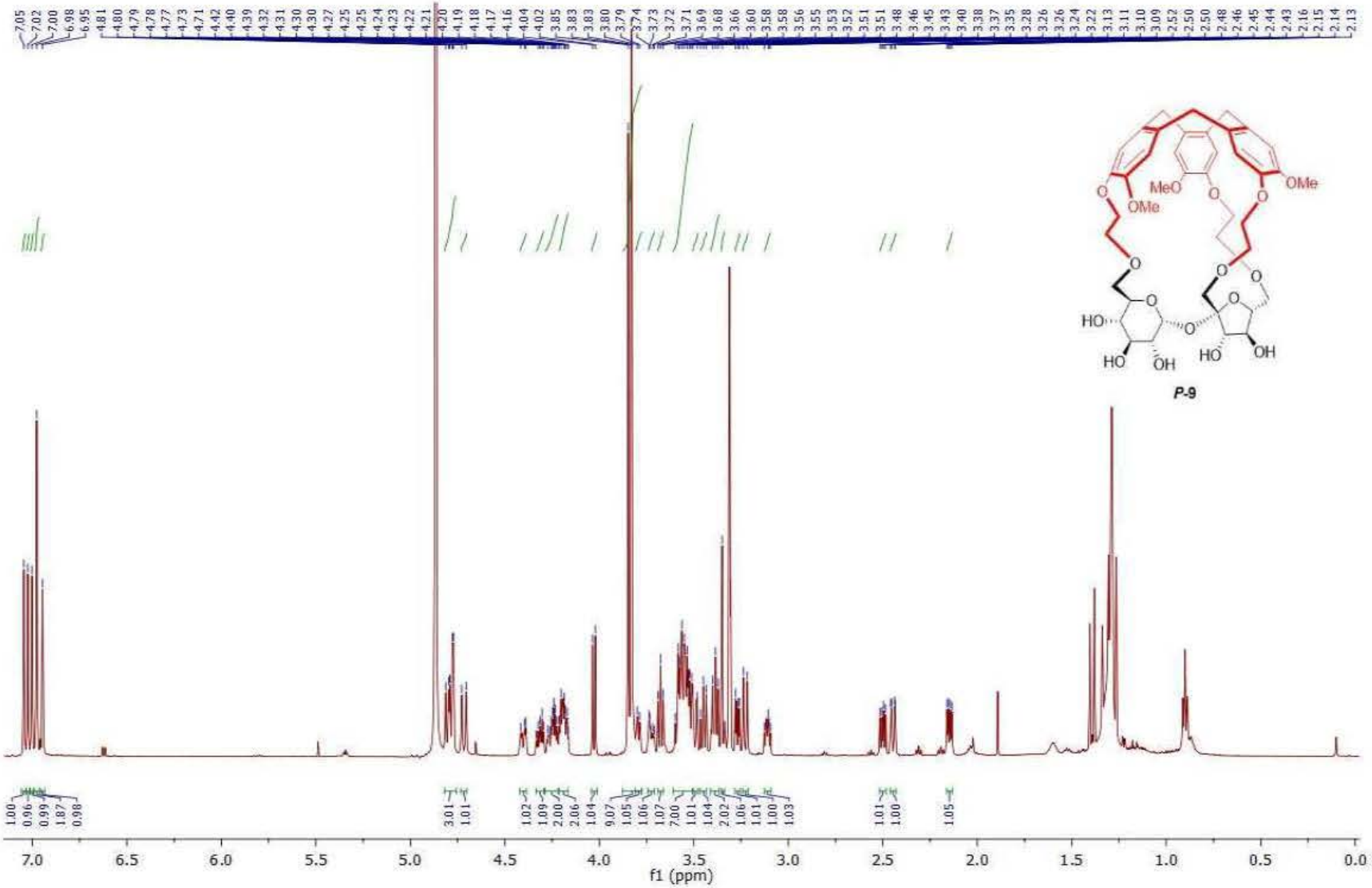

Figure S73. ^{1}H NMR spectrum of compound ***P*-9.**

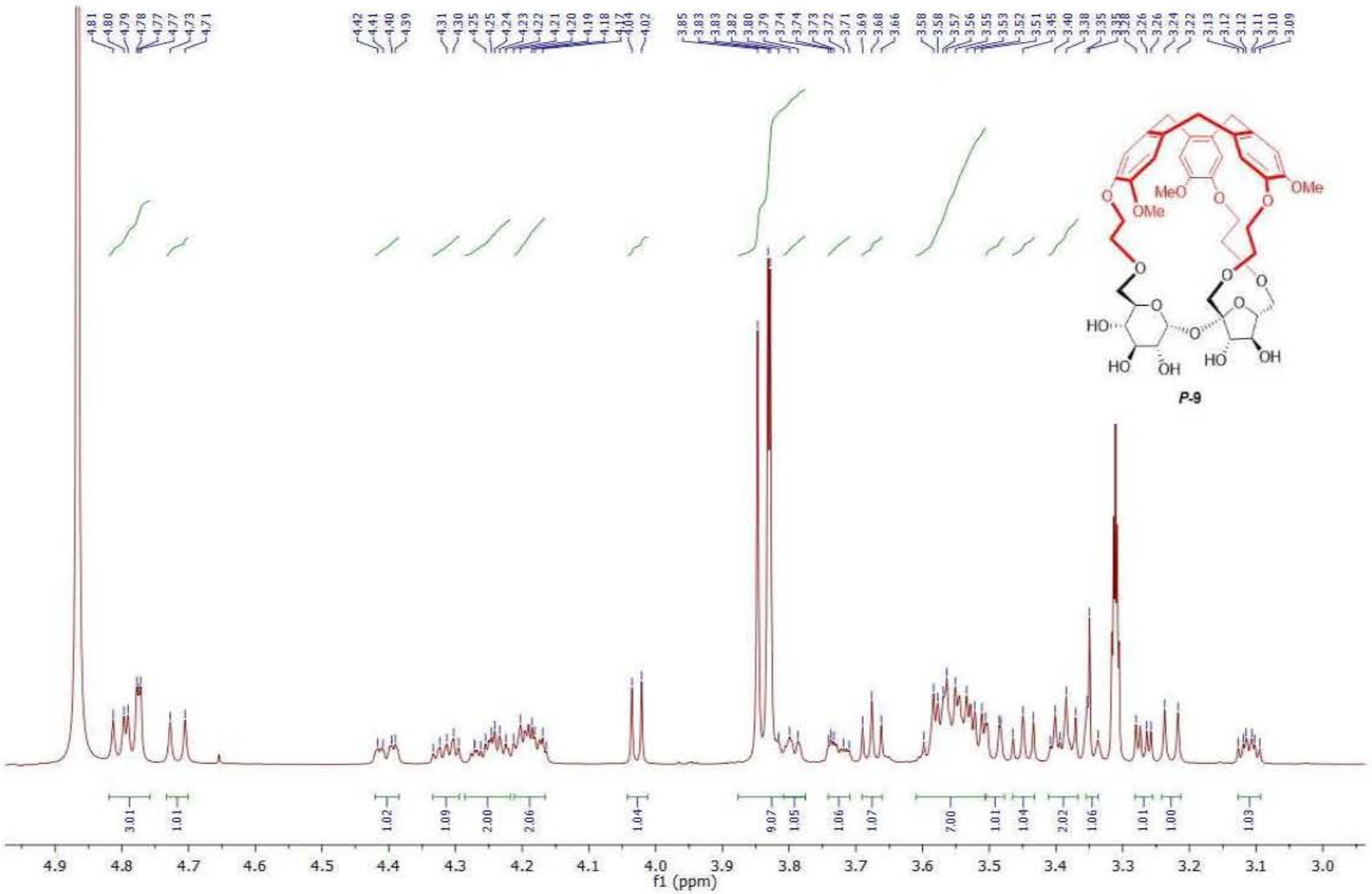

Figure S74. ^{1}H NMR spectrum of compound ***P*-9** (aliphatic part).

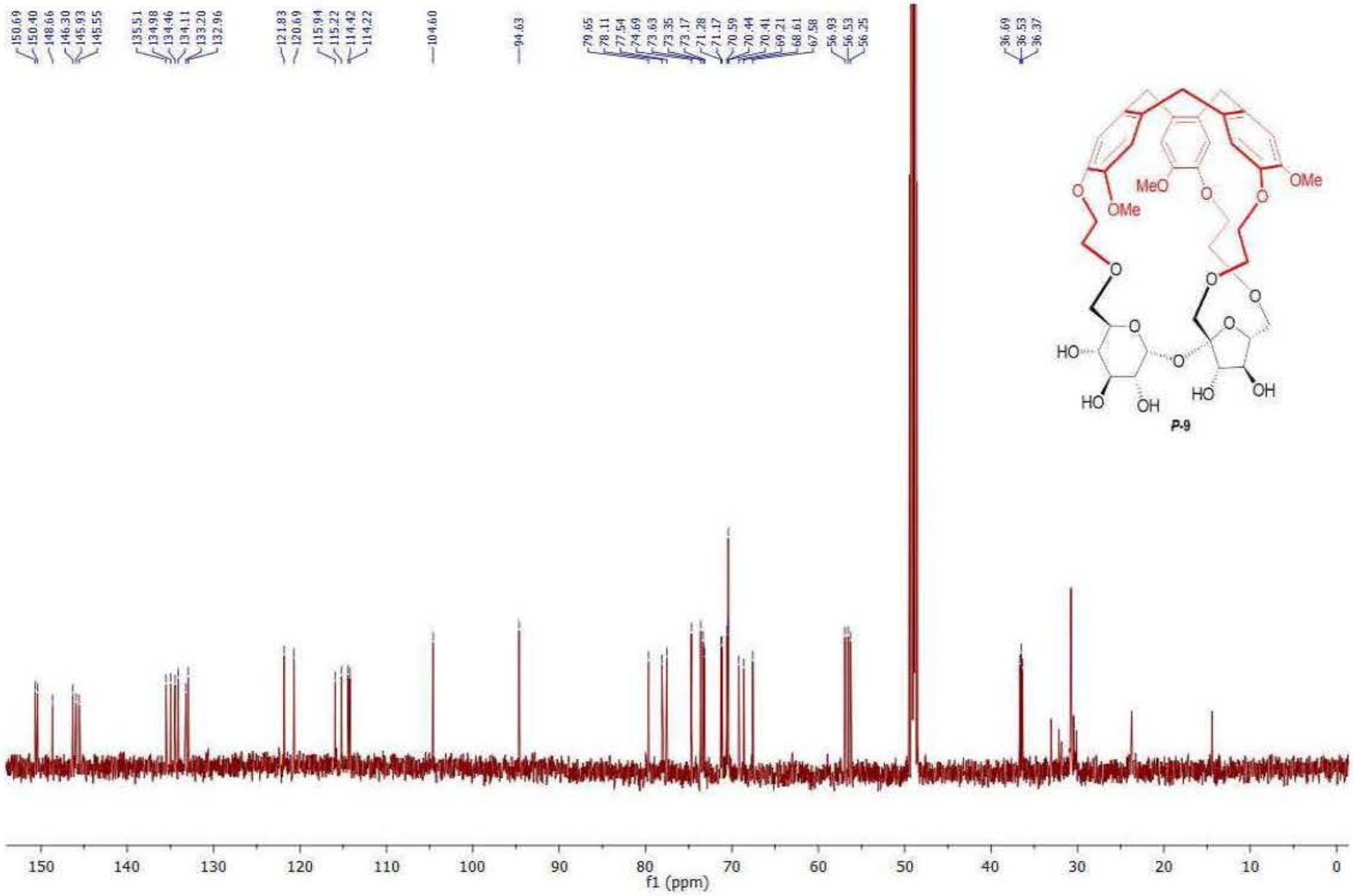

Figure S75. ^{13}C NMR spectrum of compound ***P*-9**.

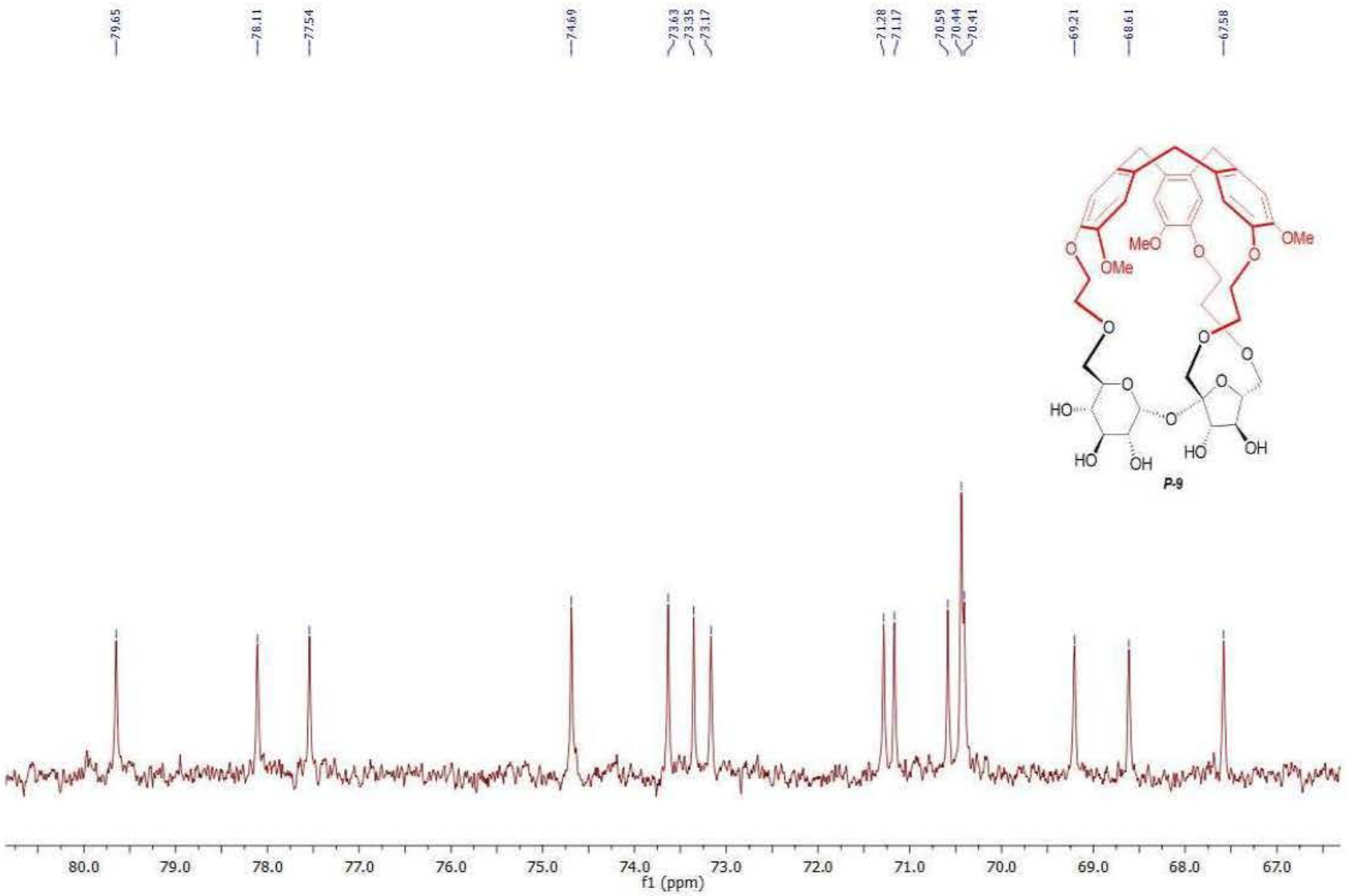

Figure S76. ^{13}C NMR spectrum of compound ***P*-9** (aliphatic part).

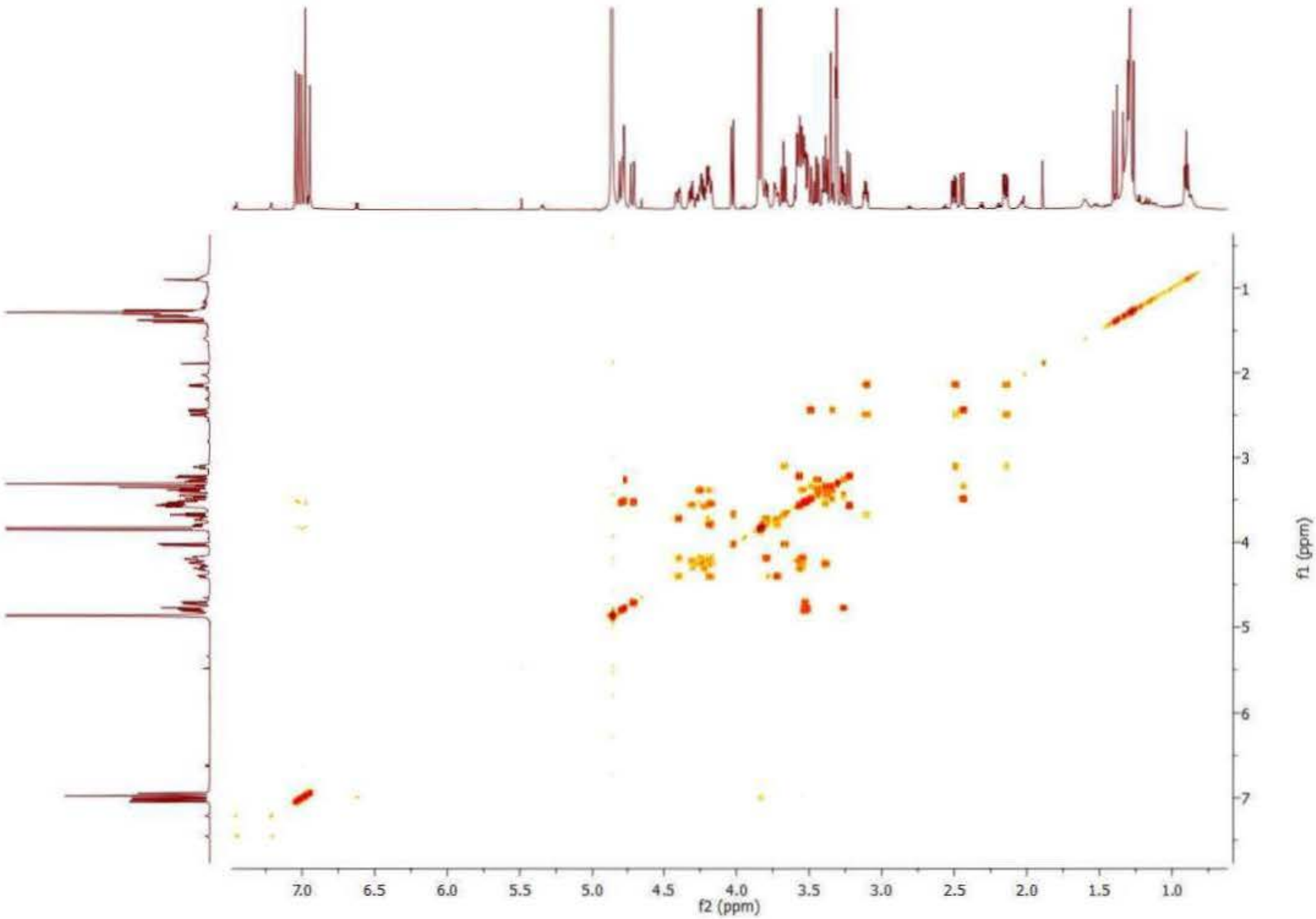

Figure S77. $^{1}H–^{1}H$ COSY spectrum of compound ***P*-9**.

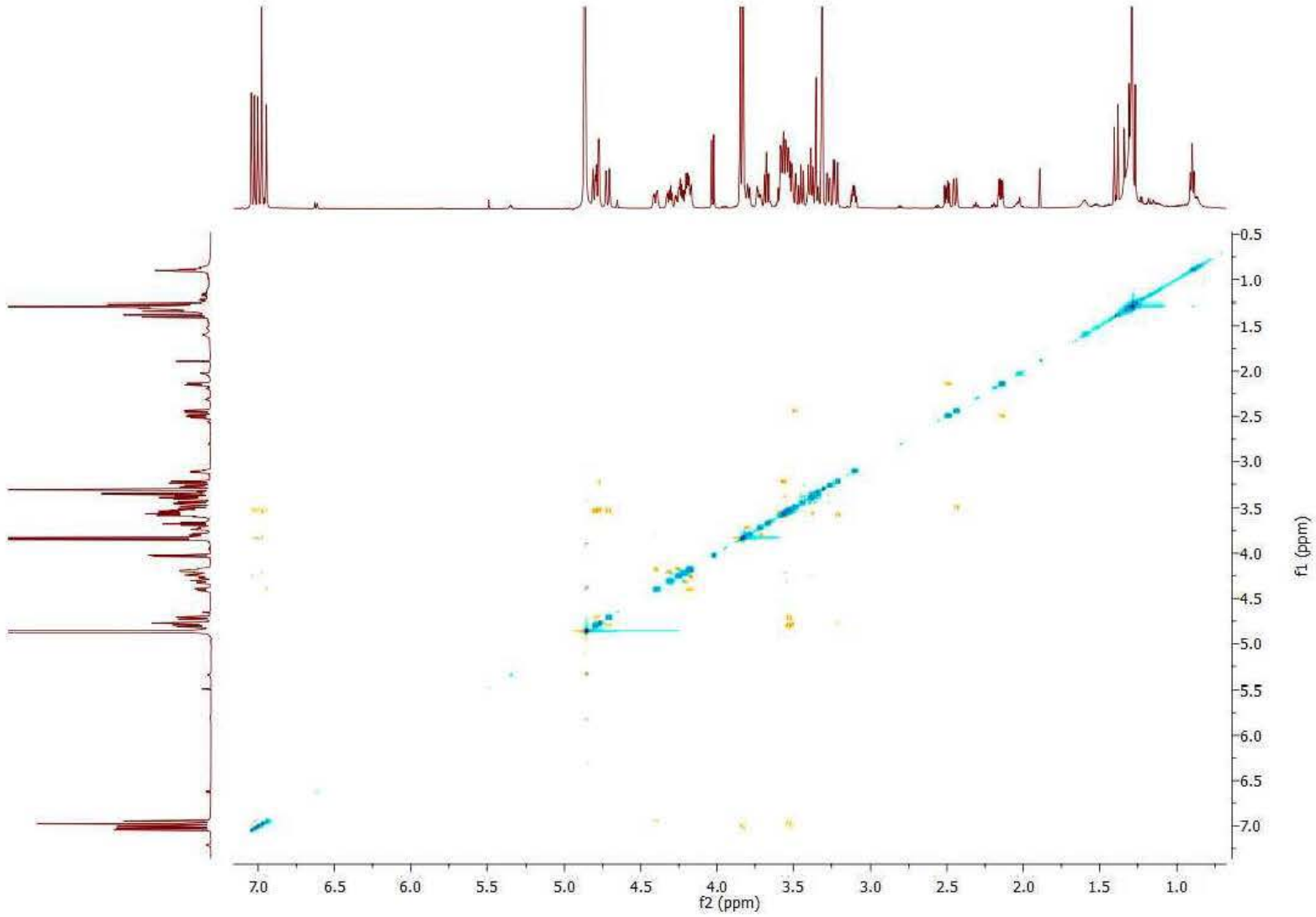

Figure S78. ^{1}H–^{1}H ROESY spectrum of compound ***P*-9**.

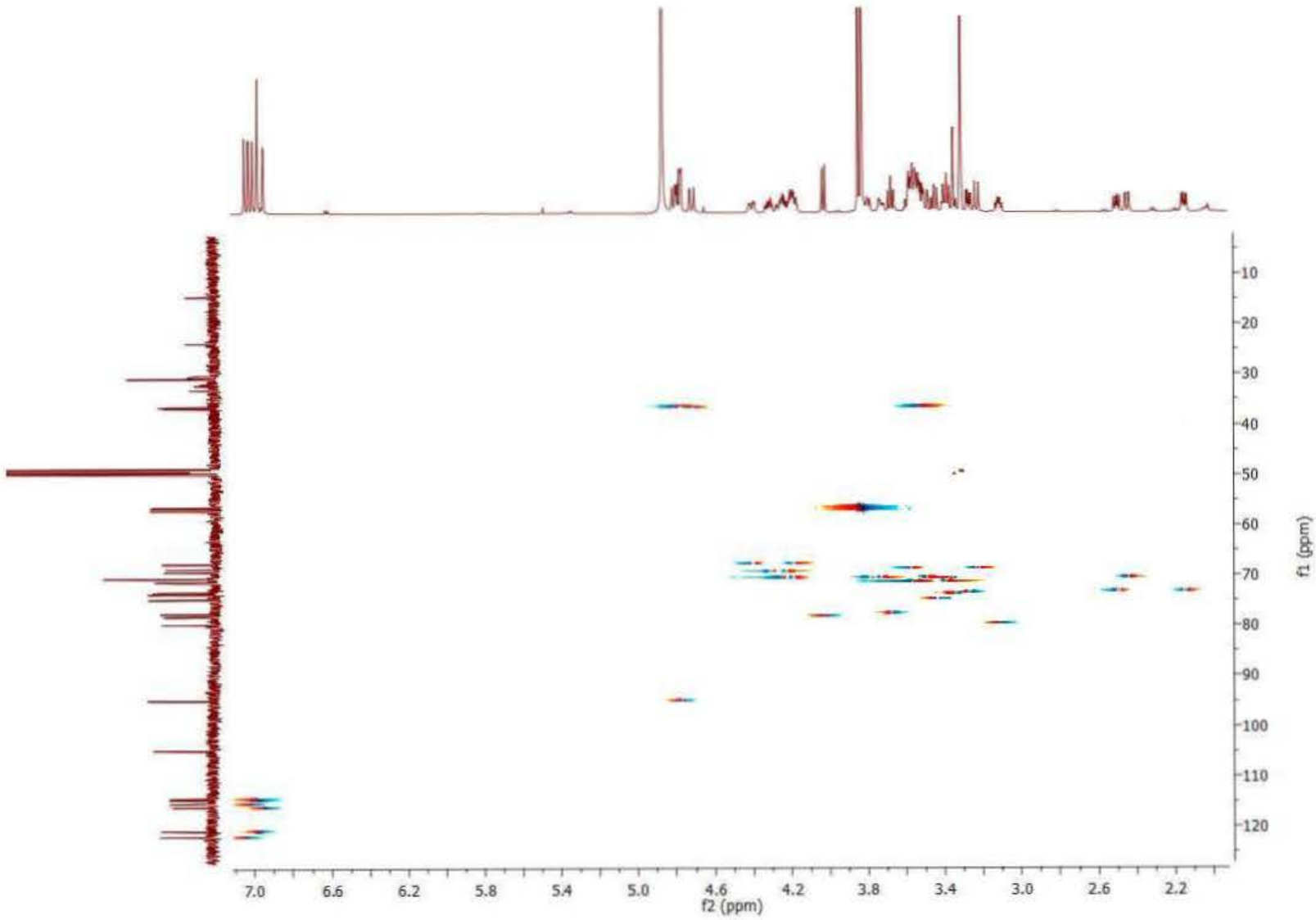

Figure S79. ^{1}H–^{13}C HSQC spectrum of compound ***P*-9**.

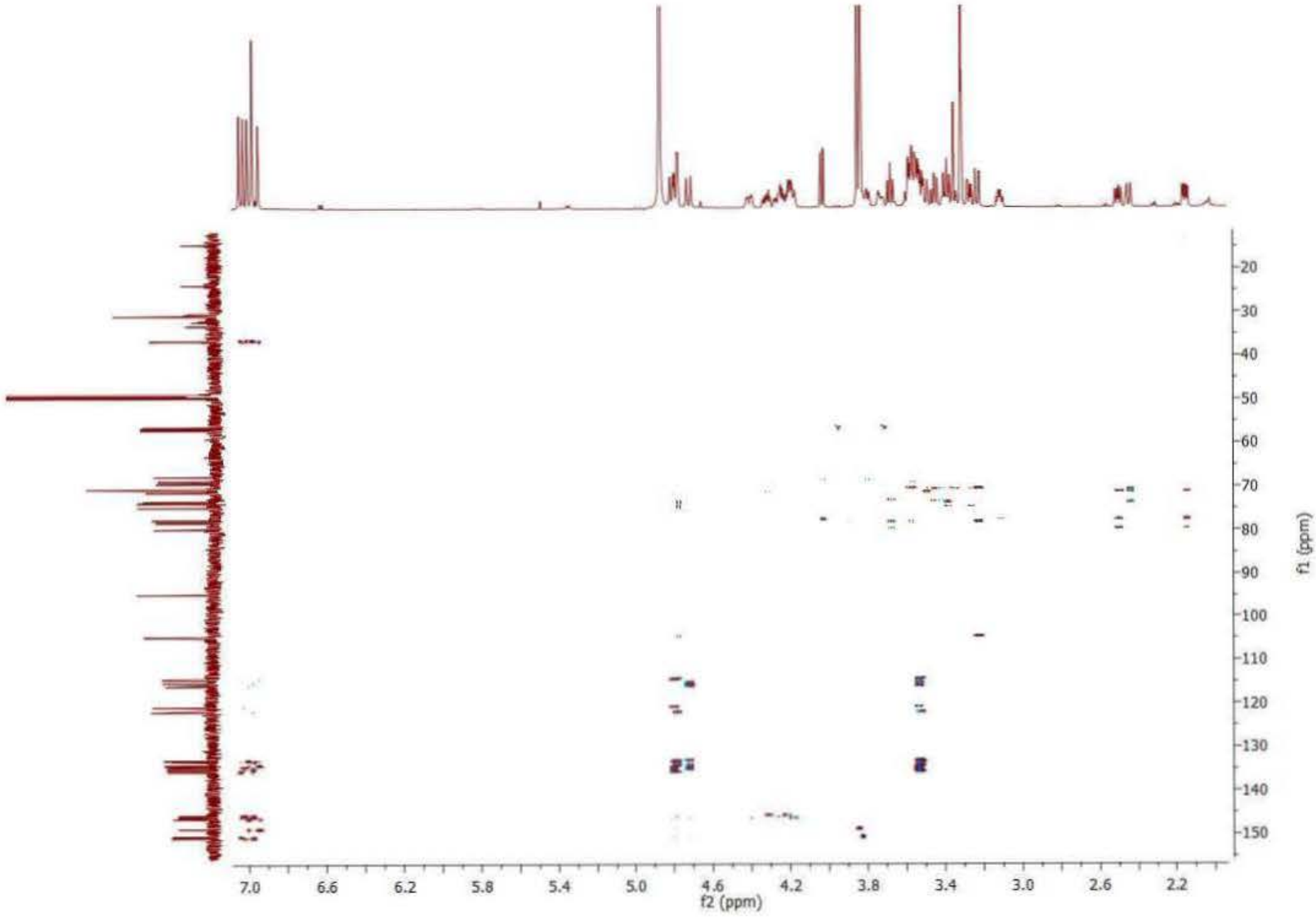

Figure S80. $^{1}H–^{13}C$ HMBC spectrum of compound ***P*-9**.

Elements Used:
C: 0-100 H: 0-100 O: 17-17 Na: 1-1

Mass	Calc. Mass	mDa	PPM	DBE	Formula	i-FIT	i-FIT Norm	Fit Conf %	C	H	O	Na
1301.5447	1301.5450	-0.3	-0.2	36.5	C77 H82 O17 Na	296.4	n/a	n/a	77	82	17	1

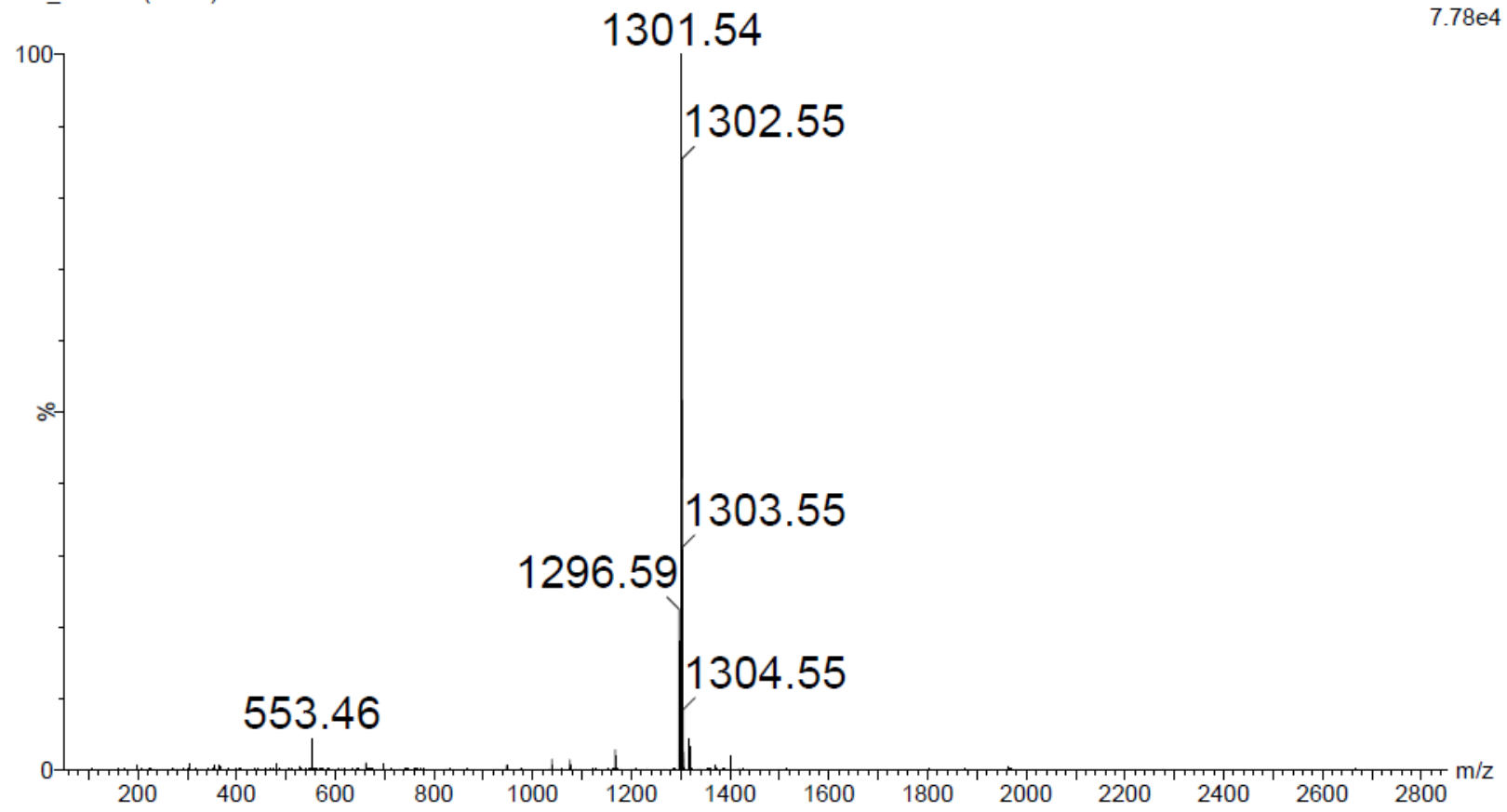

Figure S81. HRMS spectrum of compound ***M*-8**.

Elements Used:
C: 0-100 H: 0-100 O: 17-17 Na: 1-1

Mass	Calc. Mass	mDa	PPM	DBE	Formula	i-FIT	i-FIT Norm	Fit Conf %	C	H	O	Na
1301.5426	1301.5450	-2.4	-1.8	36.5	C77 H82 O17 Na	315.3	n/a	n/a	77	82	17	1

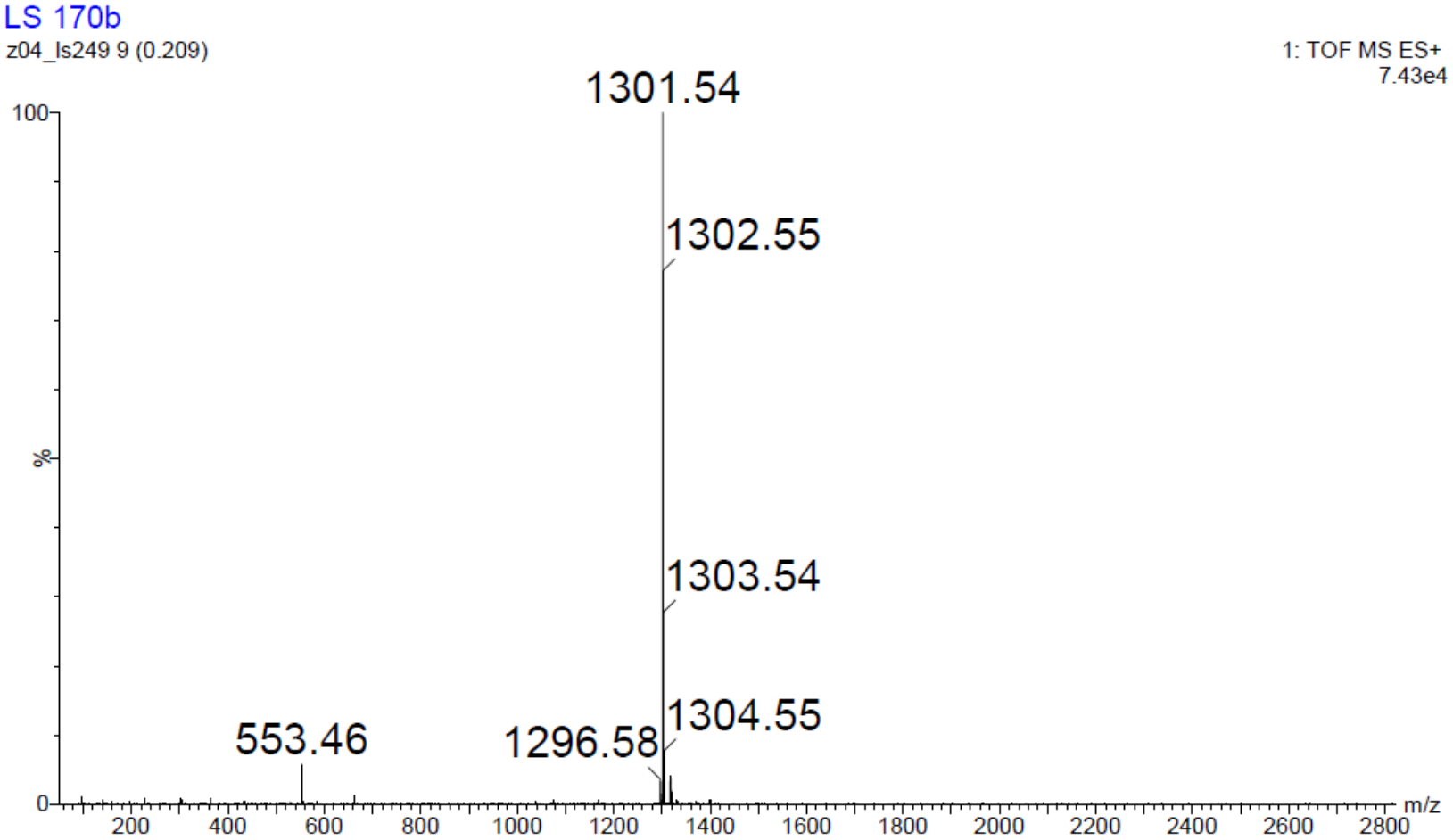

Figure S82. HRMS spectrum of compound ***P*-8**.

Elements Used:
C: 0-150 H: 0-150 O: 15-17 K: 1-1

Mass	Calc. Mass	mDa	PPM	DBE	Formula	i-FIT	i-FIT Norm	Fit Conf %	C	H	O	K
867.2832	867.2842	-1.0	-1.2	16.5	C42 H52 O17 K	273.4	n/a	n/a	42	52	17	1

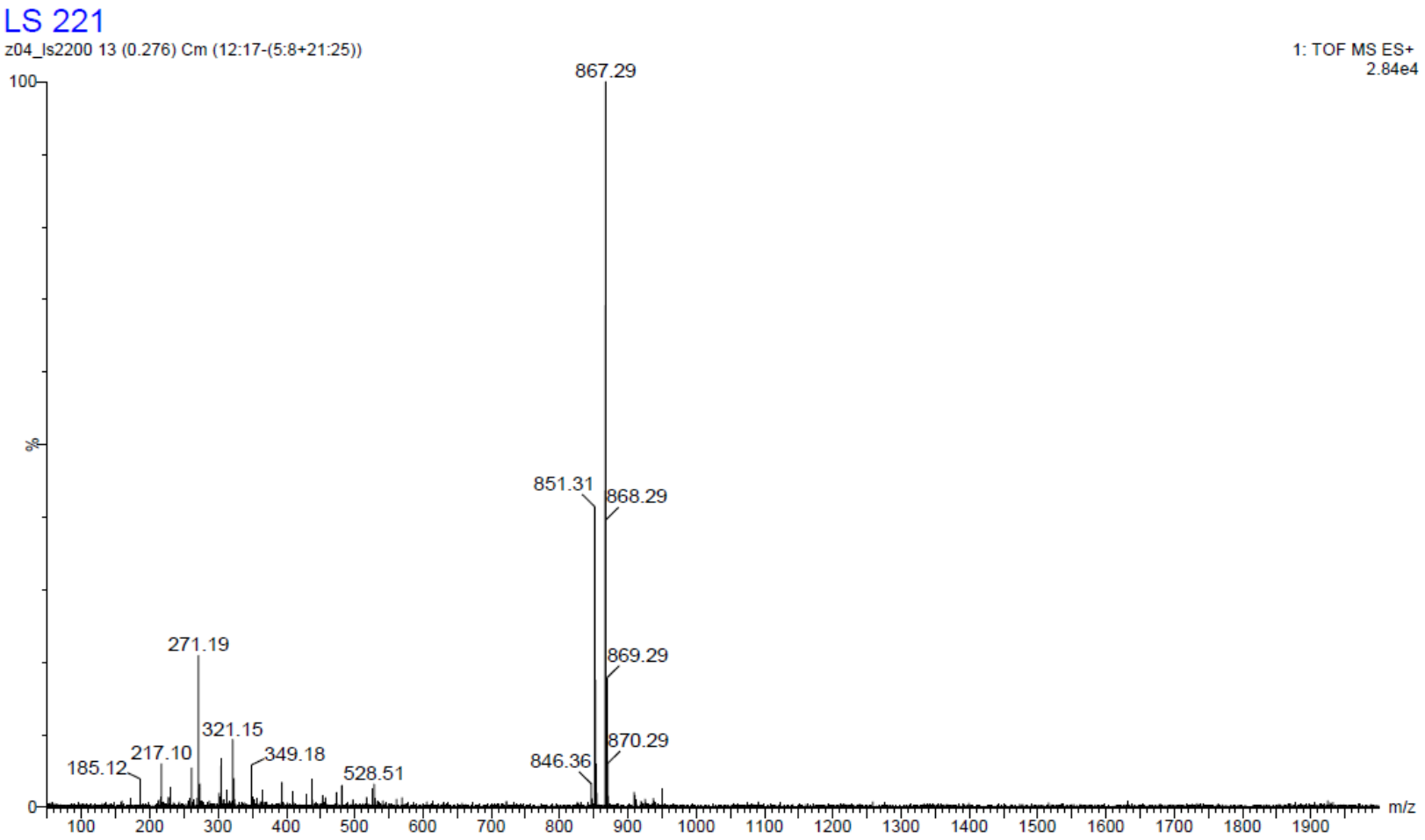

Figure S83. HRMS spectrum of compound ***M*-9**.

Elements Used:
C: 0-100 H: 0-100 O: 17-17 K: 1-1

Mass	Calc. Mass	mDa	PPM	DBE	Formula	i-FIT	i-FIT Norm	Fit Conf %	C	H	O	K
867.2838	867.2842	-0.4	-0.5	16.5	C42 H52 O17 K	398.0	n/a	n/a	42	52	17	1

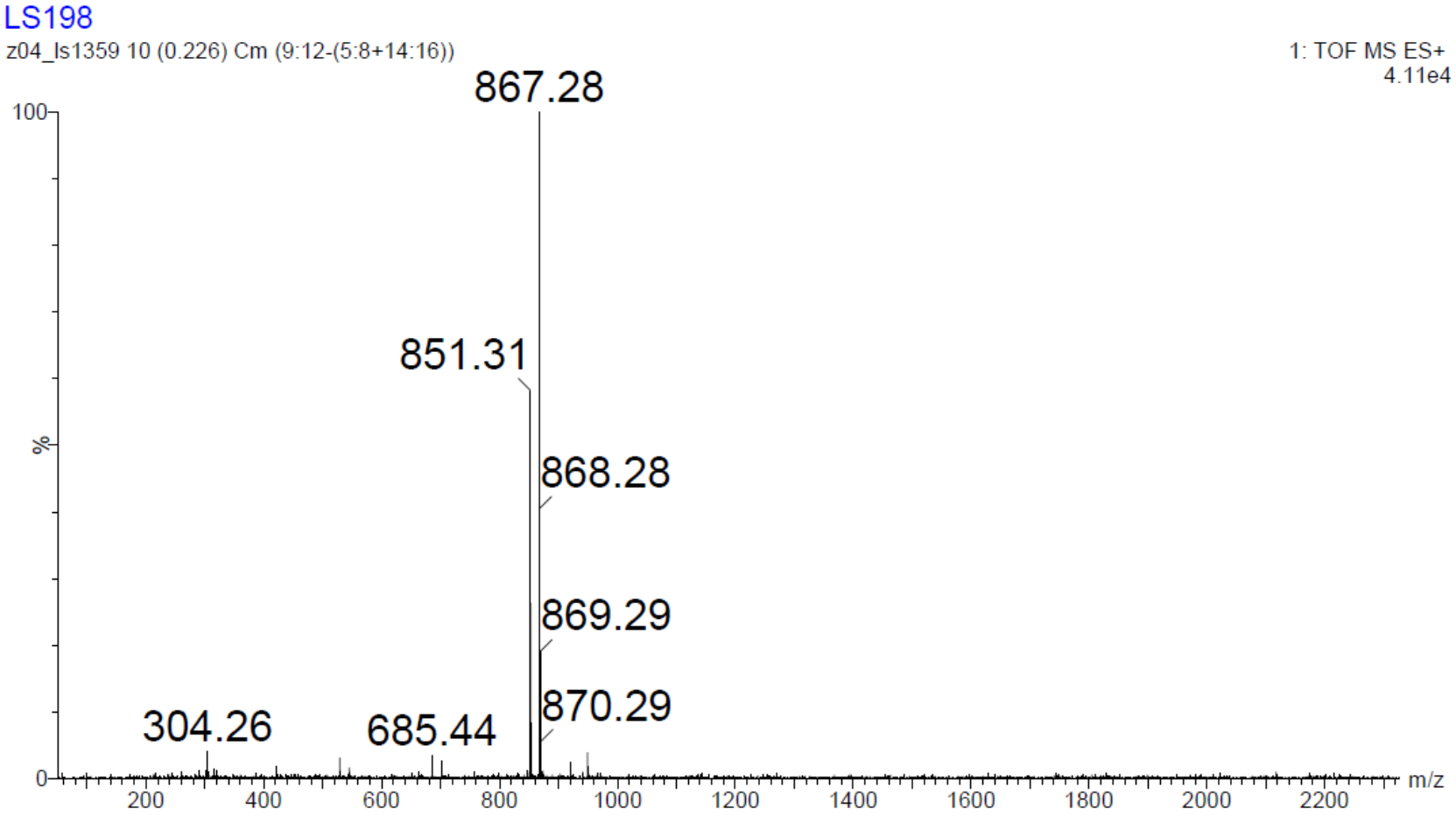

Figure S84. HRMS spectrum of compound ***P*-9**.

(1) CONFLEX 7; Conflex corporation.

(2) (a)Yanaia, T.; Tew, D.P., Handy, N.C. A new hybrid exchange–correlation functional using the Coulomb-attenuating method (CAM-B3LYP). *Chemical Physics Letters***2004**, *393*, 51–57. (b) Feller, D. The Role of Databases in Support of Computational Chemistry Calculations. *J. Comp. Chem.***1996**, *17*, 1571–1586. (c) Schuchardt, K.L.; Didier, B.T.; Elsethagen, T.; Sun, L.; Gurumoorthi, V.; Chase, J.; Li, J.; Windus, T.L. Basis Set Exchange: A Community Database for Computational Sciences. *J. Chem. Inf. Model.* **2007**, *47*, 1045–1052.

(3) Gaussian 16, Revision B.01, Frisch, M.J.; Trucks, G.W.; Schlegel, H.B.; Scuseria, G.E.; Robb, M.A.; Cheeseman, J.R.; Scalmani, G.; Barone, V.; Petersson, G.A.; Nakatsuji, H.; Li, X.; Caricato, M.; Marenich, A.V.; Bloino, J.; Janesko, B.G.; Gomperts, R.; Mennucci, B.; Hratchian, H.P.; Ortiz, J. V.; Izmaylov, A. F.; Sonnenberg, J. L.; Williams-Young, D.; Ding, F.; Lipparini, F.; Egidi, F.; Goings, J.; Peng, B.; Petrone, A.; Henderson, T.; Ranasinghe, D.; Zakrzewski, V.G.; Gao, J.; Rega, N.; Zheng, G.; Liang, W.; Hada, M.; Ehara, M.; Toyota, K.; Fukuda, R.; Hasegawa, J.; Ishida, M.; Nakajima, T.; Honda, Y.; Kitao, O.; Nakai, H.; Vreven, T.; Throssell, K.; Montgomery, J.A., Jr.; Peralta, J.E.; Ogliaro, F.; Bearpark, M.J.; Heyd, J.J.; Brothers, E.N.; Kudin, K.N.; Staroverov, V.N.; Keith, T.A.; Kobayashi, R.; Normand, J.; Raghavachari, K.; Rendell, A.P.; Burant, J.C.; Iyengar, S.S.; Tomasi, J.; Cossi, M.; Millam, J.M.; Klene, M.; Adamo, C.; Cammi, R.; Ochterski, J.W.; Martin, R.L.; Morokuma, K.; Farkas, O.; Foresman, J.B.; Fox, D.J. Gaussian, Inc., Wallingford CT, **2016**.

(4) Wei, Q.; Seward, G.K.; Hill, P.A.; Patton, B.; Dimitrov, I.E.; Kuzma, N.N.; Dmochowski, I.J.Designing ^{129}Xe NMR Biosensors for Matrix Metalloproteinase Detection. *J. Am. Chem. Soc.* **2006**, *128*, 13274–13283.

(5) Brotin, T.; Devic, T.; Lesage, A.; Emsley, L.; Collet, A. Synthesis of Deuterium-Labeled Cryptophane-A and Investigation of Xe@Cryptophane Complexation Dynamics by 1D-EXSY NMR Experiments. *Chem. Eur. J.* **2001**, *7*, 1561–1573.

EurJOC
European Journal of Organic Chemistry

Chemistry Europe
European Chemical Societies Publishing

Front Cover:
Ł. Szyszka, S. Jarosz et al.
Chiral Molecular Cages Based on Cyclotriveratrylene and Sucrose Units Connected with *p*-Phenylene Linkers

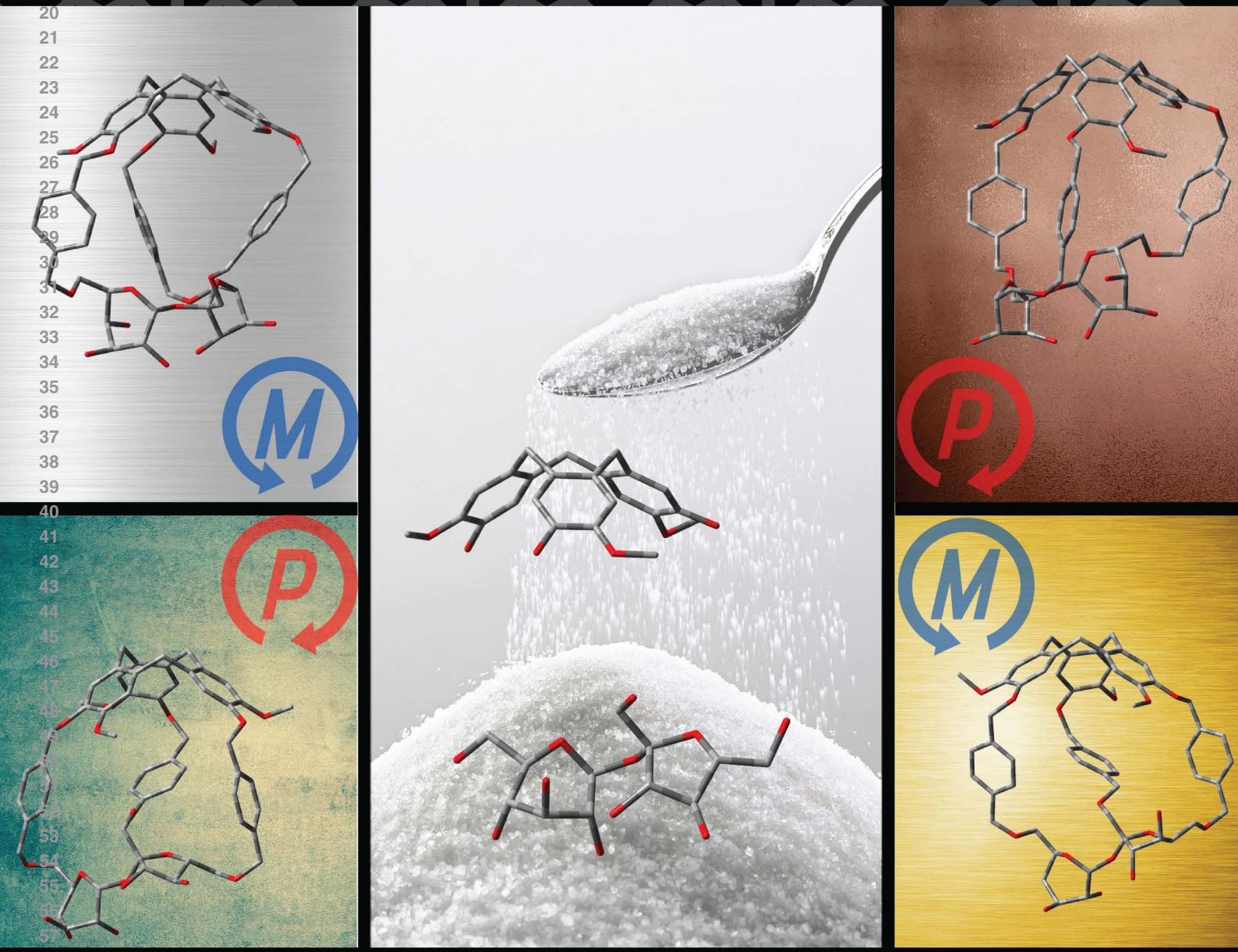

6/2021

WILEY-VCH

doi.org/10.1002/ejoc.202001482

Chiral Molecular Cages Based on Cyclotriveratrylene and Sucrose Units Connected with *p*-Phenylene Linkers

Łukasz Szyszka,*[a] Piotr Cmoch,[a] Marcin Górecki,[a] Magdalena Ceborska,[b] Mykhaylo A. Potopnyk,[a] and Sławomir Jarosz*[a]

Four diastereomeric molecular cages based on cyclotriveratrylene (CTV) and sucrose scaffolds, connected *via* *p*-phenylene linkers, were synthesized in a few steps synthesis. The absolute configuration of these diastereoisomers was determined by advanced NMR and ECD spectroscopies supported by DFT calculations. The X-Ray crystal structure of ***P*-4b** cage gave an insight into its unique structure. The binding properties of ***P*-4a** and ***M*-4a** cages towards small ammonium guests (1-methylpyridinium and 1,3-dimethylimidazolium salts) were investigated.

European Journal of Organic Chemistry

Supporting Information

Chiral Molecular Cages Based on Cyclotriveratrylene and Sucrose Units Connected with *p*-Phenylene Linkers

Łukasz Szyszka,* Piotr Cmoch, Marcin Górecki, Magdalena Ceborska, Mykhaylo A. Potopnyk, and Sławomir Jarosz*

Contents

Table S1. Crystal data of compound ***P*-4b**

Compound	***P*-4b**	
Empirical formula	$C_{390}H_{391}N_5O_{68}$	
Moiety formula	4(C95 H94 O17), 5(C2 H3 N)	
Formula weight	6236.10	
CCDC No.	CCDC 2017787	
Wavelength	1.54184	
Crystal system	monoclinic	
Space group	$P2_1$	
Unit cell dimensions	a = 11.9273(1)) Å	β = 90.8021(8) °
	b = 35.2958(3) Å	
	c = 19.5792(2) Å	
Volume	8241.7 (1)Å^3	
Z	1	
Density Calc.	1.257 g/cm^3	
Absorption coefficient	0.69 mm^{-1}	
F(000)	3310	
Crystal	Colourless block	
Crystal size	0.50 × 0.20 × 0.03 mm	
Index ranges	$-14 \leq h \leq 14$, $-42 \leq k \leq 42$, $-23 \leq l \leq 23$	
Reflections collected (all / independent)	30561 / 25595 [R_{int} = 0.151]	
Absorption correction	Multi-scan	
Refinement method	Full-matrix least-squares on F^2	
Goodness-of-fit on F^2	1.142	
Final R indices [$F^2 > 2\sigma(F^2)$]	R_1 = 0.136, ωR_2 = 0.313	
***R* indices (all data)**	R_1 = 0.152, ωR_2 = 0.321	

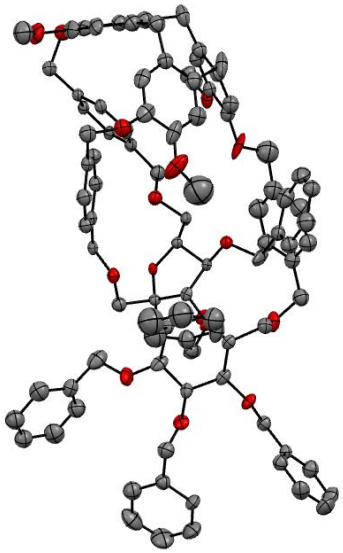

Figure S1. ORTEP diagram of the second form of compound ***P*-4b** with thermal ellipsoids at the 50% probability level. Hydrogen atoms are omitted for clarity.

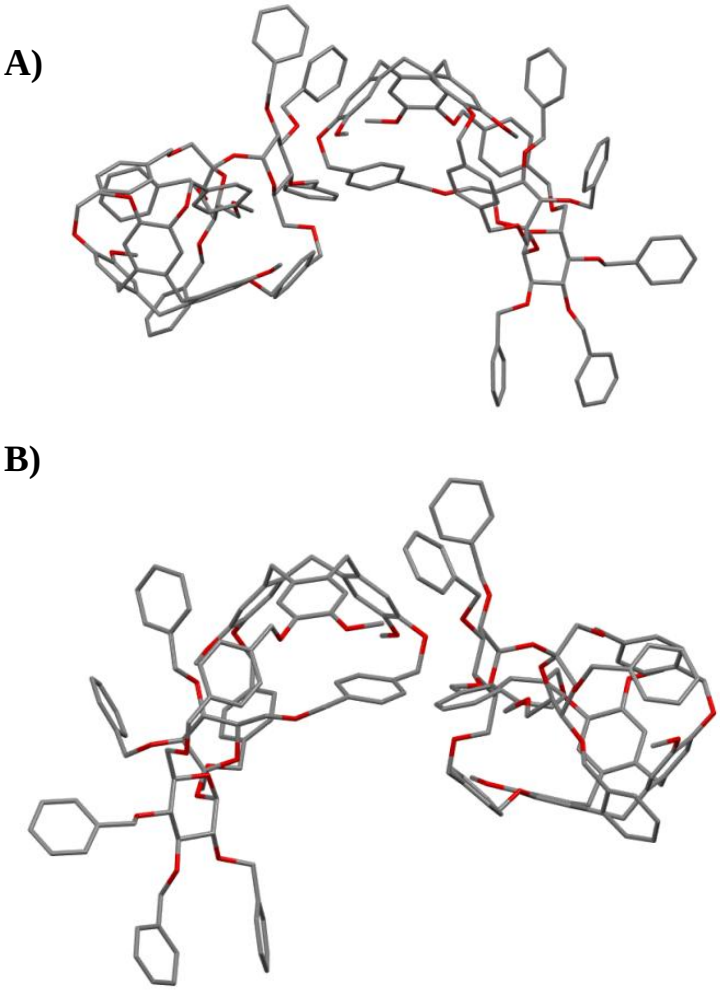

Figure S2. A) and B) Different perspectives of single crystal structure of both forms of compound ***P*-4b**. Hydrogen atoms are omitted for clarity.

Table S2. Comparison of ^{1}H and ^{13}C NMR signals of ***P*-4a**, ***P*-4b**, ***M*-4a** and ***M*-4b**.

	^{1}H and ^{13}C NMR chemical shifts δ (ppm)			
	***P*-4a**	***M*-4a**	***P*-4b**	***M*-4b**
Glucose part				
H-1 / C-1	5.18 / 91.19	5.54 / 91.48	5.62 / 88.71	5.34 / 89.22
H-2 / C-2	3.31 / 79.96	3.40 / 79.91	3.66 / 79.60	3.53 / 79.75
H-3 / C-3	3.94 / 81.29	3.86 / 81.29	3.91 / 82.37	3.94 / 82.14
H-4 / C-4	3.64 / 77.39	3.53 / 77.37	3.69 / 77.67	3.48 / 78.49
H-5 / C-5	3.75 / 70.98	3.76 / 70.21	4.33 / 69.37	4.15 / 69.63
H-6 / C-6	3.55+3.28 / 68.28	3.48+3.07 / 67.78	3.47+3.31 / 66.24	3.37+3.33 / 68.36
Fructose part				
H-1’ / C-1’	3.43+3.29 / 67.87	3.61+3.35 / 67.49	3.82+3.34 / 73.92	3.79+3.20 / 73.26
C-2’	104.06	105.34	103.38	102.79
H-3’ / C-3’	4.37 / 83.57	4.38 / 84.31	4.08 / 83.26	4.30 / 83.49
H-4’ / C-4’	3.90 / 82.96	4.03 / 83.23	3.31 / 80.72	3.47 / 81.39
H-5’ / C-5’	4.07 / 80.80	3.99 / 80.56	3.57 / 79.61	3.54 / 77.57
H-6’ / C-6’	3.68+3.44 / 73.08	3.60+3.56 / 73.71	3.43 / 73.04	3.05+2.73 / 71.96
Phenylene linkers				
H-7 /C-7	4.22+3.96 / 72.54	4.53+4.34 / 73.02	4.84+4.09 / 72.17	4.54+4.16 / 72.93
H-7’ / C-7’	4.59+4.49 / 72.89	4.41+4.31 / 73.07	4.43+4.38 / 72.25	3.44 / 70.13
H-7” / C-7”	4.70+4.02 / 72.30	4.64+4.34 / 72.80	4.50+4.40 / 75.12	4.60+4.44 / 74.64
C-8	138.04	137.46	137.97	137.88
C-8’	138.82	138.44	139.27	138.78
C-8”	136.76	137.36	138.32	138.74
H-9 / C-9	7.00 / 126.74	7.04 / 127.83	7.42 / 128.86	7.30 / 129.64
H-9’ / C-9’	6.98 / 127.11	7.01 / 127.07	6.57 / 125.66	6.10 / 124.41
H-9” / C-9”	7.17 / 128.14	7.16 / 128.18	7.14 / 128.35	7.10 / 126.79
H-10 / C-10	7.22 / 128.93	7.07 / 127.91	7.53 / 128.75	7.31 / 128.86
H-10’ / C-10’	6.98 / 127.06	7.09 / 127.30	6.44 / 129.25	6.40 / 130.23
H-10” / C-10”	7.38 / 126.79	7.26 / 127.20	6.91 / 128.86	7.22 / 125.82
C-11	135.58	136.45	137.33	136.76
C-11’	135.92	136.28	133.92	132.88
C-11”	137.72	136.06	136.21	136.56
H-12 / C-12	5.23 / 69.33	5.22+5.13 / 69.71	5.39+4.63 / 73.59	5.08+4.42 / 71.13
H-12’ / C-12’	5.28+5.20 / 70.53	5.26+5.05 / 72.40	5.09+4.85 / 73.01	5.14+4.75 / 76.08
H-12” / C-12”	5.28+5.03 / 71.68	5.17 / 70.56	5.25+4.50 / 78.71	5.59+5.19 / 68.53
CTV-ring A				
C-13	144.60	145.65	145.15	146.84
C-14	148.29	148.33	149.71	147.64
H-15 / C-15	6.70 / 113.61	6.75 / 113.69	6.34 / 112.72	6.68 / 111.73
H-18 / C-18	6.94 / 116.17	6.88 / 116.41	6.95 / 121.97	6.59 / 113.07
H-19 / C-19 (OCH_3)	3.80 / 55.84	3.74 / 56.00	3.68 / 55.22	3.43 / 54.85
H-20 / C-20	4.64+3.47 / 36.54	4.65-4.71+3.51 / 36.47	4.54+3.31 / 35.64	4.65+3.52 / 36.33
CTV-ring B				
C-13’	145.81	146.25	146.24	146.47
C-14’	148.30	149.12	151.52	147.92
H-15’ / C-15’	6.87 / 114.20	6.73 / 113.90	6.19 / 113.94	7.00 / 113.75
H-18’ / C-18’	6.74 / 117.83	6.99 / 116.41	7.12 / 123.14	7.13 / 113.49
H-19’ / C-19’ (OCH_3)	3.89 / 56.57	3.67 / 56.04	2.55 / 56.02	3.96 / 56.45
H-20’ / C-20’	4.70+3.48 / 36.58	4.65-4.71+3.50 / 36.59	4.52+3.35 / 36.17	4.65+3.53 / 35.66
CTV-ring C				
C-13”	146.99	146.89	143.31	144.16
C-14”	148.53	148.05	150.79	150.74
H-15” / C-15”	6.51 / 113.51	6.66 / 113.72	6.90 / 112.72	6.42 / 112.27
H-18” / C-18”	6.86 / 117.84	6.93 / 115.50	6.33 / 126.19	7.06 / 124.52
H-19” / C-19” (OCH_3)	3.54 / 55.67	3.64 / 56.00	3.95 / 55.94	3.53 / 55.40
H-20” / C-20”	4.62+3.40 / 36.37	4.65-4.71+3.48 / 36.49	4.72+3.56 / 36.21	4.69+3.40 / 36.05

Table S3. The quantitative evaluation of the agreement between simulated and experimental ECD spectra of ***P*-4a**, ***P*-4b**, ***M*-4a** and ***M*-4b**.

Compound	Band-width	Similarity factor (SF)	SF for enantiomer	Δ value	UV-correction
***P*-4a**	0.26 eV	0.720	0.084	0.636	+9 nm
***P*-4b**	0.28 eV	0.874	0.010	0.864	+15 nm
***M*-4a**	0.22 eV	0.867	0.046	0.821	+9 nm
***M*-4b**	0.30 eV	0.887	0.032	0.855	+10 nm

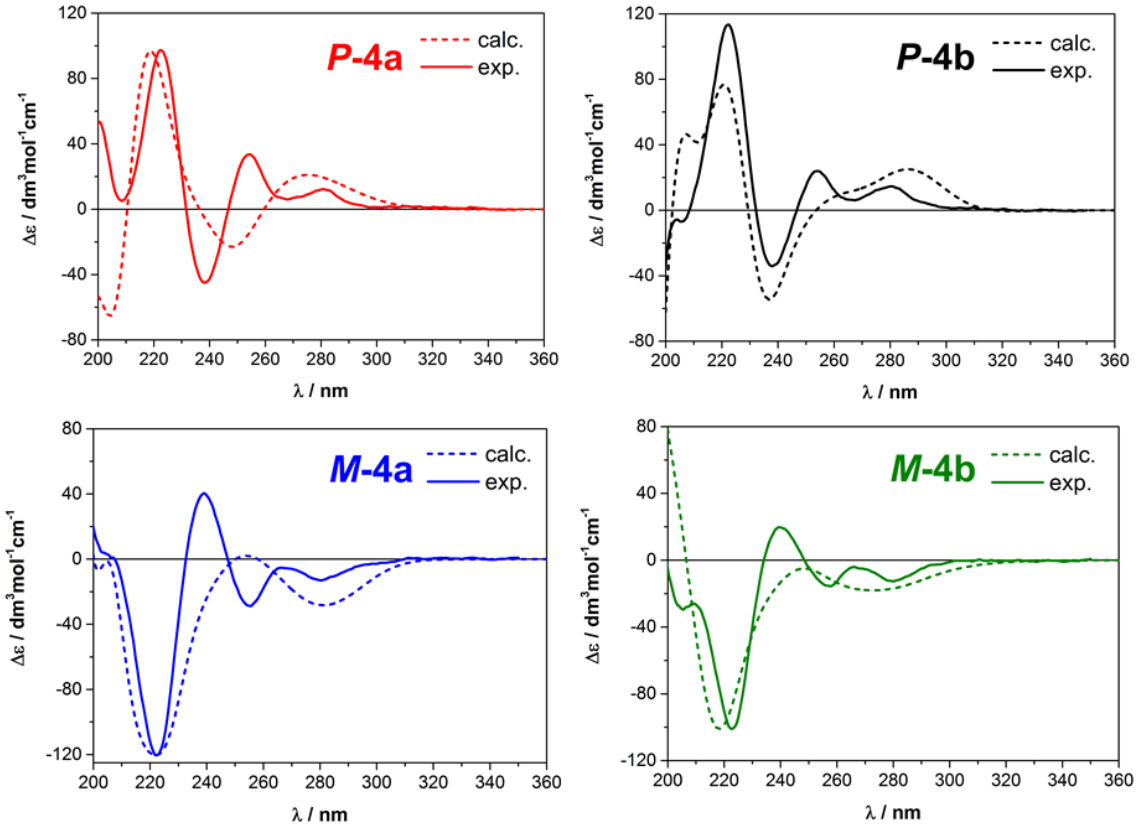

Figure S3. Comparison of the calculated ECD spectra at the TDDFT/B3LYP/SVP/PCM(CH_3CN) level for ***P*-4a**, ***P*-4b**, ***M*-4a** and ***M*-4b** with the experimental ones measured in CH_3CN at room temperature.

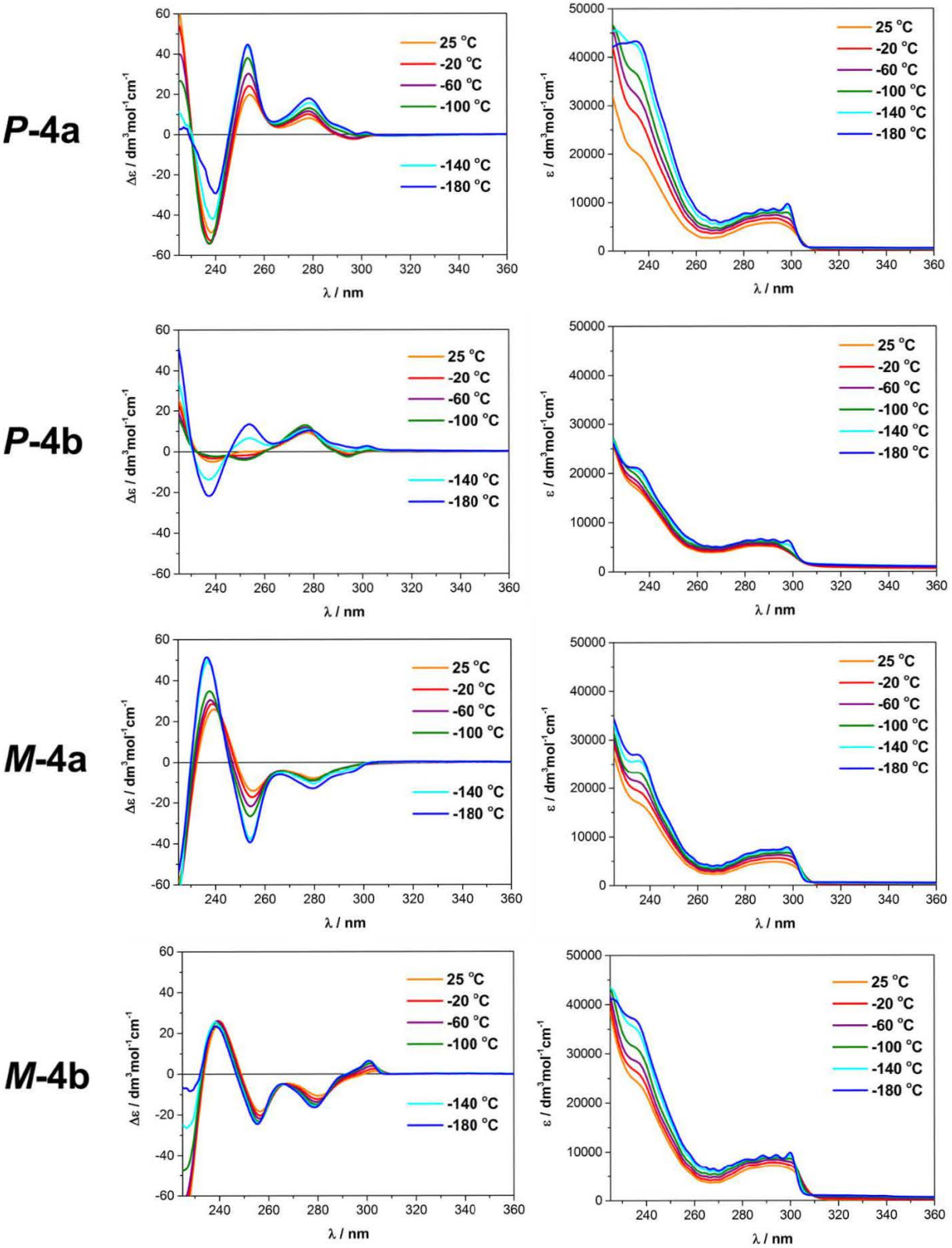

Figure S4. ECD/UV spectra of ***P*-4a**, ***P*-4b**, ***M*-4a**, and ***M*-4b** measured in EPA (diethyl ether :*iso*-pentane : ethanol, 5 : 5 : 2, *v/v*) at variable temperatures. Concentration 6.15×10^{-4} M at 25°C, cell path length 1 cm.

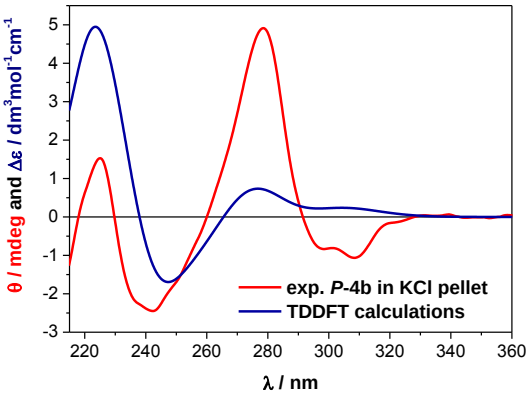

Figure S5. Comparison of the experimental ECD spectrum recorded in KCl pellet of ***P*-4b** with its calculated spectrum at the B3LYP/SVP level of theory based on geometry taken from X-ray structure.

1. NMR titration experiments

1.1. Titration of 1,3-dimethylimidazolium hexafluorophosphate with *P*-4a

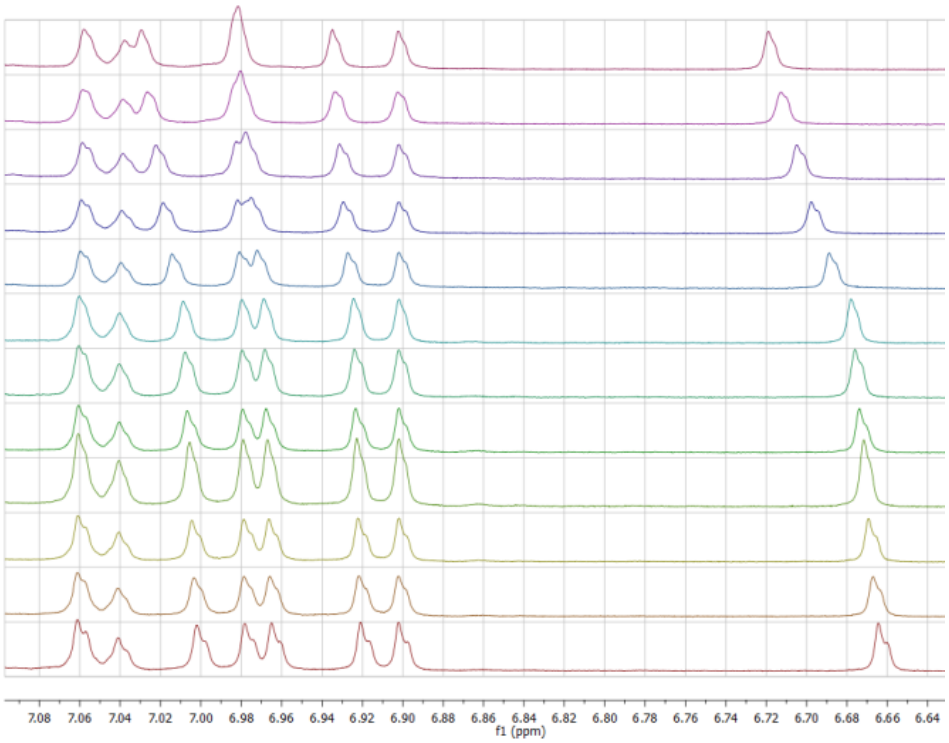

Figure S6. Chemical shifts of CTV aromatic part protons during titration of **G1** with ***P*-4a**.

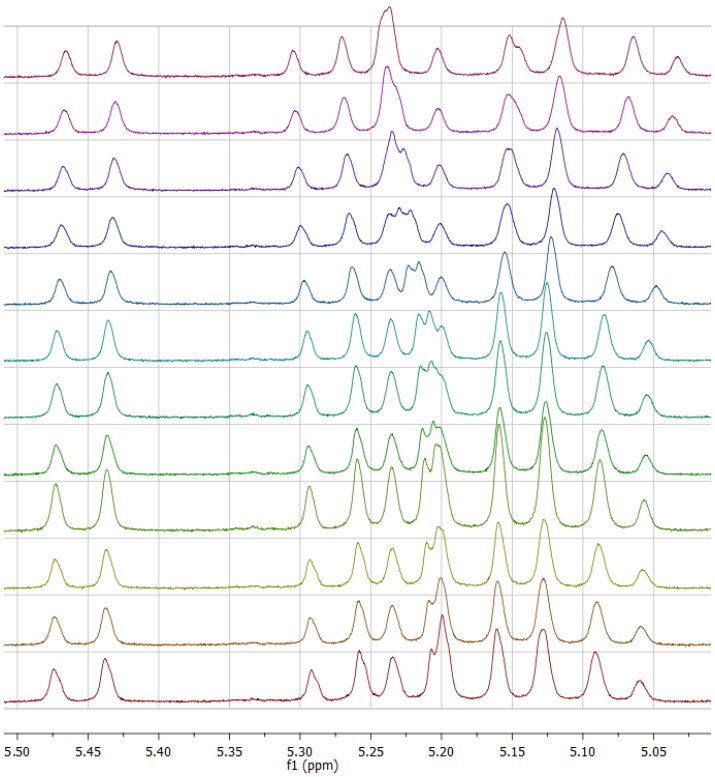

Figure S7. Chemical shifts of H-12 protons during titration of **G1** with ***P*-4a**.

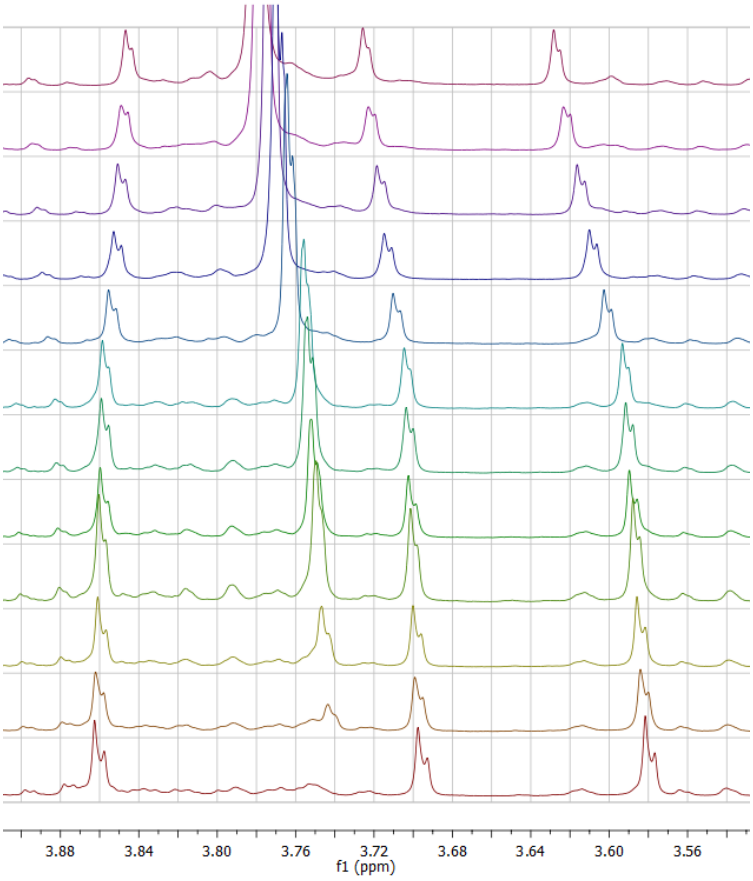

Figure S8. Chemical shifts of methoxy protons during titration of **G1** with ***P*-4a**.

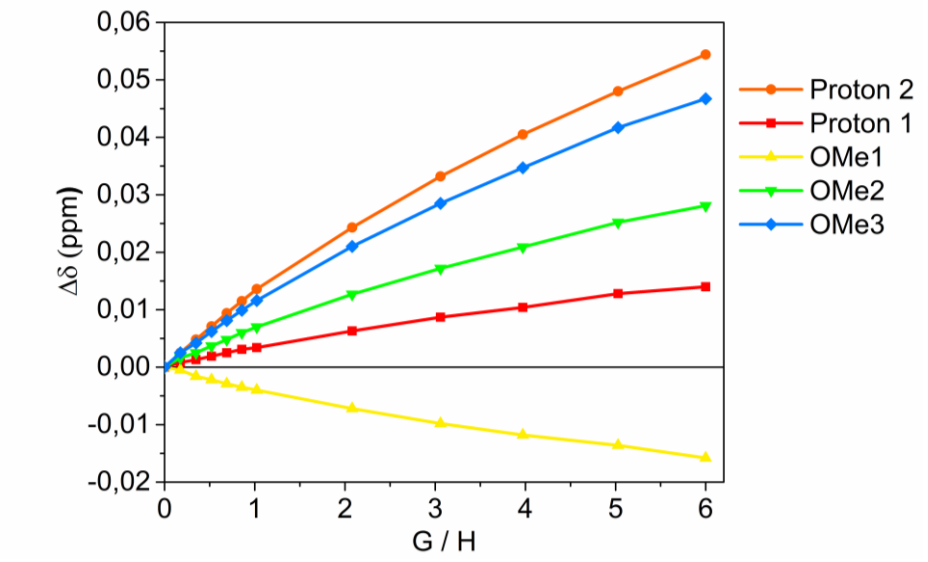

Figure S9. Titration curve for ***P*-4a** and 1,3-dimethylimidazolium hexafluorophosphate complex.

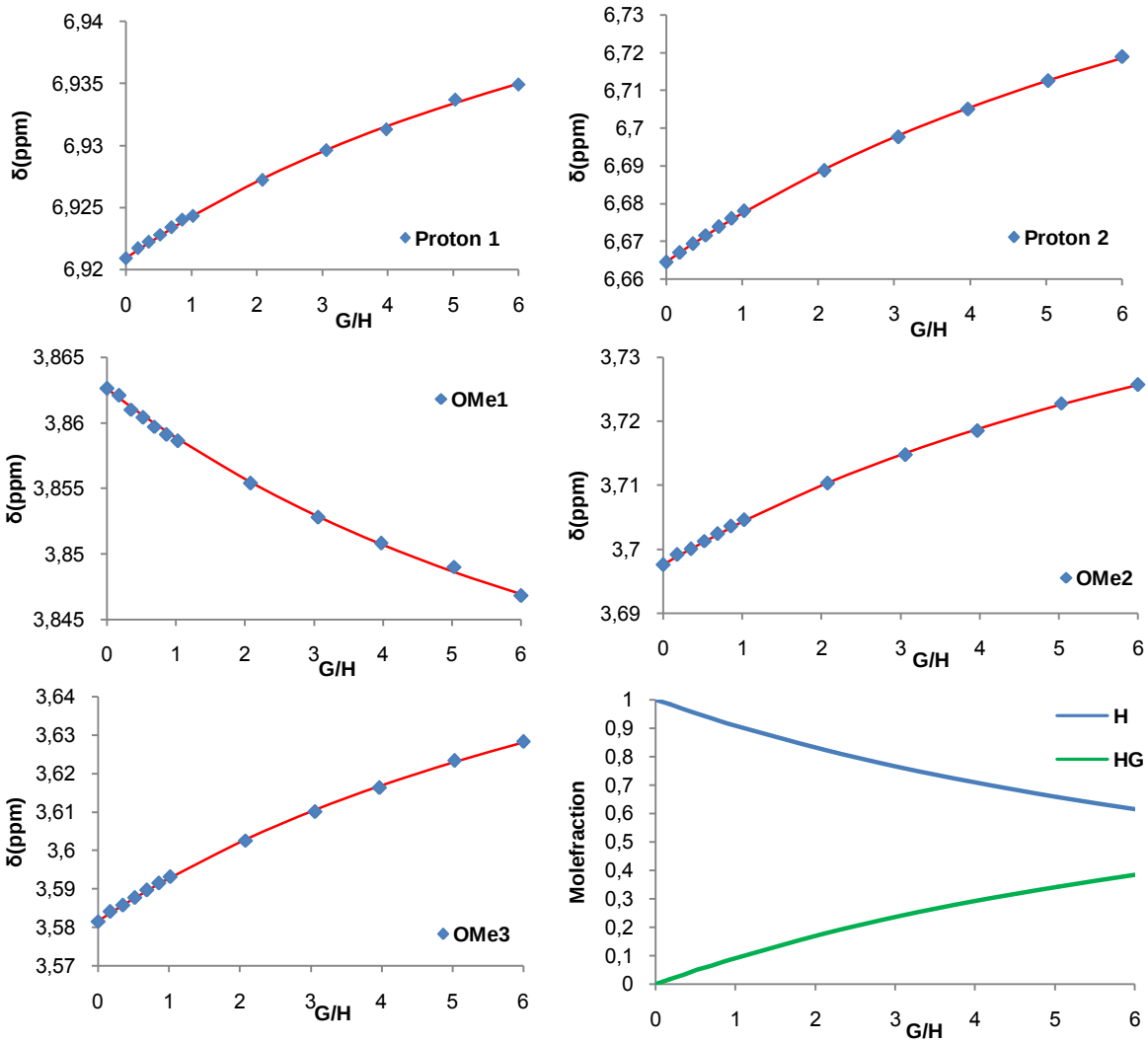

$K_a = 13.9 \pm 0.1\ M^{-1}$ RMS = $2.1478 \cdot 10^{-4}\ M^{-1}$

Figure S10. Titration curves of ***P*-4a** protons and K_a value.

1.2. Titration of 1-methylpyridinium hexafluorophosphate with *P*-4a

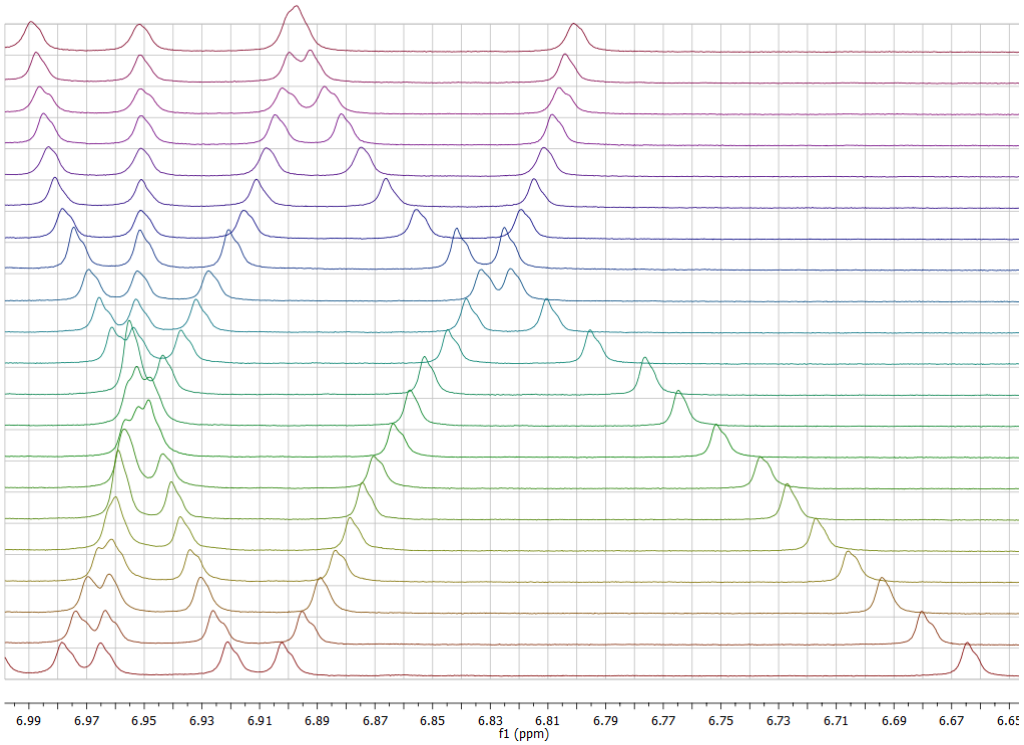

Figure S11. Chemical shifts of CTV aromatic part protons during titration of **G2** with ***P*-4a**.

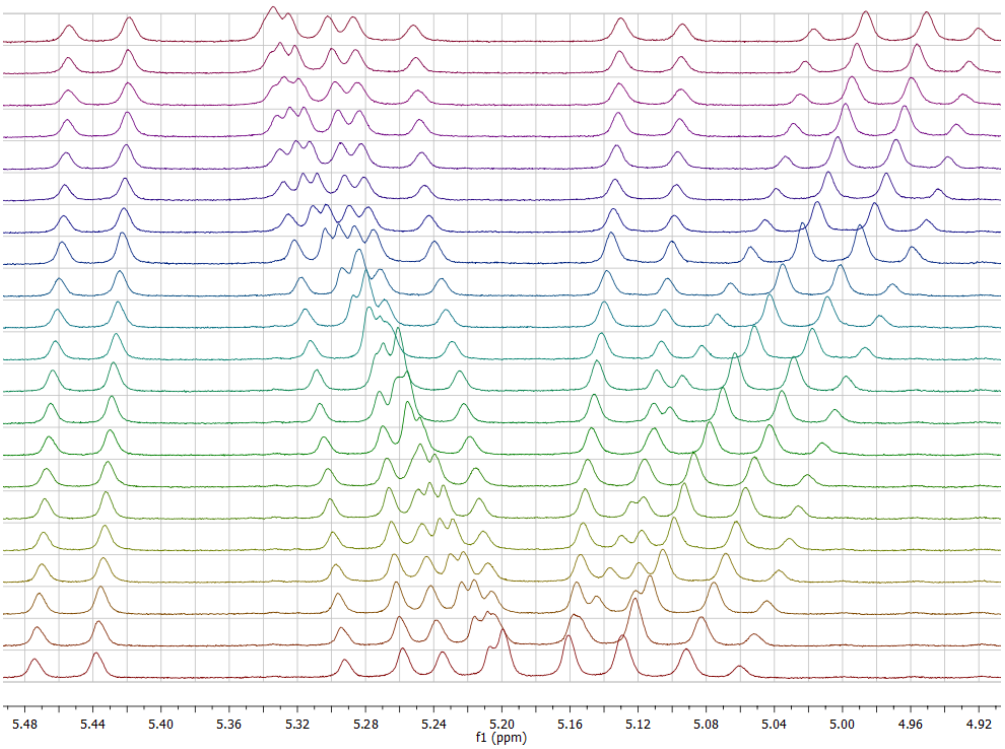

Figure S12. Chemical shifts of H-12 protons during titration of **G2** with ***P*-4a**.

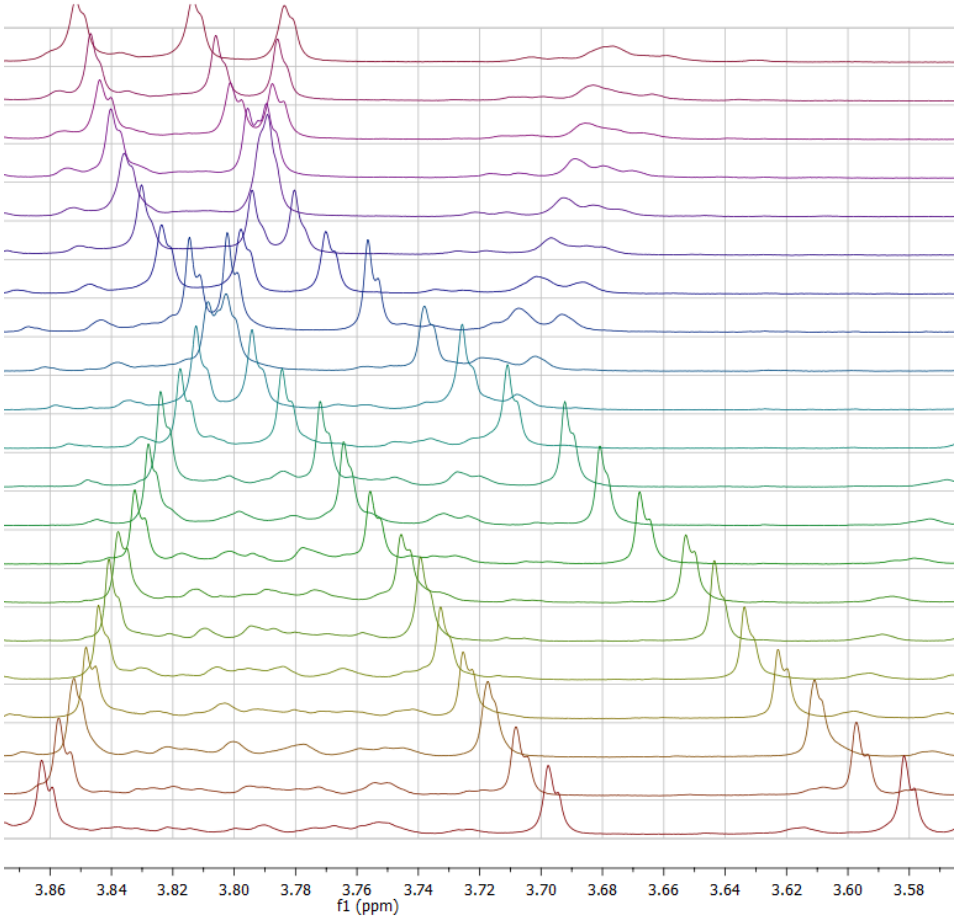

Figure S13. Chemical shifts of methoxy protons during titration of **G2** with ***P*-4a**.

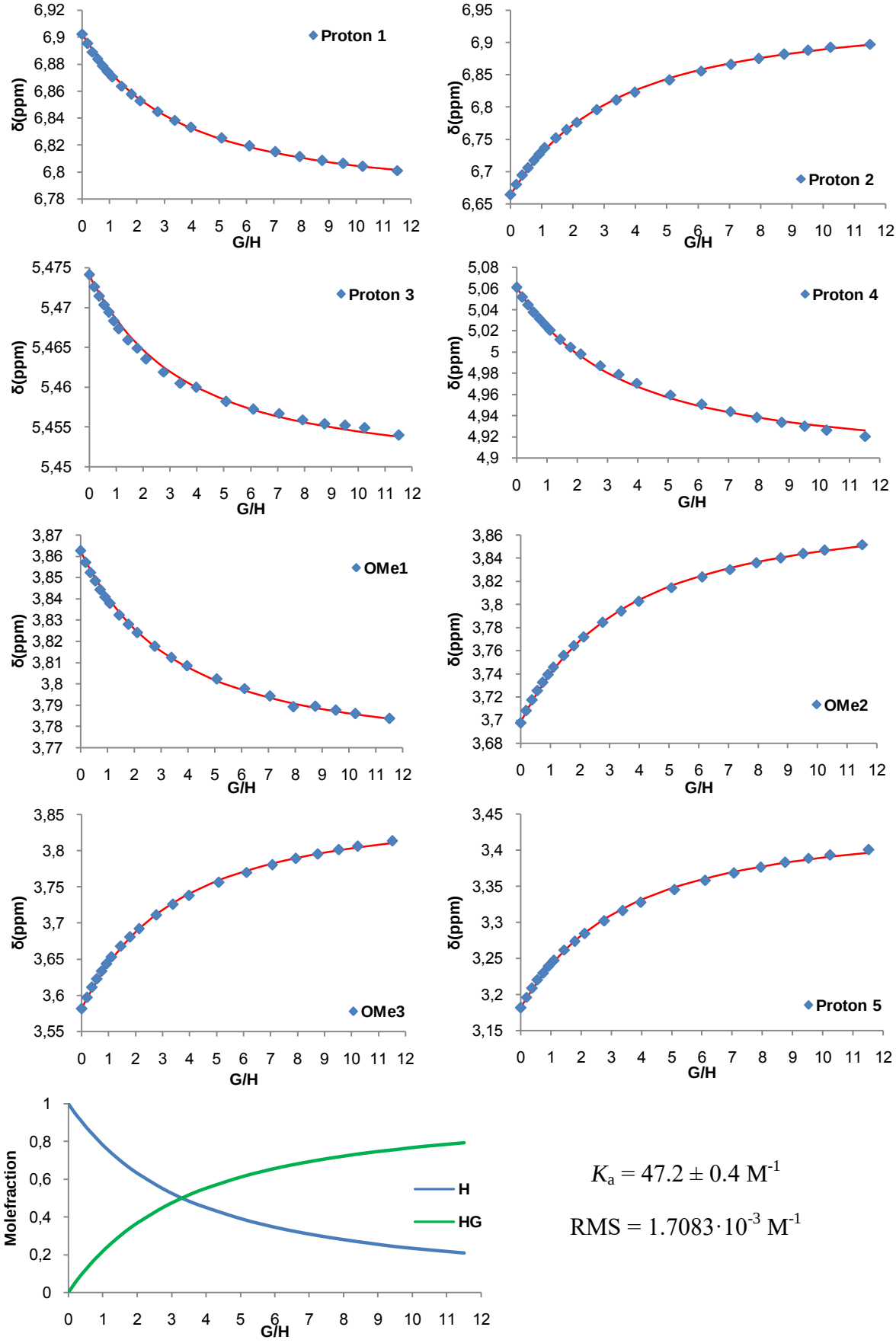

Figure S14. Titration curves of ***P*-4a** protons and K_a value.

1.3. Titration of 1,3-dimethylimidazolium hexafluorophosphate with *M*-4a

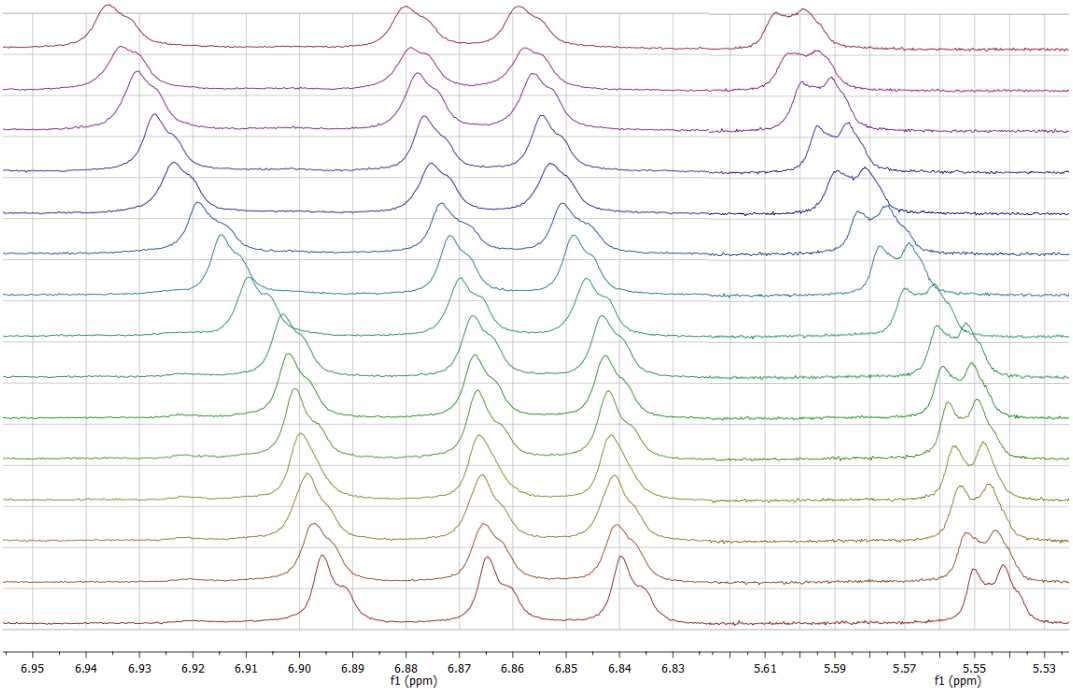

Figure S15. Chemical shifts of CTV aromatic part protons and H-1 proton during titration of **G1** with ***M*-4a**.

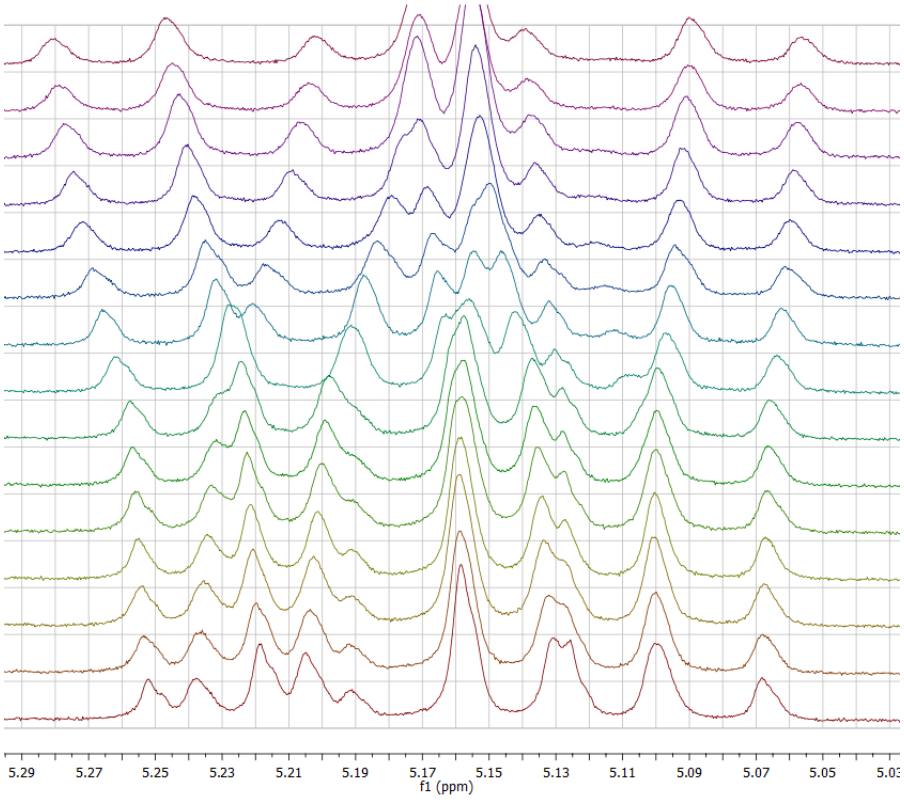

Figure S16. Chemical shifts of H-12 protons during titration of **G1** with ***M*-4a**.

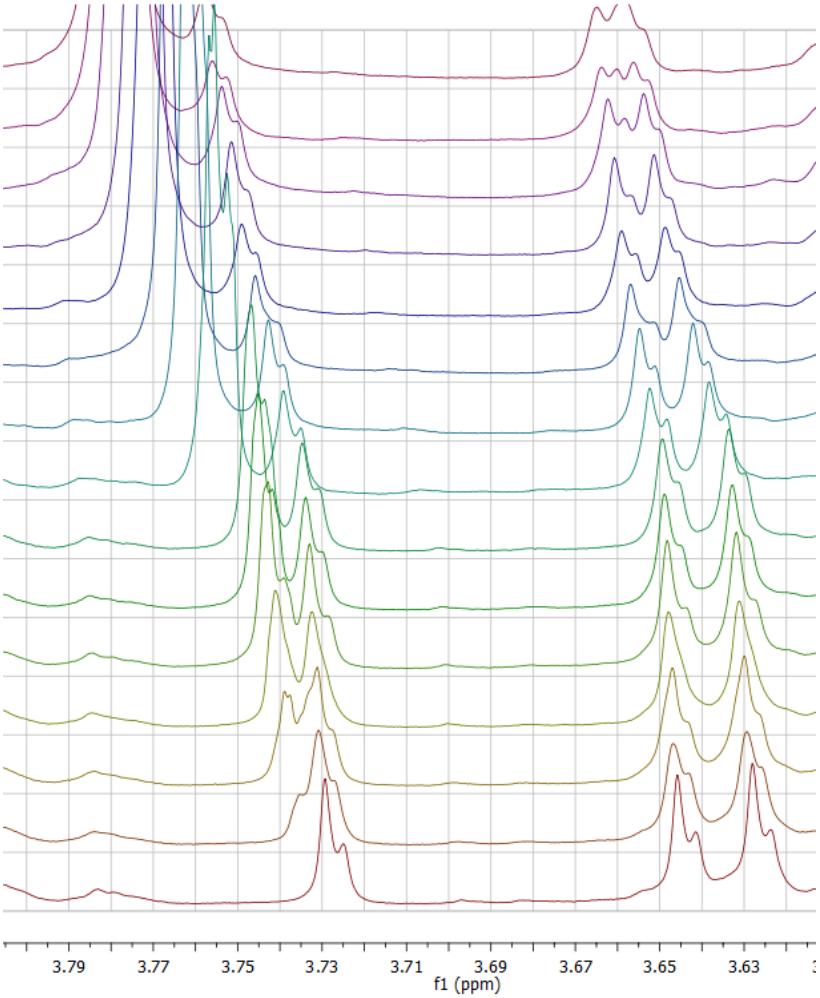

Figure S17. Chemical shifts of methoxy protons during titration of **G1** with ***M*-4a**.

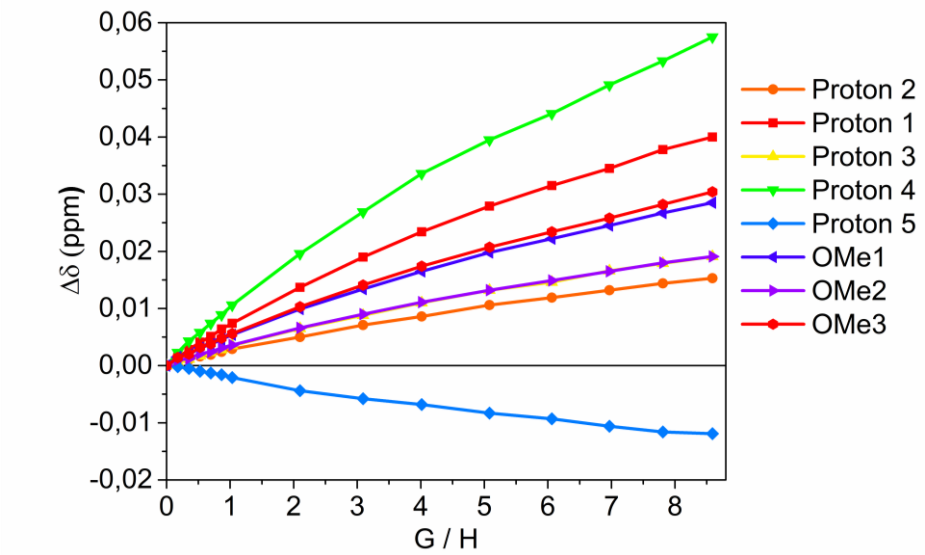

Figure S18. Titration curve for ***M*-4a** and 1,3-dimethylimidazolium hexafluorophosphate complex.

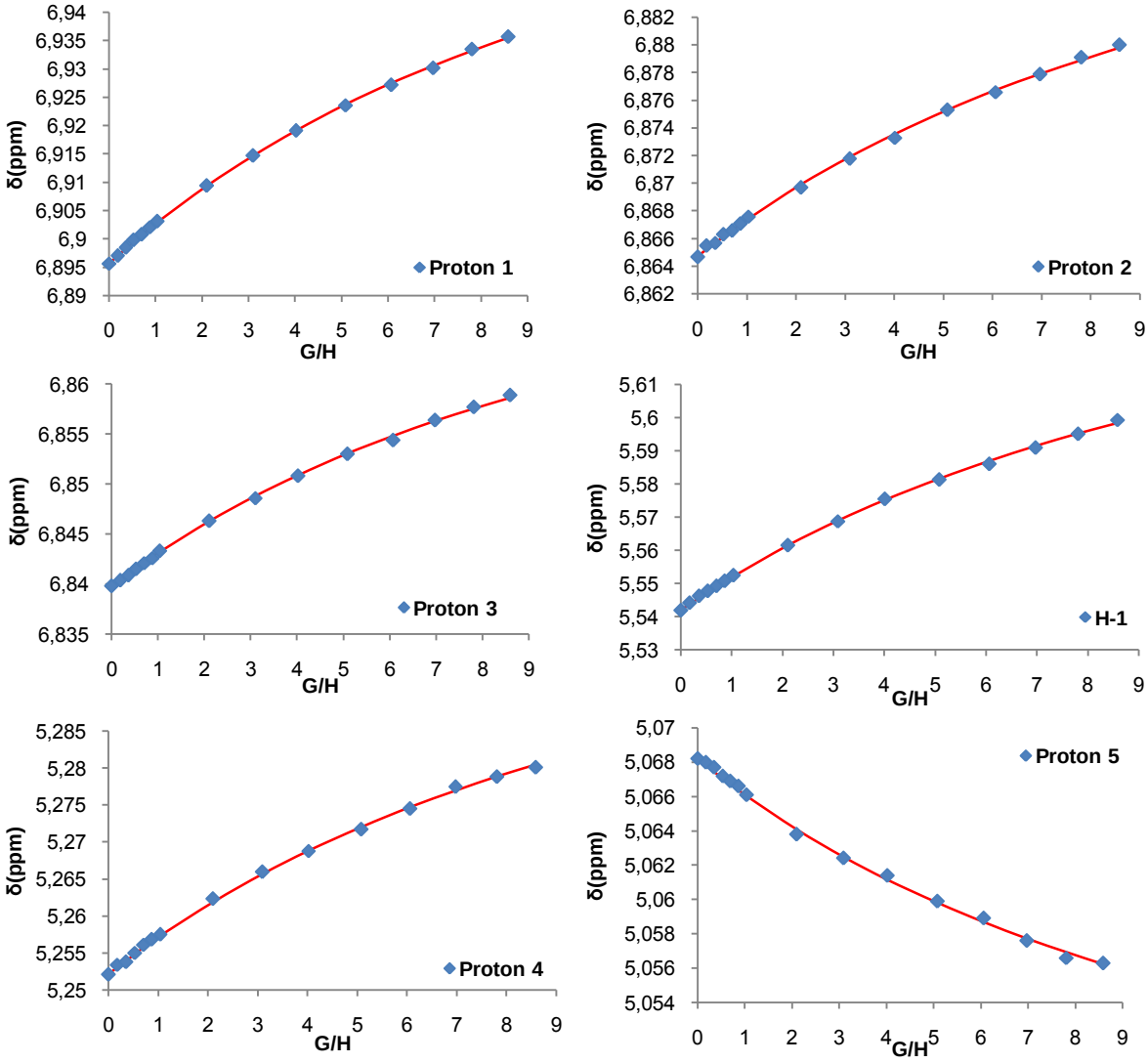

Figure S19. Titration curves of ***M*-4a** protons.

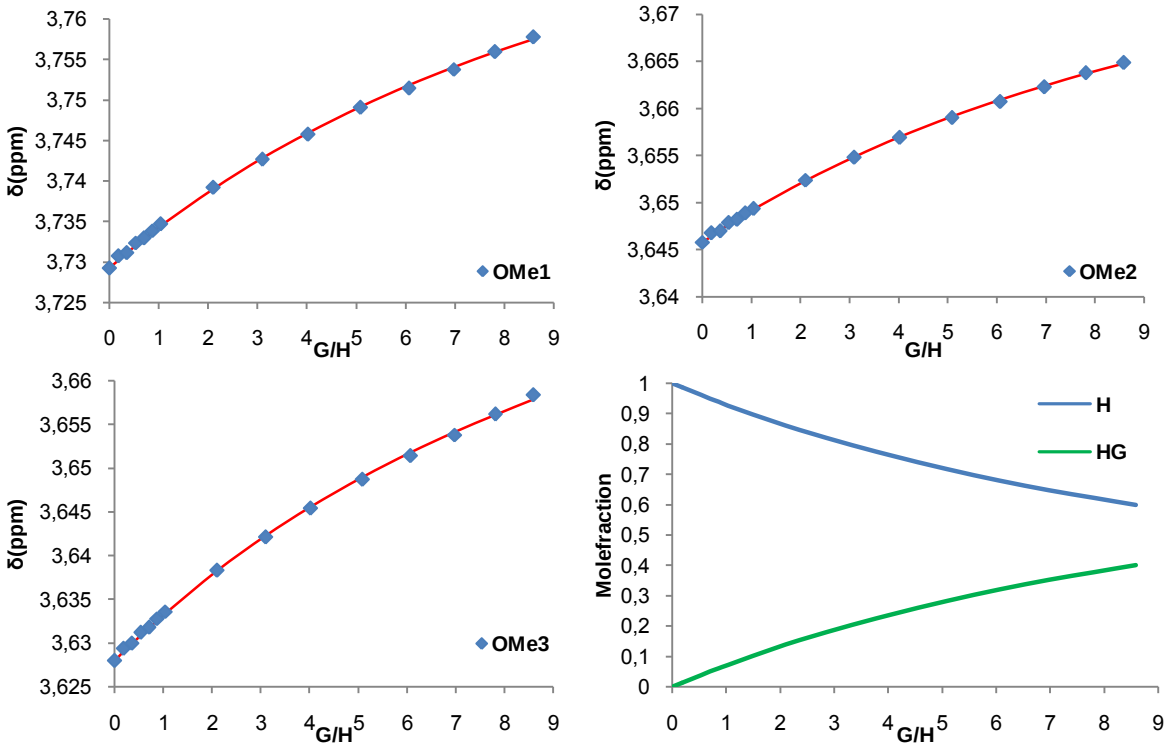

$K_a = 14.6 \pm 0.1\ M^{-1}$ RMS = $2.5607 \cdot 10^{-4}\ M^{-1}$

Figure S20. Titration curves of ***M*-4a** protons and K_a value.

1.4. Titration of 1-methylpyridinium hexafluorophosphate with *M*-4a

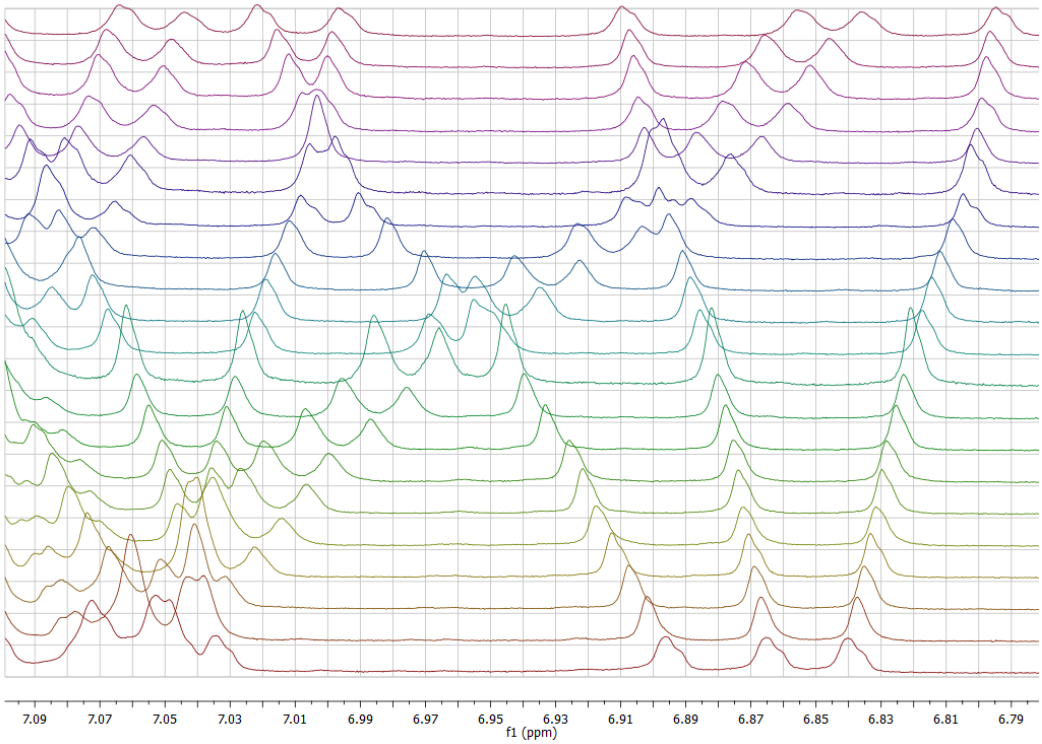

Figure S21. Chemical shifts of CTV aromatic part protons during titration of **G2** with ***M*-4a**.

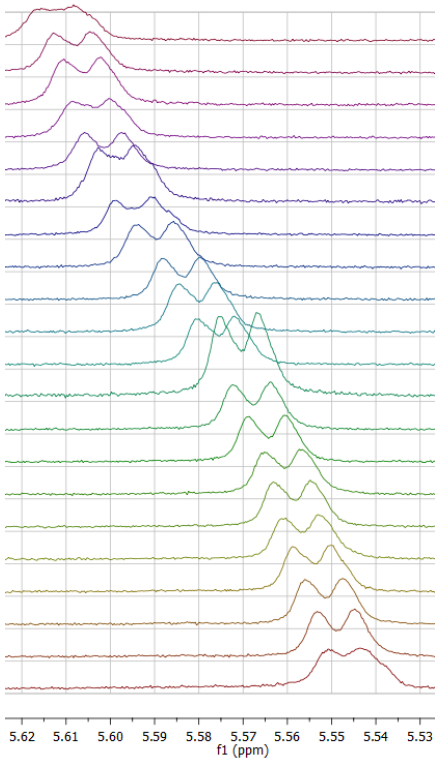

Figure S22. Chemical shifts of H-1 proton during titration of **G2** with ***M*-4a**.

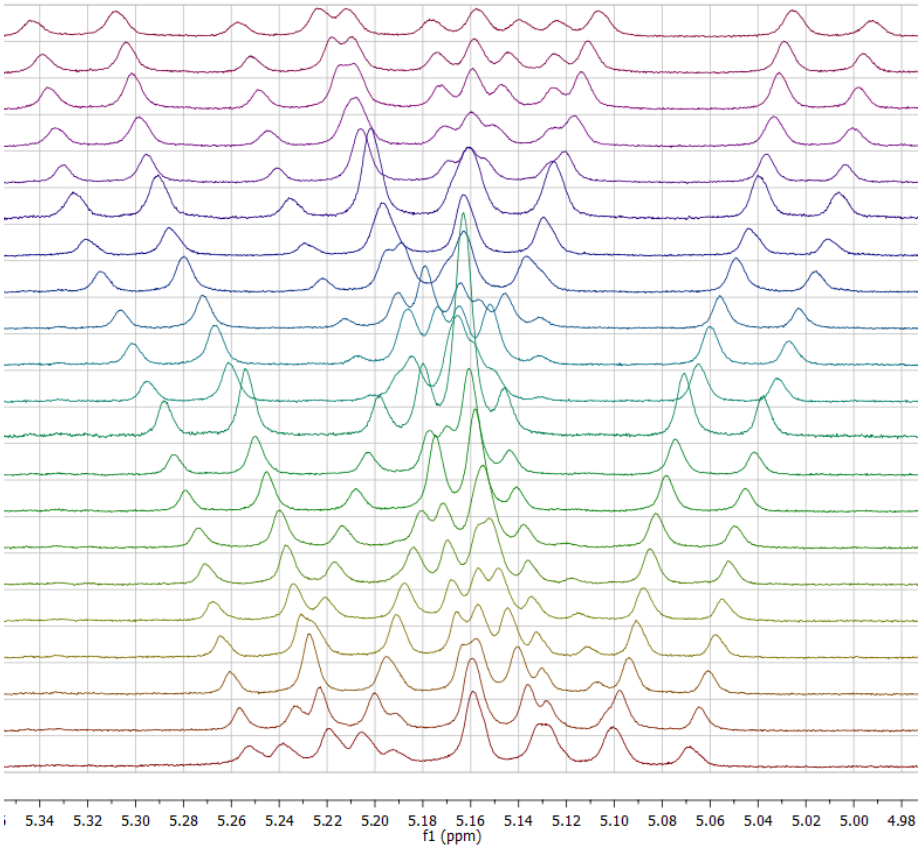

Figure S23. Chemical shifts of H-12 protons during titration of **G2** with ***M*-4a**.

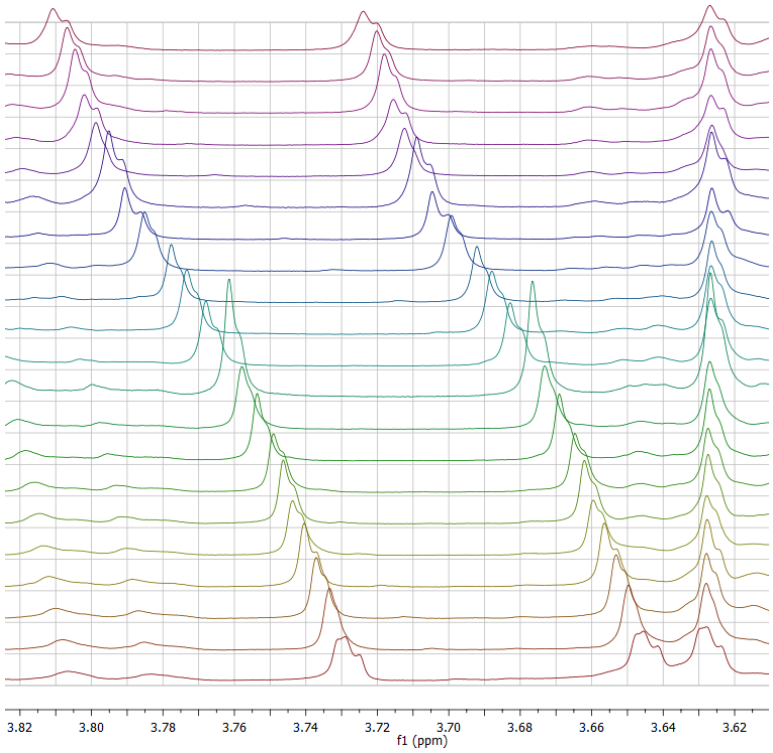

Figure S24. Chemical shifts of methoxy protons during titration of **G2** with ***M*-4a**.

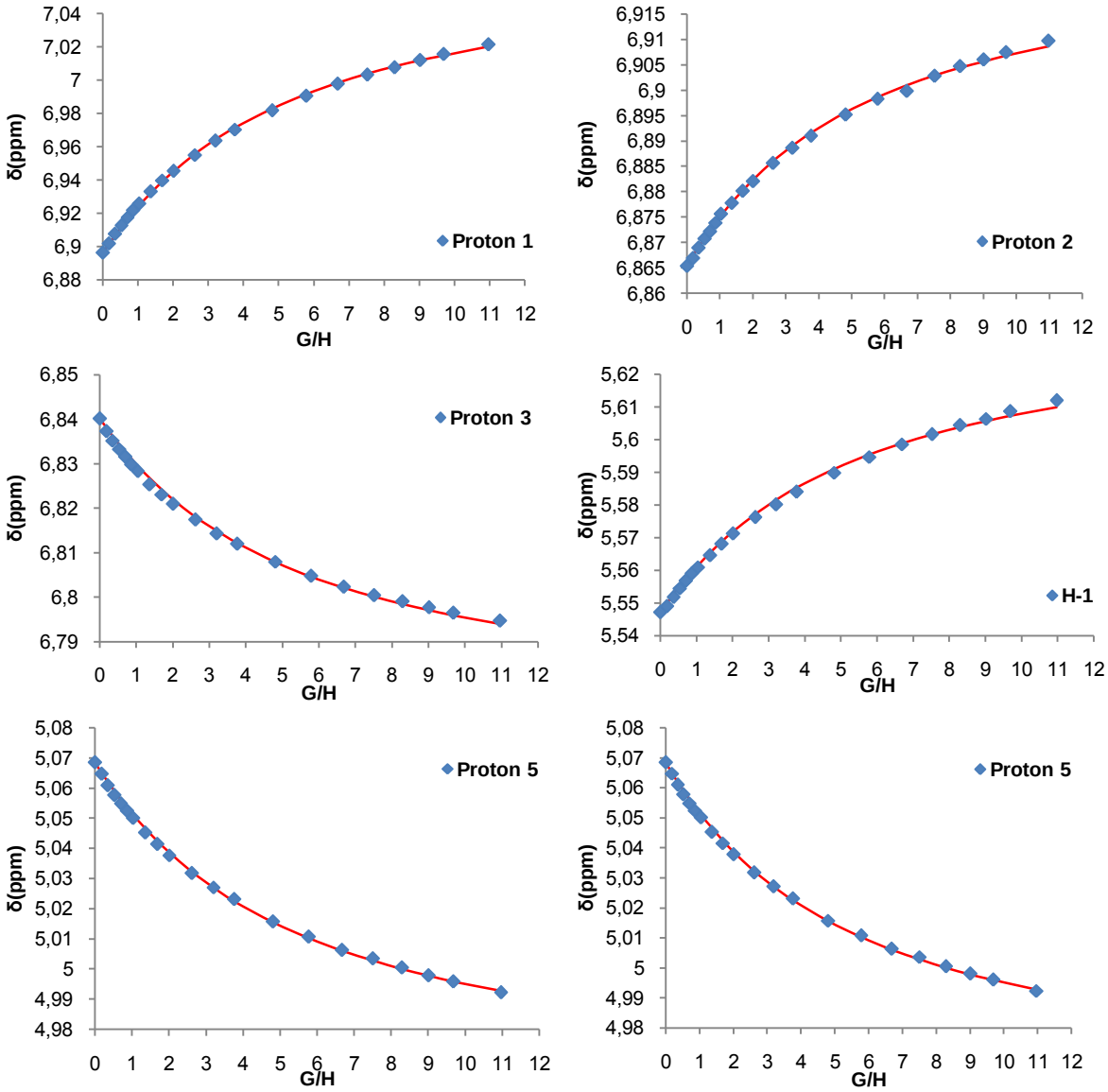

Figure S25. Titration curves of ***M*-4a** protons.

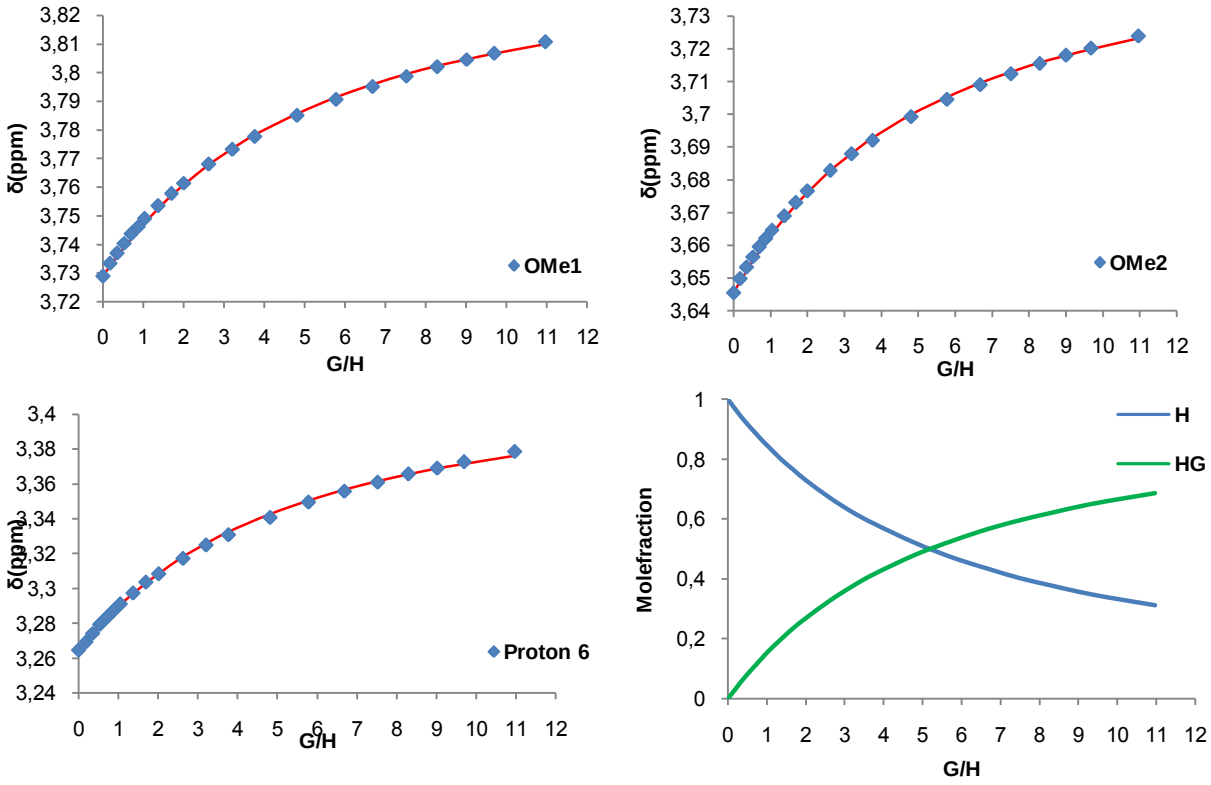

$K_a = 38.2 \pm 0.2\ M^{-1}$ RMS = $7.7804 \cdot 10^{-4}\ M^{-1}$

Figure S26. Titration curves of ***M*-4a** protons and K_a value.

2. Geometry of calculated structures

P-4a

Symbolic Z-matrix:

C	-3.833849	-3.465875	-1.302737
C	-3.764752	-2.345390	-2.361059
C	-3.308488	-0.991707	-1.789944
C	-1.841272	-2.185682	-0.221819
C	-3.047570	-3.125171	-0.022374
O	-2.097986	-1.065091	-1.103984
O	-3.376186	-4.717230	-1.810441
O	-4.997853	-2.207148	-3.057594
O	-4.312519	-0.457774	-0.895029
O	-3.938890	-2.581908	0.952168
C	-0.550764	-2.856895	-0.678866
O	-0.663519	-3.321377	-2.016871
C	-6.544732	1.556422	0.467805
C	-7.537895	0.969277	-0.551691
C	-5.225568	0.573646	-1.251303
C	-6.684930	-0.006913	-1.372947
O	-5.252937	1.486271	-0.159412
O	-6.790354	-1.349233	-0.935407
C	-4.860180	1.347730	-2.521212
C	-6.522020	0.897600	1.842127
O	-3.601756	1.974997	-2.363111
H	-3.009067	-2.631999	-3.098107
H	-7.024711	0.000469	-2.410684
H	-8.375849	0.448019	-0.072810
H	-6.771329	2.617279	0.631610
H	-4.879742	-3.565243	-0.981199
H	-2.681487	-4.063291	0.405355
H	-1.634429	-1.758094	0.767305
H	0.270170	-2.130633	-0.602793
H	-0.325876	-3.682628	0.011043
H	-5.655385	2.091058	-2.674284
H	-5.800254	1.427588	2.473520
H	-4.864153	0.671456	-3.389801
C	2.635004	4.394662	0.054296
C	3.064904	4.047127	1.336035
C	3.389909	3.941459	-1.052520
C	4.204259	3.263162	1.577296
H	2.483666	4.381895	2.187328
C	4.549125	3.207612	-0.803855
C	4.978046	2.849525	0.481473
H	5.125395	2.900122	-1.672355
C	1.472235	0.676220	3.965160
C	1.919411	-0.634480	3.681935
C	2.356968	1.733482	3.790093

C	3.253112	-0.815960	3.311957
C	3.674970	1.564736	3.341186
H	1.973939	2.730253	3.989768
C	4.143427	0.257420	3.127756
H	3.618569	-1.821727	3.136011
C	6.182976	-2.179917	-0.394359
C	6.502207	-1.203276	-1.364047
C	5.861887	-1.752198	0.893842
C	6.478370	0.141801	-0.990925
C	5.858933	-0.404106	1.283041
H	5.654997	-2.527978	1.626328
C	6.176485	0.564768	0.313286
O	6.861927	-1.641031	-2.610675
O	1.001343	-1.643396	3.788565
C	7.226653	-0.674774	-3.593805
H	7.464699	-1.244653	-4.492941
H	6.399751	0.013071	-3.805711
H	8.107308	-0.101433	-3.280875
C	1.416546	-2.971661	3.480880
H	1.772608	-3.047874	2.446541
H	2.204049	-3.313856	4.163059
H	0.530584	-3.595220	3.608452
C	4.470369	2.824334	3.014443
H	4.154385	3.624709	3.692686
H	5.537935	2.680451	3.193330
C	5.586649	-0.072526	2.748113
H	5.890115	-0.942488	3.341934
H	6.243725	0.740924	3.066960
H	6.751838	0.893830	-1.722323
C	6.275214	2.056940	0.611355
H	6.998490	2.487077	-0.091035
H	6.706774	2.207727	1.603876
H	-3.141834	-0.285574	-2.599058
H	-4.244886	-1.717719	0.615643
H	-5.685810	-2.089103	-2.368824
H	-6.511043	-1.371204	0.004281
H	-3.871462	-4.891075	-2.627764
O	1.519072	5.147573	-0.190775
C	0.695757	5.526717	0.906926
H	0.324958	4.649415	1.450375
H	1.230358	6.186105	1.601579
H	-0.145645	6.066630	0.470283
O	-6.150113	-0.476062	1.729627
H	-7.514664	0.985060	2.309047
O	6.314433	-3.537857	-0.567584
O	3.110167	4.117746	-2.386852
O	0.179203	1.015605	4.276818
C	2.119623	5.020939	-2.888855
H	2.484395	5.270009	-3.892578
H	2.097122	5.943057	-2.305272

C	0.731798	4.417159	-2.994953
C	-0.358393	5.250663	-3.269868
C	0.509185	3.040833	-2.874033
C	-1.640258	4.720136	-3.420011
H	-0.209361	6.324618	-3.360642
C	-0.773217	2.511720	-3.021876
H	1.344762	2.382140	-2.659877
C	-1.865060	3.343723	-3.301828
H	-2.475107	5.385725	-3.626668
H	-0.928721	1.441962	-2.908093
C	5.839846	-4.207290	-1.763879
H	6.252575	-5.213907	-1.657980
H	6.271392	-3.739824	-2.647896
C	4.335461	-4.272678	-1.870088
C	3.616631	-5.260685	-1.186644
C	3.629400	-3.360057	-2.667619
C	2.228789	-5.342150	-1.305350
H	4.147744	-5.976477	-0.563258
C	2.243165	-3.442882	-2.787907
H	4.175614	-2.591080	-3.208225
C	1.526121	-4.441501	-2.114235
H	1.686793	-6.119555	-0.771551
H	1.708348	-2.729996	-3.410385
C	-0.593929	0.273914	5.230585
H	-0.684469	0.892254	6.134199
H	-0.085028	-0.651320	5.507129
C	-1.964382	-0.024039	4.654893
C	-2.953890	-0.620546	5.448550
C	-2.273260	0.282150	3.327582
C	-4.207614	-0.922485	4.915675
H	-2.746359	-0.853892	6.490993
C	-3.525001	-0.024709	2.792930
H	-1.524442	0.760248	2.706516
C	-4.504821	-0.643877	3.574154
H	-4.957780	-1.390805	5.549880
H	-3.734421	0.222182	1.757859
C	0.020482	-4.544735	-2.267620
H	-0.371061	-5.337866	-1.614556
H	-0.242148	-4.805456	-3.298841
C	-5.834432	-1.088583	2.984873
H	-6.652665	-0.916225	3.698759
H	-5.798668	-2.160210	2.768308
C	-3.245775	2.766882	-3.498968
H	-3.981918	3.572101	-3.641323
H	-3.274878	2.135623	-4.402460
O	-8.003390	1.963308	-1.462253
H	-8.484736	2.636131	-0.953592

Imaginary Frequency = 0

E(RB3LYP) = -3600.99227134 a.u.

***P*-4b**

Symbolic Z-matrix:

C	7.674130	-0.519836	-0.222009
C	6.764162	0.704337	-0.400483
C	5.346620	0.348101	0.100235
C	5.621381	-1.678103	-1.237931
C	7.172356	-1.658087	-1.125949
O	4.991995	-1.008550	-0.141928
O	7.683761	-1.000374	1.117943
O	6.794111	1.146836	-1.753983
O	4.436415	1.258950	-0.496999
O	7.766180	-1.407441	-2.413951
C	5.047961	-3.100600	-1.299513
O	5.608680	-4.038736	-0.389173
C	2.471750	3.861800	-0.305037
C	3.706432	4.094579	0.560072
C	3.318828	1.733959	0.261484
C	3.747620	2.787041	1.340938
O	2.557993	2.479463	-0.679595
O	4.997491	2.488256	1.933915
O	3.615463	5.212104	1.425798
C	2.423628	0.592348	0.827986
C	2.400555	4.752468	-1.539057
O	1.359004	0.200126	-0.017703
O	2.383613	6.115710	-1.092561
H	7.111056	1.539769	0.218898
H	2.963700	2.838792	2.110639
H	4.602771	4.153856	-0.077195
H	1.574968	4.026256	0.306425
H	8.690158	-0.264845	-0.553257
H	7.532781	-2.609168	-0.721550
H	5.345850	-1.173123	-2.175834
H	3.957942	-3.042301	-1.185128
H	5.260399	-3.516269	-2.290846
H	1.929122	0.958147	1.732224
H	3.293453	4.609908	-2.159423
H	1.518116	4.518134	-2.144828
H	3.045126	-0.267758	1.101790
C	5.304532	-3.860043	1.003689
H	5.883008	-4.651036	1.495022
H	5.681367	-2.896153	1.359454
C	-0.403318	-4.358699	2.189221
H	-0.925813	-4.157333	1.245361
H	-0.676346	-5.375242	2.503950
C	1.722906	-0.487596	-1.213394
H	2.448731	0.107611	-1.782948
H	2.204180	-1.444906	-0.969473
C	-3.186452	4.214955	1.689629

H	-2.817370	3.218750	1.962375
H	-3.420627	4.745525	2.619948
C	1.136552	6.812510	-1.274658
H	1.347719	7.829644	-0.931188
H	0.899627	6.855921	-2.346153
C	-6.104763	4.629157	-1.568763
H	-7.149085	4.293852	-1.591856
H	-5.901996	5.246593	-2.446441
O	-0.824071	-3.417339	3.178582
O	-5.213465	3.507524	-1.653908
C	-5.344426	2.578104	-0.643787
C	-5.891086	1.332980	-0.934696
C	-4.887733	2.835728	0.660422
C	-5.989177	0.309867	0.020045
H	-6.244015	1.167733	-1.949075
C	-5.017589	1.838755	1.628729
C	-5.550539	0.572454	1.333844
H	-4.713297	2.061142	2.647666
C	-4.220853	-2.761825	-2.868617
C	-3.807023	-3.902419	-2.149438
C	-5.120049	-1.879960	-2.282050
C	-4.255903	-4.063149	-0.839083
C	-5.577446	-2.035039	-0.962129
H	-5.475558	-1.039887	-2.872256
C	-5.102189	-3.126938	-0.217992
H	-3.929565	-4.923964	-0.266661
C	-2.023971	-2.782445	2.999131
C	-2.149166	-1.490535	3.560507
C	-3.106613	-3.331820	2.325678
C	-3.342567	-0.797888	3.381255
C	-4.306454	-2.624230	2.118741
H	-3.023322	-4.341576	1.937835
C	-4.421371	-1.330412	2.646134
O	-1.062118	-1.024454	4.242673
O	-2.983496	-4.770170	-2.805400
O	-4.390443	4.088258	0.921553
C	-1.135641	0.283664	4.801122
H	-0.172389	0.455728	5.283634
H	-1.295851	1.042018	4.024817
H	-1.935206	0.355750	5.548596
C	-2.540900	-5.929652	-2.107206
H	-1.951578	-5.664253	-1.220740
H	-3.384242	-6.562623	-1.804963
H	-1.910880	-6.477298	-2.809789
C	-6.584764	-1.020455	-0.425158
H	-7.303023	-0.810921	-1.226213
H	-7.169765	-1.464104	0.383439
C	-5.378027	-3.306359	1.270781
H	-5.373568	-4.377425	1.502563
H	-6.373970	-2.945965	1.535574

H	-3.448200	0.193950	3.806239
C	-5.652825	-0.444757	2.469569
H	-5.806024	0.110239	3.402086
H	-6.547134	-1.058959	2.341697
H	-5.923609	5.210412	-0.659885
H	5.324191	0.446533	1.182941
C	-2.117008	4.964451	-0.492230
C	-1.076709	5.584486	-1.188755
C	-0.024106	6.210034	-0.512416
C	-0.050239	6.226040	0.890873
C	-1.087404	5.612479	1.589825
C	-2.123735	4.960194	0.905543
H	-2.926270	4.485680	-1.034228
H	-1.083339	5.574914	-2.276462
H	0.754479	6.709686	1.439315
H	-1.089356	5.635265	2.677423
C	1.736911	-5.218666	1.183607
C	3.088886	-5.095565	0.872327
C	3.834151	-4.002343	1.338551
C	3.189890	-3.051888	2.135544
C	1.832344	-3.168153	2.446690
C	1.090459	-4.248239	1.963654
H	1.174719	-6.071048	0.807335
H	3.571827	-5.846945	0.252824
H	3.753287	-2.201377	2.510855
H	1.339450	-2.412878	3.049015
H	7.452112	-2.080670	-3.039774
H	7.103258	0.406302	-2.311461
H	5.184701	3.200267	2.567577
H	3.383686	5.964187	0.850339
H	8.071301	-0.308446	1.678281
C	-3.083795	-1.357015	-4.441021
H	-2.834780	-1.436353	-5.504051
H	-3.774018	-0.512847	-4.324286
C	-1.841613	-1.135472	-3.603611
C	-0.856859	-2.127361	-3.504069
C	-1.651371	0.065859	-2.910626
C	0.280358	-1.922707	-2.723209
H	-1.002112	-3.076775	-4.010856
C	-0.504850	0.277578	-2.143327
H	-2.410646	0.842921	-2.964571
C	0.473911	-0.717673	-2.034796
H	1.023786	-2.712700	-2.641821
H	-0.374268	1.211340	-1.605996
O	-3.754415	-2.602619	-4.157241

Imaginary Frequency = 0

E(RB3LYP) = -3600.97786967 a.u.

***M*-4a**

Symbolic Z-matrix:

C	6.286494	1.394750	-0.805196
C	5.609582	0.455312	-1.848279
C	4.115107	0.167848	-1.553871
C	3.970801	1.877069	0.193658
C	5.448027	1.524742	0.480107
O	3.456740	1.277222	-1.017047
O	6.614010	2.663359	-1.357786
O	6.321727	-0.752563	-2.065415
O	3.972335	-0.945433	-0.642678
O	5.541196	0.329875	1.260481
C	3.628701	3.362843	0.103107
O	4.170263	3.921161	-1.091600
C	3.028641	-3.886871	0.577837
C	4.244856	-4.467550	-0.166610
C	3.652403	-2.272273	-1.053189
C	4.877548	-3.236316	-0.826428
O	2.625274	-2.731640	-0.179155
O	5.909076	-2.664678	-0.042863
C	3.155181	-2.389732	-2.497386
O	2.007556	-1.578204	-2.676570
H	5.638797	0.995837	-2.799602
H	5.335249	-3.515244	-1.777139
H	4.956308	-4.960244	0.507583
H	2.200237	-4.604946	0.550546
H	7.239463	0.934248	-0.527098
H	5.885191	2.316022	1.097198
H	3.397803	1.488531	1.045871
H	2.538511	3.464482	0.092725
H	4.015319	3.888304	0.988882
H	2.928969	-3.449576	-2.664180
H	3.956545	-2.096374	-3.191234
C	-4.926754	-2.862588	-1.656043
C	-5.144485	-2.556930	-0.313262
C	-5.179517	-1.861555	-2.619585
C	-5.574233	-1.300044	0.133765
H	-4.993663	-3.363104	0.399857
C	-5.556751	-0.591375	-2.176538
C	-5.755737	-0.283272	-0.821086
H	-5.744735	0.184080	-2.910550
C	-2.879589	-1.539492	3.937683
C	-2.625624	-0.220689	4.353134
C	-3.930404	-1.779072	3.054835
C	-3.428468	0.806154	3.854570
C	-4.731158	-0.751255	2.535135
H	-4.119478	-2.811443	2.772483
C	-4.466456	0.572912	2.939650

H	-3.251341	1.817735	4.209855
C	-2.881682	3.882448	0.303971
C	-3.276391	3.567169	-1.016574
C	-3.577969	3.303343	1.363625
C	-4.345482	2.693101	-1.197226
C	-4.633658	2.396113	1.176069
H	-3.284959	3.548346	2.378026
C	-5.032737	2.085168	-0.133974
O	-2.650913	3.998719	-2.162646
O	-1.657066	-0.000839	5.304030
C	-0.611088	0.962354	5.017506
H	-0.949336	1.661997	4.247785
H	-0.461452	1.516217	5.948642
C	-5.888962	-1.136911	1.618789
H	-6.278579	-2.097294	1.974855
H	-6.710099	-0.426550	1.742691
C	-5.249402	1.778417	2.427758
H	-5.259692	2.538834	3.216490
H	-6.294792	1.513872	2.255588
H	-4.637317	2.480866	-2.222241
C	-6.182406	1.138633	-0.471359
H	-6.715334	1.552410	-1.334957
H	-6.910102	1.124642	0.344126
H	3.578886	-0.055087	-2.471427
H	4.987904	-0.347594	0.823684
H	6.307190	-1.265733	-1.228616
H	5.535583	-2.487100	0.849095
H	5.788395	3.188999	-1.424431
O	-4.582416	-4.169291	-1.908341
O	4.207724	-2.466410	2.140427
C	-1.654889	-3.599287	-2.165070
C	-2.087271	-3.474150	-4.528872
C	-0.428084	-2.957357	-2.353748
H	-1.961341	-3.888749	-1.163271
C	-0.857049	-2.850944	-4.722753
H	-2.736495	-3.659565	-5.381047
C	-0.018203	-2.575739	-3.635023
H	0.218972	-2.748122	-1.508139
H	-0.556338	-2.556869	-5.726568
C	0.064272	6.399636	-1.483103
C	0.194381	4.249191	-2.554839
C	1.444456	6.378459	-1.273465
H	-0.519808	7.242195	-1.120324
C	1.574053	4.232229	-2.356898
H	-0.292526	3.404611	-3.033479
C	2.213747	5.287815	-1.693199
H	1.920291	7.205692	-0.751198
H	2.156718	3.371658	-2.672166
C	1.496942	-0.320534	5.554833
C	1.014060	0.158527	3.245333

C	2.644541	-1.013359	5.171467
H	1.239966	-0.247641	6.609021
C	2.171444	-0.519489	2.859474
H	0.378301	0.607063	2.485662
C	2.997941	-1.117504	3.820334
H	3.271545	-1.476308	5.930187
H	2.418144	-0.614852	1.806479
C	3.703385	5.237457	-1.409593
H	3.957924	5.935461	-0.599175
H	4.285259	5.525368	-2.291679
C	4.275105	-1.837502	3.426278
H	4.545080	-2.578325	4.191565
H	5.099165	-1.123853	3.334486
C	1.280167	-1.825857	-3.874990
H	1.906088	-2.363624	-4.600638
H	1.057386	-0.846440	-4.317392
O	3.849814	-5.339427	-1.222513
H	3.375315	-6.091643	-0.832589
C	-2.504003	-3.855949	-3.246824
C	0.661384	0.267752	4.596135
C	-0.580610	5.323385	-2.101072
C	-3.827432	-4.566011	-3.069475
H	-3.664580	-5.634553	-2.890405
H	-4.434121	-4.460945	-3.970910
C	-2.085880	5.319603	-2.272403
H	-2.559847	6.004998	-1.566091
H	-2.352931	5.642743	-3.286016
O	-5.074930	-2.208456	-3.938706
O	-1.829717	4.737996	0.458768
O	-2.098961	-2.595603	4.353595
C	-2.279794	-2.987563	5.720598
H	-3.319162	-3.288266	5.904657
H	-1.621801	-3.844519	5.881915
H	-2.004652	-2.179163	6.404597
C	-5.244008	-1.194167	-4.923993
H	-4.514840	-0.385447	-4.794874
H	-5.077247	-1.683923	-5.884396
H	-6.258241	-0.777496	-4.899858
C	-1.388899	5.051215	1.774917
H	-1.066010	4.151480	2.313010
H	-0.539256	5.723149	1.646326
H	-2.172371	5.557857	2.351733
C	3.248982	-3.520338	2.042875
H	3.589943	-4.403634	2.602909
H	2.295529	-3.191599	2.468235

Imaginary Frequency = 0

E(RB3LYP) = -3600.99799979 a.u.

***M*-4b**

Symbolic Z-matrix:

C	6.486408	3.404560	1.498932
C	6.597126	1.928636	1.091919
C	5.560586	1.639743	-0.028509
C	5.070011	3.763307	2.015232
O	4.479715	2.556610	-0.007219
O	6.840873	4.235030	0.388867
O	6.379317	1.126688	2.242162
O	5.170951	0.291064	0.158153
O	4.893862	3.560077	3.414599
C	5.377504	-0.518698	-2.204797
O	4.427085	-1.762475	-0.409573
O	6.729731	-0.199850	-1.904219
O	4.047687	-2.166165	-3.319794
H	7.598283	1.744248	0.675583
H	4.974487	0.126104	-2.994152
H	7.214854	3.617734	2.287802
H	4.909746	4.818940	1.760379
O	-4.410702	4.779028	-0.767970
C	-2.708052	-3.772915	-1.661402
C	-3.815265	-3.650819	-0.830924
C	-4.771224	-2.627723	-0.992764
H	-3.953808	-4.362098	-0.023958
C	-3.525528	-1.884756	-2.928374
C	-4.623875	-1.729499	-2.058628
H	-3.429870	-1.201487	-3.764695
C	-4.084912	-1.638688	3.315708
C	-4.172786	-0.235651	3.338732
C	-4.684183	-2.335014	2.268829
C	-4.971468	0.392908	2.383657
C	-5.414783	-1.697526	1.255431
H	-4.561794	-3.414897	2.255781
C	-5.612764	-0.306140	1.353174
H	-5.068526	1.473125	2.449897
C	-4.628519	3.467549	-1.149535
C	-4.086363	2.931156	-2.331283
C	-5.388720	2.638230	-0.321030
C	-4.421093	1.606873	-2.658432
C	-5.687402	1.309307	-0.627009
H	-5.766689	3.073662	0.600537
C	-5.219370	0.790193	-1.853904
C	-5.871154	-2.531264	0.062903
H	-6.108277	-3.542904	0.410885
H	-6.793958	-2.136313	-0.367418
C	-6.480247	0.495751	0.384419
H	-7.087422	1.189128	0.977353
H	-7.190834	-0.162190	-0.120582

H	-4.046282	1.232749	-3.607432
C	-5.600292	-0.598076	-2.367089
H	-5.690827	-0.528445	-3.457237
H	-6.598957	-0.856985	-2.006724
H	6.012096	1.768234	-1.010950
H	5.349033	4.282344	3.875566
H	6.091430	4.193853	-0.230593
H	6.058424	0.270777	1.903968
H	7.205849	-0.133297	-2.747810
H	4.038834	-3.055362	-3.707412
C	-5.565540	5.623564	-0.837748
H	-5.925513	5.714588	-1.870841
H	-6.378809	5.246420	-0.207306
H	-5.251173	6.603833	-0.472989
O	-3.392767	-2.342315	4.283685
C	-4.119273	-2.498573	5.510286
H	-5.054854	-3.045616	5.341192
H	-3.475294	-3.073113	6.179537
H	-4.346768	-1.527230	5.965824
O	-3.287583	3.549139	-3.255743
O	-3.573643	0.576119	4.272086
C	-2.565322	-2.872358	-2.745437
O	-1.471680	-3.063544	-3.540736
C	-1.279799	-2.171735	-4.633752
H	-2.106984	-2.232278	-5.351995
H	-1.173604	-1.134856	-4.291658
H	-0.355686	-2.489986	-5.118958
C	5.260308	-2.000918	-2.591750
H	6.126046	-2.321245	-3.184138
C	4.003983	2.906805	1.305879
H	3.833594	1.997804	1.892024
C	2.675778	3.625054	1.134704
H	2.312982	3.924955	2.129300
H	1.944788	2.941947	0.686216
O	2.882337	4.770951	0.313648
C	4.526506	-0.431842	-0.891018
C	3.111536	0.123398	-1.160380
H	3.205745	1.121598	-1.593717
H	2.623609	-0.538147	-1.888763
C	5.233052	-2.657659	-1.203396
H	6.254392	-2.684938	-0.799972
O	2.321350	0.279368	0.005668
C	4.637079	-4.049577	-1.175921
H	5.155073	-4.676127	-1.921913
H	3.577000	-3.993741	-1.451265
O	4.799449	-4.605219	0.121527
C	4.211512	-5.900603	0.253835
H	4.620988	-6.586131	-0.503737
H	4.536798	-6.254871	1.237932
C	2.698063	-5.866997	0.164613

C	1.994858	-6.692740	-0.719561
C	1.980076	-4.957100	0.951588
C	0.606583	-6.594989	-0.835003
H	2.537278	-7.406730	-1.335092
C	0.597873	-4.847860	0.825531
H	2.516451	-4.313101	1.643200
C	-0.103510	-5.655012	-0.080083
H	0.077274	-7.232634	-1.538888
H	0.058310	-4.116991	1.422936
O	-1.720807	-4.708363	-1.536089
C	-1.578750	-5.432735	-0.296497
H	-1.992506	-4.849972	0.531331
H	-2.135075	-6.375087	-0.372305
C	-2.212763	0.317910	4.687721
H	-2.188887	-0.495127	5.417777
H	-1.939155	1.244052	5.203991
C	-1.236004	0.025403	3.569219
C	-0.342721	-1.042130	3.697182
C	-1.165556	0.820313	2.414503
C	0.602898	-1.305931	2.704421
H	-0.383795	-1.672828	4.581178
C	-0.242573	0.536570	1.408681
H	-1.850220	1.655862	2.295447
C	0.655947	-0.533761	1.539664
H	1.301280	-2.128817	2.836570
H	-0.213094	1.152231	0.514082
C	1.628234	-0.894222	0.439977
H	1.087726	-1.329294	-0.416942
H	2.333871	-1.651484	0.796065
C	-2.789253	4.894510	-3.115968
H	-2.468498	5.131951	-4.135679
H	-3.592445	5.580898	-2.846565
C	1.851555	5.741783	0.356599
H	1.534497	5.917984	1.396524
H	2.317310	6.670921	0.004045
C	-1.616228	5.039733	-2.168538
C	-1.622314	6.028384	-1.177016
C	-0.468644	4.249108	-2.311840
C	-0.514637	6.221810	-0.354028
H	-2.504666	6.646461	-1.043247
C	0.646390	4.448524	-1.494089
H	-0.442457	3.476342	-3.076397
C	0.636108	5.438985	-0.505356
H	-0.544791	6.993978	0.412325
H	1.537544	3.843132	-1.630024

Imaginary Frequency = 0

E(RB3LYP) = -3600.97783393 a.u.

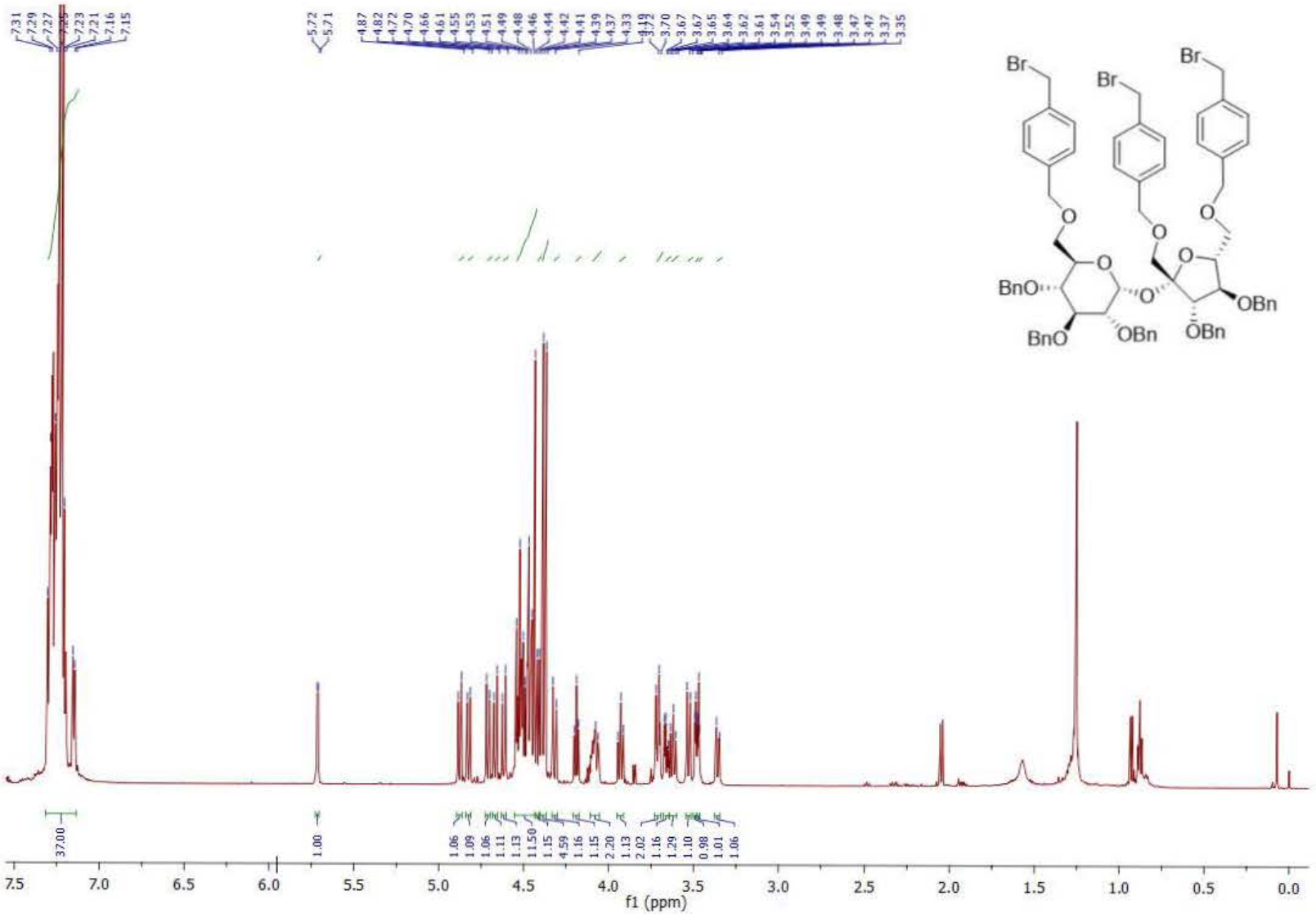

Figure S27. ^{1}H NMR spectrum of compound **2.**

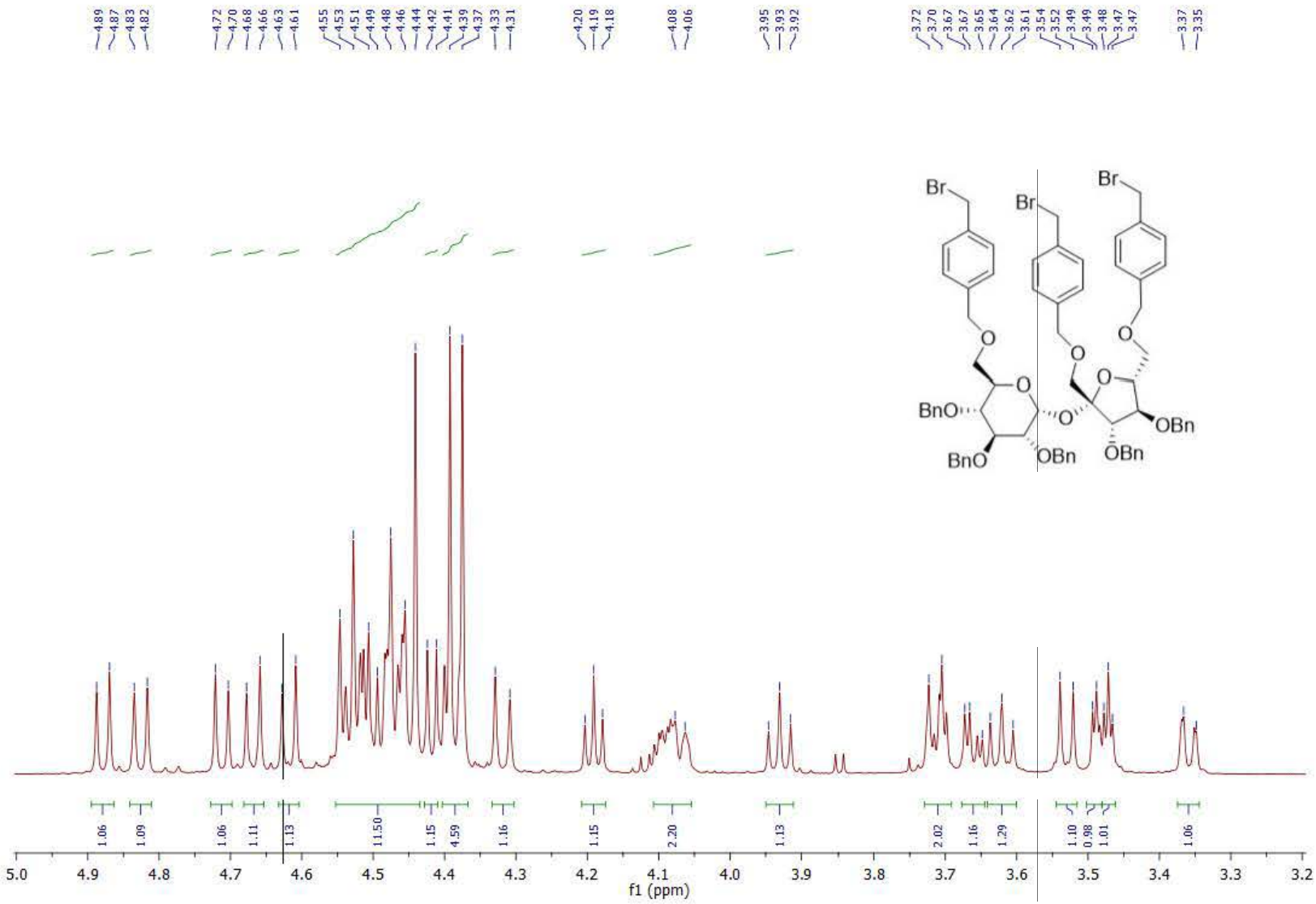

Figure S28. ^{1}H NMR spectrum of compound **2** (aliphatic part).

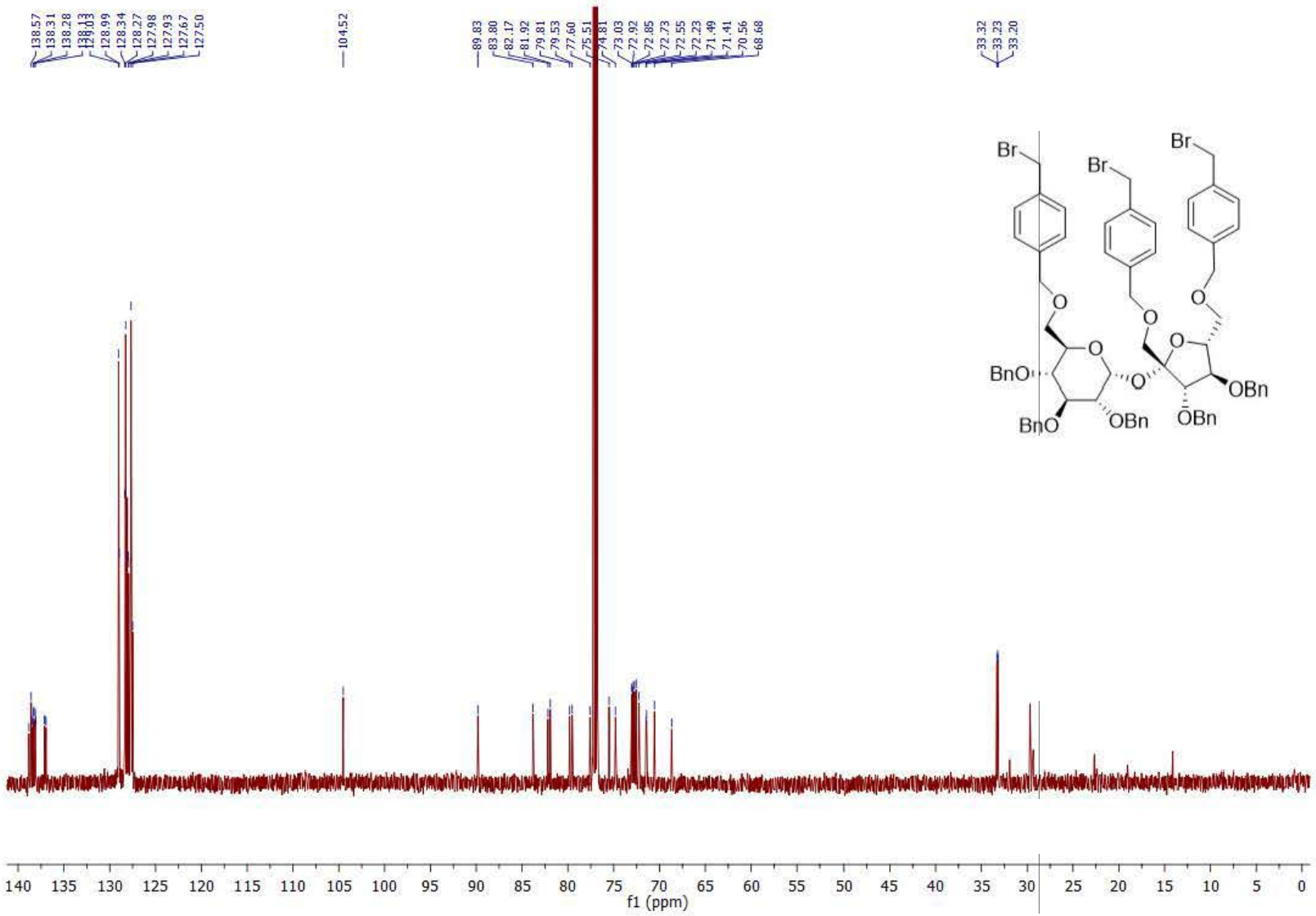

Figure S29. ^{13}C NMR spectrum of compound **2**.

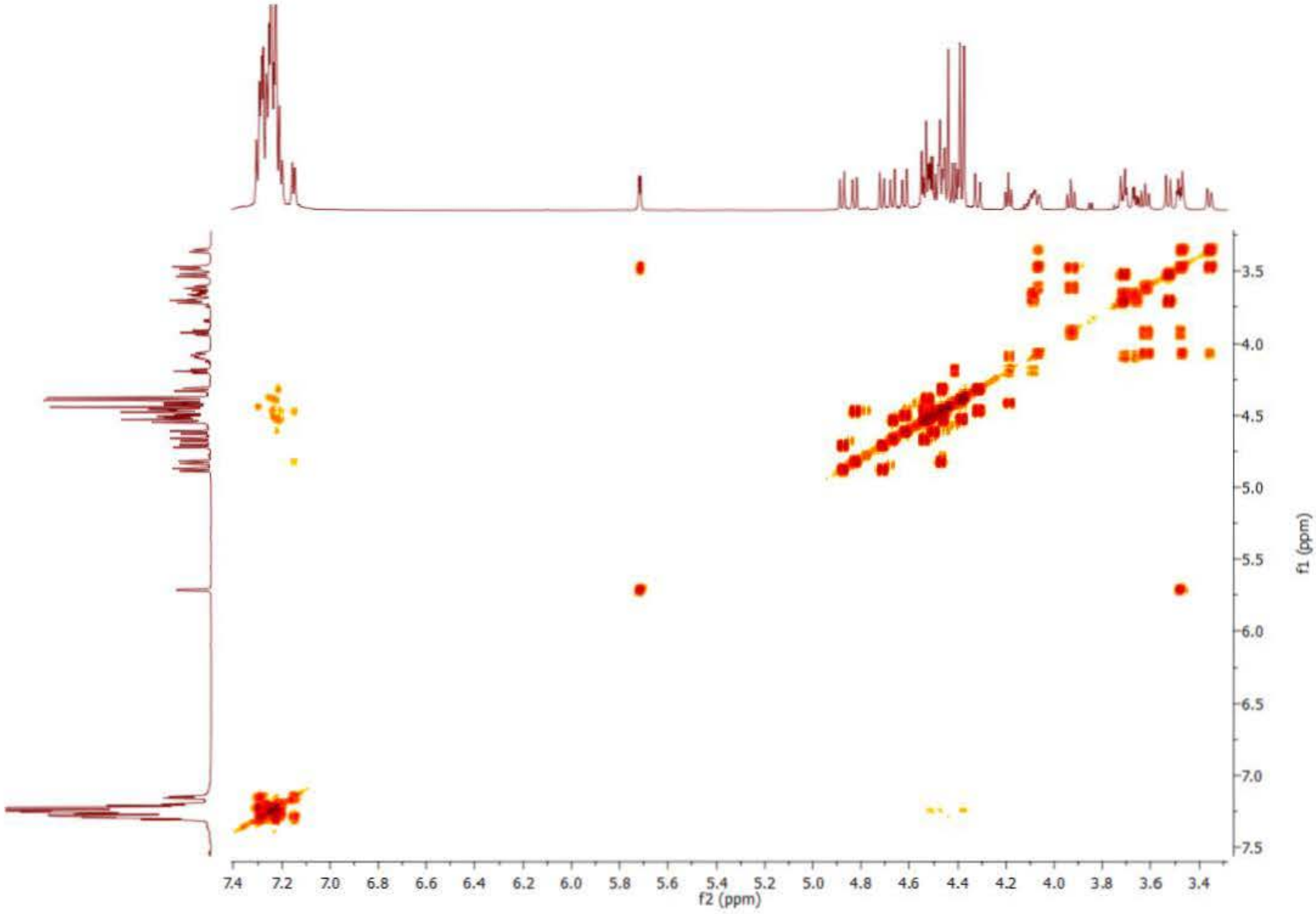

Figure S30. $^{1}H–^{1}H$ COSY spectrum of compound **2**.

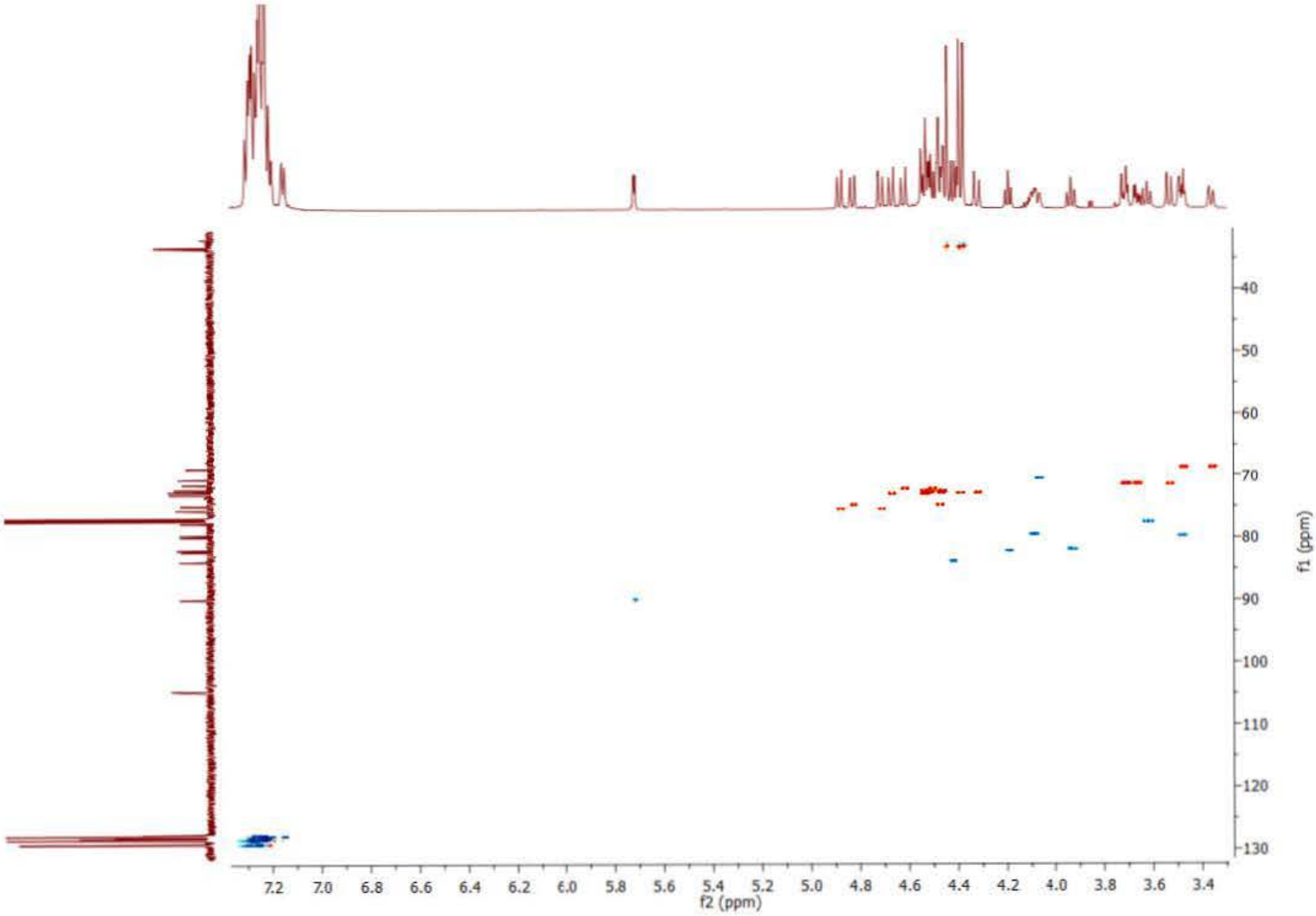

Figure S31. $^{1}H–^{13}C$ HSQC spectrum of compound **2**.

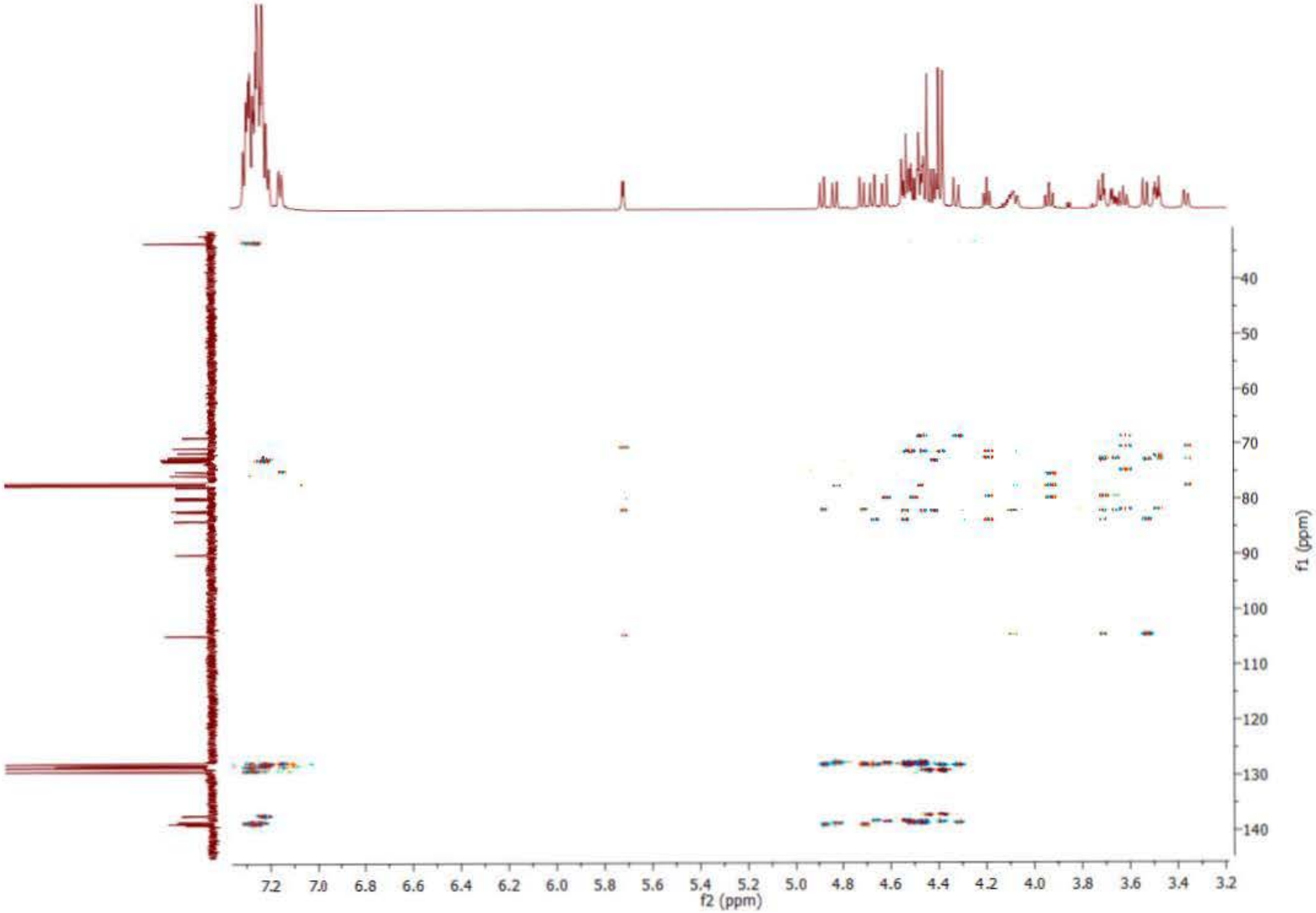

Figure S32. ^{1}H–^{13}C HMBC spectrum of compound **2**.

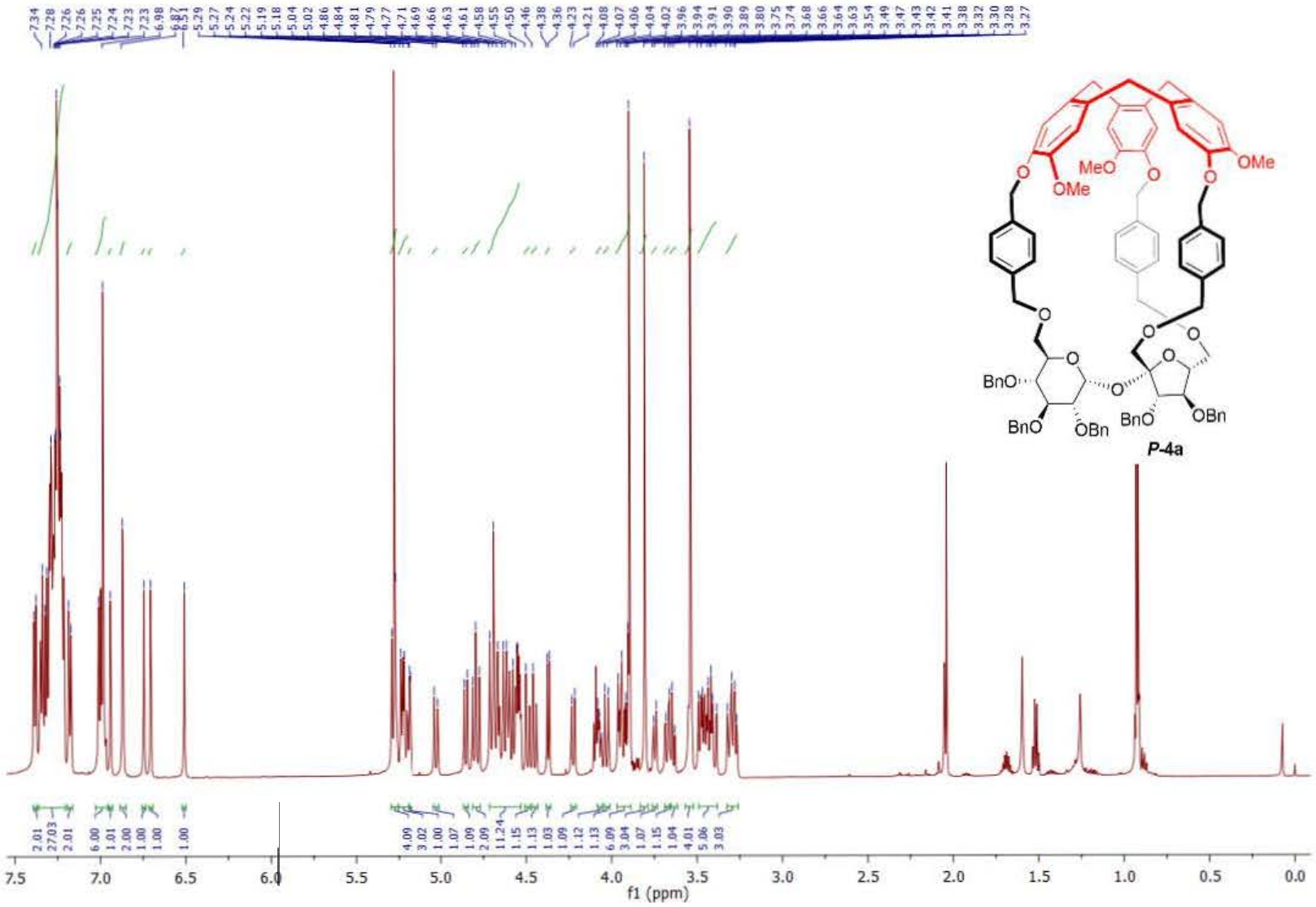

Figure S33.[1]H NMR spectrum of compound ***P*-4a.**

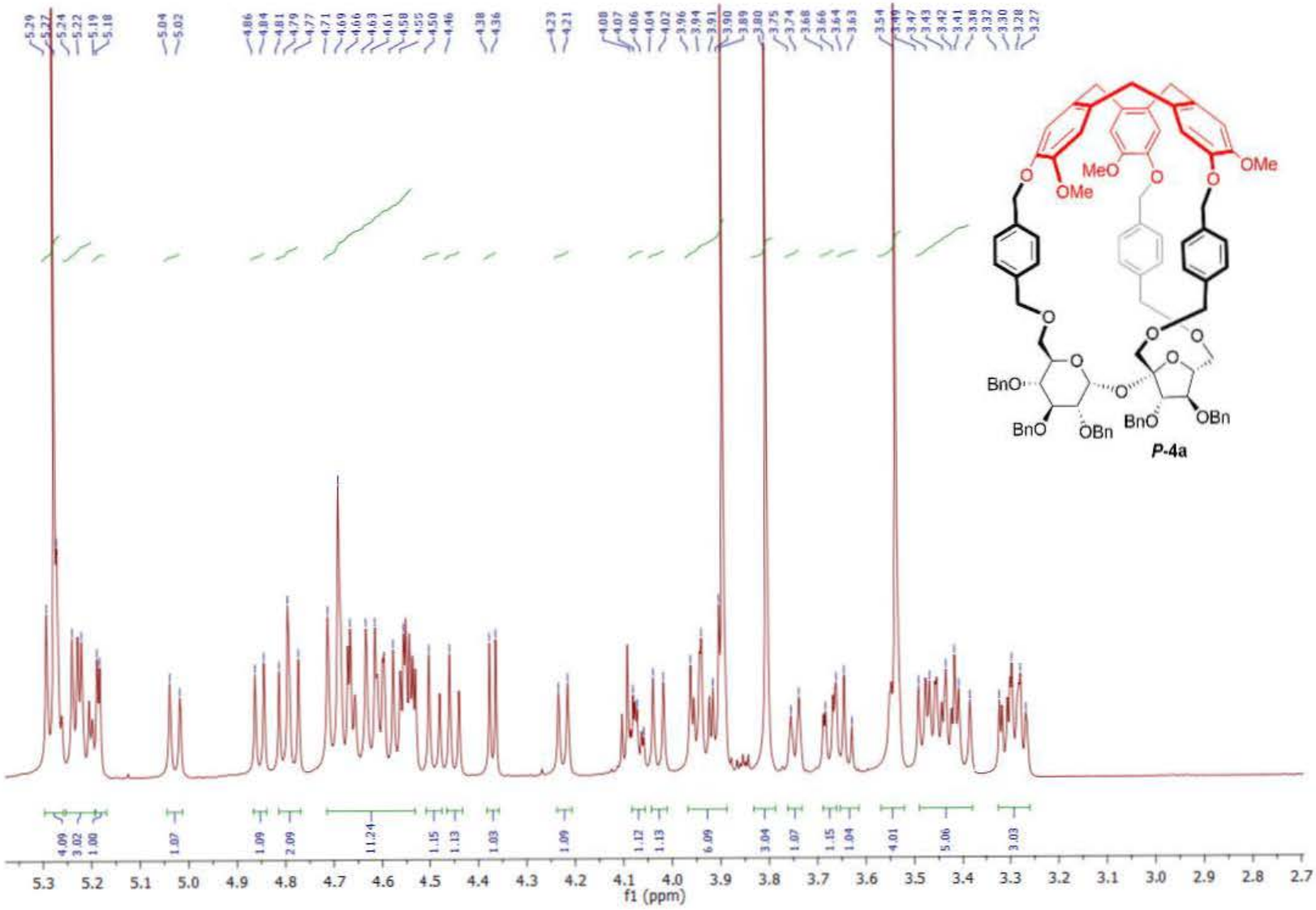

Figure S34. ^{1}H NMR spectrum of compound ***P*-4a** (aliphatic part).

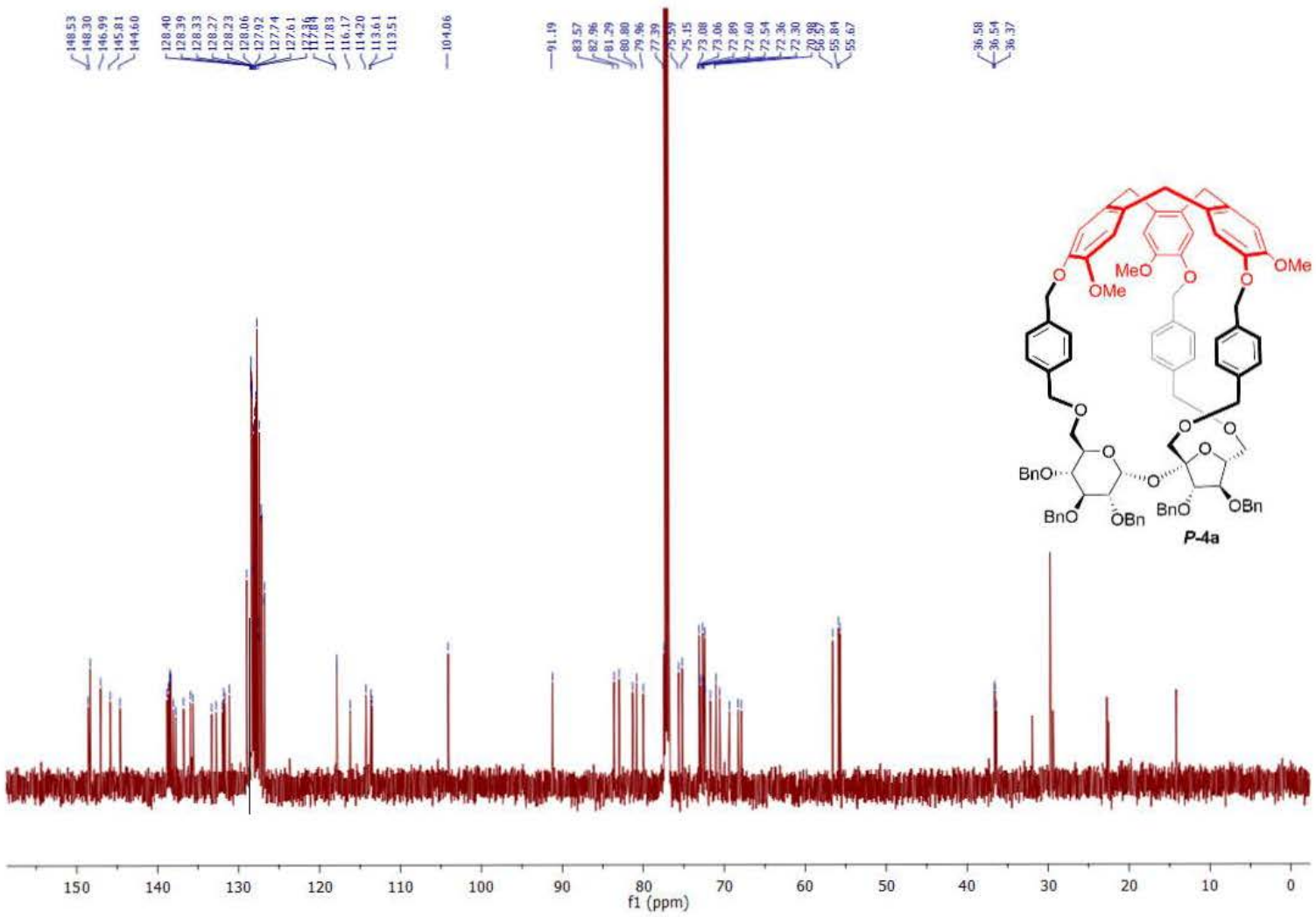

Figure S35. ^{13}C NMR spectrum of compound ***P*-4a**.

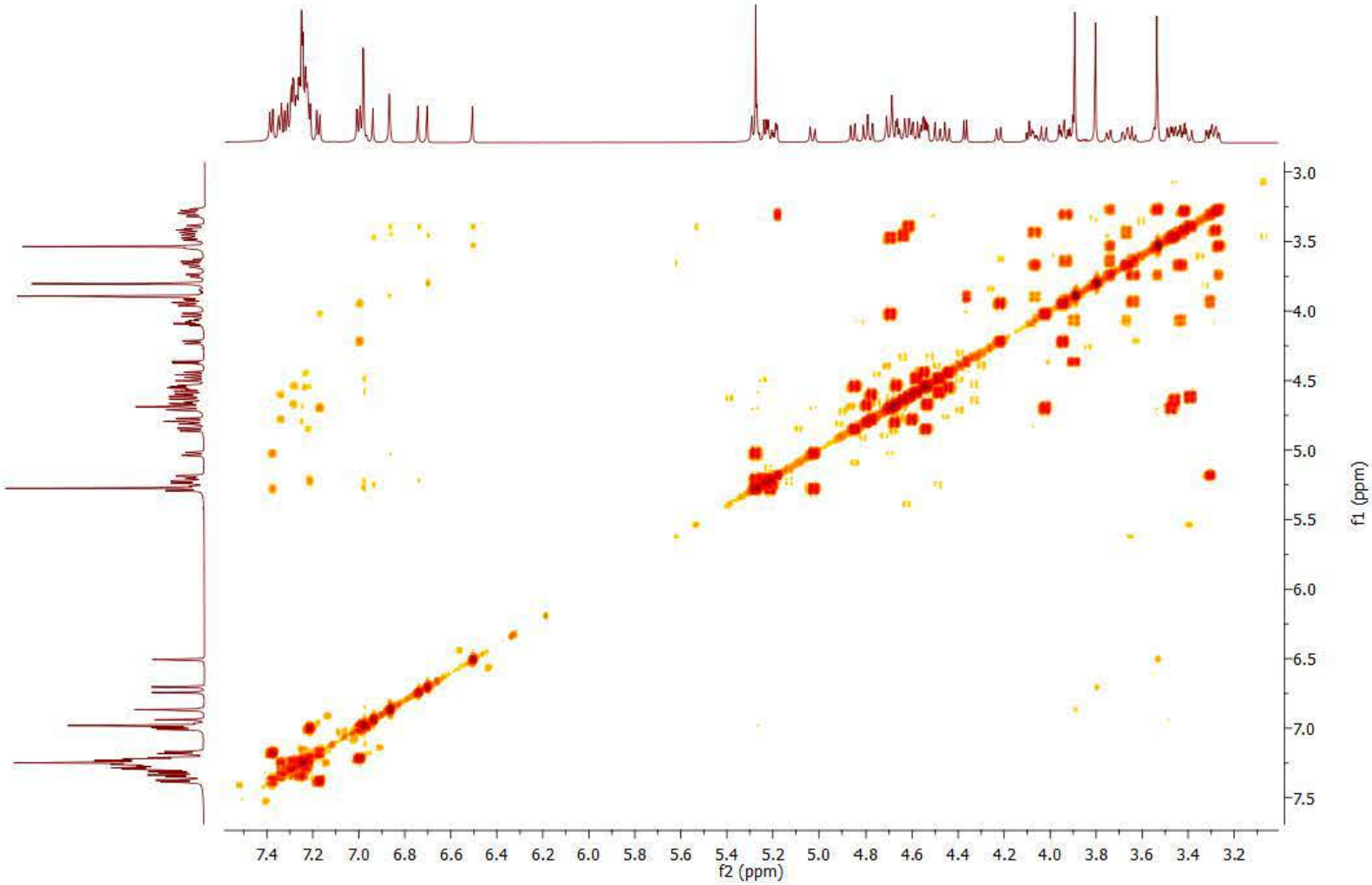

Figure S36. ^{1}H–^{1}H COSY spectrum of compound ***P*-4a**.

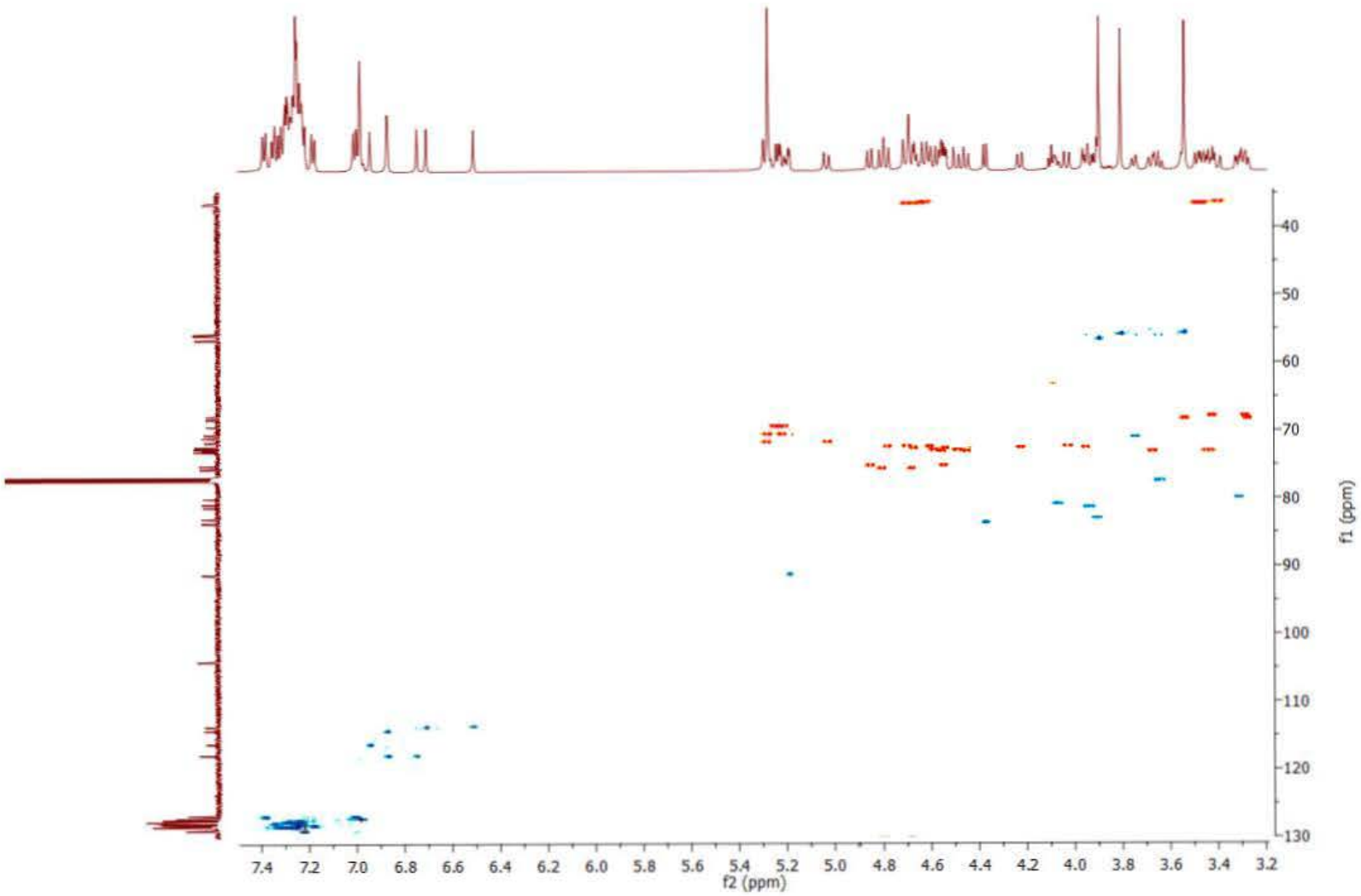

Figure S37. $^{1}H–^{13}C$ HSQC spectrum of compound ***P*-4a**.

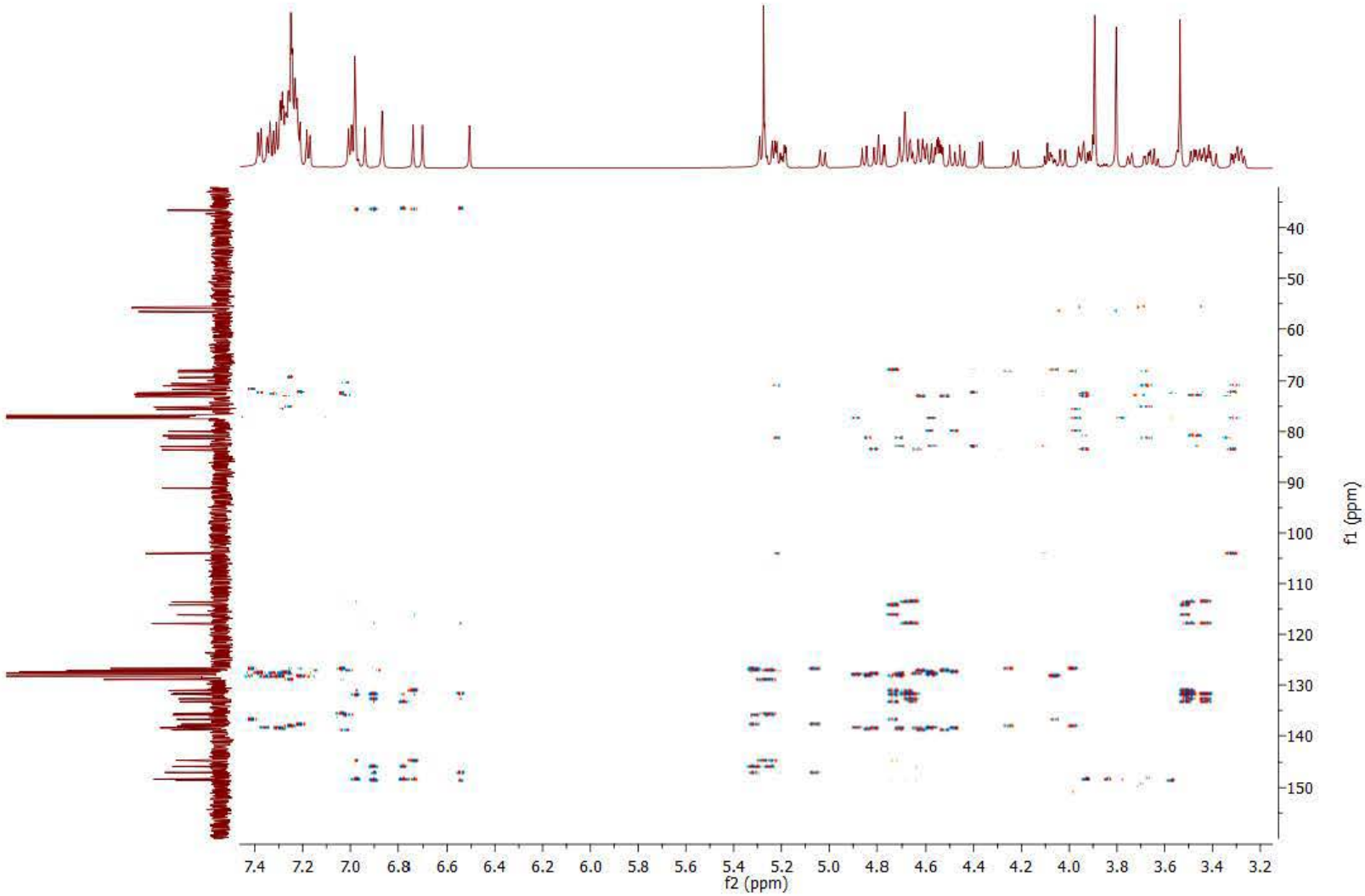

Figure S38. $^{1}H–^{13}C$ HMBC spectrum of compound ***P*-4a**.

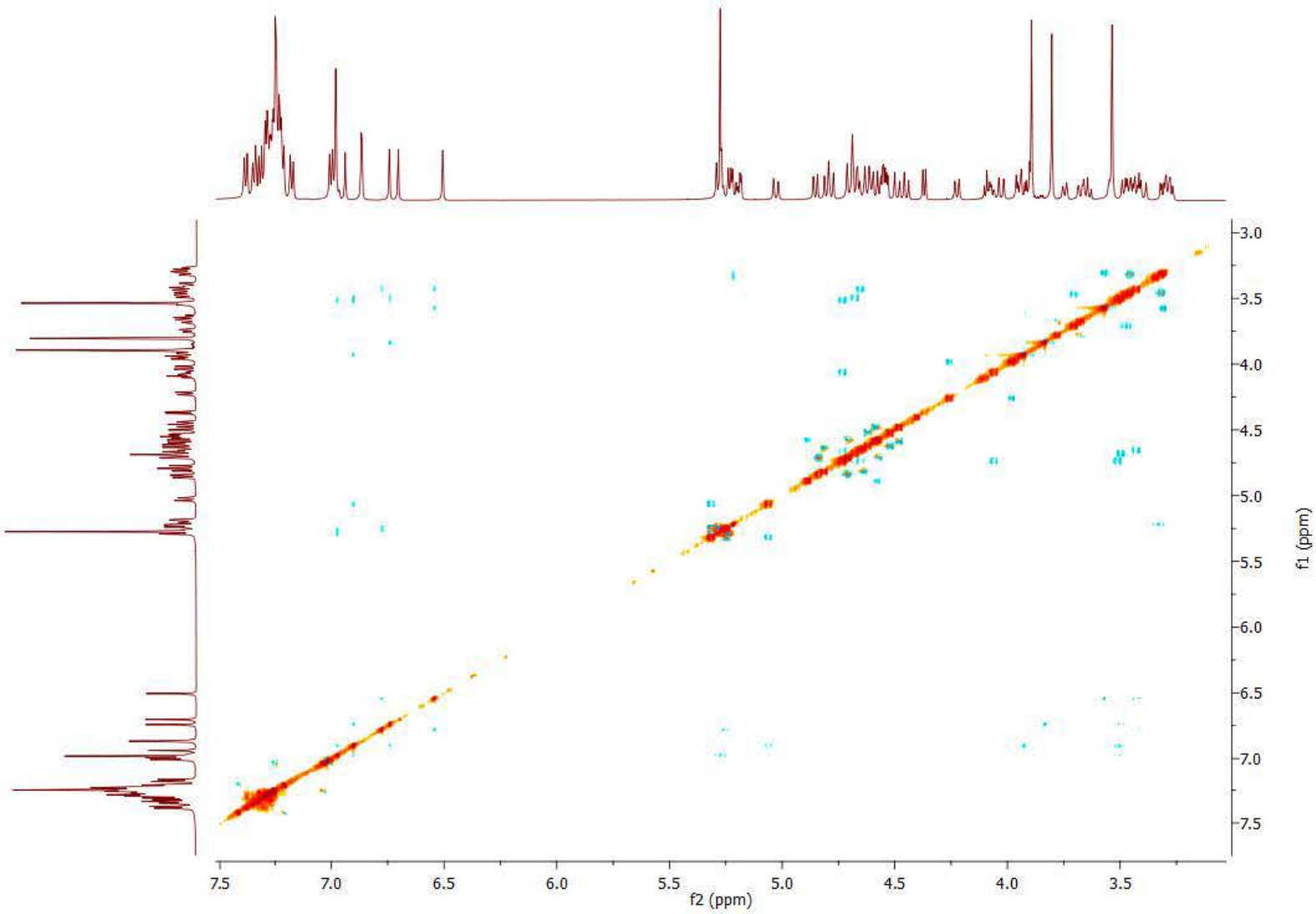

Figure S39. ^{1}H–^{1}HROESY spectrum of compound ***P*-4a**.

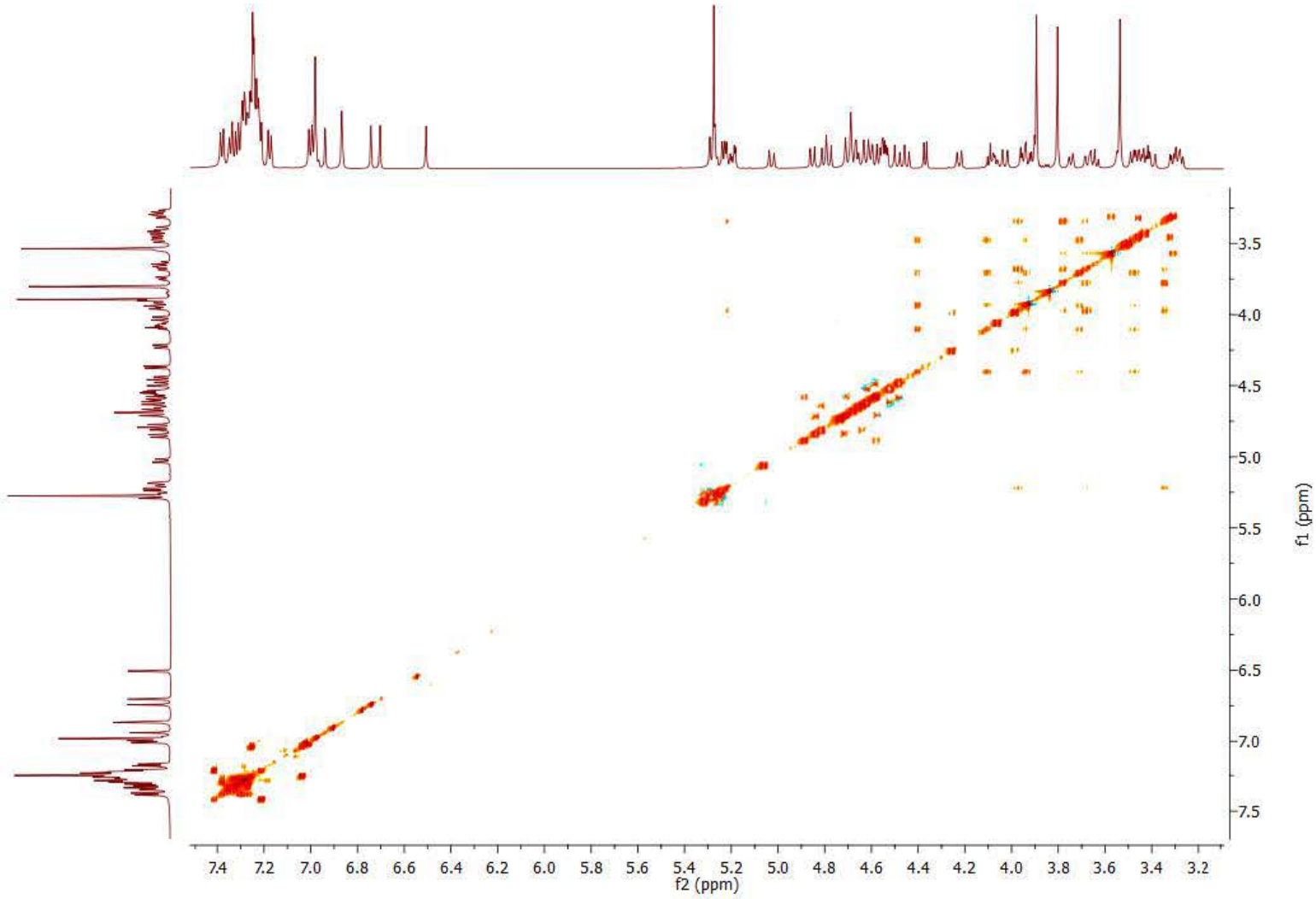

Figure S40. ^{1}H–^{1}HTOCSY spectrum of compound ***P*-4a**.

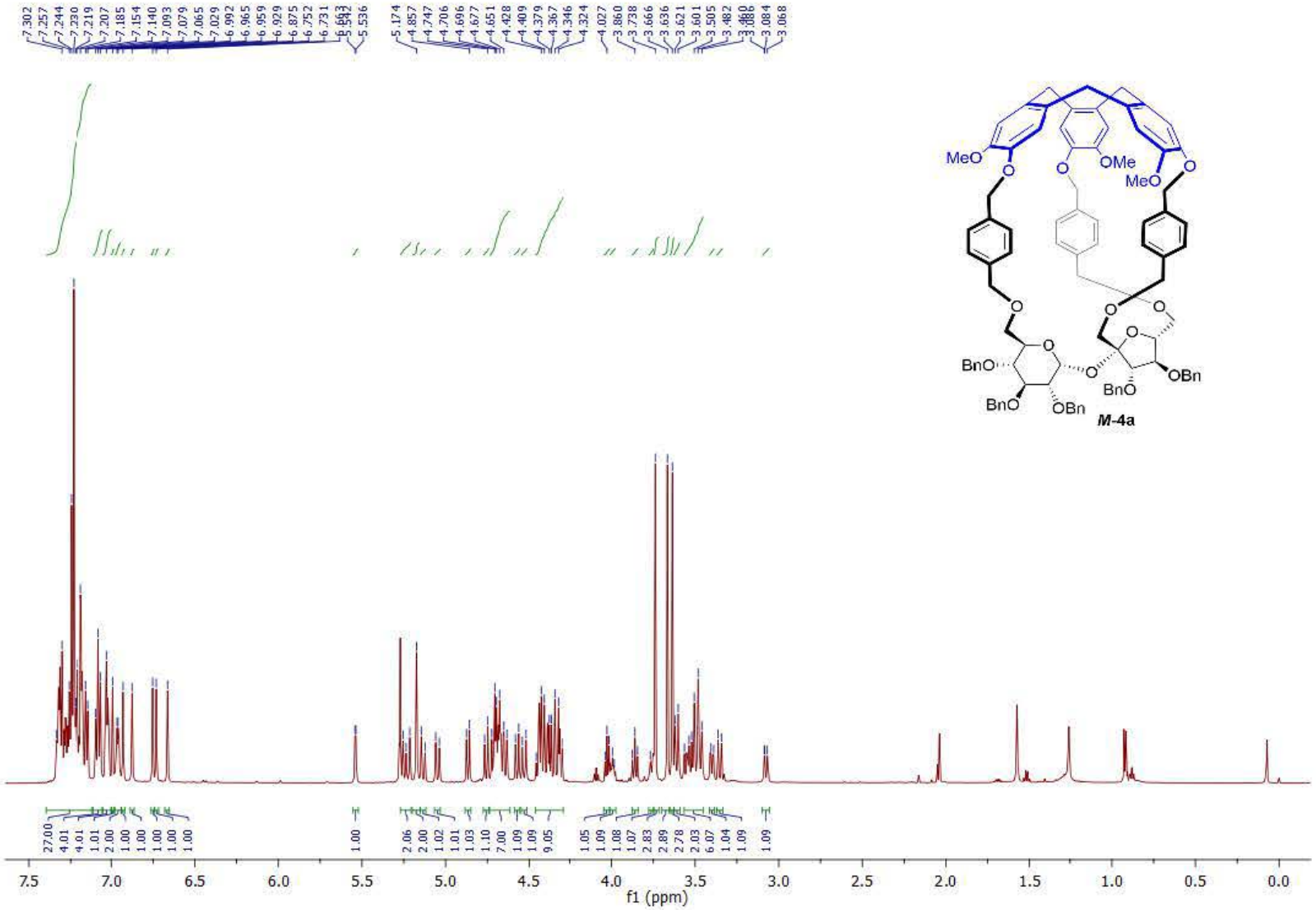

Figure S41. ^{1}H NMR spectrum of compound ***M*-4a.**

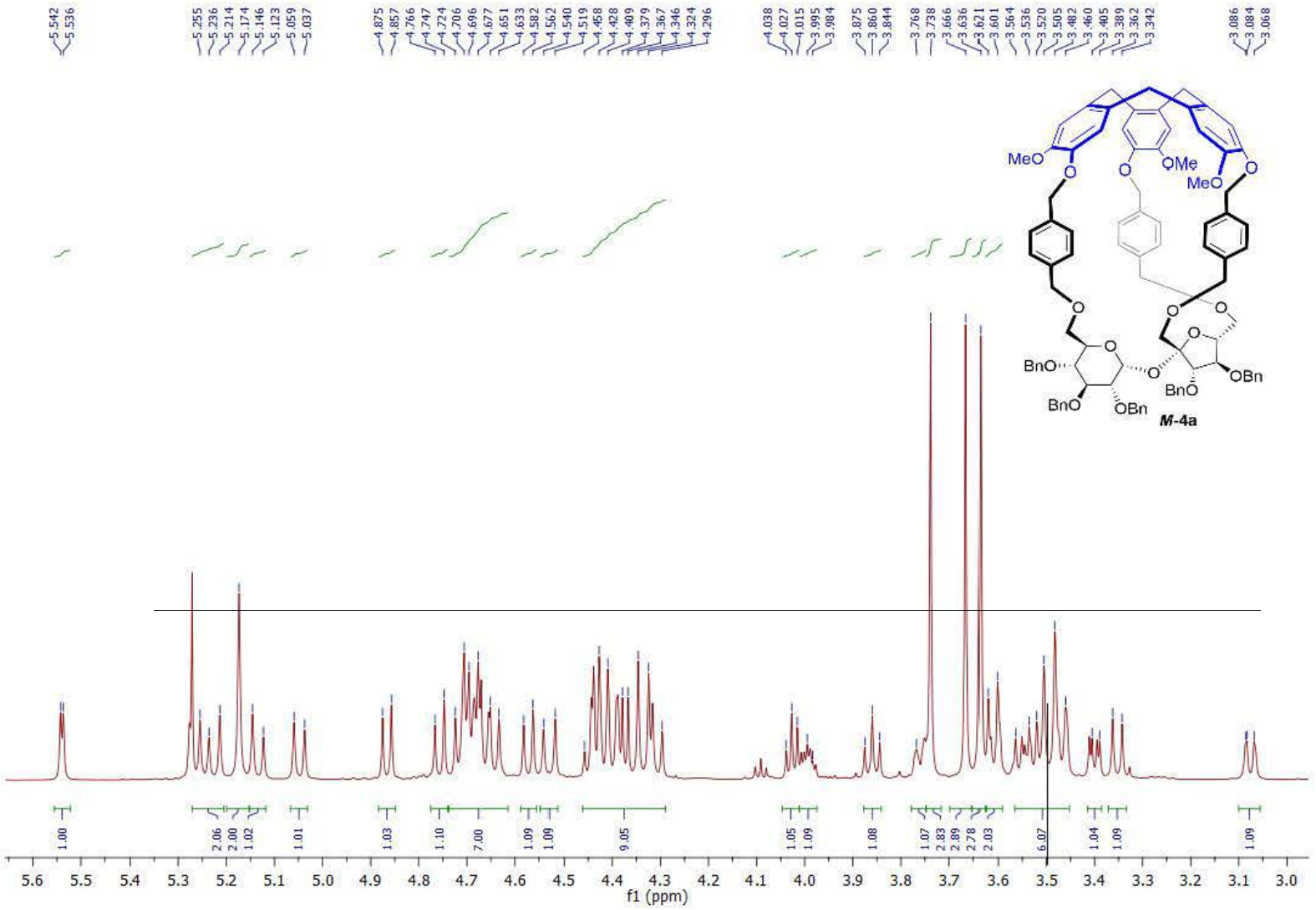

Figure S42. ^{1}H NMR spectrum of compound ***M*-4a** (aliphatic part).

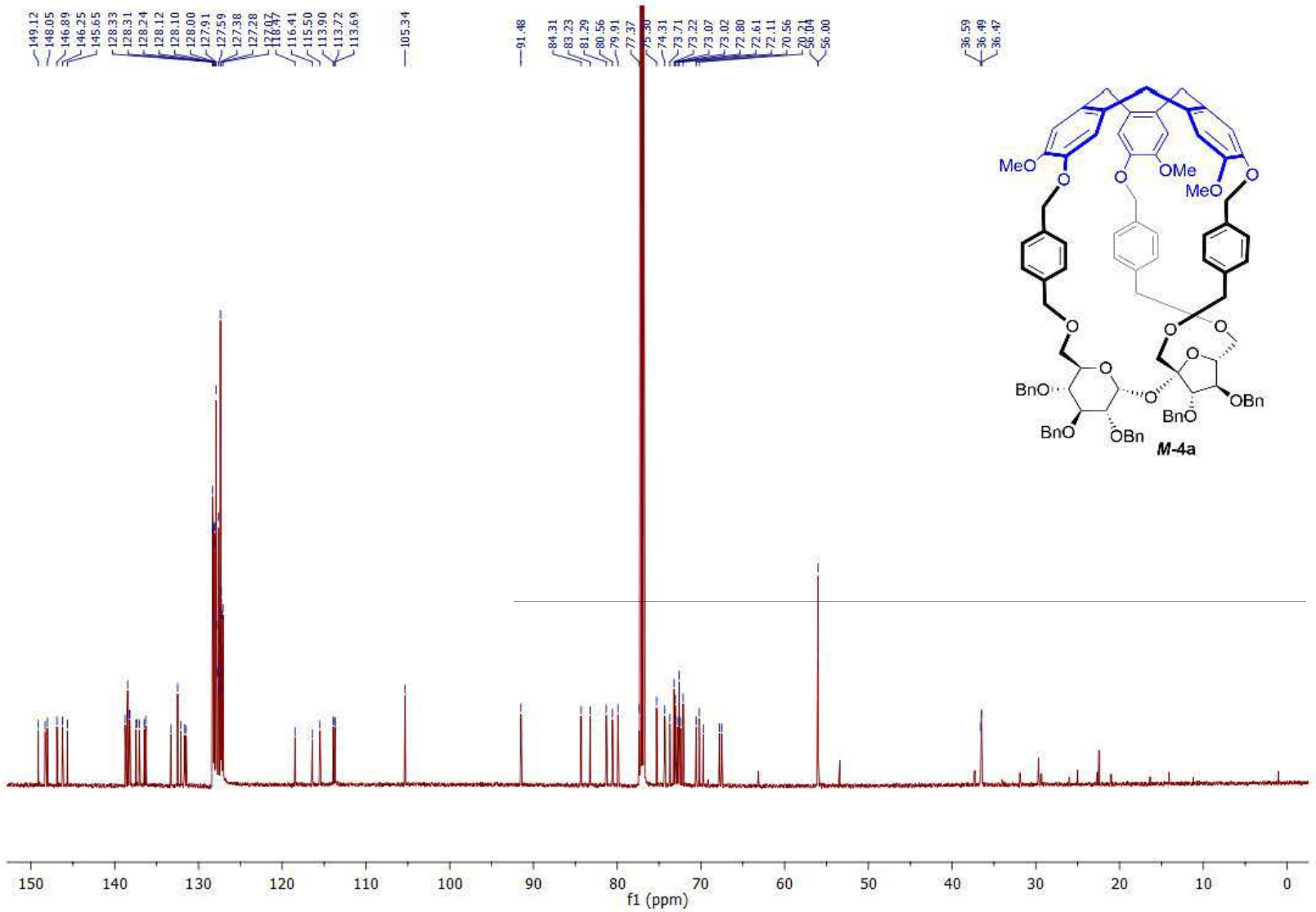

Figure S43. ^{13}C NMR spectrum of compound ***M*-4a**.

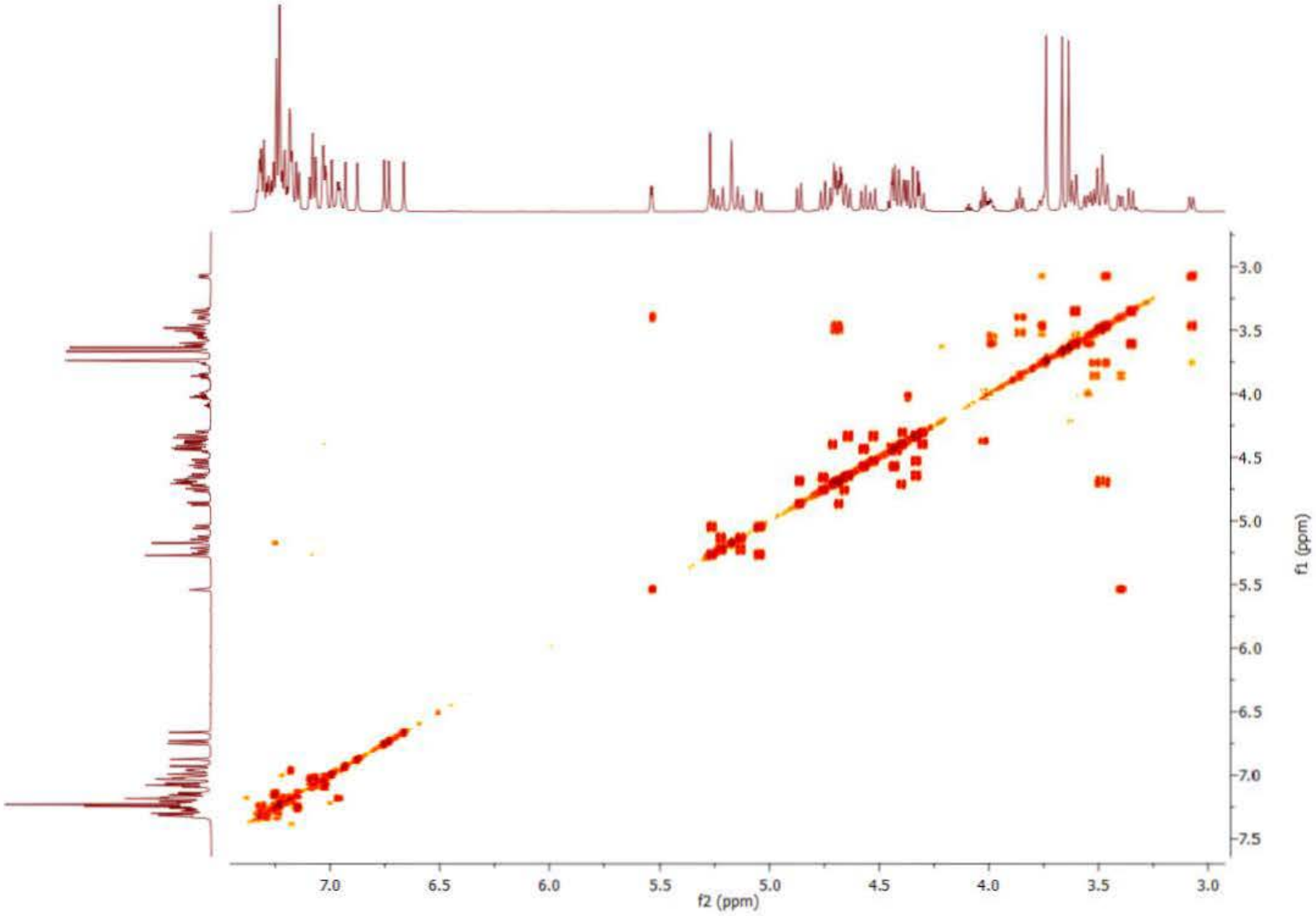

Figure S44. $^{1}H–^{1}H$ COSY spectrum of compound ***M*-4a**.

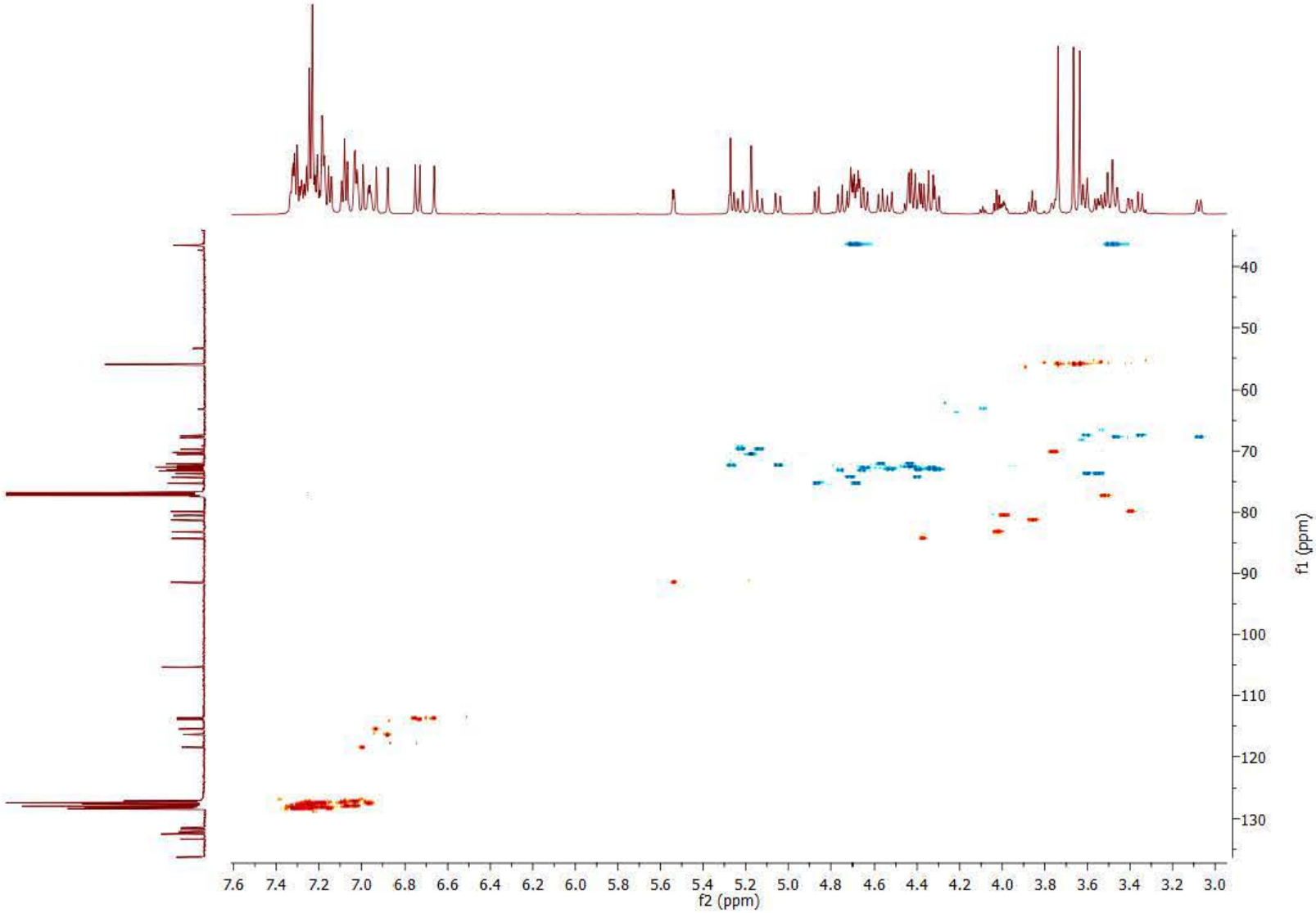

Figure S45. $^{1}H–^{13}C$ HSQC spectrum of compound ***M*-4a**.

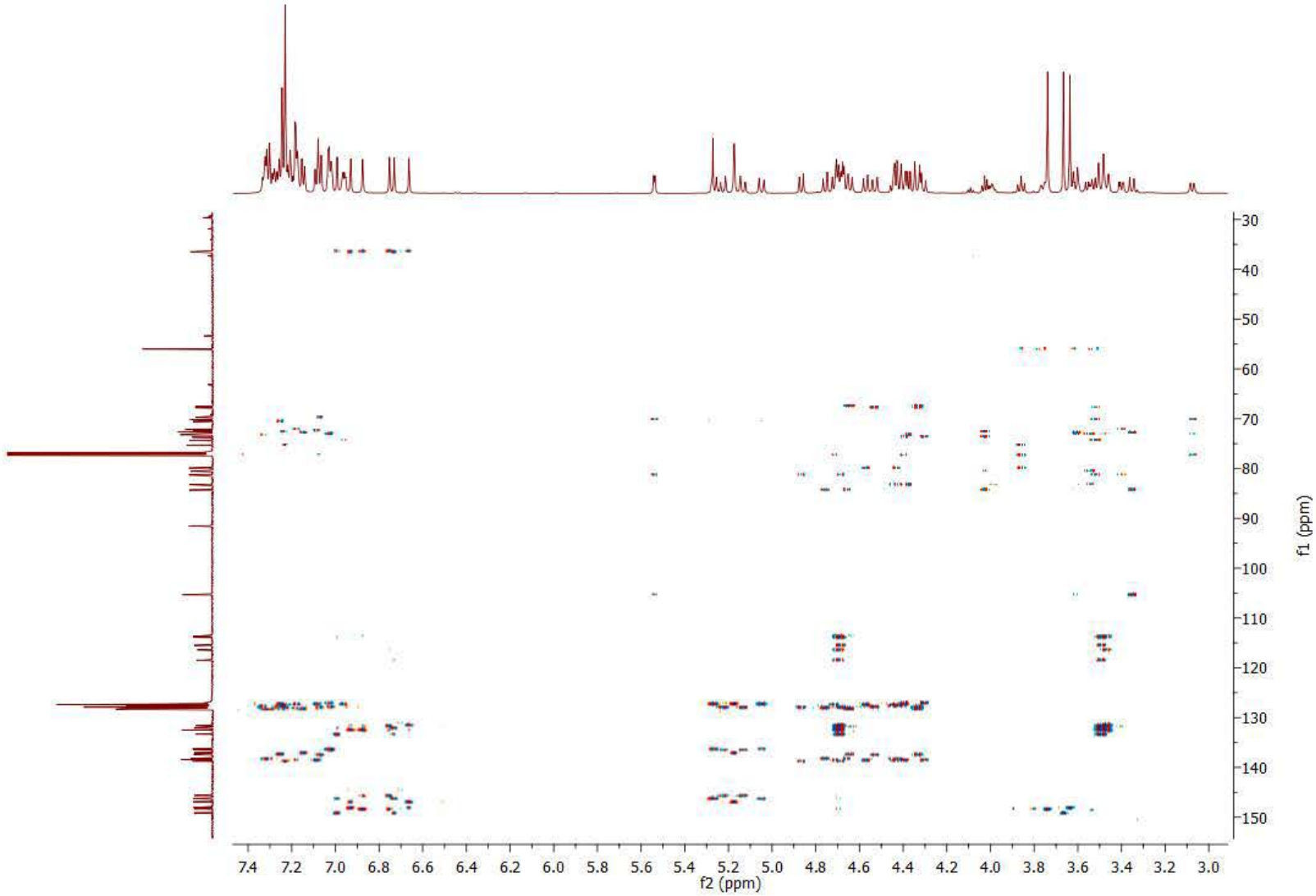

Figure S46. ^{1}H–^{13}C HMBC spectrum of compound ***M*-4a**.

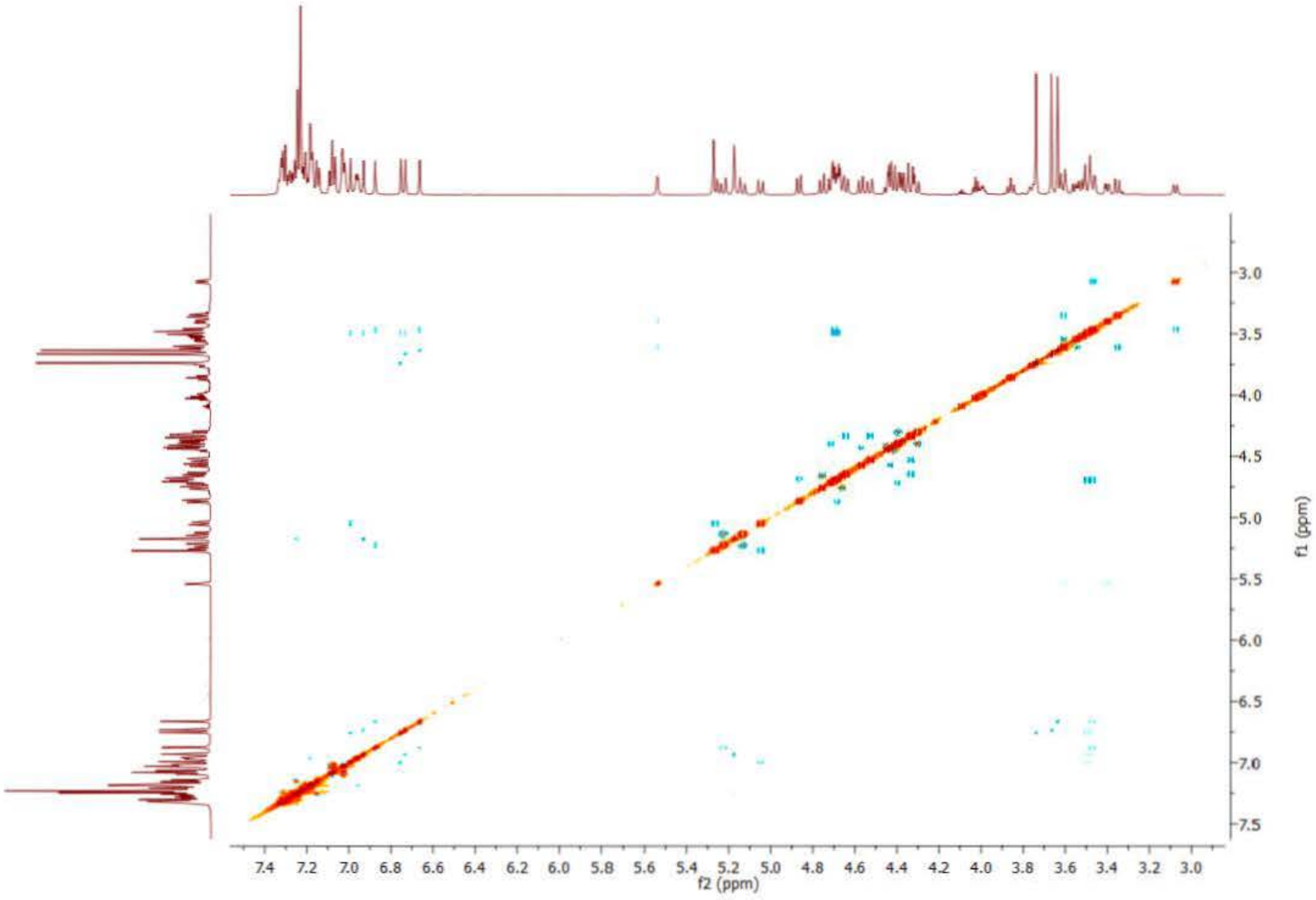

Figure S47. ^{1}H–^{1}H ROESY spectrum of compound ***M*-4a**.

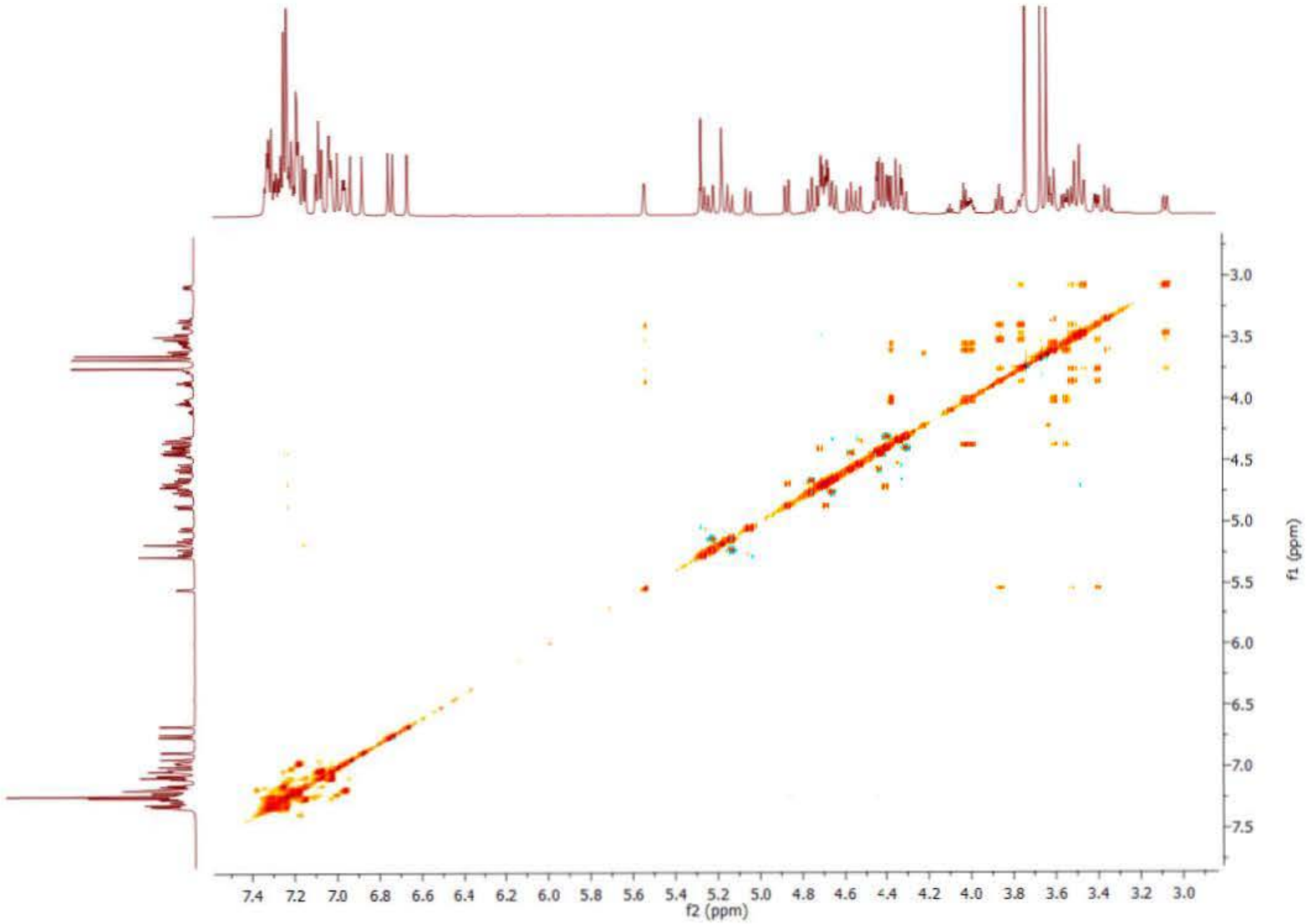

Figure S48. $^{1}H–^{1}H$ TOCSY spectrum of compound ***M*-4a**.

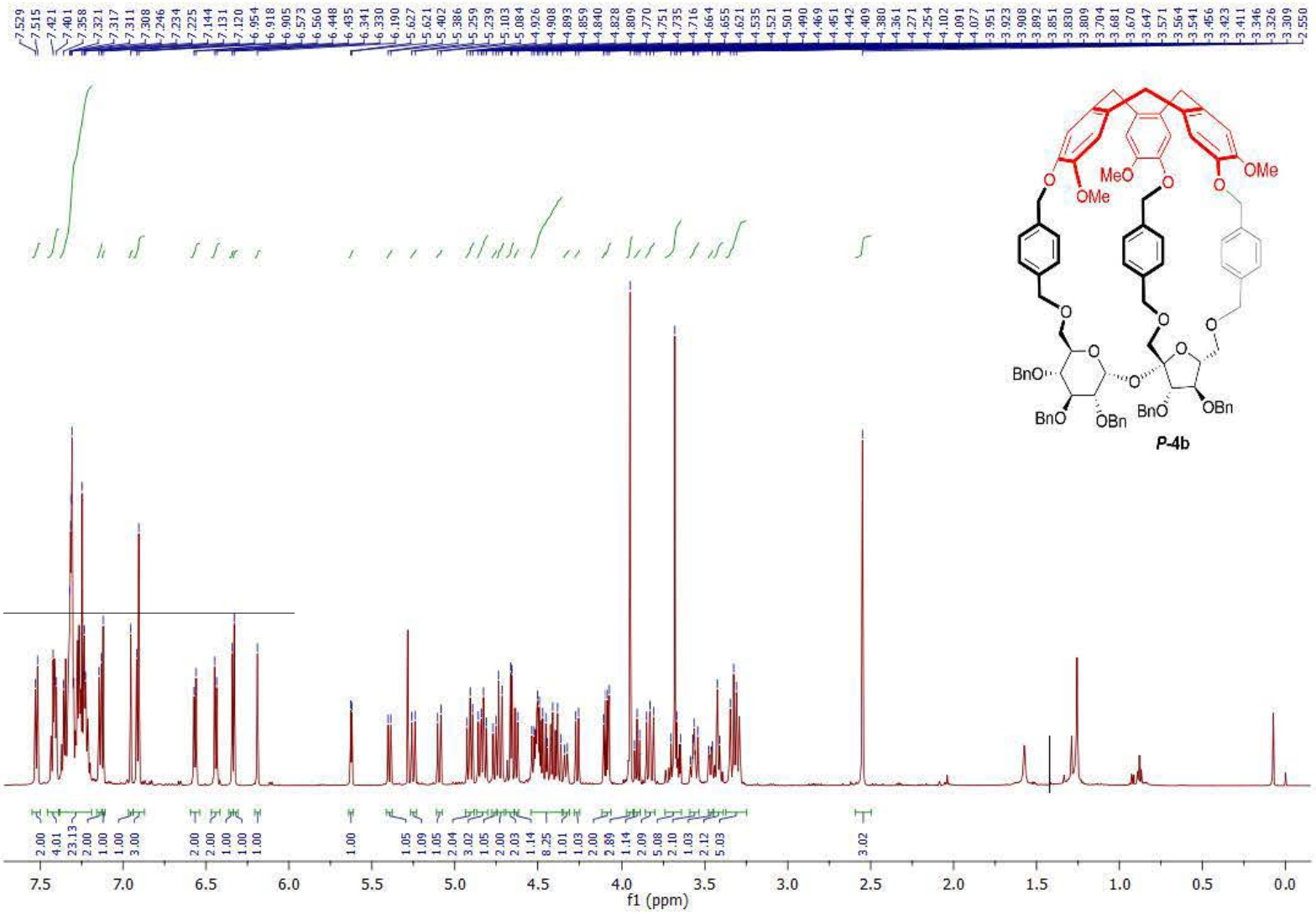

Figure S49. ^{1}H NMR spectrum of compound ***P*-4b.**

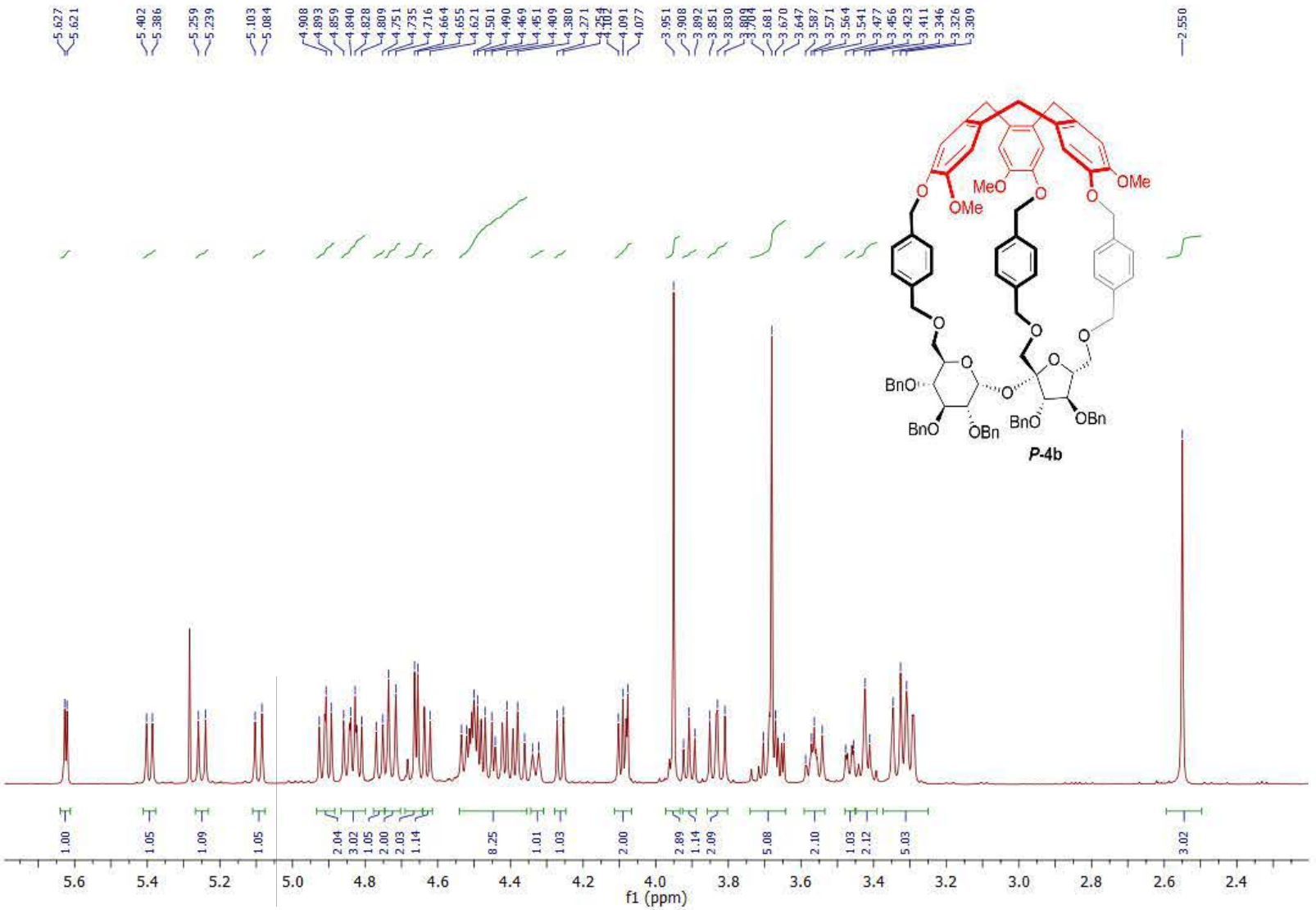

Figure S50. ^{1}H NMR spectrum of compound ***P*-4b** (aliphatic part).

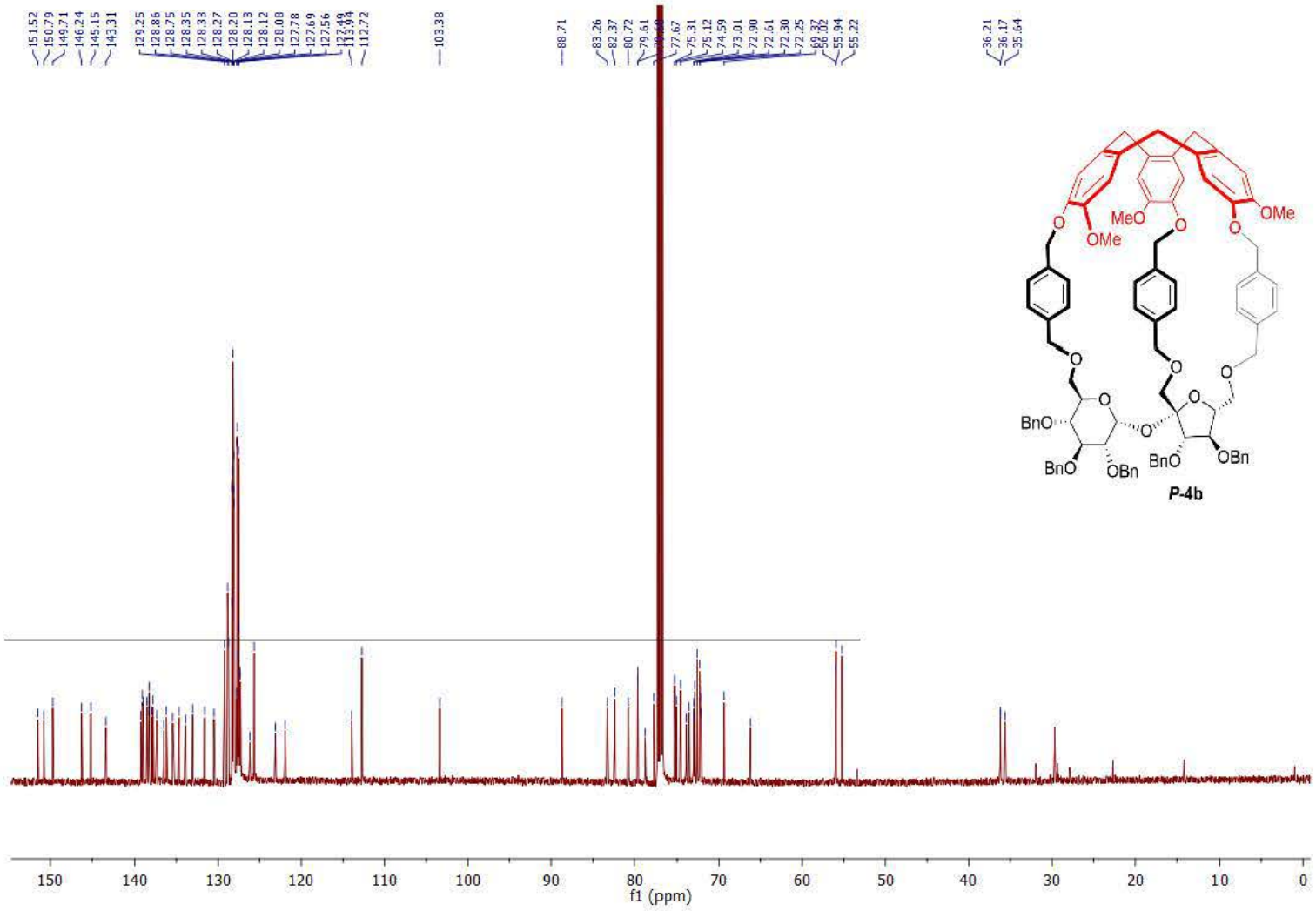

Figure S51. ^{13}C NMR spectrum of compound ***P*-4b**.

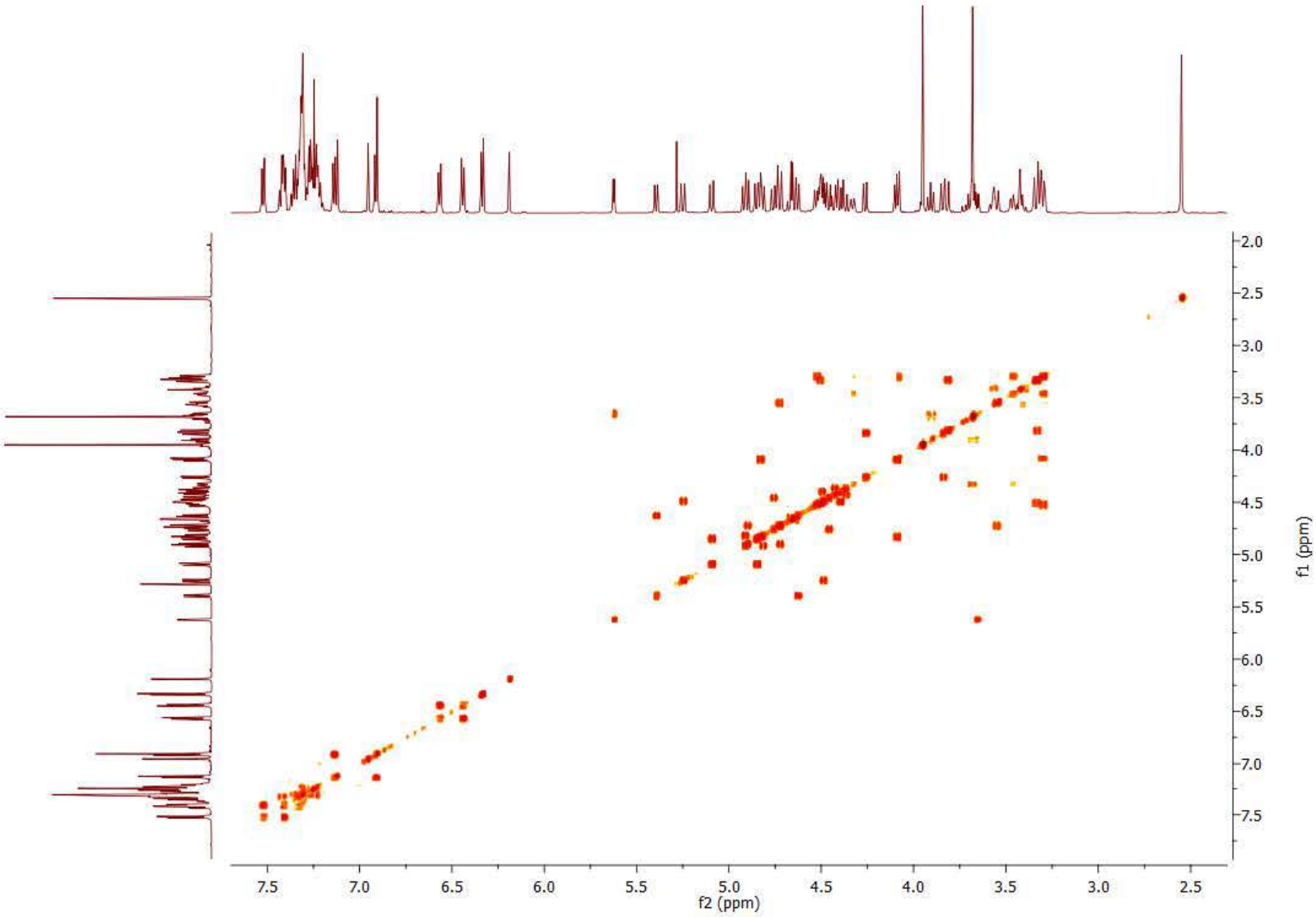

Figure S52. ^{1}H–^{1}H COSY spectrum of compound ***P*-4b**.

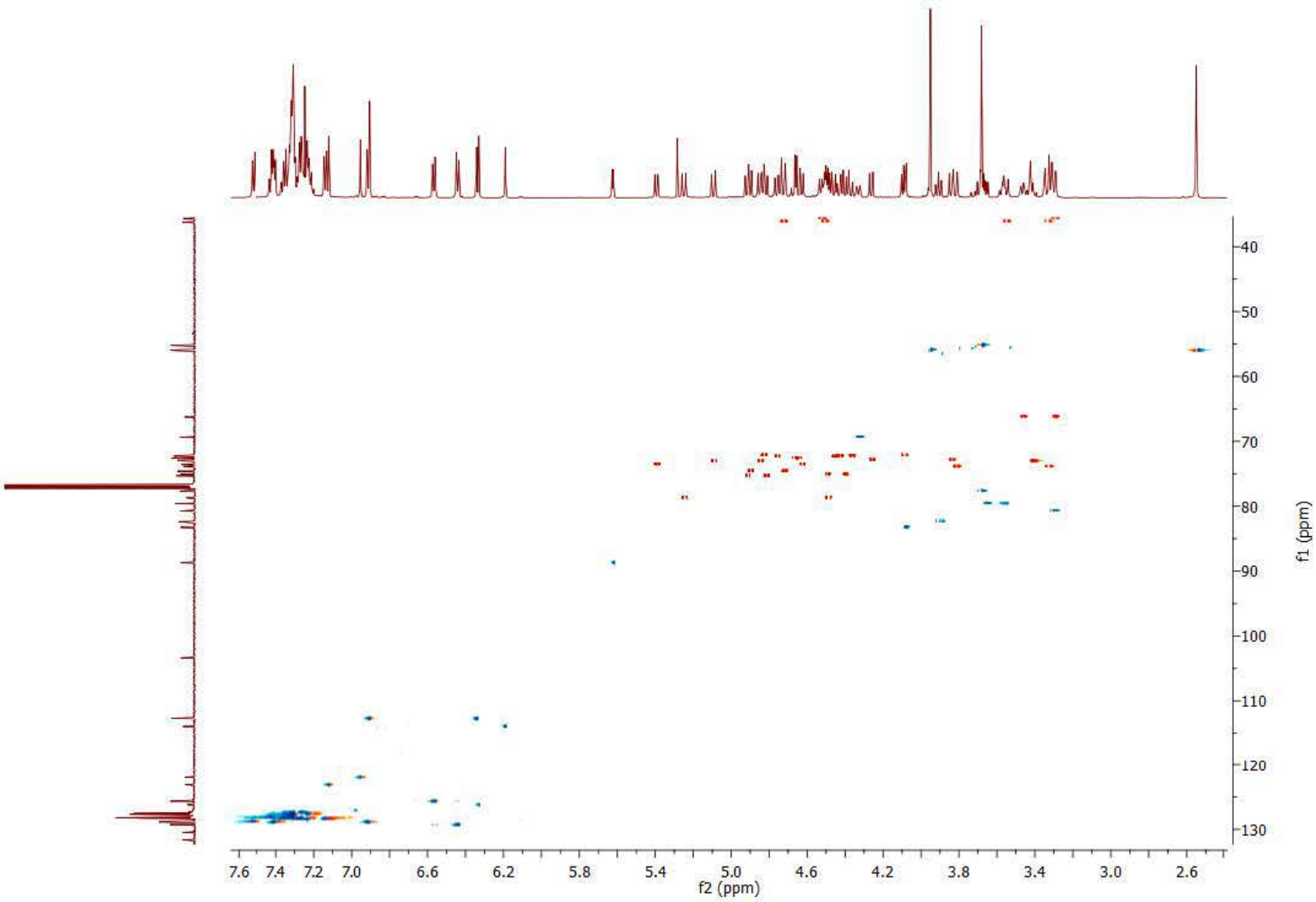

Figure S53. $^{1}H–^{13}C$ HSQC spectrum of compound ***P*-4b**.

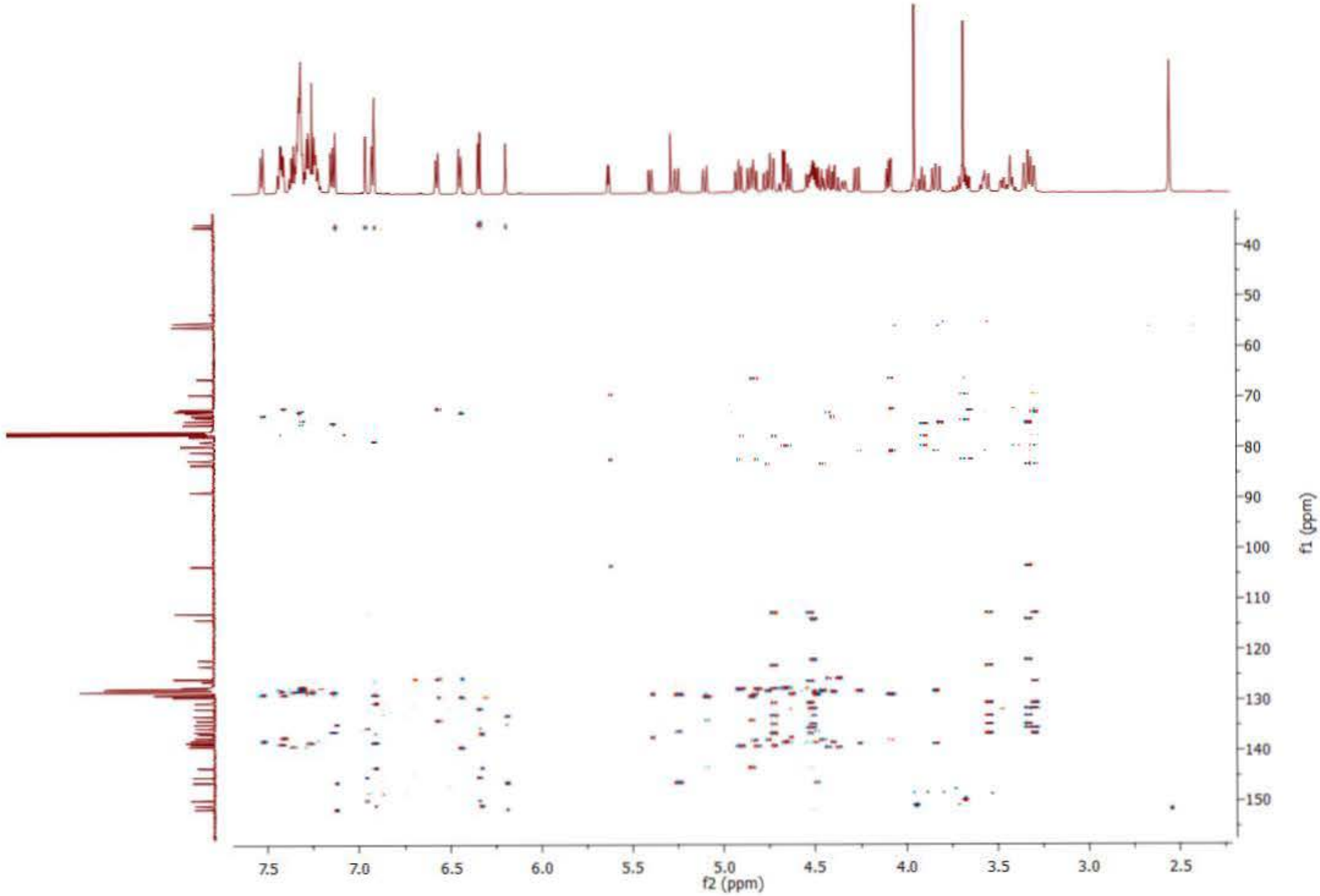

Figure S54. $^{1}H–^{13}C$ HMBC spectrum of compound ***P*-4b**.

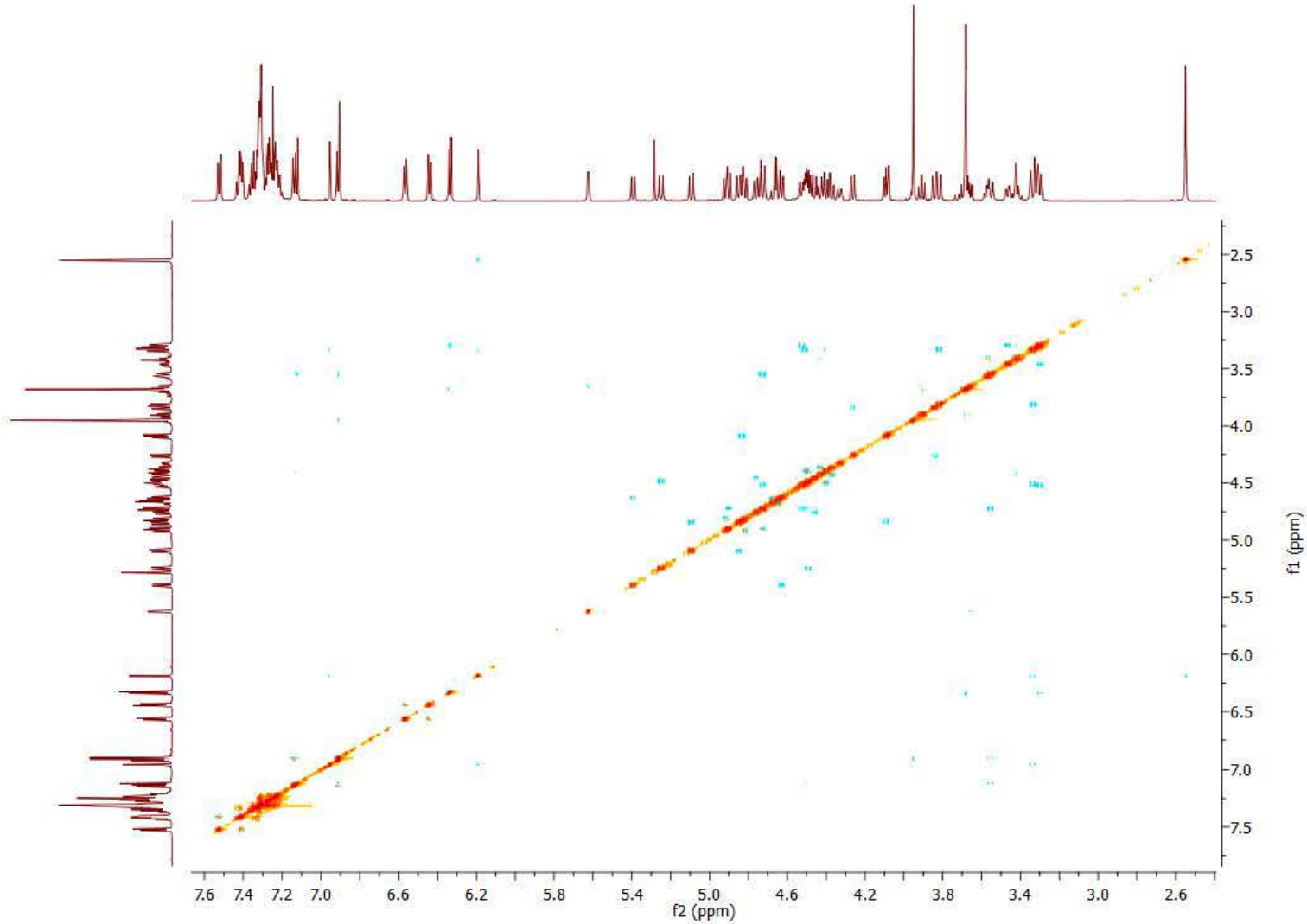

Figure S55. $^{1}H–^{1}H$ ROESY spectrum of compound ***P*-4b**.

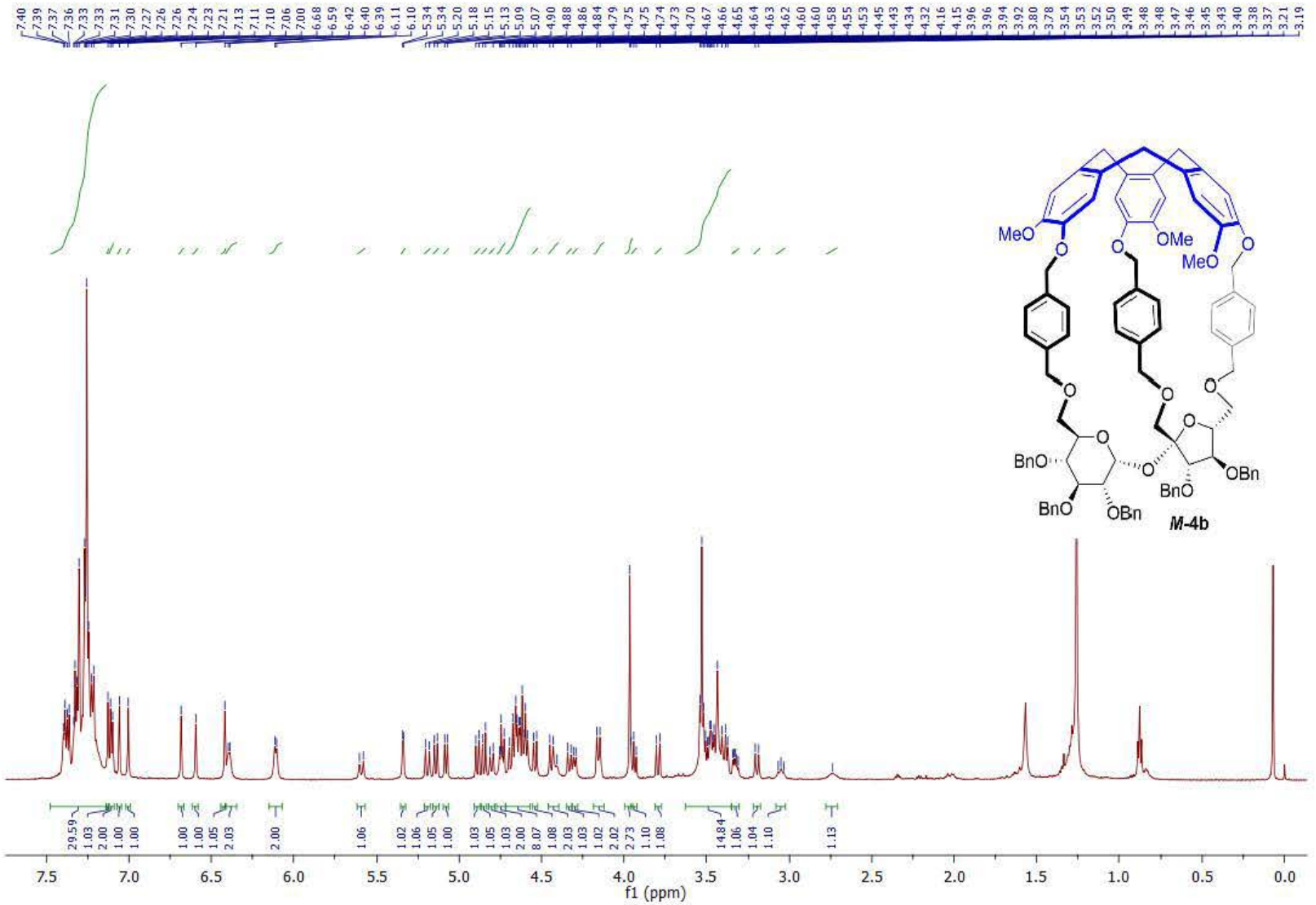

Figure S56. ^{1}H NMR spectrum of compound ***M*-4b.**

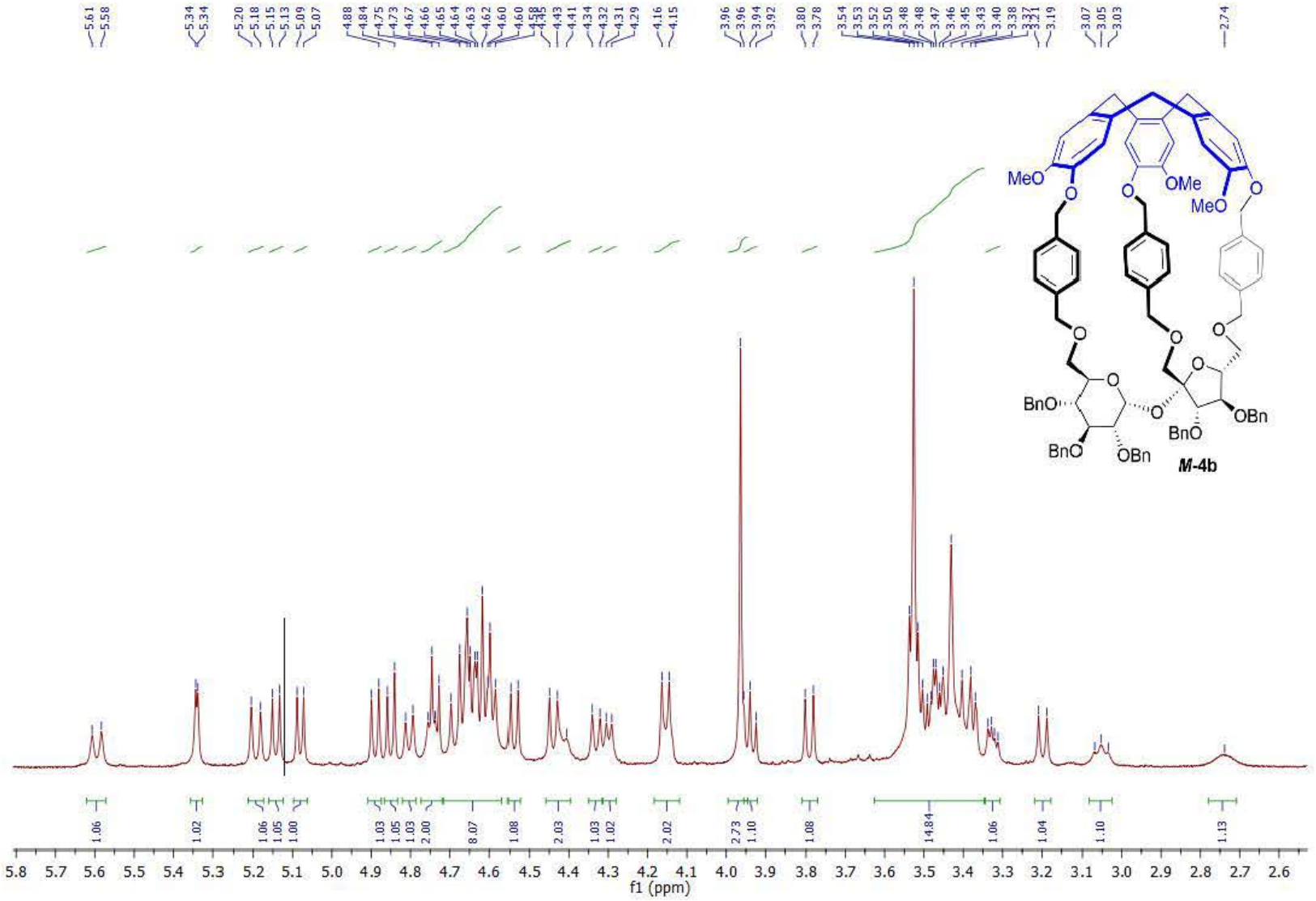

Figure S57. ^{1}H NMR spectrum of compound ***M*-4b** (aliphatic part).

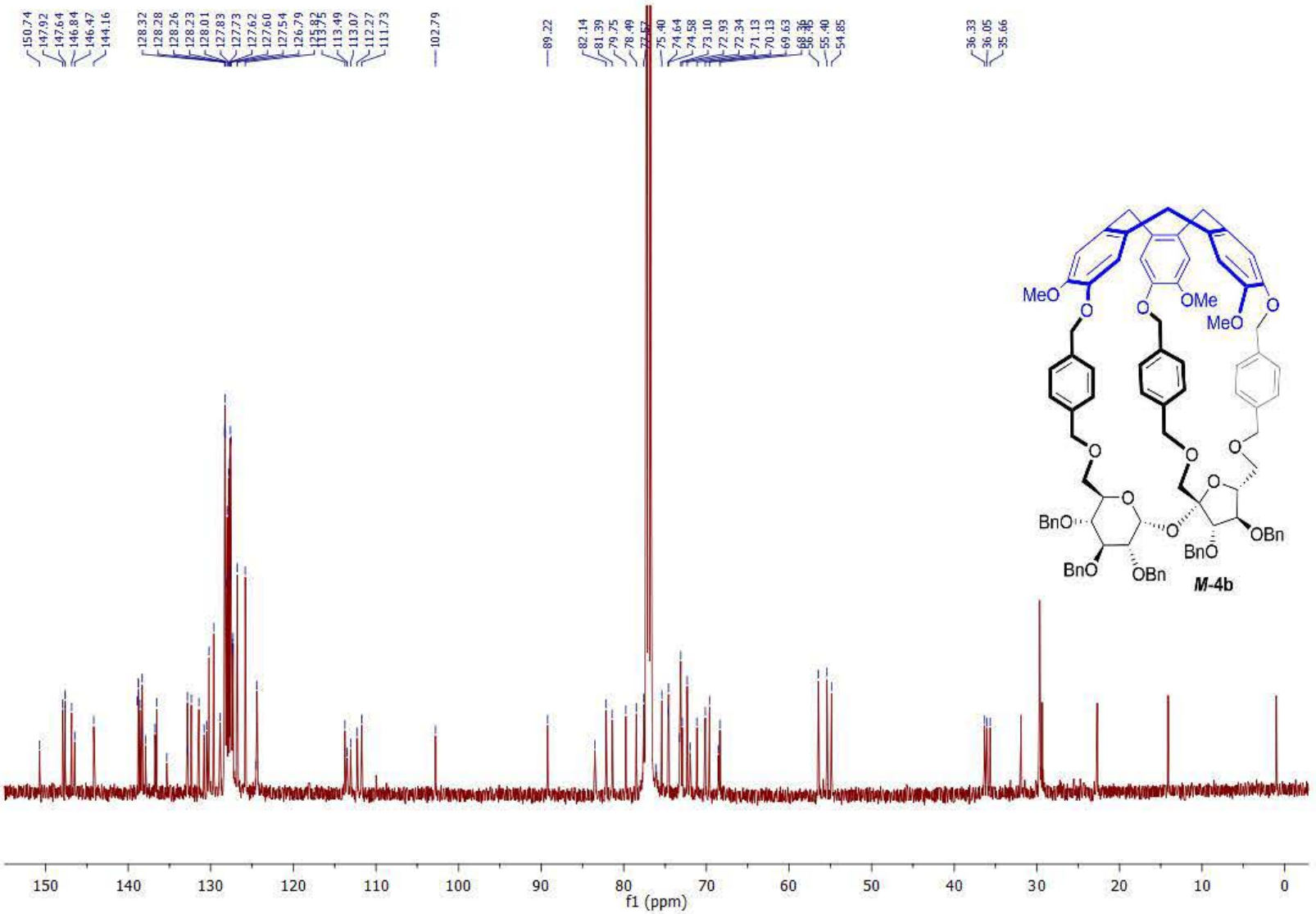

Figure S58. ^{13}C NMR spectrum of compound ***M*-4b**.

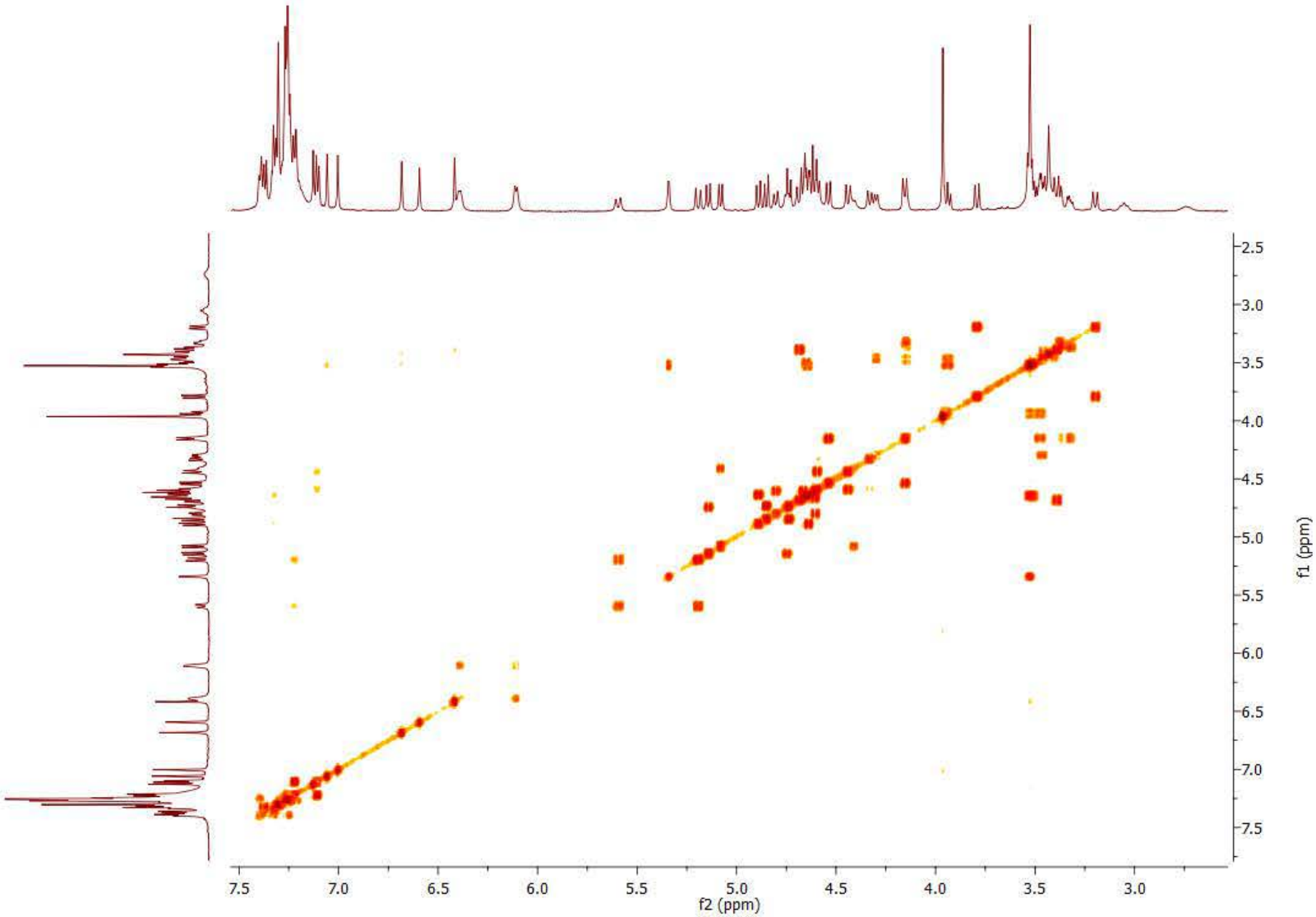

Figure S59. ^{1}H–^{1}H COSY spectrum of compound ***M*-4b**.

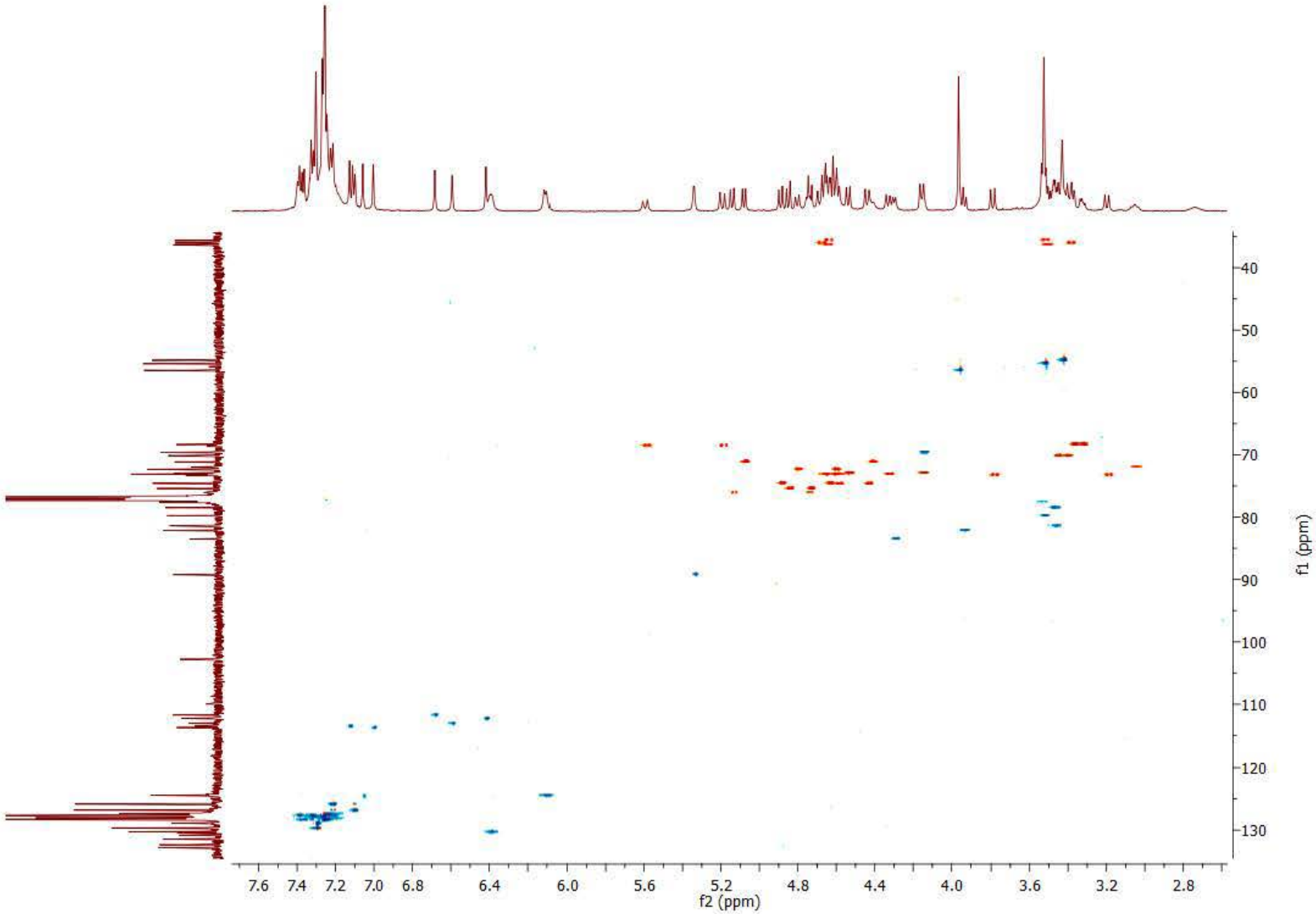

Figure S60. $^{1}H–^{13}C$ HSQC spectrum of compound ***M*-4b**.

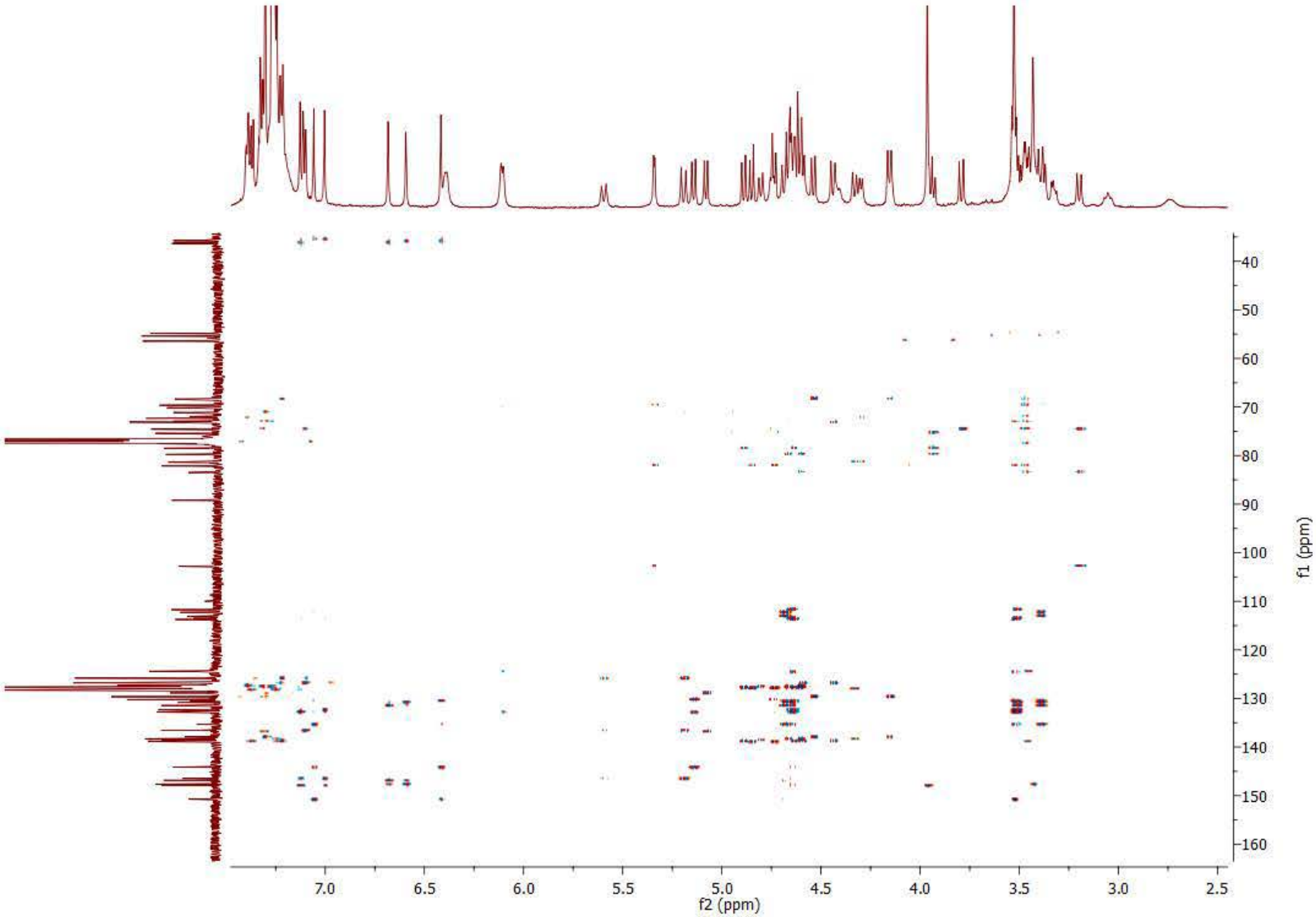

Figure S61. $^{1}H–^{13}C$ HMBC spectrum of compound ***M*-4b**.

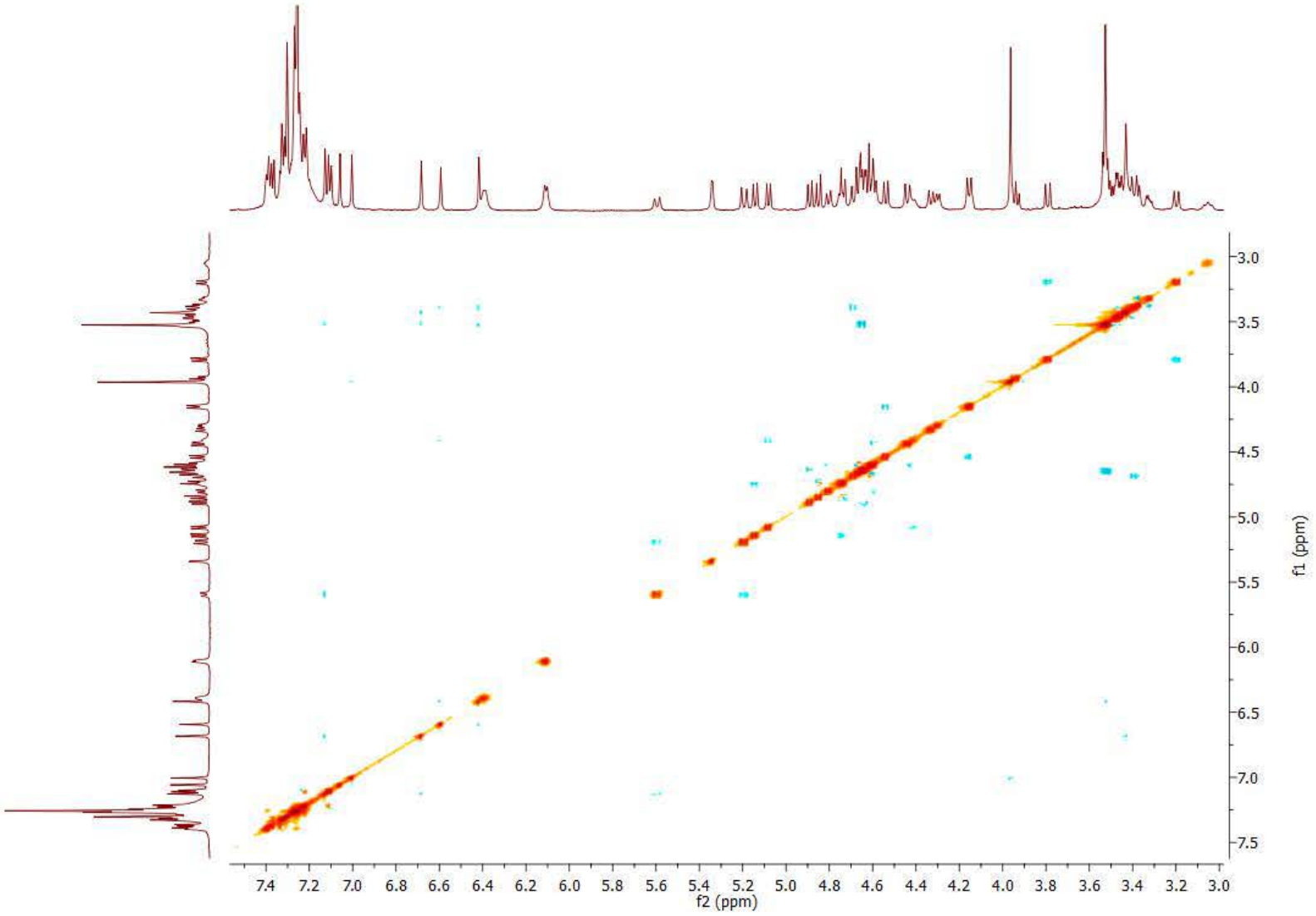

Figure S62. ^{1}H–^{1}H ROESY spectrum of compound ***M*-4b**.

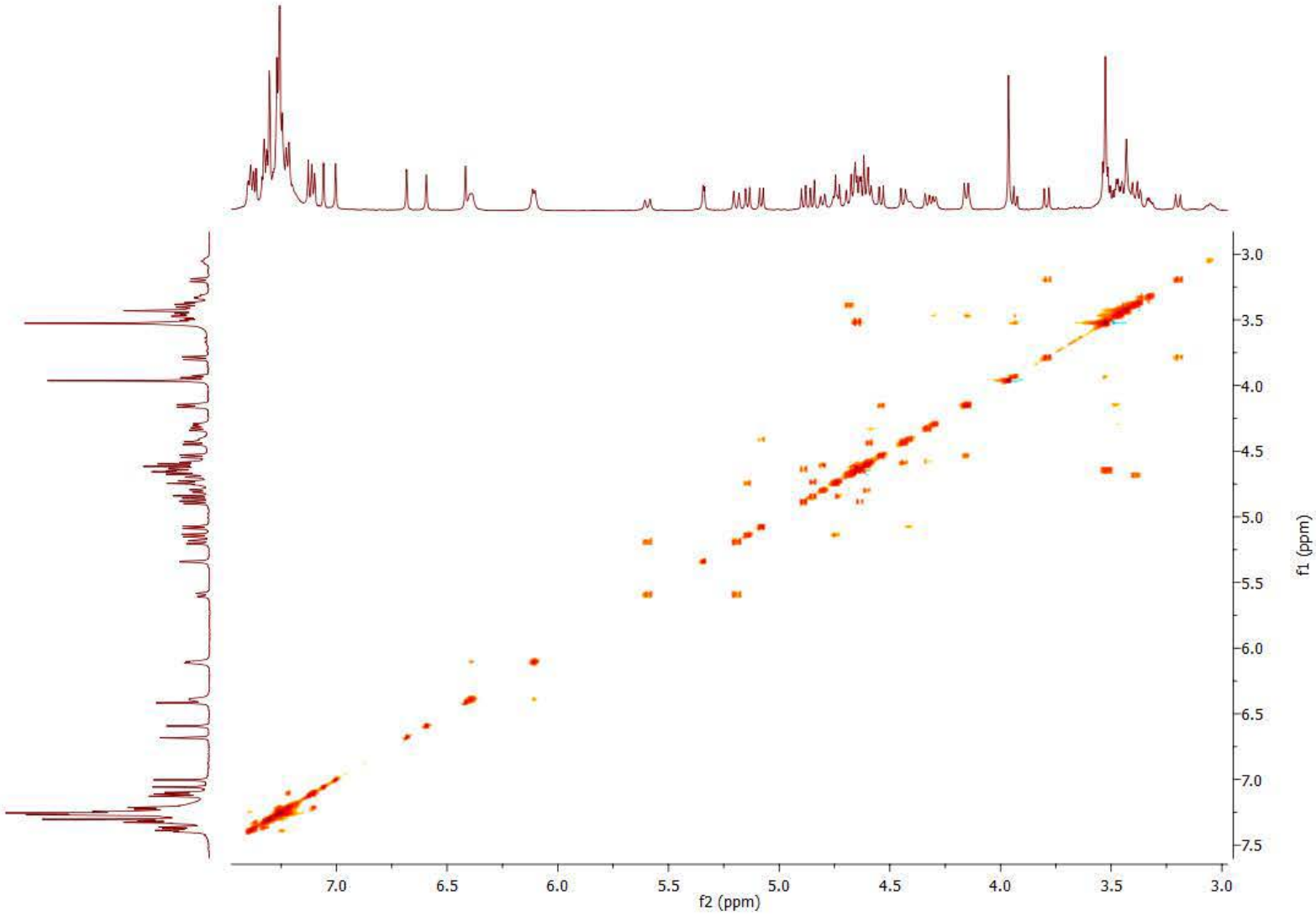

Figure S63. ^{1}H–^{1}H TOCSY spectrum of compound ***M*-4b**.

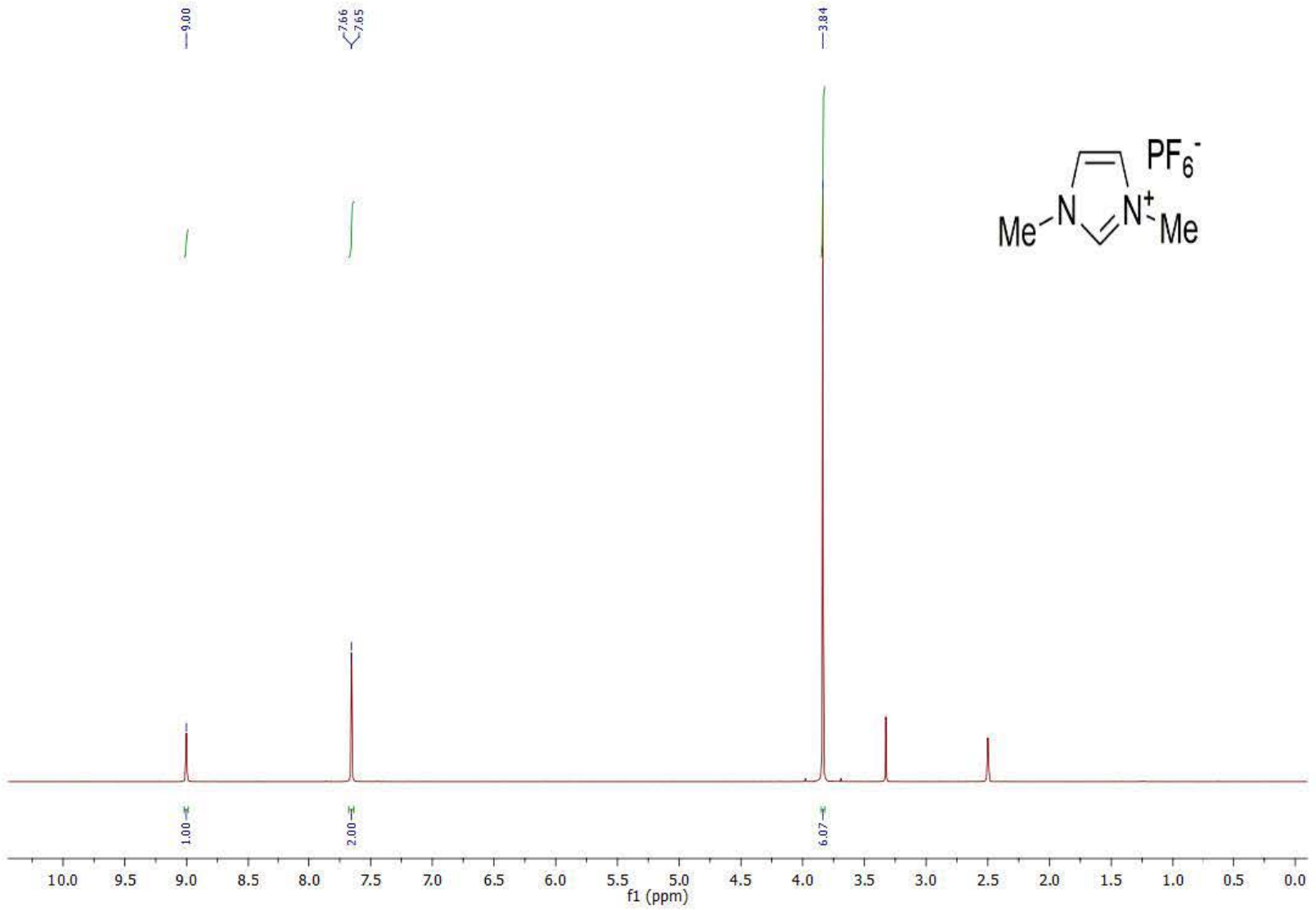

Figure S64. ^{1}H NMR spectrum of compound **G1.**

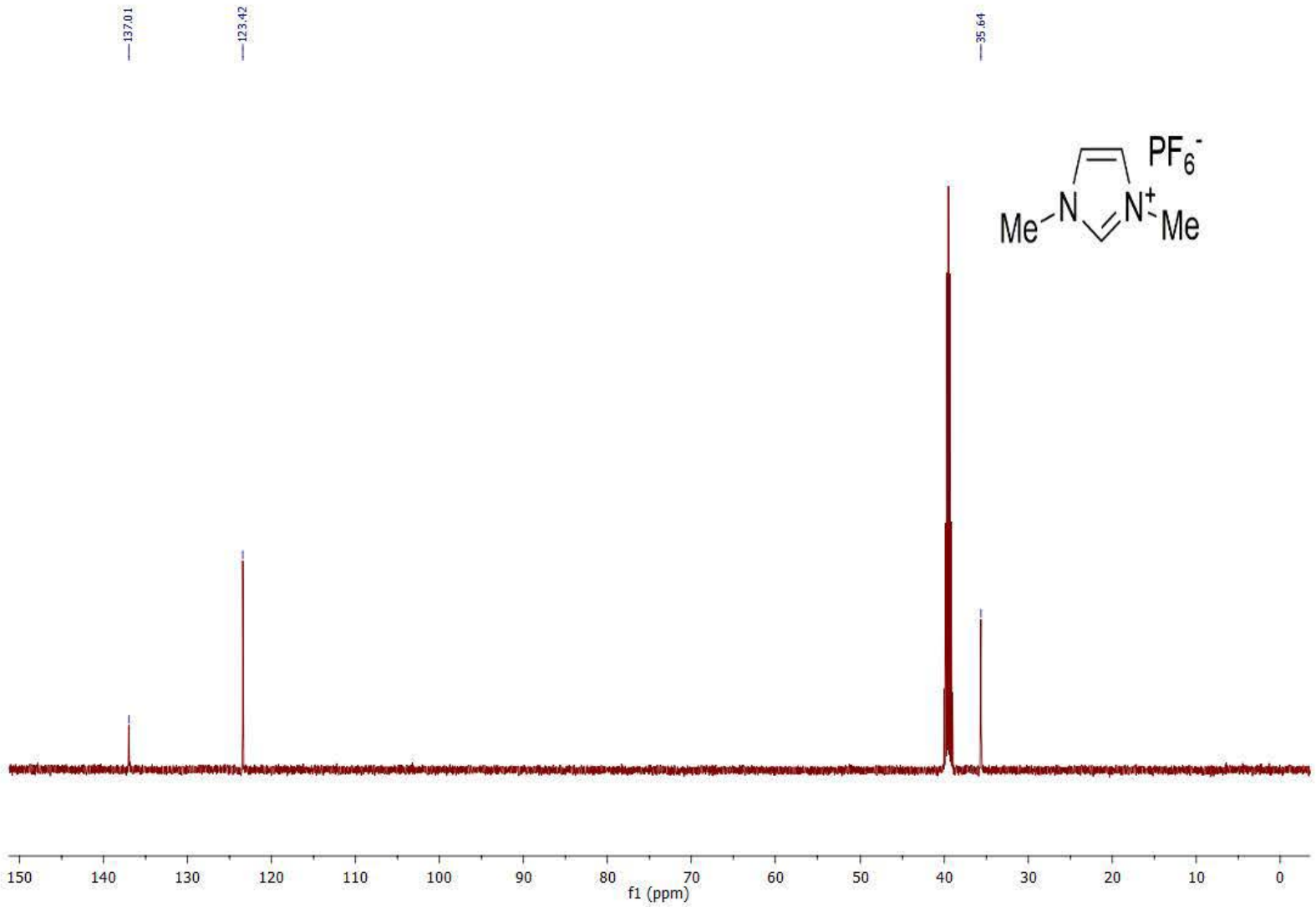

Figure S65. ^{13}C NMR spectrum of compound **G1**.

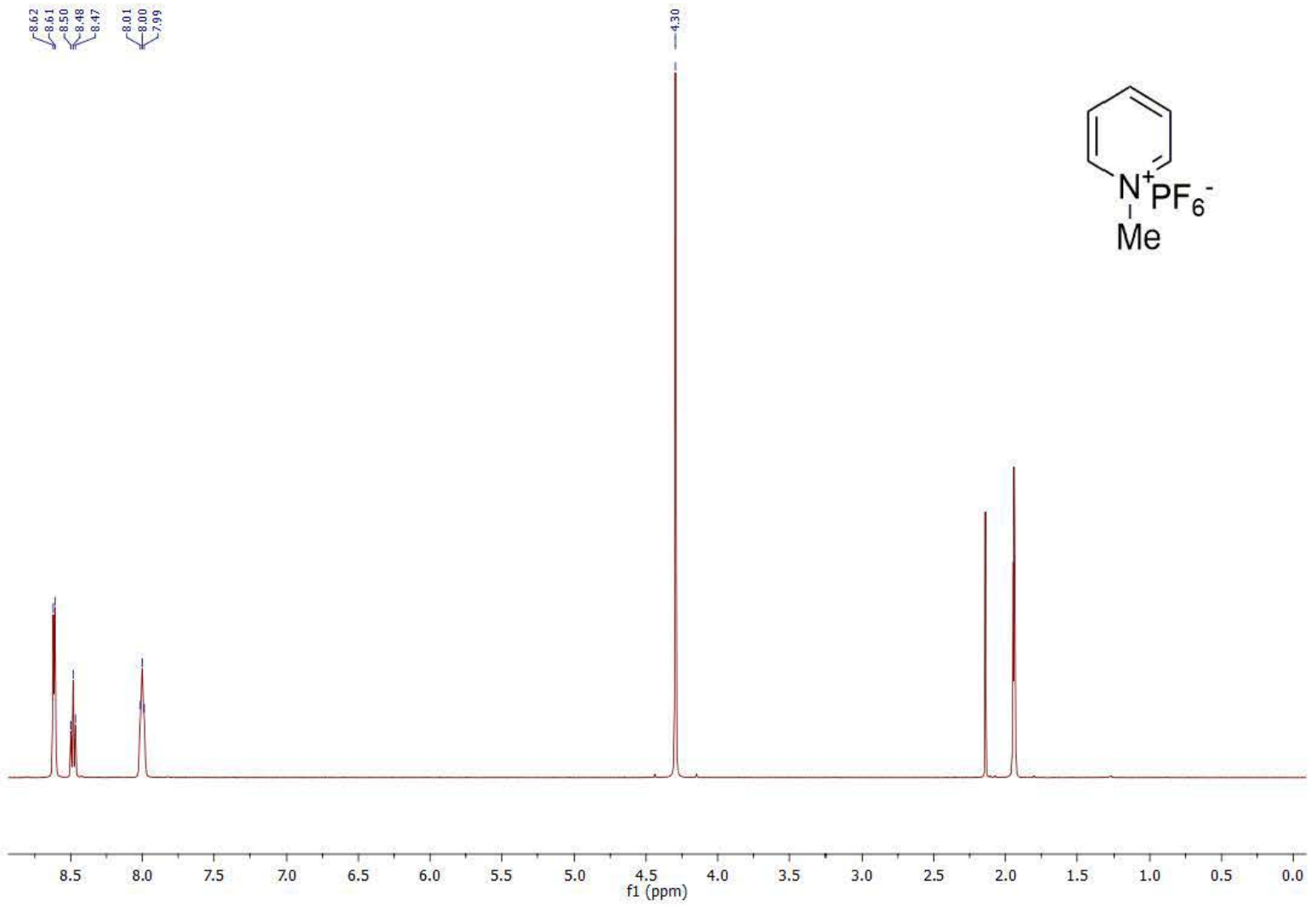

Figure S66. ^{1}H NMR spectrum of compound **G2.**

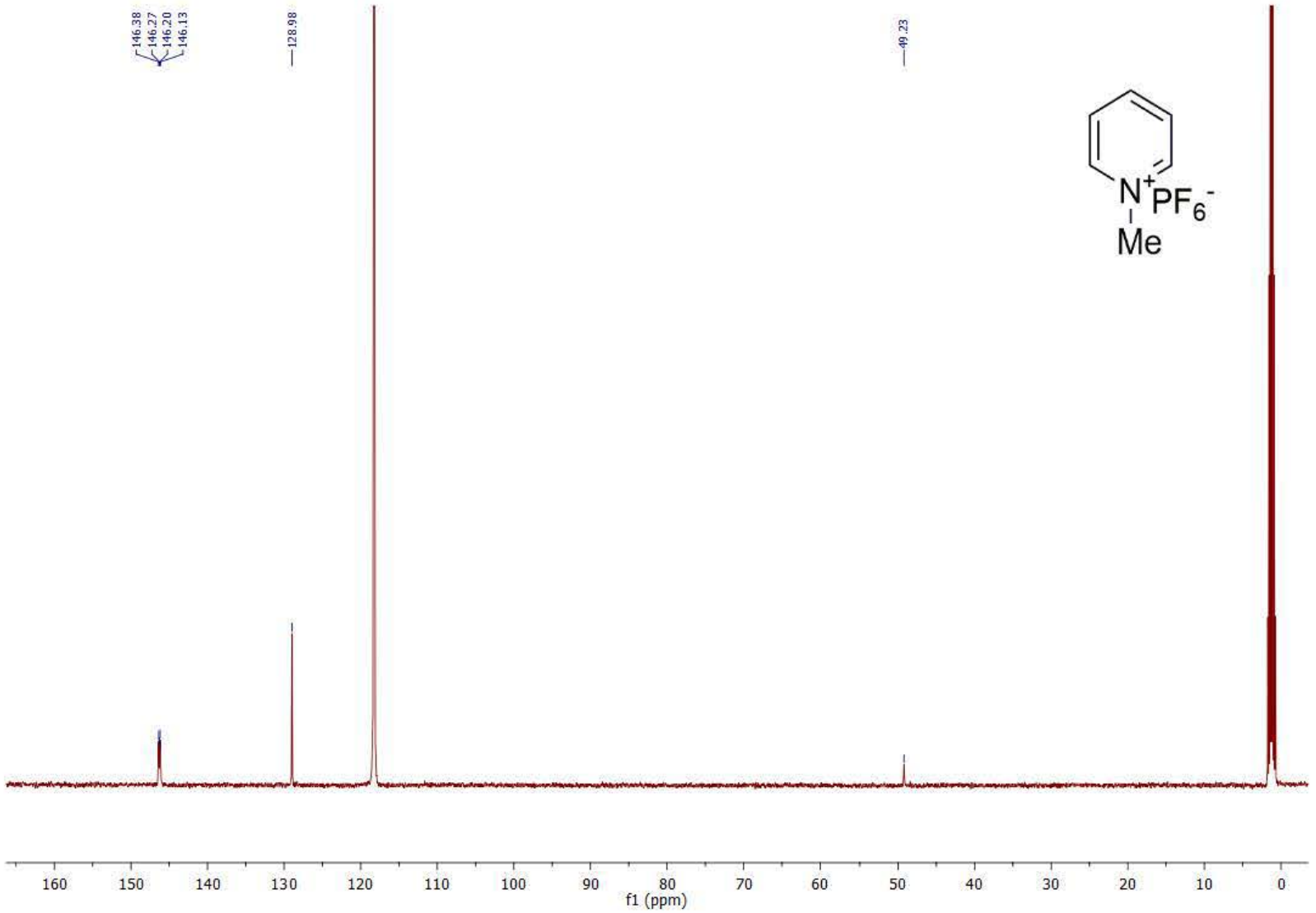

Figure S67. ^{13}C NMR spectrum of compound **G2**.

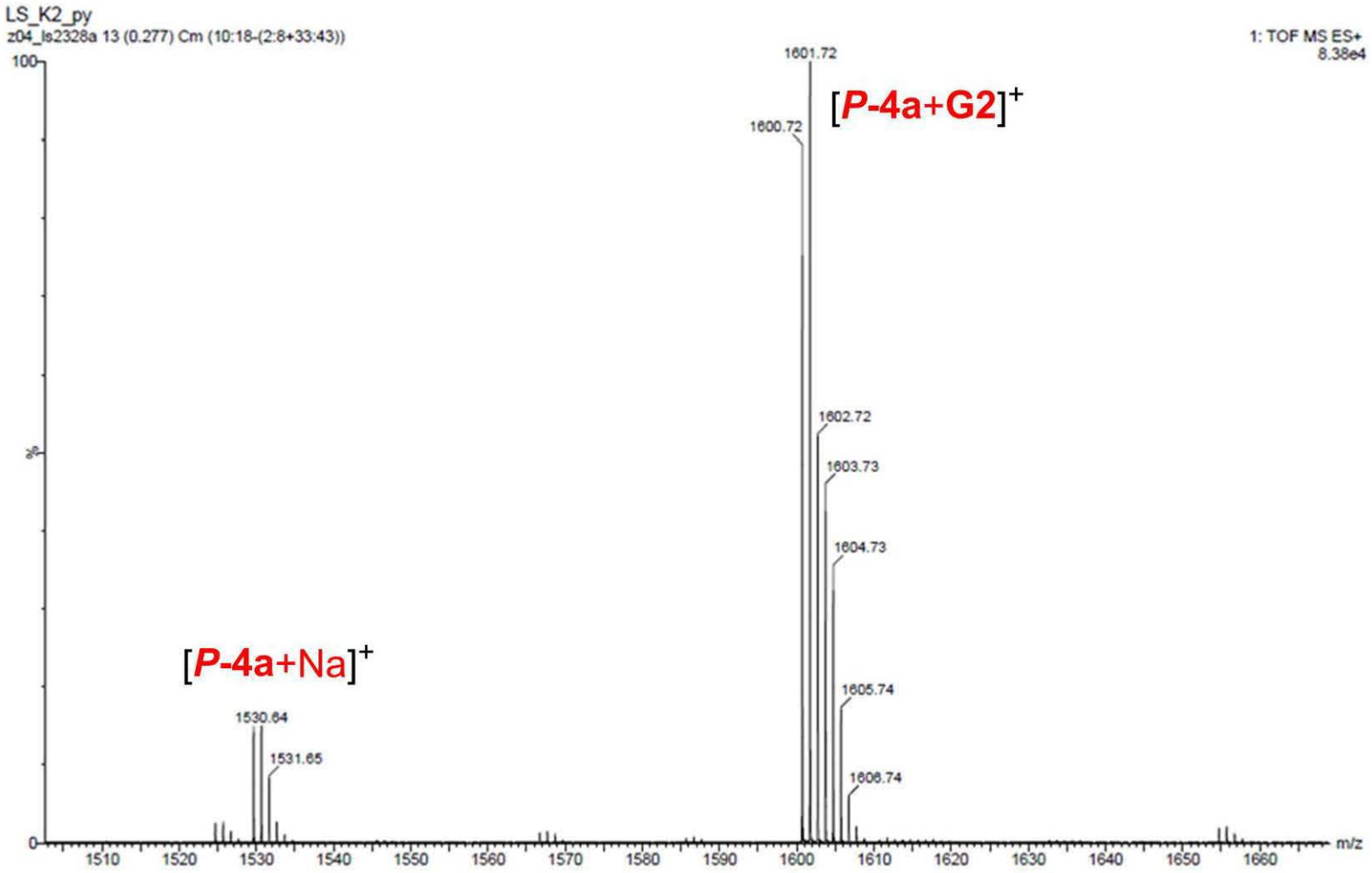

Figure S68. ESI MS spectrum of ***P*-4a** adduct with 1-methylpyridinium cation (**G2**).

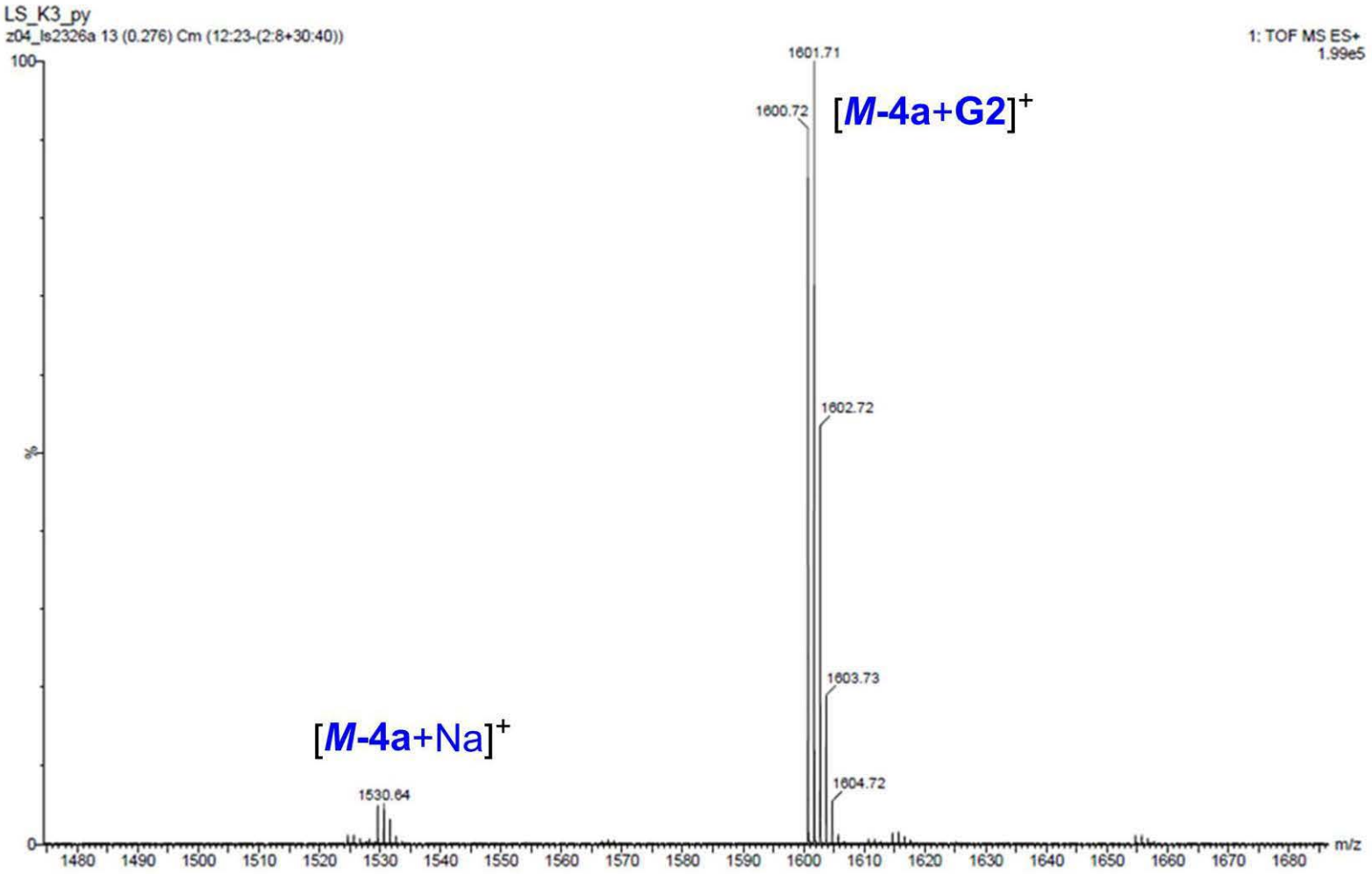

Figure S69. ESI MS spectrum of ***M*-4a** adduct with 1-methylpyridinium cation (**G2**).

JOC The Journal of Organic Chemistry

pubs.acs.org/joc Article

Fluorescent Molecular Cages with Sucrose and Cyclotriveratrylene Units for the Selective Recognition of Choline and Acetylcholine

Łukasz Szyszka,* Marcin Górecki, Piotr Cmoch, and Sławomir Jarosz*

Cite This: J. Org. Chem. 2021, 86, 5129−5141 Read Online

ACCESS | Metrics & More | Article Recommendations | Supporting Information

ABSTRACT: The synthesis of four fluorescent diastereoisomeric molecular cages containing cyclotriveratrylene and sucrose moieties connected *via* the naphthalene linkers is reported. These diastereoisomers were found to be selective and efficient receptors for acetylcholine and choline. Compound ***P*-5a** has a better affinity for choline over acetylcholine, while cage ***M*-5a** exhibits a higher association constant for acetylcholine over choline. The highest selectivity value was observed for compound ***M*-5a** (K_{ACh}/K_{Ch} = 3.1). Cages ***P*-5a**, ***P*-5b**, ***M*-5a**, and ***M*-5b** were fully characterized by the advanced NMR techniques, and ECD spectroscopy was supported by DFT calculations. The binding constants K_a of these receptors were determined by fluorescence titration experiments in acetonitrile.

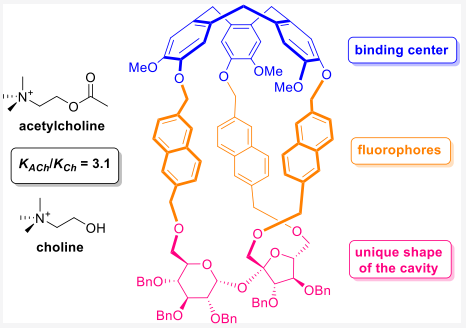

INTRODUCTION

Molecular cages with fluorescent properties able to selectively recognize various biologically essential compounds have been recently extensively studied.[1] Fluorescence imaging techniques are attractive and powerful tools for the nondestructive visualization of biological processes with high spatial resolution.[2]

The main advantages of fluorescence recognition studies are high sensitivity, fast response time, and technical simplicity, which makes this technique a useful tool for analytical detections and optical imaging.[3] In the last decades, several macrocycle derivatives containing fluorophores with different geometries and cavities capable of encapsulating guest molecules have been reported.[4]

The synthesis of molecular cages is particularly attractive due to its selective recognition properties.[5] These receptors can find application as catalysts,[6] separators,[7] sensors,[8] porous materials,[9] polymers,[10] transporters,[11] or drug delivery systems.[12] Among them, cryptophanes and hemicryptophanes are of particular interest as they are able to recognize small organic compounds.[13] This class of receptors is based on the rigid and bowl-shaped C_3-symmetrical cyclotriveratrylene (CTV) unit.[14]

The significant contribution to the synthesis of the CTV-based cages was made by Martinez group.[15] They obtained a wide range of molecular cages in which the CTV moiety is triply connected with tris(2-aminoethyl)amine or 1,3,5-tris-(bromomethyl)benzene *via* different linkers. These synthetic receptors can selectively recognize carbohydrates,[16] zwitterions,[17] or neurotransmitters.[18]

Although chiral receptors are important in selective recognition, only a few examples of such derivatives have been reported so far due to the difficulties in their syntheses.[19] Preparation of chiral macrocyclic receptors usually requires a multistep procedure, and the final yield is generally low for both steric and entropic reasons. The vast majority of these compounds are prepared as racemic mixtures.[15]

Acetylcholine (ACh) and choline (Ch), structurally related biologically important compounds, are the subject of interest for many years.[20] Acetylcholine plays a crucial role in the human central nervous system, in particular, in memory processes and transmission of the nervous impulse. This neurotransmitter, released at nerve-muscle synapse, is hydrolyzed to acetic acid and choline by acetylcholinesterase to prevent its high concentrations in the synaptic cleft.[21] Several diseases are connected with cholinergic failures, such as Parkinson's disease, Alzheimer's disease, Schizophrenia, or other mental diseases.[22] Choline (Ch) is an essential nutrient and has a critical role in neurotransmitter function because of its impact on acetylcholine synthesis and dopaminergic function.[23] Thus, the selective differentiation of both compounds could provide the understanding of the mechanism of the transmission of nervous signals.

In the last decade, several fluorescent receptors able to recognize ACh and Ch have been reported.,[20a24] Martinez *et al.* obtained three fluorescent hemicryptophanes containing naphthalene[25] or phenylacetylene[26] linkers, which can efficiently distinguish ACh over Ch. In another paper, they

Received: January 4, 2021
Published: March 12, 2021

https://dx.doi.org/10.1021/acs.joc.1c00019
J. Org. Chem. 2021, 86, 5129−5141

reported a fluorescent heteroditopic host with the naphthalene units and a Zn(II) complex for the selective recognition of choline phosphate.[27] Wu *et al.* reported a self-assembled triple anion helicate acting as a fluorescence displacement sensor, able to differentiate effectively choline, acetylcholine, glycine betaine, and L-carnitine.[28] In contrast to Martinez's hemicrypotophanes, this supramolecular host system displays high selectivity toward Ch over ACh. Sarmentero and Ballester developed a fluorescent hybrid cavitand-resorcin[4]arene receptor with the pH-modulated binding properties toward choline.[29] Moreover, this receptor is able to form thermodynamically stable complexes with complementary ammonium cations in protic solvents.

For many years, our group is involved in the synthesis of macrocyclic derivatives with sucrose scaffold able to recognize chiral and achiral guests.[30] We have prepared a vast array of chiral receptors based on this disaccharide that could effectively complex ammonium salts,[31] amino acid esters,[32] or simple anions.[33]

Our current studies are concentrated on chiral molecular cages bearing CTV and sucrose scaffolds connected *via* different linkers. In 2019, we presented, for the first time, the water-soluble chiral molecular cages consisting of cyclotriveratrylene and sucrose units.[34] Recently, we demonstrated an efficient, short, and high-yield route to four diastereoisomeric molecular cages ***P*-1a**, ***M*-1a**, ***P*-1b**, and ***M*-1b** connected *via* the *p*-phenylene linkers (Figure 1).[35] These compounds, unfortunately, are not able to recognize choline or acetylcholine.

Herein, we report the synthesis of fluorescent chiral CTV-sucrose-based cages with the naphthalene linkers and disclose their recognition properties toward choline and acetylcholine.

We decided to combine (i) a CTV unit as a binding center for an ammonium part of neurotransmitters, (ii) a sucrose unit as a chiral scaffold, which provide a unique shape of the cavity, and (iii) the naphthalene linkers as fluorophores, which will ensure the fluorescence properties, rigid cavity, and additional π-system for supporting the recognition.

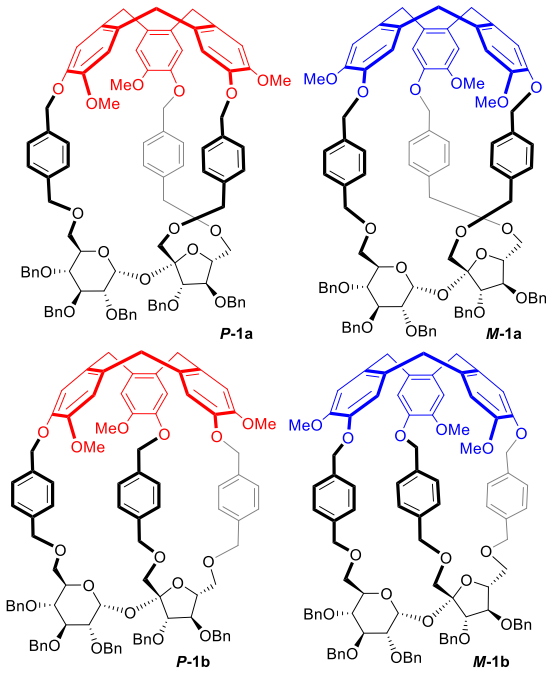

Figure 1. Structures of four molecular cages ***P*-1a**, ***M*-1a**, ***P*-1b**, and ***M*-1b** based on CTV and sucrose moieties connected *via* *p*-phenylene linkers.

RESULTS AND DISCUSSION

The synthesis of the CTV-sucrose-based cages was initiated from commercial sucrose, which was transformed into triol **2** in a three-step route, consisting of selective protection of secondary hydroxyl groups, according to our previously reported procedure.[34] Alkylation of this triol with an excess of 2,6-bis(bromomethyl)naphthalene at room temperature gave tribromide **3** in 24% yield (Scheme 1). When this reaction was carried out at reflux, the decomposition of the main product **3** was observed. Racemic cyclotriguaiacylene (**4**) was synthesized according to the previously reported literature procedure.[34]

Scheme 1. Synthesis of Sucrose Tribromide 3

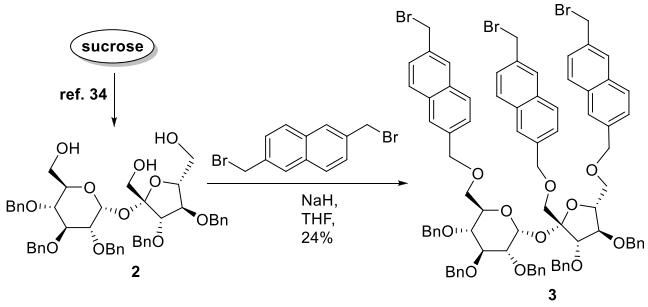

The Cs_2CO_3-catalyzed macrocyclization of sucrose tribromide **3** with racemic cyclotriguaiacylene (**4**) in acetonitrile at very low concentration (c = 0.001 M) at reflux provided four diastereoisomeric molecular cages: ***P*-5a**, ***M*-5a**, ***P*-5b**, and ***M*-5b** in 13, 13, 6, and 7% yield, respectively (total yield of macrocyclization reaction: 39%, ratio 2:2:1:1) (Scheme 2). These diastereoisomers were successfully separated by preparative HPLC using as the eluent, a mixture of three solvents: hexanes/dichloromethane/ethyl acetate in a ratio 50:50:10 v/v.

The structures of these cages were fully characterized by the advanced NMR techniques (^{1}H−^{1}H COSY, TOCSY, ROESY, and ^{1}H−^{13}C HSQC, HMBC, HSQC−TOCSY), as well as ECD spectroscopy and ESI-HRMS.

NMR Spectroscopy Results. The identification of all four separated isomers was more complex comparing to compounds described earlier.[35] Each of these structures contains three naphthalene rings, the CTV scaffold, and five benzyl groups, which significantly complicate the identification process, due to big crowding of the ^{1}H/^{13}C chemical shifts in the range typical for aromatic rings. Careful analysis of all NMR spectra supported by additional results obtained from the ECD measurements allowed us to determine unambiguously the structures of each isomer. Correct assignments of the proper structures for each compound based only on the NMR data could be misleading since such simplified analysis would give ambiguous results in proper structure determination. For example, the correct structure of isomer ***P*-5a**, in which the C-1′ atom of fructose is connected with ring C of the CTV unit and the C-6′ atom with ring B, while the CTV scaffold has a *P*-stereodescriptor, cannot be assigned only from the NMR data. The set of the ^{1}H/^{13}C chemical shifts and ROESY effects observed in the CTV part may also suggest the structure ***M*-5b**

https://dx.doi.org/10.1021/acs.joc.1c00019
J. Org. Chem. 2021, 86, 5129−5141

Scheme 2. Syntheses of Four Diastereoisomeric Molecular Cages *P*-5a, *M*-5a, *P*-5b, and *M*-5b

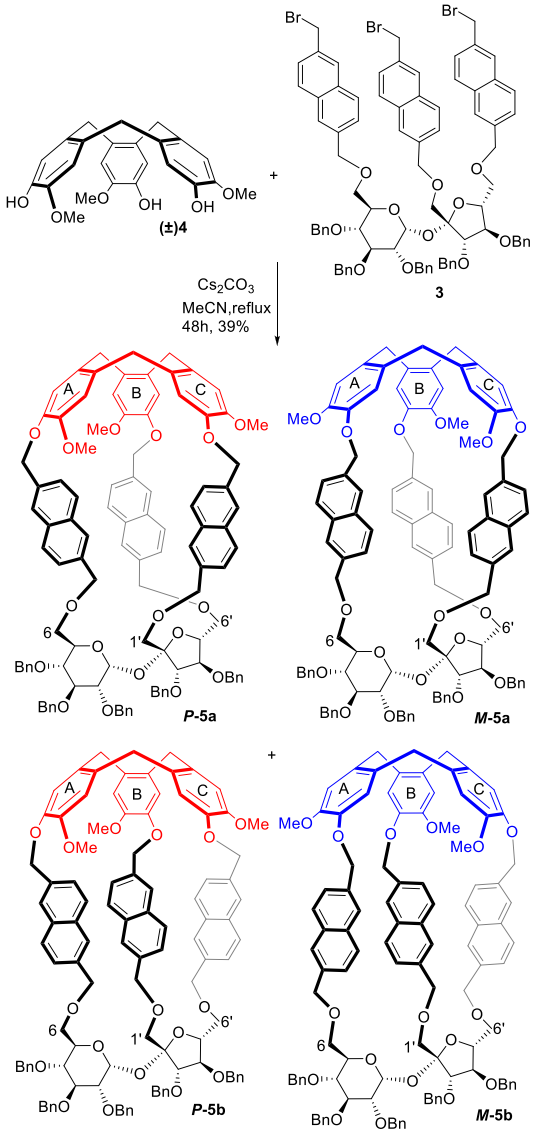

for this cage. The unambiguous assignment can be done only when the NMR spectra are supported with the ECD experiments (for more information, see the next part of this article).

Based on correct assignments of the $^{1}H/^{13}C$ signals in the NMR spectra for each individual isomer, some interesting remarks could be drawn. In the case of cages ***P*-5a** and ***M*-5a**, the value of $^{3}J(H-H)$ for the H-1 anomeric proton of glucose is *ca.* 3.3 Hz, whereas for counter pair ***P*-5b** and ***M*-5b** is *ca.* 3.8 Hz. It could be concluded that a change of direction in the CTV cap can cause an appropriate effect in the H-1/H-2 position of protons related to a change of the dihedral angle between them. Comparison of the ^{1}H and especially ^{13}C chemical shifts for both nontwisted (***P*-5a**/***M*-5a**) and twisted (***P*-5b**/***M*-5b**) molecules indicates the relatively good compatibility of these data in the sucrose part for both pairs (Table S1). The analysis of the NMR data, in particular, ^{13}C NMR chemical shifts, shows that, in the formation process of ***P*-5** and ***M*-5** derivatives, much more significant changes are observed for the fructose ring. This is manifesting, depending on the form of the cage, in strong shielding/deshielding effects at the C-1′ and C-6′ nuclei. In the case of cages ***P*-5a** and ***M*-5a**, the combination of sucrose and CTV fragments is connected with strong shielding increase by *ca.* 5 ppm of the C-1′ nucleus, as compared to shielding in cages ***P*-5b** and ***M*-5b** (Table 1). The opposite effect, however less pronounced, is noticed for the C-6′ nuclei. It suggests that its chemical shifts depend more on the position of the C-6′ methylene group in a specific product, which is clearly evident in ^{1}H chemical shifts for the H-6′ protons. In the ***M*-5b** structure, a very strong shielding effect for the C-6′ methylene protons is observed (δ = 2.25 and 2.95 ppm), as compared to other isomers (Table 1). The difference between positions of these diastereoisomeric protons is bigger for twisted structures ***P*-5b**/***M*-5b** (*ca.* 0.5−0.7 ppm) than for nontwisted ***P*-5a**/***M*-5a** (*ca.* 0−0.2 ppm). This observation is probably strongly connected with other arrangement of the fructose fragment in **5a**/**5b** isomers.

Another conclusion, which may be drawn from the NMR data is related to the signals of the benzyl groups. In the ^{1}H NMR spectra of ***P*-5b** and ***M*-5b**, the chemical shifts of such groups at the C-4′ atom are significantly different, as compared to ***P*-5a** and ***M*-5a** isomers. This is especially visible for structure ***P*-5b**, where the signals of the methylene protons of the benzyl group appear at δ = 3.51 and 3.70 ppm (Table 1). In this case, also, phenyl ring protons of the benzyl group are in the special isolated range (δ = 6.30−6.60 ppm). For isomer ***M*-5b**, the above mentioned phenomena also exist, but the results are less highlighted. A similar trend is typical for phenyl ring protons of the benzyl group attached to the C-4 atom in compound ***M*-5a**. Signals of these protons (δ = 5.92−6.50 ppm) are separated and more shielded than most aromatic protons of this cage. The position of the methoxy groups in the CTV part is also different for all isomers. The ^{1}H chemical shifts are in the typical range (δ ca. 3.0−4.0 ppm), but the structure of the cage determines the values of their shifts. The biggest difference between ^{1}H chemical shifts for these

Table 1. Comparison of the Selected ^{1}H and ^{13}C NMR Chemical Shifts δ (ppm) of *P*-5a, *P*-5b, *M*-5a, and *M*-5b Cages

	^{1}H and ^{13}C NMR chemical shifts δ (ppm)			
atom's number[a]	***P*-5a**	***P*-5b**	***M*-5a**	***M*-5b**
H-1	5.19	5.55	5.60	5.54
H-6′a/H-6′b	3.36/3.54	2.84/3.37	3.46/3.49	2.25/2.95
C4′−OC$\underline{H_2}$Ph	4.40/4.48	3.51/3.70	4.37/4.42	4.09/3.93
C4′−OCH_2−$\underline{H}$−Ph	7.19−7.29	6.58/6.41/6.30	7.16−7.27	7.07/7.06/6.96
H-26/H-26′/H-26″ (OC$\underline{H_3}$)	3.40/3.55/3.21	3.60/3.44/3.73	3.92/3.22/3.48	3.02/4.03/3.19
C-1′	69.9	74.8	69.1	74.8
C-6′	73.0	70.9	73.1	72.7

[a]For numbering of atom, see Experimental Section.

https://dx.doi.org/10.1021/acs.joc.1c00019
J. Org. Chem. 2021, 86, 5129−5141

methoxy groups is noted for compound ***M*-5b** (ca. 1.0 ppm, Table 1). Moreover, due to the specific through-space interactions of the methoxy groups and aromatic protons from the CTV fragment, the proper assignment of the $^{1}H/^{13}C$ chemical shifts and thus structure correctness can be verified. All these above-mentioned remarks can be used in the future to find a relation of the NMR data and spatial arrangements of atoms defining the specific structure.

ECD Spectroscopy Results. For more detailed structural information that would allow more deeply to explore the stereochemistry of these diastereoisomeric molecular cages, we turned our attention to the electronic circular dichroism (ECD) spectroscopy, which is one of the most suitable spectroscopic tools for this purpose. It is based on the study of interactions of circularly polarized light in the UV−vis region for exploring the 3D environment of chiral nonracemic compounds and allows to monitor even the smallest subtle changes in their structures. The successful combination of the ECD spectroscopy with quantum chemical calculations expands significantly the range of applicability of this spectroscopy.[34−36]

Thus, the UV and ECD spectra of four diastereoisomeric molecular cages ***P*-5a**, ***M*-5a**, ***P*-5b**, and ***M*-5b** were recorded in CH_3CN to assign their absolute stereochemistry (Figure 2).

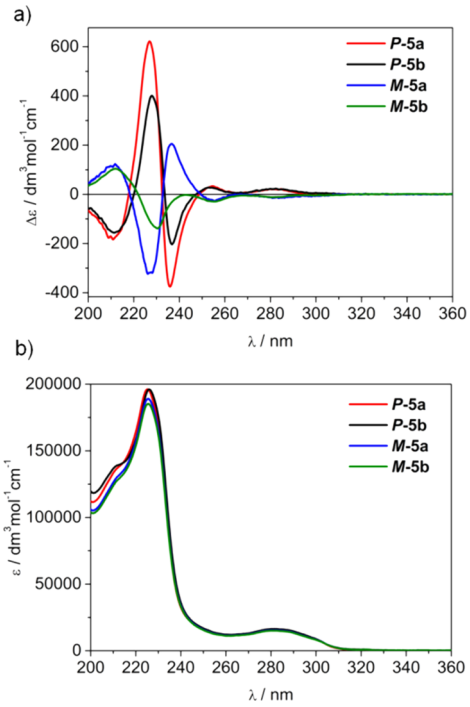

Figure 2. (a) ECD and (b) UV spectra of ***P*-5a**, ***M*-5a**, ***P*-5b**, and ***M*-5b** measured in CH_3CN at room temperature.

The UV spectra of these compounds are almost identical and showed a manifold of bands at 280 and 225 nm associated with the CTV and naphthalene chromophores.

In the ECD spectra, there are a few very intense bands centered at around 235, 225, and 210 nm and rather intense ones at lower energy wavelengths at about 282 and 255 nm. In the case of molecular cage ***M*-5b**, being eluted as the fourth compound in the elution order under our conditions (see the Experimental Section part), the ECD curve showed some aberrations in the range 220−250 nm. Remarkably, the two curves, *i.e.*, ***P*-5a** and ***M*-5a** are associated with almost perfect mirror image of the ECD pattern. This is clearly evidenced by crossing exactly at zero values. In contrast, for ***P*-5b** and ***M*-5b**, the mirror image correlation was not perfect, as evidenced in Figure 2a by different absolute values of the ECD intensities in the range 220−250 nm, and by the fact that these two spectra do not cross precisely at zero values. Nevertheless, all spectra show characteristic features related to $^{1}L_b$ and $^{1}L_a$ transitions of aromatic chromophores. According to Collet *et al.*, the signs of the $^{1}L_a$ bands can be used to assign the absolute configuration of the CTV unit: *M*-configuration is determined for molecules, which exhibit in their ECD spectra a sequence of signs *negative/positive* from *low* to *high* energy within this region, so analogously for *P*-configuration sequence is opposite.[37] Thus, *ad hoc* for the first and second eluted peaks with *positive/negative* sequence of signs, the configuration was immediately assigned as ***P*-5a**/***P*-5b**, while for the third and fourth the opposite sequence indicates ***M*-5a**/***M*-5b** configuration.

DFT Calculation Results. To support this assignment, the quantum chemical calculations were carried out. First, the conformational search was done at the molecular mechanics level using a simplified structure in which benzyl groups (Bn) in the sucrose moiety were substituted with the hydrogen atom to facilitate the further computational predictions of ECD spectra. This approach preserves the main conformational landscapes of the investigated compounds and does not have any impact on the final stereochemical assignment. Then, the lowest energy structures within 3 kcal/mol were submitted for DFT optimization using Gaussian16 program[38] at the B3LYP/6-31G(d) level of theory applying PCM for CH_3CN. In this way, for each compound, two conformers were identified for ECD calculations. They mainly fluctuate in the rotation around the C−O bond(s) linking the CTV unit with naphthalene linker(s), while the rest of the molecule is well-kept. The lowest energy structures are presented in Figure 3. For TDDFT simulations, the following functional/basis-set combination was used: B3LYP/SVP with the polarizable continuum model (PCM) for CH_3CN.

This level of approximation was indicated as one of the most successful in recent studies for investigating their ECD properties of systems with CTV moiety.[34,35,36b,c]

The simulated spectra are consistent with experimental ones (Figure 4); however, some minor inconsistencies are found in the range of $^{1}L_b$ transitions. This is a well-known issue in TDDFT calculations of the ECD spectra since this band is simulated without taking into account a vibronic effect.[39] Consequently, here, this subregion is excluded from our discussion.

The distinction of diastereoisomeric molecular cages was made by in-depth analysis of their chiroptical properties. Although the shapes of the ECD bands for two pairs of diastereoisomers are in line for ***P*-5a** and ***M*-5a**, the relative intensity of bands in the range 220−250 nm is higher in respect to the second pair ***P*-5b** and ***M*-5b**. The same observation can be found from TDDFT-calculated ECD spectra, which provides further strong evidence on the correctness of this stereochemical assignment.

Recognition Studies. Then, we investigated the recognition properties of ***P*-5a**, ***P*-5b**, ***M*-5a**, and ***M*-5b** cages toward biologically interesting compounds, acetylcholine (ACh) and choline (Ch). The binding properties were determined by the fluorescence titration evaluating the emission spectra after the progressive addition of ACh or Ch solution to the host

https://dx.doi.org/10.1021/acs.joc.1c00019
J. Org. Chem. 2021, 86, 5129−5141

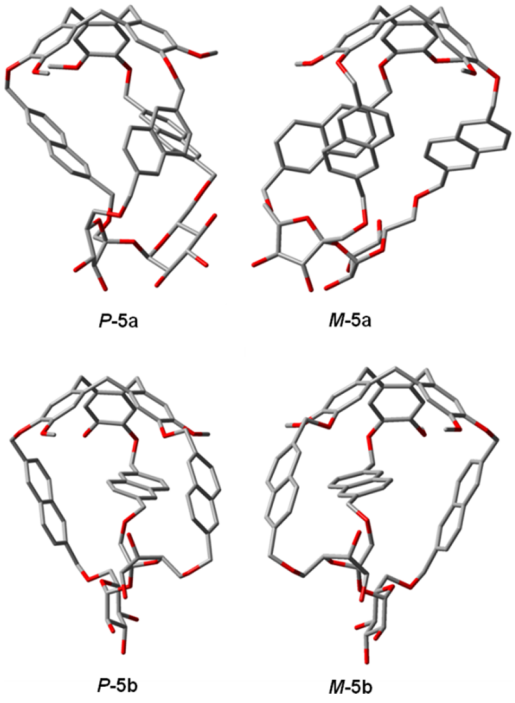

Figure 3. Lowest-energy conformers calculated at the B3LYP/6-31G(d)/PCM/CH_3CN level of theory. Note: the hydrogen atoms are omitted for the sake of clarity.

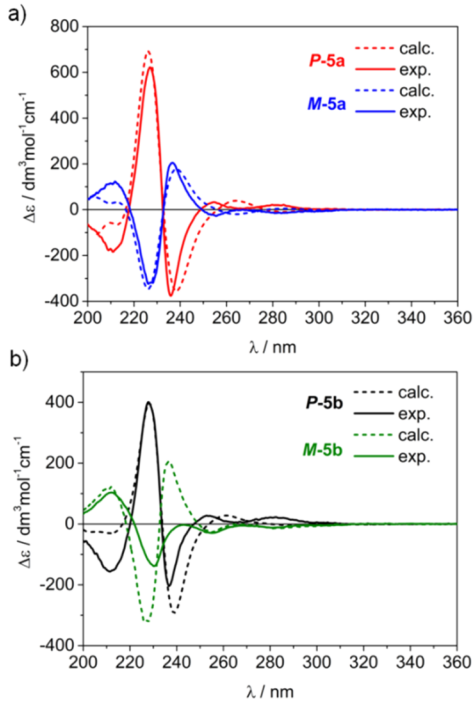

Figure 4. Comparison of calculated ECD spectra at the B3LYP/SVP/PCM (CH_3CN) level of (a) ***P*-5a**, ***M*-5a**, and (b) ***P*-5b**, ***M*-5b** with experimental ones measured in CH_3CN at room temperature. Note: all spectra are red-shifted by 5 nm and simulated using 0.15 eV Gaussian band-widths.

solution in the same solvent. We decided to choose this method due to the fast response time, high sensitivity, and the presence of the naphthalene linkers, which ensure fluorescence properties. The titration experiments were performed in acetonitrile, and iodide was chosen as a guest counter-ion because of good solubility.

Fluorescence emission spectra of the hosts strongly differ after the addition of appropriate equivalents of guests. Indeed, an increase of fluorescence is observed for ***P*-5a** and ***M*-5a** hosts, whereas receptors ***P*-5b** and ***M*-5b** display a decrease of the fluorescence intensity upon the addition of acetylcholine or choline (Figure 5 and Figures S3, S5, S9, and S11). This opposite behavior might suggest the differences in formation of the host–guest complexes and the influence of chiral twisted/non-twisted structure of each diastereoisomer. The fluorescence enhancement might be assigned to the formation of rigid host–guest complex structures of nontwisted ***P*-5a** and ***M*-5a** cages stabilized by intermolecular hydrogen bonds.[26a] Moreover, the twisted structures of compounds ***P*-5b** and ***M*-5b** ensure the different size and shape of the cavity than nontwisted ***P*-5a** and ***M*-5a**, which might also explain this binding differences.

The addition of acetylcholine resulted in a significant increase of the fluorescence of the ***P*-5a** and ***M*-5a** host at *ca.* 330 nm (Figure 5a,c). The binding constant (K_a) for ***P*-5a** was 2.2×10^3 M^{-1}, whereas for ***M*-5a** was 5.6×10^3 M^{-1}. In the case of hosts ***P*-5b** and ***M*-5b**, the K_a values were 2.4×10^3 and 0.6×10^3 M^{-1}, respectively (Table 2). These results show that compound ***M*-5a** is the most efficient host for ACh.

During our recognition studies of choline, the remarkable increase of the fluorescence intensity was observed for ***P*-5a** and ***M*-5a** cages at *ca.* 330 nm (Figure 5b,d). In the case of ***P*-5b** and ***M*-5b**, quenching of fluorescence intensity was observed (Figures S9 and S11). The most significant value of binding constant K_a (3.8×10^3 M^{-1}) was achieved by receptor ***P*-5a**.

Lower binding constants were obtained for ***P*-5b** and ***M*-5a** cages, 2.6×10^3 and 1.8×10^3 M^{-1}, respectively. The lowest K_a value was obtained for the ***M*-5b** host (0.5×10^3 M^{-1}) (Table 2). Comparing the recognition selectivity of ACh and Ch by these hosts, we can notice that compound ***P*-5a** is the most efficient sensor for choline ($K_{Ch}/K_{ACh} = 1.7$), while ***M*-5a** is a more suitable receptor for acetylcholine ($K_{ACh}/K_{Ch} = 3.1$). The ***M*-5a** host could efficiently distinguish acetylcholine over choline. This selectivity is meaningful since both guests participate in the metabolic pathway. In the case of compounds ***P*-5b** and ***M*-5b**, no binding selectivity was observed. These differences in recognition of both guests could be rationalized by the structure of the molecular cages. As we can conclude from the DFT calculated structures, the chiral sucrose platform provides the unique shapes of the cavities of these receptors, which might allow to distinguish acetylcholine over choline and vice versa.

To supply the fluorescence recognition studies and get more information about the binding sites, the ^1H NMR titration experiments of ***P*-5a** and ***M*-5a** cages with ACh and Ch were carried out (Figures S13, S16, S19, and S21). For this purpose, appropriate amounts of ACh or Ch solutions in CD_3CN/$CDCl_3$ (80:20) were gradually added to the host solution in the mixture of the same solvent. The ^1H NMR studies show changes in the chemical shifts of both host and guest protons, which is in line with fast host–guest exchange on the NMR time scale. In all cases, the signals from $(CH_3)_3N^+$ and methylene protons are shifted downfield with increasing amount of ACh or Ch guests (Figures S15 and S18). This could be explained by increasing the ratio of the unbounded guest.[26] Compared to the spectra of pure ACh or Ch, the

https://dx.doi.org/10.1021/acs.joc.1c00019
J. Org. Chem. 2021, 86, 5129–5141

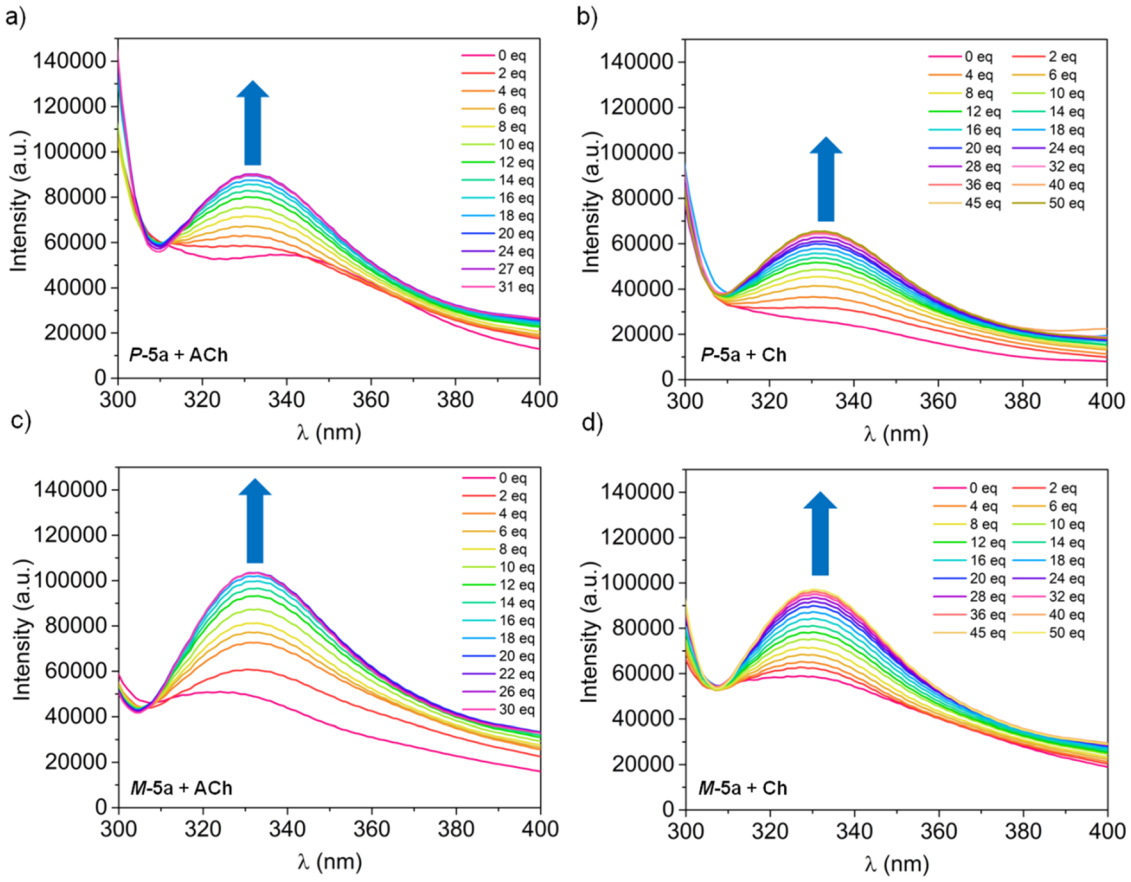

Figure 5. Fluorescent titration of hosts: (a) ***P*-5a** with ACh, (b) ***P*-5a** with Ch, (c) ***M*-5a** with ACh, and (d) ***M*-5a** with Ch in CH_3CN at 298 K excited at 280 nm (counter-ion I^-).

Table 2. Comparison of Binding Constants K_a (M^{-1}) of *P*-5a, *P*-5b, *M*-5a, and *M*-5b Hosts with ACh and Ch

Guest	Host	K_a (M^{-1})[a]	K_{ACh}/K_{Ch}
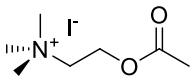 **ACh**	***P*-5a**	$2.2 \times 10^3 \pm 1.6\%$	0.6
	***P*-5b**	$2.4 \times 10^3 \pm 3.5\%$	0.9
	***M*-5a**	$5.6 \times 10^3 \pm 1.7\%$	3.1
	***M*-5b**	$0.6 \times 10^3 \pm 0.9\%$	1.2
Guest	Host	K_a (M^{-1})[a]	K_{Ch}/K_{ACh}
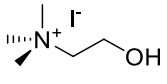 **Ch**	***P*-5a**	$3.8 \times 10^3 \pm 0.9\%$	1.7
	***P*-5b**	$2.6 \times 10^3 \pm 3.8\%$	1.1
	***M*-5a**	$1.8 \times 10^3 \pm 1.4\%$	0.3
	***M*-5b**	$0.5 \times 10^3 \pm 1.1\%$	0.8

[a]Association constants *Ka* were determined by fitting fluorescence titration curves (CH_3CN, 298 K) using Bindfit program.[40]

signals of both guests are shifted upfield during the titration studies, which confirms the encapsulation of both guests in the host cavities. There are a few reports about binding the $(CH_3)_3N^+$ part of ACh and Ch inside the electron-rich CTV cavity.,[25,26a,27] In the case of ***M*-5a**, the gradual addition of ACh provided downfield chemical shifts of the CTV aromatic protons and upfield shifts of the protons from naphthalene ring linkers (Figure S14). On the other hand, the recognition studies of Ch also show downfield shifts of the CTV aromatic protons, but upfield chemical shifts of naphthalene ring linkers were less significant (Figure S17).

The additional interactions of ACh ester group with the host may explain the higher binding constant and selectivity for ACh by ***M*-5a** cage. While the ^{1}H NMR titration studies of ***P*-5a** cage with Ch show evident changes in the chemical shifts of aromatic part of CTV unit, as well as naphthalene rings, the binding studies with ACh demonstrate only slight changes of such chemical shifts (Figures S20 and S22). In this case, most likely, the shape of the cavity may cause the preference for Ch binding.

All these results indicate the formation of the corresponding host–guest complexes. Both guests are bind inside the electron-rich cavities, which is reflected in chemical shift changes observed during ^{1}H NMR titration experiments, as well as in the changes of the fluorescence intensity. The observed differences in ACh and Ch recognition by these diastereoisomeric cages are, most likely, caused by original shapes of their cavities, created by various connections of both CTV and sucrose scaffolds. To further supply the binding properties of these cages and the stoichiometry of the complexation, ESI-MS measurements were carried out. Both hosts, ***P*-5a** and ***M*-5a**, form noncovalent complexes with choline cations $[M + Ch]^+$ with an *m/z* value of 1761.81 (Figures S77 and S79), as well as with acetylcholine cations $[M + ACh]^+$ with an *m/z* of value 1803.82 (Figures S78 and S80) in acetonitrile. These results show that adducts formed between cages ***P*-5a** or ***M*-5a** with Ach or Ch are relatively stable proving a 1:1 stoichiometry ratio. Adducts containing

https://dx.doi.org/10.1021/acs.joc.1c00019
J. Org. Chem. 2021, 86, 5129−5141

two guest molecules $[M + 2ACh]^{2+}$ or $[M + 2Ch]^{2+}$ were not detected.

Next, the DFT calculations of the host−guest inclusion complexes were performed to investigate further the selectivity of cage ***M*-5a** toward ACh over Ch. The optimized structures of both complexes show that ACh, as well as Ch, is partially encapsulated in the ***M*-5a** host cavity (Figure 6). These results

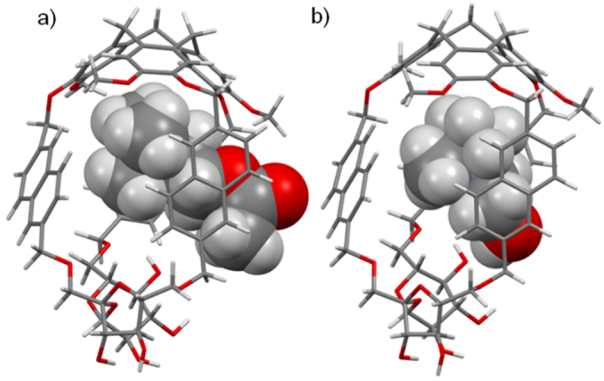

Figure 6. DFT-calculated structures of encapsulated complexes (a) ***M*-5a⊂ACh** and (b) ***M*-5a⊂Ch**.

are consistent with previously described CTV-based hemicryptophanes capable of binding ACh.[41] In the case of ***M*-5a⊂ACh** complex, the ammonium unit is situated below the bowl-shaped CTV moiety, while the ester function is located between naphthalene linkers. Several CH−π interactions between the $(CH_3)_3N^+$ part of ACh and phenyl rings of the CTV unit or naphthalene rings with distances ranging from 2.8 to 3.1 Å and from 2.5 to 3.0 Å, respectively, are observed. Moreover, cation−π interactions between positively charged nitrogen from ACh and CTV's phenyl or naphthyl centroids occur with distances from 4.8 and 4.9 or 4.1 to 4.4 Å, respectively. Additionally, the interactions between (i) C═O or −O− from ACh and CH_3 from the methoxy group (2.8 Å or 2.7 Å), (ii) $C(O)CH_3$ from the ACh and naphthalene centroid (3.4 Å), and (iii) both CH_2 from ACh and naphthalene centroids (distances from 2.4 to 3.4 Å) can be found. In the case of ***M*-5a⊂Ch**, complex similar cation-π, as well as CH−π, interactions between the $(CH_3)_3N^+$ part of choline and aromatic rings of the CTV unit or naphthalene linkers are observed, but with greater distances. Indeed, the distance between positively charged nitrogen from choline and phenyl or naphthyl centroids from the host ranging from 5.1 to 5.6 or 4.2 to 4.5 Å, respectively. These results show that the ammonium part of Ch is bound weaker than ACh by the CTV unit. The CH−π interactions between $(CH_3)_3N^+$ and phenyl or naphthyl centroids in ***M*-5a⊂Ch** are in distance ranging from 3.0 to 3.7 or 2.5 to 3.1 Å, respectively. Both CH_2 groups from choline are also in distance from 3.1 to 3.5 Å in relation to naphthyl centroids. These DFT studies of both complexes give an insight in the binding details of the ***M*-5a** cage and support its selectivity toward ACh. The additional interactions of the ester group with ***M*-5a** cage and shorter distances between the CTV moiety and ammonium part of ACh could be responsible for this selectivity compared to Ch.

CONCLUSIONS

In summary, we described the synthesis of four fluorescent diastereoisomeric molecular cages based on CTV and sucrose units connected *via* the naphthalene linkers. These compounds can act as efficient fluorogenic sensors for the detection of acetylcholine or choline. Application of the sucrose platform to the host structure is, as we assume, responsible for the unique shape of the cavity resulting in the selective recognition of these biologically important guests. Cage ***M*-5a** displays the strongest binding with acetylcholine, while cage ***P*-5a** mostly prefers choline. Both guests acetylcholine and choline could be, therefore, selectively recognized by these molecular cages using fluorescence spectroscopy.

EXPERIMENTAL SECTION

General Methods. All reagent-grade chemicals and solvents were received from commercial suppliers. TLC was performed on Merck silica gel $60F_{254}$ plates. Compounds were purified using an automatic flash chromatography system Knauer with UV and ELSD detection and Grace Resolv or Reveleris cartridges. Preparative HPLC was conducted on a Shimadzu SPD-6a spectrometer using a UV detector (254 nm) with a Vathsil 100 column (250 mm × 10 mm, particle size: 5 μm) and a 5 mL/min flow rate. The NMR spectra were recorded with a Varian VNMRS 600 MHz (at 600 MHz and 150 MHz for ^1H and ^{13}C NMR spectra, respectively) spectrometer for solutions in $CDCl_3$ and TMS as internal standards. All significant resonances were assigned by COSY ($^1H-^1H$), ROESY ($^1H-^1H$), TOCSY ($^1H-^1H$), HSQC ($^1H-^{13}C$), and HMBC ($^1H-^{13}C$) correlations. Mass spectra were measured using a Synapt G2-S HDMS (Waters Inc.) mass spectrometer equipped with an electrospray ion source and q-TOF type mass analyzer or using an AutoSpec Premier (Waters Inc.) double-focusing magnetic sector mass spectrometer with an EBE geometry equipped with an EI (electron impact) ion source. Optical rotations were measured with a Jasco P 2000 apparatus in $CHCl_3$ or CH_2Cl_2 with a sodium lamp at room temperature. Elemental analyses were obtained with a Perkin-Elmer 2400 CHN analyzer. The ECD and UV spectra were recorded in a CH_3CN on a Jasco J-715 spectropolarimeter. The fluorescence titration experiments were performed using a Shimadzu RF-6000 fluorescence spectrometer.

2,6-Bis(bromomethyl)naphthalene was synthesized according to the literature procedure.[42] All reactions were carried out under an argon atmosphere. Organic solutions were dried over anhydrous Na_2SO_4.

*Synthesis of 2,3,3′,4,4′-Penta-O-benzyl-1′,6,6′-tri-O-[5-(bromomethyl)-naphthyl]-sucrose (**3**).*

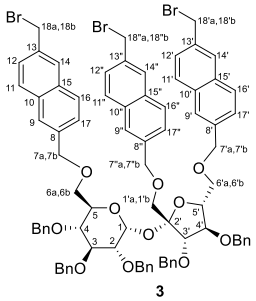

3

Sodium hydride (453.6 mg, 18.9 mmol, 60% dispersion in mineral oil) was added portionwise to a solution of triol **2** (1 g, 1.26 mmol) in dry THF (20 mL). After stirring for 20 min. at room temperature, 2,6-bis(bromomethyl)naphthalene (2.37 g, 7.56 mmol) was added in one portion, and the mixture was stirred at room temperature overnight. The reaction was quenched by careful addition of methanol (2 mL), and the mixture was poured onto dichloromethane (20 mL) and water (20 mL). The layers were separated, the aqueous one was extracted with dichloromethane (3 × 20 mL), combined organic phases were washed with brine (60 mL), dried over Na_2SO_4, and concentrated, and the residue was purified by flash chromatography (hexanes/ethyl acetate = from 100:0 to 75:25) to afford **3** (446 mg, 0.3 mmol, 24%) as a yellowish oil. $[\alpha]_D^{25}$ + 34.3 (*c* 0.5, $CHCl_3$). ^1H NMR (600 MHz, $CDCl_3$): δ = 7.76 (s, 1H, H-Naphth), 7.65−7.74 (m, 9H, 9 × H-Naphth), 7.62 (d, *J* = 7.6 Hz, 1H, H-Naphth), 7.62 (s,

https://dx.doi.org/10.1021/acs.joc.1c00019
J. Org. Chem. 2021, 86, 5129−5141

1H, H-Naphth), 7.43 (dd, J = 18.2 Hz, J = 1.7 Hz, 1H, H-Naphth), 7.43 (t, 1H, H-Naphth), 7.35−7.41 (m, 4H, 4 × H-Naphth), 7.11−7.24 (m, 23H, 23 × H-Ph), 7.01−7.04 (m, 2H, 2 × H-Ph), 5.78 (d, $J_{1,2}$ = 3.5 Hz, 1H, H-1), 4.83 (d, J = 10.8 Hz, 1H, benzylic H), 4.80 (d, J = 11.0 Hz, 1H, benzylic H), 4.64 (s, 2H, 2 × C$\underline{H}_2$−Br), 4.61 (s, 2H, 2 × C$\underline{H}_2$−Br), 4.70 (m, 1H, H-7″a), 4.67 (m, 2H, H-7′a, benzylic H), 4.66 (m, 1H, benzylic H), 4.64 (m, 1H, H-7′b), 4.60 (m, 1H, H-7a), 4.58 (s, 2H, 2 × C$\underline{H}_2$−Br), 4.57 (m, 1H, H-7″b), 4.56 (d, J = 12.4 Hz, 1H, benzylic H), 4.52 (d, J = 11.1 Hz, 1H, benzylic H), 4.50 (d, J = 11.0 Hz, 1H, benzylic H), 4.46 (m, 1H, H-3′), 4.43 (m, 1H, H-7b), (4.41−4.47 (m, 3H, 3 × benzylic H), 4.24 (dd, $J_{4',3'}$ = 7.5 Hz, $J_{4',5'}$ = 7.5 Hz 1H, H-4′), 4.14−4.17 (m, 1H, H-5′), 4.09 (m, 1H, H-5), 3.92 (dd, $J_{3,4}$ = 9.3 Hz, $J_{3,2}$ = 9.3 Hz, 1H, H-3), 3.72−3.80 (m, 3H, H-1′a, H-6′a, H-6′b), 3.62 (dd, $J_{4,5}$ = 9.8 Hz, $J_{4,3}$ = 9,4 Hz, 1H, H-4), 3.59 (d, $J_{1'b,1'a}$ = 11.0 Hz, 1H, H-1′b), 3.48 (dd, $J_{6b,5}$ = 3.5 Hz, $J_{6b,6a}$ = 10.3 Hz 1H, H-6a), 3.46 (dd, $J_{2,1}$ = 3.5 Hz, $J_{2,3}$ = 9.5 Hz, 1H, H-2), 3.39 (dd, $J_{6b,5}$ = 1.7 Hz, $J_{6b,6a}$ = 10.6 Hz, 1H, H-6b) ppm. $^{13}C\{^1H\}$ NMR (150 MHz, $CDCl_3$): δ = 139.0, 138.6, 138.4, 138.2, 138.2 (C_{quat}, 5 × C-Ph), 136.7, 136.5, 136.4 (C-8, C-8′, C-8″), 135.3, 135.2, 135.1 (C-13, C-13′, C-13″), 133.1, 133.0, 132.9, 132.8, 132.8, 132.7 (C-10, C-10′, C-10″, C-15, C-15′, C-15″), 125.9−128.9 (m, 43C, 25 × C-Ph, 18 × C-Naphth), 104.7 (C-2′), 90.0 (C-1), 84.0 (C-3′), 82.3 (C-4′), 82.1 (C-3), 80.0 (C-2), 79.7 (C-5′), 77.8 (C-4), 75.6 (C3−O$\underline{C}H_2$Ph), 74.9 (C4−O$\underline{C}H_2$Ph), 73.5 (C-7″), 73.4 (C-7), 73.3 (C-7′), 73.2 (C3′−O$\underline{C}H_2$Ph), 72.7 (C4′−O$\underline{C}H_2$Ph), 72.3 (C2−O$\underline{C}H_2$Ph), 71.6 (C-1′), 71.6 (C-6′), 70.7 (C-5), 68.8 (C-6), 34.2, 34.2, 34.2 (C-18, C-18′, C-18″) ppm. MS (ESI-TOF) m/z: $[M + Na]^+$ calcd for $C_{83}H_{79}O_{11}Br_3Na$ 1511.31; found 1511.35. Anal. calcd for $C_{83}H_{79}O_{11}Br_3$: C, 66.81; H, 5.34; found: C, 66.69; H, 5.54.

*Syntheses of CTV-Sucrose-Based Cages **P-5a**, **M-5a**, **P-5b**, and **M-5b**.* To a solution of (±)**4** (24.5 mg, 0.06 mmol) in dry acetonitrile (40 mL), Cs_2CO_3 (175 mg, 0.54 mmol) was added and the mixture was stirred at room temperature for 30 min. The solution of compound **3** (89 mg, 0.06 mmol) in dry acetonitrile (20 mL) was added dropwise by a syringe pump within 4 h, and the mixture was stirred at reflux for additional 48 h. After cooling to room temperature, the mixture was filtered through Celite and the solvent was removed under vacuum. The residue was dissolved in CH_2Cl_2 (20 mL) and washed with water (20 mL). The aqueous phase was extracted with CH_2Cl_2 (3 × 20 mL), and the combined organic solutions were washed with brine (30 mL), dried, and concentrated. The resulting residue was purified by preparative HPLC (hexanes/dichloromethane/ethyl acetate = 50:50:10) to afford pure compounds ***P*-5a** (13 mg, 0.0078 mmol, 13%, colorless solid), ***P*-5b** (6 mg, 0.0036 mmol, 6%, white solid), ***M*-5a** (13 mg, 0.0078 mmol, 13%, colorless solid), and ***M*-5b** (7 mg, 0.0042 mmol, 7%, colorless solid). Total yield: 39%.

*Characterization of Compound **P-5a**.*

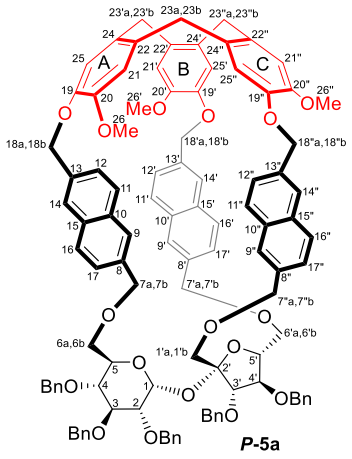

$[\alpha]_D^{25}$ + 129.5 (c 0.22, CH_2Cl_2). ^1H NMR (600 MHz, $CDCl_3$): δ = 7.77 (s, 1H, H-14″), 7.65 (d, $J_{11'',12''}$ = 8.7 Hz, 1H, H-11″), 7.64 (s, 1H, H-9″), 7.58 (d, $J_{16'',17''}$ = 8.5 Hz, 1H, H-16″), 7.51 (d, $J_{11,12}$ = 8.1 Hz, 1H, H-11), 7.51 (s, 1H, H-9′), 7.47 (s, 1H, H-9), 7.46 (s, 1H, H-14), 7.44 (d, $J_{11',12'}$ = 8.5 Hz, 1H, H-11′), 7.39 (d, $J_{16,17}$ = 8.4 Hz, 1H, H-16), 7.36 (m, 1H, H-17″), 7.35 (m, 1H, H-12″), 7.34−7.36 (m, 2H, 2 × H-Ph), 7.21−7.29 (m, 15H, 15 × H-Ph), 7.16−7.19 (m, 4H, 4 × H-Ph), 7.16 (m, 1H, H-12), 7.11 (d, 1H, H-12′), 7.03 (d, 1H, H-17), 7.00−7.02 (m, 4H, 4 × H-Ph), 6.99 (s, 1H, H-25″), 6.95 (s, 1H, H-25′), 6.94 (s, 1H, H-14′), 6.88 (m, 1H, H-17′), 6.86 (m, 1H, H-25), 6.68 (d, $J_{16,17}$ = 7.8 Hz, 1H, H-16′), 6.67 (s, 1H, H-21′), 6.64 (s, 1H, H-21), 6.61 (s, 1H, H-21″), 5.36 (d, $J_{18''a,18''b}$ = 13.1 Hz, 1H, H-18″a), 5.26 (d, $J_{18''a,18''b}$ = 12.9 Hz, 1H, H-18′a), 5.24 (d, $J_{18a,18b}$ = 10.8 Hz, 1H, H-18a), 5.19 (d, $J_{1,2}$ = 3.3 Hz, 1H, H-1), 5.16 (d, 1H, H-18″b), 5.15 (d, 1H, H-18′b), 4.81 (d, 1H, H-18b), 4.76 (d, $J_{7''a,7''b}$ = 12.4 Hz, 1H, H-7″a), 4.76 (d, J = 11.2 Hz, 1H, C3′−OC$\underline{H}_2$Ph), 4.70 (m, 3H, H-23a, H-23′a, C4−OC$\underline{H}_2$Ph), 4.68 (m, 2H, H-23″a, C3−OC$\underline{H}_2$Ph), 4.63 (d, J = 11.4 Hz, 1H, C3′−OC$\underline{H}_2$Ph), 4.49 (m, 1H, C3−OC$\underline{H}_2$Ph), 4.48 (m, 3H, 2 × C2−OC$\underline{H}_2$Ph, C4′−OC$\underline{H}_2$Ph) 4.46 (m,1 H, H-7′a), 4.45 (m, 1H, H-7a), 4.41 (m, 1H, C4−OC$\underline{H}_2$Ph), 4.40 (m, 1H, C4′−OC$\underline{H}_2$Ph), 4.38 (m, 1H, H-3′), 4.30 (d, $J_{7'b,7'a}$ = 13.4 Hz, 1H, H-7′b), 4.27 (d, 1H, H-7″b), 4.15 (d, $J_{7b,7a}$ = 12.4 Hz, 1H, H-7b), 4.07 (m, 1H, H-5′), 3.83 (m, 1H, H-4′), 3.81 (m, 1H, H-5), 3.79 (m, 1H, H-3), 3.65 (d, $J_{1'a,1'b}$ = 11.0 Hz, 1H, H-1′a), 3.56 (m, 1H, H-4), 3.55 (s, 3H, H-26′), 3.54 (m, 1H, H-6′a), 3.53 (m, 1H, H-6a), 3.51 (m, 1H, H-23b), 3.48 (m, 1H, H-23″b), 3.47 (m, 1H, H-23′b), 3.45 (d, 1H, H-1′b), 3.40 (s, 3H, H-26), 3.36 (dd, $J_{6'b,5'}$ = 8.00 Hz, $J_{6'b,6'a}$ = 11.9 Hz 1H, H-6′b), 3.30 (dd, $J_{2,3}$ = 9.7 Hz, $J_{2,1}$ = 3.4 Hz, 1H, H-2), 3.21 (s, 3H, H-26″), 3.17 (dd, $J_{6b,5}$ = 1.4 Hz, $J_{6b,6a}$ = 10.8 Hz, 1H, H-6b) ppm. $^{13}C\{^1H\}$ NMR (150 MHz, $CDCl_3$): δ = 149.1 (C-20′), 148.8 (C-20″), 148.5 (C-20), 147.0 (C-19″), 146.1 (C-19), 145.9 (C-19′), 138.8, 138.6, 138.3, 138.2, 138.2 (C_{quat}, 5 × C-Ph), 136.9 (C-8′), 135.9 (C-8), 135.8 (C-8″), 135.3 (C-13″), 134.2 (C-13), 133.7 (C-22′), 133.3 (C-13′), 133.3 (C-22″), 132.8 (C-10/C-15), 132.7 (C-22), 132.6 (C-15″), 132.6 (C-10″), 132.6 (C-10′), 132.5 (C-15′), 132.0 (C-24″), 132.0 (C-10/C-15), 131.7 (C-24′), 131.6 (C-24), 128.1 (C-11″), 127.9 (C-16″), 127.8 (C-11), 127.7 (C-16′), 127.7 (C-16), 127.2−128.3 (m, 25 × C-Ph), 126.8 (C-14′), 126.3 (C-14), 126.3 (C-17″), 126.2 (C-9″), 126.2 (C-17), 126.1 (C-9), 126.1 (C-11′), 125.6 (C-17′), 125.6 (C-12′), 125.4 (C-14″), 125.4 (C-12), 124.8 (C-12″), 124.5 (C-9′), 118.6 (C-25′), 117.6 (C-25″), 116.3 (C-25), 113.4 (C-21″), 113.4 (C-21′), 113.0 (C-21), 104.1 (C-2′), 90.7 (C-1), 84.1 (C-3′), 82.4 (C-4′), 81.6 (C-3), 80.9 (C-5′), 79.9 (C-2), 77.5 (C-4), 75.4 (C3−O$\underline{C}H_2$Ph), 74.7 (C4−O$\underline{C}H_2$Ph), 73.1 (C-7), 73.0 (C-7″), 73.0 (C-6′), 72.9 (C3′−O$\underline{C}H_2$Ph), 72.7 (C-18″), 72.6 (C-18′), 72.5 (C2−O$\underline{C}H_2$Ph), 72.5 (C-7′), 72.4 (C4′−O$\underline{C}H_2$Ph), 71.4 (C-18), 70.6 (C-5), 69.9 (C-1′), 68.1 (C-6), 55.9 (C-26′), 55.5 (C-26), 55.5 (C-26″), 36.4 (C-23), 36.4 (C-23′), 36.2 (C-23″) ppm. HRMS (ESI-TOF) m/z: $[M + Na]^+$ calcd for $C_{107}H_{100}O_{17}Na$ 1679.6858; found 1679.6844. Anal. calcd for $C_{107}H_{100}O_{17} + H_2O$: C, 76.68; H, 6.13; found: C, 76.55; H, 6.25.

*Characterization of Compound **P-5b**.*

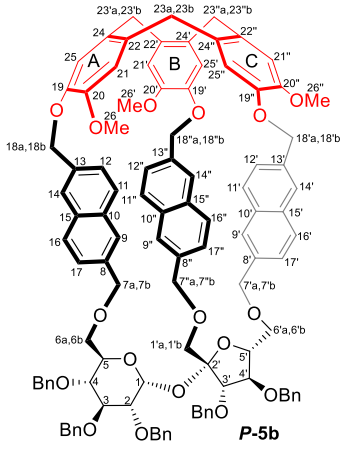

$[\alpha]_D^{25}$ + 103.2 (c 0.22, CH_2Cl_2). ^1H NMR (600 MHz, $CDCl_3$): δ = 7.65 (d, $J_{11,12}$ = 8.3 Hz, 1H, H-11), 7.62 (s, 1H, H-9), 7.57 (s, 1H, H-14), 7.56 (s, 1H, H-14″), 7.55 (m, 2H, H-11′, H-16), 7.52 (d, $J_{16'',17''}$ = 8.4 Hz, 1H, H-16″), 7.49 (s, 1H, H-9″), 7.47 (s, 1H, H-9′), 7.38 (m, 1H, H-17), 7.32 (m, 1H, H-12′), 7.27 (m, 1H, H-12), 7.26−7.40

https://dx.doi.org/10.1021/acs.joc.1c00019
J. Org. Chem. 2021, 86, 5129−5141

(m, 16H, 16 × H-Ph), 7.23 (d, $J_{11'',12''}$ = 8.2 Hz, 1H, H-11″), 7.09 (s, 1H, H-25′), 7.07 (s, 1H, H-25″), 7.06 (s, 1H, H-14′), 7.02−7.05 (m, 5H, H-17″, 4 × H-Ph), 6.91 (d, $J_{17',16'}$ = 8.1 Hz, 1H, H-17′), 6.88 (s, 1H, H-25), 6.87 (m, 1H, H-12″), 6.86 (s, 1H, H-21″), 6.81 (s, 1H, H-21′), 6.79 (d, $J_{16',17'}$ = 8.4 Hz 1H, H-16′), 6.70 (s, 1H, H-21), 6.58 (t, J = 7.6 Hz, 2H, 2 × H-Ph), 6.41 (d, J = 7.4 Hz, 2H, 2 × H-Ph), 6.30 (t, J = 7.4 Hz, 1H, H-Ph), 5.55 (d, $J_{1,2}$ = 3.8 Hz, 1H, H-1), 5.46 (d, $J_{18'a,18'b}$ = 13.3 Hz, 1H, H-18′a), 5.35 (d, 1H, H-18′b), 5.27 (d, $J_{18''a,18''b}$ = 12.7 Hz, 1H, H-18″a), 5.09 (d, $J_{18a,18b}$ = 11.7 Hz, 1H, H-18a), 4.94 (d, 1H, H-18″b), 4.93 (d, J = 11.0 Hz, 1H, C3−OC$\underline{H}_2$Ph), 4.89 (d, J = 11.6 Hz, 1H, C4−OC$\underline{H}_2$Ph), 4.87 (d, 1H, H-18b), 4.79 (m, 1H, C3−OC$\underline{H}_2$Ph), 4.78 (m, 1H, H-7a), 4.77 (m, 3H, H-23a, H-23′a, H-23″a), 4.74 (d, J = 12.0 Hz, 1H, C2−OC$\underline{H}_2$Ph), 4.67 (d, J = 11.6 Hz, 1H, C2−OC$\underline{H}_2$Ph), 4.66 (m, 2H, H-7″a, C4−OC$\underline{H}_2$Ph), 4.58 (d, $J_{7''b,7''a}$ = 12.1 Hz, 1H, H-7″b), 4.46 (d, J = 11.2 Hz, 1H, C3′−OC$\underline{H}_2$Ph), 4.24 (d, $J_{3',4'}$ = 8.2 Hz, 1H, H-3′), 4.23 (d, $J_{7b,7a}$ = 11.9 Hz, 1H, H-7b), 4.21 (d, $J_{7'a,7'b}$ = 12.9 Hz, 1H, H-7′a), 4.19 (d, J = 11.4 Hz, 1H, C3′−OC$\underline{H}_2$Ph), 4.13 (m, 1H, H-5), 3.95 (d, 1H, H-7′b), 3.92 (dd, $J_{3,2}$ = 9.1 Hz, $J_{3,4}$ = 9.3, 1H, H-3), 3.73 (s, 3H, H-26″), 3.71 (d, $J_{1'a,1'b}$ = 11.9 Hz, 1H, H-1′a), 3.70 (d, J = 11.5 Hz, 1H, C4′−OC$\underline{H}_2$Ph) 3.61 (m, 1H, H-2), 3.60 (s, 3H, H-26), 3.59 (m, 1H, H-23″b), 3.58 (m, 1H, H-1′b), 3.57 (m, 2H, H-4, H-23′b), 3.55 (m, 1H, H-23b), 3.53 (m, 1H, H-4′), 3.51 (d, J = 10.9 Hz, 1H, C4′−OC$\underline{H}_2$Ph), 3.44 (s, 3H, H-26′), 3.37 (dd, $J_{6'a,6'b}$ = 10.9 Hz, $J_{6'a,5'}$ = 11.1 Hz, 1H, H-6′a), 3.32 (m, 1H, H-5′), 3.31 (m, 1H, H-6a), 3.26 (dd, $J_{6b,5}$ = 4.0 Hz, $J_{6b,6a}$ = 10.5 Hz, 1H, H-6b), 2.84 (dd, $J_{6'a,5'}$ = 1.9 Hz, 1H, H-6′b) ppm. $^{13}C\{^1H\}$ NMR (150 MHz, $CDCl_3$): δ = 149.7 (C-20″), 149.1 (C-20′), 148.4 (C-20), 147.6 (C-19′) 147.3 (C-19), 145.3 (C-19″), 139.0, 138.8, 138.4, 137.8, 137.8 (C_{quat}, 5 × C-Ph), 136.5 (C-8″), 136.1 (C-8′), 135.3 (C-8), 135.1 (C-13), 134.7 (C-13″), 134.0 (C-22″), 133.6 (C-22′), 133.5 (C-13′), 132.8 (C-22), 132.8 (C-10″/C-15″), 132.8 (C-15), 132.6 (C-10), 132.5 (C-24′), 132.4 (C-10′), 132.3 (C-10″/C-15″), 132.3 (C-24″), 132.2 (C-15′), 131.6 (C-24), 128.2 (C-16), 127.8 (C-11), 127.7 (C-16″), 127.6 (C-16′, C-11′), 127.4−128.4 (m, 22 × C-Ph), 127.0 (C-9), 126.8, 126.7 (3 × C-Ph), 126.5 (C-17), 126.3 (C-14″, C-14′), 126.3 (C-17′), 126.0 (C-9′), 125.9 (C-14), 125.8 (C-12′), 125.5 (C-9″), 125.4 (C-12″, C-17″), 125.3 (C-11″, C-12), 120.0 (C-25″), 118.5 (C-25′), 116.4 (C-25), 114.4 (C-21′), 113.9 (C-21″), 113.5 (C-21), 104.0 (C-2′), 88.7 (C-1), 82.5 (C-3′), 82.3 (C-3), 81.3 (C-4′), 79.3 (C-2), 79.2 (C-5′), 78.0 (C-4), 75.4 (C3−O$\underline{C}H_2$Ph), 74.8 (C-1′), 74.7 (C4−O$\underline{C}H_2$Ph), 74.4 (C-7″), 73.9 (C-18″), 73.0 (C-7), 72.6 (C-7′), 72.3 (C-18′), 72.2 (C2−O$\underline{C}H_2$Ph), 72.2 (C3′−O$\underline{C}H_2$Ph), 71.4 (C4′−O$\underline{C}H_2$Ph), 71.3 (C-18), 70.9 (C-6′), 69.9 (C-5), 67.6 (C-6), 56.3 (C-26″), 56.2 (C-26′), 56.0 (C-26), 36.6 (C-23′), 36.5 (C-23″), 36.3 (C-23) ppm. HRMS (ESI-TOF) m/z: $[M + Na]^+$ calcd for $C_{107}H_{100}O_{17}Na$ 1679.6858; found 1679.6836. Anal. calcd for $C_{107}H_{100}O_{17} + H_2O$: C, 76.68; H, 6.13; found: C, 76.23; H, 6.25.

*Characterization of Compound **M-5a**.*

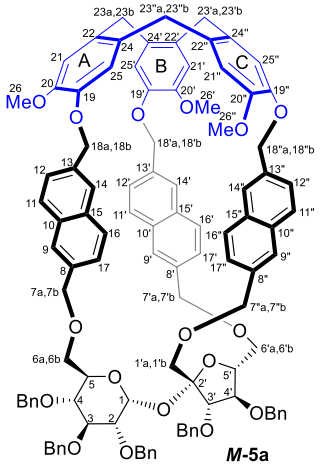

M-5a

$[\alpha]_D^{25}$ − 90.5 (*c* 0.22, CH_2Cl_2). ^1H NMR (600 MHz, $CDCl_3$): δ = 7.83 (s, 1H, H-9″), 7.79 (d, $J_{16'',17''}$ = 8.4 Hz, 1H, H-16″), 7.76 (d, $J_{11'',12''}$ = 8.4 Hz, 1H, H-11″), 7.73 (s, 1H, H-14″), 7.48 (d, 1H, H-17″), 7.45 (s, 1H, H-14), 7.44 (d, 1H, H-11′), 7.40 (s, 1H, H-9′), 7.38 (m, 1H, H-12″), 7.36 (m, 1H, H-9), 7.30 (m, 1H, H-11), 7.29−7.40 (m, 5H, 5 × H-Ph), 7.23 (m, 1H, H-16), 7.21 (m, 1H, H-12), 7.17 (m, 1H, H-12′), 7.16−7.27 (m, 13H, 13 × H-Ph), 7.12 (s, 1H, H-25′), 7.09 (s, 1H, H-25), 7.02 (m, 1H, H-17), 7.01 (m, 1H, H-17′), 6.99 (m, 1H, H-21), 6.98 (d, $J_{16',17'}$ = 8.6 Hz, 1H, H-16′), 6.98−7.04 (m, 2H, 2 × H-Ph), 6.93 (s, 1H, H-21″), 6.84 (s, 1H, H-14′), 6.76 (s, 1H, H-25″), 6.64 (s, 1H, H-21′), 6.50 (d, J = 7.5 Hz, 2H, 2 × H-Ph), 6.39 (t, J = 7.6 Hz, 2H, 2 × H-Ph), 5.92 (t, J = 7.3 Hz, 1H, 1 × H-Ph), 5.60 (d, $J_{1,2}$ = 3.3 Hz, 1H, H-1), 5.40 (d, $J_{18a,18b}$ = 13.5 Hz, 1H, H-18a), 5.31 (d, 1H, H-18b), 5.21 (d, $J_{18''a,18''b}$ = 11.9 Hz, 1H, H-18″a), 5.20 (d, $J_{18'a,18'b}$ = 11.9 Hz, 1H, H-18′a), 5.07 (d, $J_{7''a,7''b}$ = 12.5 Hz, 1H, H-7″a), 4.97 (d, 1H, H-18″b), 4.79 (m, 1H, H-23a), 4.76 (m, 2H, 2 × C3′−OC$\underline{H}_2$Ph), 4.74 (m, 2H, H-23′a, H-23″a), 4.64 (d, $J_{7a,7b}$ = 12.7 Hz, 1H, H-7a), 4.60 (d, J = 11.9 Hz, 1H, C2−OC$\underline{H}_2$Ph), 4.55 (d, 1H, C2−OC$\underline{H}_2$Ph), 4.54 (d, J = 10.8 Hz, 1H, C3−OC$\underline{H}_2$Ph), 4.50 (d, J = 10.8 Hz, 1H, C4−OC$\underline{H}_2$Ph), 4.50 (d, 1H, H-7″b), 4.42 (d, J = 11.4 Hz, 1H, C4′−OC$\underline{H}_2$Ph), 4.40 (d, 1H, H-18′b), 4.37 (d, 1H, C4′−OC$\underline{H}_2$Ph), 4.35 (m, 1H, H-3′), 4.34 (m, 2H, H-7′a, H-7′b), 4.15 (d, 1H, C3−OC$\underline{H}_2$Ph), 4.04 (m, 2H, H-7b, C4−OC$\underline{H}_2$Ph), 4.03 (m, 1H, H-4′), 3.92 (m, 1H, H-5′), 3.92 (s, 3H, H-26), 3.90 (m, 1H, H-5), 3.72 (m, 2H, H-1′a, H-3), 3.66 (d, $J_{1'b,1'a}$ = 12.2 Hz, 1H, H-1′b), 3.61 (m, 2H, H-23b, H-23′b), 3.51 (d, $J_{23''b,23''a}$ = 13.5 Hz, 1H, H-23″b), 3.49 (m, 1H, H-6′a), 3.48 (s, 3H, H-26″), 3.46 (m, 1H, H-6′b), 3.41 (m, 1H, H-4), 3.39 (m, 1H, H-6a), 3.38 (m, 1H, H-2), 3.22 (s, 3H, H-26′), 3.06 (dd, $J_{6b,5}$ = 1.2 Hz, $J_{6b,6a}$ = 10.4 Hz, 1H, H-6b) ppm. $^{13}C\{^1H\}$ NMR (150 MHz, $CDCl_3$): δ = 150.3 (C-20′), 148.6 (C-20), 148.0 (C-20″), 147.3 (C-19″), 146.8 (C-19′), 145.8 (C-19), 138.7, 138.6, 138.1, 138.0, 137.8 (C_{quat}, 5 × C-Ph), 136.3 (C-8′), 135.9 (C-8″), 135.4 (C-8), 134.9 (C-13″), 134.7 (C-22′), 134.3 (C-13), 133.6 (C-13′), 133.2 (C-22), 132.8, 132.8, 132.6, 132.5, 132.5 (C_{quat}, 5 × C-Naphth) 132.4 (C-24″), 132.1 (C_{quat}, C-Naphth), 132.1 (C-24′), 131.9 (C-24), 131.8 (C-22″), 128.4 (C-11″), 128.2 (C-14′), 128.0 (C-16″), 128.0 (C-16), 127.9 (C-16′), 127.8 (C-11), 127.4 (C-9″), 127.3−128.3 (m, 25 × C-Ph), 127.2 (C-17″), 127.2 (C-11′), 126.7 (C-9), 126.6 (C-14), 126.6 (C-12′), 126.3 (C-17), 126.3 (C-14″), 125.9 (C-12), 125.5 (C-12″), 125.0 (C-17′), 124.4 (C-9′), 121.9 (C-25′), 116.7 (C-25), 115.0 (C-21″), 113.8 (C-21), 113.5 (C-21′), 113.3 (C-25″), 104.6 (C-2′), 91.4 (C-1), 84.9 (C-3′), 83.1 (C-4′), 81.4 (C-3), 80.8 (C-5′), 79.7 (C-2), 77.7 (C-4), 76.2 (C-18′), 75.1 (C3−O$\underline{C}H_2$Ph), 74.3 (C4−O$\underline{C}H_2$Ph), 73.9 (C-7″), 73.9 (C-7), 73.3 (C3′−O$\underline{C}H_2$Ph), 73.1 (C-6′), 72.7 (C4′−O$\underline{C}H_2$Ph), 72.5 (C2−O$\underline{C}H_2$Ph), 72.3 (C-7′), 71.3 (C-18″), 70.4 (C-5), 70.2 (C-18), 69.1 (C-1′), 67.9 (C-6), 56.3 (C-26), 55.7 (C-26″), 55.5 (C-26′), 36.5 (C-23′), 36.4 (C-23″), 36.2 (C-23) ppm. HRMS (ESI-TOF) m/z: $[M + Na]^+$ calcd for $C_{107}H_{100}O_{17}Na$ 1679.6858; found 1679.6866. Anal. calcd for $C_{107}H_{100}O_{17} + H_2O$: C, 76.68; H, 6.13; found: C, 76.40; H, 6.28.

*Characterization of Compound **M-5b**.*

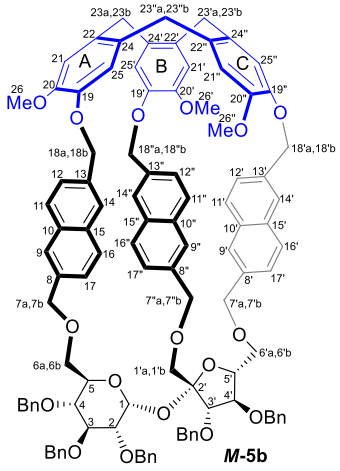

M-5b

$[\alpha]_D^{25}$ − 82.1 (*c* 0.21, CH_2Cl_2). ^1H NMR (600 MHz, $CDCl_3$): δ = 7.78 (s, 1H, H-9), 7.70 (s, 1H, H-14″), 7.69 (d, $J_{16,17}$ = 8.6 Hz, 1H, H-16), 7.67 (s, 1H, H-11), 7.62 (s, 1H, H-9″), 7.58 (s, 1H, H-14), 7.52

https://dx.doi.org/10.1021/acs.joc.1c00019
J. Org. Chem. 2021, 86, 5129−5141

(d, 1H, H-17), 7.49 (d, $J_{11'',12''}$ = 8.4 Hz, 1H, H-11″), 7.49 (d, $J_{16'',17''}$ = 8.3 Hz, 1H, H-16″), 7.34 (s, 1H, H-25″), 7.32 (m, 1H, H-12″), 7.24–7.42 (m, 20H, 20 × H-Ph), 7.21 (d, 1H, H-17″), 7.19 (s, 1H, H-21′), 7.18 (d, 1H, H-11′), 7.16 (s, 1H, H-9′), 7.14 (m, 1H, H-12), 7.13 (s, 1H, H-25′), 7.12 (d, $J_{12',11'}$ = 8.4 Hz, 1H, H-12′), 7.04–7.09 (m, 4H, 4 × H-Ph), 6.96 (t, J = 6.9 Hz, 1H, H-Ph), 6.55 (s, 1H, H-14′), 6.54 (s, 1H, H-21), 6.49 (d, $J_{17',16'}$ = 8.2 Hz, 1H, H-17′), 6.42 (s, 1H, H-25), 6.33 (s, 1H, H-21″), 6.14 (d, 1H, H-16′), 5.64 (d, $J_{18''a,18''b}$ = 14.7 Hz, 1H, H-18″a), 5.54 (d, $J_{1,2}$ = 3.8 Hz, 1H, H-1), 5.45 (d, 1H, H-18″b), 5.35 (d, $J_{18'a,18'b}$ = 11.2 Hz, 1H, H-18′a), 5.00 (d, 1H, H-18′b), 4.94 (m, 1H, H-7a), 4.93 (m, 2H, C3−OC$\underline{H}_2$Ph, C4−OC$\underline{H}_2$Ph), 4.87 (d, $J_{18a,18b}$ = 9.3 Hz, 1H, H-18a), 4.83 (d, J = 11.1 Hz, 1H, C3−OC$\underline{H}_2$Ph), 4.79 (d, $J_{23'a,23'b}$ = 13.5 Hz, 1H, H-23′a), 4.77 (d, J = 11.2 Hz, 1H, C4−OC$\underline{H}_2$Ph), 4.74 (d, $J_{23a,23b}$ = 13.4 Hz, 1H, H-23a), 4.71 (d, 1H, H-23″a), 4.70 (d, J = 13.0 Hz, 1H, C3′−OC$\underline{H}_2$Ph), 4.69 (m, 2H, C2−OC$\underline{H}_2$Ph), 4.67 (d, 1H, H-7″a), 4.59 (d, $J_{7''b,7''a}$ = 11.9 Hz, 1H, H-7″b), 4.45 (d, J = 11.1 Hz, 1H, C3′−OC$\underline{H}_2$Ph), 4.29 (d, $J_{3',4'}$ = 8.1 Hz, 1H, H-3′), 4.23 (d, $J_{7b,7a}$ = 12.0 Hz, 1H, H-7b), 4.19 (m, 1H, H-5), 4.09 (d, J = 11.2 Hz, 1H, C4′−OC$\underline{H}_2$Ph), 4.03 (s, 3H, H-26′), 3.96 (m, 1H, H-7′a), 3.94 (m, 1H, H-18b), 3.93 (m, 2H, H-3, C4′−OC$\underline{H}_2$Ph), 3.80 (d, $J_{1'a,1'b}$ = 11.5 Hz, 1H, H-1′a), 3.76 (m, 1H, H-5′), 3.73 (m, 1H, H-7′b), 3.70 (m, 1H, H-4), 3.67 (d, 1H, H-23′b), 3.64 (dd, $J_{2,3}$ = 9.6 Hz, 1H, H-2), 3.57 (d, 1H, H-23b), 3.46 (dd, $J_{6a,5}$ = 2.7 Hz, $J_{6a,6b}$ = 10.4 Hz, 1H, H-6a), 3.43 (d, $J_{1'b,1'a}$ = 11.6 Hz, 1H, H-1′b), 3.37 (d, $J_{23''b,23''a}$ = 13.6 Hz, 1H, H-23″b), 3.20 (dd, $J_{6b,5}$ = 2.2 Hz, 1H, H-6b), 3.19 (s, 3H, H-26″), 3.06 (dd, $J_{4',3'}$ = 9.1 Hz, $J_{4',5'}$ = 9.2 Hz, 1H, H-4′), 3.02 (s, 3H, H-26), 2.95 (dd, $J_{6'a,5'}$ = 8.7 Hz, $J_{6'a,6'b}$ = 11.9 Hz, 1H, H-6′a), 2.25 (d, 1H, H-6′b) ppm. $^{13}C\{^1H\}$ NMR (150 MHz, $CDCl_3$): δ = 151.1 (C-20″), 148.0 (C-20′), 147.6 (C-20), 147.1 (C-19), 146.9 (C-19′), 144.4 (C-19″), 139.1, 139.1, 138.3, 138.2, 138.1 (C_{quat}, 5 × C-Ph), 136.6 (C-8″), 136.5 (C-8′), 135.6 (C-22″), 135.4 (C-8), 135.2 (C-13″), 134.2 (C-13), 133.0 (C-22′), 132.8 (C-15), 132.8 (C-10″), 132.8 (C-10), 132.5 (C-15″), 132.4 (C-24′), 132.2 (C-10′), 131.6 (C-24″), 131.4 (C-24), 131.1 (C-15′), 131.1 (C-13′), 130.9 (C-22), 129.9 (C-14′), 128.8 (C-11″), 128.5 (C-9), 128.2 (C-16), 128.2 (C-17), 128.1 (C-14), 128.0 (C-12′), 128.0 (C-11), 127.6 (C-16″), 127.2 (C-12), 127.2–128.3 (m, 25 × C-Ph), 126.9 (C-16′), 126.4 (C-11′), 125.3 (C-17″), 125.1 (C-9″), 124.9 (C-17′), 124.1 (C-14″), 124.1 (C-25″), 123.7 (C-12″), 123.1 (C-9′), 113.8 (C-25′), 113.7 (C-21′), 112.9 (C-21″), 112.4 (C-25), 111.8 (C-21), 103.0 (C-2′), 88.9 (C-1), 83.4 (C-3′), 82.4 (C-3), 81.8 (C-4′), 79.5 (C-2), 77.9 (C-4), 77.6 (C-5′), 77.0 (C-18′), 75.4 (C3−O$\underline{C}H_2$Ph), 74.8 (C-1′), 74.6 (C4−O$\underline{C}H_2$Ph), 74.2 (C-7″), 72.8 (C-7), 72.7 (C-6′), 72.6 (C2−O$\underline{C}H_2$Ph), 72.5 (C4′−O$\underline{C}H_2$Ph), 72.4 (C3′−O$\underline{C}H_2$Ph), 71.6 (C-7′), 70.6 (C-18), 69.4 (C-5), 69.4 (C-18″), 65.9 (C-6), 56.4 (C-26′), 55.4 (C-26″), 54.5 (C-26), 36.6 (C-23), 36.2 (C-23″), 36.0 (C-23′) ppm. HRMS (ESI-TOF) m/z: $[M + Na]^+$ calcd for $C_{107}H_{100}O_{17}Na$ 1679.6858; found 1679.6860. Anal. calcd for $C_{107}H_{100}O_{17} + H_2O$: C, 76.68; H, 6.13; found: C, 76.62; H, 6.22.

ECD Spectra. ECD spectra were measured in acetonitrile at room temperature. All spectra were collected between 180–400 nm at room temperature using solutions at concentrations 2.5 × 10^{-5} M in quartz cells with path length 0.2 or 0.5 cm. All spectra were recorded using a 100 nm/min scanning speed, a step size of 0.2 nm, a bandwidth of 1 nm, a response time of 0.5 s, and an accumulation of 3 scans. The spectra were background corrected using acetonitrile.

Computational Details. Conformational search was carried out at the molecular mechanics level using a simplified structure in which all benzyl groups (Bn) in a sucrose moiety were exchanged by a hydrogen atom to save computational time and facilitate the computational predictions of ECD spectra for all investigated diastereoisomers. Next, the lowest energy structures (#10) within 3 kcal/mol were submitted for DFT optimization using Gaussian16 program[38] at the B3LYP/6-31G(d) level of theory applying PCM for CH_3CN. In each case, structures were confirmed to contain no imaginary frequencies. Finally, for the most abundant structures (#2), TDDFT calculations were carried out using the B3LYP and CAM-B3LYP functionals with SVP basis set using the PCM model for CH_3CN. Since they gave fully coherent results, we are only presenting results from the B3LYP functional and SVP basis set. Other basis sets, *i.e.*, TZVP, 6-311+G(d,p), were also checked for improving consistency of the obtained results. The UV and ECD spectra are simulated by overlapping Gaussian functions for 350 transitions. An optimum Gaussian band-shape and UV-correction were selected according to the similarity analysis with experimental data in CH_3CN performed using SpecDis.[43] The ***M*-5a⊂ACh** and ***M*-5a⊂Ch** encapsulated complexes were optimized at the B3LYP/6-31G(d) level of theory using Gaussian16 program.[38]

Fluorescence Titration Experiments. The stock solutions of the hosts ***P*-5a**, ***P*-5b**, ***M*-5a**, and ***M*-5b** were prepared at concentrations *ca.* 0.001 M in acetonitrile. A volume of 2.5 mL of acetonitrile was taken to the quartz cuvette, and the appropriate amount of host stock solution was added to obtain concentrations between 2.26 and 2.44 × 10^{-5} M. The guest solutions were prepared by dissolving the required amount of acetylcholine iodide or choline iodide in a host stock solution to provide constant host concentration during the titration studies. Portions of the guest solution were gradually added to the cuvette containing appropriate host solution, mixed, and incubated for 30 s before irradiation at 280 nm at 25 °C. The corresponding emission spectra during titration were recorded. The measured emission spectra for the host during the titration studies were plotted as a function of the guest/host ratio using nonlinear regression *via* Bindfit program.[40] The value of association constant K_a was calculated by nonlinear least-squares using as input parameters 1:1 binding model and the Nelder–Mead method.

^{1}H NMR Titration Experiments. The ^{1}H NMR titration experiments were conducted by measuring the ^{1}H NMR spectra at 400 MHz with a Bruker Avance II apparatus at 303 K. The solutions of the hosts ***P*-5a** and ***M*-5a** were prepared at concentrations 3.73 × 10^{-3} and 1.78 × 10^{-3} M, respectively, in the mixture of solvents CD_3CN/$CDCl_3$ = 80:20. The guest solutions were prepared by dissolving the required amount of acetylcholine iodide or choline iodide salts in a host stock solution to ensure constant host concentration during the experiment. Next, to the NMR tube containing appropriate host solution, portions of the guest solution were gradually added and the ^{1}H NMR spectrum was recorded.

■ ASSOCIATED CONTENT

Supporting Information

The Supporting Information is available free of charge at https://pubs.acs.org/doi/10.1021/acs.joc.1c00019.

Table with comparison of ^{1}H and ^{13}C NMR signals of ***P*-5a**, ***M*-5a**, ***P*-5b**, and ***M*-5b**; fluorescence titration data; Cartesian coordinates of calculated structures; and copies of NMR spectra (PDF)

■ AUTHOR INFORMATION

Corresponding Authors

Sławomir Jarosz − *Institute of Organic Chemistry, Warsaw 01-224, Poland;* orcid.org/0000-0002-9212-6203; Email: slawomir.jarosz@icho.edu.pl

Łukasz Szyszka − *Institute of Organic Chemistry, Warsaw 01-224, Poland;* orcid.org/0000-0002-7739-9713; Email: lukasz.szyszka@icho.edu.pl

Authors

Marcin Górecki − *Institute of Organic Chemistry, Warsaw 01-224, Poland;* orcid.org/0000-0001-7472-3875

Piotr Cmoch − *Institute of Organic Chemistry, Warsaw 01-224, Poland;* orcid.org/0000-0002-8413-9290

Complete contact information is available at: https://pubs.acs.org/10.1021/acs.joc.1c00019

Notes

The authors declare no competing financial interest.

https://dx.doi.org/10.1021/acs.joc.1c00019
J. Org. Chem. 2021, 86, 5129−5141

■ ACKNOWLEDGMENTS

This work was financed by the Polish National Science Centre (grant UMO-2016/21/B/ST5/03382). We would like to thank the Wroclaw Centre for Networking and Supercomputing (WCSS) and PLGrid platform for the computational support. We thank Mr. Wiktor Ignacak for preparative HPLC equipment support. Dr. Shashuk's Group (Institute of Physical Chemistry, PAS) is acknowledgment for fluorescence spectrometer support.

■ REFERENCES

(1) (a) Santos-Figueroa, L. E.; Moragues, M. E.; Climent, E.; Agostini, A.; Martínez-Máñez, R.; Sancenón, F. Chromogenic and fluorogenic chemosensors and reagents for anions. A comprehensive review of the years 2010−2011. *Chem. Soc. Rev.* **2013**, *42*, 3489−3613. (b) Pinalli, R.; Pedrini, A.; Dalcanale, E. Biochemical sensing with macrocyclic receptors. *Chem. Soc. Rev.* **2018**, *47*, 7006−7026. (c) Wu, D.; Sedgwick, A. C.; Gunnlaugsson, T.; Akkaya, E. U.; Yoon, J.; James, T. D. Fluorescent chemosensors: the past, present and future. *Chem. Soc. Rev.* **2017**, *46*, 7105−7123.

(2) Park, S.-H.; Kwon, N.; Lee, J.-H.; Yoon, J.; Shin, I. Synthetic ratiometric fluorescent probes for detection of ions. *Chem. Soc. Rev.* **2020**, *49*, 143−179.

(3) (a) de Silva, A. P.; Gunaratne, H. Q. N.; Gunnlaugsson, T.; Huxley, A. J. M.; McCoy, C. P.; Rademacher, J. T.; Rice, T. E. Signaling Recognition Events with Fluorescent Sensors and Switches. *Chem. Rev.* **1997**, *97*, 1515−1566. (b) Czarnik, A. W. *Fluorescent Chemosensors for Ion and Molecule Recognition*; American Chemical Society: Washington, DC, 1992. (c) Chen, X.; Tian, X.; Shin, I.; Yoon, J. Fluorescent and luminescent probes for detection of reactive oxygen and nitrogen species. *Chem. Soc. Rev.* **2011**, *40*, 4783−4804.

(4) For example: (a) Lai, W.-F.; Rogach, A. L.; Wong, W.-T. Chemistry and engineering of cyclodextrins for molecular imaging. *Chem. Soc. Rev.* **2017**, *46*, 6379−6419. (b) Li, J.; Yim, D.; Jang, W.-D.; Yoon, J. Recent progress in the design and applications of fluorescence probes containing crown ethers. *Chem. Soc. Rev.* **2017**, *46*, 2437−2458. (c) Li, Y.; Dong, Y.; Cheng, L.; Qin, C.; Nian, H.; Zhang, H.; Yu, Y.; Cao, L. Aggregation-Induced Emission and Light-Harvesting Function of Tetraphenylethene-Based Tetracationic Dicyclophane. *J. Am. Chem. Soc.* **2019**, *141*, 8412−8415. (d) Han, X.-N.; Han, Y.; Chen, C.-F. Pagoda[4]arene and i-Pagoda[4]arene. *J. Am. Chem. Soc.* **2020**, *142*, 8262−8269.

(5) (a) Kolesnichenko, I. V.; Anslyn, E. V. Practical applications of supramolecular chemistry. *Chem. Soc. Rev.* **2017**, *46*, 2385−2390. (b) Liu, Z.; Nalluri, S. K. M.; Stoddart, J. F. Surveying macrocyclic chemistry: from flexible crown ethers to rigid cyclophanes. *Chem. Soc. Rev.* **2017**, *46*, 2459−2478. (c) You, L.; Zha, D.; Anslyn, E. V. Recent Advances in Supramolecular Analytical Chemistry Using Optical Sensing. *Chem. Rev.* **2015**, *115*, 7840−7892.

(6) (a) Brevé, T. G.; Filius, M.; Araman, C.; van der Helm, M. P.; Hagedoorn, P.-L.; Joo, C.; van Kasteren, S. I.; Eelkema, R. Conditional Copper-Catalyzed Azide−Alkyne Cycloaddition by Catalyst Encapsulation. *Angew. Chem., Int. Ed.* **2020**, *59*, 9340−9344. (b) de Simone, N. A.; Meninno, S.; Talotta, C.; Gaeta, C.; Neri, P.; Lattanzi, A. Solvent-Free Enantioselective Michael Reactions Catalyzed by a Calixarene-Based Primary Amine Thiourea. *J. Org. Chem.* **2018**, *83*, 10318−10325. (c) Sashuk, V.; Butkiewicz, H.; Fiałkowski, M.; Danylyuk, O. Triggering autocatalytic reaction by host−guest interactions. *Chem. Commun.* **2016**, *52*, 4191−4194. (d) Tang, B.; Zhao, J.; Xu, J.-F.; Zhang, X. Cucurbit[n]urils for Supramolecular Catalysis. *Chem.−Eur. J.* **2020**, *26*, 15446−15460.

(7) (a) Hua, B.; Shao, L.; Zhang, Z.; Liu, J.; Huang, F. Cooperative Silver Ion-Pair Recognition by Peralkylated Pillar[5]arenes. *J. Am. Chem. Soc.* **2019**, *141*, 15008−15012. (b) Moosa, B.; Alimi, L. O.; Shkurenko, A.; Fakim, A.; Bhatt, P. M.; Zhang, G.; Eddaoudi, M.; Khashab, N. M. A Polymorphic Azobenzene Cage for Energy-Efficient and Highly Selective p-Xylene Separation. *Angew. Chem., Int. Ed.* **2020**, *59*, 21367−21371.

(8) (a) Sun, X.; Wang, Y.; Lei, Y. Fluorescence based explosive detection: from mechanisms to sensory materials. *Chem. Soc. Rev.* **2015**, *44*, 8019−8061. (b) Liu, Y.; Song, Y.; Chen, Y.; Li, X.-Q.; Ding, F.; Zhong, R.-Q. Biquinolino-Modified *β*-Cyclodextrin Dimers and Their Metal Complexes as Efficient Fluorescent Sensors for the Molecular Recognition of Steroids. *Chem.−Eur. J.* **2004**, *10*, 3685−3696.

(9) (a) Huang, Y.; Gao, R.-H.; Liu, M.; Chen, L.-X.; Ni, X.-L.; Xiao, X.; Cong, H.; Zhu, Q.-J.; Chen, K.; Tao, Z. Cucurbit[n]uril-Based Supramolecular Frameworks Assembled through Outer-Surface Interactions. *Angew. Chem., Int. Ed.* **2021**, DOI: 10.1002/anie.202002666. (b) Mastalerz, M. Permanent Porous Materials from Discrete Organic Molecules—Towards Ultra-High Surface Areas. *Chem.−Eur. J.* **2012**, *18*, 10082−10091. (c) Schaub, T. A.; Prantl, E. A.; Kohn, J.; Bursch, M.; Marshall, C. R.; Leonhardt, E. J.; Lovell, T. C.; Zakharov, L. N.; Brozek, C. K.; Waldvogel, S. R.; Grimme, S.; Jasti, R. Exploration of the Solid-State Sorption Properties of Shape-Persistent Macrocyclic Nanocarbons as Bulk Materials and Small Aggregates. *J. Am. Chem. Soc.* **2020**, *142*, 8763−8775.

(10) (a) Kim, H.-J.; Whang, D. R.; Gierschner, J.; Park, S. Y. Highly Enhanced Fluorescence of Supramolecular Polymers Based on a Cyanostilbene Derivative and Cucurbit[8]uril in Aqueous Solution. *Angew. Chem., Int. Ed.* **2016**, *55*, 15915−15919. (b) Liang, T.; Collin, D.; Galerne, M.; Fuks, G.; Vargas Jentzsch, A.; Maaloum, M.; Carvalho, A.; Giuseppone, N.; Moulin, E. Covalently Trapped Triarylamine-Based Supramolecular Polymers. *Chem.−Eur. J.* **2019**, *25*, 14341−14348. (c) Zeng, R.; Gong, Z.; Yan, Q. Chalcogen-Bonding Supramolecular Polymers. *J. Org. Chem.* **2020**, *85*, 8397−8404.

(11) (a) Davis, J. T.; Gale, P. A.; Quesada, R. Advances in anion transport and supramolecular medicinal chemistry. *Chem. Soc. Rev.* **2020**, *49*, 6056−6086. (b) Grauwels, G.; Valkenier, H.; Davis, A. P.; Jabin, I.; Bartik, K. Repositioning Chloride Transmembrane Transporters: Transport of Organic Ion Pairs. *Angew. Chem., Int. Ed.* **2019**, *58*, 6921−6925. (c) Tapia, L.; Pérez, Y.; Bolte, M.; Casas, J.; Solà, J.; Quesada, R.; Alfonso, I. pH-Dependent Chloride Transport by Pseudopeptidic Cages for the Selective Killing of Cancer Cells in Acidic Microenvironments. *Angew. Chem., Int. Ed.* **2019**, *58*, 12465−12468.

(12) (a) Dasgupta, S.; Mukherjee, P. S. Carboxylatopillar[n]arenes: a versatile class of water soluble synthetic receptors. *Org. Biomol. Chem.* **2017**, *15*, 762−772. (b) Hu, X.-Y.; Jia, K.; Cao, Y.; Li, Y.; Qin, S.; Zhou, F.; Lin, C.; Zhang, D.; Wang, L. Dual Photo- and pH-Responsive Supramolecular Nanocarriers Based on Water-Soluble Pillar[6]arene and Different Azobenzene Derivatives for Intracellular Anticancer Drug Delivery. *Chem.−Eur. J.* **2015**, *21*, 1208−1220. (c) Xia, D.; Li, Y.; Jie, K.; Shi, B.; Yao, Y. A Water-Soluble Cyclotriveratrylene-Based Supra-amphiphile: Synthesis, pH-Responsive Self-Assembly in Water, and Its Application in Controlled Drug Release. *Org. Lett.* **2016**, *18*, 2910−2913.

(13) (a) He, Q.; Vargas-Zúñiga, G. I.; Kim, S. H.; Kim, S. K.; Sessler, J. L. Macrocycles as Ion Pair Receptors. *Chem. Rev.* **2019**, *119*, 9753−9835. (b) Brotin, T.; Dutasta, J.-P. Cryptophanes and Their Complexes—Present and Future. *Chem. Rev.* **2009**, *109*, 88−130.

(14) Hardie, M. J. Recent advances in the chemistry of cyclotriveratrylene. *Chem. Soc. Rev.* **2010**, *39*, 516−527.

(15) Zhang, D.; Martinez, A.; Dutasta, J.-P. Emergence of Hemicryptophanes: From Synthesis to Applications for Recognition, Molecular Machines, and Supramolecular Catalysis. *Chem. Rev.* **2017**, *117*, 4900−4942.

(16) Long, A.; Perraud, O.; Albalat, M.; Robert, V.; Dutasta, J.-P.; Martinez, A. Helical Chirality Induces a Substrate-Selectivity Switch in Carbohydrates Recognitions. *J. Org. Chem.* **2018**, *83*, 6301−6306.

(17) Perraud, O.; Robert, V.; Martinez, A.; Dutasta, J.-P. A Designed Cavity for Zwitterionic Species: Selective Recognition of Taurine in Aqueous Media. *Chem.−Eur. J.* **2011**, *17*, 13405−13408.

https://dx.doi.org/10.1021/acs.joc.1c00019
J. Org. Chem. 2021, 86, 5129−5141

(18) Yang, J.; Chatelet, B.; Dufaud, V.; Hérault, D.; Jean, M.; Vanthuyne, N.; Mulatier, J.-C.; Pitrat, D.; Guy, L.; Dutasta, J.-P.; Martinez, A. Enantio- and Substrate-Selective Recognition of Chiral Neurotransmitters with C_3-Symmetric Switchable Receptors. *Org. Lett.* **2020**, *22*, 891−895.
(19) (a) Taratula, O.; Kim, M. P.; Bai, Y.; Philbin, J. P.; Riggle, B. A.; Haase, D. N.; Dmochowski, I. J. Synthesis of Enantiopure, Trisubstituted Cryptophane-A Derivatives. *Org. Lett.* **2012**, *14*, 3580−3583. (b) Cochrane, J. R.; Schmitt, A.; Wille, U.; Hutton, C. A. Synthesis of cyclic peptide hemicryptophanes: enantioselective recognition of a chiral zwitterionic guest. *Chem. Commun.* **2013**, *49*, 8504−8506.
(20) (a) Pradhan, T.; Jung, H. S.; Jang, J. H.; Kim, T. W.; Kang, C.; Kim, J. S. Chemical sensing of neurotransmitters. *Chem. Soc. Rev.* **2014**, *43*, 4684−4713. (b) Park, Y. S.; Kim, Y.; Paek, K. Specific Encapsulation of Acetylcholine Chloride by a Self-Assembled Molecular Capsule with Sulfonamido Moiety. *Org. Lett.* **2019**, *21*, 8300−8303. (c) Ballester, P.; Shivanyuk, A.; Far, A. R.; Rebek, J. A Synthetic Receptor for Choline and Carnitine. *J. Am. Chem. Soc.* **2002**, *124*, 14014−14016.
(21) (a) Tsai, T.-H. Separation methods used in the determination of choline and acetylcholine. *J. Chromatogr. B: Biomed. Sci. Appl.* **2000**, *747*, 111−122. (b) Hasselmo, M. E.; Sarter, M. Modes and models of forebrain cholinergic neuromodulation of cognition. *Neuropsychopharmacology* **2011**, *36*, 52−73.
(22) (a) White, K. E.; Cummings, J. L. Schizophrenia and Alzheimer's disease: clinical and pathophysiologic analogies. *Compr. Psychiatry* **1996**, *37*, 188−195. (b) Doody, R. S. Current treatments for Alzheimer's disease: cholinesterase inhibitors. *J. Clin. Psychiatry* **2003**, *64*, 11−17. (c) Higley, M. J.; Picciotto, M. R. Neuromodulation by acetylcholine: examples from schizophrenia and depression. *Curr. Opin. Neurobiol.* **2014**, *29*, 88−95.
(23) Zeisel, S. H.; da Costa, K.-A. Choline: An Essential Nutrient for Public Health. *Nutr. Rev.* **2009**, *67*, 615−623.
(24) (a) Korbakov, N.; Timmerman, P.; Lidich, N.; Urbach, B.; Sa'ar, A.; Yitzchaik, S. Acetylcholine Detection at Micromolar Concentrations with the Use of an Artificial Receptor-Based Fluorescence Switch. *Langmuir* **2008**, *24*, 2580−2587. (b) Liu, Y.; Perez, L.; Mettry, M.; Gill, A. D.; Byers, S. R.; Easley, C. J.; Bardeen, C. J.; Zhong, W.; Hooley, R. J. Site selective reading of epigenetic markers by a dual-mode synthetic receptor array. *Chem. Sci.* **2017**, *8*, 3960−3970. (c) Erieau-Peyrard, L.; Coiffier, C.; Bordat, P.; Bégué, D.; Chierici, S.; Pinet, S.; Gosse, I.; Baraille, I.; Brown, R. Selective, direct detection of acetylcholine in PBS solution, with self-assembled fluorescent nano-particles: experiment and modelling. *Phys. Chem. Chem. Phys.* **2015**, *17*, 4168−4174. (d) Dumartin, M.-L.; Givelet, C.; Meyrand, P.; Bibal, B.; Gosse, I. A fluorescent cyclotriveratrylene: synthesis, emission properties and acetylcholine recognition in water. *Org. Biomol. Chem.* **2009**, *7*, 2725−2728.
(25) Long, A.; Fantozzi, N.; Pinet, S.; Genin, E.; Pétuya, R.; Bégué, D.; Robert, V.; Dutasta, J.-P.; Gosse, I.; Martinez, A. Selective recognition of acetylcholine over choline by a fluorescent cage. *Org. Biomol. Chem.* **2019**, *17*, 5253−5257.
(26) (a) Long, A.; Antonetti, E.; Insuasty, A.; Pinet, S.; Gosse, I.; Robert, V.; Dutasta, J.-P.; Martinez, A. Hemicryptophanes with Improved Fluorescent Properties for the Selective Recognition of Acetylcholine over Choline. *J. Org. Chem.* **2020**, *85*, 6400−6407. (b) Fantozzi, N.; Pétuya, R.; Insuasty, A.; Long, A.; Lefevre, S.; Schmitt, A.; Robert, V.; Dutasta, J.-P.; Baraille, I.; Guy, L.; Genin, E.; Bégué, D.; Martinez, A.; Pinet, S.; Gosse, I. A new fluorescent hemicryptophane for acetylcholine recognition with an unusual recognition mode. *New J. Chem.* **2020**, *44*, 11853−11860.
(27) Zhang, D.; Gao, G.; Guy, L.; Robert, V.; Dutasta, J.-P.; Martinez, A. A fluorescent heteroditopic hemicryptophane cage for the selective recognition of choline phosphate. *Chem. Commun.* **2015**, *51*, 2679−2682.
(28) Jia, C.; Zuo, W.; Yang, D.; Chen, Y.; Cao, L.; Custelcean, R.; Hostaš, J.; Hobza, P.; Glaser, R.; Wang, Y.-Y.; Yang, X.-J.; Wu, B. Selective binding of choline by a phosphate-coordination-based triple helicate featuring an aromatic box. *Nat. Commun.* **2017**, *8*, 938.
(29) Ballester, P.; Sarmentero, M. A. Hybrid Cavitand−Resorcin-[4]arene Receptor for the Selective Binding of Choline and Related Compounds in Protic Media. *Org. Lett.* **2006**, *8*, 3477−3480.
(30) Jarosz, S.; Sokołowska, P.; Szyszka, Ł. Synthesis of fine chemicals with high added value from sucrose: Towards sucrose-based macrocycles. *Tetrahedron Lett.* **2020**, *61*, 151888.
(31) (a) Potopnyk, M. A.; Jarosz, S. Synthesis and Complexation Properties of "Unsymmetrical" Sucrose-Based Receptors. *Eur. J. Org. Chem.* **2013**, 5117−5126. (b) Lewandowski, B.; Jarosz, S. Chiral recognition of α-phenylethylamine by sucrose-based macrocyclic receptors. *Chem. Commun.* **2008**, 6399−6401.
(32) Potopnyk, M. A.; Lewandowski, B.; Jarosz, S. Novel sucrose-based macrocyclic receptors for enantioselective recognition of chiral ammonium cations. *Tetrahedron: Asymmetry* **2012**, *23*, 1474−1479.
(33) (a) Łęczycka-Wilk, K.; Dąbrowa, K.; Cmoch, P.; Jarosz, S. Chloride-Templated Macrocyclization and Anion-Binding Properties of C2-Symmetric Macrocyclic Ureas from Sucrose. *Org. Lett.* **2017**, *19*, 4596−4599. (b) Łęczycka-Wilk, K.; Ulatowski, F.; Cmoch, P.; Jarosz, S. "Choose-a-size" control in the synthesis of sucrose based urea and thiourea macrocycles. *Org. Biomol. Chem.* **2018**, *16*, 6063−6069.
(34) Szyszka, Ł.; Cmoch, P.; Butkiewicz, A.; Potopnyk, M. A.; Jarosz, S. Synthesis of Cyclotriveratrylene-Sucrose-Based Capsules. *Org. Lett.* **2019**, *21*, 6523−6528.
(35) Szyszka, Ł.; Cmoch, P.; Górecki, M.; Ceborska, M.; Potopnyk, M. A.; Jarosz, S. Chiral Molecular Cages Based on Cyclotriveratrylene and Sucrose Units Connected with *p*-Phenylene Linkers. *Eur. J. Org. Chem.* **2021**, 897−906.
(36) (a) Górecki, M. A configurational and conformational study of (−)-Oseltamivir using a multi-chiroptical approach. *Org. Biomol. Chem.* **2015**, *13*, 2999−3010. (b) Long, A.; Colomban, C.; Jean, M.; Albalat, M.; Vanthuyne, N.; Giorgi, M.; Di Bari, L.; Górecki, M.; Dutasta, J.-P.; Martinez, A. Enantiopure C_1-Cyclotriveratrylene with a Reversed Spatial Arrangement of the Substituents. *Org. Lett.* **2019**, *21*, 160−165. (c) Long, A.; Jean, M.; Albalat, M.; Vanthuyne, N.; Giorgi, M.; Górecki, M.; Dutasta, J.-P.; Martinez, A. Synthesis, resolution, and chiroptical properties of hemicryptophane cage controlling the chirality of propeller arrangement of a C_3 triamide unit. *Chirality* **2019**, *31*, 910−916.
(37) Canceill, J.; Collet, A.; Gabard, J.; Gottarelli, G.; Spada, G. P. Exciton approach to the optical activity of C_3-cyclotriveratrylene derivatives. *J. Am. Chem. Soc.* **1985**, *107*, 1299−1308.
(38) Frisch, M.J.; Trucks, G.W.; Schlegel, H.B.; Scuseria, G.E.; Robb, M.A.; Cheeseman, J.R.; Scalmani, G.; Barone, V.; Petersson, G.A.; Nakatsuji, H.; Li, X.; Caricato, M.; Marenich, A.V.; Bloino, J.; Janesko, B.G.; Gomperts, R.; Mennucci, B.; Hratchian, H.P.; Ortiz, J. V.; Izmaylov, A. F.; Sonnenberg, J. L.; Williams-Young, D.; Ding, F.; Lipparini, F.; Egidi, F.; Goings, J.; Peng, B.; Petrone, A.; Henderson, T.; Ranasinghe, D.; Zakrzewski, V.G.; Gao, J.; Rega, N.; Zheng, G.; Liang, W.; Hada, M.; Ehara, M.; Toyota, K.; Fukuda, R.; Hasegawa, J.; Ishida, M.; Nakajima, T.; Honda, Y.; Kitao, O.; Nakai, H.; Vreven, T.; Throssell, K.; Montgomery, J.A., Jr.; Peralta, J.E.; Ogliaro, F.; Bearpark, M.J.; Heyd, J.J.; Brothers, E.N.; Kudin, K.N.; Staroverov, V.N.; Keith, T.A.; Kobayashi, R.; Normand, J.; Raghavachari, K.; Rendell, A.P.; Burant, J.C.; Iyengar, S.S.; Tomasi, J.; Cossi, M.; Millam, J.M.; Klene, M.; Adamo, C.; Cammi, R.; Ochterski, J.W.; Martin, R.L.; Morokuma, K.; Farkas, O.; Foresman, J.B.; Fox, D.J. *Gaussian 16*, Revision B.01; Gaussian, Inc.: Wallingford CT, 2016.
(39) (a) Pescitelli, G.; Barone, V.; Di Bari, L.; Rizzo, A.; Santoro, F. Vibronic Coupling Dominates the Electronic Circular Dichroism of the Benzene Chromophore ^1L_b band. *J. Org. Chem.* **2013**, *78*, 7398−7405. (b) Del Bello, F.; Bonifazi, A.; Giorgioni, G.; Piergentili, A.; Sabbieti, M. G.; Agas, D.; Dell'Aera, M.; Matucci, R.; Górecki, M.; Pescitelli, G.; Vistoli, G.; Quaglia, W. Novel Potent Muscarinic Receptor Antagonists: Investigation on the Nature of Lipophilic Substituents in the 5- and/or 6-Positions of the 1,4-Dioxane Nucleus. *J. Med. Chem.* **2020**, *63*, 5763−5782.

https://dx.doi.org/10.1021/acs.joc.1c00019
J. Org. Chem. 2021, 86, 5129−5141

(40) Brynn Hibbert, D.; Thordarson, P. The death of the Job plot, transparency, open science and online tools, uncertainty estimation methods and other developments in supramolecular chemistry data analysis. *Chem. Commun.* **2016**, *52*, 12792−12805.
(41) Makita, Y.; Katayama, N.; Lee, H.-H.; Abe, T.; Sogawa, K.; Nomoto, A.; Fujiwara, S.-I.; Ogawa, A. A tri-aromatic amide hemicryptophane host: synthesis and acetylcholine binding. *Tetrahedron Lett.* **2016**, *57*, 5112−5115.
(42) Łukasik, B.; Milczarek, J.; Pawlowska, R.; Żurawiński, R.; Chworos, A. Facile synthesis of fluorescent distyrylnaphthalene derivatives for bioapplications. *New J. Chem.* **2017**, *41*, 6977−6980.
(43) Bruhn, T.; Schaumlöffel, A.; Hemberger, Y.; Pescitelli, G. *SpecDis Version 1.70*, 2017, Brerlin, Germany; https://specdis-software.jimdo.com.

https://dx.doi.org/10.1021/acs.joc.1c00019
J. Org. Chem. 2021, 86, 5129−5141

Supporting Information for

Fluorescent Molecular Cages with Sucrose and Cyclotriveratrylene Units for the Selective Recognition of Choline and Acetylcholine

Łukasz Szyszka,* Marcin Górecki, Piotr Cmoch, and Sławomir Jarosz*

Institute of Organic Chemistry, Polish Academy of Sciences, Kasprzaka 44/52,

01-224 Warsaw, Poland

Table of Contents

Table S1. Comparison of ^{1}H and ^{13}C NMR signals of ***P*-5a**, ***P*-5b**, ***M*-5a,** and ***M*-5b**.

	^{1}H and ^{13}C NMR chemical shifts δ (ppm)			
Glucose part	***P*-5a**	***P*-5b**	***M*-5a**	***M*-5b**
H-1/C-1	5.19/90.7	5.55/88.7	5.60/91.4	5.54/88.9
H-2/C-2	3.30/79.9	3.61/79.3	3.38/79.7	3.64/79.5
H-3/C-3	3.79/81.6	3.92/82.3	3.72/81.4	3.93/82.4
H-4/C-4	3.56/77.5	3.57/78.0	3.41/77.7	3.70/77.9
H-5/C-5	3.81/70.6	4.13/69.9	3.90/70.4	4.19/69.4
H-6a+H-6b/C-6	3.17+3.53/68.1	3.26+3.31/67.6	3.06+3.39/67.9	3.20+3.46/65.9
Fructose part				
H-1'a+H-1'b/C-1'	3.45+3.65/69.9	3.58+3.71/74.8	3.66+3.72/69.1	3.43+3.80/74.8
C-2'	104.1	104.0	104.6	103.0
H-3'/C-3'	4.38/84.1	4.24/82.5	4.35/84.9	4.29/83.4
H-4'/C-4'	3.83/82.4	3.53/81.3	4.03/83.1	3.06/81.8
H-5'/C-5'	4.07/80.9	3.32/79.2	3.92/80.8	3.76/77.6
H-6'a+H-6'b/C-6'	3.36+3.54/73.0	2.84+3.37/70.9	3.46+3.49/73.1	2.25+2.95/72.7
Naphthalene linkers				
H-7a+H-7b/C-7	4.15+4.45/73.1	4.23+4.78/73.0	4.04+4.64/73.4	4.23+4.94/72.8
H-7'a+H-7'b/C-7'	4.30+4.46/72.5	3.95+4.21/72.6	4.34/72.3	3.73+3.96/71.6
H-7"a+H-7"b/C-7"	4.27+4.76/73.0	4.58+4.66/74.4	4.50+5.07/73.9	4.59+4.67/74.2
C-8	135.9	135.3	135.4	135.4
C-8'	136.9	136.1	136.3	136.5
C-8"	135.8	136.5	135.9	136.6
H-9/C-9	7.47/126.1	7.62/127.0	7.36/126.7	7.78/128.5
H-9'/C-9'	7.51/124.5	7.47/126.0	7.40/124.4	7.16/123.1
H-9"/C-9"	7.64/126.2	7.49/125.5	7.83/127.4	7.62/125.1
C-10	132.78/132.0	132.6	nd	132.8
C-10'	132.6	132.4	nd	132.2
C-10"	132.6	132.82/132.3	nd	132.8
H-11/C-11	7.51/127.8	7.65/127.8	7.30/127.8	7.67/128.0
H-11'/C-11'	7.46/126.1	7.55/127.6	7.44/127.2	7.18/126.4
H-11"/C-11"	7.65/128.1	7.23/125.3	7.76/128.4	7.49/128.8
H-12/C-12	7.16/125.4	7.27/125.3	7.21/125.9	7.14/127.2
H-12'/C-12'	7.11/125.6	7.32/125.8	7.17/126.6	7.12/128.0
H-12"/C-12"	7.35/124.8	6.87/125.4	7.38/125.5	7.32/123.7
C-13	134.2	135.1	134.3	134.2
C-13'	133.3	133.5	133.6	131.1
C-13"	135.3	134.7	134.9	135.2
H-14/C-14	7.46/126.3	7.57/125.9	7.45/126.6	7.58/128.1
H-14'/C-14'	6.94/126.8	7.06/126.3	6.84/128.2	6.55/129.9
H-14"/C-14"	7.77/125.4	7.56/126.3	7.73/126.3	7.70/124.1
C-15	132.78/132.0	132.8	nd	132.8
C-15'	132.5	132.2	nd	131.1
C-15"	132.6	132.82/132.3	nd	132.5
H-16/C-16	7.39/127.7	7.55/128.2	7.23/128.0	7.69/128.2
H-16'/C-16'	6.68/127.7	6.79/127.6	6.98/127.9	6.14/126.9
H-16"/C-16"	7.58/127.9	7.52/127.7	7.79/128.0	7.49/127.6
H-17/C-17	7.02/126.2	7.38/126.5	7.02/126.3	7.52/128.2
H-17'/C-17'	6.88/125.6	6.91/126.3	7.01/125.0	6.49/124.9
H-17"/C-17"	7.36/126.3	7.04/125.4	7.48/127.2	7.21/125.3
H-18a+H-18b/C-18	4.81+5.24/71.4	4.87+5.09/71.3	5.31+5.40/70.2	3.94+4.87/70.6
H-18'a+H-18'b/C-18'	5.15+5.26/72.6	5.35+5.46/72.3	4.40+5.20/76.2	5.00+5.35/77.0
H-18"a+H-18"b/C-18"	5.15+5.36/72.7	4.94+5.27/73.9	4.97+5.21/71.3	5.45+5.64/69.4
CTV-ring A				
C-19	146.1	147.3	145.8	147.1
C-20	148.5	148.4	148.6	147.6
H-21/C-21	6.64/113.0	6.70/113.5	6.99/113.8	6.54/111.8
C-22	132.7	132.8	133.2	130.9

H-23a+H-23b/C-23	3.51+4.70/36.4	3.55+4.77/36.3	3.61+4.79/36.2	3.57+4.74/36.6
C-24	131.6	131.6	131.9	131.4
H-25/C-25	6.86/116.3	6.88/116.4	7.09/116.7	6.42/112.4
H-26/C-26 (OCH_3)	3.40/55.5	3.60/56.0	3.92/56.3	3.02/54.5
CTV-ring B				
C-19’	145.9	147.6	146.8	146.9
C-20’	149.1	149.1	150.3	148.0
H-21’/C-21’	6.67/113.4	6.81/114.4	6.64/113.5	7.19/113.7
C-22’	133.7	133.6	134.7	133.0
H-23’a+H-23’b/C-23’	3.47+4.70/36.4	3.57+4.77/36.6	3.51+4.74/36.5	3.67+4.79/36.0
C-24’	131.7	132.5	132.1	132.4
H-25’/C-25’	6.95/118.6	7.09/118.5	7.12/121.9	7.13/113.8
H-26’/C-26’ (OCH_3)	3.55/55.9	3.44/56.2	3.22/55.5	4.03/56.4
CTV-ring C				
C-19”	147.0	145.3	147.3	144.4
C-20”	148.8	149.7	148.0	151.1
H-21”/C-21”	6.61/113.4	6.86/113.9	6.93/115.0	6.33/112.9
C-22”	133.3	134.0	131.8	135.6
H-23”a+H-23”b/C-23”	3.48+4.68/36.2	3.59+4.77/36.5	3.51+4.74/36.4	3.37+4.71/36.2
C-24”	132.0	132.3	132.4	131.6
H-25”/C-25”	6.99/117.6	7.07/120.0	6.76/113.3	7.34/124.1
H-26”/C-26” (OCH_3)	3.21/55.5	3.73/56.3	3.48/55.7	3.19/55.4

Fluorescence titration experiments

Fluorescence titration curves for acetylcholine iodide

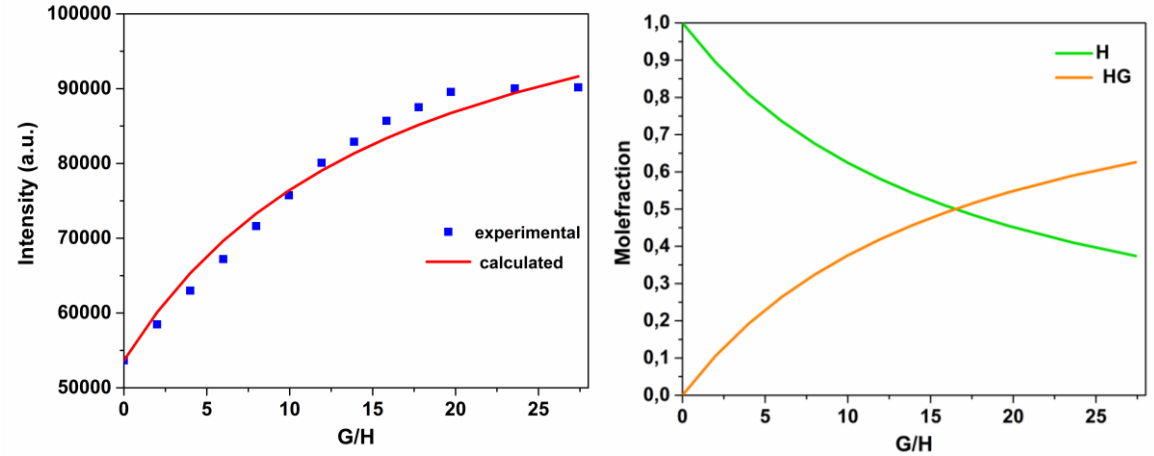

FigureS1. Fluorescence intensity and molefraction as a functions of guest/host ratio for cage ***P*-5a.**

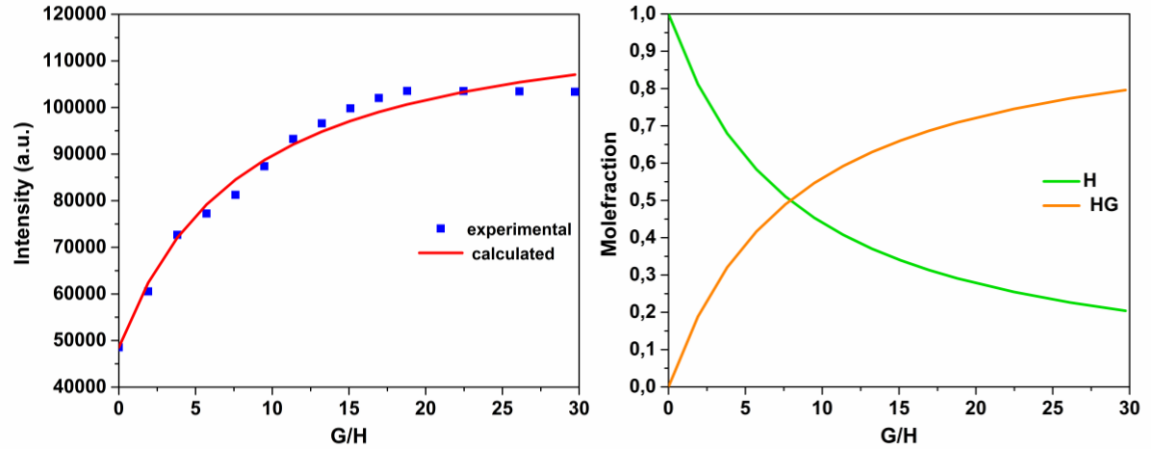

FigureS2. Fluorescence intensity and molefraction as a functions of guest/host ratio for cage ***M*-5a.**

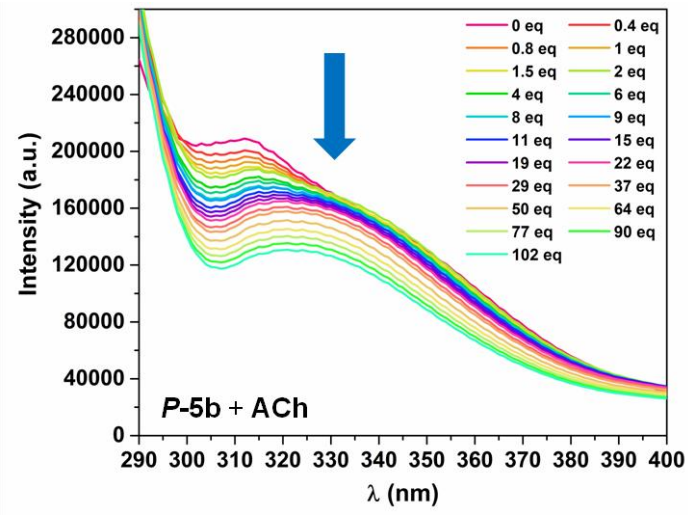

FigureS3. Fluorescence titration of host ***P*-5b** with ACh in CH_3CN excited at 280 nm.

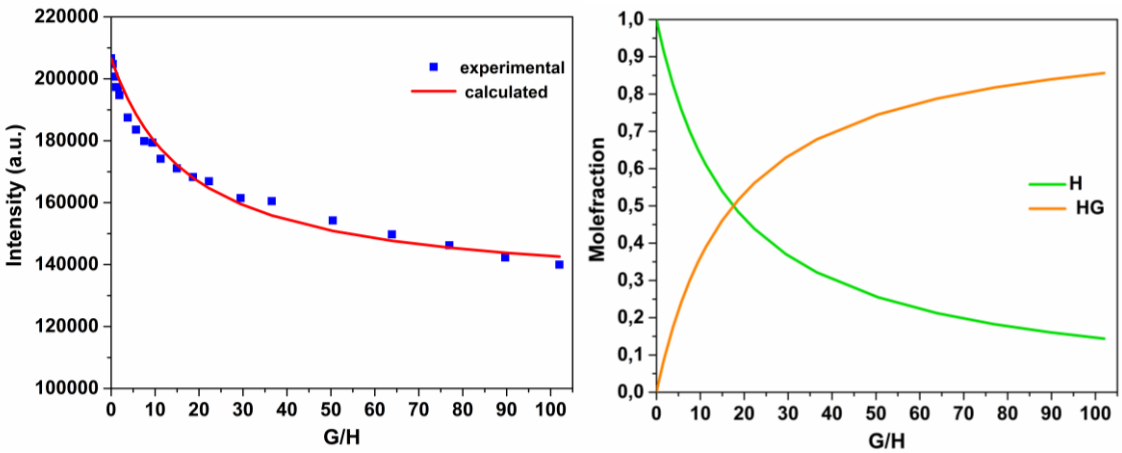

FigureS4. Fluorescence intensity and molefraction as a functions of guest/host ratio for cage ***P*-5b.**

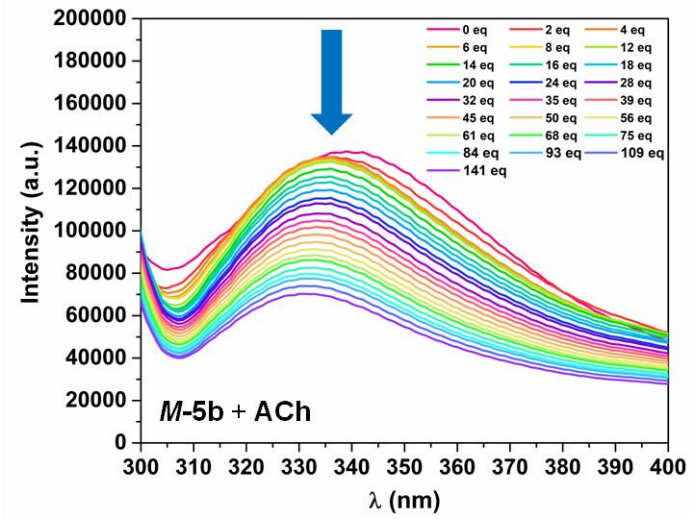

Figure S5. Fluorescence titration of host ***M*-5b** with ACh in CH_3CN excited at 280 nm.

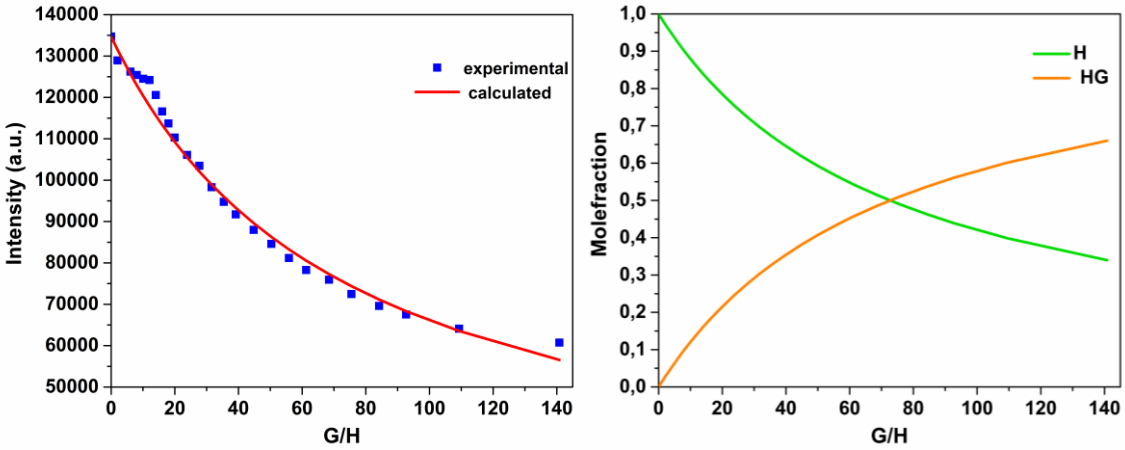

Figure S6. Fluorescence intensity and molefraction as a functions of guest/host ratio for cage ***M*-5b.**

Fluorescence titration curves for choline iodide

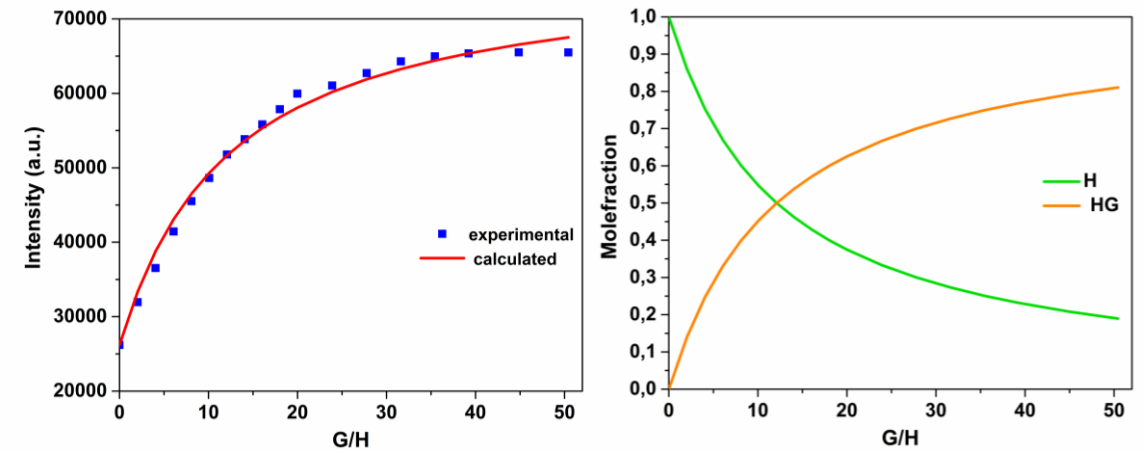

Figure S7. Fluorescence intensity and molefraction as a functions of guest/host ratio for cage ***P*-5a.**

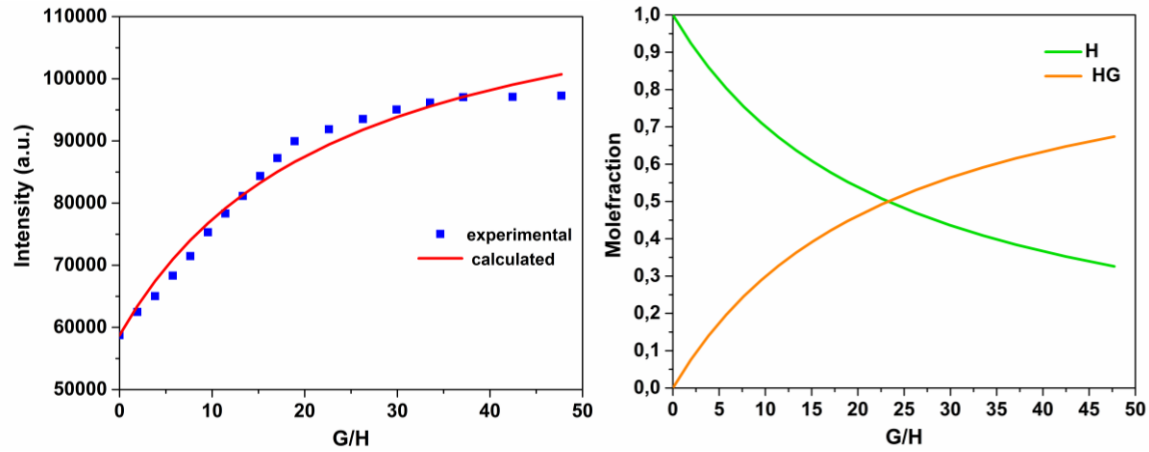

Figure S8. Fluorescence intensity and molefraction as a functions of guest/host ratio for cage ***M*-5a.**

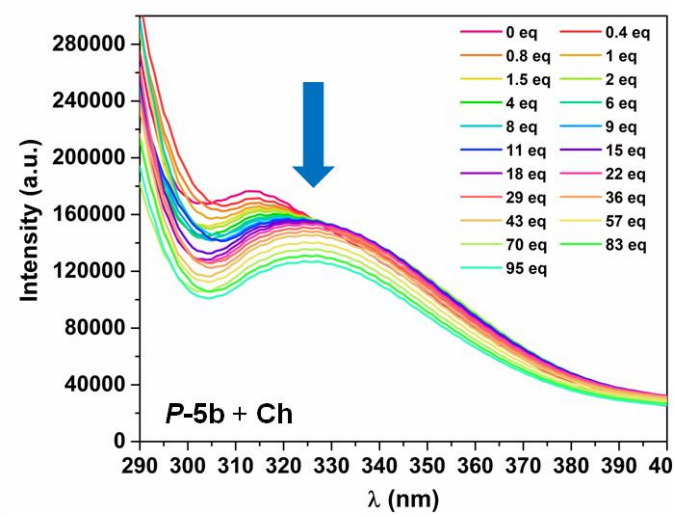

Figure S9. Fluorescence titration of host ***P*-5b** with Ch in CH_3CN excited at 280 nm.

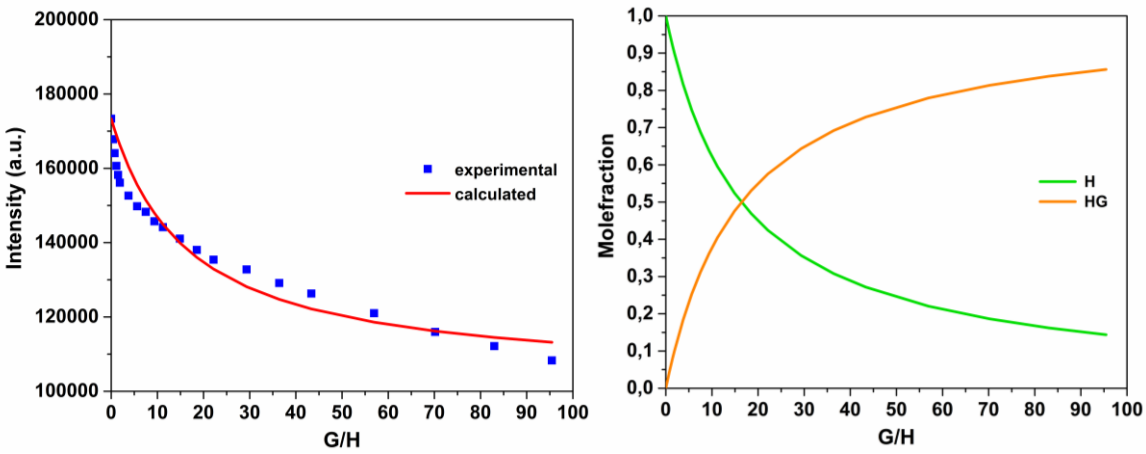

Figure S10. Fluorescence intensity and molefraction as a functions of guest/host ratio for cage ***P*-5b.**

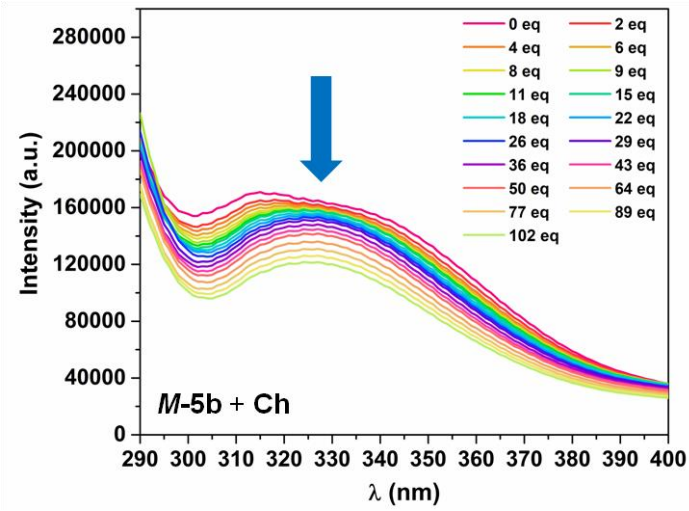

Figure S11. Fluorescence titration of host ***M*-5b** with Ch in CH_3CN excited at 280 nm.

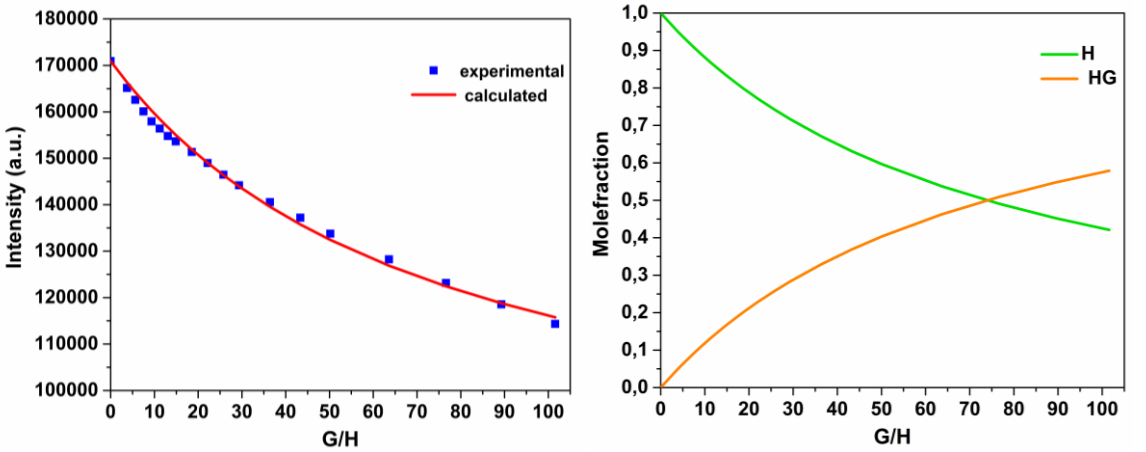

Figure S12. Fluorescence intensity and molefraction as a functions of guest/host ratio for cage ***M*-5b.**

Fit parameters

Table S2. Fit parameters obtained from the fluorescence titrations.

Host	Guest	K_a (M^{-1})	**RMS** (Intensity a.u.)	**Covariance**
***P*-5a**	ACh	$2.2 \times 10^3 \pm 1.6\%$	1.0×10^3	2.1×10^{-2}
	Ch	$3.8 \times 10^3 \pm 0.9\%$	1.6×10^3	8.5×10^{-3}
***M*-5a**	ACh	$5.6 \times 10^3 \pm 1.7\%$	2.2×10^3	1.8×10^{-2}
	Ch	$1.8 \times 10^3 \pm 1.4\%$	1.8×10^3	2.2×10^{-2}
***P*-5b**	ACh	$2.4 \times 10^3 \pm 3.5\%$	6.1×10^3	7.2×10^{-2}
	Ch	$2.6 \times 10^3 \pm 3.8\%$	2.6×10^3	2.8×10^{-2}
***M*-5b**	ACh	$0.6 \times 10^3 \pm 0.9\%$	2.8×10^3	1.7×10^{-2}
	Ch	$0.5 \times 10^3 \pm 1.1\%$	2.6×10^3	2.8×10^{-2}

^{1}H NMR titration experiments

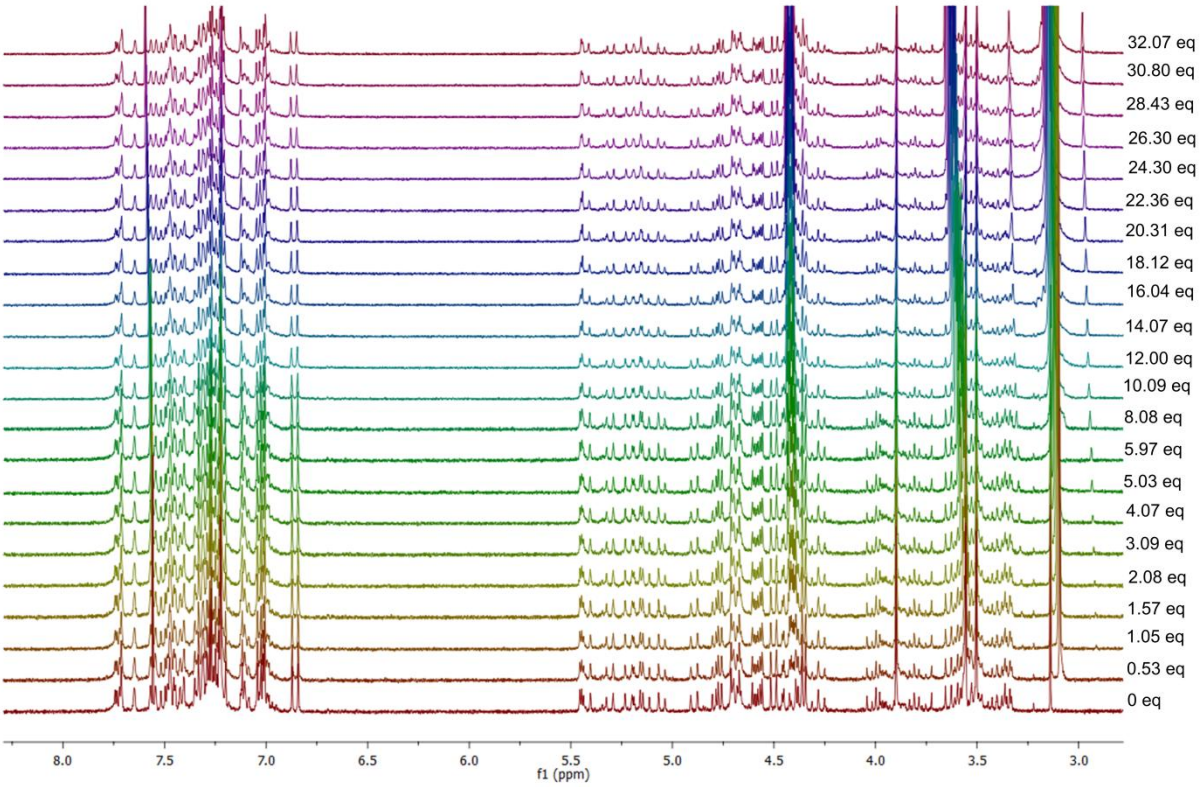

Figure S13. ^{1}H NMR (400 MHz, $CD_3CN/CDCl_3$ = 80:20) spectra of ***M*-5a** after gradual addition of acetylcholine iodide in the same solvent**.**

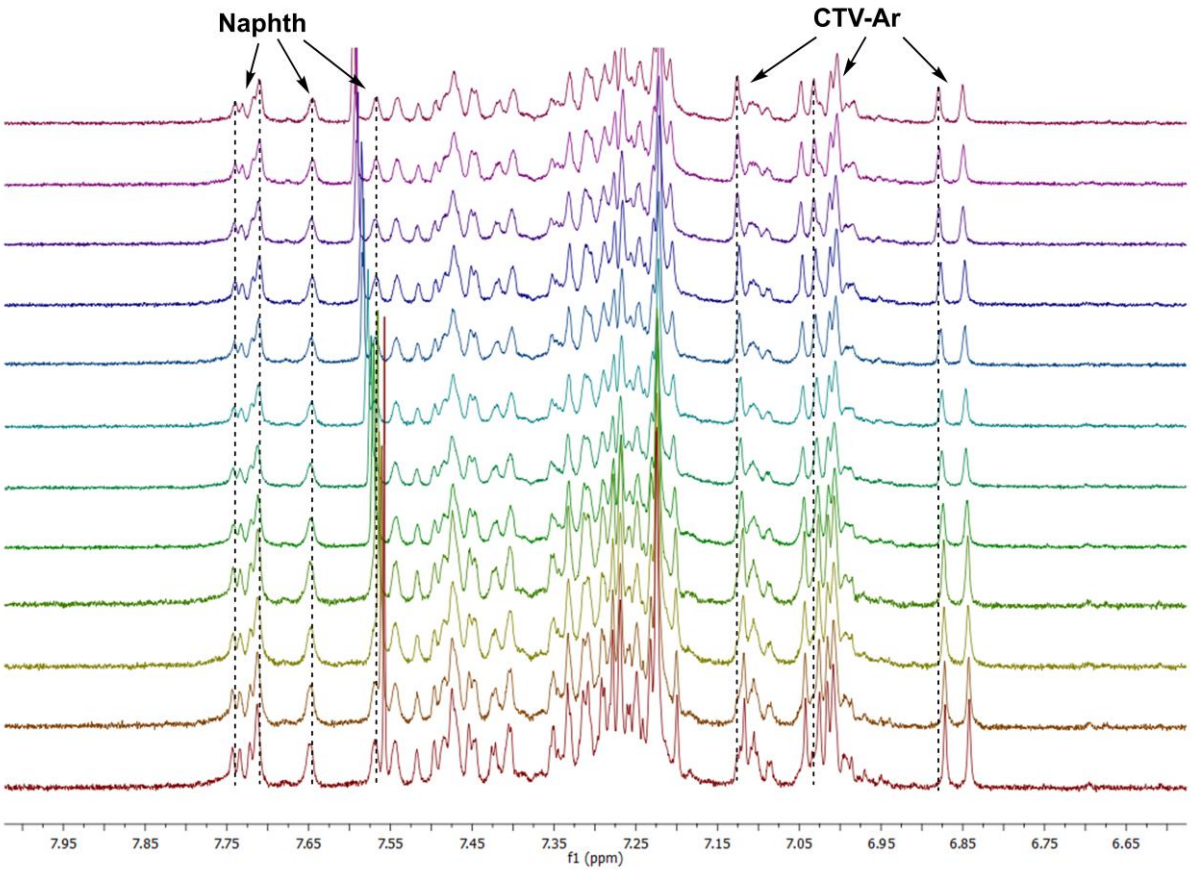

Figure S14. ^{1}H NMR (400 MHz, $CD_3CN/CDCl_3$ = 80:20) spectra of aromatic part of ***M*-5a** after gradual addition of acetylcholine iodide in the same solvent**.**

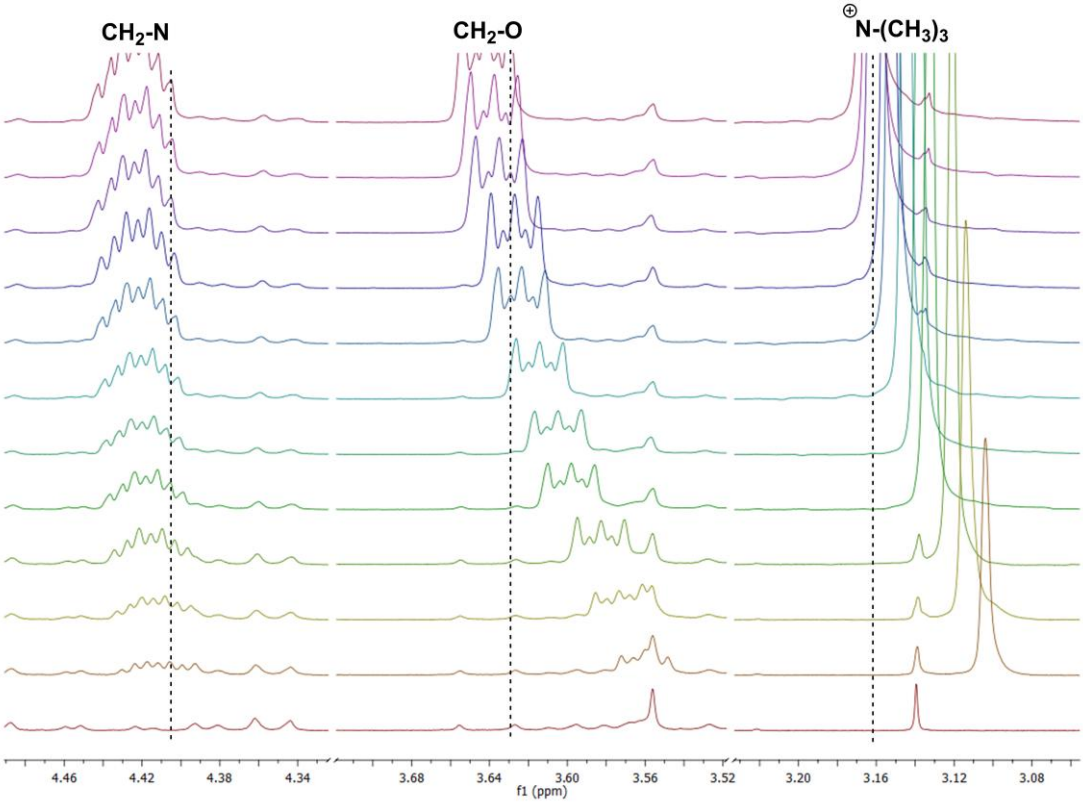

Figure S15. ^{1}H NMR (400 MHz, $CD_3CN/CDCl_3$ = 80:20) spectra of ACh chemical shifts during titration studies of ***M*-5a** with acetylcholine iodide**.**

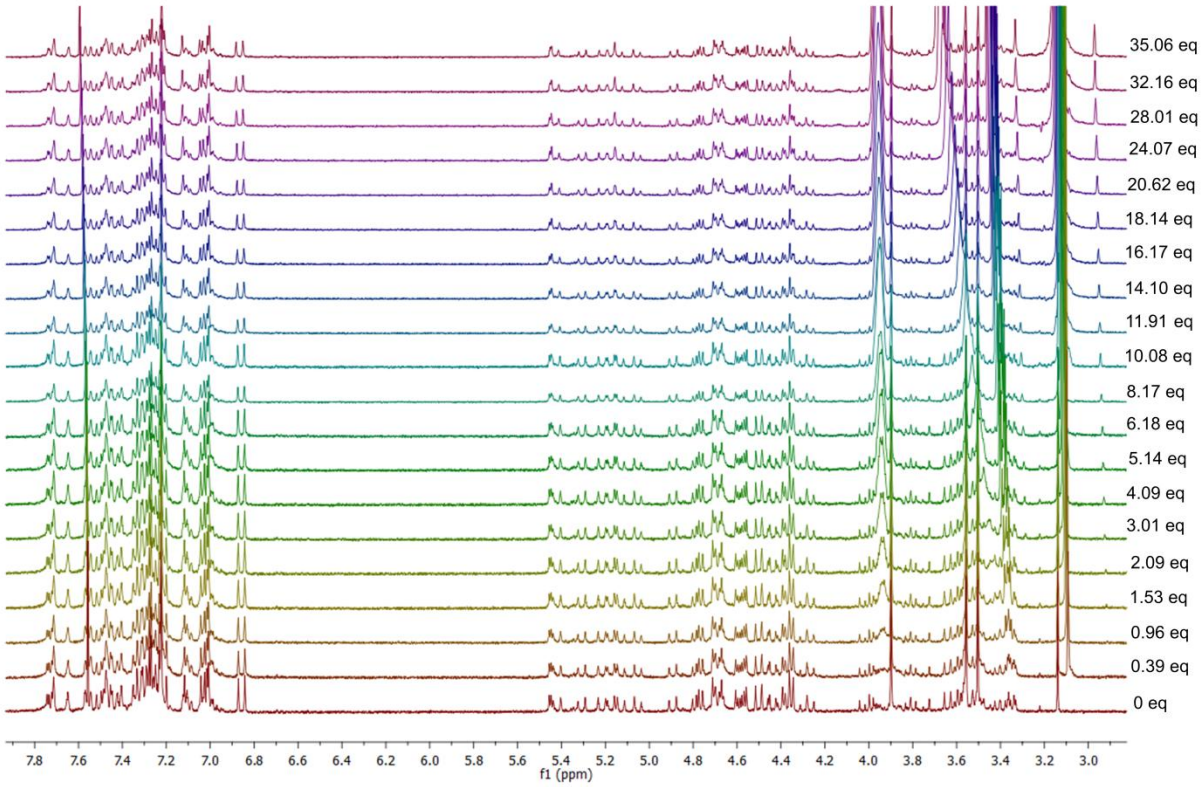

Figure S16. ^{1}H NMR (400 MHz, $CD_3CN/CDCl_3$ = 80:20) spectra of ***M*-5a** after gradual addition of choline iodide in the same solvent**.**

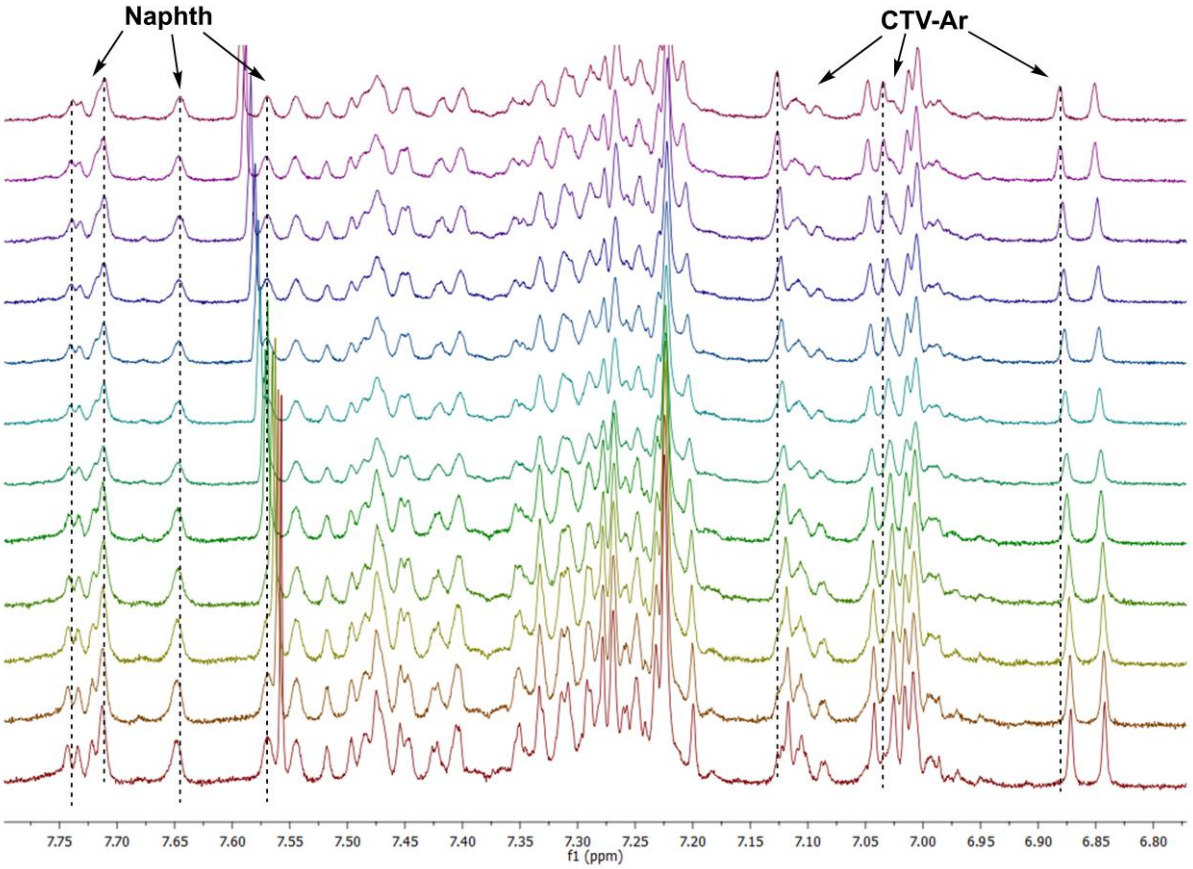

Figure S17. ^{1}H NMR (400 MHz, $CD_3CN/CDCl_3$ = 80:20) spectra of aromatic part of ***M*-5a** after gradual addition of choline iodide in the same solvent**.**

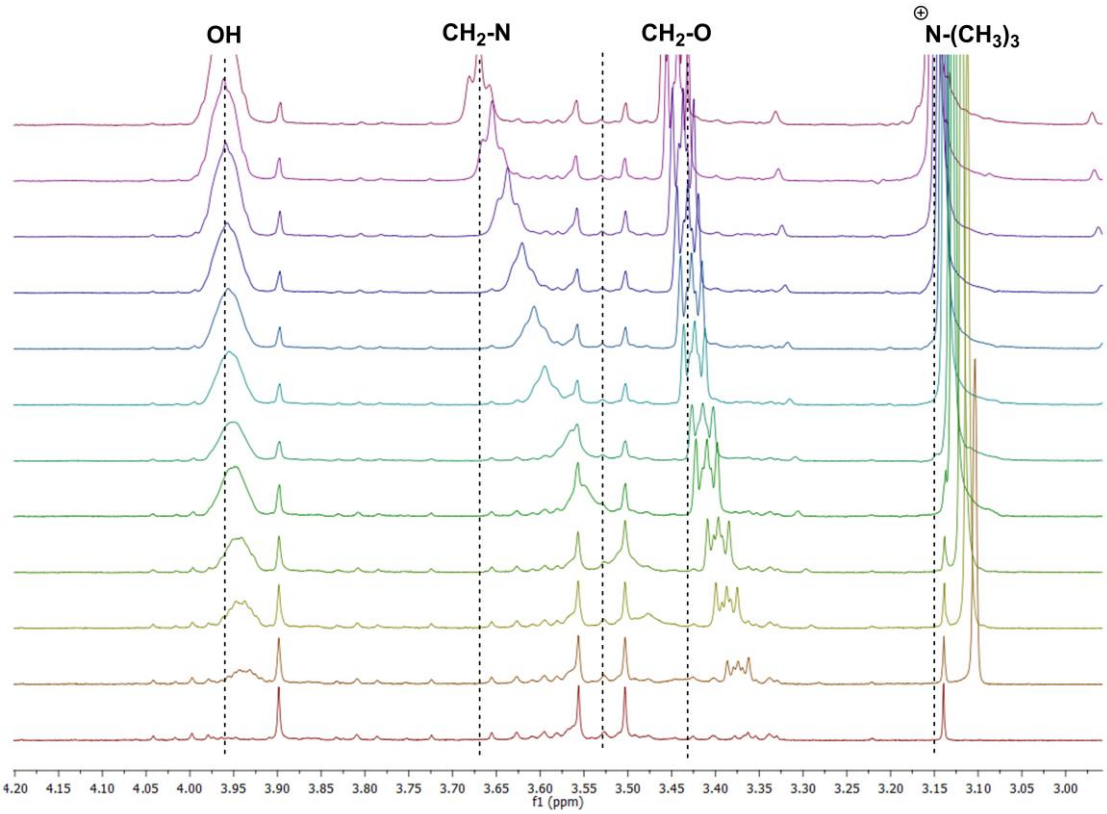

Figure S18. ^{1}H NMR (400 MHz, $CD_3CN/CDCl_3$ = 80:20) spectra of Ch chemical shifts during titration studies of ***M*-5a** with choline iodide**.**

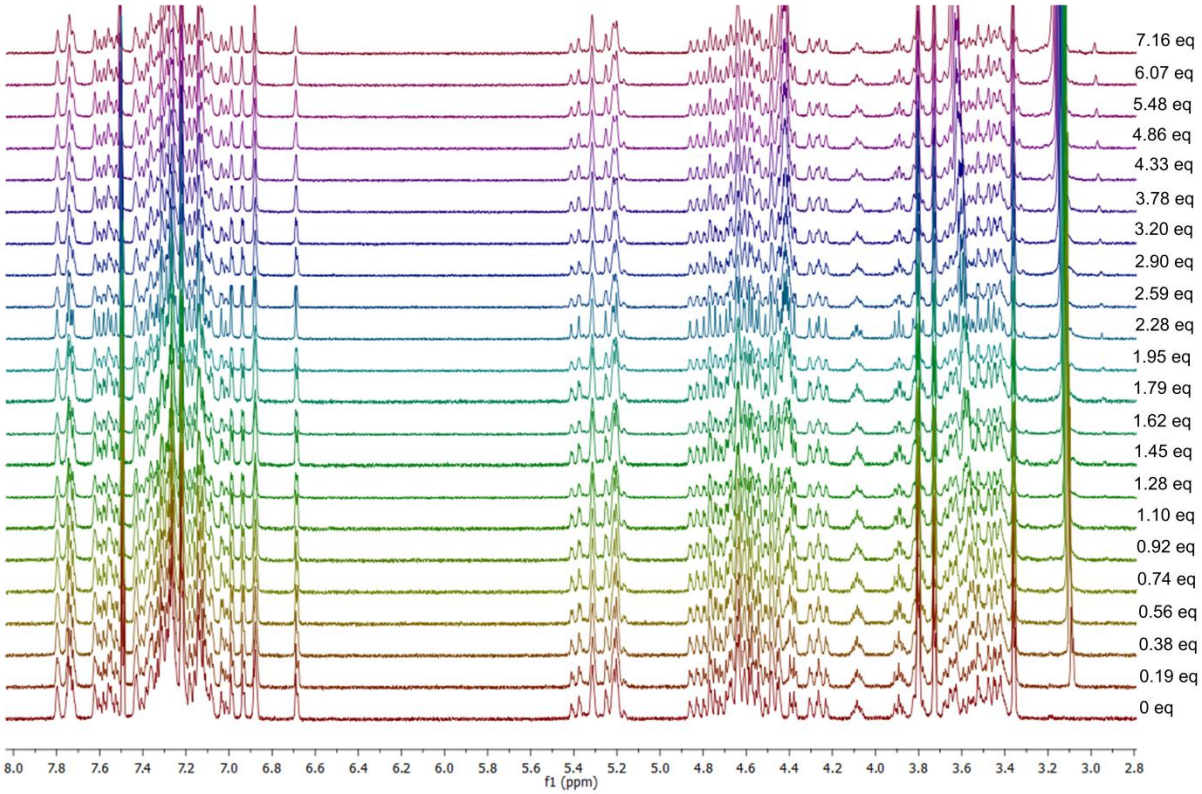

Figure S19. ^{1}H NMR (400 MHz, $CD_3CN/CDCl_3$ = 80:20) spectra of ***P*-5a** after gradual addition of acetylcholine iodide in the same solvent**.**

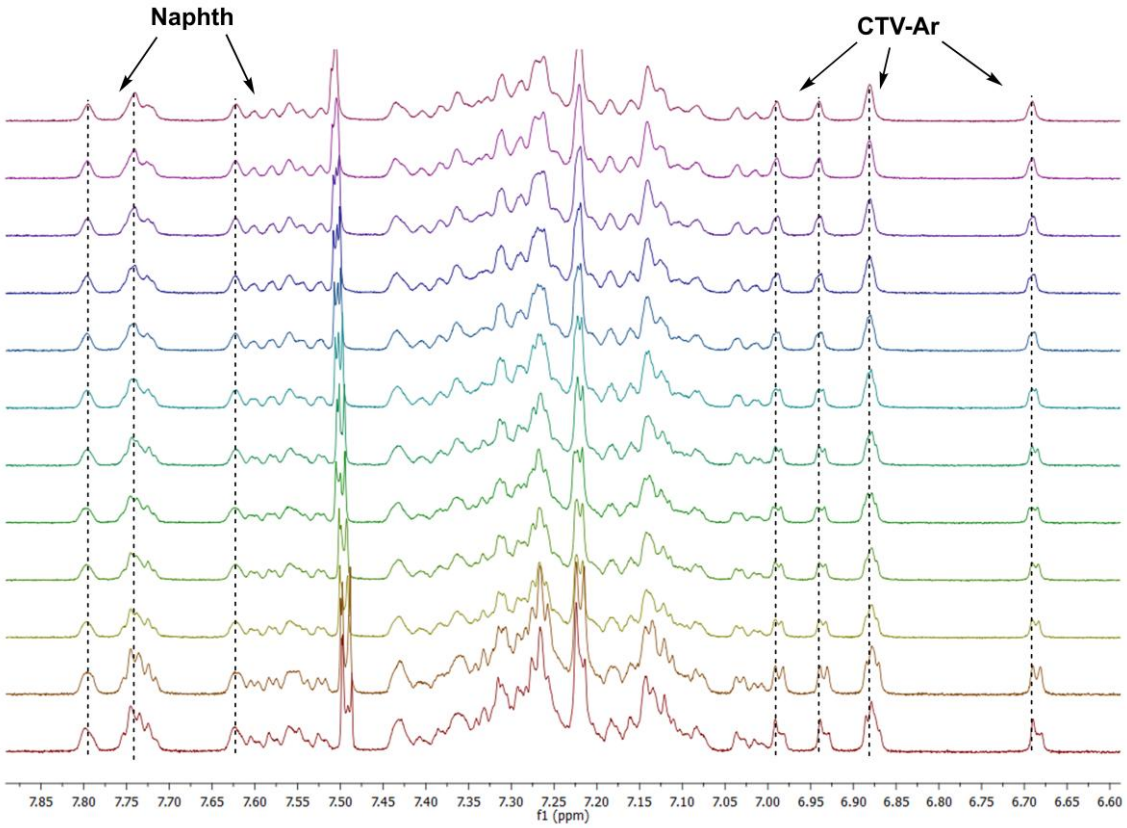

Figure S20. ^{1}H NMR (400 MHz, $CD_3CN/CDCl_3$ = 80:20) spectra of aromatic part of ***P*-5a** after gradual addition of acetylcholine iodide in the same solvent**.**

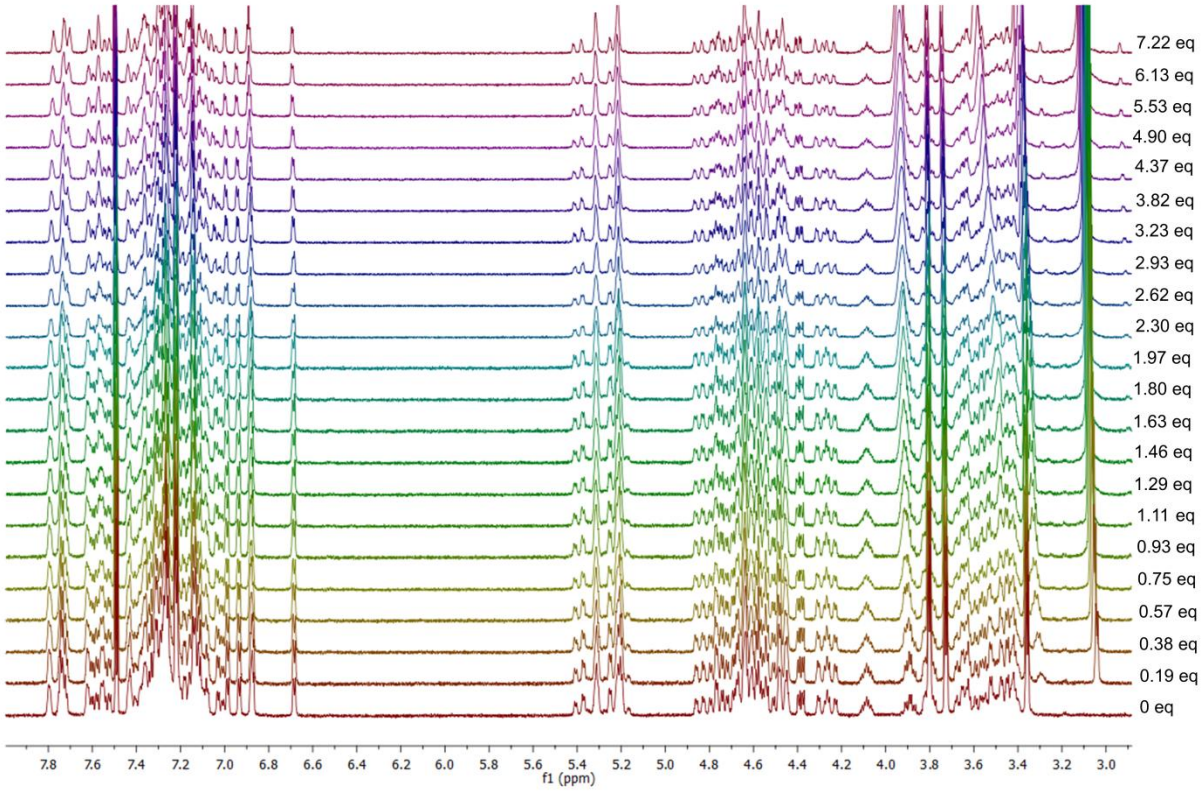

Figure S21. ^{1}H NMR (400 MHz, $CD_3CN/CDCl_3$ = 80:20) spectra of ***P*-5a** after gradual addition of choline iodide in the same solvent**.**

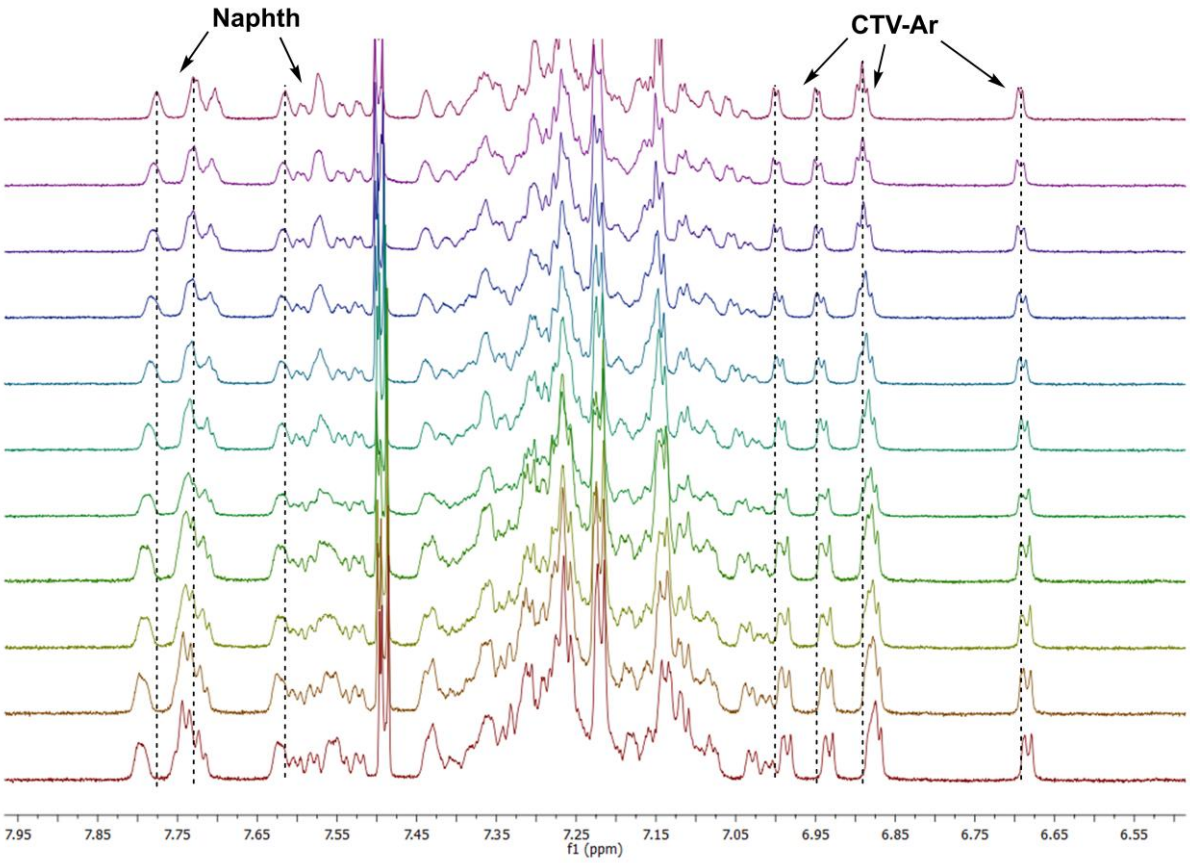

Figure S22. ^{1}H NMR (400 MHz, $CD_3CN/CDCl_3$ = 80:20) spectra of aromatic part of ***P*-5a** after gradual addition of choline iodide in the same solvent**.**

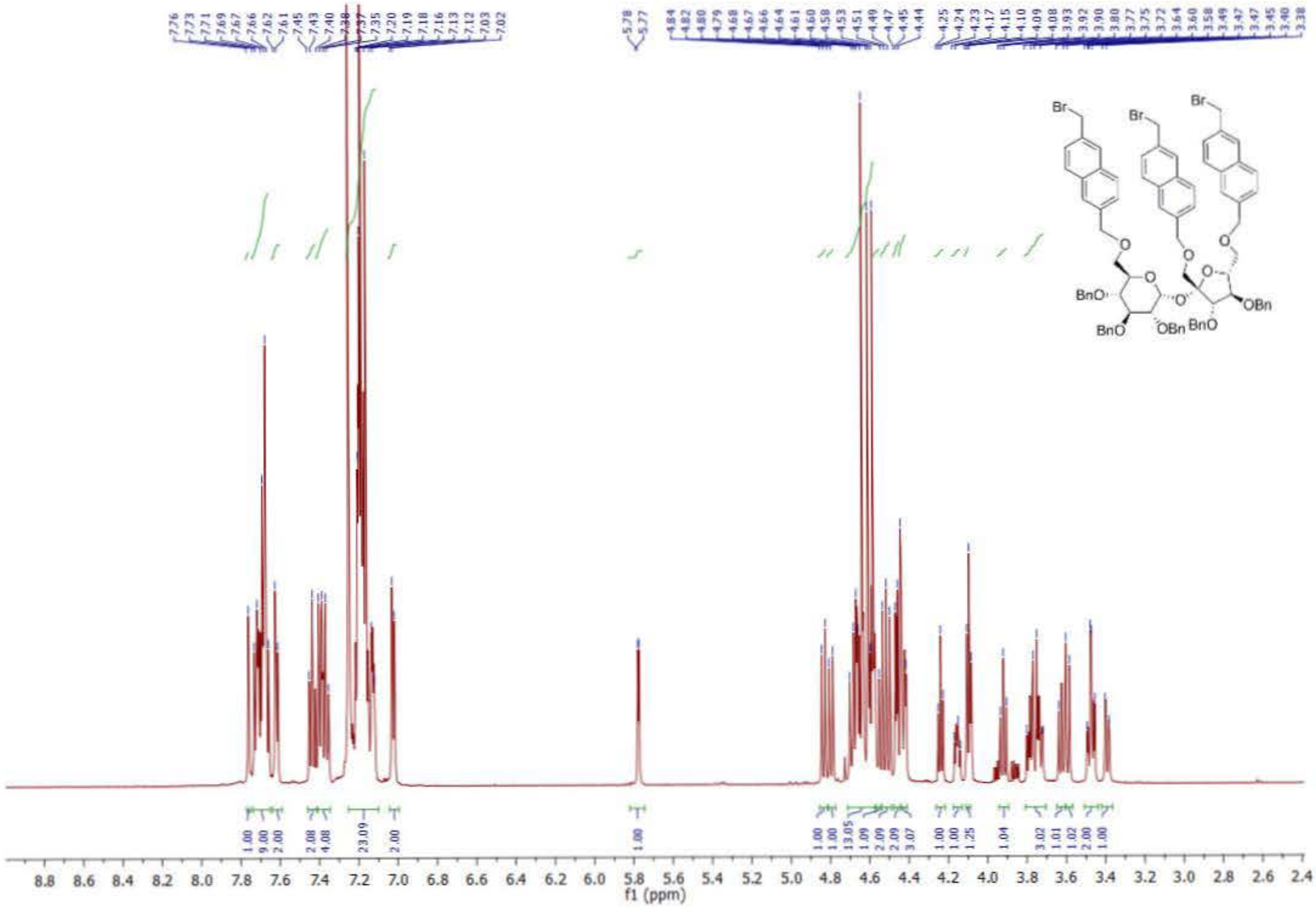

Figure S23. ^{1}H NMR (600 MHz, $CDCl_3$) spectrum of compound **3.**

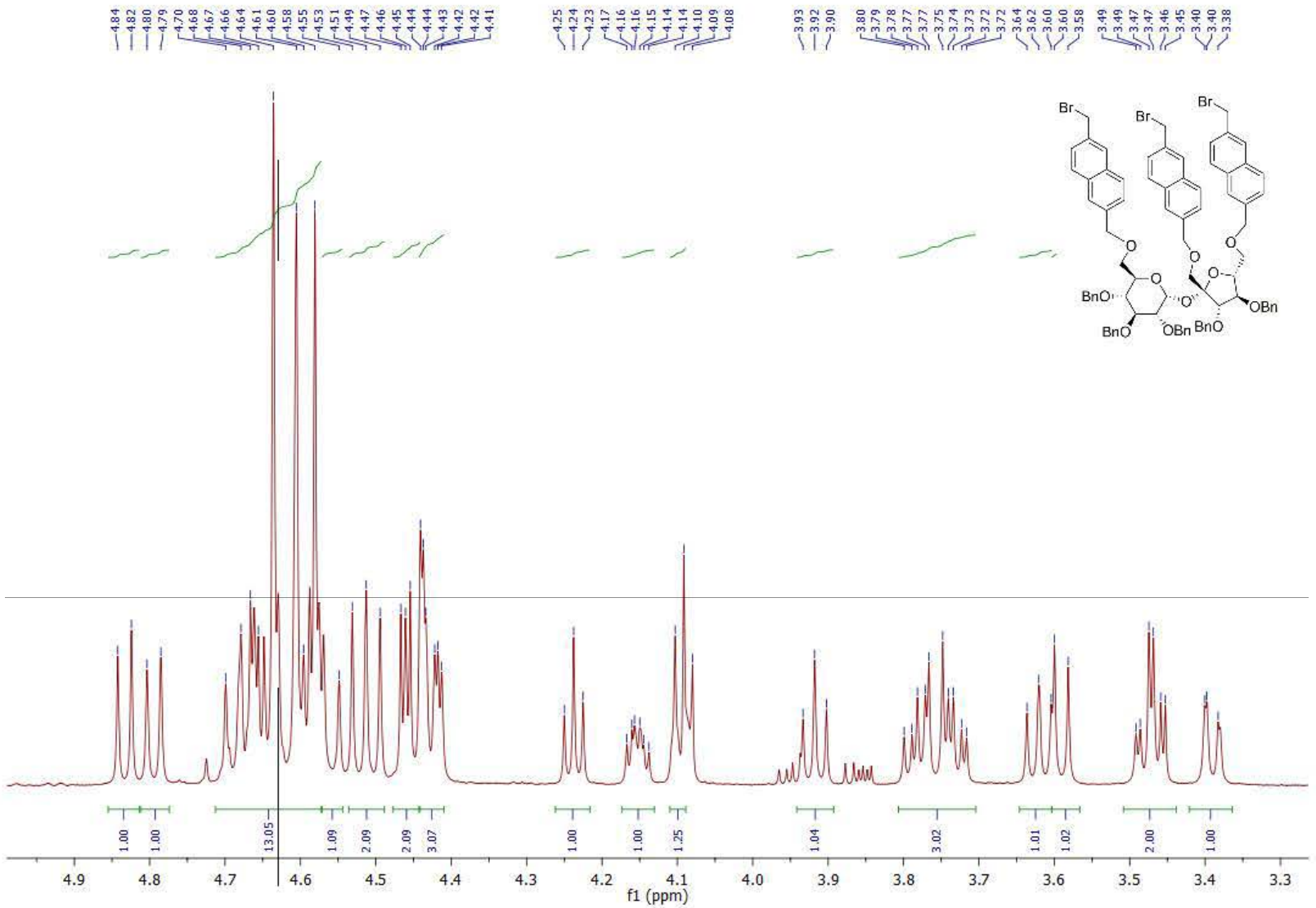

Figure S24. ^{1}H NMR (600 MHz, $CDCl_3$) spectrum of compound **3** (aliphatic part).

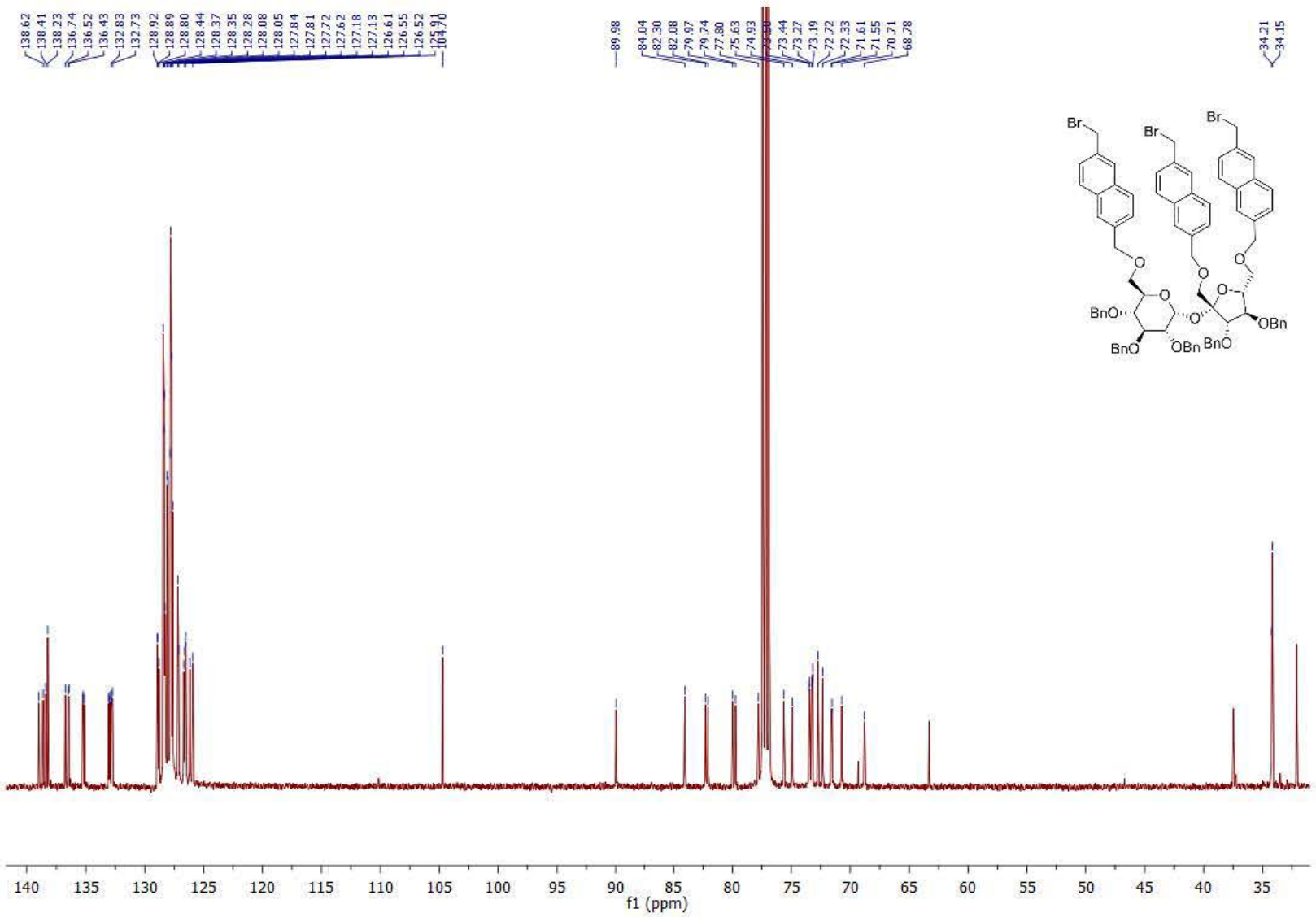

Figure S25. $^{13}C\{^{1}H\}$ NMR (150 MHz, $CDCl_3$) spectrum of compound **3**.

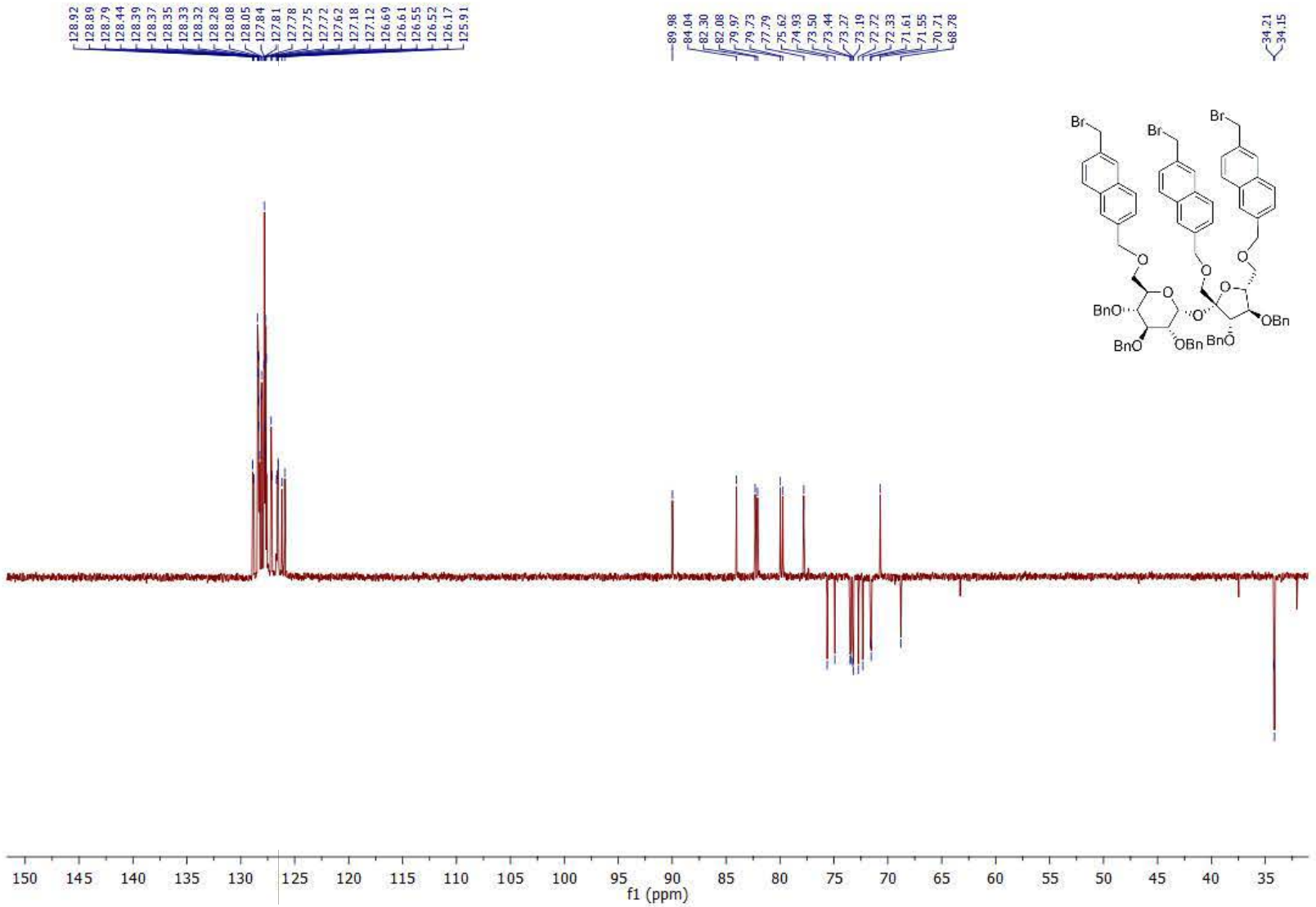

Figure S26. $^{13}C\{^{1}H\}$ DEPT (150 MHz, $CDCl_3$) spectrum of compound **3**.

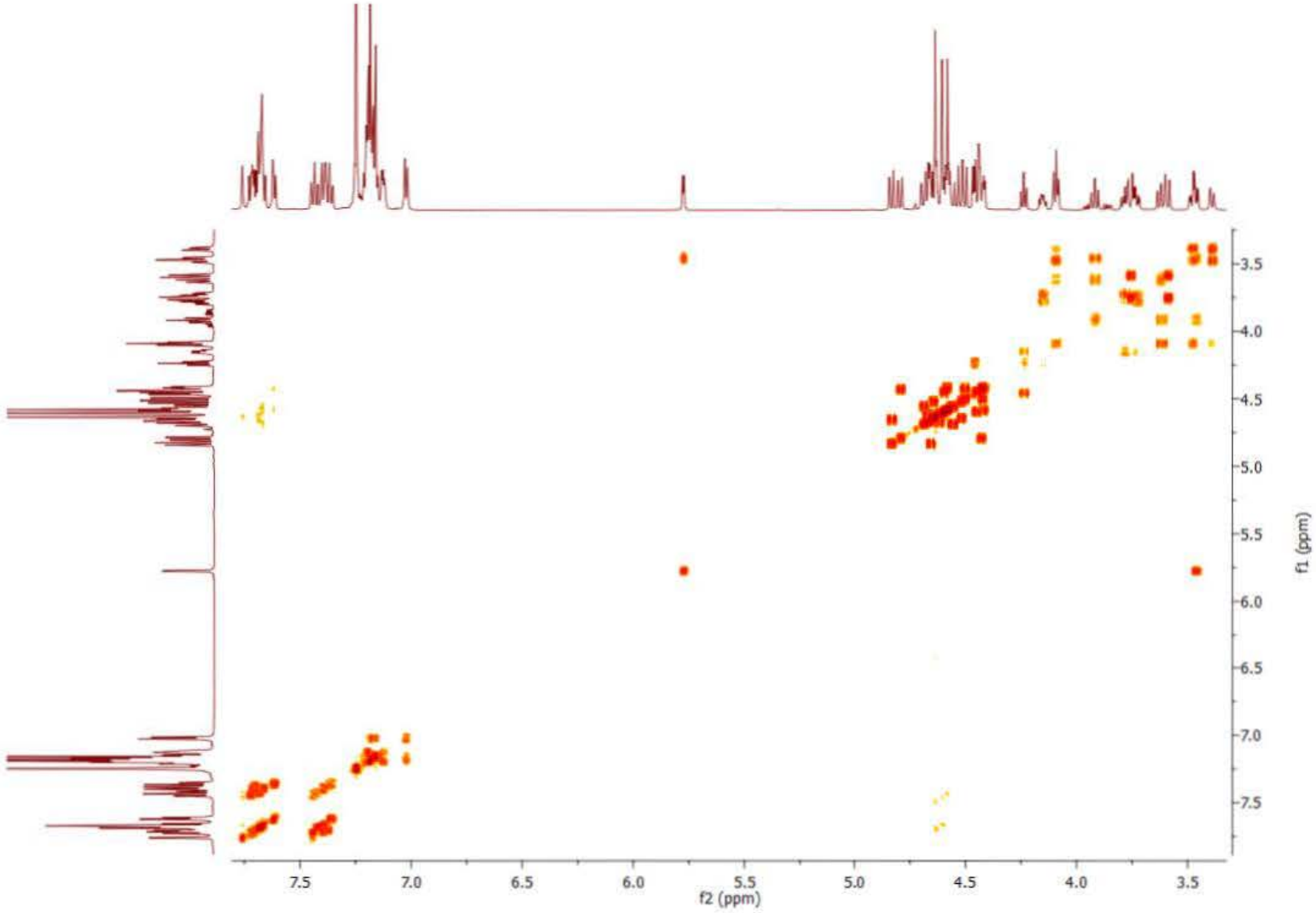

Figure S27. ^{1}H–^{1}H COSY (600 MHz, $CDCl_3$) spectrum of compound **3**.

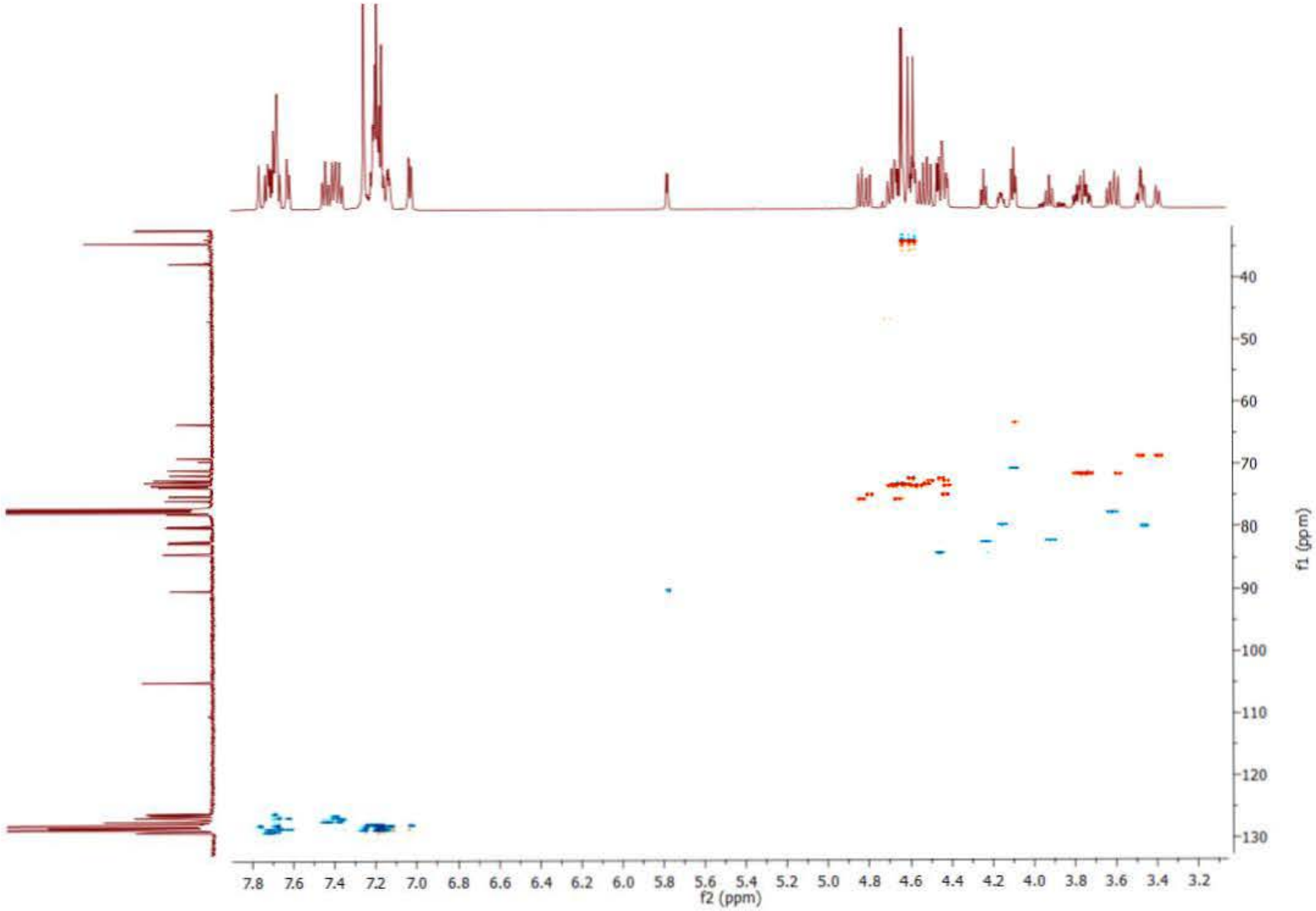

Figure S28. $^{1}H–^{13}C$ HSQC (600/150 MHz, $CDCl_3$) spectrum of compound **3**.

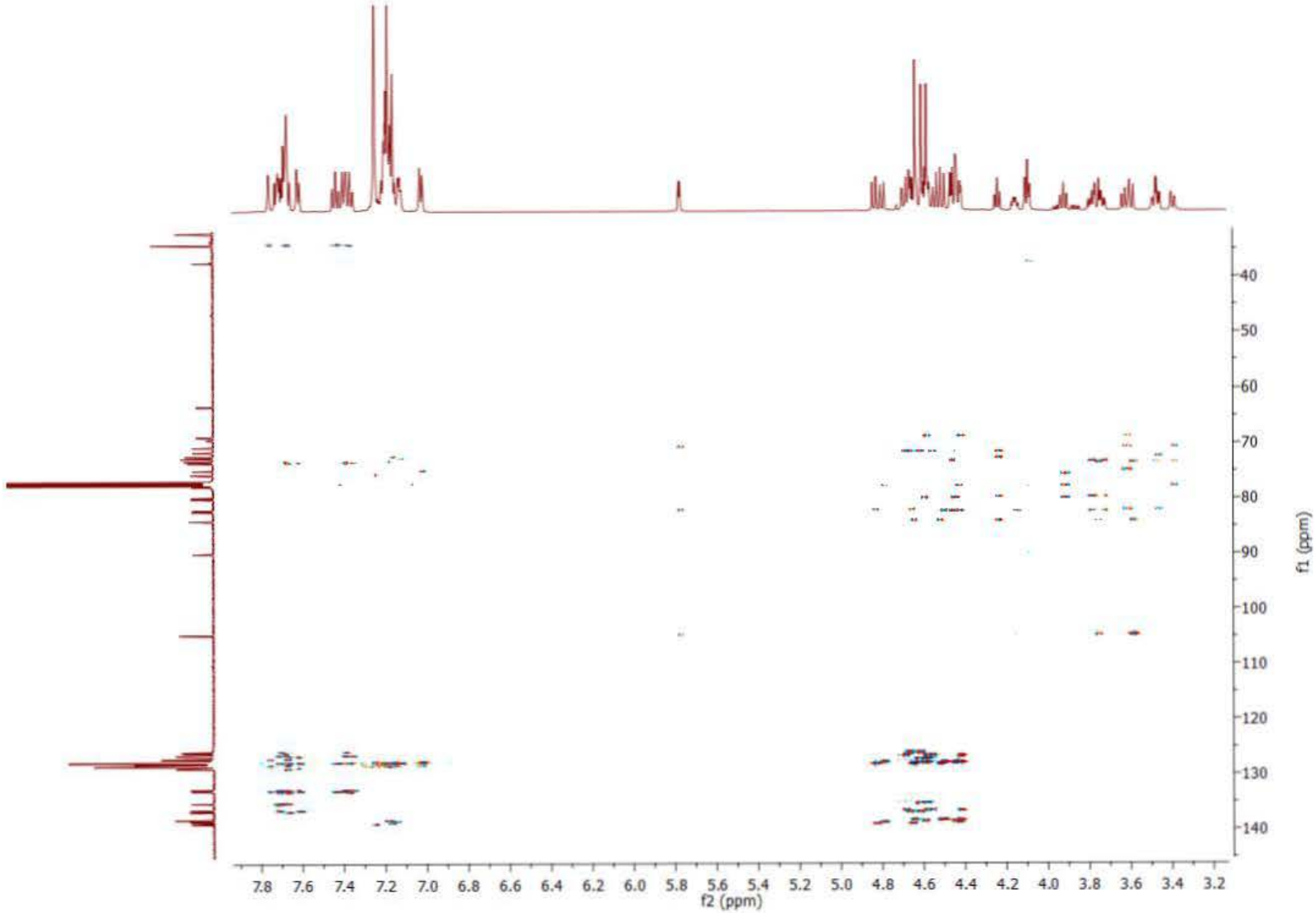

Figure S29. $^{1}H–^{13}C$ HMBC (600/150 MHz, $CDCl_3$) spectrum of compound **3**.

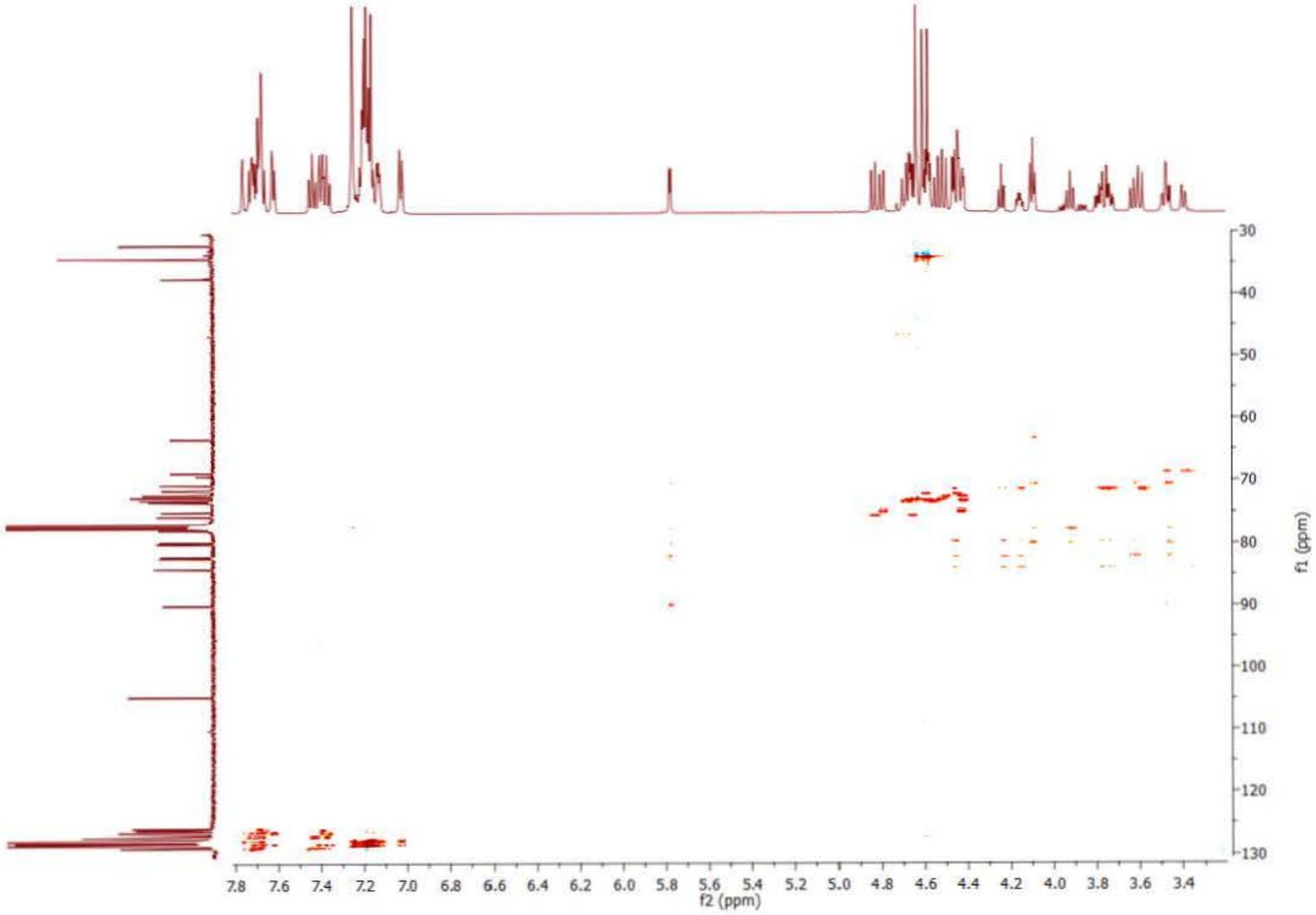

Figure S30. $^{1}H–^{13}C$ HSQC-TOCSY (600/150 MHz, $CDCl_3$) spectrum of compound **3**.

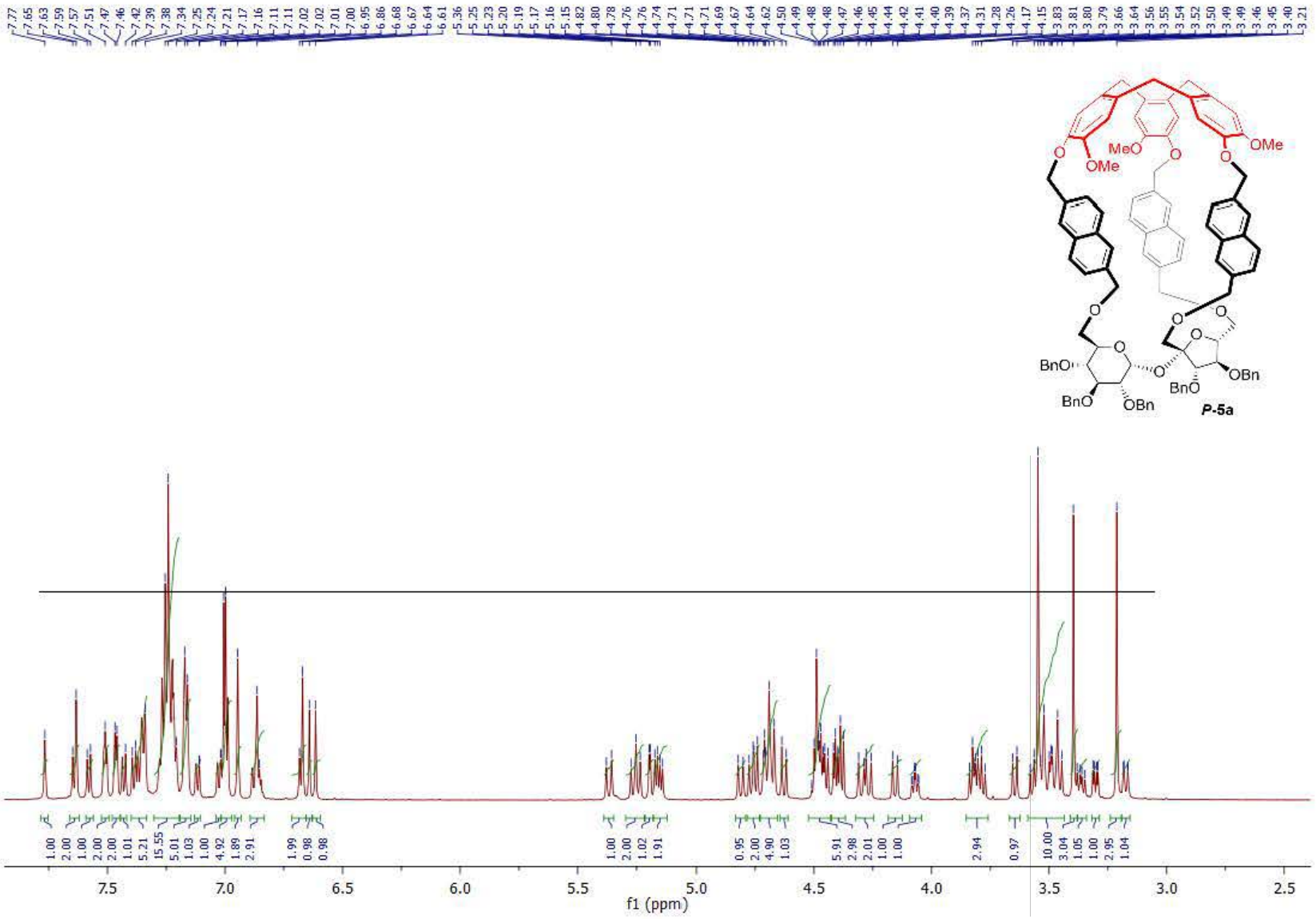

Figure S31. ^{1}H NMR (600 MHz, $CDCl_3$) spectrum of compound ***P*-5a.**

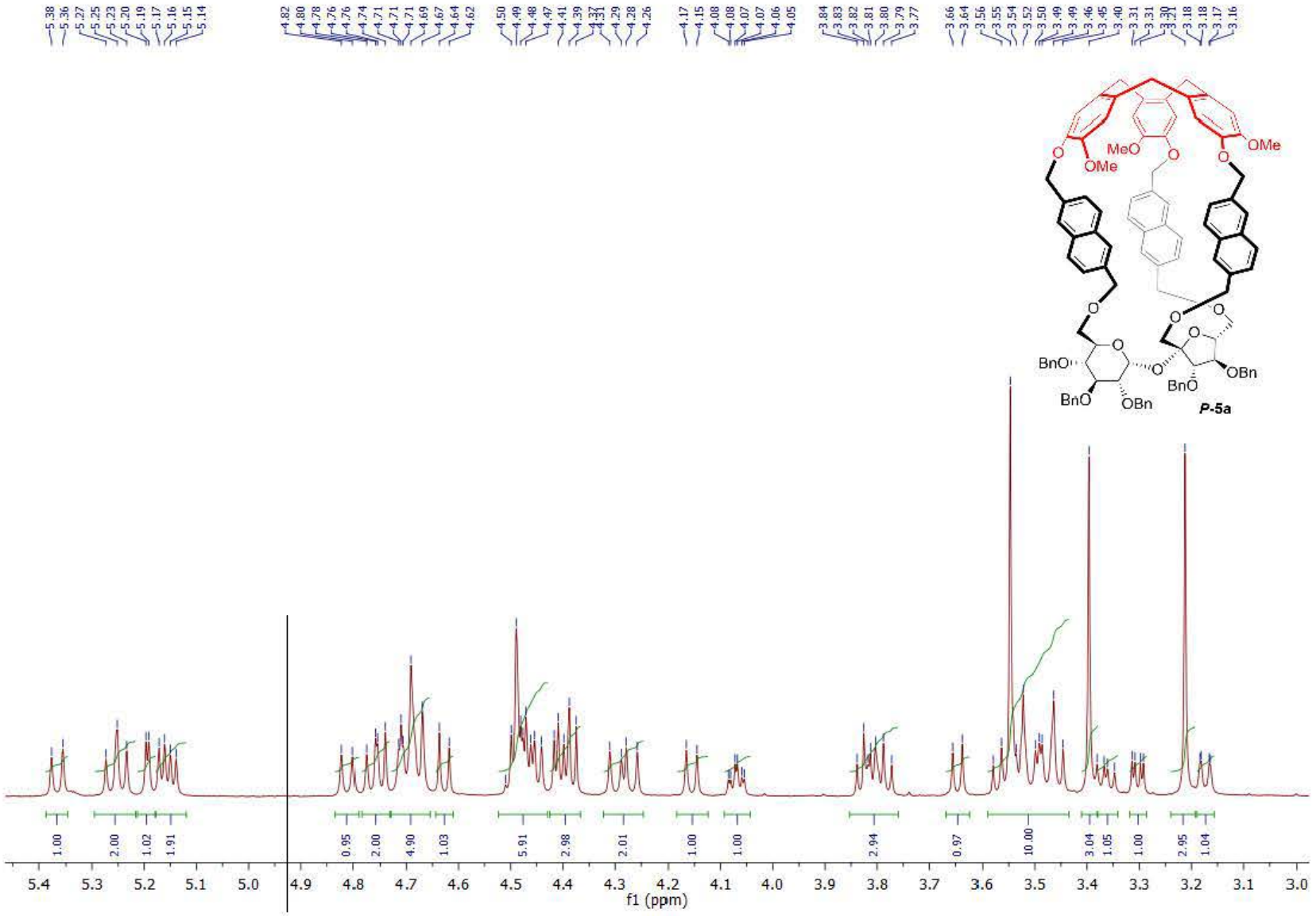

Figure S32. ^{1}H NMR (600 MHz, $CDCl_3$) spectrum of compound ***P*-5a** (aliphatic part).

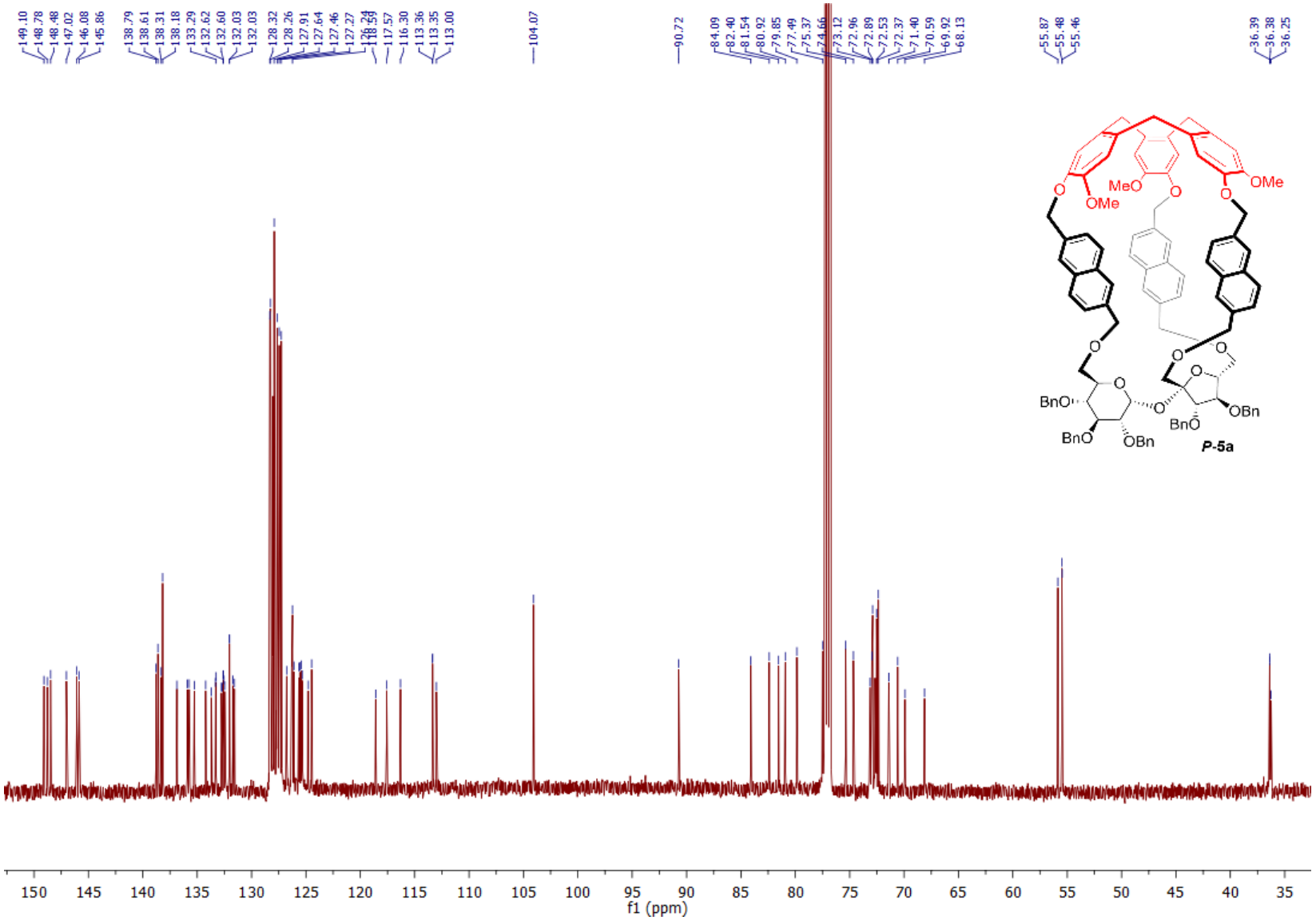

Figure S33. $^{13}C\{^{1}H\}$ NMR (150 MHz, $CDCl_3$) spectrum of compound ***P*-5a.**

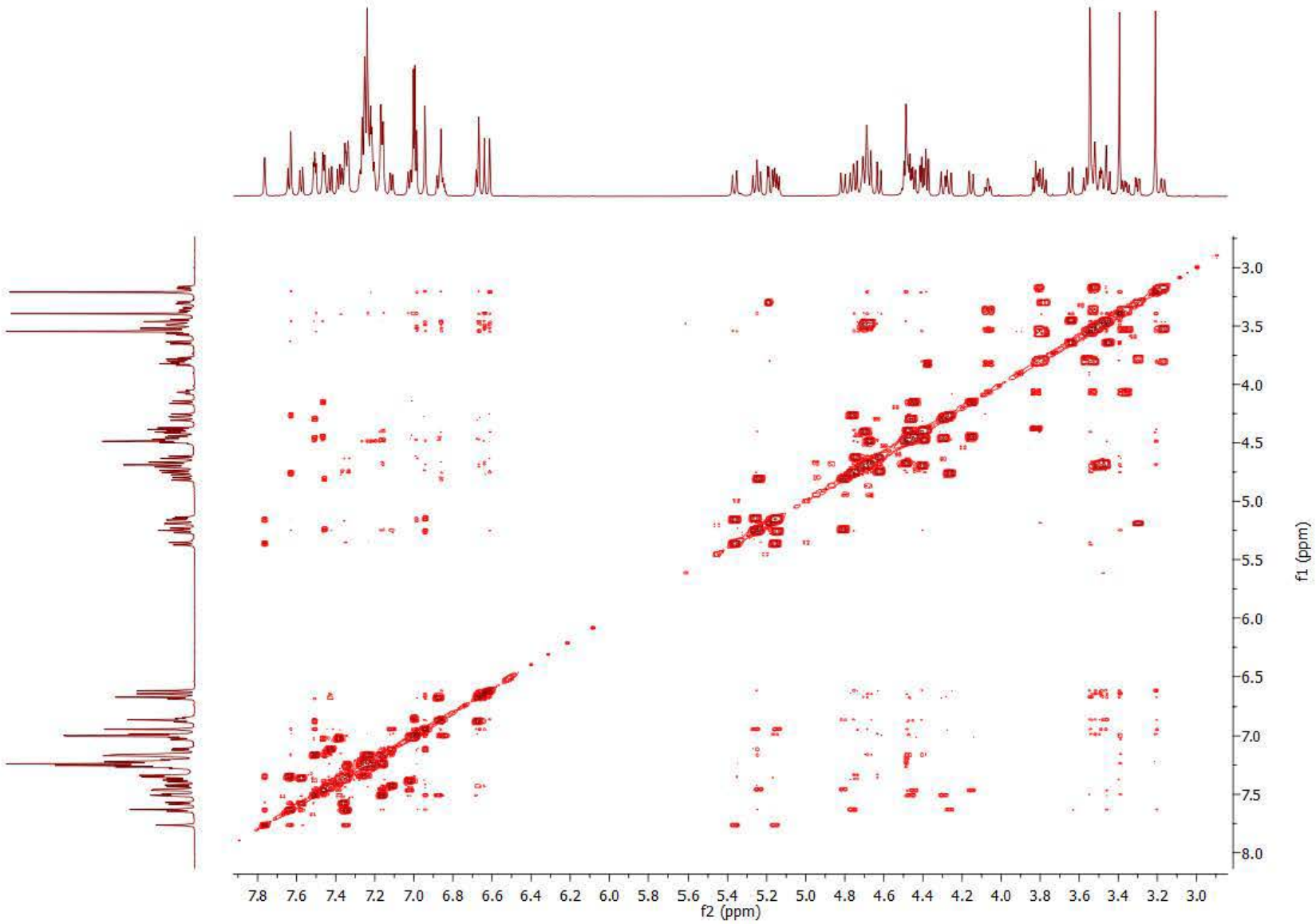

Figure S34. $^{1}H–^{1}H$ COSY (600 MHz, $CDCl_3$) spectrum of compound ***P*-5a**.

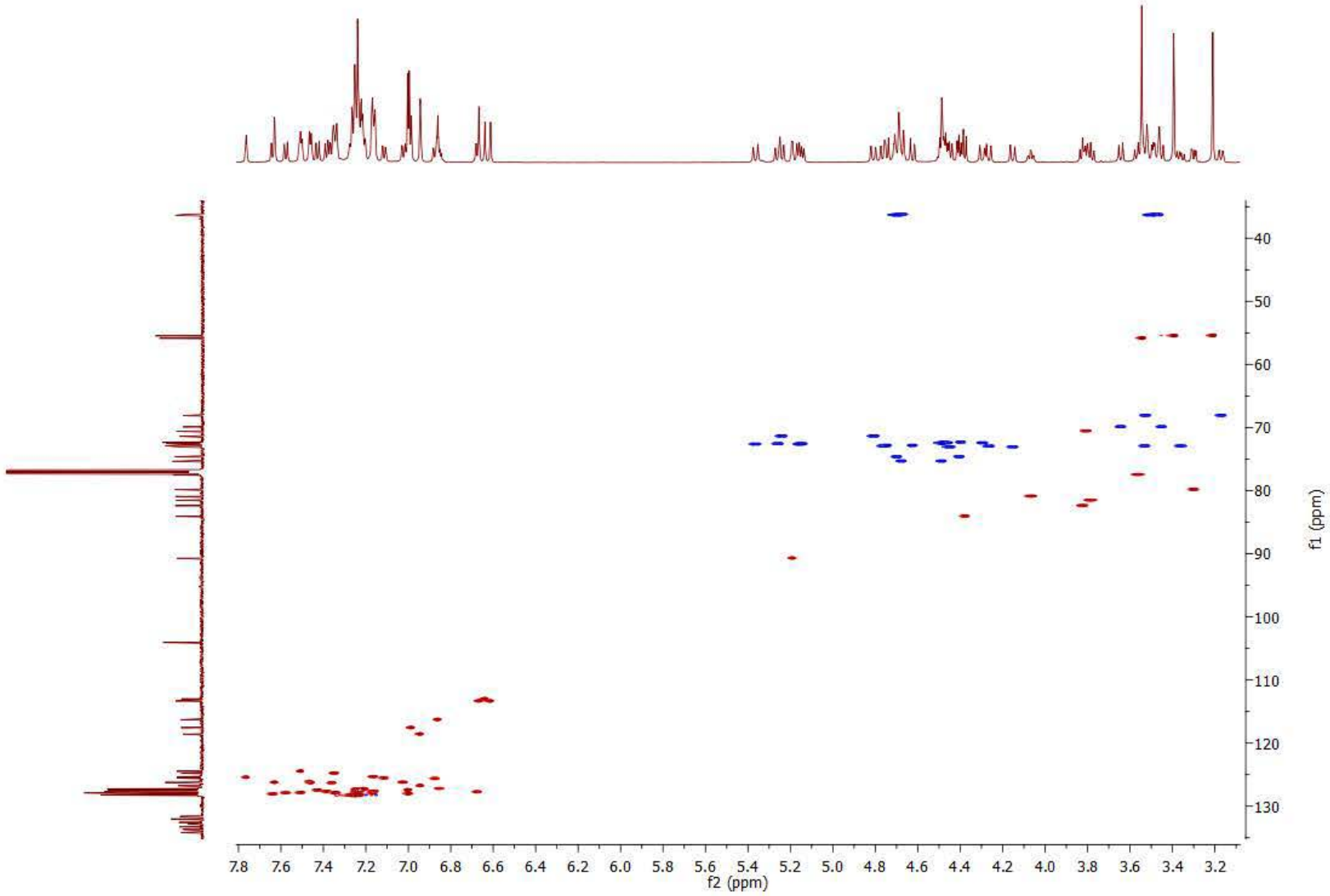

Figure S35. $^{1}H–^{13}C$ HSQC (600/150 MHz, $CDCl_3$) spectrum of compound ***P*-5a**.

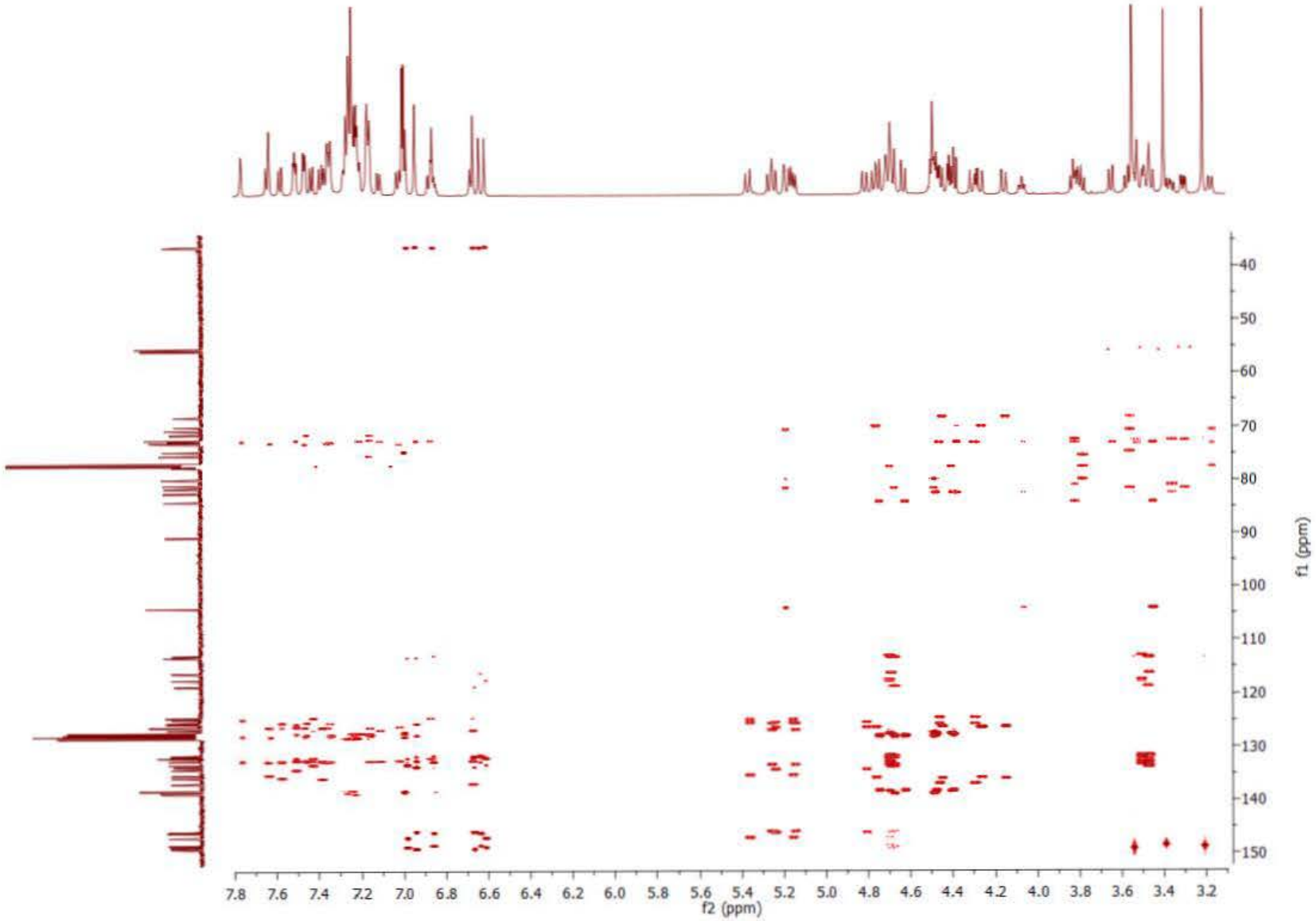

Figure S36. $^{1}H–^{13}C$ HMBC (600/150 MHz, $CDCl_3$) spectrum of compound ***P*-5a.**

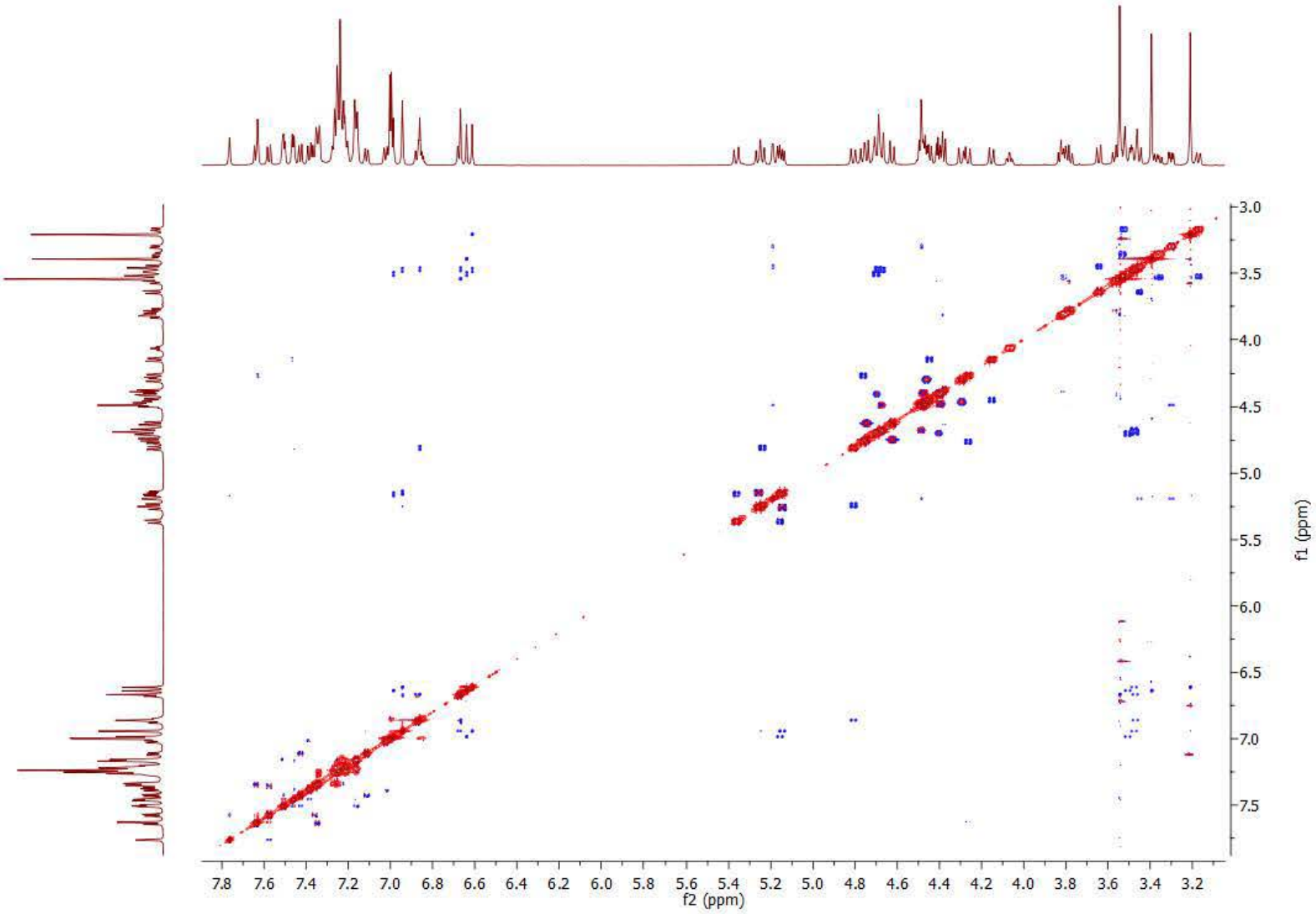

Figure S37. ^{1}H–^{1}H ROESY (600 MHz, $CDCl_3$) spectrum of compound ***P*-5a.**

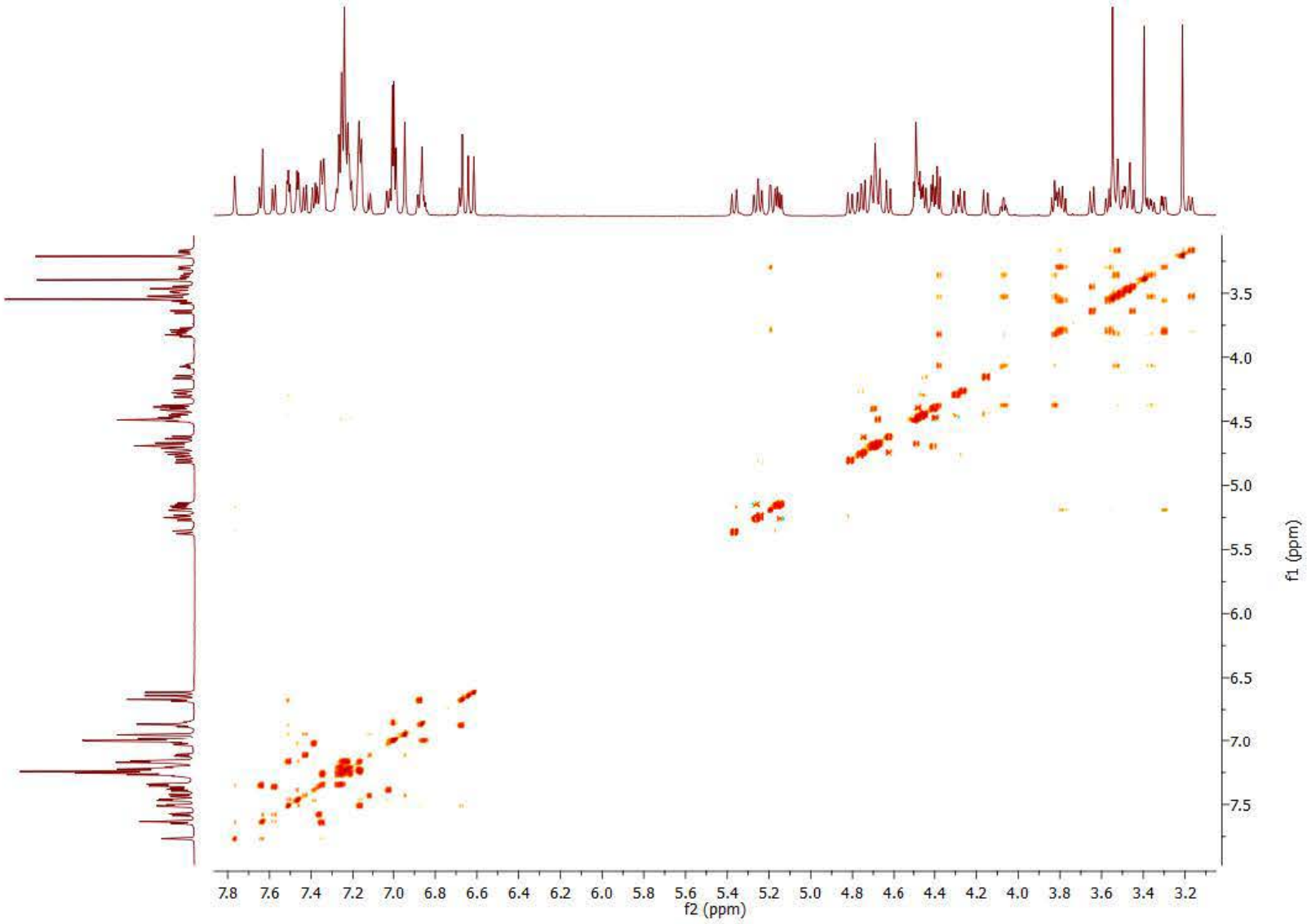

Figure S38. ^{1}H–^{1}H TOCSY (600 MHz, $CDCl_3$) spectrum of compound ***P*-5a.**

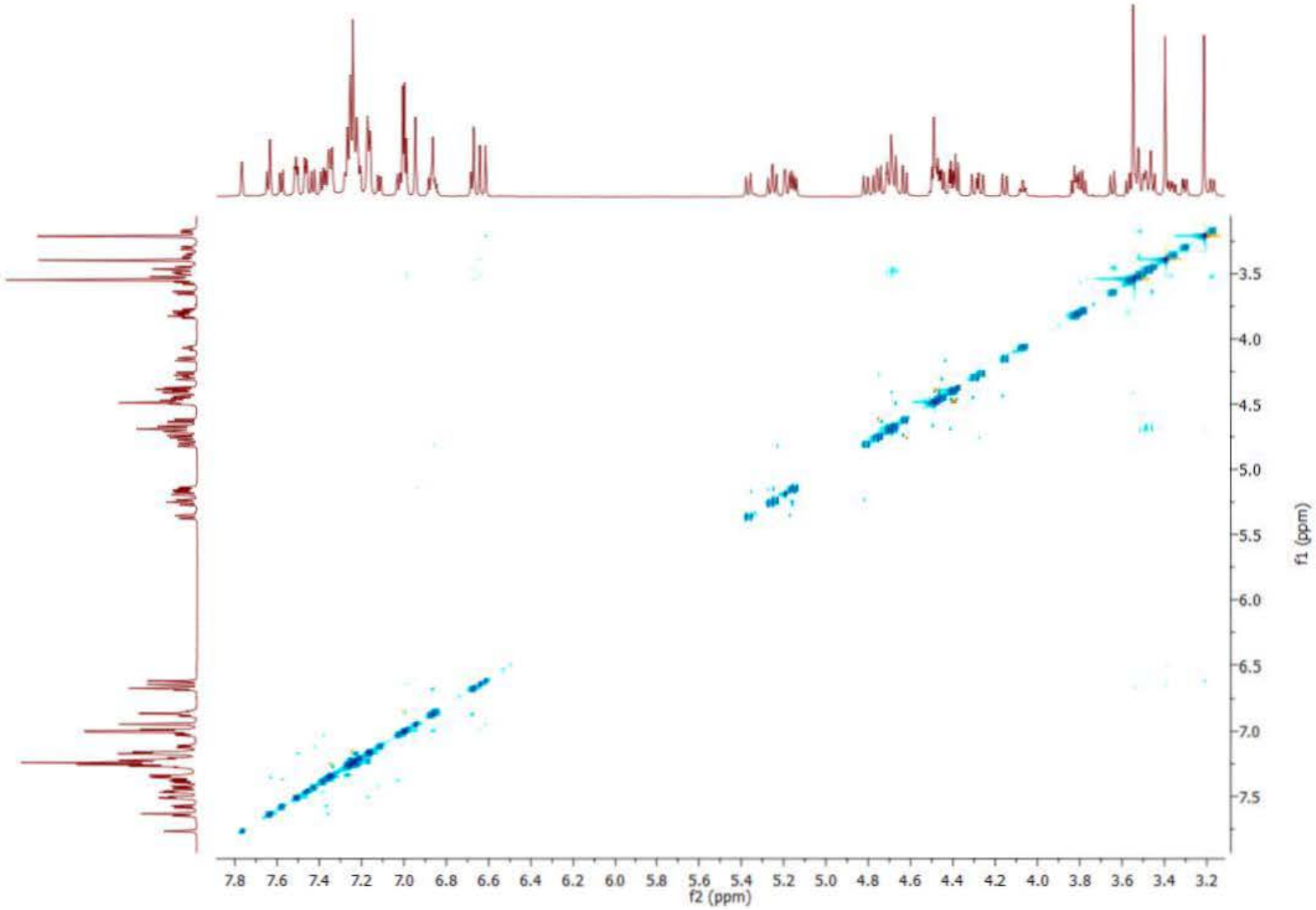

Figure S39. $^{1}H–^{1}H$ NOESY (600 MHz, $CDCl_3$) spectrum of compound ***P*-5a.**

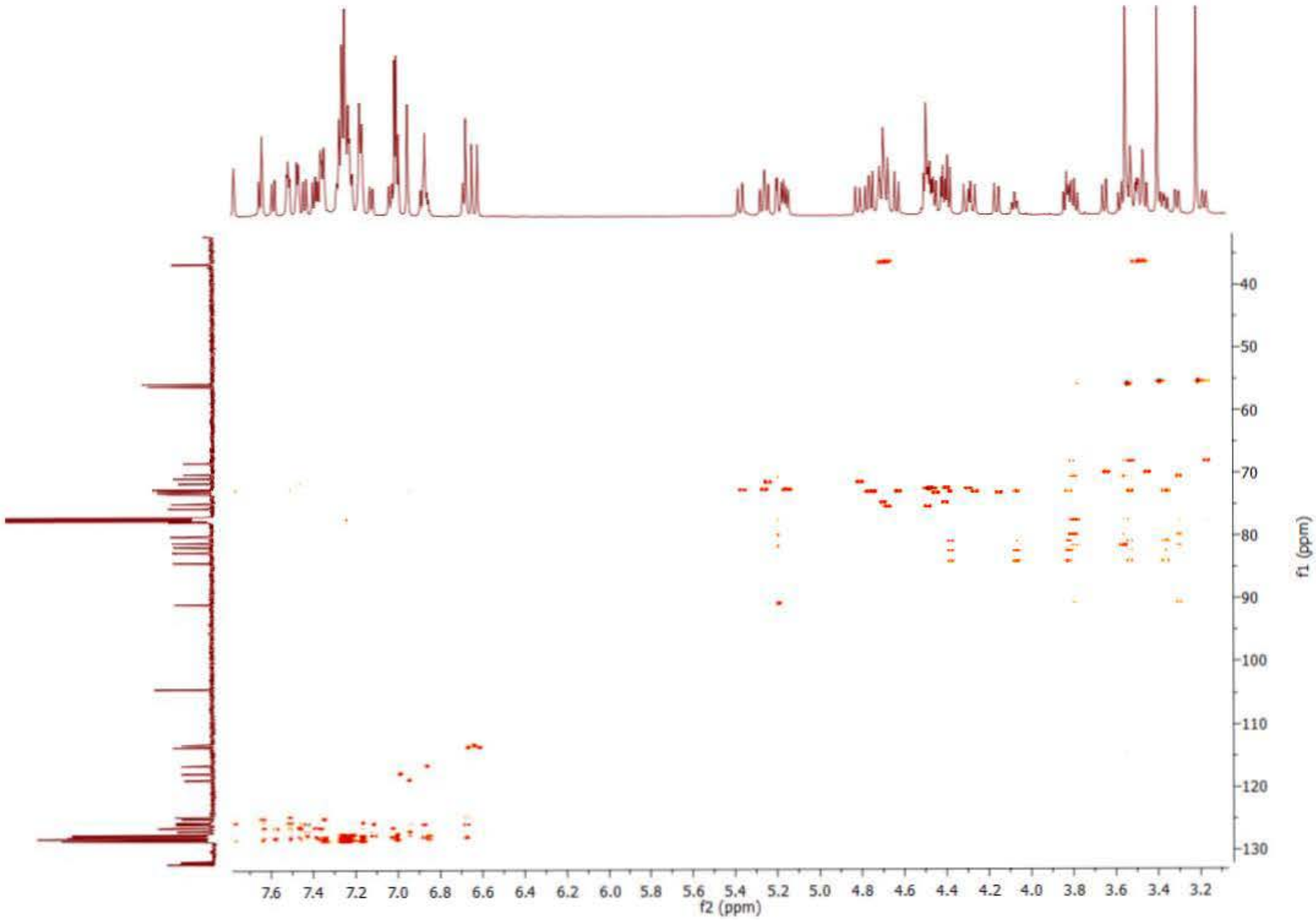

Figure S40. $^{1}H–^{13}C$ HSQC-TOCSY (600/150 MHz, $CDCl_3$) spectrum of compound ***P*-5a.**

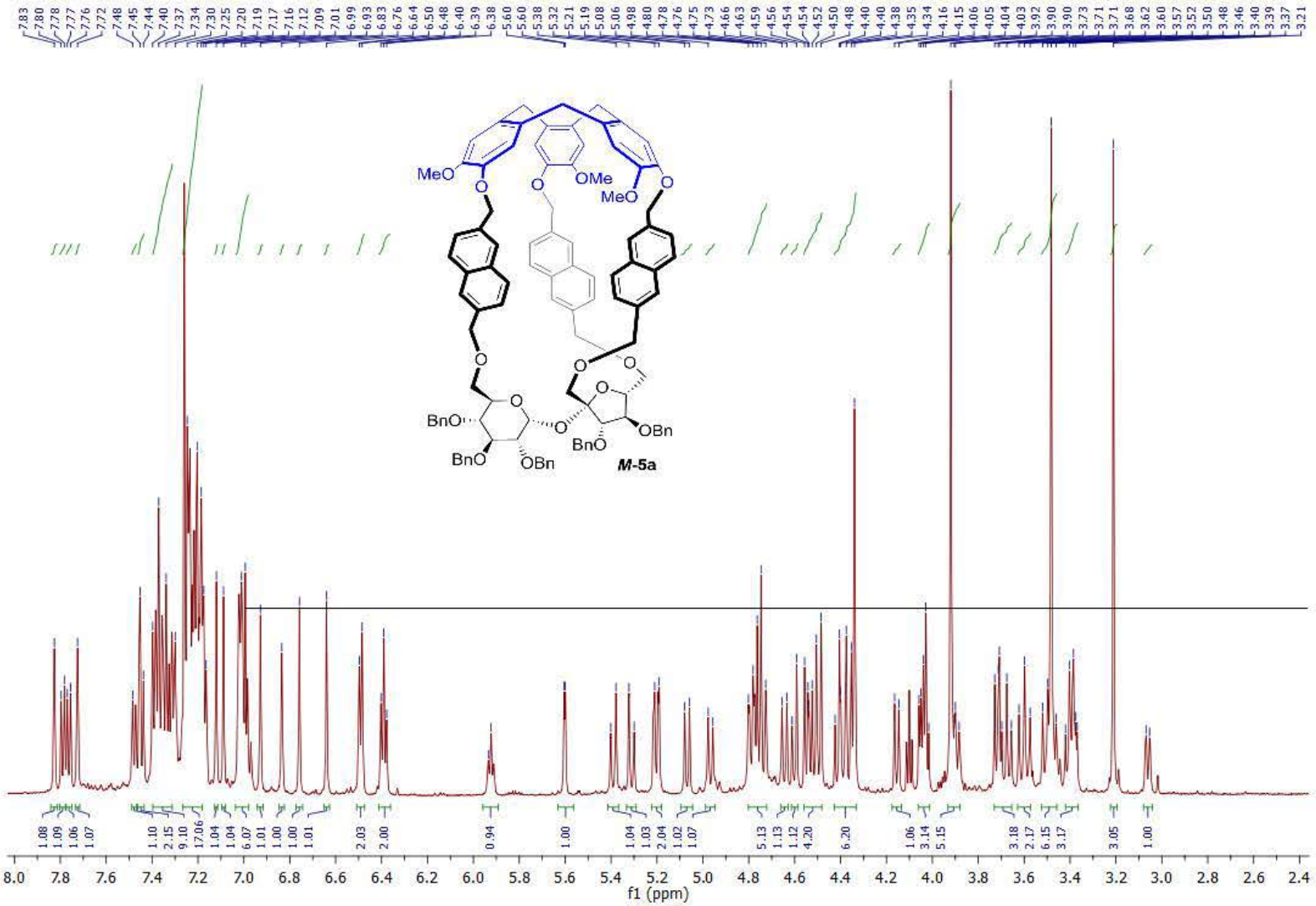

Figure S41. ^{1}H NMR (600 MHz, $CDCl_3$) spectrum of compound ***M*-5a.**

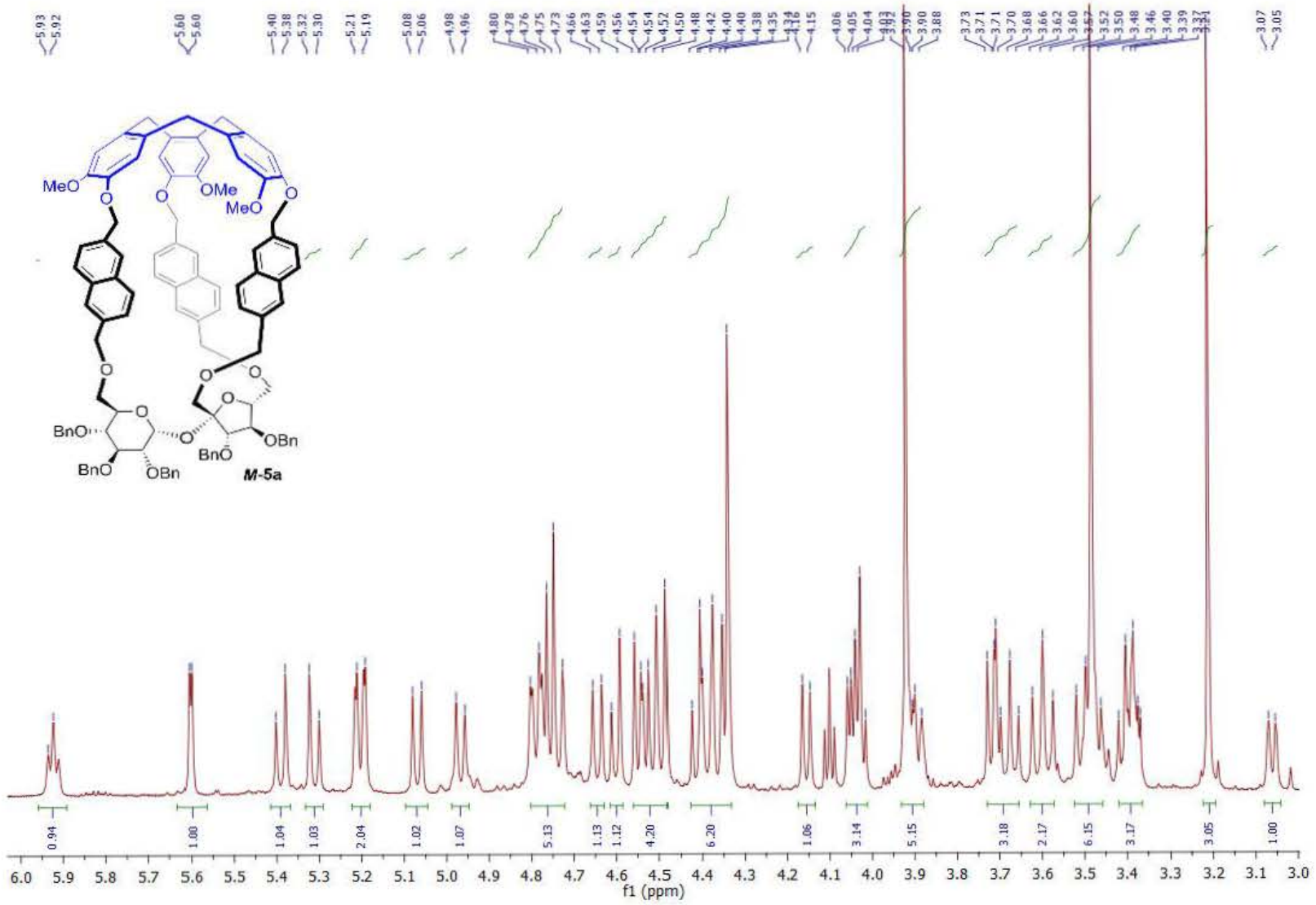

Figure S42. ^{1}H NMR (600 MHz, $CDCl_3$) spectrum of compound ***M*-5a** (aliphatic part).

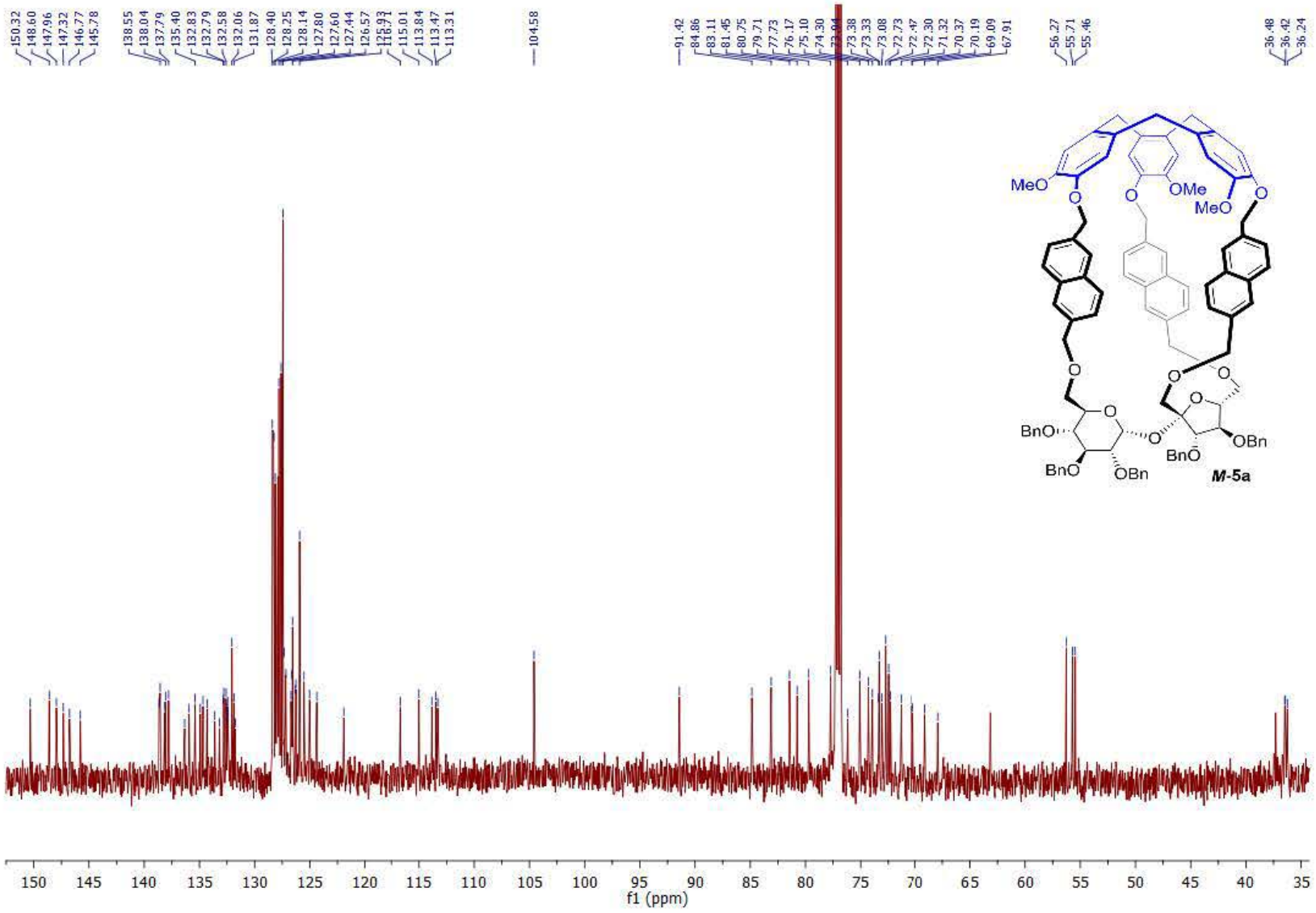

Figure S43. $^{13}C\{^{1}H\}$ NMR (150 MHz, $CDCl_3$) spectrum of compound ***M*-5a.**

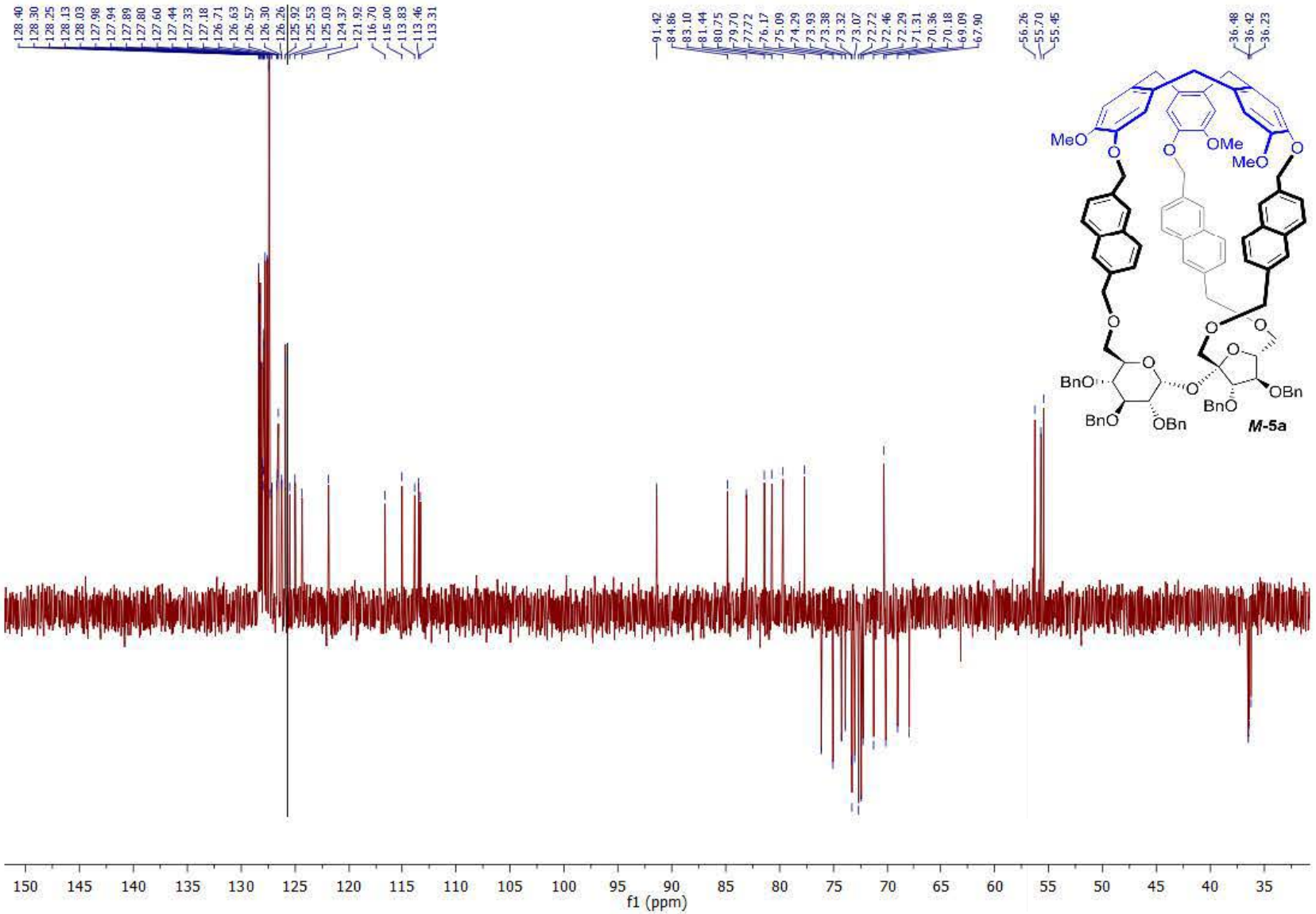

Figure S44. $^{13}C\{^{1}H\}$ DEPT (150 MHz, $CDCl_3$) spectrum of compound ***M*-5a.**

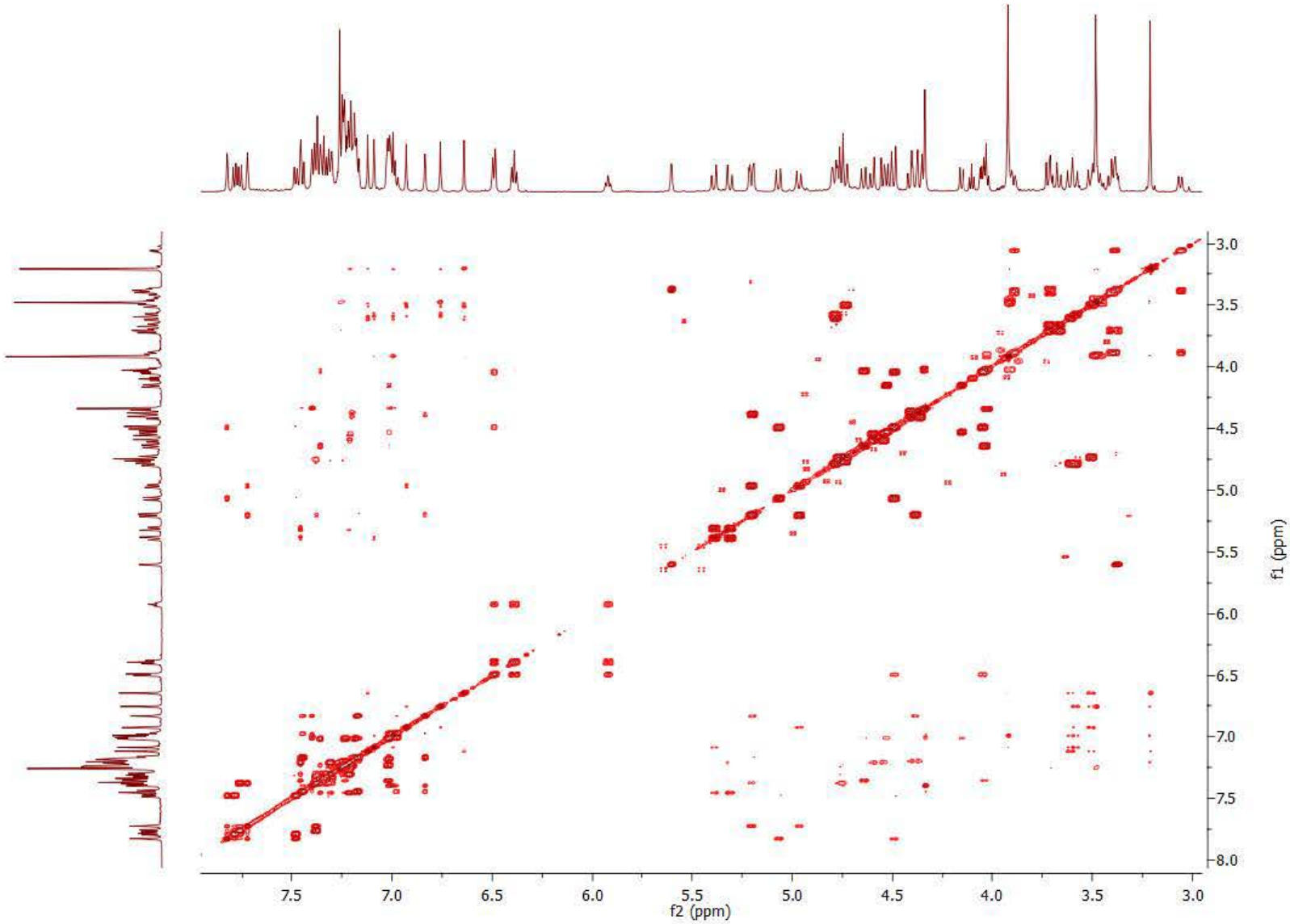

Figure S45. ^{1}H–^{1}H COSY (600 MHz, $CDCl_3$) spectrum of compound ***M*-5a.**

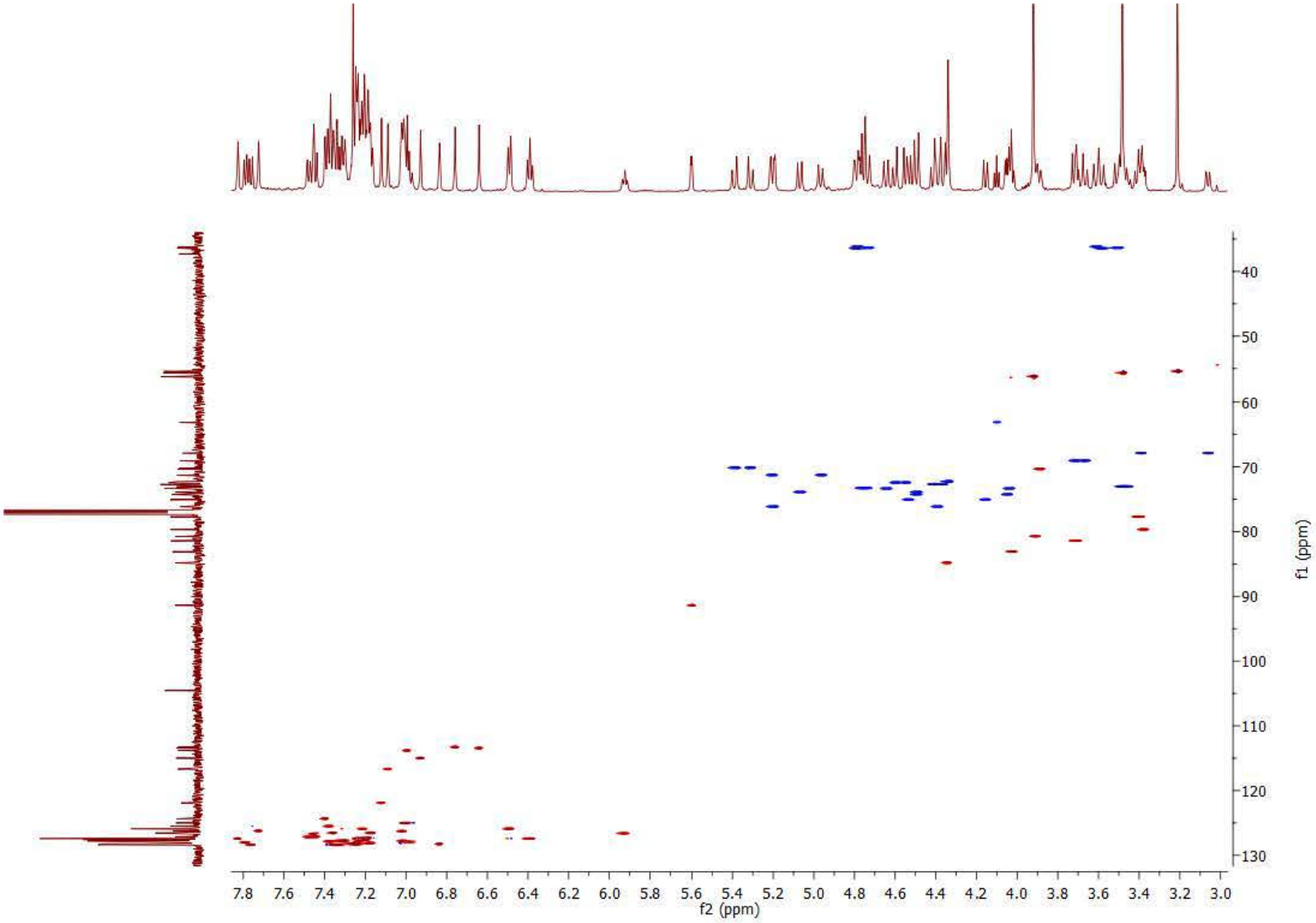

Figure S46. $^{1}H–^{13}C$ HSQC (600/150 MHz, $CDCl_3$) spectrum of compound ***M*-5a**.

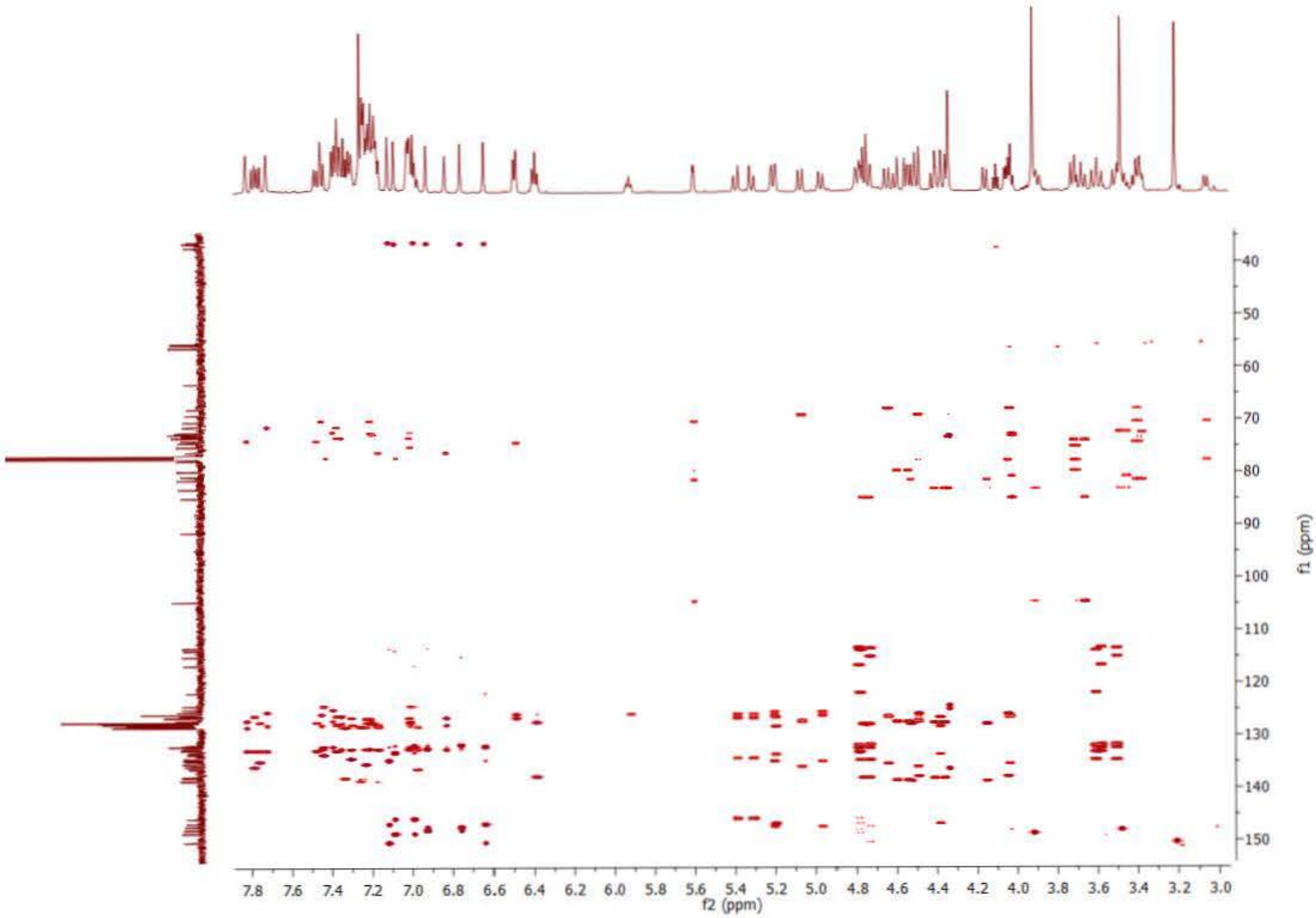

Figure S47. $^{1}H–^{13}C$ HMBC (600/150 MHz, $CDCl_3$) spectrum of compound ***M*-5a.**

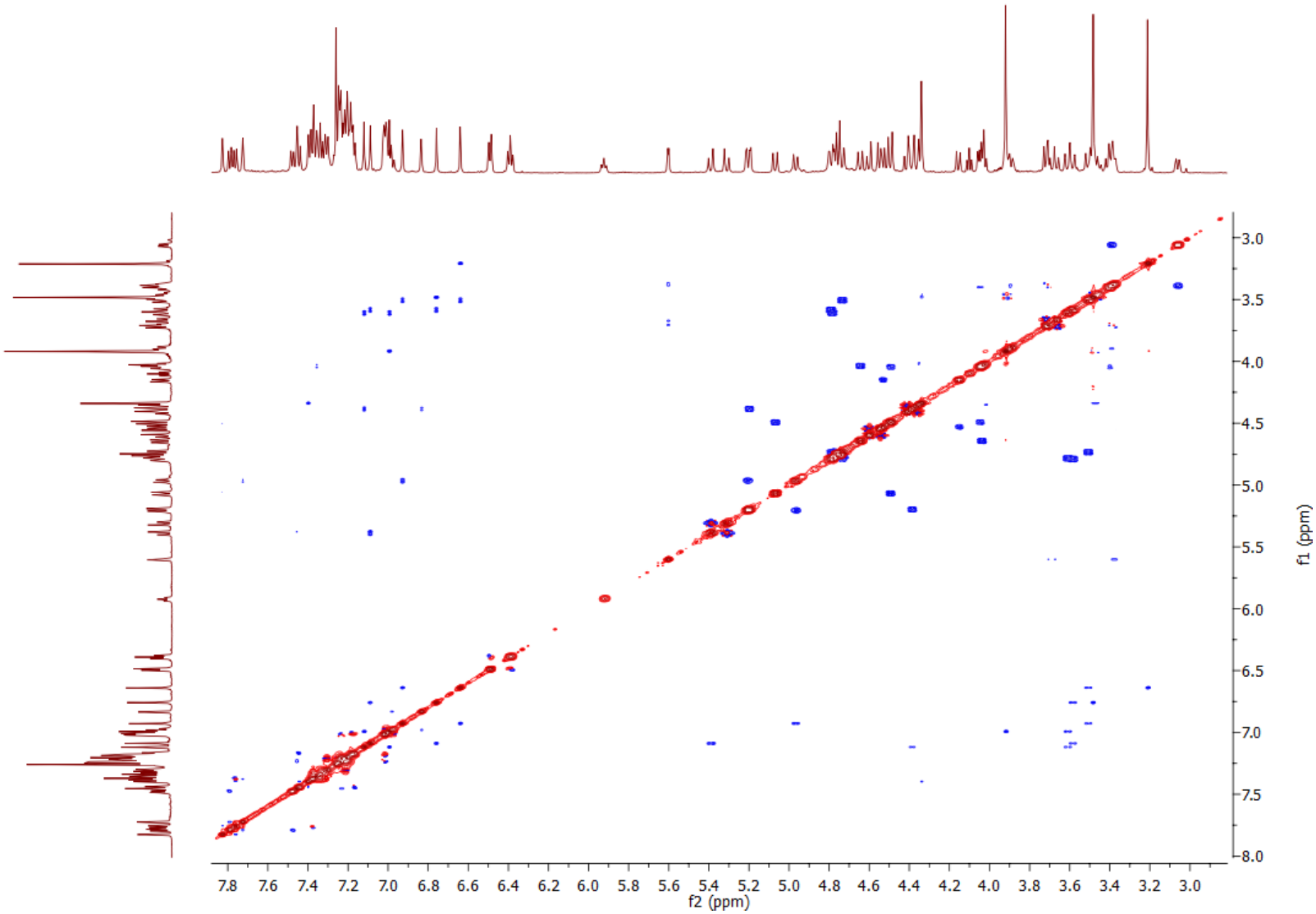

Figure S48. $^{1}H–^{1}H$ ROESY (600 MHz, $CDCl_3$) spectrum of compound ***M*-5a.**

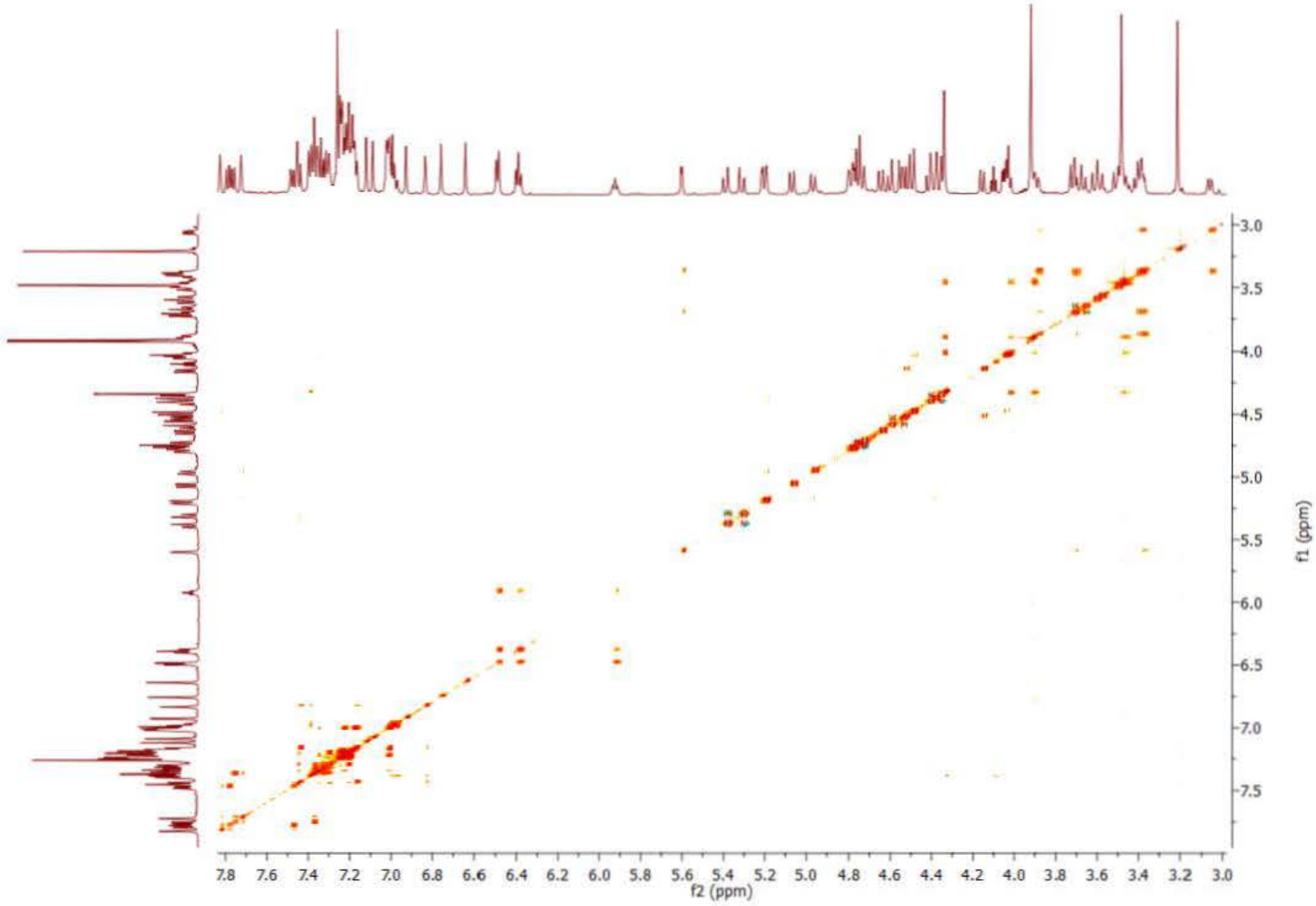

Figure S49. $^{1}H–^{1}H$ TOCSY (600 MHz, $CDCl_3$) spectrum of compound ***M*-5a.**

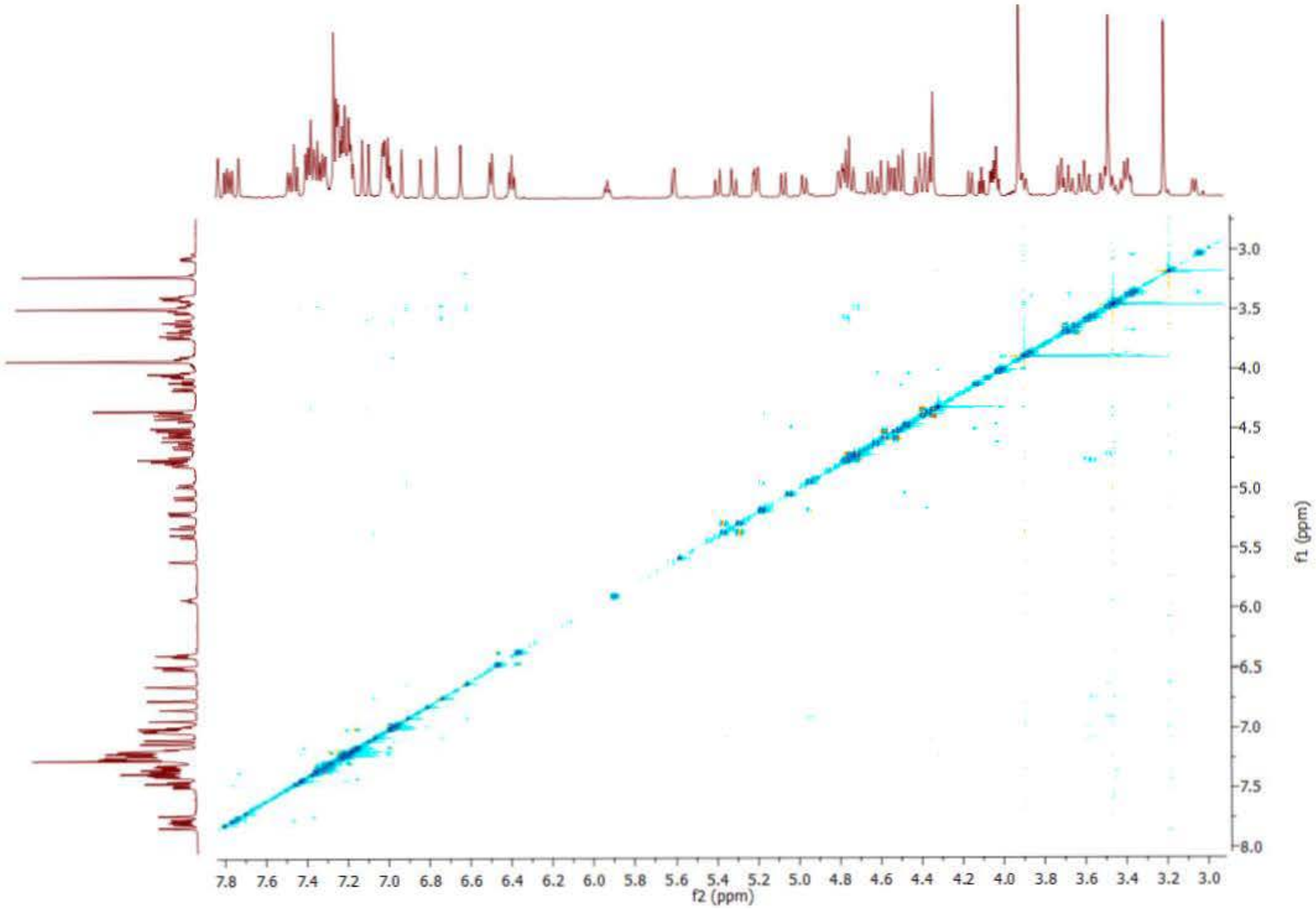

Figure S50. $^{1}H–^{1}H$ NOESY (600 MHz, $CDCl_3$) spectrum of compound ***M*-5a.**

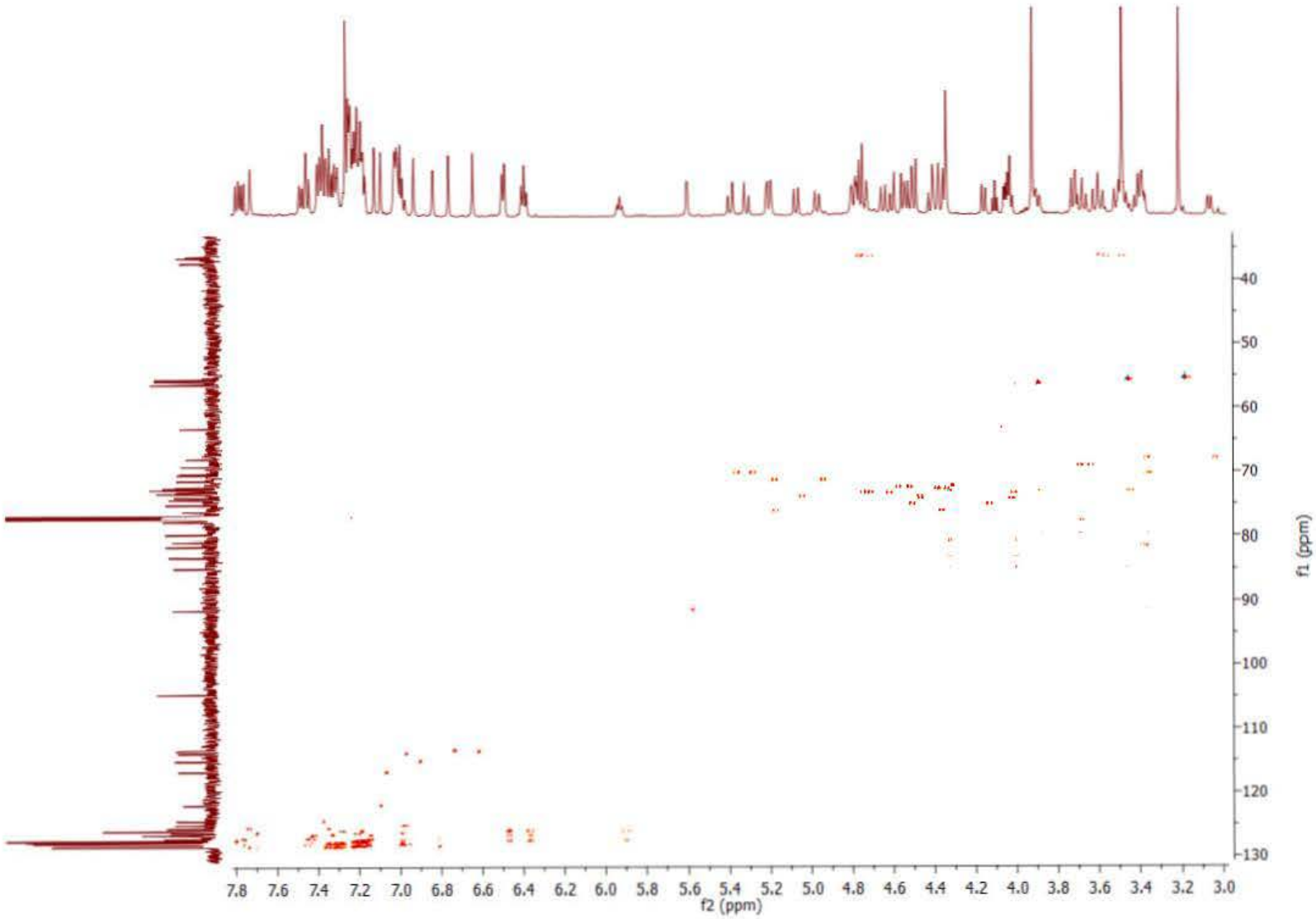

Figure S51. ^{1}H–^{13}C HSQC-TOCSY (600/150 MHz, $CDCl_3$) spectrum of compound ***M*-5a.**

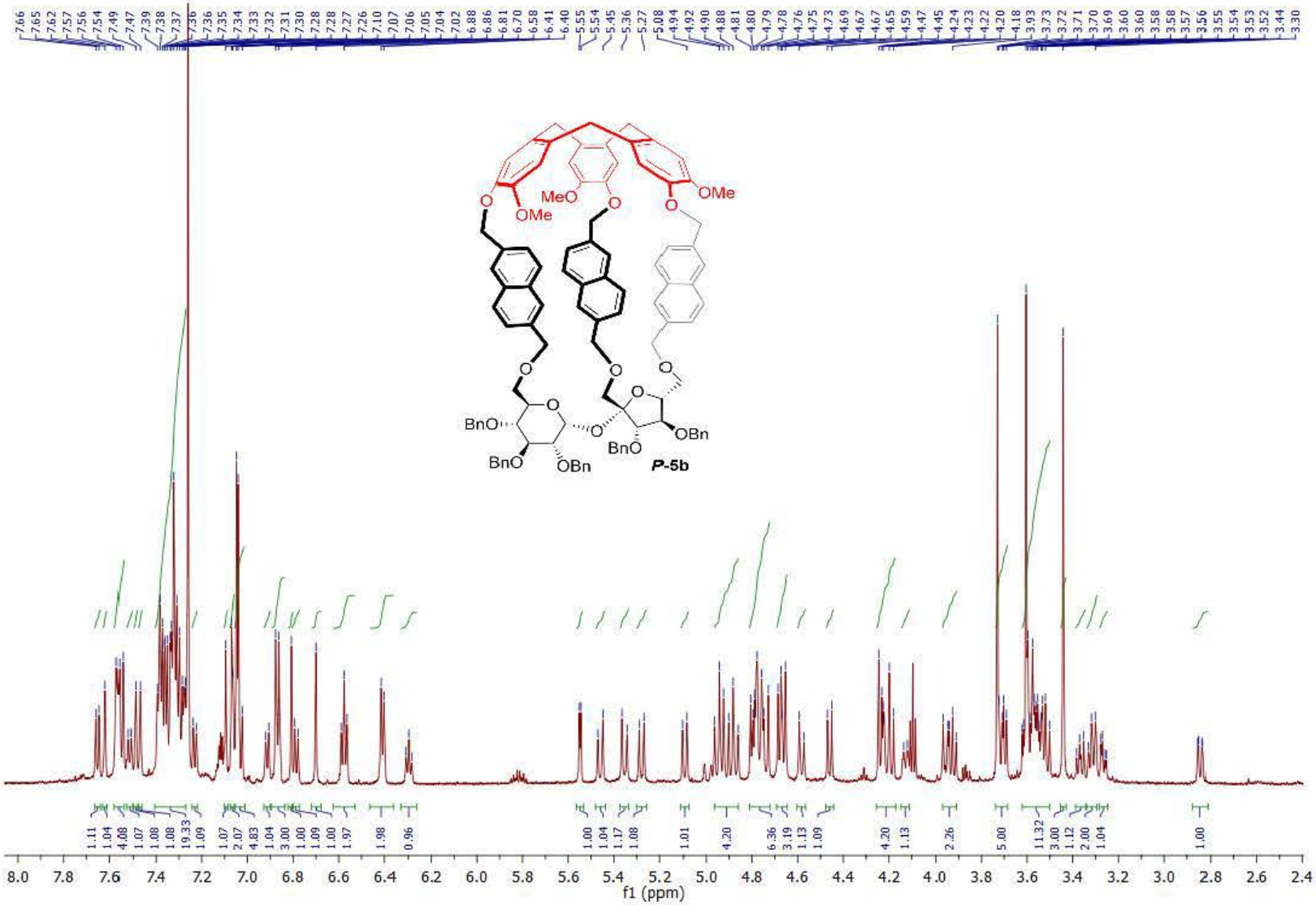

Figure S52. ^{1}H NMR (600 MHz, $CDCl_3$) spectrum of compound ***P*-5b.**

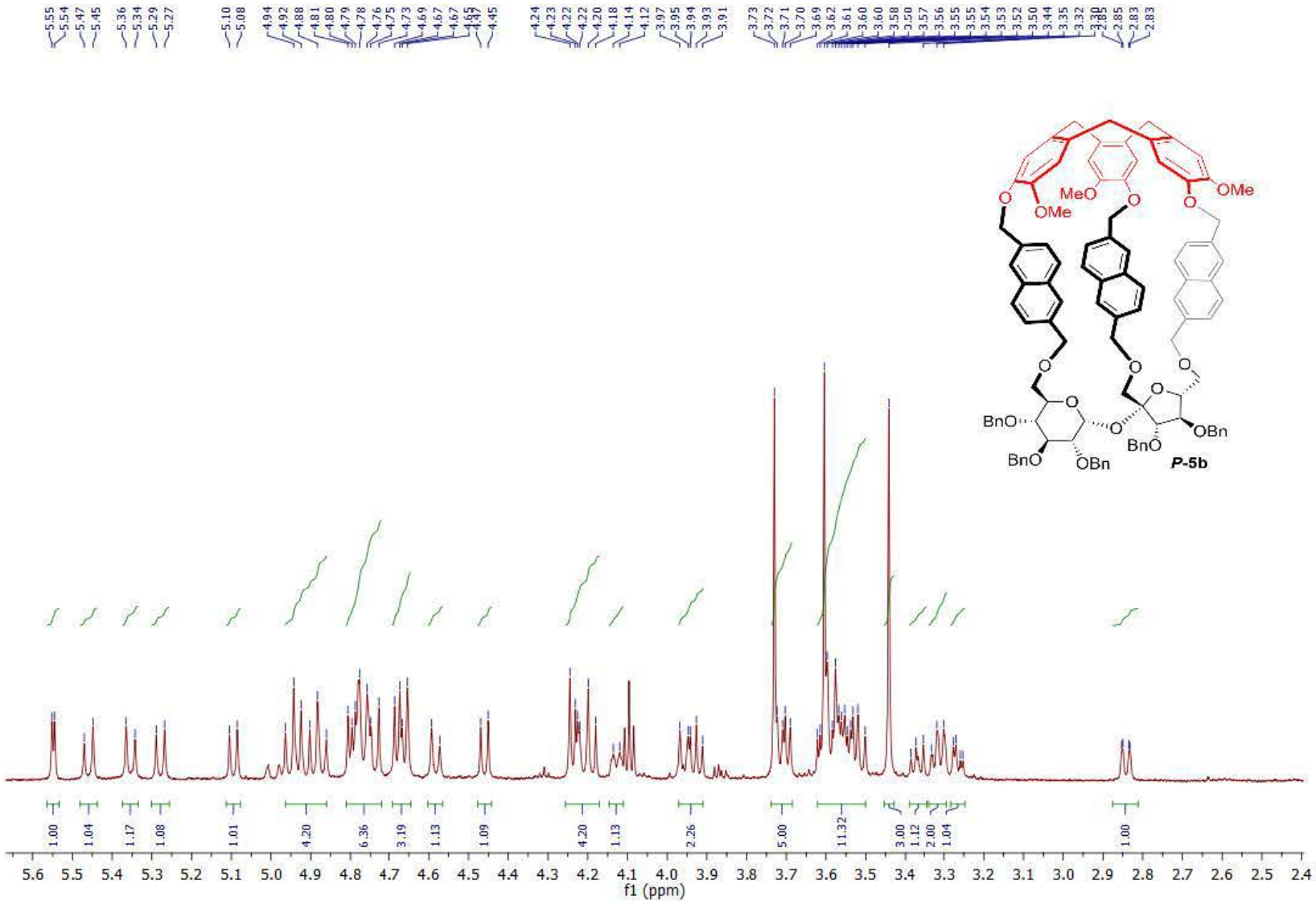

Figure S53. ^{1}H NMR (600 MHz, $CDCl_3$) spectrum of compound ***P*-5b** (aliphatic part).

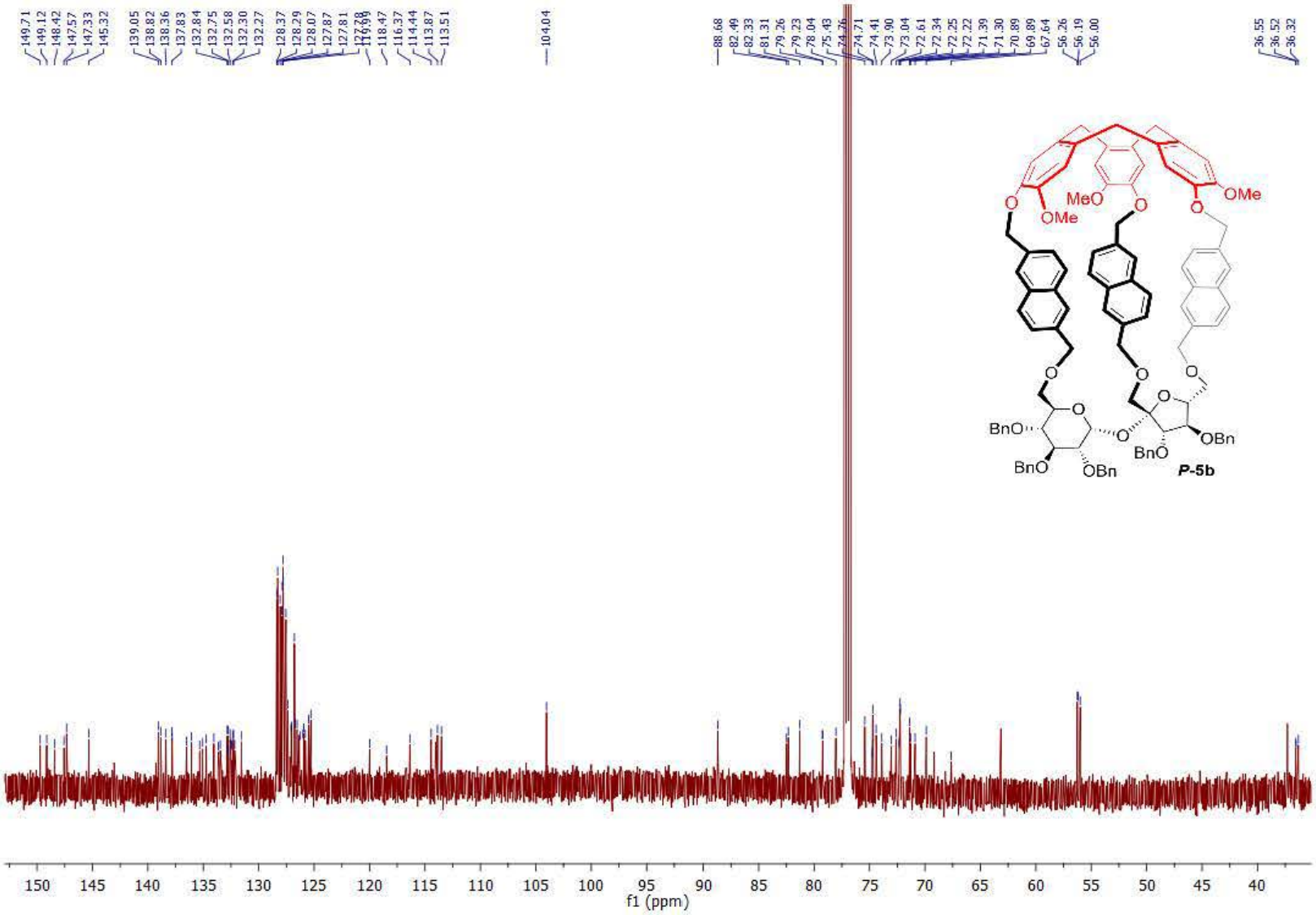

Figure S54. $^{13}C\{^{1}H\}$ NMR (150 MHz, $CDCl_3$) spectrum of compound ***P*-5b.**

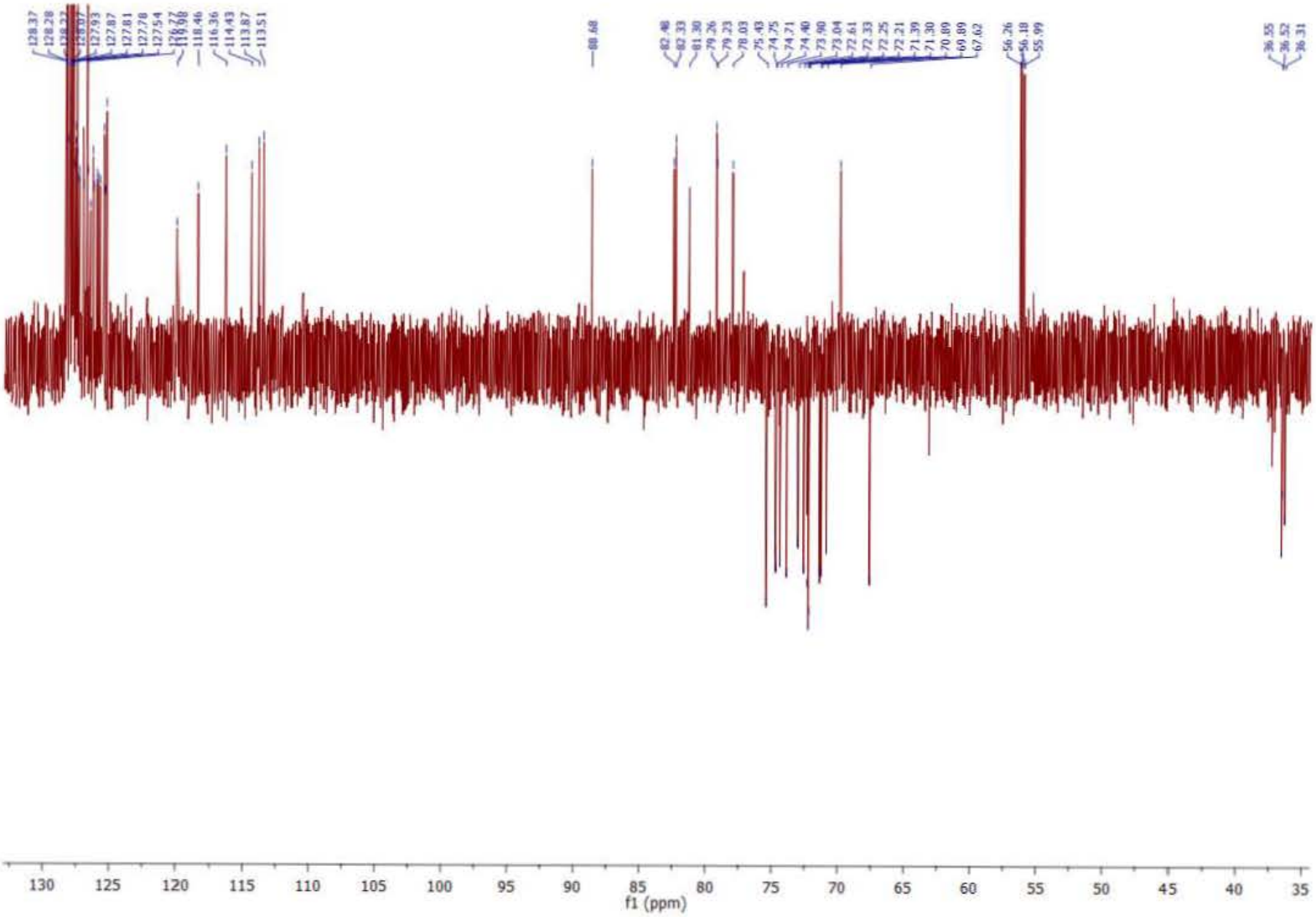

Figure S55. $^{13}C\{^{1}H\}$ DEPT (150 MHz, $CDCl_3$) spectrum of compound ***P*-5b.**

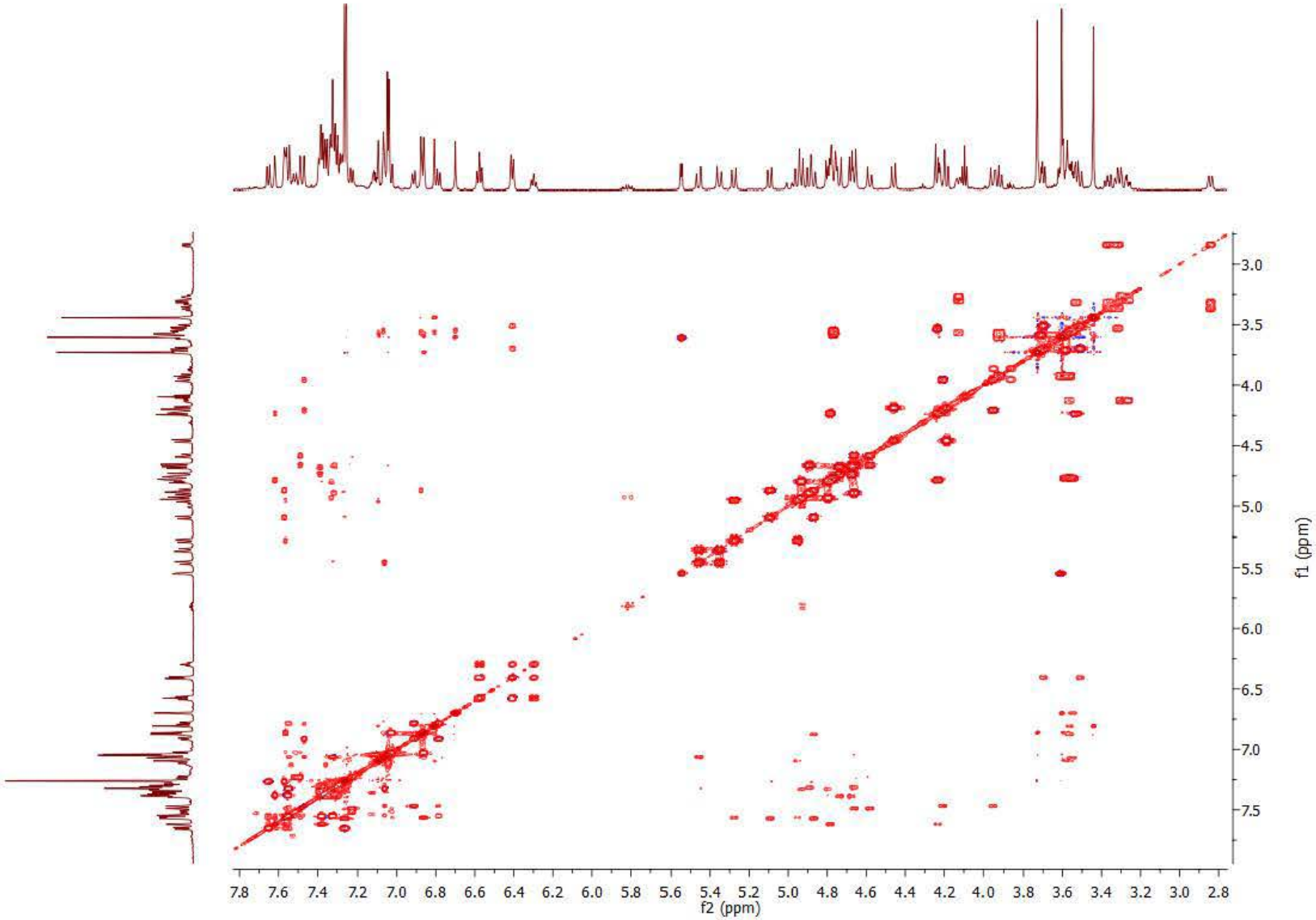

Figure S56. ^{1}H–^{1}H COSY (600 MHz, $CDCl_3$) spectrum of compound ***P*-5b**.

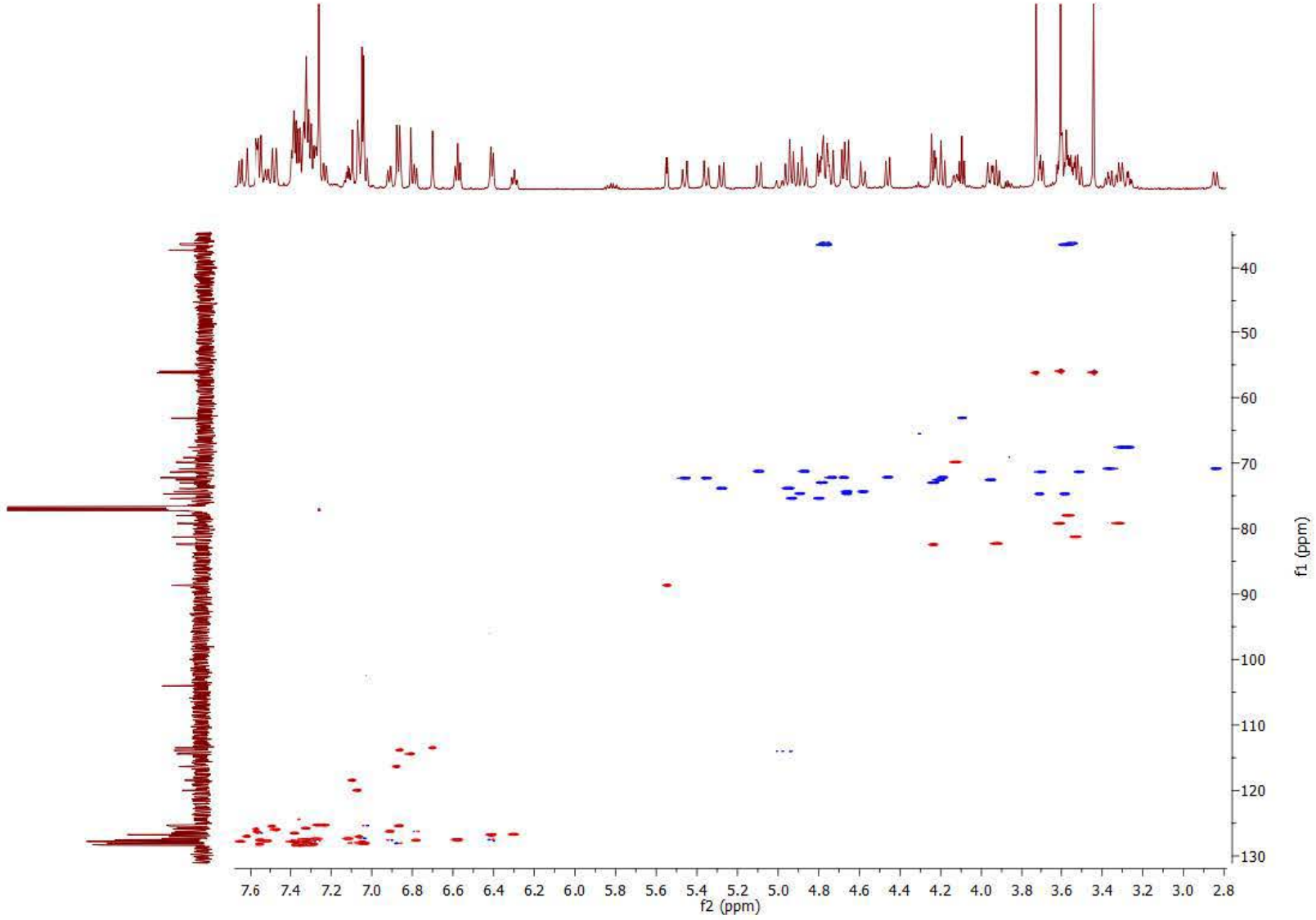

Figure S57. $^{1}H–^{13}C$ HSQC (600/150 MHz, $CDCl_3$) spectrum of compound ***P*-5b**.

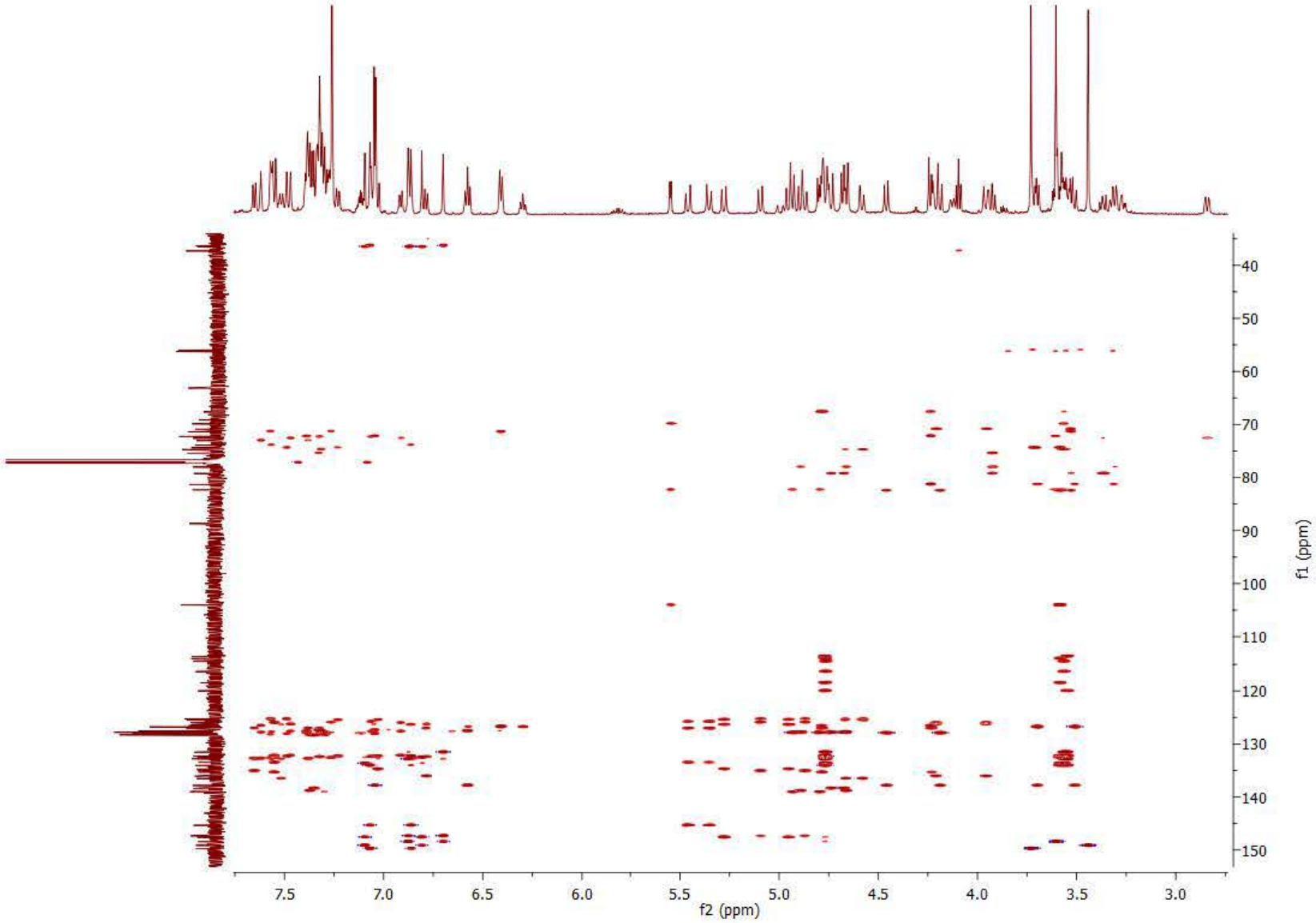

Figure S58. $^{1}H–^{13}C$ HMBC (600/150 MHz, $CDCl_3$) spectrum of compound ***P*-5b.**

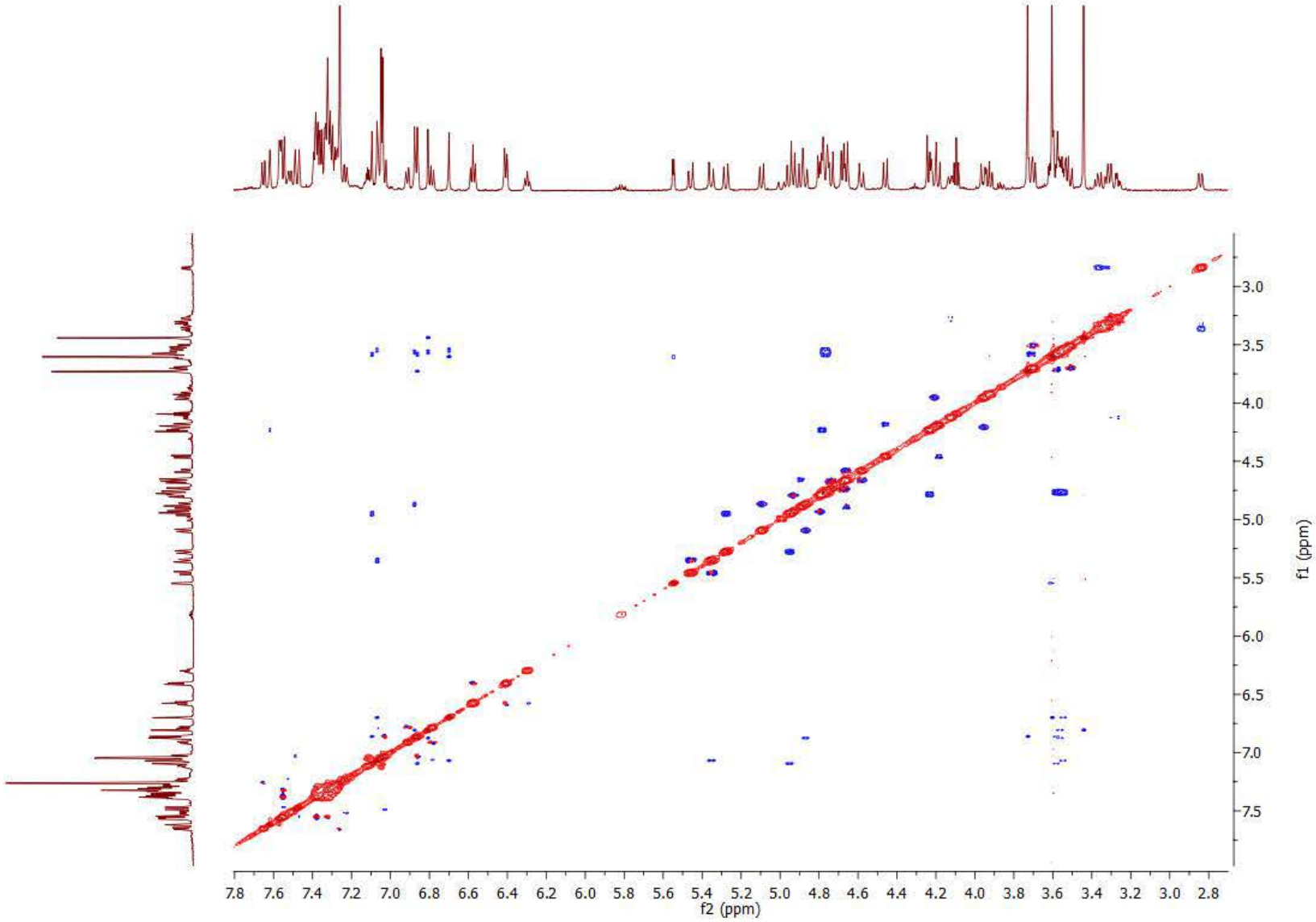

Figure S59. $^{1}H–^{1}H$ ROESY (600 MHz, $CDCl_3$) spectrum of compound ***P*-5b.**

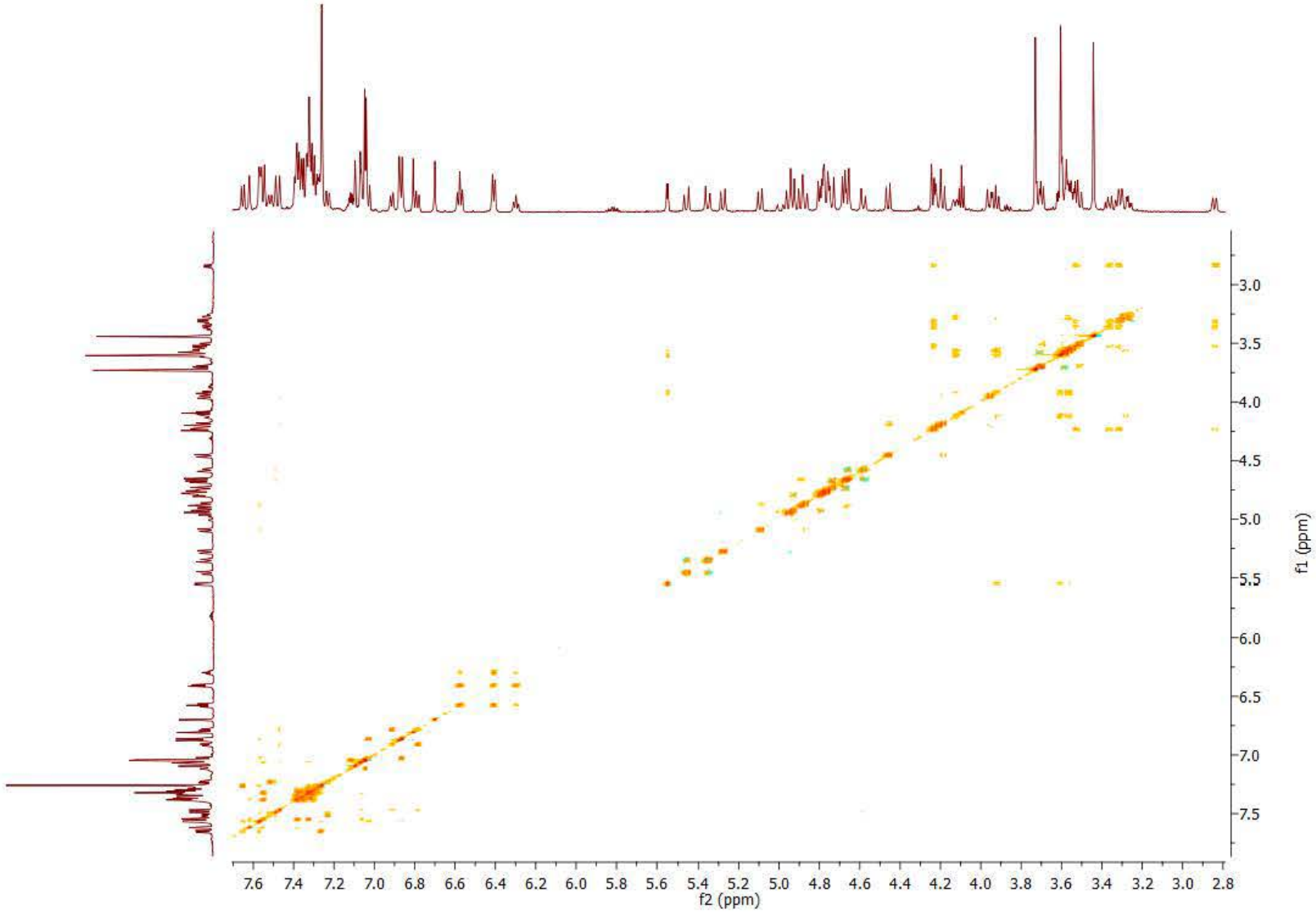

Figure S60. $^{1}H–^{1}H$ TOCSY (600 MHz, $CDCl_3$) spectrum of compound ***P*-5b.**

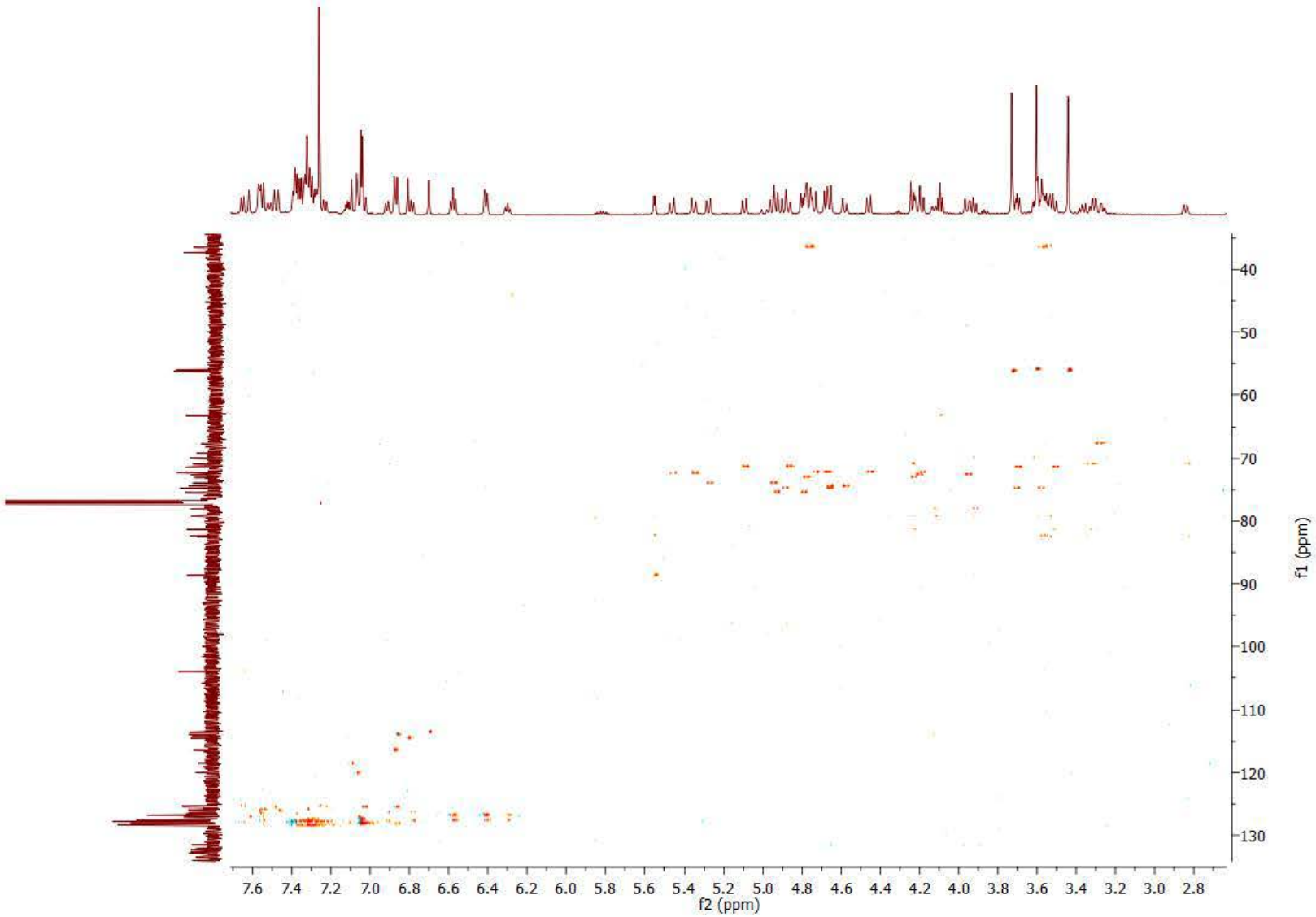

Figure S61. $^{1}H–^{13}C$ HSQC-TOCSY (600/150 MHz, $CDCl_3$) spectrum of compound ***P*-5b.**

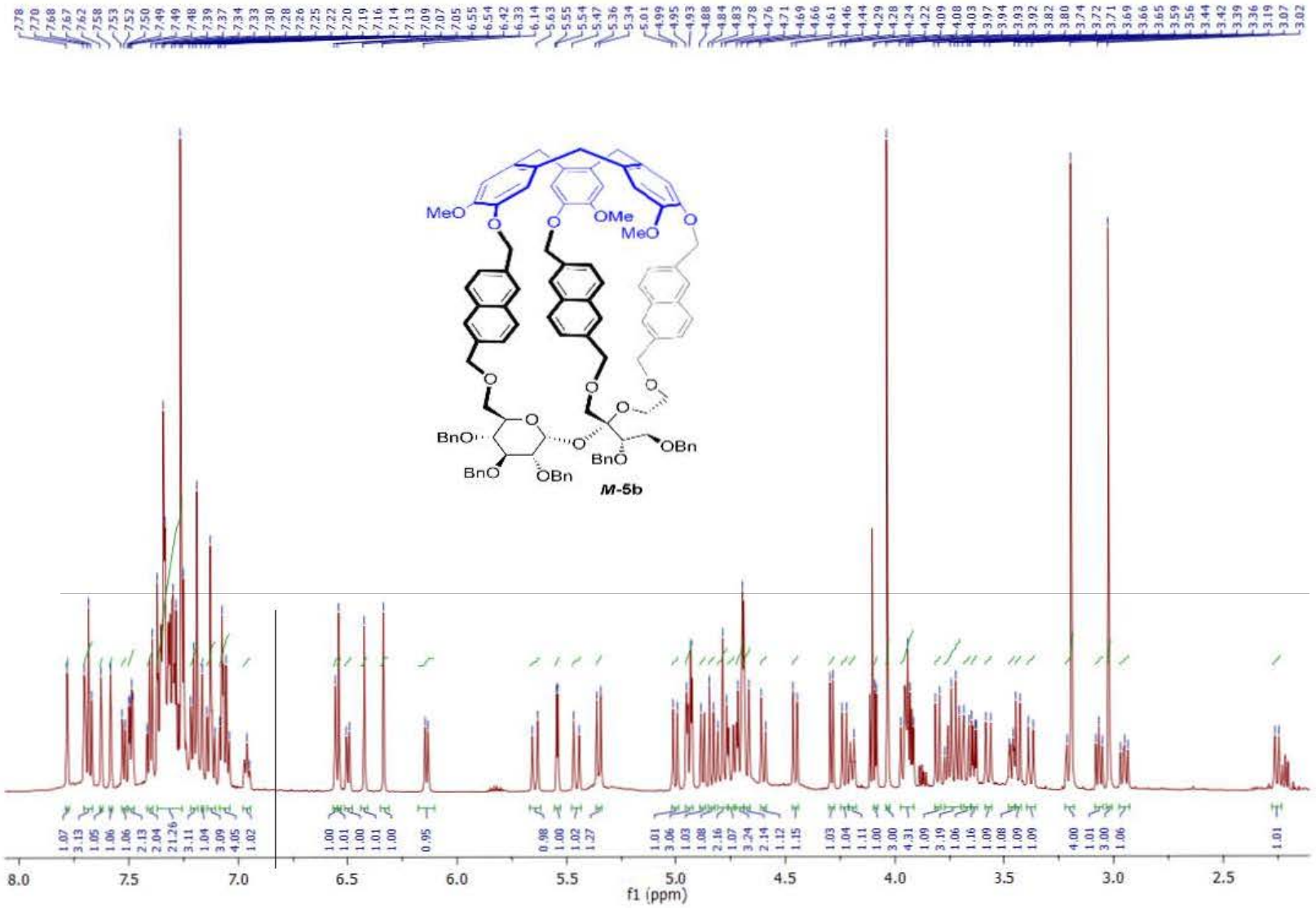

Figure S62. ^{1}H NMR (600 MHz, $CDCl_3$) spectrum of compound ***M*-5b.**

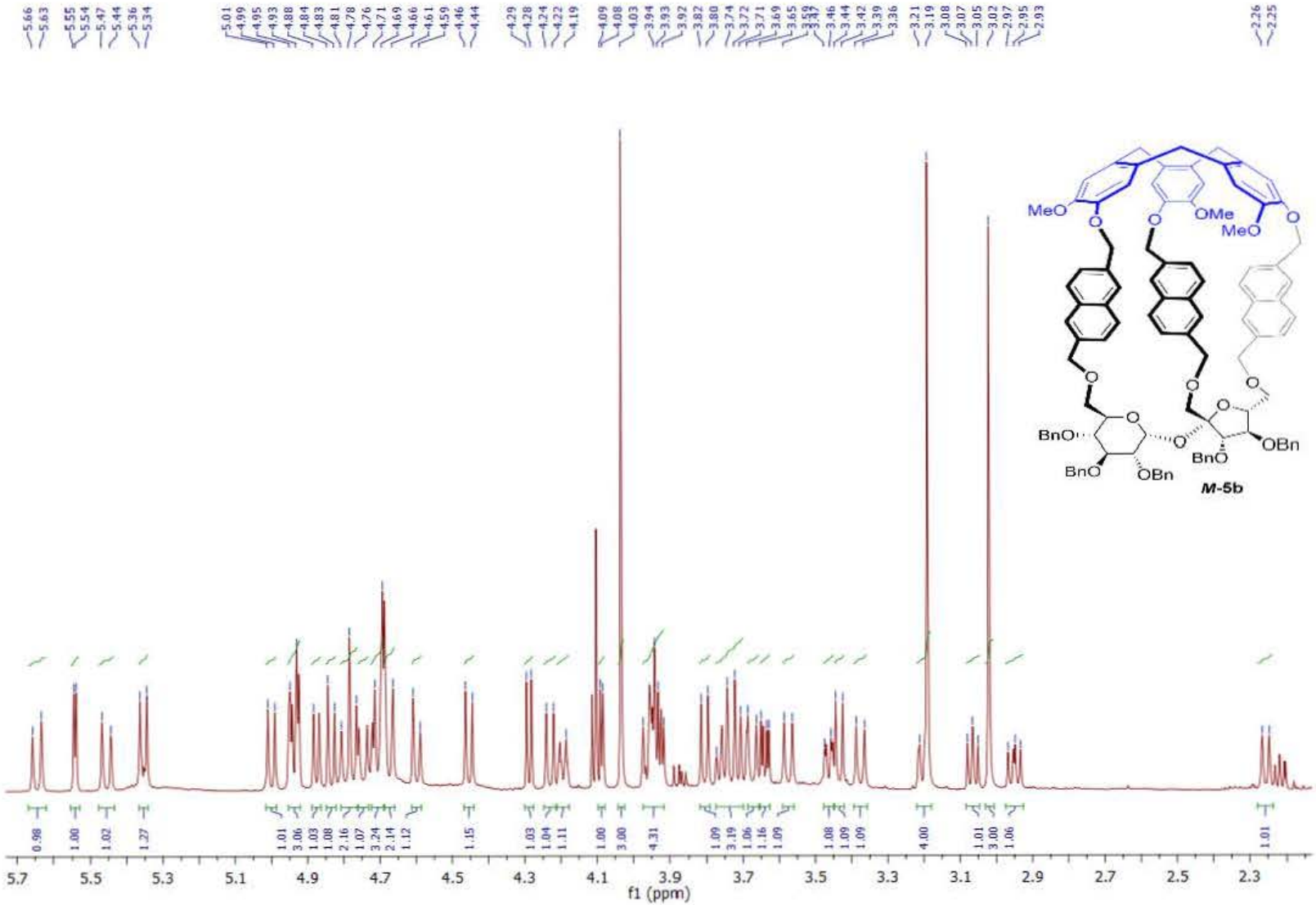

Figure S63. ^{1}H NMR (600 MHz, $CDCl_3$) spectrum of compound ***M*-5b** (aliphatic part).

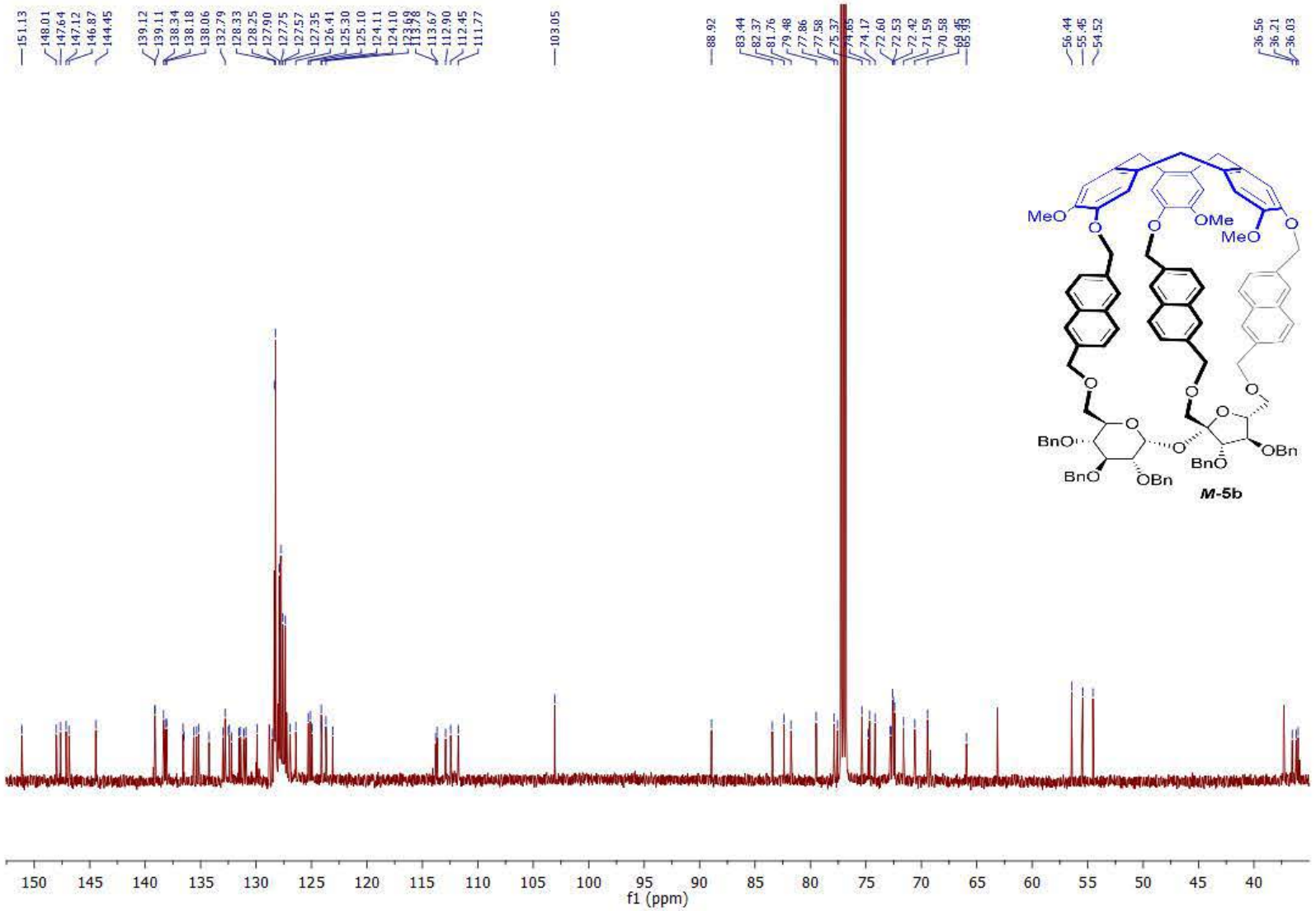

Figure S64. $^{13}C\{^{1}H\}$ NMR (150 MHz, $CDCl_3$) spectrum of compound ***M*-5b.**

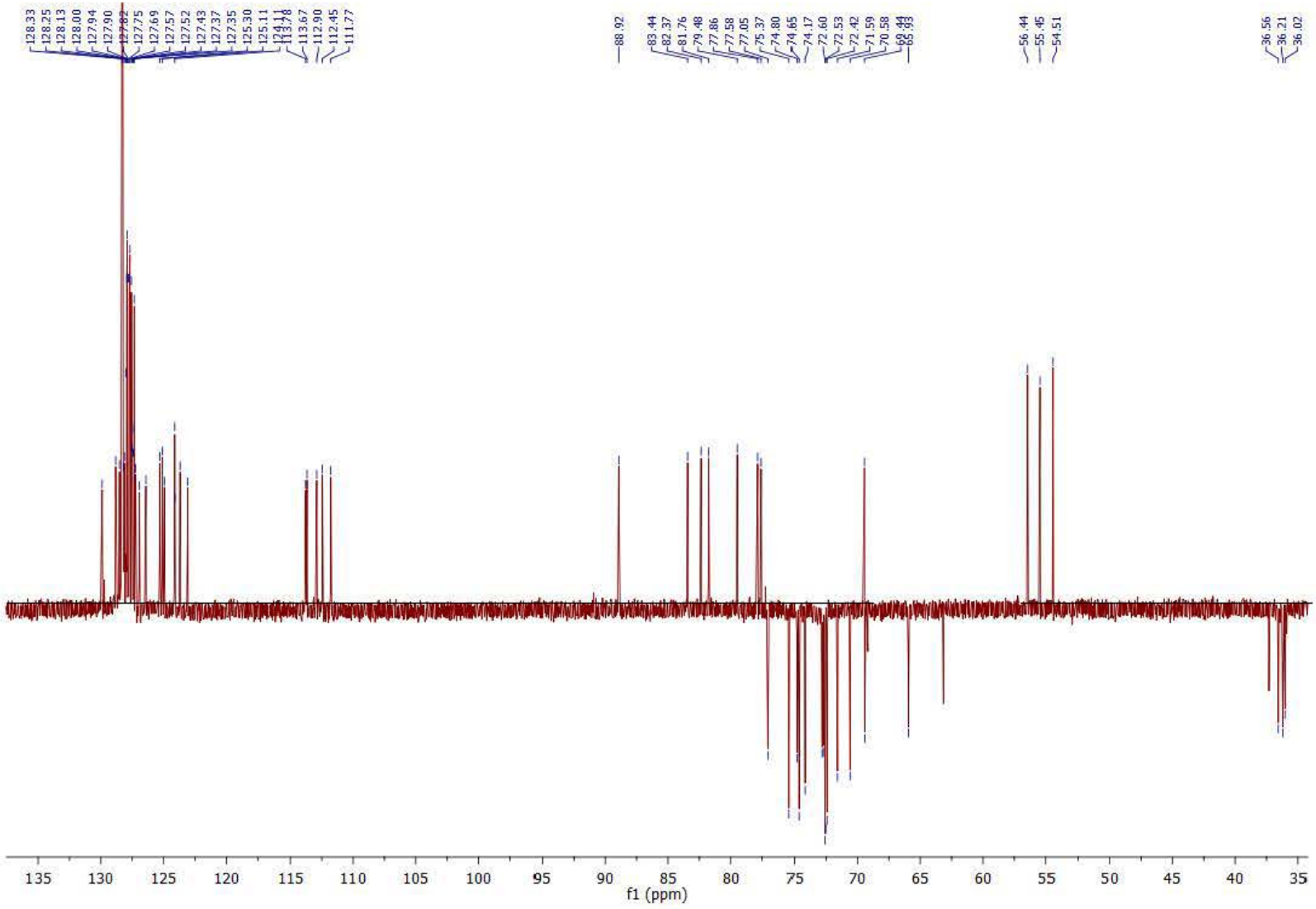

Figure S65. $^{13}C\{^{1}H\}$ DEPT (150 MHz, $CDCl_3$) spectrum of compound ***M*-5b.**

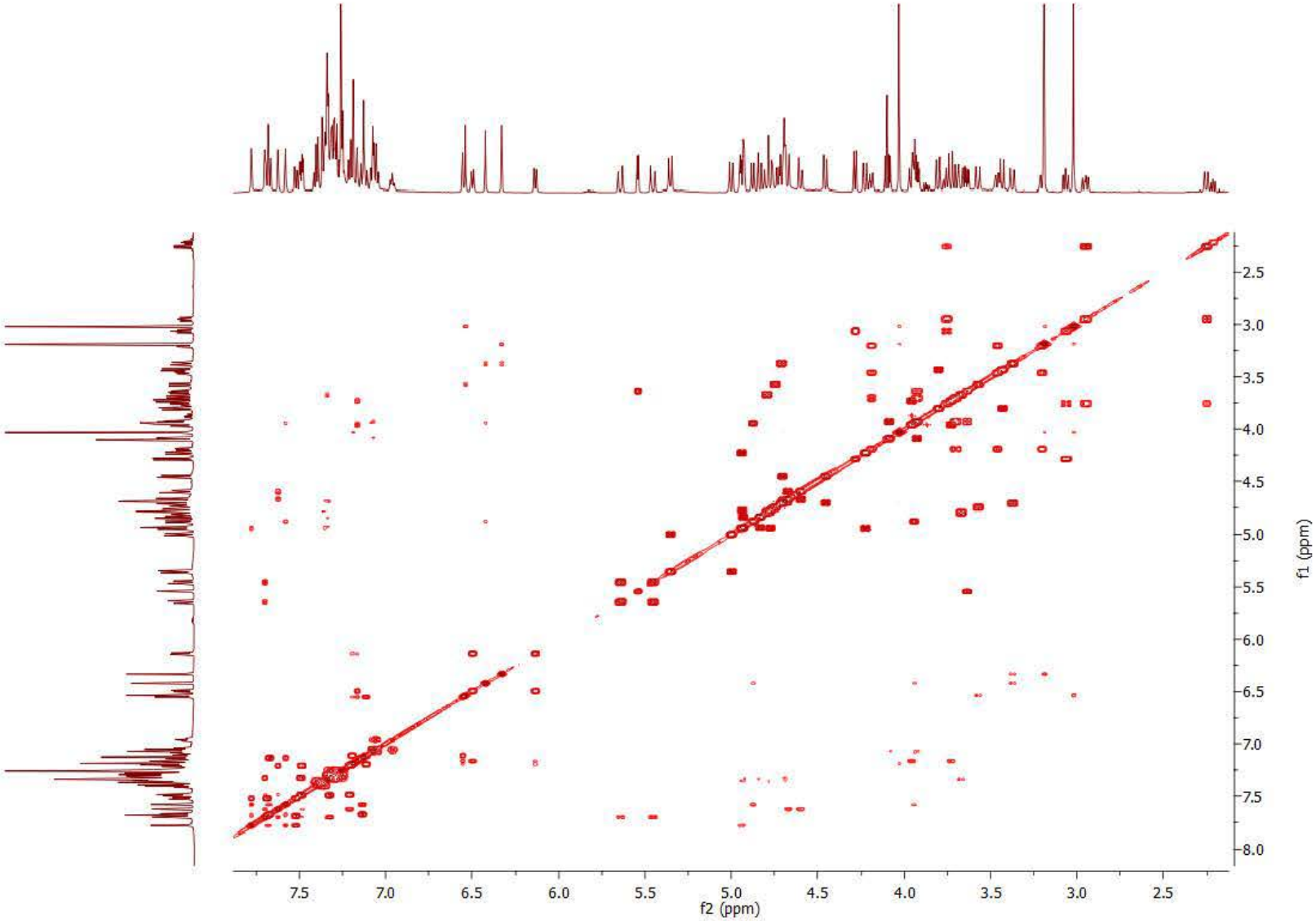

Figure S66. $^{1}H–^{1}H$ COSY (600 MHz, $CDCl_3$) spectrum of compound ***M*-5b**.

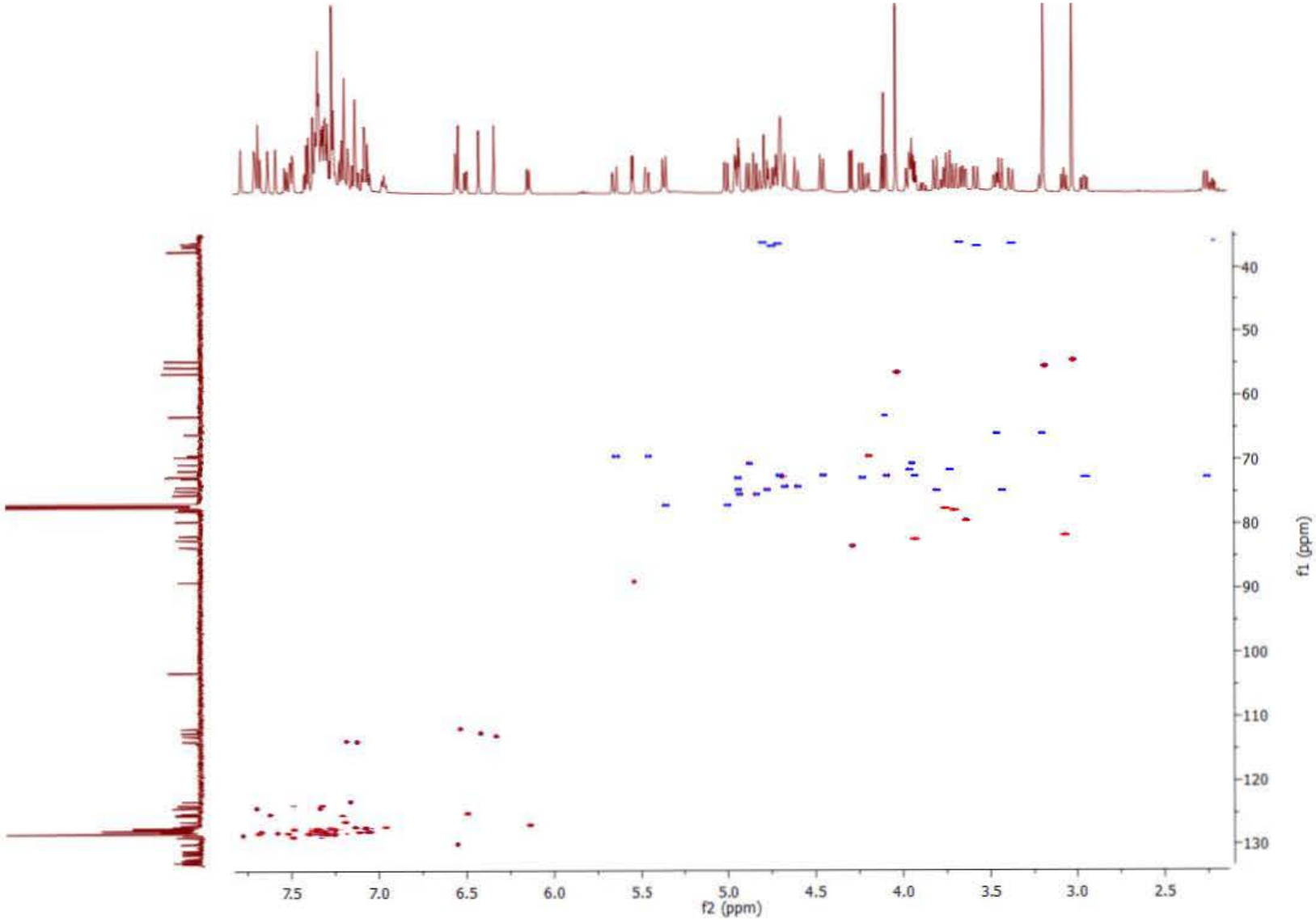

Figure S67. $^{1}H–^{13}C$ HSQC (600/150 MHz, $CDCl_3$) spectrum of compound ***M*-5b**.

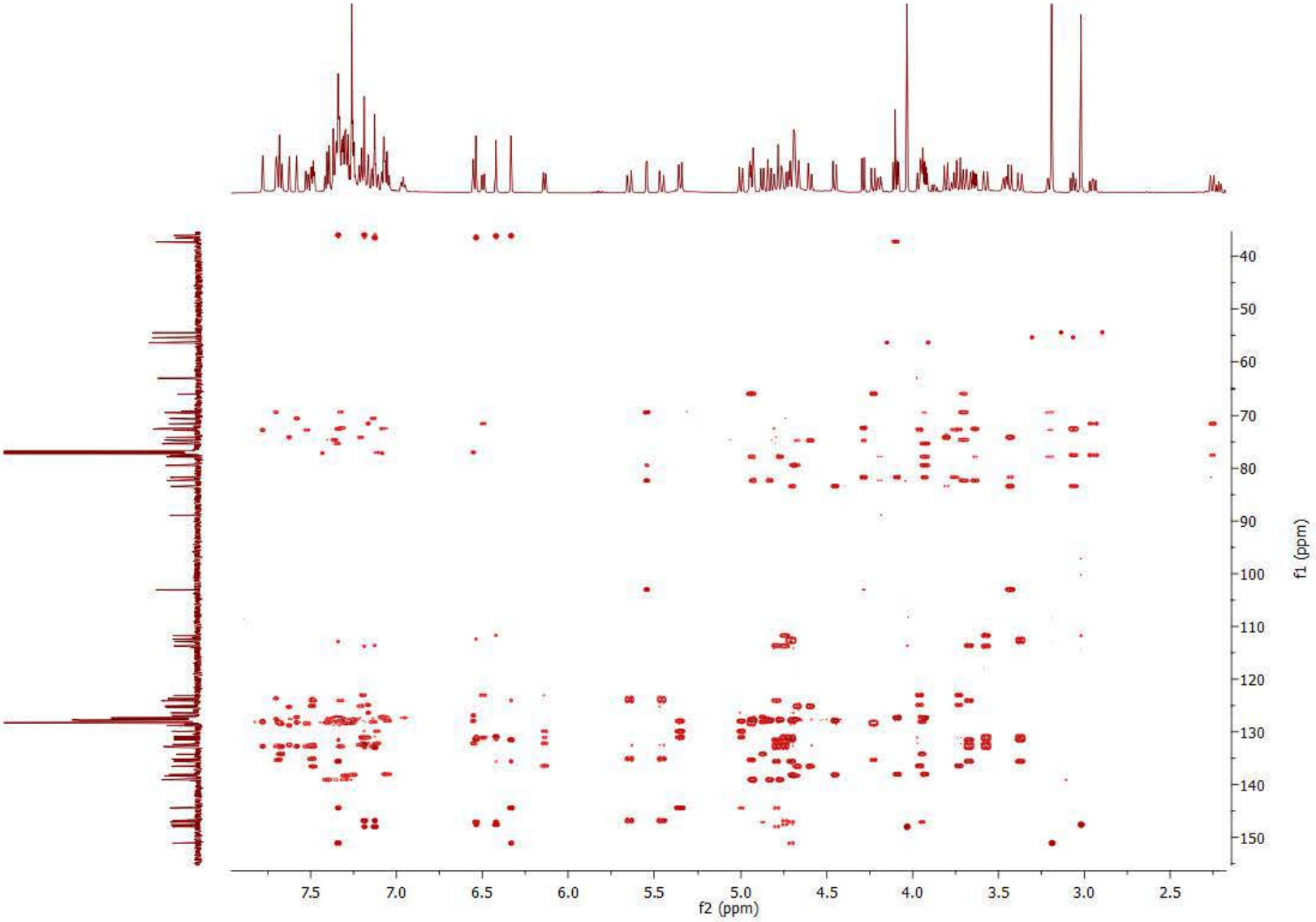

Figure S68. $^{1}H–^{13}C$ HMBC (600/150 MHz, $CDCl_3$) spectrum of compound ***M*-5b.**

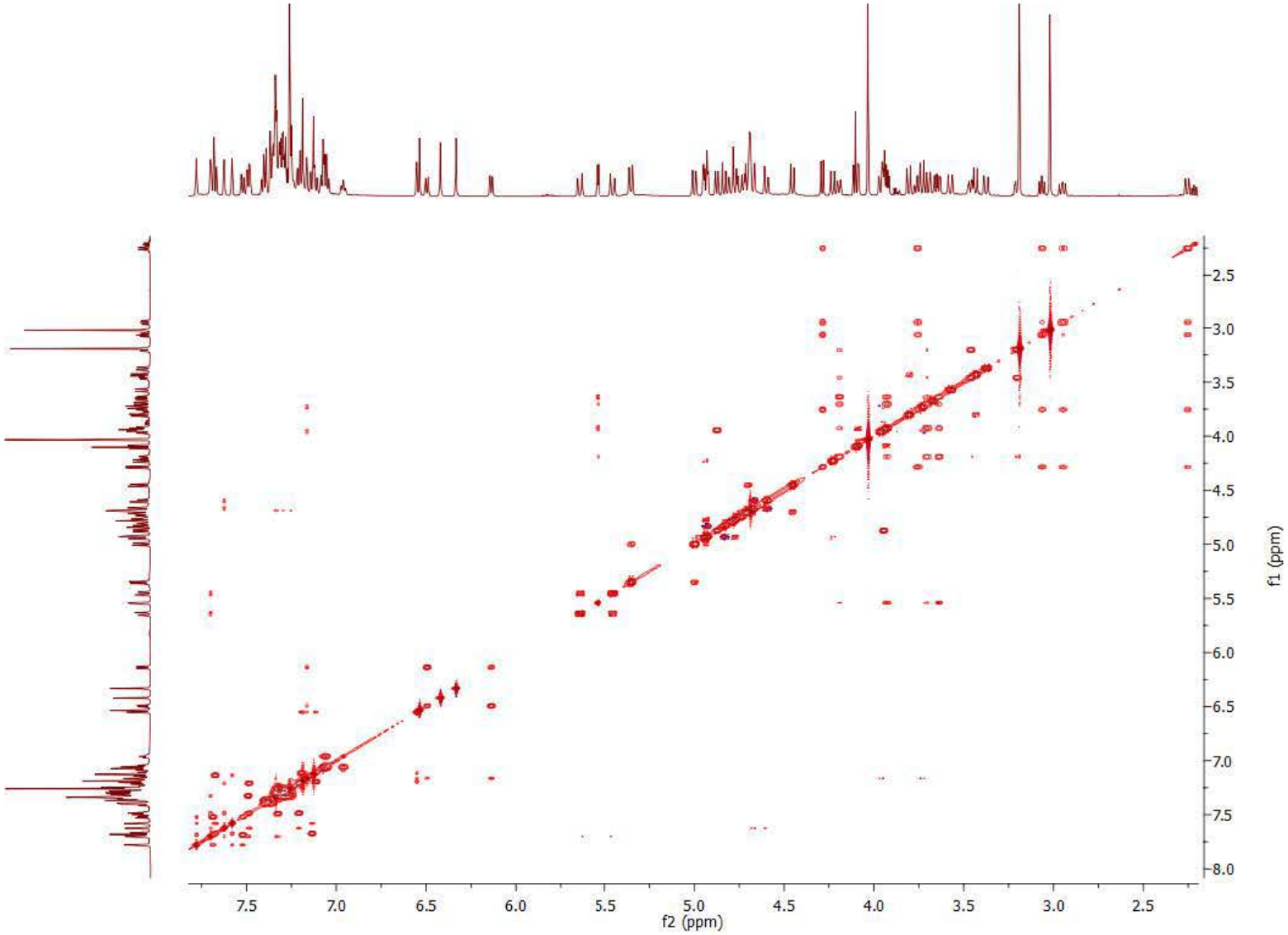

Figure S69. ^{1}H–^{1}H TOCSY (600 MHz, $CDCl_3$) spectrum of compound ***M*-5b.**

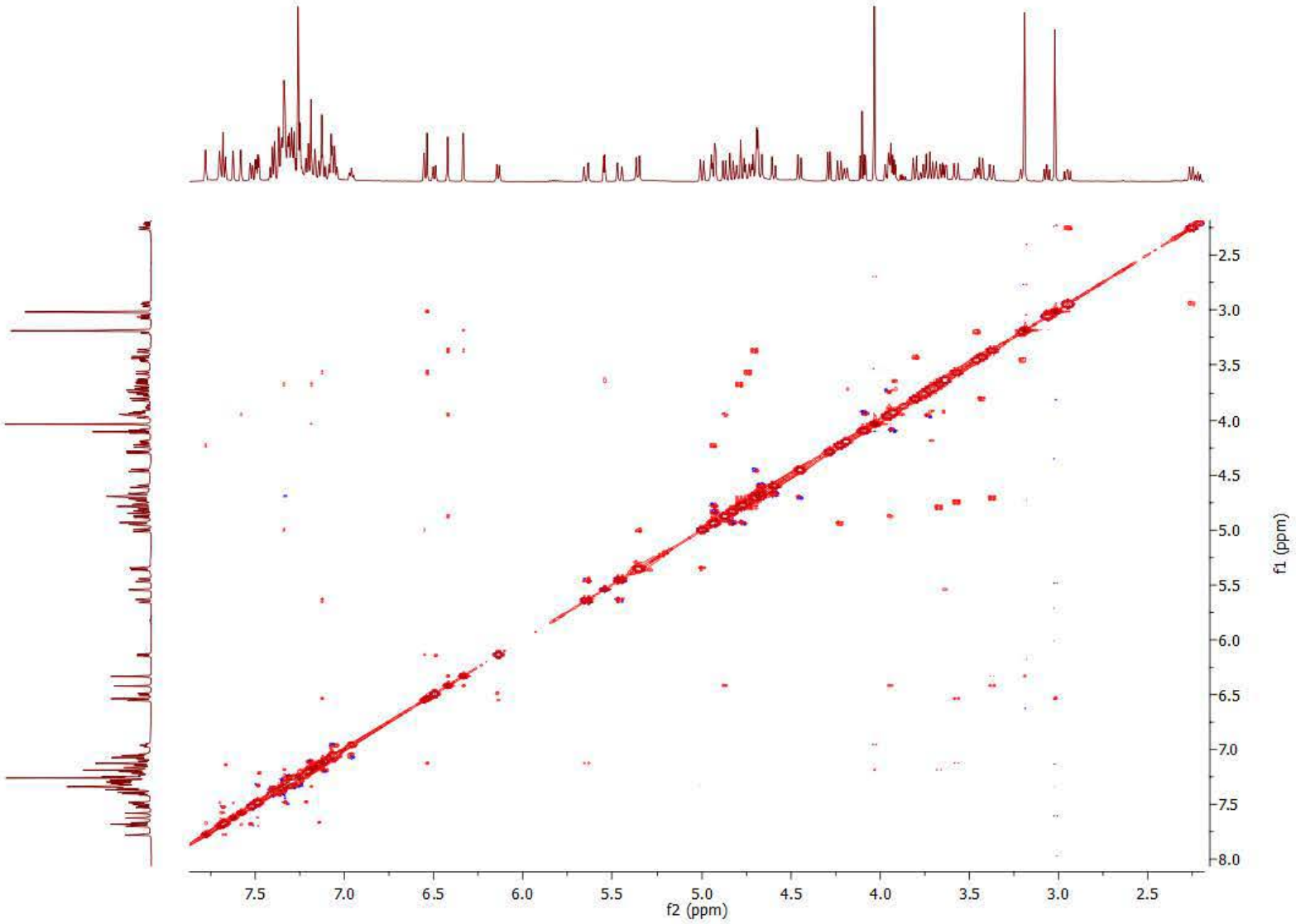

Figure S70. ^{1}H–^{1}H NOESY (600 MHz, $CDCl_3$) spectrum of compound ***M*-5b.**

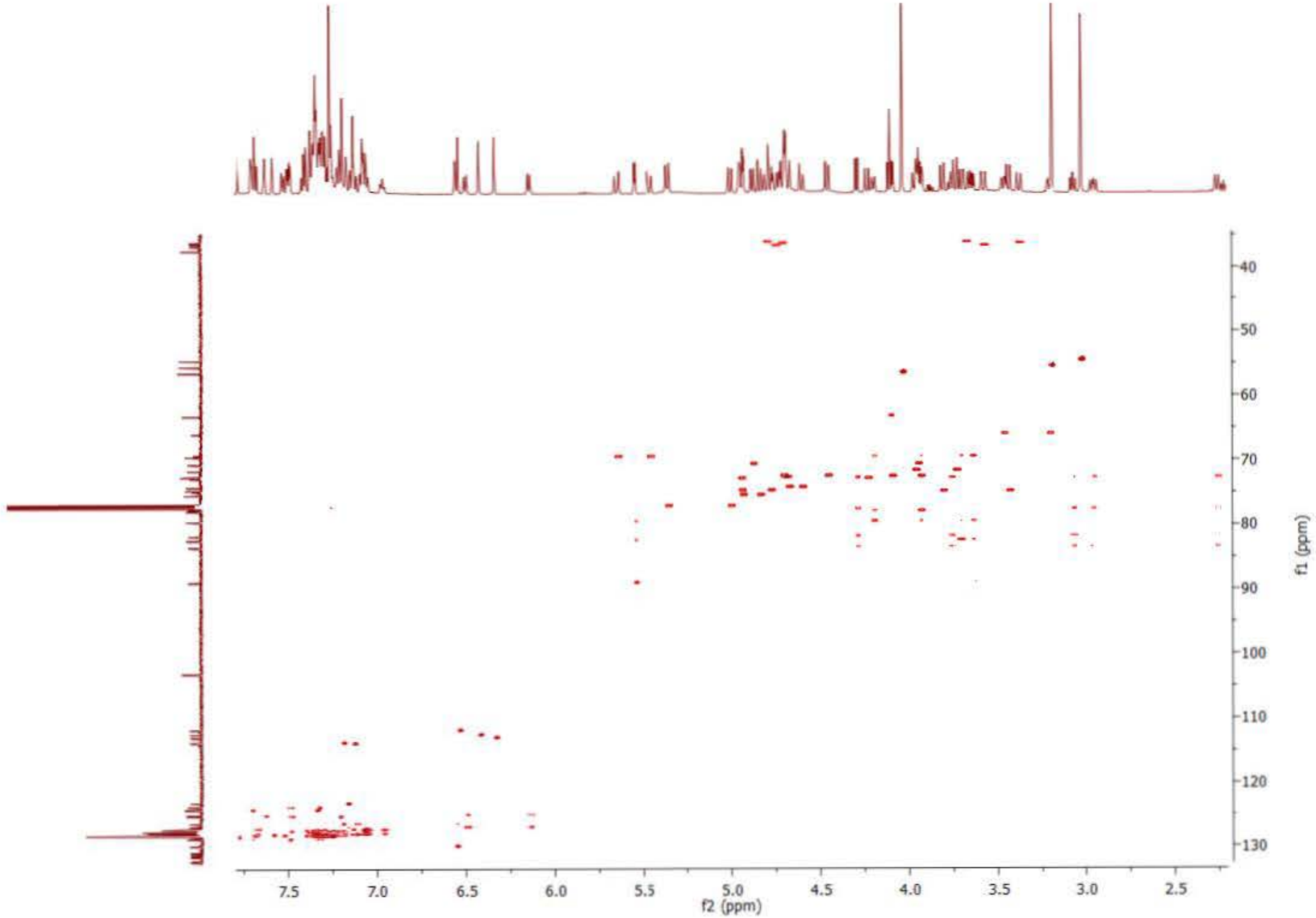

Figure S71. $^{1}H–^{13}C$ HSQC-TOCSY (600/150 MHz, $CDCl_3$) spectrum of compound ***M*-5b.**

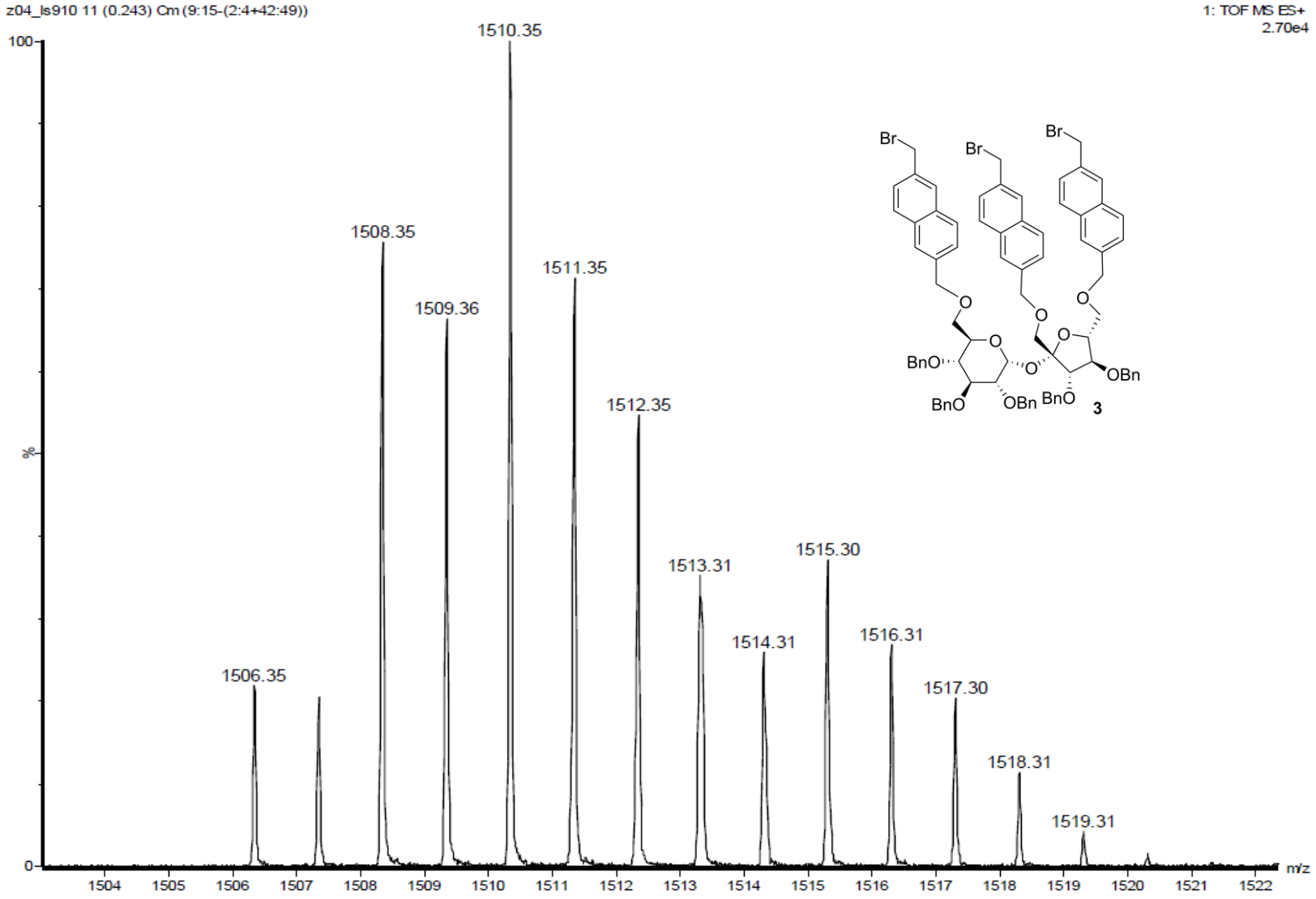

Figure S72. ESI-MS spectrum of compound **3.**

Elements Used:
C: 0-150 H: 0-150 O: 0-17 Na: 1-1

Mass	Calc. Mass	mDa	PPM	DBE	Formula	C	H	O	Na
1679.6844	1679.6858	-1.4	-0.8	57.5	C107 H100 O17 Na	107	100	17	1
	1679.6799	4.5	2.7	66.5	C114 H96 O12 Na	114	96	12	1
	1679.6893	-4.9	-2.9	79.5	C125 H92 O4 Na	125	92	4	1

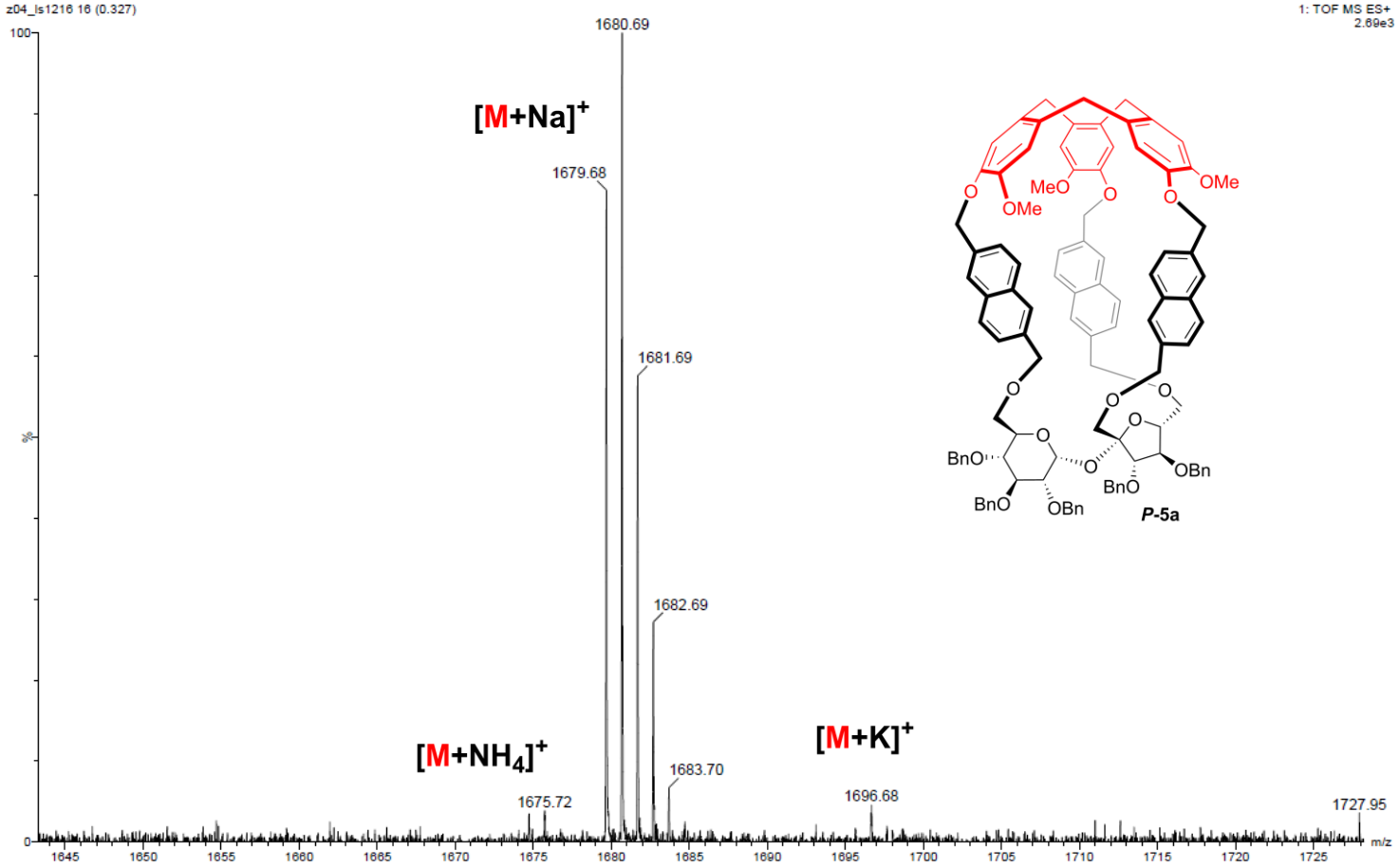

Figure S73. HRMS spectrum of compound ***P*-5a.**

Elements Used:
C: 0-150 H: 0-150 O: 0-17 Na: 0-1

Mass	Calc. Mass	mDa	PPM	DBE	Formula	i-FIT	i-FIT Norm	Fit Conf %	C	H	O	Na
1679.6866	1679.6858	0.8	0.5	57.5	C107 H100 O17 Na	152.4	0.155	85.63	107	100	17	1
	1679.6882	-1.6	-1.0	60.5	C109 H99 O17	154.2	1.940	14.36	109	99	17	
	1679.6893	-2.7	-1.6	79.5	C125 H92 O4 Na	162.4	10.119	0.00	125	92	4	1

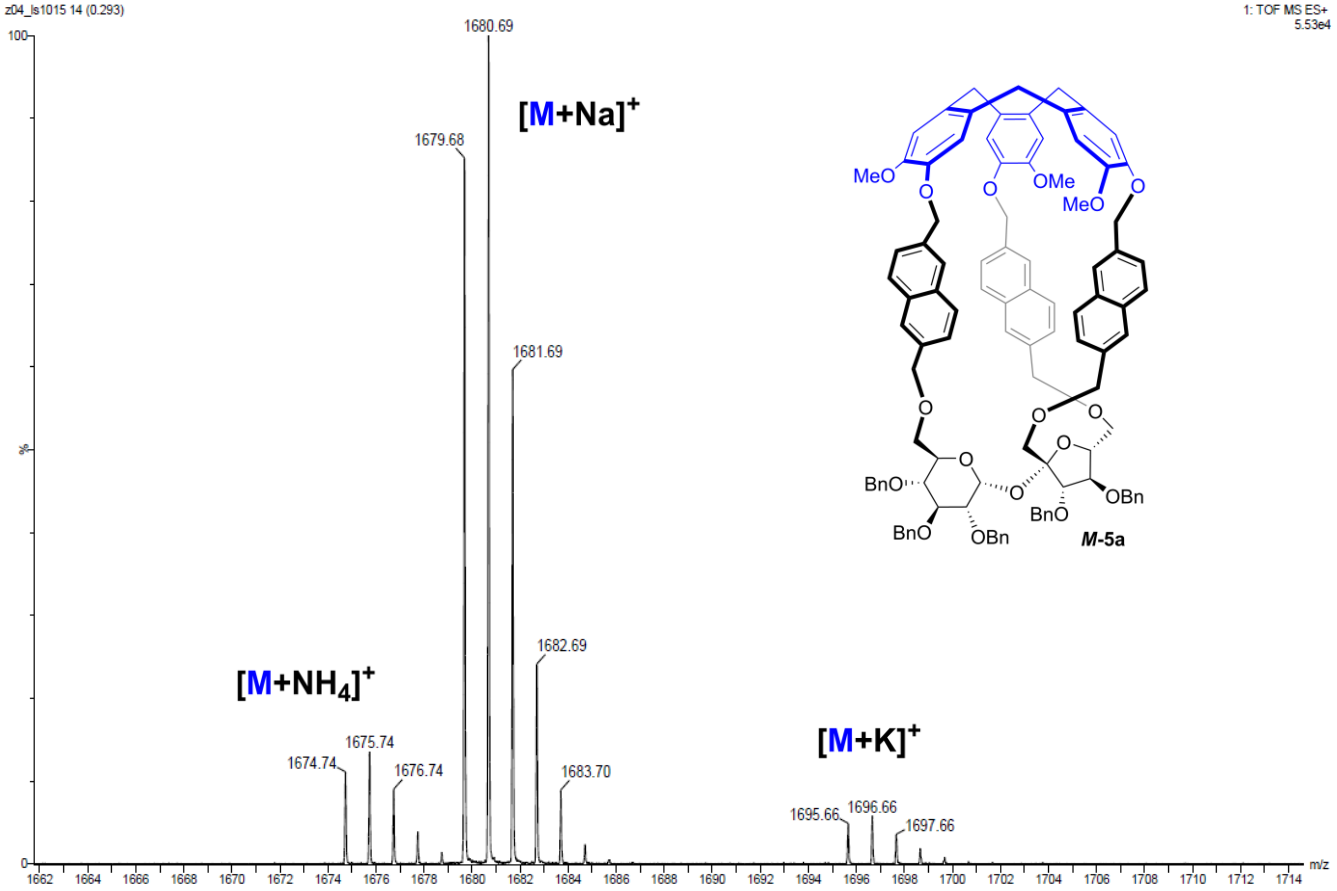

Figure S74. HRMS spectrum of compound ***M*-5a.**

Elements Used:
C: 0-150 H: 0-150 O: 0-20 Na: 1-1

Mass	Calc. Mass	mDa	PPM	DBE	Formula	i-FIT	i-FIT Norm	Fit Conf %	C	H	O	Na
1679.6836	1679.6858	-2.2	-1.3	57.5	C107 H100 O17 Na	97.7	n/a	n/a	107	100	17	1

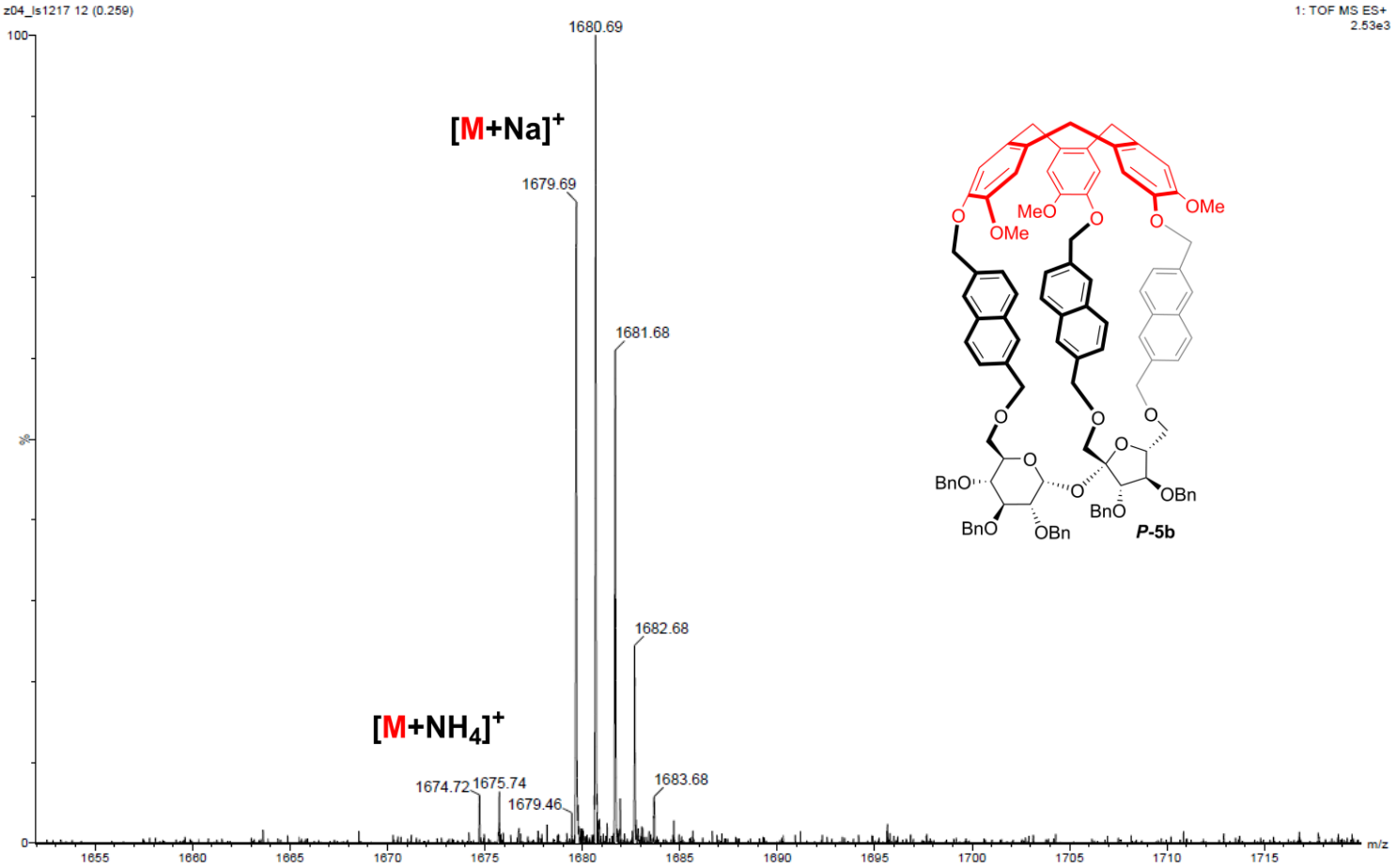

Figure S75. HRMS spectrum of compound ***P*-5b.**

Elements Used:
C: 0-150 H: 0-150 O: 0-17 Na: 0-1

Mass	Calc. Mass	mDa	PPM	DBE	Formula	i-FIT	i-FIT Norm	Fit Conf %	C	H	O	Na
1679.6860	1679.6882	-2.2	-1.3	60.5	C109 H99 O17	154.8	1.985	13.73	109	99	17	
	1679.6858	0.2	0.1	57.5	C107 H100 O17 Na	152.9	0.148	86.27	107	100	17	1

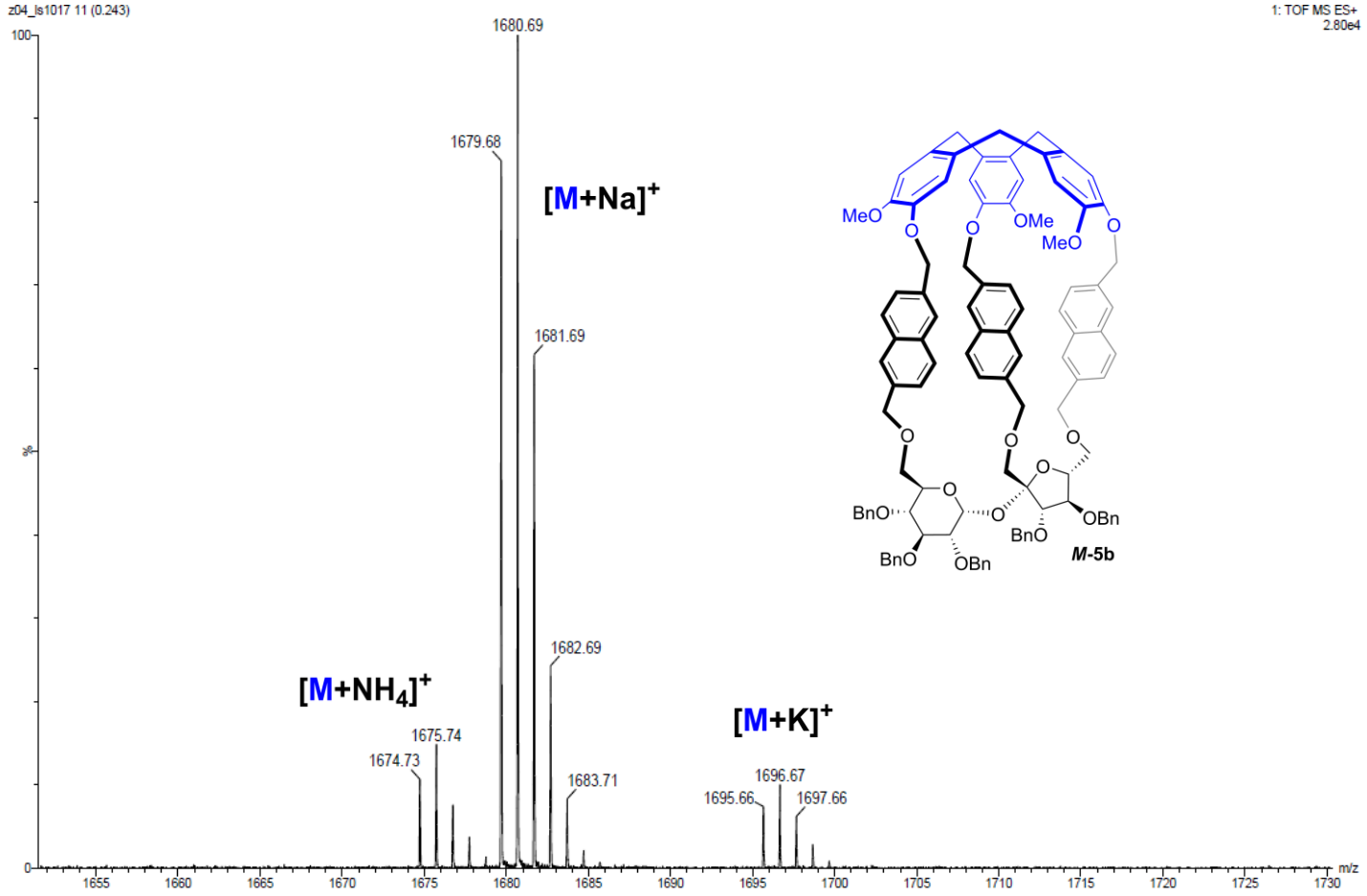

Figure S76. HRMS spectrum of compound ***M*-5b.**

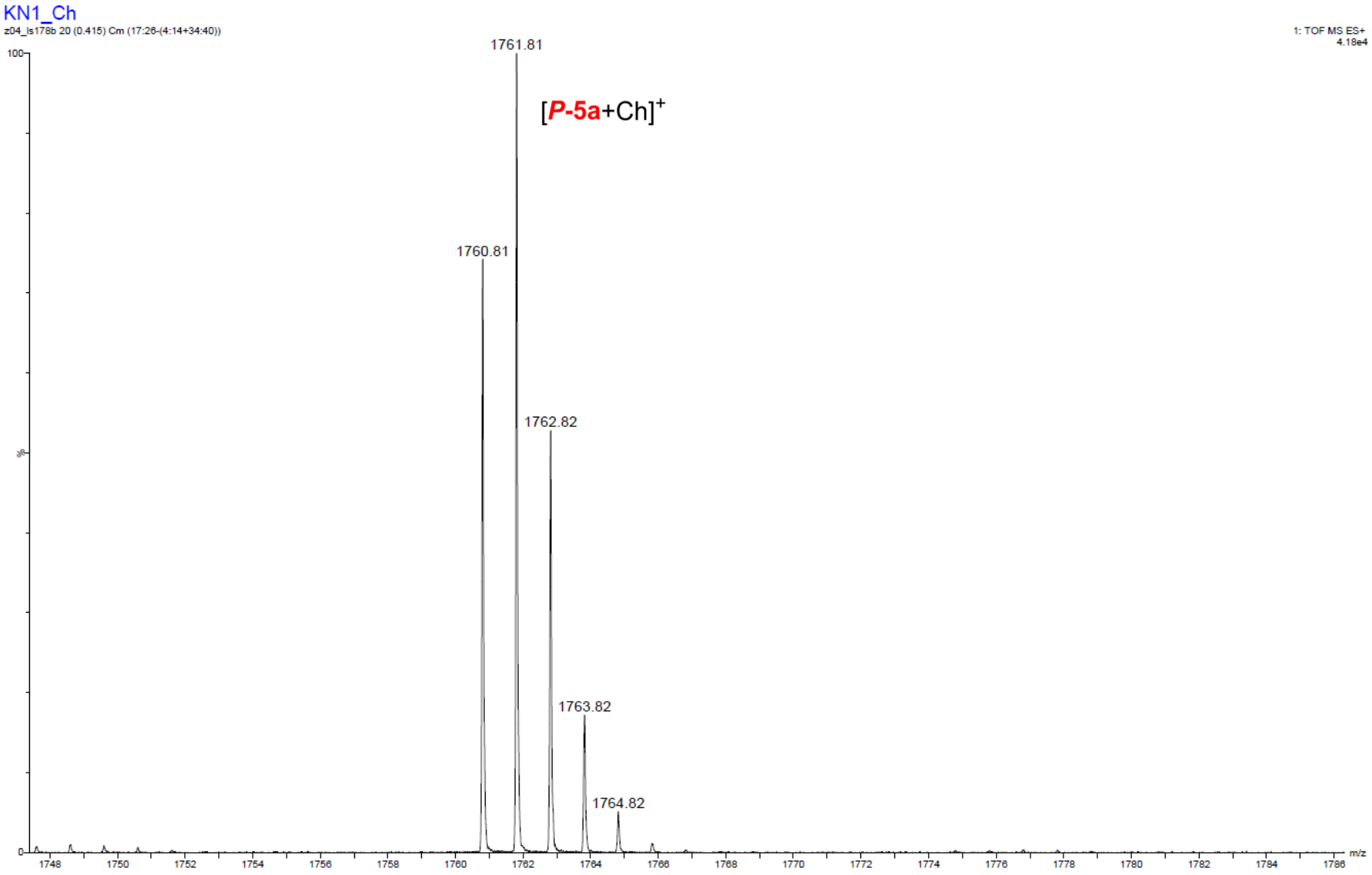

Figure S77. ESI-MS spectrum of adduct [***P*-5a** + Ch]$^+$.

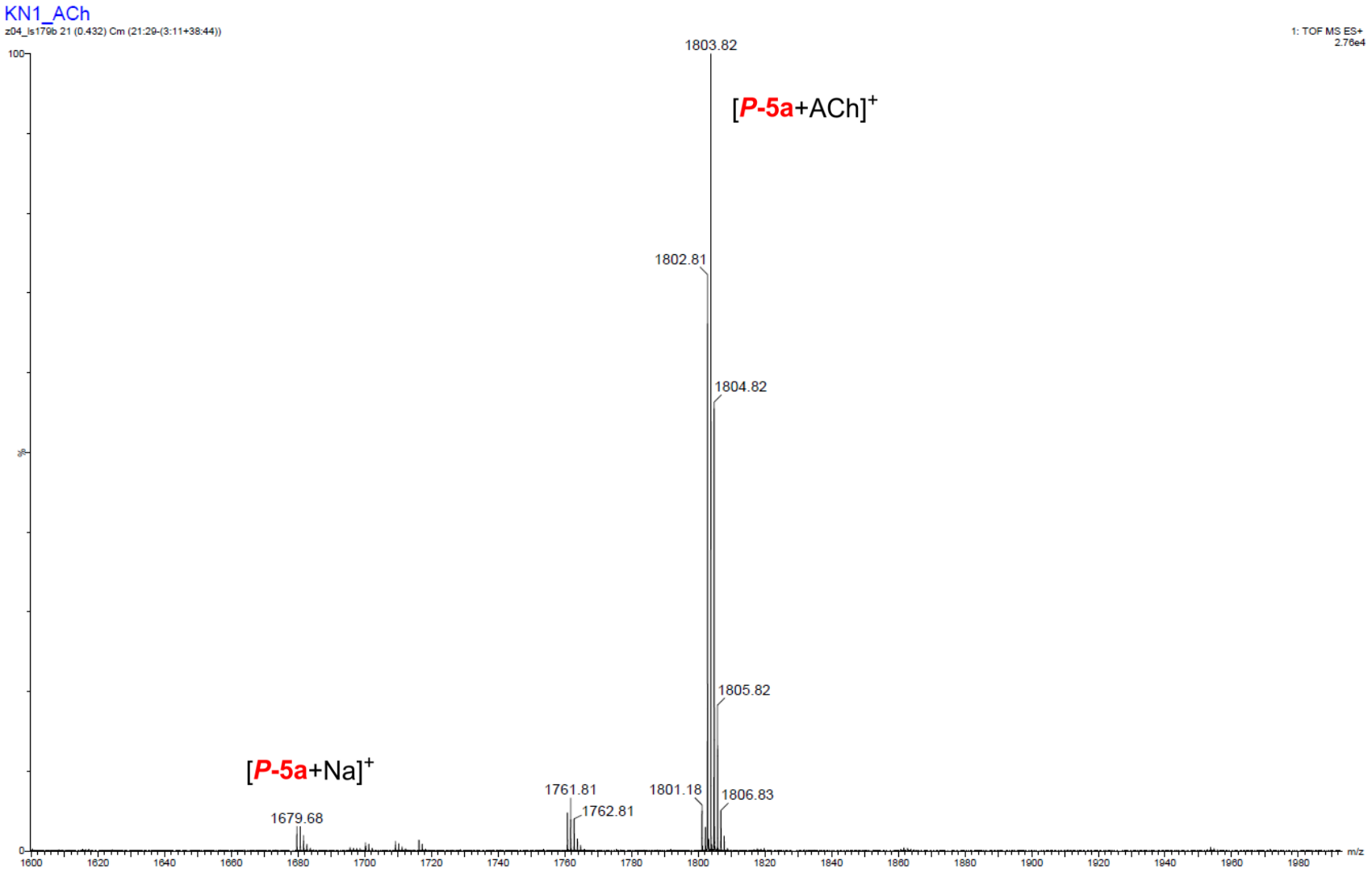

Figure S78. ESI-MS spectrum of adduct [***P*-5a** + ACh]$^+$.

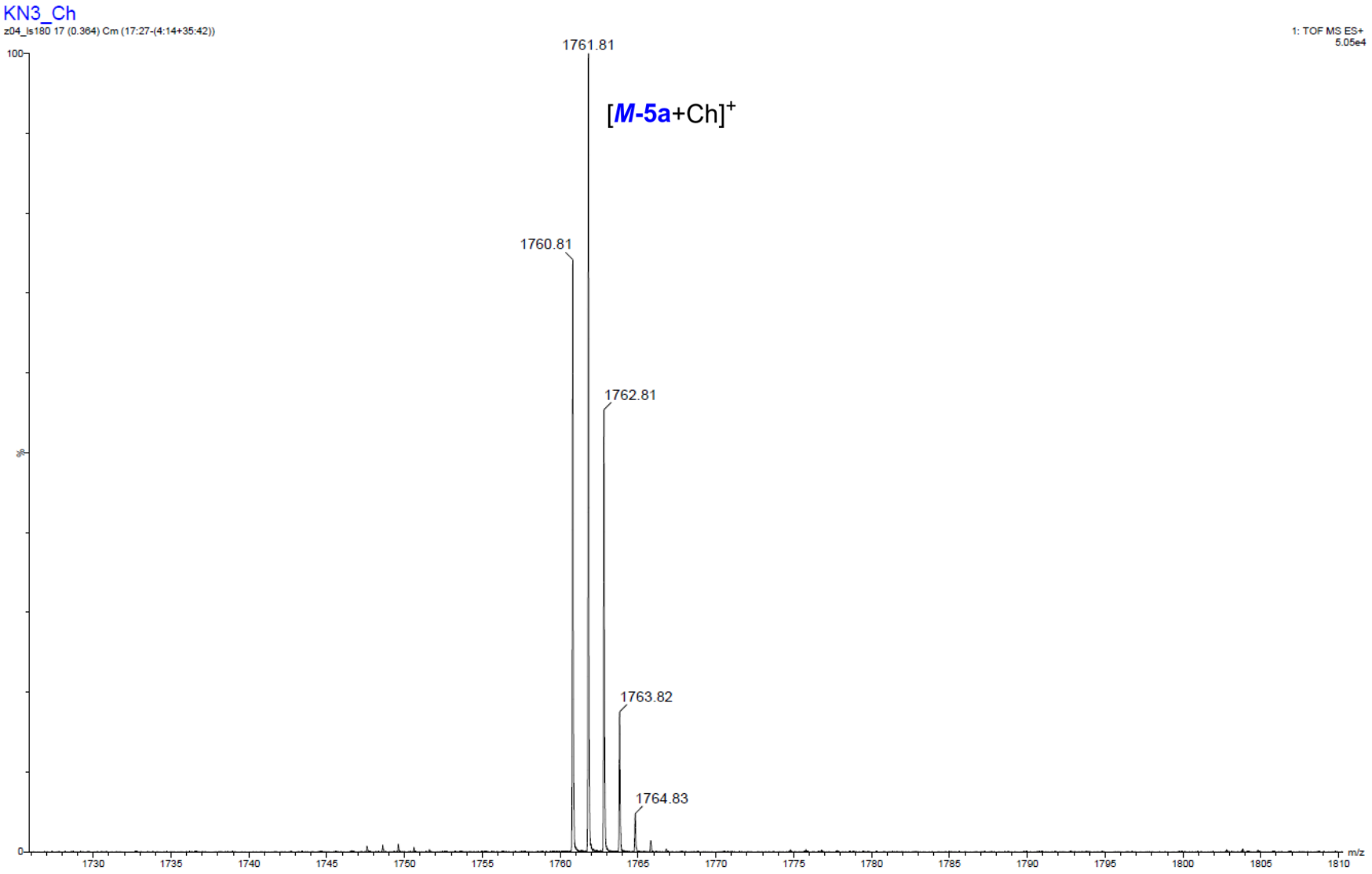

Figure S79. ESI-MS spectrum of adduct [***M*-5a** + Ch]$^+$.

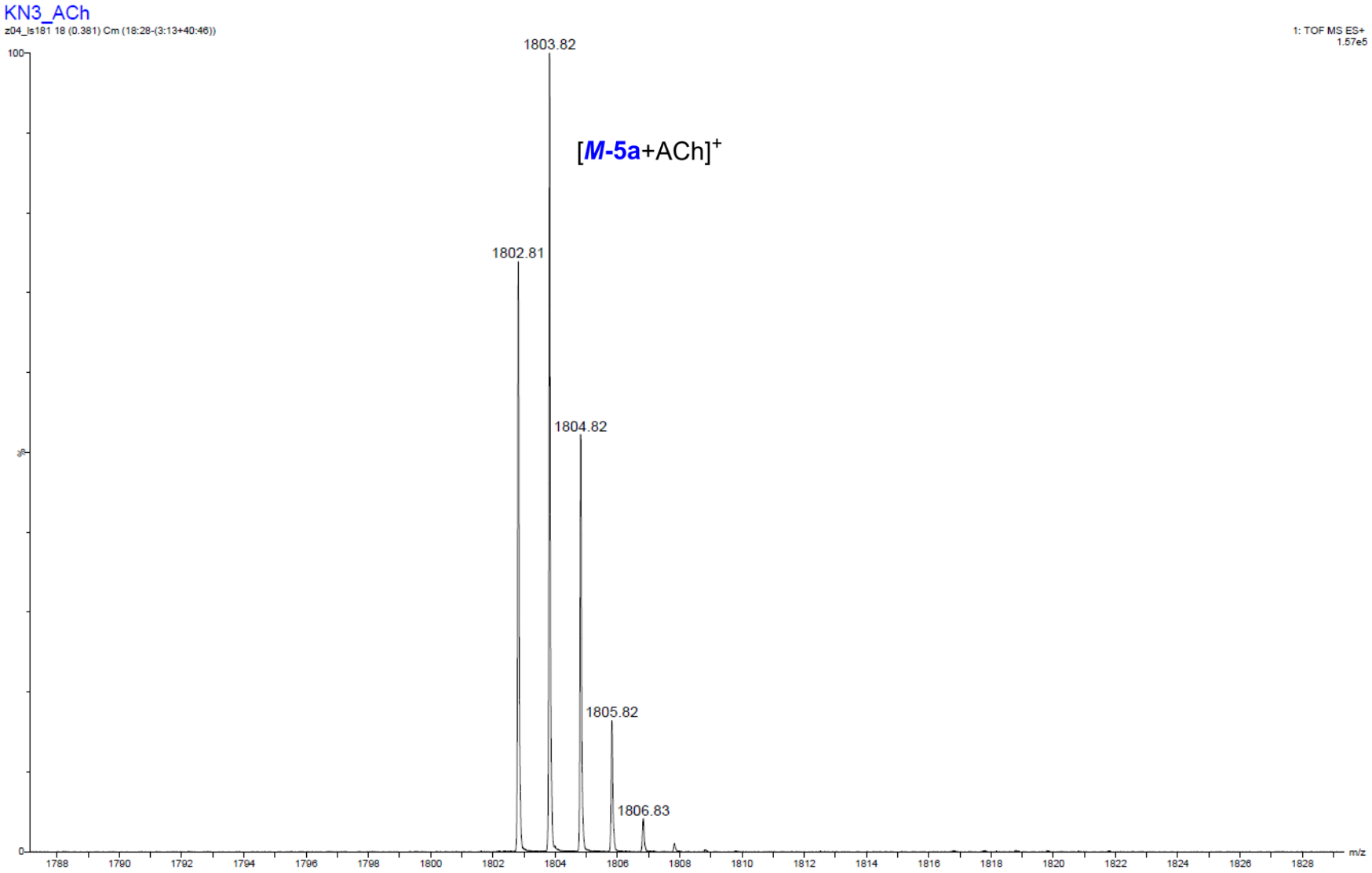

Figure S80. ESI-MS spectrum of adduct [***M*-5a** + ACh]$^+$.

Geometry of calculated structures

P-5a

Conformation #1 (Pop. = 68.98%)

Symbolic Z-matrix:

C	7.04048300	2.16352500	0.03090500
C	7.39308900	1.65453100	-1.36290000
C	6.15137000	1.04199700	-2.03362000
C	4.70910400	2.52736100	-0.81529100
C	5.88632200	3.15908300	-0.04844500
O	5.14509900	2.03469400	-2.08835300
O	8.23163000	2.74531400	0.55846900
O	8.43143400	0.68181500	-1.29949700
O	5.76710000	-0.09268500	-1.27973100
O	5.52997300	3.51344000	1.28554900
C	3.59479100	3.52440700	-1.12896300
O	3.04611100	3.96104700	0.11556800
C	5.78723300	-3.21146000	-0.47286000
C	7.13560800	-2.82310900	-1.06694500
C	5.42737000	-1.34221700	-1.89827700
C	6.69760500	-2.11835900	-2.35525100
O	4.90001800	-2.12649200	-0.83860900
O	7.69496700	-1.36726700	-3.00401900
C	4.38803900	-1.21957600	-3.03351500
C	5.72144800	-3.45721300	1.02269700
O	3.37239700	-0.25443300	-2.86726100
H	7.71678400	2.50380400	-1.98078800
H	6.38495900	-2.89239500	-3.06824900
H	7.64124500	-2.10057000	-0.41267500
H	5.44250100	-4.13044600	-0.96944500
H	6.72932200	1.31028400	0.64925800
H	6.23206700	4.04788700	-0.60103500
H	4.29579100	1.70708400	-0.21597800
H	3.99499700	4.38130200	-1.69133600
H	2.83073200	3.03592700	-1.74565100
H	3.97809400	-2.22910400	-3.18777100
H	4.66352700	-3.50728800	1.31666400
H	4.90559400	-0.92962500	-3.95451600
C	-3.91871600	-4.22891900	1.07533900
C	-4.24732300	-3.31916200	2.08119500
C	-4.74506300	-4.30039100	-0.06495900
C	-5.36360800	-2.46839500	1.99093700
H	-3.62937800	-3.26423800	2.97038700
C	-5.86599600	-3.48308500	-0.14066100
C	-6.19771800	-2.55626300	0.86226700
H	-6.51555400	-3.58276000	-1.00598700
C	-2.93528500	1.13594000	3.72625400
C	-3.60205000	2.32731800	3.36573000
C	-3.61897300	-0.07222200	3.62803600
C	-4.88042900	2.23454600	2.81708500
C	-4.92811100	-0.16774500	3.12797800
H	-3.10086600	-0.96407800	3.97056600
C	-5.54983300	1.00862300	2.67200300
H	-5.39399900	3.14048700	2.51561900
C	-6.49849900	1.81162900	-1.71158100

C	-6.87819400	0.59694300	-2.32822800
C	-6.53004600	1.89873800	-0.32563100
C	-7.18659700	-0.49533400	-1.52112800
C	-6.87856000	0.81174100	0.49627200
H	-6.28044700	2.85868100	0.11780300
C	-7.17278600	-0.41695400	-0.11614900
O	-6.92835600	0.59662200	-3.69387500
O	-2.94794100	3.50327900	3.60478400
C	-7.35670600	-0.59186100	-4.35330400
H	-7.34630400	-0.36000700	-5.41920600
H	-6.67641300	-1.42931200	-4.15640600
H	-8.37247400	-0.87142300	-4.04914000
C	-3.57219200	4.71924800	3.20152600
H	-3.75084500	4.73712900	2.11982100
H	-4.52002000	4.87617500	3.73015900
H	-2.87314700	5.51318400	3.46805700
C	-5.62458900	-1.52806000	3.16474400
H	-5.29029600	-2.03887000	4.07489800
H	-6.70021700	-1.38238800	3.29137700
C	-6.91916500	1.03571200	2.00665600
H	-7.36665100	2.01945900	2.18848300
H	-7.59071000	0.31441900	2.47754300
H	-7.46399600	-1.43645000	-1.98242100
C	-7.44697200	-1.70258000	0.65703000
H	-8.17342600	-2.29611800	0.09055700
H	-7.92378000	-1.48543900	1.61531100
H	6.35759800	0.78008800	-3.07191800
H	4.67478000	3.98218300	1.22328100
H	9.09858900	1.01390700	-0.67391100
H	8.08963200	-0.74649600	-2.35320900
H	8.04976200	2.98128600	1.48271600
O	-2.85708800	-5.08452700	1.11457900
C	-1.99695400	-5.03240400	2.24872000
H	-1.53224700	-4.04458000	2.35486100
H	-2.53444300	-5.28125100	3.17203500
H	-1.22269800	-5.77975400	2.06864100
O	6.40144200	-2.43619800	1.73430800
H	6.17509900	-4.43805600	1.23680900
O	-6.21349100	2.93729400	-2.45149000
O	-1.66539800	1.11615200	4.25930500
C	-0.66778500	1.92290100	3.61979200
H	-0.59496200	2.88821600	4.13264500
H	-0.97008300	2.13412200	2.58652700
O	7.93010200	-3.97890100	-1.27194100
H	8.75219300	-3.68481400	-1.69768600
C	1.97535100	4.90032200	-0.00080400
H	2.28806800	5.75900200	-0.61169400
H	1.81705900	5.26091800	1.02167700
C	0.69146500	4.30565200	-0.55131900
C	-0.17740000	5.08306200	-1.28909700
C	0.34388000	2.95529100	-0.26839800
C	-1.41320400	4.56665200	-1.76549600
H	0.07569800	6.11664600	-1.51802500
C	-0.83290100	2.41575700	-0.73773400
H	1.02802400	2.34849400	0.31666000
C	-2.32711200	5.35410300	-2.51699300
C	-1.74379000	3.19776800	-1.50123500
H	-1.07783300	1.37706400	-0.53057200

C	-3.49646700	4.80922200	-2.99652200
H	-2.08388500	6.39485400	-2.71655600
C	-2.95075500	2.66449200	-2.02753500
C	-3.82013800	3.44311000	-2.76913900
H	-4.18077600	5.42298800	-3.57739600
H	-3.17610800	1.61484400	-1.85056000
C	2.50701500	-0.38592400	-1.72752200
H	2.05328900	0.60415000	-1.62661000
H	3.09250900	-0.58638700	-0.82612000
C	1.40888900	-1.41854600	-1.87891700
C	0.21130000	-1.07749200	-2.47792200
C	1.56768000	-2.73157000	-1.35241600
C	-0.87563700	-1.98899000	-2.53996400
H	0.07253600	-0.07514500	-2.87855500
C	0.53885000	-3.64391400	-1.40339700
H	2.51234200	-2.99460700	-0.88630300
C	-2.13529500	-1.63648900	-3.09487300
C	-0.71648600	-3.29664000	-1.97398400
H	0.66462100	-4.63799400	-0.98074800
C	-3.19368400	-2.51671000	-3.05265600
H	-2.26039700	-0.64778600	-3.52988900
C	-1.82460000	-4.18128700	-1.96023000
C	-3.05202300	-3.80362700	-2.46887200
H	-4.15874900	-2.22106000	-3.45669300
H	-1.71160000	-5.15522900	-1.49255200
C	6.10148700	-2.43140000	3.13521400
H	6.89726500	-1.83392500	3.59088800
H	6.16689000	-3.45035300	3.54351200
C	4.74497900	-1.82073300	3.42546900
C	4.53009200	-0.48654700	3.13633900
C	3.66845100	-2.59347500	3.93401700
C	3.26199500	0.11604200	3.31515500
H	5.34508300	0.12071900	2.74803000
C	2.41928200	-2.03745800	4.12193500
H	3.83488200	-3.64154800	4.17226300
C	3.03102700	1.48511200	3.00458800
C	2.17250800	-0.67499900	3.80654300
H	1.60211400	-2.64543800	4.50275600
C	1.77997400	2.02967200	3.15287400
H	3.85628800	2.08616900	2.63124200
C	0.88466200	-0.07852400	3.93442600
C	0.68079000	1.24226800	3.60333500
H	1.61501500	3.07676300	2.90976900
H	0.05263500	-0.68293200	4.28270700
C	-5.08237300	2.86100900	-3.36173500
H	-5.38510600	3.43452300	-4.24231900
H	-4.92797500	1.82501900	-3.66697000
O	-4.44770300	-5.23859400	-1.03376600
C	-4.24212400	-4.73543700	-2.36916800
H	-4.09311600	-5.63889200	-2.96847200
H	-5.14748200	-4.23773200	-2.73685000

Imaginary Frequency = 0

E(RB3LYP) = -4064.5336189 a.u.

Conformation #2 (Pop. = 20.28%)

Symbolic Z-matrix:

C	-6.57531800	-2.47382400	-0.12229800
C	-7.20312100	-1.92903900	-1.39453600
C	-6.28117300	-0.87372100	-2.02995600
C	-4.34046600	-2.01955400	-1.16166700
C	-5.20835700	-3.06896200	-0.43508500
O	-5.02548300	-1.47830400	-2.30487900
O	-7.48712800	-3.44142900	0.39667000
O	-8.48104800	-1.36226500	-1.12405100
O	-6.15239100	0.22317400	-1.15447500
O	-4.64187800	-3.47641600	0.80228200
C	-3.04690900	-2.61804200	-1.71547700
O	-2.29699200	-3.10713300	-0.60188300
C	-6.97461500	2.84635600	0.27404700
C	-8.21068900	2.12200000	-0.25535600
C	-6.31873100	1.58936900	-1.61865300
C	-7.83355600	1.92176100	-1.73031800
O	-5.87696600	2.39970600	-0.56019700
O	-8.64237000	1.02461500	-2.45081000
C	-5.48329000	1.92358500	-2.88205500
C	-6.62774400	2.66676300	1.74087000
O	-4.19768300	2.45299900	-2.62465100
H	-7.31012500	-2.74750500	-2.12031000
H	-7.92711000	2.89303000	-2.23111300
H	-8.32232800	1.14387000	0.22837600
H	-7.11480700	3.92355800	0.10592200
H	-6.44520000	-1.65208500	0.59488400
H	-5.34834300	-3.93408100	-1.10518600
H	-4.09833900	-1.21821600	-0.45221100
H	-3.28308800	-3.43998500	-2.40680100
H	-2.48184500	-1.85554600	-2.26585900
H	-6.00603500	2.71230300	-3.43058400
H	-5.68513000	3.19641400	1.93641100
H	-5.42118000	1.04638000	-3.54001900
C	3.58460100	3.46648200	2.48785000
C	4.03641000	2.31871600	3.14065900
C	4.38391700	4.01711700	1.46490200
C	5.25025300	1.69181100	2.80641600
H	3.43759400	1.88917100	3.93578400
C	5.60154300	3.42097800	1.16177700
C	6.05660500	2.25736700	1.80398300
H	6.22697000	3.88876100	0.40637100
C	3.15713700	-2.42855800	2.98176800
C	3.88716000	-3.30718200	2.15202200
C	3.76080500	-1.24954900	3.40541600
C	5.15916300	-2.92311200	1.72882700
C	5.05372700	-0.87006200	3.01049200
H	3.18790600	-0.61607800	4.07710700
C	5.75358700	-1.71417600	2.13001900
H	5.72676500	-3.58801600	1.08749600
C	6.97048600	-0.77280900	-2.19094100
C	7.19045000	0.61947700	-2.28896500
C	6.96342900	-1.36613400	-0.93517100
C	7.33453600	1.35746100	-1.11598400

C	7.13222500	-0.63355900	0.25304000
H	6.83108600	-2.44374900	-0.89651600
C	7.29349500	0.75850500	0.15634300
O	7.26540000	1.13820300	-3.55073300
O	3.29327400	-4.49928800	1.84366700
C	7.48444400	2.53951400	-3.69197500
H	7.50830400	2.72922800	-4.76593900
H	6.67262400	3.11965500	-3.23640700
H	8.44018100	2.84055100	-3.24658900
C	3.96012600	-5.37204700	0.93568300
H	4.11831200	-4.89084400	-0.03699200
H	4.92347600	-5.70834500	1.33761000
H	3.30028600	-6.23218100	0.81319800
C	5.62440700	0.42856300	3.57651100
H	5.24844500	0.53724400	4.60014700
H	6.71015500	0.35069900	3.66899600
C	7.13809500	-1.39754600	1.57548200
H	7.66036300	-2.34680900	1.41014900
H	7.73199100	-0.85994400	2.31810900
H	7.50177900	2.42686300	-1.17721600
C	7.40049200	1.68184300	1.36539100
H	8.05709600	2.51811900	1.09992300
H	7.89013600	1.17295500	2.19833600
H	-6.67314900	-0.56892100	-3.00188900
H	-3.68856600	-3.61192800	0.63947700
H	-8.91992000	-1.94440600	-0.47895200
H	-8.73750300	0.20216000	-1.92272400
H	-7.13014900	-3.73718500	1.25009700
O	2.42356900	4.12170800	2.77670200
C	1.58421000	3.58109400	3.79263800
H	1.24861900	2.56795600	3.53885200
H	2.09166600	3.56169200	4.76488200
H	0.72085800	4.24579800	3.84896300
O	-6.52149200	1.29132500	2.06696900
H	-7.41261300	3.15428000	2.34183900
O	6.86909600	-1.56495000	-3.31441300
O	1.90084900	-2.71508500	3.46212600
C	0.90668100	-3.16362600	2.50868600
H	0.84845900	-4.25517500	2.53992800
H	1.21940100	-2.86854200	1.50253100
O	-9.36068200	2.92864600	-0.05139600
H	-10.11382700	2.44790500	-0.43223200
C	-1.20169600	-3.96076500	-0.92737400
H	-1.52991800	-4.75172500	-1.61681300
H	-0.93953300	-4.44043400	0.02239800
C	0.00992100	-3.24088700	-1.49103700
C	0.93919500	-3.93990500	-2.23578500
C	0.24184900	-1.86947200	-1.19983200
C	2.12999700	-3.32266000	-2.70117700
H	0.77330800	-4.99038800	-2.46817700
C	1.37232800	-1.23300100	-1.66288700
H	-0.48966000	-1.32571300	-0.61040700
C	3.11604800	-4.03114100	-3.44349100
C	2.34764200	-1.93447000	-2.42176600
H	1.53283700	-0.17975900	-1.44728200
C	4.25091500	-3.39581100	-3.89085900
H	2.95562000	-5.08515800	-3.65702100
C	3.52334200	-1.30751300	-2.91642200

C	4.46555100	-2.01105000	-3.64083400
H	4.99436900	-3.95008200	-4.45875700
H	3.66918500	-0.24770000	-2.71853500
C	-3.23000200	1.51827300	-2.13627600
H	-2.98509800	0.78329700	-2.91691000
H	-3.63797700	0.97583200	-1.27564700
C	-2.00729200	2.29391100	-1.71657100
C	-0.79268000	2.14132600	-2.34964700
C	-2.11756400	3.20911200	-0.63017300
C	0.35690100	2.86889100	-1.93035700
H	-0.69701500	1.45145500	-3.18552800
C	-1.02770500	3.92432600	-0.19639100
H	-3.08447600	3.33005900	-0.15047700
C	1.62041000	2.73188600	-2.56449100
C	0.24105200	3.77507700	-0.82637400
H	-1.11977100	4.61731300	0.63659200
C	2.71366700	3.44587300	-2.12170000
H	1.71683100	2.04771600	-3.40412000
C	1.38495900	4.49482400	-0.39893000
C	2.60699300	4.34109300	-1.02530700
H	3.67505600	3.32178400	-2.61466800
H	1.29799900	5.16121400	0.45404600
C	-5.93850300	1.01752400	3.35057500
H	-6.58862400	0.29251400	3.85261100
H	-5.92876500	1.93134900	3.95906600
C	-4.54349600	0.44585600	3.21264400
C	-4.29837500	-0.88463900	3.48130500
C	-3.46715700	1.26659200	2.76391800
C	-3.00766600	-1.45641200	3.30579600
H	-5.10732100	-1.52670300	3.82355500
C	-2.20848900	0.74832200	2.57752200
H	-3.64464100	2.32046300	2.56930600
C	-2.74295200	-2.82828100	3.55642900
C	-1.94004600	-0.62651500	2.83243900
H	-1.40143600	1.38497200	2.22343800
C	-1.49124500	-3.35775400	3.32646400
H	-3.54798000	-3.46098600	3.92110500
C	-0.66497200	-1.20414900	2.60870900
C	-0.43362600	-2.54900400	2.83344900
H	-1.30597300	-4.41277300	3.51296100
H	0.13647600	-0.57171400	2.23247700
C	5.71079100	-1.33656400	-4.16223100
H	6.00019100	-1.75914100	-5.12834000
H	5.55478700	-0.26289700	-4.28637000
O	3.96897800	5.18487500	0.85523000
C	3.81498400	5.13891900	-0.57414200
H	3.71546000	6.18997500	-0.86453700
H	4.72383600	4.75068500	-1.04854300

Imaginary Frequency = 0

E(RB3LYP) = -4064.5324641 a.u.

***M*-5a**

Conformation #1 (Pop. = 81.87%)

Symbolic Z-matrix:

C	-5.80016800	-0.71927100	3.10539100
C	-6.86809800	-1.52981300	2.38272100
C	-6.42566900	-1.82120200	0.94043400
C	-4.11168000	-1.81589900	1.59341900
C	-4.46098100	-1.45032300	3.04999700
O	-5.19618600	-2.51798400	0.96911900
O	-6.26107600	-0.53720000	4.44345000
O	-6.34247200	-0.58743500	0.25625900
C	-2.92890400	-2.77726700	1.49683700
O	-1.79427300	-2.16753000	2.11023900
C	-7.42087800	1.81154100	-1.50694600
C	-8.57397700	1.17992300	-0.73347800
C	-6.84792800	-0.44765300	-1.08363900
O	-6.38044700	0.80581400	-1.53225000
C	-6.33043800	-1.52750200	-2.03393300
O	-4.91984300	-1.56355600	-1.98220700
H	-6.98820900	-2.49541900	2.89382600
H	-8.42902500	1.32204800	0.34537500
H	-7.75614300	1.99295300	-2.53843800
H	-5.69366800	0.25353300	2.60619300
H	-4.55445800	-2.38203900	3.63268600
H	-3.88748900	-0.89682700	1.03841400
H	-3.18253400	-3.71608800	2.01207000
H	-2.72080100	-3.00695500	0.44362500
H	-6.68570300	-1.27423000	-3.04435400
H	-6.75682500	-2.50833600	-1.77054600
C	4.97649600	-3.41454300	-1.45188500
C	5.13722200	-2.40565100	-2.39325900
C	5.80674100	-3.42348100	-0.30960300
C	6.05895200	-1.35711800	-2.23292400
H	4.51273900	-2.45381500	-3.28084300
C	6.70790300	-2.37558900	-0.13078000
C	6.83550900	-1.32877600	-1.06197600
H	7.34762200	-2.36837200	0.74465500
C	2.77679100	1.45275400	-3.60871000
C	3.00315900	2.66765000	-2.91907200
C	3.82976500	0.55629800	-3.74590300
C	4.27747300	2.94405900	-2.43997500
C	5.10670500	0.80627100	-3.20457100
H	3.66600500	-0.37742600	-4.27161000
C	5.34056800	2.02564300	-2.55498900
H	4.46345700	3.89963800	-1.96071800
C	6.22350900	2.95537800	1.81699900
C	6.62532300	1.71405000	2.35644400
C	6.27760300	3.13111800	0.43444200
C	7.12829200	0.74447500	1.49579900
C	6.74699200	2.13191100	-0.43629100
H	5.96382500	4.07759900	0.00911400
C	7.21491100	0.92280200	0.10598100
O	6.65234100	1.43635600	3.70450300
O	1.92062500	3.49430900	-2.79587900

C	1.90294700	4.46718900	-1.74229200
H	2.54295500	4.12489600	-0.91905500
H	2.30593700	5.42075000	-2.10602900
C	6.14576200	-0.30220400	-3.33355800
H	5.98975500	-0.80549300	-4.29471300
H	7.15345600	0.11639400	-3.37901500
C	6.67948200	2.41626800	-1.93316700
H	6.82532900	3.49195700	-2.08524200
H	7.50320400	1.92744400	-2.45780200
H	7.46905700	-0.18298200	1.94752900
C	7.81448100	-0.20890900	-0.72702600
H	8.64209200	-0.64241400	-0.15386700
H	8.26412200	0.19161000	-1.63826600
H	-7.12895600	-2.49920500	0.45555200
H	-5.60396800	0.01867200	4.89375200
O	4.07414200	-4.42097200	-1.70642000
O	-6.57034600	2.99877400	0.41062400
O	-9.80567500	1.73618100	-1.16340200
H	-10.50716400	1.29965800	-0.65286500
C	3.06497700	-4.67528800	-0.69399800
H	3.19208100	-5.70885100	-0.35859000
H	3.23319000	-4.01880200	0.16218100
C	5.46290800	1.66122700	4.50362300
H	5.28361200	2.73309600	4.60398700
H	5.74620800	1.25905000	5.48001100
O	5.66776100	-4.48900000	0.53492500
O	5.82103900	3.91672600	2.70323500
O	1.51175700	1.25994400	-4.08571100
C	1.25496300	0.07205800	-4.82888400
H	1.41063000	-0.82594100	-4.21891000
H	0.20665200	0.12806800	-5.12594500
H	1.88647000	0.01700500	-5.72416900
C	6.45173600	-4.51142700	1.72466500
H	6.23640400	-3.64456300	2.36098700
H	6.17081900	-5.42635000	2.24830700
H	7.52407000	-4.53753600	1.49642500
C	5.41858000	5.18432600	2.18951900
H	4.54955400	5.09011500	1.52744300
H	5.14908700	5.78439600	3.05967300
H	6.23774400	5.67255500	1.64839400
C	-6.87247500	3.12158200	-0.97090000
H	-7.62408700	3.91081400	-1.13139900
H	-5.97588600	3.38742000	-1.54635100
C	-0.67801000	-3.04780200	2.19136500
H	-0.91391000	-3.89156700	2.85821300
H	-0.47975300	-3.47206200	1.19456500
C	-5.70817100	4.01731500	0.90547000
H	-5.72619200	3.89200800	1.99460100
H	-6.11276600	5.01617200	0.68212700
C	0.54732700	-2.31805500	2.68872200
C	0.67718200	-0.94849100	2.59861700
C	1.61709500	-3.08559100	3.23067800
C	1.85609900	-0.29019900	3.04705200
H	-0.13221600	-0.35434700	2.18502500
C	2.77291100	-2.48099300	3.66512200
H	1.51054000	-4.16523900	3.30609200
C	2.00974300	1.11994500	2.97625700
C	2.92905100	-1.06846600	3.59238600

H	3.57987900	-3.07809800	4.08280100
C	3.16032500	1.72770700	3.42860800
H	1.20249000	1.71603800	2.55761200
C	4.09654700	-0.40851900	4.05507400
C	4.22279900	0.96658300	3.98597000
H	3.26479400	2.80757500	3.36781100
H	4.90043300	-1.00663400	4.47994300
C	-4.28465700	3.90213100	0.38917500
C	-3.51924300	5.02410400	0.14860100
C	-3.72195800	2.61230000	0.17319400
C	-2.17471600	4.91981300	-0.30388900
H	-3.94239200	6.01583300	0.29882300
C	-2.43017600	2.47630600	-0.27491900
H	-4.34518100	1.73761400	0.32886100
C	-1.36297800	6.05599200	-0.56521700
C	-1.61992500	3.61784300	-0.52880000
H	-2.01098700	1.48753400	-0.44728600
C	-0.07358700	5.91262400	-1.03202200
H	-1.77776500	7.04770500	-0.40173000
C	-0.29154800	3.50690200	-1.00743200
C	0.47793600	4.62562300	-1.26105200
H	0.52967500	6.79403800	-1.23590100
H	0.11653200	2.51744900	-1.19528900
C	-2.89198100	-2.65250300	-2.59831900
C	-2.35128400	-3.91836800	-2.51697400
C	-2.06353200	-1.52432000	-2.33412000
C	-0.99315400	-4.12345400	-2.14818500
H	-2.97256900	-4.78958400	-2.71362300
C	-0.74855700	-1.68630500	-1.96573100
H	-2.49191900	-0.52891500	-2.40426200
C	-0.42832200	-5.42036100	-2.02434700
C	-0.17660100	-2.98540000	-1.84462200
H	-0.12899800	-0.81865500	-1.75187500
C	0.86763000	-5.58487500	-1.58747700
H	-1.04142000	-6.28599900	-2.26287800
C	1.15298800	-3.19320600	-1.39388000
C	1.67445100	-4.46663000	-1.24758800
H	1.28039000	-6.58513800	-1.48114500
H	1.75653100	-2.32586400	-1.13463900
C	-4.34878100	-2.45247100	-2.93951300
H	-4.46728900	-2.02816200	-3.95089300
H	-4.87201900	-3.41999900	-2.92820900
O	-9.10964400	-1.19065300	-0.23259600
H	-8.90801500	-0.96507100	0.70129100
O	-3.48780400	-0.58997600	3.63014300
H	-2.62452300	-1.01918600	3.47352000
O	-8.11441200	-0.83949600	2.35533600
H	-8.28207700	-0.50854300	3.25430400
C	-8.39747400	-0.30670500	-1.06733400
H	-8.77223400	-0.47382600	-2.08459400

Imaginary Frequency = 0

E(RB3LYP) = -4064.5398342 a.u.

Conformation #2 (Pop. = 12.04%)

Symbolic Z-matrix:

C	-5.79521100	-0.67942100	3.06253500
C	-6.84753000	-1.48341600	2.31054600
C	-6.39366400	-1.73257600	0.86277600
C	-4.08482100	-1.72349800	1.54199700
C	-4.44988200	-1.39699700	3.00392500
O	-5.15695700	-2.41790600	0.88694800
O	-6.27423400	-0.53391600	4.39918600
O	-6.31213400	-0.48570600	0.20493300
C	-2.89576500	-2.67547100	1.43504200
O	-1.77080400	-2.08148300	2.08135500
C	-7.36411200	2.00044900	-1.36809700
C	-8.52265700	1.34182300	-0.62239500
C	-6.84710400	-0.29604600	-1.11807000
O	-6.36942000	0.96132700	-1.54016600
C	-6.38751500	-1.35919700	-2.11477800
O	-4.97855600	-1.45851900	-2.10517600
H	-6.95788900	-2.46413200	2.79441300
H	-8.36327500	1.40487100	0.46146000
H	-7.72193800	2.30150100	-2.36283100
H	-5.69295000	0.30619800	2.58863200
H	-4.54074500	-2.34325900	3.56320500
H	-3.86107400	-0.78795700	1.01477200
H	-3.15393900	-3.62939100	1.91959200
H	-2.67117300	-2.87570300	0.37964800
H	-6.75884100	-1.06015900	-3.10698900
H	-6.84919000	-2.32938600	-1.87133900
C	4.75469700	-3.55627000	-1.41835500
C	4.94268000	-2.56876800	-2.37680100
C	5.59714300	-3.57976200	-0.28580900
C	5.90420100	-1.55427600	-2.24321500
H	4.30787000	-2.60794200	-3.25742700
C	6.54383500	-2.56656500	-0.13682000
C	6.70139600	-1.54043300	-1.08607000
H	7.19668200	-2.57356900	0.72891300
C	2.71902600	1.41178600	-3.48157900
C	3.05239300	2.64943100	-2.89676600
C	3.70866100	0.45138800	-3.63871200
C	4.36969300	2.87208200	-2.50059000
C	5.02777100	0.64628500	-3.19662800
H	3.42149000	-0.49013100	-4.09842500
C	5.36201300	1.88200300	-2.61530500
H	4.63730800	3.83703300	-2.08159300
C	6.39319500	2.85500400	1.69214100
C	6.72368300	1.60289800	2.25465900
C	6.43646300	2.99606300	0.30552600
C	7.14796700	0.58320600	1.41041800
C	6.82656000	1.94868800	-0.54796900
H	6.17567000	3.95052200	-0.13720500
C	7.22293900	0.72361600	0.01527800
O	6.75274300	1.36001700	3.60938600
O	2.04141500	3.56185900	-2.77272700
C	2.05447600	4.48697400	-1.67687600
H	2.74958100	4.13118100	-0.90604500

H	2.41376200	5.46339400	-2.02448000
C	6.00427600	-0.51419900	-3.35434400
H	5.78440000	-1.01411400	-4.30455000
H	7.02886600	-0.14706800	-3.44338300
C	6.74409700	2.20291400	-2.05036000
H	6.95358600	3.26264900	-2.23420400
H	7.51868100	1.64744400	-2.58296800
H	7.43520900	-0.35412300	1.87859700
C	7.74065100	-0.46274600	-0.79641400
H	8.55543200	-0.92413700	-0.22663400
H	8.19335700	-0.11222100	-1.72669800
H	-7.08658900	-2.40661900	0.35739200
H	-5.63403000	0.02590800	4.86839700
O	3.81122200	-4.52824700	-1.65794900
O	-6.38256400	2.93312000	0.62455200
O	-9.74469400	1.95868400	-0.99650500
H	-10.45059200	1.51154000	-0.50154100
C	2.81320400	-4.76202100	-0.63788600
H	2.93100500	-5.79031400	-0.28226800
H	2.99307000	-4.09523200	0.20963900
C	5.57214100	1.64632700	4.40376400
H	5.42556500	2.72607200	4.46798300
H	5.84495900	1.26808900	5.39246300
O	5.42675400	-4.62468800	0.57842700
O	6.06479900	3.85783900	2.56230800
O	1.41990100	1.10463200	-3.82800600
C	0.90996600	1.78889700	-4.98142100
H	1.51983200	1.56296600	-5.86499000
H	-0.10386800	1.41323600	-5.13439400
H	0.88142600	2.87025000	-4.81929500
C	6.22438100	-4.65928900	1.75886800
H	6.05327100	-3.77341300	2.38224100
H	5.91240500	-5.55257700	2.30189500
H	7.29166600	-4.73428300	1.51812700
C	5.73803200	5.13813000	2.02658000
H	4.85409200	5.08732700	1.37964100
H	5.52242900	5.77289900	2.88706200
H	6.57866800	5.55970700	1.46281900
C	-6.74474000	3.22456700	-0.71667100
H	-7.47532600	4.04874500	-0.74822300
H	-5.86759200	3.52859000	-1.30275100
C	-0.66094900	-2.97134200	2.16302500
H	-0.90934300	-3.81967500	2.81916800
H	-0.45916900	-3.38761300	1.16354500
C	-5.46547600	3.85901600	1.19411600
H	-5.43487000	3.60024900	2.25922200
H	-5.84880700	4.88809200	1.11754100
C	0.56591100	-2.25614200	2.67663700
C	0.74294500	-0.89729200	2.52208400
C	1.59052000	-3.02688700	3.29482900
C	1.92866700	-0.25418300	2.97313300
H	-0.03293000	-0.30095900	2.05109600
C	2.75146800	-2.43689200	3.73624400
H	1.44547700	-4.09703300	3.42255000
C	2.13422700	1.14408500	2.82929500
C	2.95760500	-1.03671300	3.59266700
H	3.52420300	-3.03606600	4.21168500
C	3.29388800	1.73616400	3.27879900

H	1.36085800	1.74262000	2.35400900
C	4.13545700	-0.39201500	4.05074900
C	4.31407100	0.97105800	3.90612900
H	3.43885000	2.80669900	3.16098300
H	4.90648000	-0.99262700	4.52960300
C	-4.07082400	3.77665200	0.59622400
C	-3.25210300	4.88630100	0.55069500
C	-3.59025700	2.53313400	0.09862100
C	-1.93430200	4.81180700	0.02259000
H	-3.61194000	5.84589900	0.91828800
C	-2.32793900	2.43183800	-0.43687100
H	-4.25454300	1.67517100	0.10915500
C	-1.06806300	5.93700500	-0.03868000
C	-1.46487900	3.56056500	-0.49415000
H	-1.97550000	1.48171000	-0.83205000
C	0.19067400	5.83165500	-0.58887000
H	-1.41792000	6.89179600	0.34650000
C	-0.16589900	3.48719500	-1.05746500
C	0.65557300	4.59532700	-1.10997600
H	0.83573500	6.70596200	-0.63562900
H	0.17303100	2.54496700	-1.47856300
C	-3.03554100	-2.66335100	-2.78778400
C	-2.62484000	-3.90287900	-2.34532600
C	-2.07145600	-1.62482300	-2.93381500
C	-1.26959900	-4.15534700	-1.99677700
H	-3.34854800	-4.70743300	-2.23264700
C	-0.75012500	-1.83354500	-2.61305500
H	-2.39490500	-0.65323100	-3.29810100
C	-0.83966700	-5.41194100	-1.49640700
C	-0.31160800	-3.09533500	-2.11508600
H	-0.02433800	-1.03228400	-2.73421800
C	0.46583100	-5.60139200	-1.09918800
H	-1.56031600	-6.22236600	-1.41894500
C	1.02476800	-3.32752400	-1.69836800
C	1.41597800	-4.54966700	-1.17963700
H	0.77768600	-6.56634800	-0.70705400
H	1.74176500	-2.51285600	-1.77018200
C	-4.49131500	-2.39233800	-3.07229100
H	-4.63028300	-1.97842500	-4.08428800
H	-5.06489900	-3.32905500	-3.01618300
O	-9.10767600	-1.04819000	-0.27776000
H	-8.90103000	-0.87859500	0.66689100
O	-3.48864200	-0.54314200	3.61239400
H	-2.62021200	-0.95947400	3.44850500
O	-8.10206500	-0.80792600	2.30169700
H	-8.26248000	-0.48581100	3.20544400
C	-8.39055900	-0.12229200	-1.06045500
H	-8.78435700	-0.20862900	-2.08070000

Imaginary Frequency = 0

E(RB3LYP) = -4064.5380266 a.u.

***P*-5b**

Conformation #1 (Pop. = 75.32%)

Symbolic Z-matrix:

C	-5.74916800	4.67505000	-1.18282900
C	-5.74829200	4.39628600	0.31511100
C	-4.69552300	3.33385500	0.65252800
C	-3.34115300	3.98482800	-1.22653300
C	-4.34621300	5.07931300	-1.63043600
O	-3.42680700	3.74490600	0.19491800
O	-6.70400100	5.70577700	-1.41050700
O	-7.01343000	3.94676800	0.78279500
O	-5.12283000	2.11066700	0.06935000
O	-4.39509700	5.24859900	-3.04762700
C	-1.89380300	4.32524900	-1.53925600
O	-1.58506900	5.60583700	-1.00634000
C	-5.86001400	-1.21335500	0.51959700
C	-5.86225500	-0.85441600	2.02426400
C	-4.78213100	0.88561900	0.72722600
C	-5.65849500	0.67123400	1.99890800
O	-5.17436100	-0.13518000	-0.16817100
O	-6.94016600	1.25703500	1.85334400
O	-4.88065700	-1.54667800	2.77432100
C	-3.24948800	0.83058800	0.91966000
O	-2.78650900	-0.45646600	1.33694500
O	-7.99860900	-2.44097500	0.43561100
H	-5.46158800	5.31865200	0.84010600
H	-5.15693600	1.01970000	2.91270900
H	-6.82491600	-1.08808900	2.48377200
H	-5.28116900	-2.12671500	0.37028500
H	-6.04268600	3.76105200	-1.71990900
H	-4.07267900	6.01887400	-1.13722700
H	-3.59120900	3.06240500	-1.76683300
H	-1.24627800	3.55028000	-1.10806000
H	-1.75043200	4.32004000	-2.63052200
H	-2.92372400	1.55160200	1.67436300
H	-2.78811700	1.10436300	-0.03181100
C	5.20040600	2.55837300	3.91397700
H	6.24063200	2.43710600	3.59389700
H	5.20443600	3.22032200	4.78472400
C	1.57382400	-4.04251200	-3.96615800
H	1.94918100	-3.02659600	-4.13548700
H	0.66816200	-4.19826300	-4.55408500
O	4.66603300	1.32988000	4.43296600
O	1.18949000	-4.22802300	-2.60537900
C	2.14565300	-4.08416800	-1.64076700
C	3.48563100	-3.79115400	-1.88601100
C	1.72469000	-4.24830100	-0.30392400
C	4.41818400	-3.62506100	-0.84619400
H	3.82609400	-3.67237800	-2.90818200
C	2.65515300	-4.12425700	0.71947600
C	4.00367000	-3.80372400	0.48464800
H	2.29938900	-4.27303700	1.73542800
C	5.68876300	0.28298000	-2.74794000
C	6.31958600	1.06948200	-1.76699600

C	5.59050100	-1.09014300	-2.54180100
C	6.74902800	0.46138900	-0.59110400
C	6.02693400	-1.71149300	-1.36237500
H	5.12938300	-1.67885400	-3.32938600
C	6.58431900	-0.91040700	-0.34648100
H	7.22372800	1.09395100	0.15381500
C	4.78200600	0.17867800	3.69421900
C	3.85297000	-0.84421600	3.99686500
C	5.76499600	-0.07056400	2.74443400
C	3.95544200	-2.06354200	3.33412100
C	5.86517300	-1.29898000	2.06270500
H	6.49539700	0.69923800	2.52305200
C	4.94131200	-2.31140500	2.35927300
O	2.92271700	-0.54550000	4.95061500
O	6.47601900	2.43458100	-1.90476800
O	0.39628200	-4.44351400	0.00409500
C	1.95701900	-1.54055200	5.27433300
H	2.42995600	-2.44148600	5.68454800
H	1.31213600	-1.09369100	6.03268400
H	1.35503000	-1.81469700	4.39916100
C	7.40557700	2.83376400	-2.92480800
H	8.40717600	2.44540400	-2.70383600
H	7.08611500	2.48456500	-3.91140100
H	7.42576300	3.92524000	-2.90829600
C	5.83529500	-3.22187900	-1.24006000
H	6.05878600	-3.66926300	-2.21504600
H	6.56404500	-3.64387000	-0.54515600
C	6.97983300	-1.43967400	1.02733200
H	7.84572300	-0.86734500	1.37893600
H	7.31486000	-2.47708100	0.96316300
H	3.25606300	-2.85660500	3.57341700
C	4.93610700	-3.68197100	1.68748700
H	4.61603700	-4.41921100	2.43285100
H	5.95193400	-3.97019600	1.40705800
H	2.33459100	-4.77120600	-4.27048600
H	-4.59283100	3.23415300	1.73738600
H	-3.72796400	5.90753700	-3.29497800
H	-7.69159200	4.46424700	0.31523900
H	-6.88107200	2.08232600	1.32953900
H	-4.01120200	-1.31300000	2.38527000
H	-6.67651600	5.89772500	-2.36316200
C	4.09343500	1.75550100	-3.76259100
H	4.42103400	2.58432800	-3.12980500
H	3.92297300	2.12825700	-4.77540800
O	5.19503900	0.81423500	-3.92149800
C	-0.20147700	5.93348900	-1.05095200
H	0.20861300	5.75690000	-2.05665300
H	-0.16484100	7.01418700	-0.86816100
C	-2.19009500	-1.26360500	0.30089000
H	-2.91782500	-1.45354600	-0.49532800
H	-1.96640800	-2.21459400	0.79537700
C	0.63519300	5.21014800	-0.00877100
C	1.96296400	4.91981900	-0.24518100
C	0.06515800	4.88316700	1.25347300
C	2.78088600	4.32424300	0.75447400
H	2.40969200	5.15461800	-1.20969200
C	0.82232700	4.29058700	2.23620900
H	-0.98721000	5.09113000	1.41852400

C	4.15602400	4.03510700	0.54469900
C	2.19922000	3.99973100	2.02423100
H	0.37596600	4.03887800	3.19532600
C	4.91843900	3.46650400	1.54282600
H	4.60583400	4.26093000	-0.41876600
C	3.01274600	3.41041300	3.02519700
C	4.35262600	3.14928200	2.80518700
H	5.96999400	3.25929600	1.36229500
H	2.56516600	3.16419100	3.98547000
C	-0.92940500	-0.64887000	-0.26873400
C	-0.68571200	-0.67028000	-1.62720700
C	0.02481600	-0.05067100	0.60097400
C	0.49828500	-0.10564400	-2.17558600
H	-1.40882300	-1.12333100	-2.30230800
C	1.16892900	0.52538800	0.10187800
H	-0.17258300	-0.03738700	1.66887600
C	0.77625300	-0.11816000	-3.57059700
C	1.43646800	0.52300100	-1.29558800
H	1.88624100	0.99047000	0.77305600
C	1.91974900	0.46683900	-4.06753000
H	0.06529800	-0.59144700	-4.24343300
C	2.59371700	1.13403100	-1.84519200
C	2.84526000	1.11563000	-3.20427600
H	2.11585600	0.45072200	-5.13699400
H	3.28751000	1.62969500	-1.17058800
C	-0.17703600	-5.73382200	-0.33427500
H	-0.01384000	-6.41989900	0.50599800
H	0.32063700	-6.13639400	-1.22039600
C	-6.57714800	-4.35227000	-0.16319000
C	-5.68705200	-4.36534700	-1.21759600
C	-6.16831900	-4.87327000	1.09652300
C	-4.34897300	-4.81305500	-1.05076600
H	-5.98812100	-3.97607200	-2.18821300
C	-4.88780800	-5.33606800	1.28770200
H	-6.87734600	-4.87844700	1.92053200
C	-3.39011000	-4.74186400	-2.09829600
C	-3.93192100	-5.28779100	0.23468400
H	-4.58026400	-5.71794100	2.25816900
C	-2.07432900	-5.06964300	-1.86974800
H	-3.70839600	-4.39524600	-3.07854900
C	-2.56978400	-5.64211000	0.42799400
C	-1.64492800	-5.51510600	-0.58885700
H	-1.33887200	-4.97451300	-2.66261400
H	-2.25362800	-5.98490700	1.41113200
C	-7.25227400	-1.35696800	-0.11353700
H	-7.14561200	-1.46539200	-1.20175800
H	-7.82184000	-0.44498700	0.08782100
C	-7.92538200	-3.67904500	-0.28676200
H	-8.71382600	-4.29875500	0.15256300
H	-8.17112900	-3.50874600	-1.34454500

Imaginary Frequency = 0

E(RB3LYP) = -4064.5350289 a.u

Conformation #2 (Pop. = 21.14%)

Symbolic Z-matrix:

C	-5.87160200	4.53565500	-1.29345700
C	-5.91307200	4.25748200	0.20403600
C	-4.84564000	3.22310900	0.57976200
C	-3.44959500	3.90043000	-1.26335500
C	-4.46490600	4.97316900	-1.69770400
O	-3.57412100	3.65814800	0.15450100
O	-6.84275700	5.54288000	-1.55358600
O	-7.18021800	3.77535700	0.63116900
O	-5.22776200	1.98317300	0.00074500
O	-4.47594200	5.14054800	-3.11598400
C	-1.99855500	4.26716300	-1.52646700
O	-1.71727900	5.53116800	-0.94083600
C	-5.86437700	-1.35765200	0.53958900
C	-5.87709400	-0.95475400	2.03357500
C	-4.85999000	0.77994500	0.68369100
C	-5.72550600	0.57535400	1.96284800
O	-5.23804800	-0.26811200	-0.18598500
O	-7.02601200	1.11464800	1.80017100
O	-4.87273500	-1.59130800	2.80236400
C	-3.32526000	0.76273500	0.87049000
O	-2.82888300	-0.51075500	1.29008900
O	-7.94158800	-2.68457700	0.52639600
H	-5.66703100	5.18768600	0.73603600
H	-5.23632500	0.96757200	2.86542000
H	-6.83102900	-1.20660100	2.50145900
H	-5.24236300	-2.24575200	0.41391200
H	-6.12512000	3.61450900	-1.83892000
H	-4.22791100	5.91893200	-1.19707000
H	-3.66417800	2.97414200	-1.81257300
H	-1.35547200	3.48440800	-1.10367200
H	-1.82538600	4.29965700	-2.61286100
H	-3.01400500	1.49639700	1.61918200
H	-2.87537500	1.04287100	-0.08448500
C	4.43786300	2.23803800	4.60332000
H	4.90263300	3.03179400	5.19892400
H	3.72155500	1.71168700	5.23712300
C	1.45926300	-3.80385100	-4.03985000
H	1.81335200	-2.78245500	-4.22151900
H	0.51821700	-3.96152500	-4.56876200
O	5.55274800	1.38440500	4.28400500
O	1.16712700	-4.00898700	-2.65904000
C	2.18356700	-3.86927400	-1.75861200
C	3.50163000	-3.55986200	-2.08769000
C	1.85432600	-4.06101700	-0.40017100
C	4.50171300	-3.41248900	-1.11019600
H	3.77267000	-3.42058300	-3.12785500
C	2.84946900	-3.94670800	0.56190300
C	4.17837200	-3.61654500	0.24268000
H	2.56493500	-4.11954400	1.59649900
C	5.62522000	0.56290300	-2.92906300
C	6.33124700	1.30777700	-1.96657900
C	5.54333100	-0.81816300	-2.77833100
C	6.86289600	0.64885700	-0.86247700

C	6.07983500	-1.49017800	-1.66968900
H	5.01614100	-1.37228100	-3.54939100
C	6.72669400	-0.73492800	-0.67291500
H	7.39150000	1.25023300	-0.12802900
C	5.36029200	0.22345400	3.56635600
C	4.42367300	-0.77677100	3.90716300
C	6.24345400	-0.01950500	2.52049000
C	4.40518700	-1.95546100	3.15887600
C	6.23968300	-1.20547300	1.77135500
H	6.97401500	0.75515600	2.30510000
C	5.29233500	-2.19252500	2.09416600
O	3.61924500	-0.53518800	4.98590000
O	6.46555700	2.67901400	-2.05162600
O	0.54999400	-4.29181500	-0.01937300
C	2.64963500	-1.51759600	5.34220700
H	3.12600500	-2.46378100	5.62557800
H	2.11615300	-1.10881400	6.20139700
H	1.94260800	-1.69641200	4.52348100
C	7.31359200	3.13607000	-3.11701000
H	8.33295800	2.75259400	-2.98722900
H	6.92671800	2.82709500	-4.09283500
H	7.32344400	4.22599300	-3.05236800
C	5.88904200	-3.00319400	-1.59321100
H	6.03509500	-3.41396200	-2.59846800
H	6.66348100	-3.45615000	-0.97112100
C	7.24749400	-1.32680200	0.63185200
H	8.15390000	-0.78234300	0.91901800
H	7.55397800	-2.36594600	0.49490400
H	3.70189300	-2.73659600	3.42476700
C	5.19551300	-3.53822400	1.37890800
H	4.91461700	-4.29042200	2.12500800
H	6.18185900	-3.83900000	1.01726200
H	2.20488900	-4.52146500	-4.40242000
H	-4.77038600	3.13668600	1.66801600
H	-3.82196700	5.81864600	-3.34565300
H	-7.85658400	4.28423500	0.15188600
H	-6.99373000	1.91714300	1.24038500
H	-4.01339200	-1.36282000	2.38874900
H	-6.78624500	5.73697300	-2.50457000
C	3.94624200	2.06236200	-3.74502500
H	4.29530500	2.83342500	-3.05332300
H	3.73028400	2.52470500	-4.71131400
O	5.04365400	1.14882100	-4.03457400
C	-0.32983300	5.82646000	-0.83362500
H	0.17893100	5.66821700	-1.79646200
H	-0.28945900	6.90070100	-0.61686500
C	-2.20384200	-1.29747200	0.25429600
H	-2.92180300	-1.50341600	-0.54681600
H	-1.95586400	-2.24364100	0.74589800
C	0.37863500	5.05307300	0.26763000
C	1.73272700	4.79337600	0.19046400
C	-0.34355500	4.64069800	1.42052500
C	2.42342500	4.14232700	1.24835700
H	2.29690400	5.09588500	-0.69013100
C	0.29063300	3.98704600	2.45206900
H	-1.41158200	4.82764000	1.46009800
C	3.82302000	3.88498900	1.20855800
C	1.68650300	3.72401800	2.40330300

H	-0.27258300	3.66676800	3.32559700
C	4.46048600	3.26586500	2.26014300
H	4.39022600	4.19320300	0.33314600
C	2.37176400	3.05983000	3.45572900
C	3.73373500	2.84115800	3.40677600
H	5.53128500	3.09129700	2.22031900
H	1.80034800	2.73484800	4.32317800
C	-0.95936500	-0.64098600	-0.30303700
C	-0.73553900	-0.58797400	-1.66397100
C	-0.00216900	-0.07148900	0.58264700
C	0.42783500	0.02967200	-2.19921700
H	-1.46084000	-1.01792100	-2.35167700
C	1.12446600	0.54945300	0.09799300
H	-0.18343700	-0.11625800	1.65264900
C	0.68017100	0.10065200	-3.59736700
C	1.36861800	0.62856600	-1.30154500
H	1.84396900	0.99117300	0.78208000
C	1.80010100	0.73970000	-4.08038500
H	-0.03296700	-0.35028300	-4.28315700
C	2.50289200	1.29480300	-1.83598300
C	2.72717000	1.36038200	-3.19808300
H	1.97634800	0.78888300	-5.15227700
H	3.19958400	1.76594500	-1.14660700
C	0.02232400	-5.61824400	-0.28748600
H	0.23867200	-6.26096100	0.57475000
H	0.51520800	-6.03655000	-1.16962800
C	-6.43498300	-4.54588100	-0.02185500
C	-5.56806900	-4.56371100	-1.09521000
C	-5.97345500	-4.98756000	1.24996900
C	-4.20593200	-4.93644100	-0.93992200
H	-5.90900900	-4.23575000	-2.07525800
C	-4.66720200	-5.37645400	1.43168900
H	-6.66354000	-4.98999100	2.08987300
C	-3.27575400	-4.86925400	-2.01295700
C	-3.73724100	-5.32840400	0.35561700
H	-4.32012700	-5.69709300	2.41094100
C	-1.94057300	-5.12050100	-1.80160000
H	-3.63307000	-4.58759100	-3.00054300
C	-2.35455900	-5.60391600	0.53231200
C	-1.46012600	-5.47972200	-0.51199100
H	-1.22903400	-5.03028300	-2.61631600
H	-1.99993400	-5.88382700	1.52224200
C	-7.25253100	-1.59027900	-0.07513800
H	-7.15079900	-1.73775100	-1.15917500
H	-7.86253900	-0.69833300	0.09569900
C	-7.81795800	-3.94714300	-0.14493400
H	-8.56549000	-4.58613100	0.33629900
H	-8.09167800	-3.83523600	-1.20363800

Imaginary Frequency = 0

E(RB3LYP) = -4064.5338306 a.u

***M*-5b**

Conformation #1 (Pop. = 52.95%)

Symbolic Z-matrix:

C	7.28986400	-2.78527500	-2.16707300
C	6.36770200	-1.69230000	-2.72740900
C	6.46688500	-0.44477000	-1.84339600
C	6.92881700	-3.07787100	-0.69188400
O	6.06553100	-0.75992500	-0.51859300
O	8.62321500	-2.30392400	-2.31966000
O	5.03220200	-2.20045200	-2.72957200
O	5.58923900	0.51314600	-2.40594300
O	5.72002400	-3.82818900	-0.63322000
C	5.55318600	2.35399000	-0.69546400
O	4.15557800	2.22111700	-2.61994700
O	6.85089900	1.96081700	-0.30245800
O	5.86480400	4.81885700	-0.84082400
H	6.68391800	-1.42963400	-3.74574500
H	4.92399600	2.59234500	0.17089100
H	7.13452600	-3.70927400	-2.73981800
H	7.70891100	-3.71360000	-0.25402200
O	-0.86786500	-3.53945600	2.16725300
C	-6.36437400	2.74559900	1.01693800
C	-7.01704100	1.53558600	0.81524800
C	-6.81396300	0.41539000	1.63837800
H	-7.72599400	1.47898400	-0.00700000
C	-5.27151800	1.77029400	2.93141200
C	-5.90615200	0.53565000	2.70609900
H	-4.60052300	1.85639300	3.77868100
C	-6.87843000	-2.28916600	-2.11979800
C	-5.97436700	-3.33504100	-1.83057200
C	-7.36709700	-1.51532200	-1.06664300
C	-5.64313300	-3.57876100	-0.50157800
C	-7.01735100	-1.75638500	0.27323400
H	-8.06682100	-0.71514300	-1.27985000
C	-6.15056300	-2.82270700	0.56625500
H	-4.97561700	-4.41399700	-0.30850200
C	-1.99011900	-2.81357200	2.50749700
C	-1.90507900	-1.65428700	3.29884400
C	-3.24381600	-3.27385300	2.12045900
C	-3.07650900	-0.98401000	3.64151000
C	-4.42991000	-2.60720200	2.46304500
H	-3.28284000	-4.18916900	1.53623100
C	-4.34416400	-1.42714000	3.22907700
C	-7.62012100	-0.84604400	1.33808300
H	-8.61046300	-0.53148400	0.98976600
H	-7.79762600	-1.40749200	2.25838200
C	-5.74308700	-3.21606800	1.98250300
H	-5.63228700	-4.30588000	2.00724500
H	-6.54771400	-2.98589600	2.68424100
H	-2.98488200	-0.09527900	4.25999300
C	-5.56163600	-0.60944700	3.65570200
H	-5.35002800	-0.17974800	4.64089200
H	-6.42639100	-1.26172300	3.79642400
H	7.48588100	-0.04487100	-1.85035000

H	5.11569300	-3.37682900	-1.25974100
H	9.23012000	-3.02807700	-2.09723500
H	4.41686100	-1.46871300	-2.48804600
H	6.82266900	1.17604400	0.27929200
H	6.69449100	4.73653100	-0.34265200
C	-0.06427200	-2.94621100	1.13461100
H	-0.63473900	-2.86164400	0.20186300
H	0.30087400	-1.95975500	1.43596100
H	0.78231700	-3.61908000	0.98340600
O	-7.23344900	-2.11931400	-3.43032000
C	-8.17755200	-1.09910300	-3.75029900
H	-7.80097800	-0.10573800	-3.47936600
H	-8.31584200	-1.15294600	-4.83091100
H	-9.13679000	-1.27473000	-3.24925800
O	-0.68805000	-1.14789600	3.70366700
O	-5.49068800	-4.21857400	-2.76796300
C	-5.48441200	2.87966700	2.11061800
O	-4.92020300	4.10540200	2.29516800
C	-3.99653100	4.26463600	3.36763000
H	-3.13672900	3.59253500	3.25844800
H	-3.65653800	5.29997500	3.31457300
H	-4.47394200	4.08802700	4.33934600
C	5.70227700	3.61064500	-1.55921100
H	6.56437900	3.43565100	-2.21993000
C	6.81763300	-1.79152100	0.15665100
H	6.18940400	-2.04106200	1.01389800
C	8.15509700	-1.24509600	0.67581400
H	8.82266000	-0.99579700	-0.15243900
H	8.64627300	-2.01902500	1.28211600
O	8.00329100	-0.04481800	1.43559800
C	4.76192600	1.38627500	-1.63371500
C	3.62599000	0.60581100	-0.93941900
H	4.00357600	0.08864300	-0.05971000
H	2.86746700	1.33456800	-0.63765200
C	4.43280400	3.61790400	-2.41244400
H	4.61790100	4.05651100	-3.39949100
O	3.04742500	-0.40478600	-1.76517900
C	3.23250100	4.35520900	-1.82534300
H	2.37213200	4.21603300	-2.49626100
H	3.46798100	5.42907300	-1.79108400
O	2.93989800	3.87392800	-0.52125300
O	-6.63113200	3.83095400	0.20523600
C	-5.97428900	3.81580300	-1.08926300
H	-6.10154300	2.82819300	-1.54759900
H	-6.52711500	4.54981900	-1.68144200
C	-4.85218600	-3.72609900	-3.97542100
H	-5.58795800	-3.20484900	-4.59038300
H	-4.55074200	-4.64422000	-4.48523000
C	0.05321900	-1.96349900	4.63157500
H	-0.23709700	-1.67169000	5.65181400
H	-0.20823300	-3.01657900	4.49866700
C	7.72611200	-0.19731400	2.83871200
H	8.14238700	0.70525100	3.29981000
H	8.27559900	-1.06224700	3.23153300
C	2.17152000	0.05833100	-2.81229600
H	1.83833600	1.07602800	-2.59465700
H	2.74121400	0.09952300	-3.75019100
C	1.94494400	4.61965400	0.17636900

H	2.10910700	4.38135700	1.23417300
H	2.11638700	5.69812600	0.04916200
C	6.25224300	-0.31205600	3.16501000
C	5.73069100	-1.43675300	3.77062400
C	5.37944400	0.76335800	2.83604300
C	4.33882200	-1.55805700	4.03581400
H	6.38557500	-2.26308500	4.04037400
C	4.02731000	0.67663300	3.07149200
H	5.79607900	1.66150900	2.38715800
C	3.77645800	-2.71748900	4.63405500
C	3.46249200	-0.48988400	3.65949500
H	3.37032200	1.50170100	2.80726500
C	2.41707900	-2.82532100	4.81919400
H	4.43492700	-3.53208000	4.92536500
C	2.06490500	-0.63084700	3.86931100
C	1.53857600	-1.78001800	4.42354000
H	2.00264500	-3.72919800	5.25937500
H	1.40335000	0.17328800	3.56122800
C	0.97962300	-0.85913200	-2.94653500
C	-0.28207100	-0.32225400	-3.09811700
C	1.13847300	-2.27355400	-2.97144900
C	-1.42297100	-1.14551600	-3.29474200
H	-0.41976200	0.75655500	-3.07392900
C	0.05230700	-3.10096300	-3.14324000
H	2.13117200	-2.69842400	-2.85307200
C	-2.72283400	-0.60529300	-3.48575800
C	-1.25686800	-2.56812500	-3.31597800
H	0.18462500	-4.18009900	-3.16080700
C	-3.80301500	-1.43071300	-3.69987400
H	-2.85005500	0.47452200	-3.47348600
C	-2.39582900	-3.38921000	-3.52816600
C	-3.65123500	-2.84448600	-3.72512100
H	-4.78867000	-1.00599500	-3.86724200
H	-2.26327500	-4.46922000	-3.55164600
C	0.51976300	4.26558700	-0.20250100
C	-0.43438500	5.24474900	-0.38976500
C	0.13240200	2.89894600	-0.28384900
C	-1.79839900	4.91672100	-0.62374100
H	-0.15454800	6.29504400	-0.33321800
C	-1.17203700	2.54549500	-0.53669300
H	0.88015000	2.12795800	-0.12787300
C	-2.80898100	5.90773100	-0.76309300
C	-2.17711900	3.53789900	-0.70069800
H	-1.45528300	1.49729500	-0.59072000
C	-4.12675100	5.55004100	-0.93237300
H	-2.52575400	6.95662800	-0.71868200
C	-3.54265100	3.20561000	-0.90326900
C	-4.51361500	4.18296400	-0.99585300
H	-4.89078000	6.31919100	-1.01651300
H	-3.81989200	2.15521300	-0.96051200

Imaginary Frequency = 0

E(RB3LYP) = -4064.5224152 a.u.

Conformation #2 (Pop. = 40.31%)

Symbolic Z-matrix:

C	-7.28565600	2.80017600	-2.15052900
C	-6.36295200	1.70456900	-2.71924400
C	-6.46544300	0.45336100	-1.84150400
C	-6.92819300	3.07877600	-0.67757700
O	-6.06490800	0.76104600	-0.51519000
O	-8.65158600	2.39592500	-2.20225600
O	-5.02551800	2.20834000	-2.72495100
O	-5.59203100	-0.50631400	-2.40734700
O	-5.71554100	3.82174600	-0.61373400
C	-5.55854100	-2.35126200	-0.70111500
O	-4.16197800	-2.21654300	-2.62681200
O	-6.85744300	-1.95893300	-0.31142500
O	-5.86723300	-4.81644500	-0.84699800
H	-6.67492600	1.44175800	-3.74133000
H	-4.93129200	-2.58935700	0.16667200
H	-7.12738100	3.73050000	-2.71209300
H	-7.71054500	3.71239500	-0.24485800
O	0.87072900	3.54757700	2.15640700
C	6.36112800	-2.74627600	1.02811400
C	7.01506100	-1.53756200	0.82274300
C	6.81284100	-0.41453500	1.64221600
H	7.72436100	-1.48428800	0.00057200
C	5.26884100	-1.76384600	2.93925200
C	5.90474100	-0.53054300	2.71016800
H	4.59762700	-1.84663900	3.78667400
C	6.88060100	2.27866000	-2.12429200
C	5.97779000	3.32651100	-1.83834600
C	7.36815100	1.50737400	-1.06873900
C	5.64662400	3.57458600	-0.51014500
C	7.01852300	1.75289800	0.27036000
H	8.06696200	0.70573200	-1.27944900
C	6.15296600	2.82113200	0.56003600
H	4.98009600	4.41120900	-0.31967700
C	1.99208400	2.82163900	2.49948300
C	1.90567000	1.66465100	3.29404400
C	3.24639600	3.27976600	2.11186300
C	3.07637800	0.99451000	3.63941200
C	4.43174900	2.61311300	2.45697700
H	3.28648500	4.19332900	1.52497300
C	4.34462600	1.43541000	3.22646000
C	7.62024700	0.84518100	1.33806100
H	8.61030300	0.52857100	0.99079900
H	7.79821900	1.40928400	2.25663900
C	5.74566400	3.21923400	1.97500400
H	5.63597800	4.30922700	1.99642100
H	6.54989400	2.99034400	2.67761600
H	2.98362300	0.10760200	4.26033500
C	5.56117000	0.61791300	3.65604900
H	5.34889100	0.19157300	4.64255300
H	6.42653700	1.26977600	3.79489600
H	-7.48669200	0.05896000	-1.85165800
H	-5.11022700	3.37023100	-1.23903300

H	-8.90217400	2.29178900	-3.13480000
H	-4.41137100	1.47360900	-2.48877600
H	-6.83089800	-1.17961800	0.27781700
H	-6.69637700	-4.73422400	-0.34788500
C	0.06664100	2.95176100	1.12561700
H	0.63730800	2.86306300	0.19337800
H	-0.29998800	1.96690300	1.43036800
H	-0.77893100	3.62529400	0.97171700
O	7.23568600	2.10449000	-3.43423800
C	8.17874800	1.08230900	-3.75098100
H	7.80102700	0.09015300	-3.47723400
H	8.31736400	1.13282500	-4.83171200
H	9.13805500	1.25835700	-3.25021900
O	0.68808100	1.15984500	3.69916600
O	5.49541600	4.20794500	-2.77838700
C	5.48072900	-2.87598900	2.12195300
O	4.91515500	-4.10055200	2.31015900
C	3.99152800	-4.25556800	3.38328600
H	3.13236200	-3.58296300	3.27220900
H	3.65050800	-5.29073200	3.33350600
H	4.46930500	-4.07642100	4.35435700
C	-5.70555000	-3.60802900	-1.56516000
H	-6.56756700	-3.43377300	-2.22622800
C	-6.81938500	1.78795200	0.16430600
H	-6.19280200	2.03469000	1.02351700
C	-8.15636000	1.23768800	0.68050400
H	-8.82341200	0.98713800	-0.14744600
H	-8.64982400	2.00909100	1.28792700
O	-8.00071900	0.03628000	1.43858200
C	-4.76579300	-1.38279900	-1.63780400
C	-3.62764800	-0.60603300	-0.94303500
H	-4.00360300	-0.08843400	-0.06290600
H	-2.87104600	-1.33702800	-0.64204400
C	-4.43599000	-3.61375300	-2.41807500
H	-4.62003700	-4.05324100	-3.40492300
O	-3.04646100	0.40360000	-1.76835600
C	-3.23472600	-4.34910900	-1.83031600
H	-2.37409900	-4.20844500	-2.50058800
H	-3.46865600	-5.42332500	-1.79658700
O	-2.94379900	-3.86795400	-0.52579900
O	6.62707200	-3.83457000	0.22010200
C	5.97198100	-3.82238100	-1.07528300
H	6.10098700	-2.83624200	-1.53628100
H	6.52476000	-4.55870800	-1.66463000
C	4.85679100	3.71287100	-3.98469300
H	5.59219700	3.18918500	-4.59801800
H	4.55647100	4.62992800	-4.49707600
C	-0.05377200	1.97811100	4.62402900
H	0.23935600	1.69314500	5.64542000
H	0.20393600	3.03130400	4.48460700
C	-7.72317600	0.18706600	2.84176500
H	-8.13636400	-0.71760600	3.30153800
H	-8.27513700	1.04958700	3.23639500
C	-2.17142700	-0.06113000	-2.81549200
H	-1.83933900	-1.07906100	-2.59725900
H	-2.74135900	-0.10229200	-3.75324200
C	-1.95128800	-4.61472700	0.17420800
H	-2.11744000	-4.37577800	1.23155600

H	-2.12398200	-5.69300100	0.04705700
C	-6.24944300	0.30590400	3.16729800
C	-5.73094000	1.43124400	3.77438200
C	-5.37341400	-0.76585600	2.83516900
C	-4.33909700	1.55697700	4.03756000
H	-6.38828400	2.25486900	4.04640900
C	-4.02123900	-0.67486500	3.06877800
H	-5.78755300	-1.66468500	2.38532400
C	-3.77976900	2.71748300	4.63665800
C	-3.45962100	0.49264500	3.65781700
H	-3.36174900	-1.49712600	2.80203600
C	-2.42044000	2.83007900	4.81910000
H	-4.44065500	3.52915000	4.93063100
C	-2.06210200	0.63843500	3.86494600
C	-1.53889500	1.78870400	4.41973700
H	-2.00842200	3.73480800	5.25982000
H	-1.39820100	-0.16266500	3.55410400
C	-0.97848100	0.85480200	-2.95072700
C	0.28264700	0.31618100	-3.10084300
C	-1.13568700	2.26936600	-2.97840900
C	1.42455800	1.13772200	-3.29877100
H	0.41908300	-0.76273400	-3.07450000
C	-0.04851000	3.09516300	-3.15158400
H	-2.12790000	2.69567200	-2.86106100
C	2.72383500	0.59559500	-3.48834200
C	1.26008900	2.56046900	-3.32299700
H	-0.17957300	4.17441400	-3.17131000
C	3.80499700	1.41931500	-3.70404700
H	2.84981800	-0.48433500	-3.47367200
C	2.40001800	3.37979100	-3.53680300
C	3.65481900	2.83319500	-3.73244100
H	4.79020900	0.99312200	-3.87026500
H	2.26871800	4.45989900	-3.56263400
C	-0.52472300	-4.26287200	-0.20159800
C	0.42882100	-5.24351300	-0.38423100
C	-0.13550700	-2.89686000	-0.28455700
C	1.79383100	-4.91754300	-0.61527100
H	0.14762600	-6.29336800	-0.32627600
C	1.17000600	-2.54544500	-0.53471900
H	-0.88269600	-2.12464600	-0.13208500
C	2.80363500	-5.90998600	-0.75001600
C	2.17433800	-3.53932700	-0.69421100
H	1.45459700	-1.49768400	-0.59011500
C	4.12218200	-5.55415100	-0.91718400
H	2.51914300	-6.95846600	-0.70389400
C	3.54068600	-3.20901700	-0.89453900
C	4.51074000	-4.18765700	-0.98305000
H	4.88551500	-6.32435300	-0.99795200
H	3.81920000	-2.15905900	-0.95362000

Imaginary Frequency = 0

E(RB3LYP) = -4064.5221581 a.u

***M*-5a⊂Ach**

Symbolic Z-matrix:

C	-5.498030	-0.383334	2.720378
C	-6.721538	-1.171521	2.276302
C	-6.476420	-1.690676	0.852081
C	-4.139629	-2.006684	1.314958
C	-4.270402	-1.284733	2.677047
O	-5.380700	-2.580580	0.882503
O	-5.767596	0.094652	4.040015
O	-6.246423	-0.562649	0.035516
C	-3.186685	-3.197706	1.423700
O	-1.934671	-2.737743	1.925576
C	-7.119786	1.896969	-1.579752
C	-8.307092	1.411306	-0.752283
C	-6.860678	-0.428615	-1.251027
O	-6.305332	0.728763	-1.834351
C	-6.564971	-1.619343	-2.160904
O	-5.171807	-1.828898	-2.225398
H	-6.857885	-2.039497	2.936833
H	-8.088601	1.512242	0.319038
H	-7.500504	2.266142	-2.542050
H	-5.354235	0.458284	2.031573
H	-4.389310	-2.044908	3.467639
H	-3.784296	-1.288918	0.566108
H	-3.631494	-3.929006	2.115449
H	-3.059476	-3.678850	0.445799
H	-6.982059	-1.397765	-3.156605
H	-7.080087	-2.515630	-1.777361
C	4.613090	-3.415787	-1.837405
C	4.839327	-2.307300	-2.648422
C	5.419758	-3.585065	-0.687776
C	5.775671	-1.309357	-2.335551
H	4.258634	-2.243205	-3.565113
C	6.314541	-2.572099	-0.345553
C	6.493100	-1.423063	-1.134346
H	6.909184	-2.673439	0.555386
C	2.976600	1.857785	-4.455871
C	3.110134	3.050829	-3.707124
C	3.907332	0.840480	-4.272388
C	4.128421	3.137108	-2.762558
C	4.968267	0.945810	-3.353250
H	3.843784	-0.052798	-4.884371
C	5.069755	2.104877	-2.566361
H	4.247048	4.051330	-2.190286
C	5.300601	2.317419	2.138257
C	5.932049	1.135220	2.596697
C	5.384577	2.635419	0.778087
C	6.588037	0.340462	1.660540
C	6.072958	1.837103	-0.156879
H	4.951678	3.569372	0.434410
C	6.681980	0.655029	0.297808
O	6.073640	0.747293	3.896574
O	2.253927	4.053641	-4.067449
C	1.999584	5.161150	-3.213292
H	2.898151	5.471855	-2.666095

H	1.754752	5.980420	-3.899860
C	5.994369	-0.181710	-3.338334
H	5.999364	-0.630900	-4.338542
H	6.994648	0.238219	-3.207092
C	6.212866	2.362409	-1.586065
H	6.346027	3.448825	-1.521003
H	7.144986	1.986454	-2.017829
H	7.073637	-0.551812	2.045499
C	7.416997	-0.335130	-0.601197
H	8.210195	-0.808829	-0.012011
H	7.924122	0.182267	-1.419124
H	-7.321021	-2.284039	0.498357
H	-4.957486	0.536315	4.342315
O	3.674042	-4.322712	-2.257231
O	-5.748303	2.546968	0.275482
O	-9.471430	2.139490	-1.109516
H	-10.211083	1.733043	-0.629292
C	2.793989	-4.914081	-1.287355
H	3.066065	-5.968778	-1.169036
H	2.941303	-4.435025	-0.313621
C	5.034375	0.895945	4.894605
H	4.834911	1.953536	5.077993
H	5.526694	0.480050	5.782138
O	5.271240	-4.752838	0.008418
O	4.683534	3.094266	3.073573
O	1.934669	1.822410	-5.336288
C	1.809808	0.688092	-6.178542
H	1.650385	-0.233135	-5.600689
H	0.935413	0.876312	-6.803747
H	2.693483	0.560669	-6.817355
C	6.105680	-4.977214	1.136312
H	5.923244	-4.239077	1.927801
H	5.845208	-5.970959	1.504347
H	7.167129	-4.957492	0.858207
C	4.034939	4.291148	2.660034
H	3.285939	4.097303	1.884808
H	3.517173	4.671137	3.540710
H	4.763820	5.028649	2.297873
C	-6.288691	3.005914	-0.952844
H	-6.938002	3.882946	-0.791985
H	-5.491279	3.296407	-1.648513
C	-1.192013	-3.735262	2.671055
H	-1.821429	-4.048587	3.521233
H	-1.022900	-4.613567	2.032982
C	-4.750740	3.375452	0.842015
H	-4.549511	2.929112	1.824061
H	-5.138313	4.392735	1.019828
C	0.107374	-3.133678	3.108008
C	0.110771	-1.947040	3.872092
C	1.329752	-3.678961	2.695150
C	1.311860	-1.253683	4.162466
H	-0.828254	-1.532145	4.234946
C	2.539172	-3.055681	3.007502
H	1.332412	-4.596238	2.108451
C	1.339992	-0.000454	4.834890
C	2.570066	-1.813542	3.715777
H	3.480824	-3.507921	2.702228
C	2.532845	0.696778	5.019795

H	0.403080	0.418099	5.198555
C	3.762610	-1.097663	3.964679
C	3.755419	0.158524	4.593579
H	2.514860	1.672029	5.501816
H	4.708140	-1.526340	3.640689
C	-3.469355	3.458210	0.026627
C	-2.624061	4.546147	0.169250
C	-3.129490	2.429432	-0.888072
C	-1.435170	4.670604	-0.596591
H	-2.878932	5.346326	0.863026
C	-2.001465	2.542131	-1.678512
H	-3.795714	1.578115	-0.995821
C	-0.547073	5.771902	-0.459708
C	-1.134218	3.665013	-1.574544
H	-1.782255	1.775987	-2.419584
C	0.566085	5.888022	-1.264538
H	-0.759912	6.527922	0.292262
C	0.000126	3.836535	-2.413934
C	0.839529	4.924189	-2.267345
H	1.232695	6.739754	-1.143449
H	0.192961	3.114516	-3.202628
C	-3.336987	-3.173571	-2.945324
C	-2.843894	-4.281018	-2.278509
C	-2.421824	-2.243872	-3.500125
C	-1.450737	-4.490142	-2.106547
H	-3.534504	-5.007430	-1.854554
C	-1.060345	-2.423676	-3.366164
H	-2.808198	-1.376696	-4.029794
C	-0.930975	-5.601426	-1.390732
C	-0.530058	-3.534616	-2.652021
H	-0.369590	-1.705475	-3.805075
C	0.425868	-5.738528	-1.184585
H	-1.622482	-6.343648	-0.998869
C	0.862908	-3.715243	-2.430858
C	1.341939	-4.782399	-1.688191
H	0.803748	-6.591916	-0.625434
H	1.563687	-3.004152	-2.861520
C	-4.821522	-2.935894	-3.050633
H	-5.113545	-2.725230	-4.094121
H	-5.370902	-3.835784	-2.731397
O	-9.134685	-0.848917	-0.202227
H	-8.860876	-0.608527	0.708009
O	-3.130683	-0.469204	2.944976
H	-2.364370	-1.062808	2.813709
O	-7.899538	-0.368607	2.298839
H	-7.837090	0.196453	3.087846
C	-8.368488	-0.079997	-1.100951
H	-8.844915	-0.184270	-2.083972
C	1.717219	0.983690	1.285769
H	2.060367	0.416960	2.152248
H	2.509072	1.673846	0.988041
C	0.454828	1.765891	1.654711
H	-0.059807	2.188757	0.784649
H	-0.241296	1.130629	2.205924
O	0.951109	2.829915	2.472804
C	1.450950	0.732519	-1.170999
H	1.334456	-0.004607	-1.966371
H	0.586979	1.394842	-1.153173

H	2.364483	1.306686	-1.328922
C	2.783884	-0.869914	0.107578
H	2.798091	-1.482120	1.010502
H	2.733759	-1.502060	-0.778435
H	3.666413	-0.230915	0.058551
C	0.335346	-0.871269	0.330693
H	0.343529	-1.645142	-0.438494
H	0.371735	-1.327479	1.319429
H	-0.561888	-0.260145	0.225509
N	1.552279	0.001810	0.138232
C	0.181167	3.458798	3.411951
C	-1.260530	3.024335	3.560780
H	-1.797481	3.108683	2.609393
H	-1.339226	1.983680	3.893731
H	-1.727952	3.671981	4.303105
O	0.695262	4.337190	4.060599

Imaginary Frequency = 0

E(RB3LYP) = -4545.97271 a.u.

***M*-5a⊂Ch**

Symbolic Z-matrix:

C	-5.304476	-1.134014	2.743393
C	-6.550413	-1.748385	2.116832
C	-6.360365	-1.838035	0.594812
C	-4.006441	-2.244373	0.873044
C	-4.105799	-2.005821	2.395686
O	-5.256852	-2.685162	0.332367
O	-5.550825	-1.075760	4.148602
O	-6.177658	-0.526475	0.113753
C	-3.024104	-3.375663	0.558997
O	-1.750371	-3.064488	1.132626
C	-7.176336	2.263488	-0.752640
C	-8.288104	1.546889	0.007653
C	-6.872836	-0.059917	-1.053641
O	-6.358267	1.221744	-1.335338
C	-6.639448	-0.959121	-2.266408
O	-5.256321	-1.145484	-2.456838
H	-6.678084	-2.770228	2.501863
H	-7.980727	1.363366	1.046011
H	-7.638585	2.837689	-1.567828
H	-5.163156	-0.125003	2.333409
H	-4.239971	-2.975929	2.899249
H	-3.698381	-1.313263	0.381348
H	-3.419727	-4.303632	0.997845
H	-2.934957	-3.512970	-0.524382
H	-7.103174	-0.472064	-3.139532
H	-7.150902	-1.924829	-2.117013
C	4.489213	-2.682073	-2.609511
C	4.673800	-1.372831	-3.043168
C	5.370782	-3.202235	-1.635283
C	5.663473	-0.528040	-2.517813
H	4.029418	-1.026390	-3.847246
C	6.323753	-2.353266	-1.075131
C	6.476664	-1.018675	-1.484679
H	6.984500	-2.733124	-0.303972

C	2.935255	3.275551	-3.407291
C	3.232035	4.222626	-2.401278
C	3.777891	2.179027	-3.568269
C	4.305371	3.979046	-1.549059
C	4.902617	1.966777	-2.749665
H	3.598788	1.487251	-4.384328
C	5.151137	2.861334	-1.694699
H	4.549751	4.711240	-0.785481
C	5.634017	1.577070	2.804968
C	6.228409	0.293665	2.839029
C	5.660055	2.300069	1.608529
C	6.802357	-0.187199	1.666825
C	6.267882	1.814406	0.434864
H	5.245173	3.302915	1.590589
C	6.845844	0.534787	0.467300
O	6.415913	-0.476280	3.949886
O	2.491974	5.374535	-2.443643
C	2.233479	6.137386	-1.272460
H	3.086974	6.129765	-0.582752
H	2.131404	7.168184	-1.632766
C	5.854813	0.844996	-3.150677
H	5.758011	0.716382	-4.235340
H	6.883761	1.178618	-2.994387
C	6.360852	2.754355	-0.768637
H	6.564534	3.759793	-0.381233
H	7.243330	2.493021	-1.360347
H	7.262358	-1.169340	1.725420
C	7.481873	-0.155521	-0.734200
H	8.293644	-0.796825	-0.372993
H	7.951590	0.570500	-1.402172
H	-7.213805	-2.329094	0.125215
H	-4.765131	-0.687115	4.565001
O	3.520487	-3.423206	-3.234243
O	-5.617615	2.490390	1.051420
O	-9.480451	2.313290	-0.048144
H	-10.180532	1.766703	0.344393
C	2.671051	-4.263148	-2.437574
H	2.970554	-5.307595	-2.579444
H	2.813171	-4.027902	-1.376393
C	5.392575	-0.671850	4.957424
H	5.209705	0.263257	5.492165
H	5.894487	-1.365328	5.643078
O	5.233349	-4.526767	-1.322176
O	5.116556	2.051923	3.980849
O	1.843666	3.547030	-4.181952
C	1.564326	2.681660	-5.270334
H	1.355729	1.656710	-4.932724
H	0.675348	3.089325	-5.754554
H	2.392621	2.659013	-5.990307
C	6.150712	-5.099296	-0.401769
H	6.064133	-4.643487	0.592885
H	5.885575	-6.155993	-0.336844
H	7.185045	-5.003614	-0.756552
C	4.556981	3.352204	3.997564
H	3.700189	3.435756	3.314244
H	4.215435	3.518216	5.020905
H	5.300361	4.116602	3.734161
C	-6.326548	3.222274	0.067170

H	-6.994203	3.966981	0.532924
H	-5.636410	3.759001	-0.596531
C	-0.964299	-4.241161	1.485265
H	-1.569203	-4.824672	2.200074
H	-0.817363	-4.851190	0.584944
C	-4.660255	3.238461	1.776415
H	-4.323514	2.569076	2.577594
H	-5.128765	4.114827	2.255470
C	0.347724	-3.810810	2.061279
C	0.390872	-2.921277	3.155640
C	1.557496	-4.260161	1.509937
C	1.615269	-2.392550	3.636481
H	-0.530365	-2.608921	3.645012
C	2.785125	-3.825113	2.008808
H	1.533394	-4.958712	0.675106
C	1.673555	-1.371928	4.624179
C	2.855849	-2.850480	3.052719
H	3.709995	-4.194268	1.571579
C	2.886755	-0.801473	4.998441
H	0.743912	-1.009157	5.057745
C	4.070573	-2.283583	3.499249
C	4.098100	-1.251028	4.451502
H	2.898838	0.000519	5.734489
H	5.004119	-2.637954	3.068069
C	-3.450777	3.682199	0.968442
C	-2.604202	4.645664	1.488239
C	-3.136467	3.080272	-0.275309
C	-1.411960	5.024903	0.821590
H	-2.834743	5.112195	2.444911
C	-2.009675	3.467558	-0.976625
H	-3.797119	2.314727	-0.672610
C	-0.490544	5.957295	1.372620
C	-1.111564	4.436039	-0.451731
H	-1.794859	3.027268	-1.948393
C	0.673405	6.278105	0.708802
H	-0.711617	6.403517	2.339365
C	0.078825	4.819923	-1.128409
C	0.967922	5.709530	-0.556830
H	1.373318	6.982253	1.155235
H	0.291838	4.402927	-2.108725
C	-3.476018	-2.235159	-3.597706
C	-2.973736	-3.477355	-3.247852
C	-2.571098	-1.191342	-3.910439
C	-1.578130	-3.716612	-3.148687
H	-3.659017	-4.289975	-3.013958
C	-1.207245	-1.392639	-3.841278
H	-2.965910	-0.219175	-4.195135
C	-1.044759	-4.967796	-2.737958
C	-0.667250	-2.645445	-3.435103
H	-0.521962	-0.584487	-4.091295
C	0.314456	-5.134718	-2.562657
H	-1.727079	-5.793872	-2.550954
C	0.725153	-2.860018	-3.262455
C	1.216873	-4.069775	-2.801262
H	0.703063	-6.097139	-2.236014
H	1.417440	-2.052883	-3.486511
C	-4.958291	-1.970008	-3.581823
H	-5.282621	-1.462222	-4.506399

H	-5.514103	-2.918714	-3.514278
O	-9.080949	-0.793936	-0.033917
H	-8.760994	-0.804977	0.892485
O	-2.917465	-1.381970	2.896292
H	-2.183667	-1.922076	2.527232
O	-7.711153	-0.979743	2.415359
H	-7.633691	-0.709346	3.346590
C	-8.369360	0.205460	-0.726738
H	-8.901840	0.364415	-1.673144
C	0.267284	0.358419	1.820783
H	0.032426	-0.682131	2.056664
H	0.980682	0.709379	2.569861
C	-1.009273	1.214830	1.853790
H	-0.782854	2.273105	1.702954
H	-1.708503	0.912060	1.065555
O	-1.599713	1.095059	3.132058
H	-2.143367	0.279876	3.123937
C	1.539293	1.670393	0.111928
H	2.069619	1.590268	-0.838615
H	0.715204	2.375506	0.017078
H	2.234293	1.997748	0.886776
C	2.181354	-0.632571	0.623869
H	1.803704	-1.638414	0.801183
H	2.759361	-0.600374	-0.301960
H	2.800738	-0.318576	1.464260
C	0.107790	-0.206638	-0.599379
H	0.711952	-0.405361	-1.484670
H	-0.355585	-1.133197	-0.254372
H	-0.652686	0.539503	-0.827940
N	1.012651	0.314164	0.487669

Imaginary Frequency = 0

E(RB3LYP) = -4393.317892 a.u.

Tetrahedron Letters 61 (2020) 151888

Contents lists available at ScienceDirect

Tetrahedron Letters

journal homepage: www.elsevier.com/locate/tetlet

Digest paper

Synthesis of fine chemicals with high added value from sucrose: Towards sucrose-based macrocycles

Sławomir Jarosz *, Patrycja Sokołowska, Łukasz Szyszka

Institute of Organic Chemistry, Polish Academy of Sciences, Kasprzaka 44/52, 01-224 Warsaw, Poland

ARTICLE INFO

Article history:
Received 9 January 2020
Revised 2 March 2020
Accepted 28 March 2020
Available online 4 April 2020

Keywords:
Sucrose
Macrocyclic receptors
Cryptands
Complexation

ABSTRACT

Application of sucrose for the preparation of fine chemicals is presented. Special attention is paid to macrocyclic receptors with sucrose scaffold: their synthesis and properties. This account will emphasize the work done in the laboratory of the authors.

https://doi.org/10.1016/j.tetlet.2020.151888
0040-4039/

Scheme 12. Synthesis of polymeric nanoparticles derived from sucrose and cholic acid.

Institute of Organic Chemistry
Polish Academy of Sciences

mgr inż. Łukasz Szyszka

Institute of Organic Chemistry
Polish Academy of Sciences
Kasprzaka 44/52
01-224 Warsaw, Poland

Warsaw, 08-07-2021

Statement of contribution

Hereby, I would like to claim my contribution to the papers:

1. Ł. Szyszka, P. Cmoch, A. Butkiewicz, M. A. Potopnyk, S. Jarosz „Synthesis of Cyclotriveratrylene-Sucrose-Based Capsules" *Org. Lett.* 2019, *21*, 6523–6528.

I conducted all the syntheses, optimized the cyclization reaction conditions, isolated all compounds, and determined the structures of most of them. In addition, I co-wrote the manuscript and supporting information.

2. Ł. Szyszka, P. Cmoch, M. Górecki, M. Ceborska, M. A. Potopnyk, S. Jarosz „Chiral Molecular Cages Based on Cyclotriveratrylene and Sucrose Units Connected with *p*-Phenylene Linkers" *Eur. J. Org. Chem.* 2021, 897–906. (Front Cover)

I designed and plan the research, conducted all the syntheses, optimized the cyclization reaction conditions, isolated all compounds, and determined the structures of most of them. I obtained suitable crystals for the X-Ray analysis. I performed all recognition experiments (^{1}H NMR titrations) and elaborated the results. In addition, I co-wrote the manuscript, supporting information, and responses for reviewers. I created the graphic illustration for the Front Cover.

3. Ł. Szyszka, M. Górecki, P. Cmoch, S. Jarosz „Fluorescent Molecular Cages with Sucrose and Cyclotriveratrylene Units for the Selective Recognition of Choline and Acetylcholine" *J. Org. Chem.* 2021, *86*, 5129–5141.

I designed and plan the research, conducted all the syntheses, optimized the cyclization reaction conditions, isolated all compounds, and determined the structures of most of them. I performed all recognition experiments (fluorescent and ^{1}H NMR titrations) and elaborated the results. In addition, I co-wrote the manuscript, supporting information, and responses for reviewers.

4. S. Jarosz, P. Sokołowska, Ł. Szyszka „Synthesis of fine chemicals with high added value from sucrose: Towards sucrose-based macrocycles" *Tetrahedron Lett.* 2020, *61*, 151888. (Digest paper)

I found the literature references, participated in the writing of this review paper and responses for reviewers.

S. Jarosz

Łukasz Szyszka

Łukasz Szyszka

Institute of Organic Chemistry
Polish Academy of Sciences

prof. Sławomir Jarosz

Institute of Organic Chemistry
Polish Academy of Sciences
Kasprzaka 44/52
01-224 Warsaw, Poland

Warsaw, 08-07-2021

Statement of contribution

Hereby, I would like to declare that my contribution to the papers:

1. Ł. Szyszka, P. Cmoch, A. Butkiewicz, M. A. Potopnyk, S. Jarosz „Synthesis of Cyclotriveratrylene-Sucrose-Based Capsules" *Org. Lett.* 2019, *21*, 6523–6528.

2. Ł. Szyszka, P. Cmoch, M. Górecki, M. Ceborska, M. A. Potopnyk, S. Jarosz „Chiral Molecular Cages Based on Cyclotriveratrylene and Sucrose Units Connected with *p*-Phenylene Linkers" *Eur. J. Org. Chem.* 2021, 897–906. (Front Cover)

3. Ł. Szyszka, M. Górecki, P. Cmoch, S. Jarosz „Fluorescent Molecular Cages with Sucrose and Cyclotriveratrylene Units for the Selective Recognition of Choline and Acetylcholine" *J. Org. Chem.* 2021, *86*, 5129–5141.

concerned the supervision of research, consultation of results, recommendations for further work, writing and correction of manuscripts.

The review paper
4. S. Jarosz, P. Sokołowska, Ł. Szyszka „Synthesis of fine chemicals with high added value from sucrose: Towards sucrose-based macrocycles" *Tetrahedron Lett.* 2020, *61*, 151888. (Digest paper)

I put the concept, wrote the manuscript based on my results and the literature study; the latter was strongly supported by Łukasz.

Sławomir Jarosz

Institute of Organic Chemistry
Polish Academy of Sciences

dr Mykhaylo A. Potopnyk

Institute of Organic Chemistry
Polish Academy of Sciences
Kasprzaka 44/52
01-224 Warsaw, Poland

Warsaw, 08-07-2021

Statement of contribution

Hereby, I would like to claim my contribution to the papers:

1. Ł. Szyszka, P. Cmoch, A. Butkiewicz, M. A. Potopnyk, S. Jarosz „Synthesis of Cyclotriveratrylene-Sucrose-Based Capsules" *Org. Lett.* 2019, *21*, 6523–6528.

I conceived the project, supervised research, consulted the results, and gave recommendations for further work. I co-wrote and corrected the manuscript and responses for reviewers.

2. Ł. Szyszka, P. Cmoch, M. Górecki, M. Ceborska, M. A. Potopnyk, S. Jarosz „Chiral Molecular Cages Based on Cyclotriveratrylene and Sucrose Units Connected with *p*-Phenylene Linkers" *Eur. J. Org. Chem.* 2021, 897–906.

I supervised research, consulted results, and gave recommendations for further work. I corrected the final version of manuscript.

Mykhaylo Potopnyk

Institute of Organic Chemistry
Polish Academy of Sciences

dr Piotr Cmoch

Institute of Organic Chemistry
Polish Academy of Sciences
Kasprzaka 44/52
01-224 Warsaw, Poland

Warsaw, 09-07-2021

Statement of contribution

Hereby, I would like to claim my contribution to the papers:

1. Ł. Szyszka, P. Cmoch, A. Butkiewicz, M. A. Potopnyk, S. Jarosz „Synthesis of Cyclotriveratrylene-Sucrose-Based Capsules" *Org. Lett.* 2019, *21*, 6523–6528.

I optimized and registered NMR experiments, determined the structures of cages, and wrote a section concerning NMR spectroscopy results.

2. Ł. Szyszka, P. Cmoch, M. Górecki, M. Ceborska, M. A. Potopnyk, S. Jarosz „Chiral Molecular Cages Based on Cyclotriveratrylene and Sucrose Units Connected with *p*-Phenylene Linkers" *Eur. J. Org. Chem.* 2021, 897–906. (Front Cover)

I optimized and registered NMR experiments, determined the structures of cages, and wrote a section concerning NMR spectroscopy results.

3. Ł. Szyszka, M. Górecki, P. Cmoch, S. Jarosz „Fluorescent Molecular Cages with Sucrose and Cyclotriveratrylene Units for the Selective Recognition of Choline and Acetylcholine" *J. Org. Chem.* 2021, *86*, 5129–5141.

I optimized and registered NMR experiments, determined the structures of cages, and wrote a section concerning NMR spectroscopy results.

Piotr Cmoch

Institute of Organic Chemistry
Polish Academy of Sciences
Institute of Organic Chemistry
Polish Academy of Sciences
Kasprzaka 44/52
01-224 Warsaw, Poland

dr inż. Marcin Górecki

Warsaw, 08-07-2021

Statement of contribution

Hereby, I would like to claim my contribution to the papers:

1. Ł. Szyszka, P. Cmoch, M. Górecki, M. Ceborska, M. A. Potopnyk, S. Jarosz „Chiral Molecular Cages Based on Cyclotriveratrylene and Sucrose Units Connected with *p*-Phenylene Linkers" *Eur. J. Org. Chem.* 2021, 897–906.

2. Ł. Szyszka, M. Górecki, P. Cmoch, S. Jarosz „Fluorescent Molecular Cages with Sucrose and Cyclotriveratrylene Units for the Selective Recognition of Choline and Acetylcholine" *J. Org. Chem.* 2021, *86*, 5129–5141.

I performed ECD experiments, DFT calculations, and participated in the writing of the paper.

Marcin Górecki

Instytut Chemii Organicznej
Polskiej Akademii Nauk

Dr Aleksandra Butkiewicz

+48 22 343 23 26
aleksandra.butkiewicz@icho.edu.pl

Warszawa, 8 lipca 2021 r.

Statement of contribution

Hereby, I would like to claim my contribution to the paper:

Ł. Szyszka, P. Cmoch, A. Butkiewicz, M. A. Potopnyk, S. Jarosz „Synthesis of Cyclotriveratrylene-Sucrose-Based Capsules" *Org. Lett.* **2019**, *21*, 6523–6528.

I performed ECD experiments, DFT calculations, and participated in the writing of the paper.

Aleksandra Butkiewicz

Institute of Physical Chemistry
Polish Academy of Sciences

Dr hab. Magdalena Ceborska

Kasprzaka 44/52, PL-01 224 Warsaw, Poland

Tel. +(48 22) 343 32 14
+(48 22) 343 20 00
Fax +(48 22) 343 33 33
+(48 22) 632 52 76
E-mail: mceborska@ichf.edu.pl

July 7, 2021

Statement of contribution

Hereby, I would like to claim my contribution to the paper:

Ł. Szyszka, P. Cmoch, M. Górecki, M. Ceborska, M. A. Potopnyk, S. Jarosz „Chiral Molecular Cages Based on Cyclotriveratrylene and Sucrose Units Connected with *p*-Phenylene Linkers" *Eur. J. Org. Chem.* **2021**, 897–906.

I performed X-ray crystallography measurement, solved and refined the crystal structure of compound ***P*-251b**, and participated in the writing of supporting information concerning X-ray data.

M Ceborska

Magdalena Ceborska

Institute of Organic Chemistry
Polish Academy of Sciences

mgr Patrycja Sokołowska

Institute of Organic Chemistry
Polish Academy of Sciences
Kasprzaka 44/52
01-224 Warsaw, Poland

Warsaw, 22-06-2021

Statement of contribution

Hereby, I would like to claim my contribution to the paper:

S. Jarosz, P. Sokołowska, Ł. Szyszka „Synthesis of fine chemicals with high added value from sucrose: Towards sucrose-based macrocycles" *Tetrahedron Lett.* **2020**, *61*, 151888. (Digest paper)

I found the literature references concerning sucrose-based polymers, prepared schemes, participated in the writing of this review paper and responses for reviewers.

Patrycja Sokołowska

Sokołowska Patrycja